UAM
Ph.D. Thesis

Individual and mixture toxicity of pharmaceuticals towards microalgae. Role of intracellular free Ca^{2+}

Miguel González Pleiter
2017

UAM
Ph.D. Thesis

Individual and mixture toxicity of pharmaceuticals towards microalgae. Role of intracellular free Ca^{2+}

Miguel González Pleiter
Madrid, 18 de mayo de 2017

Programa de Doctorado de Microbiología

Dirigida por:

Dr. Francisca Fernández Piñas
Departamento de Biología
Facultad de Ciencias
Universidad Autónoma de Madrid

Dr. Francisco Leganés Nieto
Departamento de Biología
Facultad de Ciencias
Universidad Autónoma de Madrid

Memoria presentada para optar al título de Doctor por la Universidad Autónoma de Madrid

AGRADECIMIENTOS

A Francisca Fernández Piñas y a Francisco Leganés Nietos sin ellos nada de esto hubiera sido posible. Así como a mis compañeros ya amigos Ismael, Keila, Gerardo, Jara, Idoia y Tamayo gracias a vosotros esta tesis ha salido adelante.
A mis padres, a mi hermana y a mi familia. Así como a todos los amigos que habéis vivido este trabajo a mi lado.

FUNDING

The thesis was supported by the Spanish Government (Projects MICIN CGL2010-15675 and MINECO CTM2013-45775-C2-2-R) and the Dirección General de Universidades e Investigación de la Comunidad de Madrid, Research Network (Comunidad de Madrid S-2009/AMB/1511). Miguel González Pleiter was supported by a FPI grant from Ministerio de Economía, Industria y Competitividad.

ABBREVIATIONS

$[Ca^{2+}]_c$ (Cytoplasmic free calcium)

$[Ca^{2+}]_i$ (Intracellular free calcium)

*A.*CPB4337 (*Anabaena* sp. PCC7120 CPB4337)

AAS (atomic absorption spectroscopy)

AMO (amoxicillin)

Anabaena CPB4337 (*Anabaena* sp. PCC7120 CPB4337)

ANOVA (Analysis of Variance)

AOPs (Advanced Oxidation Processes)

ASTM (American Society for Testing and Materials)

ATP (Adenosine triphosphate)

BAPTA-AM (Glycine, N,N'-[1,2-ethanediylbis(oxy-2,1-phenylene)]bis[N-[2-[(acetyloxy)methoxy]-2-oxoethyl]]-, bis[(acetyloxy)methyl] ester)

BCECF (2',7'-Bis-(2-Carboxyethyl)-5-(and-6)-Carboxyfluorescein, Acetoxymethyl Ester)

C1 (ATE; atenolol)

C10 (ERY; erythromycin)

C11 (OFLO; ofloxacin)

C12 (NICO, nicotine)

C13 (CAFE; caffeine)

C14 (VENLA; venlafaxine)

C15 (PRIMI; primidone)

C16 (CARBA; carbamazepine)

C2 (BEZA; benzafibrate)

C3 (FURO; furosemide)

C4 (GEM; gemfibrozil)

C5 (HYDRO; hydrochlorothiazide)

C6 (DICLO, diclofenac)

C7 (IBU; ibuprofen)

C8 (KETO; ketoprofen)

C9 (PARA; paracetamol)

CA (Concentration Addition)

Calcium Green-1/AM (Glycine, N-[2-[(acetyloxy)methoxy]-2-oxoethyl]-N-[2-[2-[5-[[[3',6'-bis(acetyloxy)-2',7'-dichloro-3-oxospiro[isobenzofuran-1(3H),9'-[9H]xanthen]-5-yl]carbonyl]amino]-2-[bis[2-[(acetyloxy)methoxy]-2-oxoethyl]amino]phenoxy]ethoxy]phenyl]-, (acetyloxy)methyl ester)

Calcium Green-5/AM (Glycine, N-[2-[(acetyloxy)methoxy]-2-oxoethyl]-N-[4-[[[3',6'-bis(acetyloxy)-2',7'-dichloro-3-oxospiro[isobenzofuran-1(3H),9'-[9H]xanthen]-5-yl]carbonyl]amino]-2-[2-[2-[bis[2-[(acetyloxy)methoxy]-2-oxoethyl]amino]-5-nitrophenoxy]ethoxy]phenyl]-, (acetyloxy)methyl ester)

CaM (Calmodulin)

CBL (Calcineurin-like protein)

CCaMK (Calcium-calmodulin-dependent kinase)

CDPK (Calcium-dependent protein kinase)

CI (Combination Index)

CML (CaM-like protein)

CNGC (cyclic nucleotide-gated channel)

DGGE (denaturing gradient gel electrophoresis)

DHR123 (Benzoic acid, 2-(3,6-diamino-9H-xanthene-9-yl)-, methyl ester)

$DiBAC_4(3)$ (2,4,6(1H,3H,5H)-Pyrimidinetrione, 1,3-dibutyl-5-(3-(1,3-dibutyl-1,2,3,4-tetrahydro-6-hydroxy-2,4-dioxo-5-pyrimidinyl)-2-propenylidene))

DMSO (Dimethyl sulfoxide)

DNA (Deoxyribonucleic acid)

DU (Discrete uniform)

E1 (Estrone)

E2 (17-beta-estradiol)

EC (effective concentration)

EE2 (17-alpha-ethinylestradiol)

EES (Elementary Effects)

EGTA (ethylene glycol-bis(β-aminoethyl ether)-N,N,N',N'-tetraacetic acid)

EINECS (European INventory of Existing Commercial chemical Substances)

EMEA (European Medicines Evaluation Agency)

EPs (Emerging Pollutants)

EROs (Especies Reactivas de Oxígeno)

ERY (Erythromycin)

EU (European Union)

FDA (Fluorescein diacetate)

FISH (fluorescence in situ hybridization)

Fluo-3/AM (Glycine, N-[4-[6-[(acetyloxy)methoxy]-2,7-dichloro-3-oxo-3H-xanthen-9-yl]-2-[2-[2-[bis[2-[(acetyloxy)methoxy]-2-oxyethyl]amino]-5-methylphenoxy]ethoxy]phenyl]-N-[2-[(acetyloxy)methoxy]-2-oxyethyl]-, (acetyloxy)methyl ester)

Fluo-4/AM (Glycine, N-[4-[6-[(acetyloxy)methoxy]-2,7-difluoro-3-oxo-3H-xanthen-9-yl]-2-[2-[2-[bis[2-[(acetyloxy)methoxy]-2-oxoethyl]amino]-5-methylphenoxy]ethoxy]phenyl]-N-[2-[(acetyloxy)methoxy]-2-oxoethyl]-,(acetyloxy)methyl ester)

FRET (Fluorescence Resonance Energy Transfer)

FS (Forward Scatter)

Fura-2/AM (5-Oxazolecarboxylic acid, 2-(6-(bis(2-((acetyloxy)methoxy)-2-oxoethyl)amino)-5-(2-(2-(bis(2-((acetyloxy)methoxy)-2-oxoethyl)amino)-5-methylphenoxy)ethoxy)-2-benzofuranyl)-, (acetyloxy)methyl ester)

GC (Gas Chromatography)

GLM_{mv} (Multivariate Generalized Linear Models)

GRL (ionotropic glutamate receptors)

GSA-QHTS (Global Sensitivity Analysis with Quantitative High Throughput Screening)

GSUA (Global Sensitivey and Uncertainty Analysis)

HE (Dihydroethidium)

HEPES (4-(2-hydroxyethyl)-1-piperazineethanesulfonic acid)

HPCL (High Performance Liquid Chromatography)

IA (Independent Action)

Indo-1/AM (1H-Indole-6-carboxylic acid, 2-[4-[bis[2-[(acetyloxy)methoxy]-2-oxoethyl]amino]-3-[2-[2-[bis[2-[(acetyloxy)methoxy]-2-oxoethyl]amino]-5-methylphenoxy]ethoxy]phenyl]-, (acetyloxy)methyl ester)

ISO (International Organization for Standardization)

JC-1 (1H-Benzimidazolium, 5,6-dichloro-2-[3-(5,6-dichloro-1,3-diethyl-1,3-dihydro-2H-benzimidazol-2-ylidene)-1-propenyl]-1,3-diethyl-, iodide)

LC-MS (Liquid Chromatography–Mass Spectrometry)

LD (Lethal Concentration)

LEV (Levofloxacin)

Lmax (Sum of all L_0 values)

Lo (Light intensity at time intervals of 1 s)

LT50 (Length of the Ca2+ transients)

MALDI TOF/TOF

MDA (Malondialdehyde)

MEC (Measured environmental concentration)

MOA (Mode of Action)

MS (Mass Spectrometry)

NAC (N-acetyl-L-cysteine)

NOEC (No Observed Effect Concentration)

NOR (Norfloxacin)

OD (Optical Density)

OECD (Organization for Economic Cooperation and Development)

PAHs (Polycyclic Aromatic Hydrocarbons)

PAM (Pulse Amplitude Modulated)

PCBs (Polychlorinated Biphenyls)

PEC (Predictive Environmental Concentrations)

PFOS (Perfluorooctanesulfonic acid)

pHi (intracellular pH)

PI (Propidium iodide)

PNEC (Predicted No Effect Concentration)

PPCPs (Pharmaceutical and Personal Care Products)

Quin-2/AM (N-[2-[(acetyloxy)methoxy]-2-oxoethyl]-N-[2-[[8-[bis[2-[(acetyloxy)methoxy]-2-oxoethyl]amino]-6-methoxy-2-quinolinyl]methoxy]-4-methylphenyl]-glycine(acetyloxy)methyl este)

RNA (Ribonucleic acid)

RNA-seq (RNA sequencing)

ROS (Reactive Oxygen Species)

RQ (Risk Quotients)

RT-qPCR (Real-Time Reverse-Transcription Polymerase Chain Reaction)

SDS-PAGE (Sodium Dodecyl Sulphate Polyacrylamide Gel Electrophoresis)

SEM (Scanning Electron Microscopy)

SS (Side Scatter)

TBARS (Thiobarbituric Acid Reactive Substances)

TCS (Triclosan)

TET (Tetracycline)

TGGE (Temperature Gradient Gel Electrophoresis)

TRP (Receptor Potential Channels)

USEPA (U.S. Environmental Protection Agency)

UV (Ultraviolet)

VDCC (Voltage-Dependent Ca^{2+} Channel)

WWTPs (Wastewater Treatment Plants)

RESUMEN ---- **1**

CHAPTER 1: GENERAL INTRODUCTION ---- **9**

1.1 EMERGING POLLUTANTS IN FRESHWATER ECOSYSTEMS ---- **11**

1.1.1 What are emerging pollutants? ---- 12

1.1.2 Sources of EPs ---- 14

1.1.3 Transport of EPs ---- 14

1.1.4 Occurrence of EPs ---- 16

1.2 BIOASSAYS IN FRESHWATER TOXICOLOGY ---- **19**

1.2.1 Bioassays based on relevant photosynthetic microorganisms - 22

1.2.1.1 Bioassays based on cyanobacteria ---- 22

1.2.1.2 Bioassays based on algae ---- 26

1.2.1.3 Bioassays based on environmental biofilms as model communities in freshwater toxicology ---- 28

1.2.2 Bioassays based on intracellular free calcium ($[Ca^{2+}]_i$) ---- 30

1.2.2.1 Calcium and life ---- 30

1.2.2.2 The $[Ca^{2+}]i$ homeostasis system ---- 31

1.2.2.3 $[Ca^{2+}]i$ in environmental relevant microorganisms (cyanobacteria and green algae) ---- 33

1.2.2.3.1 $[Ca^{2+}]i$ in cyanobacteria ---- 33

1.2.2.3.2 $[Ca^{2+}]i$ in green algae ---- 35

1.2.2.4 Measurements of $[Ca^{2+}]_i$ ---- 37

1.2.2.5 $[Ca^{2+}]_i$ and pollutants ---- 38

1.2.2.6 Bioassays based on $[Ca^{2+}]_i$: $[Ca^{2+}]_i$ as a biomarker of exposure to pollutants ---- 42

1.2.2.6.1 Bioassays based on $[Ca^{2+}]_i$ in microorganisms ---- 42

1.3 TOXICITY OF MIXTURES OF POLLUTANTS ---- 44

1.3.1 Concentration Addition (CA) ---- 46

1.3.2 Independent Action (IA) ---- 47

1.3.3 Combination index (CI) ---- 47

1.3.4 CA and IA in bioassays ---- 51

1.3.5 CI in bioassays ---- 53

1.3.6 Fractional approaches (CA, IA and CI): Limitations ---- 54

1.3.7 Global Sensitivity and Uncertainty Analysis (GSUA) ---- 57

1.3.7.1 Morris method ---- 57

1.4 REFERENCES ---- 61

OBJECTIVES ---- **79**

CHAPTER 2: TOXICITY OF FIVE ANTIBIOTICS AND THEIR MIXTURES TOWARDS PHOTOSYNTHETIC AQUATIC ORGANISMS: IMPLICATIONS FOR ENVIRONMENTAL RISK ASSESSMENT ---- **83**

2.1 INTRODUCTION ---- 85

2.2 MATERIALS AND METHODS ---- 88

2.2.1 Chemicals ---- 88

2.2.2 Stability of antibiotics ---- 88

2.2.3 Toxicity bioassays ---- 89

2.2.4 Experimental design of antibiotic mixtures ---- 91

2.2.5 Median-Effect and combination index (CI)-isobologram equations for determining individual and combined toxicities ---- 91

2.2.6 Analysis of results ---- 93

2.2.7 Mixture toxicity predictions based on CA, IA and CI equations ---- 94

2.2.8 Risk quotients assessment of antibiotic mixtures ---- 95

2.3 RESULTS AND DISCUSSION ---- 96

2.3.1 Toxicity of individual antibiotics ---- 96

2.3.2 Toxicological interactions of the tested antibiotics in mixtures ---- 101

2.3.3 Experimental and predicted toxicity of the antibiotic mixtures under CA, IA and CI methods ---- 107

2.3.4 Risk quotients assessment of antibiotic mixtures ---- 110

2.4 CONCLUSIONS ---- 113

2.5 REFERENCES ---- 114

CHAPTER 3: HIDDEN DRIVERS OF LOW-DOSE PHARMACEUTICAL POLLUTANT MIXTURES REVEALED BY THE NOVEL GSA-QHTS SCREENING METHOD ---- **119**

3.1 INTRODUCTION ---- 121

3.2 MATERIALS AND METHODS ---- 124

3.2.1 Chemicals ---- 124

3.2.2 GSA-QHTS ---- 124
3.2.3 GSA-Sampling ---- 125
3.2.4 QHTS: Bioactivity determinations based on *Anabaena* sp. PCC7120 CPB4337 ---- 125
3.2.5 GSA-Screening ---- 127
3.2.6 Individual effect of PPCPs and mixture effect prediction based on additive CA model ---- 127
3.2.7 Effects of selected mixtures on experimental benthic microbial communities ---- 128
3.2.8 Experimental design and statistical analysis ---- 128
3.3 RESULTS AND DISCUSSION ---- 130
3.3.1 Generating a low-dose PPCP mixture experimental design based on the EE method ---- 130
3.3.2 Exposure to low-doses of PPCPs produced significant sublethal effects ---- 131
3.3.3 The classical additive mixture approach does not predict the sublethal effects of low-dose PPCPs mixtures ---- 134
3.3.4 GSA-QHTS identified hidden drivers of low-dose mixture sublethal effects ---- 136
3.3.5 Important drivers of mixture bioactivity identified by GSA-QHTS are also relevant at higher ecological complexity scales ---- 138
3.3.6 Main findings ---- 141
3.3.7 Limitations and further research ---- 141
3.4 CONCLUSIONS ---- 143
3.5 REFERENCES ---- 144
CHAPTER 4: INTRACELLULAR FREE Ca^{2+} SIGNALS ANTIBIOTIC EXPOSURE IN CYANOBACTERIA ---- **149**
4.1 INTRODUCTION ---- 151
4.2 MATERIALS AND METHODS ---- 154
4.2.1 Chemicals ---- 154
4.2.2 Organism and growth conditions ---- 154
4.2.3 *In vivo* aequorin reconstitution and luminescence measurements ---- 154
4.2.4 Cell lysis check ---- 155
4.2.5 Statistical analysis ---- 155
4.3 RESULTS AND DISCUSSION ---- 156

4.3.1 Ca^{2+} signatures induced in *Anabaena* sp. PCC 7120 (pBG2001a) in response to exposure to antibiotics applied singly -- 156
4.3.2 Ca^{2+} signatures induced by selected mixtures of antibiotics in *Anabaena* sp. PCC7120 (pBG2001a) ---------- 160
4.4 CONCLUSIONS ---------- 166
4.5 REFERENCES ---------- 167

CHAPTER 5: CALCIUM MEDIATES THE CELLULAR RESPONSE OF CHLAMYDOMONAS REINHARDTII TO THE EMERGING AQUATIC POLLUTANT TRICLOSAN -- 171

5.1 INTRODUCTION ---------- 173
5.2 MATERIALS AND METHODS ---------- 175
5.2.1 Chemicals ---------- 176
5.2.2 Microalgal cultures and bioassays ---------- 176
5.2.3 Flow cytometric analysis (FCM) ---------- 177
5.2.4 Lipid peroxidation ---------- 177
5.2.5 Chlorophyll determination ---------- 178
5.2.6 Oxygen evolution ---------- 178
5.2.7 RT-qPCR ---------- 178
5.2.8 Protein isolation and analysis ---------- 179
5.2.9 Data analysis ---------- 179
5.3 RESULTS ---------- 180
5.3.1 Triclosan-induced alterations in intracellular free Ca^{2+} in *C. reinhardtii* ---------- 180
5.3.2 Triclosan-induced ROS formation in *C. reinhardtii* ---------- 182
5.3.3 Effects of antioxidant N-acetylcysteine on TCS-induced increases in $[Ca^{2+}]_c$ and ROS formation ---------- 184
5.3.4 TCS alterations in membrane integrity ---------- 187
5.3.5 Triclosan-induced alterations in cytoplasmic membrane potential ---------- 189
5.3.6 Triclosan-induced changes in mitochondrial functions --------- 190
5.3.7 Triclosan alters intracellular pH (pH_i) ---------- 193
5.3.8 Triclosan-induced alterations on the metabolic activity of *C. reinhardtii* ---------- 194
5.3.9 Photosynthetic responses of *C. reinhardtii* to Triclosan -------- 195

5.3.10Effect of Triclosan on transcription of selected genes involved in photosynthesis, oxidative stress defense, calcium signaling and apoptosis ---------- 196
5.3.11 Effect of Triclosan on the protein pattern of *C. reinhardtii* --- 199
5.4 DISCUSSION ---------- 202
5.5 REFERENCES ---------- 207
GENERAL DISCUSSION ---------- **213**
CONCLUSIONES ---------- **235**
ANNEXES: SUPPLEMENTARY MATERIAL ---------- **239**
CHAPTER 2: SUPPLEMENTARY MATERIAL ---------- 241
CHAPTER 3: SUPPLEMENTARY MATERIAL ---------- 255
CHAPTER 5: SUPPLEMENTARY MATERIAL ---------- 337

RESUMEN

Millones de toneladas de productos químicos son producidos anualmente en el mundo. Muchos de estos químicos son empleados en nuestro día a día y acaban alcanzando las aguas superficiales. Los químicos que llegan a las aguas superficiales y no sé encuentran legislados se denominan contaminantes emergentes.

En el capítulo 1 se describe la problemática de los contaminantes emergentes y los bioensayos que se utilizan con el fin de evaluar su efecto sobre los ecosistemas, así como los métodos empleados para el estudio de mezclas de contaminantes. Entre los contaminantes emergentes se encuentran los fármacos, los cuales son utilizados para salvaguardar la salud humana y animal. Su elevado consumo y relativamente baja tasa de eliminación en las plantas de tratamiento de aguas residuales provocan su entrada en las aguas superficiales. Entre los fármacos destacan los antibióticos que han sido empleado de forma generalizada en las últimas décadas por la industria alimentaria, además de para fines humanos, provocando su entrada masiva en las aguas superficiales. En las aguas superficiales de todo el mundo se encuentran un gran número de contaminantes emergentes a concentraciones que van desde ng/L a µg/L. Por tanto, los organismos que habitan estos ecosistemas están expuestos a ellos. Las algas y cianobacterias, productores primarios de los ecosistemas acuáticos, juegan un papel clave en el ciclo del carbono y el nitrógeno (en el caso de las cianobacterias fijadoras de nitrógeno) y pueden verse afectados por los contaminantes emergentes, lo cual desencadenaría daños en el funcionamiento global del ecosistema. Mientras que las concentraciones individuales de los contaminantes emergentes son relativamente bajas, causando efectos limitados, las mezclas de estos contaminantes pueden encontrarse en concentraciones de µg/L y resultar en una toxicidad significativa. Los componentes de las mezclas puede no interaccionar o interaccionar, sinérgica o antagónicamente. Por tanto, las mezclas de contaminantes emergentes pueden tener un efecto tóxico sobre los ecosistemas mayor al esperado de la suma de sus efectos individuales.

El objetivo principal de esta tesis es estudiar los efectos biológicos de los contaminantes emergentes, poniendo especial hincapié en los productos farmacéuticos, sobre microorganismos fotosintéticos acuáticos de gran relevancia ecológica, entre ellos algas verdes y cianobacterias.

El objetivo principal de los capítulos 2 y 3 de esta tesis es evaluar el riesgo potencial para el medioambiente de las mezclas de contaminantes emergentes, investigando las interacciones que se producen entre ellos y desarrollando nuevas herramientas que permitan reconocer que contaminantes emergentes son los principales responsables de los efectos tóxicos observados en mezclas complejas a concentraciones reales. Para este fin se emplearan los organismos fotosintéticos de gran relevancia ecológica: *Pseudokirchneriella subcapitata*, un alga verde unicelular en la que se estudió la toxicidad en base a la inhibición de la fluorescencia de la clorofila, y *Anabaena* sp. PCC7120 CBP4337, una cianobacteria recombinante bioluminiscente en la que se estudió la toxicidad en base a la inhibición de su bioluminiscencia constitutiva reflejo de su actividad metabólica; así como biopelículas de comunidades microbianas de ríos.

En el capítulo 2, con el fin de evaluar el riesgo potencial para el medioambiente de las mezclas de contaminantes emergentes e investigar las interacciones que se producen entre ellos, se estudió la toxicidad individual y en mezcla de cinco antibióticos (amoxicilina, eritromicina, levofloxacino, norfloxacino y tetraciclina), que habitualmente se encuentran en aguas superficiales, sobre los dos organismos fotosintéticos: una cianobacteria (*Anabaena* sp. PCC7120 CBP4337) y un alga verde (*Pseudokirchneriella subcapitata*).

Los resultados obtenidos muestran que la eritromicina es el antibiótico más tóxico para ambas. Por lo general, la cianobacteria fue más sensible, probablemente debido a su naturaleza procariotica, que el alga verde; la amoxicilina no causó efectos tóxicos sobre el alga verde. Se estudiaron las interacciones toxicológicas producidas por las mezclas de antibióticos utilizando el método del "*Combination Index*", el cual permite determinar y cuantificar la naturaleza de la interacción, sinérgica o antagónica, de los componentes de una mezcla a todos los niveles de efecto, independientemente de cual sea su número y su mecanismo de acción, teniendo en cuenta la potencia y la forma de la curva dosis-respuesta de cada uno de ellos. Se encontraron predominantemente interacciones sinérgicas en las mezclas binarias y complejas de los antibióticos en ambos organismos. Cabe destacar que el antibiótico tetraciclina interactuó sinérgicamente con los otros antibióticos en casi todas las mezclas en las que se encontraba presente. Con el fin de evaluar que método predecía mejor las interacciones

toxicologías observadas en las mezclas de antibióticos se compararon los resultados obtenidos utilizando el método del "*Combination Index*" con otros dos métodos ampliamente empleados en toxicología de mezclas, "*Concentration addition*", basado en el supuesto de que todos los componentes de la mezcla tienen un mecanismos de acción similar, e "*Independent action*", basado en el supuesto de que todos los componentes de la mezcla tiene distinto mecanismo de acción. El método del "*Combination Index*" fue el que ofreció una mejor predicción de la toxicidad de las mezclas de antibióticos. Utilizando los resultados toxicológicos obtenidos de los antibióticos individuales y en mezclas, se realizó una evaluación de riesgo ambiental estudiando si las concentraciones de antibióticos presentes en las aguas superficiales podían producir efectos negativos sobre los dos organismos fotosintéticos. Los resultados muestran que las concentraciones que aparecen en las aguas superficiales de eritromicina y de la mezcla eritromicina y tetraciclina, la cual fue fuertemente sinérgica a bajos niveles de efecto, podrían dañar a microrganismos acuáticos productores primarios, como las cianobacterias y las algas verdes.

Las contaminantes emergentes aparecen en las aguas superficiales en mezclas complejas, a bajas concentraciones y con la capacidad de interaccionar entre sí y con otros factores abióticos de forma lineal y no lineal. Para evaluar los efectos de las mezclas complejas a concentraciones reales de contaminantes emergentes es necesario desarrollar nuevas herramientas que nos permitan encontrar cuales son los principales contaminantes responsables de la toxicidad de las mezclas.

En el capítulo 3, se desarrolló una nueva herramienta que permite reconocer que contaminantes emergentes son los principales contaminantes responsables de los efectos tóxicos observados en mezclas complejas a concentraciones reales empleando el método de Morris, un Análisis de Sensibilidad Global, acoplado con un cribado de alto rendimiento, basado en el bioensayo de inhibición de la bioluminiscencia por efecto tóxico con alto número de réplicas al usar placas de 96 pocillos totalmente aleatorizados utilizando *Anabaena* sp. PCC7120 CBP4337.

Para evaluar el efecto de las mezclas complejas a concentraciones reales de contaminantes emergentes la cianobacteria *Anabaena* sp. PCC7120 CBP4337 fue expuesta a mezclas de 16 fármacos, a tres niveles de concentraciones representativos de

las aguas superficiales, y un factor abiótico (intensidad de luz) de forma individual y en mezclas (un total de 180 mezclas diferentes). Los resultaron mostraron que 67 de las 180 mezclas causaron un efecto tóxico sobre la cianobacteria. Para estudiar si los modelos actuales permiten predecir la toxicidad de mezclas complejas a concentraciones reales se compararon los resultados obtenidos de los efectos tóxicos de las mezclas complejas a concentraciones reales de los 16 fármacos y un factor ambiental con la predicción del método del "*Concentration addition*". Los resultados mostraron que el "*Concentration addition*" únicamente fue capaz de explicar entre 0 y el 0.026 % del efecto observado en las mezclas. Por otro lado, el método de Morris acoplado al un cribado de alto rendimiento utilizando *Anabaena* sp. PCC7120 CBP4337 fue capaz de identificar los principales contaminantes responsables de la toxicidad de mezclas complejas a concentraciones reales proporcionando una clasificación cualitativa de los mismos basada en su efecto e interacción. Los fármacos carbamazepina (antiepiléptico), furosemida (diurético), eritromicina (antibiótico), hidroclorotiazida (diurético), gemfibrozil (regulador lipídico), venlafaxina (antidepresivo), atenolol (beta bloqueantes) y diclofenaco (analgésico) fueron identificados como los principales responsables de la toxicidad en las 180 mezclas. Para evaluar los resultados obtenidos del método de Morris y estudiar si dichos resultados eran extrapolables a niveles superiores a población se expuso a comunidades complejas microbianas de aguas superficiales (biopelículas de río) a: la mezcla más tóxica, la mezcla más tóxica diluida 10 veces y la mezcla más tóxica sin los cuatro principales contaminantes responsables de la toxicidad. Los resultados muestran que la mezcla más tóxica sin los cuatro principales contaminantes responsables de la toxicidad evolucionó de igual forma que el control a lo largo del tiempo (no mostró toxicidad significativa respecto al control no tratado), mientras la mezcla más toxica y la mezcla más toxica diluida 10 veces evolucionaron de forma diferente al control (mostrando toxicidad significativa respecto al mismo). Por tanto, la eliminación de los cuatro principales contaminantes responsables de la toxicidad fue más efectiva en prevenir la toxicidad de la mezcla que diluirla 10 veces. Los resultados confirmaron que el método de Morris es capaz de encontrar los principales contaminantes responsables de la toxicidad de las mezclas complejas a concentraciones reales.

Para evaluar el efecto de los contaminantes emergentes sobre los organismos acuáticos se emplean bioensayos de toxicidad y también de exposición. Los bioensayos basados

en biomarcadores de exposición proporcionan información sobre la percepción de ciertos contaminantes por parte de los organismos de una forma rápida y reproducible. El Ca^{2+} libre intracelular, $[Ca^{2+}]_i$, es un segundo mensajero que está involucrado en la percepción y señalización de un gran número de estreses abióticos, incluidos los contaminantes.

El objetivo principal de los capítulos 4 y 5 de esta tesis es evaluar si el $[Ca^{2+}]_i$ puede ser utilizado como un biomarcador de exposición a contaminantes emergentes de forma individual y en mezclas, así como estudiar el papel del $[Ca^{2+}]_i$ en la respuesta celular global a contaminantes emergentes. Para estudiar el papel del $[Ca^{2+}]_i$ como biomarcador de exposición a contaminantes se empleó la cianobacteria recombinante *Anabaena* sp. PCC7120 pBG2001a, la cual expresa constitutivamente la apoecuorina, una proteína indicadora de unión a Ca^{2+} que permite medir de forma continua e *in vivo* el $[Ca^{2+}]_i$. Para estudiar el papel del $[Ca^{2+}]_i$ en la respuesta celular provocada por contaminantes emergentes se utilizó el alga verde *Chlamydomonas reinhardtii*.

En el capítulo 4, con el fin de evaluar el uso del $[Ca^{2+}]_i$ como un biomarcador de exposición a contaminantes emergentes en organismos de relevancia ecológica, se expuso a la cianobacteria *Anabaena* sp. PCC7120 pBG2001a a los cinco antibióticos (amoxicilina, eritromicina, levofloxacino, norfloxacino y tetraciclina) individualmente y en mezclas, cuya toxicidad individual e interacciones toxicológicas en mezclas había sido previamente investigadas en el capítulo 2 de esta tesis usando *Anabaena* sp. PCC7120 CBP4337.

Los resultados obtenidos muestran que los cinco antibióticos indujeron un rápido cambio (2-3 segundos) en el $[Ca^{2+}]_i$, dependiente de la concentración y diferente para cada uno de los antibióticos, por tanto, indujeron lo que se denomina "firmas de Ca^{2+}" específicas (una combinación concreta de cambios en $[Ca^{2+}]_i$). Los resultados sugieren que el $[Ca^{2+}]_i$ puede ser empleado como un buen biomarcador de exposición a antibióticos. Respecto a las mezclas, se registraron los cambios producidos en el $[Ca^{2+}]_i$ en respuesta a mezclas binarias y complejas de los antibióticos. Al comparar los resultados con los obtenido previamente, de las interacciones toxicológicas usando *Anabaena* sp. PCC7120 CBP4337 (capítulo 2), determinamos que la naturaleza de las interacciones toxicológicas, antagónicas y sinérgicas, de mezclas binarias y compleja

de antibióticos podían ser predichas usando el biomarcador temprano de exposición $[Ca^{2+}]_i$, antes de que el efecto tóxico se produzca.

El $[Ca^{2+}]_i$ puede ser considerado un biomarcador temprano de la exposición a contaminantes, pero es importante conocer los mecanismos que utiliza la célula para responder a los contaminantes y qué papel desempeña el $[Ca^{2+}]_i$ en ello.

En el capítulo 5, con el fin de evaluar el papel del $[Ca^{2+}]_i$ en la respuesta celular provocada por un contaminante emergente en organismos de relevancia ecológica, estudiamos el papel del $[Ca^{2+}]_i$ en la respuesta celular del alga verde *Chlamydomonas reinhardti* utilizando un contaminante emergente modelo, el antimicrobiano triclosan. Para estudiar la respuesta celular se emplearon principalmente distintos fluorocromos indicadores de respuestas celulares usando la técnica de citometría de flujo así como medidas fotosintéticas y de expresión génica. El triclosan indujo cambios significativos en la homeostasis del $[Ca^{2+}]_i$ y una sobreproducción de especies reactivas de oxígeno (EROs), lo cual condujo a estrés oxidativo, pérdida de la integridad de membrana citoplasmática, despolarización de la membrana citoplasmática, reducción de la actividad metabólica, acidificación del pH intracelular, inhibición de la fotosíntesis, despolarización de la membrana mitocondrial y apoptosis. Para investigar el papel del $[Ca^{2+}]_i$ en la respuesta celular tras la exposición a triclosan se empleó el BAPTA-AM, un quelante intracelular de Ca^{2+} que al querlarlo evita los cambios en $[Ca^{2+}]_i$ así, sin señal de $[Ca^{2+}]_i$, se puede estudiar si la respuesta celular al tóxico depende total o parcialmente del $[Ca^{2+}]_i$. La preincubación con BAPTA-AM previno los efectos tóxicos del triclosan sobre la mayoría de los distintos parámetros de respuesta celular estudiados. Por tanto, se ha demostrado que el $[Ca^{2+}]_i$ tiene un papel clave en las respuestas celulares desencadenadas por el triclosan y probablemente por otros contaminantes. Hay una controversia importante en la literatura sobre si, una vez se ha producido la exposición al contaminante, los cambios en $[Ca^{2+}]_i$ dan lugar a la formación de EROs ó si la formación de EROs es la primera respuesta celular a la exposición al contaminante y el $[Ca^{2+}]_i$ sería una respuesta posterior en la cascada de señalización celular, por ello se empleó el NAC (un antioxidante) para estudiar el papel de los EROs en las respuestas celulares tras la exposición al triclosan. Su uso demostró que existe una relación bidireccional entre el $[Ca^{2+}]_i$ y la formación de EROs en la

respuesta de *Chlamydomonas reinhardti* tras la exposición a contaminantes emergente como el triclosan.

En conclusión, los antibióticos a las concentraciones que aparecen en las aguas superficiales interaccionan entre si pudiendo causar efectos tóxicos mayores a los esperados de la suma de sus efectos tóxicos individuales sobre organismos fotosintéticos. El método de Morris acoplado a un cribado de alto rendimiento es capaz de identificar los principales contaminantes responsables de la toxicidad de mezclas complejas a concentraciones reales. El $[Ca^{2+}]_i$ es un buen biomarcador de exposición a antibióticos y es capaz de identificar la naturaleza de sus interacciones toxicológicas de forma temprana. El $[Ca^{2+}]_i$ juega un papel clave en la respuesta celular global al triclosan.

CHAPTER 1: GENERAL INTRODUCTION

1.1. EMERGING POLLUTANTS IN FRESHWATER ECOSYSTEMS

Nowadays, chemicals play a key role in our society. They surround us; and our social and economic development depends on them. Chemicals constitute the basis of the industries that sustain quality of life for present and future generations. Today, there are more than 100.000 registered chemicals listed in EINECS (the European Inventory of Existing Commercial Chemical Substances) and 70 new chemicals are registered each hour in the America Chemical Society (Kuzmanovic et al. 2015, McKnight et al. 2015). More than 300 million tonnes of chemicals are produced annually in Europe and many of them are used on a daily basis (Eurostat 2014). Many of these chemicals finally reach the freshwaters (rivers, streams, lakes, natural ponds, wetlands and springs) (Kuzmanovic et al. 2015).

As a response to the increasing levels of chemicals in freshwaters, consequence of human activity, the European Union (EU) has established regulatory strategies to reduce the occurrence of a few number of them (Directive 2013/39/EC). These chemicals subject to the regulation are the so-called priority pollutants. From now on, the term pollutants will be used here instead of contaminants, following Mandaric et al. (2015), who reported that: "*all pollutants are contaminants, but only those contaminants that can result in adverse biological effects are pollutants*".

Priority pollutants are 45 chemicals regulated by Directive 2013/39/EC in EU and, which should be monitored in freshwaters. Priority pollutants includes several heavy metals (cadmium, lead, mercury, nickel and their derivatives), pesticides (aldrin, dichlorodiphenyltrichloroethane, dicofol, dieldrin, endrin, endosulfan, isodrin, heptachlor, lindane, pentachlorophenol, chlorpyrifos, chlorfenvinphos, dichlorvos, atrazine, simazine, terbutryn, diuron, isoproturon, trifluralin, cypermethrin, alachlor, aclonifen, bifenox, cybutryne and quinoxyfen), solvents (dichloromethane, dichloroethane, trichloromethane and carbon tetrachloride), perfluorooctane sulfonic acid and its derivatives (PFOS), polychlorinated biphenyls (PCBs), polycyclic aromatic hydrocarbons (PAHs), nonylphenol, octylphenol, organotin compounds (tributyltin), dioxins and dioxin-like compounds, brominated diphenylethers,

hexabromocyclododecanes and di(2-ethylhexyl) phthalate (Directive 2013/39/EC; (Ribeiro et al. 2015a, Ribeiro et al. 2015b).

Due to their occurrence and potential to cause adverse effects in freshwaters, new chemicals are continuously monitored and evaluated. Recently, ten chemicals (or group of chemicals) have been included in the First Watch List of EU in order to collect data about them in freshwaters (Decision 2015/495/EC, Ribeiro et al. 2015a, Ribeiro et al. 2015b). Over the time, some of them may be embodied in future legislation as priority pollutants depending on research on their toxicology and on their occurrence in freshwaters (Mandaric et al. 2015). The First Watch List include pesticides (methiocarb, tri-allate, oxadiazon, imidacloprid, thiacloprid, thiamethoxam, clothianidin and acetamiprid), hormones (17-Beta-estradiol (E2), Estrone (E1) and 17-Alpha-ethinylestradiol (EE2)), industrial compound (2,6-Ditert-butyl-4-methylphenol), personal care products (2-Ethylhexyl 4-methoxycinnamate) and pharmaceuticals such as diclofenac or macrolide antibiotics (erythromycin, clarithromycin and azithromycin) (Decision 2015/495/EC; (Ribeiro et al. 2015a, Ribeiro et al. 2015b). However, there are still many chemicals reaching the freshwater that are not regulated by the current legislation. Many of these chemicals belong to the so-called emerging pollutants (EPs).

1.1.1 What are emerging pollutants?

There are a wide number of definitions for EPs. They can be defined as synthetic or natural chemical reaching, or having the potential to enter or occur, in the environment from various anthropogenic sources; they are not commonly monitored and may cause known or suspected adverse effects ecological and (or) human health (Gavrilescu et al. 2015, Geissen et al. 2015). EPs are not legislated and, therefore, are not included in routine monitoring programs of the EU (Mandaric et al. 2015). Currently, there are around 700 chemicals that can be grouped under this definition, which may reach the freshwaters (Gavrilescu et al. 2015, Geissen et al. 2015).

EPs can be classified into different groups according to their use and/or composition. EPs includes pharmaceuticals (used in human and veterinary medicine, including hormones), personal care products, nanomaterials (organic and inorganic), plasticizers (phthalates, non-phthalates and biobased), plastics (including microplastics and

nanoplastics), surfactants, organotin compounds [organic derivatives of tin(IV), tin(III)), tin(II) and tin(I)], plant protection products, industrial compounds, cyanotoxins, algal toxins, flame retardants, endocrine disruptors, polycyclic aromatic hydrocarbons and derivatives, illicit drugs, biocides, disinfection by-products and intermediates in the industrial manufacture (Murray et al. 2010, Noguera-Oviedo and Aga 2016, Sauvé and Desrosiers 2014, Shi et al. 2012, Vandermeersch et al. 2015).

One of the most important groups of EPs are the pharmaceuticals. They are chemicals with medicinal properties, and that have been used by human for centuries to treat diseases (Hughes et al. 2013). Over the last decades, the use of pharmaceuticals has been extended to agriculture, aquiculture and livestock industries, which has led to an increase of their production and consumption worldwide (Osorio et al. 2016, Sarmah et al. 2006). Nowadays, the presence of pharmaceuticals in freshwaters is well established in all continents (Archer et al. 2017, Esteban et al. 2016, Hughes et al. 2013). Table 1.1 shows the pharmaceuticals most frequently found in freshwaters classified according to their therapeutic effects.

Table 1.1 Pharmaceuticals most frequently found in freshwaters classified according to their therapeutic effects [modified from Ferrando-Climent et al. (2014), Nica et al. (2015); Ahmed et al. (2016) and Mandaric et al. (2016)].

Therapeutic class	Representative groups/compounds
Anticancer	Acridone, cyclophosphamide, methotrexate and tamoxifen
Analgesic	Acetaminophen, codein, diclofenac, ibuprofen, ketoprofen, naproxen and salicylic acid
Antidepressants	Citalopram, diazepam, fluoxetine, paroxetine, pirimidone and venlafaxine
Antidiabetic	Glibenclamide
Antiepileptic	Carbamazepine
Antimicrobial	Aminoglycosides (gentamycin, neomycin and streptomycin) beta-lactam (amoxicillin), macrolides (azithromycin, clarithromycin and erythromycin), quinolones (ciprofloxacin, levofloxacin, norfloxacin and ofloxacin), tetracyclines (chlortetracycline, tetracycline and oxytetraciclyne), triclosan, trimethroprim and sulfamides (sulfamethoxazole)
Beta-blockers	Atenolol, metropolol, propanol and sotalol
Diuretic	Furosemide and hydroclorotiazida
Gastric protectors	Crimetedine, famotidine, omeprazole and ranitidine
Lipid regulators	Bezafibrate, clofibric acid and gemfibrozil
Stimulants	Caffeine and nicotine
X-ray contrast media	Diatrizoate, iopamidol and iopromida

From now on, the term pollutants will be used here as a collective term, encompassing priority and emerging pollutants. In addition, particular attention will be given to pharmaceuticals, since they are one of the most important groups of EPs and those used in this thesis.

1.1.2 Sources of EPs

The major sources of EPs in freshwaters are hospitals, households, livestock, agriculture, freshwater aquaculture and industries (Fairbairn et al. 2016, Jiang et al. 2013, Noguera-Oviedo and Aga 2016, Pal et al. 2010, Pal et al. 2014); as well as sources not controlled such as septic tanks, leaking sewer lines, landfills and inappropriately disposed wastes (Gavrilescu et al. 2015, Pal et al. 2014).

One of the groups of EPs to be emphasised in this connection are pharmaceuticals. They are present in the major sources of EPs in freshwaters. Pharmaceuticals are produced worldwide on a 100.000 t scale (Mandaric et al. 2015). The worldwide annual per capita consumption of pharmaceuticals is 15 g and developed countries consume three to ten times higher (50 - 150 g) (Carere et al. 2015, Zhang et al. 2008). Its use in livestock industry has multiplied by 100 in less than 50 years in the Unites State of America (U.S.), the same as in other places of world (Sarmah et al. 2006). Due to their widespread use are present in many sources. Hospital, households, livestock industry, agriculture industry and freshwater aquaculture are continuously sources of pharmaceuticals in freshwaters (Noguera-Oviedo and Aga 2016).

1.1.3 Transport of EPs

The major pathway for the entry of EPs into freshwater is the effluents of wastewater treatment plants (WWTPs) (Luo et al. 2014). WWTPs are designed to remove pathogens and suspended or flocculated matter and they are unable to remove completely the EPs (Bueno et al. 2012, Luo et al. 2014, Rosal et al. 2010b). In fact, it is well documented that many EPs escape the activated sludge wastewater treatment process (Fig 1.1), which is the most widely used treatment system around the world (Luo et al. 2014, Noguera-Oviedo and Aga 2016, Rosal et al. 2010b).

Many pharmaceuticals are typically resistant to degradation by WWTPs. Among these pharmaceuticals are highlighted: carbamazepine (anti-epileptic), erythromycin (antibiotic), diclofenac (analgesic), bezafibrate (beta-blocker) and ketoprofen (analgesic), which are not efficiently removed in WWTPs (Luo et al. 2014, Noguera-Oviedo and Aga 2016, Rosal et al. 2010b). Other pharmaceuticals are removed at moderate levels such as atenolol (beta-blocker), gemfibrozil (beta-blocker) and triclosan (antimicrobial) and some of them are almost completely removed (caffeine, ibuprofen and acetaminophen) (Luo et al. 2014, Rosal et al. 2010b). However, due to their continued release, EPs highly removed in WWTPs also manage to reach the freshwaters and they are commonly considered as pseudo-persistent (high removal efficiency and high release) (Ribeiro et al. 2015a, Ribeiro et al. 2015b).

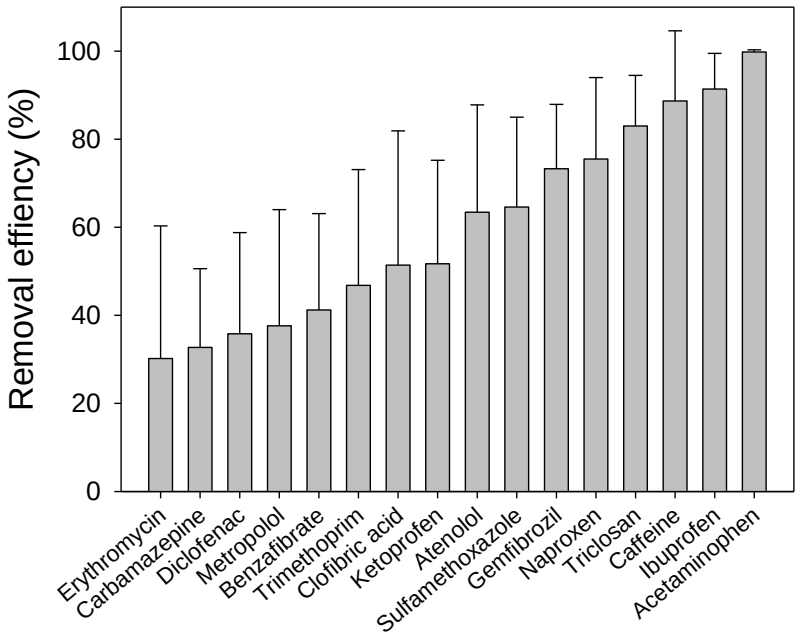

Figure 1.1 Removal efficiency of the selected EPs in WWTPs. X-axis displays the selected compounds. Error bars represent the standard deviations of the data. Figure adapted from Luo et al. (2014).

Due to the relative inefficiency of conventional WWTPs in removing EPs, it is necessary to implement new technologies in order to remove them. Since 1980s, new treatment technologies have been developed to remove EPs (Mandaric et al. 2015). These new technologies can be classified into four groups: conventional (biological activated carbon, microalgae reactor and activated sludge), non-conventional (constructed wetland and membrane bioreactor), chemical processes (Fenton, photo-

Fenton, ozonation, coagulation, photocatalysis (TiO_2) and Fenton, ozonation, photolysis and advanced oxidation processes (AOPs)) and physical processes (micro- or ultra-filtration, nanofiltration and reverse osmosis) (Ahmed et al. 2017, Rosal et al. 2010b). These technologies generally increase the cost for the process of wastewater treatment (Luo et al. 2014). However, they greatly increase the removal efficiency of EPs and, therefore, its use could prevent EPs from entering freshwaters (Ahmed et al. 2017).

Those EPs that reach the freshwater can be removed through natural processes (Mandaric et al. 2015). Removal processes in freshwater include dilution, biodegradation, photolysis, volatilization, sorption processes and abiotic oxidation, reduction and hydrolysis (Luo et al. 2014, Mandaric et al. 2015). These processes can reduce pollutant loadings. However, the capacity of freshwater for removing EPs is very limited and strongly dependent on environmental conditions (oxygen concentration, temperature, redox potential and pH) (Luo et al. 2014, Mandaric et al. 2015). In addition, EPs most efficiently removed in freshwater are also those efficiently removed in the WWTPs (Acuña et al. 2015). Therefore, many EPs cannot be removed neither by WWTPs nor by natural processes in freshwaters (Mandaric et al. 2015). On the other hand, some of these EPs are partially degraded by natural processes in freshwaters. In some cases, the degradation products have been found to be more toxic than the parent EPs. Therefore, these studies highlight the fact that the absence of the parent EPs does not necessarily mean lack of pharmaceutical persistence in the environment, but that the parent EPs may simply be transformed into more toxic pollutants (Noguera-Oviedo and Aga 2016). In conclusion, the capacities of the current technologies and natural processes to remove EPs are limited; therefore, they cannot prevent the occurrence of EPs in freshwaters.

1.1.4 Occurrence of EPs

EPs have been detected in WWTP effluents, freshwaters, drinking water and groundwater. Recently, their presence in freshwaters of all continents has been established, including in the rivers in Africa and in streams in the Antarctica (Archer et al. 2017, Ebele et al. 2017, Esteban et al. 2016, Hughes et al. 2013).

The first evidence of the presence of EPs in freshwaters was probably materialized in 2002 (Noguera-Oviedo and Aga 2016). The U.S. Geological Survey conducted the first large freshwater quality study. They reported pharmaceuticals and hormones in several freshwaters in U.S. Until then, there were few reports about the occurrence of EPs in freshwaters. The research about EPs has been carried out in more depth only during the last 15 years due to the lack of analytical methods sensitive enough to detect their relatively low concentration (typically in ng L^{-1} levels) in environmental samples (Noguera-Oviedo and Aga 2016). Therefore, the development of new technologies has allowed to increasingly detect EPs, which were probably already there long ago (Noguera-Oviedo and Aga 2016).

Pharmaceuticals stand out among EPs regarding their occurrence in freshwaters. Although some pharmaceuticals have low excretion rates (e.g., ibuprofen, carbamazepine, diclofenac and primidione), they are not necessarily present at low levels in freshwaters (Luo et al. 2014). As mentioned above, this is possibly because the low excretion rates are offset by the massive use of these pharmaceuticals and many of them can resist totally o partially the removal processes. Several studies have pointed to seasonal variability in the concentrations of EPs in freshwaters (Kolpin et al., 2004; Valcárcel et al 2012; Luo et al 2014). This may be in part due to local common diseases, which are able to induce a higher consumption of specific pharmaceuticals in certain periods (Kolpin et al., 2004, Valcárcel et al 2012, Luo et al. 2014, Valcarcel et al. 2013). Moreover, climatic conditions could also cause fluctuations in the concentration of EPs in freshwaters; since environmental conditions can decrease the capacity of freshwaters for removing EPs (Luo et al. 2014, Mandaric et al. 2015). The occurrence of individual EPs in freshwaters is currently in the concentration range from $\mu g L^{-1}$ to ng L^{-1} (Jiang et al. 2013, Jiang et al. 2014, Acuña et al. 2015).

Different EPs have been detected simultaneously in freshwaters. While the individual concentrations of EPs in freshwaters as described may be low ($\mu g\ L^{-1}$ to ng L^{-1}), the combined concentrations can be higher. Bueno et al. (2012) evaluated the occurrence of a group of 100 priority and EPs in the effluent of 5 WWTPs in Spain. They detected in at least one occasion 88 pollutants in the effluent; 20 of them were identified frequently as responsible for 83% of the total load of priority and EPs in effluents. Similarly, Kuzmanovic et al. (2016) reported that more than 50 pharmaceuticals were detected in

each sample (they collected at 77 sampling sites) of 4 river basins. Rodriguez-Gil et al. (2010) reported 56 pharmaceuticals in four river waters in Spain. Therefore, EPs co-occur in freshwater (Archer et al. 2017, Esteban et al. 2016, Hughes et al. 2013, Jiang et al. 2013, Ternes et al. 2004).

1.2. BIOASSAYS IN FRESHWATER TOXICOLOGY

Once released in freshwaters, pollutants have the potential to cause adverse effect on aquatic organism even at relatively low concentrations, which should be evaluated (Jiang et al. 2013, Luo et al. 2014, Muñoz et al. 2009).

Chemical and physical analyses techniques have been commonly used to evaluate the effects of pollutants in freshwaters. These techniques includes atomic absorption spectroscopy (AAS), gas chromatography (GC) and high performance liquid chromatography (HPLC) coupled to ultraviolet (UV), mass spectrometry (MS) or fluorescence detectors (Hassan et al. 2016, Noguera-Oviedo and Aga 2016, Rosal et al. 2010b). Chemical and physical techniques allow to accurately determine the concentration of pollutants in freshwaters (Hassan et al. 2016). However, these techniques do not respond to an important question: Is the sample toxic? In addition, chemical and physical analysis techniques are time consuming and expensive and they cannot detect bioavailable concentrations or cumulative toxicity of co-occurring pollutants (Hassan et al. 2016). Furthermore, chemical and physical analyses are only able to determine the components and concentrations of previously known pollutants. In contrast, bioassays can globally reflect the detrimental effects on organisms and reveal the toxicity mechanism (Ma et al. 2014). For this reason, bioassays are being used as a complement of chemical analysis techniques (Hassan et al. 2016).

The idea of using bioassays to evaluate the toxicity of pollutants in freshwater was developed by Anderson et al. (1944). They used invertebrate *Daphnia magna* to determine the toxicity of various pollutants found in industrial waste. In 1960s, Henderson et al. (1963) used several fishes to test the effect of pollutants in water and Jackson et al. (1966) applied bioassays for monitoring freshwaters ecosystems (Kokkali and van Delft 2014). Probably, in 1970s was the first time that a bioassay was implemented for environmental protection: Bioassays methods of the National Swedish Environment Protection Board (Kokkali and van Delft 2014). Nowadays, bioassays are used for analysing toxicity of freshwater ecosystems and to study the toxicity mechanisms of pollutants (Kokkali and van Delft 2014).

The organisms most frequently used in bioassays conducted in freshwater are shown in Table 1.2. A wide variety of commercial bioassay kits based on these organisms and statistical packages are available in the market for processing the results according to standard methods, which are validated by organizations such as the International Organization for Standardization (ISO), the American Society for Testing and Materials (ASTM), the Organization for Economic Cooperation and Development (OECD), the U.S. Environmental Protection Agency (USEPA) and Environment Canada (Kokkali and van Delft 2014).

Table 1.2 List of the organisms most commonly used in bioassays in freshwater ecosystems [modified from OECD 2011; Kokkali et al. (2014) and Hassan et al. (2016)].

Taxonomy	Species
Fish	*Danio rerio*
	Lepomis macrochirus
	Oncorhynchus mykiss
	Pimephales promelas
Invertebrate	*Artemia salina*
	Branchionus calyciflorus
	Chironomus riparius
	Daphnia magna
	Physa acuta
Protozoa	*Euglena gracilis*
	Tetrahymena sp.
Algae	*Chlamydomonas reinhardtii*
	Chlorella vulgaris
	Desmodesmus subspicatus
	Navicula pelliculosa
	Raphidocelis subcapitata
	Scenedesmus obliquus
Bacteria	*Aliivibrio fischeri*
	Anabaena flos-aquae
	Synechococcus leopoliensis

Bioassays are based on changes (at the physiological, cellular or genetic levels) in the response of living organisms in the presence of chemical, physical or biological stressors, which can lead to toxicity (Hassan et al. 2016). Toxicity is usually expressed as: no observed effect concentrations (NOECs), effective concentration (ECx) or lethal concentration (LDx). NOEC is the highest concentration of a chemical or mixture of chemicals at which no statistically significant effects on the studied toxicity endpoint with respect to the control are observed (Wagner and Løkke 1991). ECx or LDx are the concentrations of a chemical or mixture of chemicals which induce an x percent of the

measure effect on the studied endpoint parameter with respect to the control. The most used effective concentration is that producing 50% of effect (EC_{50}).

Most of the bioassays described above use endpoints of survival or growth to assess the effect of the pollutants. The main disadvantages of these endpoints are their low sensitivity to low pollutant concentrations, long test periods and that they are not useful to assess the sublethal effects of pollutants. In this context, physiological, cellular and genetic endpoints, also called biomarkers, have been used in bioassays in the last years. Bioluminescence is perhaps the most used of these endpoints (Ma et al. 2014). This is exclusive to bacteria. However, given the fact it is fast, easy to use and cost-effective, many countries use it and have established the official standard for bioluminescent bioassays applied in freshwater toxicology (French DIN 38412-1990, USA ASTM D5660-1995, Chinese GB/T 15441-1995 and Europe ISO 11348) (Ma et al. 2014). The most used organism in bioluminescent bioassays is *Aliivibrio fischeri* (also known as *Vibrio fischeri*). Bioluminescence bioassays are based on the inhibition of constitutive luminescence, which is related to the metabolic activity of the organism, caused by the presence of a stressor (Ma et al. 2014). The light emitted by bioluminescent organisms is created by a bioluminescent enzyme system which consists of a luciferase. The genes (*lux* genes) responsible for luciferase production are encoded by the operon *luxCDABE* (*lux* operon) (Ma et al. 2014).

$$FMNH_2 + RCHO + O_2 \xrightarrow{\text{bacterial luciferase}} FMN + RCOOH + H_2O + \text{light (490 nm)}$$

LuxAB encodes bacterial luciferase which catalyzes the oxidation of a long chain aliphatic aldehyde and $FMNH_2$, producing light at 490 nm. The aldehyde substrate of luciferase is synthesized by the reductase, transferase and synthetase genes encoded by *luxC, D* and *E*, respectively. Consequently, as it has been previously mentioned, light emission is closely related to cellular metabolism and light intensity reflects the metabolic status (Ma et al. 2014).

Other of these endpoints is intracellular free calcium ($[Ca^{2+}]_i$). $[Ca^{2+}]_i$ has been found to be the most versatile second messenger. Bioassays using $[Ca^{2+}]_i$ are based on the fact that biotic and abiotic stressors, including pollutants, generate changes in $[Ca^{2+}]_i$

homeostasis, which evoke specific, reproducible and doses-dependent Ca^{2+} signals, even well before toxicity is evident (Barran-Berdon et al. 2011, Kozlova et al. 2005). Therefore, $[Ca^{2+}]_i$ can be used as early endpoint of exposure to pollutants (Barran-Berdon et al. 2011, Kozlova et al. 2005, Ruta et al. 2016). The role of $[Ca^{2+}]_i$ in organisms and as a bioassay of exposure will be described in more depth in section 2.2.

Bioassays are, therefore, rapid, sensitive and effective methods to assess the toxicity of pollutants in freshwater ecosystems (Hassan et al. 2016). They are useful to detect bioavailable concentrations of pollutants. They can also be used to estimate the global response for the total pollutants load in the samples (Hassan et al. 2016). As a consequence, bioassays can be used to evaluate the toxicity of environmental samples even if the pollutants present in samples cannot be identified or quantified by chemical or physical analysis techniques (Hassan et al. 2016, Ma et al. 2014). In this thesis, particular attention will be given to bioassays based on photosynthetic microorganisms (cyanobacteria and green algae) given the key role played by these organisms in freshwater ecosystems.

1.2.1. Bioassays based on relevant photosynthetic microorganisms

Cyanobacteria and algae are primary producers in freshwater ecosystems. They are involved in the carbon cycle, including global CO_2 sequestration (Low-Decarie et al. 2014). In addition, cyanobacteria are crucial in biogeochemical cycles, such as nitrogen and phosphorus cycles (Heimann and Cirés 2015, Van Mooy et al. 2015). Therefore, changes affecting the primary producers may have effects on the entire ecosystem (Valitalo et al. 2017). As a consequence, bioassays based on primary producers are pivotal to assess the risk of pollution in freshwater ecosystems.

1.2.1.1 Bioassays based on cyanobacteria

Cyanobacteria are gran negative prokaryotic organisms able to perform oxygenic photosynthesis. Many species are able to fix nitrogen. They originated 3500 million years ago (Knoll 2015, Schopf 1993). The development of an oxygen-containing atmosphere is attributed to the photosynthetic activity of cyanobacteria (approximately 2.45 - 2.22 billion years ago) (Schirrmeister et al. 2015). Cyanobacteria are considered as ancestors of the chloroplasts in plants and algae (Hagemann et al. 2016). They exist

in almost every environment and frequently in great abundance (Adams et al. 2013). In fact, quantitatively, they are among the most important organisms on Earth (global biomass is 3×10^{14} g C) (Whitton and Potts 2012). In addition, cyanobacteria have established symbiotic relationships with plants, fungi, and animals such as corals, sponges, and ascidians (sea squirts) (Adams et al. 2013).

Cyanobacteria are considered to be a widely and ubiquitously distributed phylum. Cyanobacteria include unicellular and filamentous species. Some filamentous strains differentiate into several different cell types such as akinetes (resistant spore-like cells) and heterocystes (cells that express the enzyme nitrogenase and therefore are able to fix nitrogen; e.g., *Anabaena* sp. PCC7120) (Kaneko 2001). Currently, cyanobacteria play a key role in global biogeochemical cycle, such as carbon and nitrogen (in freshwater N_2-fixation can provide up to 1.5 g N m^{-2} $year^{-1}$) (Berman-Frank et al. 2003) (Heimann and Cirés 2015). Cyanobacterial taxonomy is an issue of controversy. The most accepted classification for cyanobacteria is the developed by Komareck et al. (2015). In its study, he classified cyanobacteria into nine sections: Nostocales, Chroococcidiopsidales, Rubidibacter/Halothece, Spirulinales, Pleurocapsales, Chroococales, Oscillatoriales, Synechococcales and Gloeobacteriales (Komárek 2015). As to date, more than 90 species of cyanobacteria have been sequenced (http://www.genome.jp/kegg/catalog/org_list.html).

Due to their ecological relevance, cyanobacteria have been included in routine monitoring programs of water quality in several countries during the last years (Mateo et al. 2015). The presence or absence of different cyanobacterial species indicates the overall ecological quality of freshwater ecosystems (Mateo et al. 2015). Besides, a few species of cyanobacteria, such as *Microcystis aeruginosa*, *Synechococcus leopoliensis*, *Anabaena flos-aquae* and *Anabaena* sp. PCC7120, have been used in bioassays (OECD, 2011;(Valitalo et al. 2017).

Among these cyanobacteria, *Anabaena* sp. PCC7120 (also known as *Nostoc* sp. PCC7120) is probably the free-living cyanobacterium most frequently used as model organism for studying cyanobacterial cell differentiation and nitrogen fixation (Komárek 2015, Stebegg et al. 2012, Zheng et al. 2017). Furthermore, over the last years, its use has been extended as model to bioassays. Several studies reported the

effect of pollutants in *Anabaena* sp. PCC7120 (Ando et al. 2007, Gonzalo et al. 2015, Panda et al. 2017, Pandey et al. 2012, Singh et al. , Thompson et al. 2002, Wannigama et al. 2012). *Anabaena* sp. PCC7120 has been sequenced, annotated and can be accessed via public databases and its cell biology is well-known; which allows to study the toxicity mechanism of pollutants (Kaneko 2001).

Fig. 1.2 shows the schematic diagram of a typical filament of *Anabaena* sp. PCC7120. Cyanobacterial cells are divided into six intracellular compartments: periplasmic space, cytoplasmic membrane, carboxysomes, thylakoid lumen, thylakoid membrane and cytosol (Malatinszky et al. 2017). They have a plasma membrane and outer membrane separated by a periplasmic space. Although gram-negative, its cell wall shares some similarities with that of the gram positive bacteria in the type and proportion of lipid components, the thickness of the peptidoglican layer and in the degree of crosslinking between the peptidoglican chains (Hoiczyk and Hansel 2000). *Anabaena sp.* PCC7120 has carboxysomes, RuBisCO-encapsulating bacterial microcompartments for CO_2 fixation, and thylakoid membranes, a system of inner membranes which host the photosynthetic apparatus (Malatinszky et al. 2017). Attached to the thylakoid membrane, they have phycobilisomes, which act as light havesting antennae complexes used during photosynthesis. *Anabaena sp.* PCC7120 presents several photosynthetic pigments such as: chlorophyll a, carotenoids, phycocyanin, allophycocyanin and phycoerytrhin. *Anabaena* sp. PCC7120 presents a single chromosome (6413771 bp) and six plasmids. There are designated as: pCC7120α (408101 bp), pCC7120β (186614 bp), pCC7120γ (101965 bp), pCC7120δ (55414 bp), pCC7120ε (40,340 bp), and pCC7120ζ (5584 bp) (Kaneko 2001). *Anabaena sp.* PCC7120 grows photoautotrophically (using light, H_2O and CO_2). It has been reported that it can also grow mixotrophically using fructose (Stebegg et al. 2012). The generation times of vegetative cells are approximately 24 hours under photoautotrophic conditions (Zhao et al. 2007a, Zhao et al. 2007b), and they can fix N_2 at rates of 7.5 to 10 pmol N_2/(mg Chl/hr) (Levine et al 1987). *Anabaena* sp. PCC7120 is a relevant bacterium in freshwater ecosystems because it is a primary producer tacking part in several biochemical cycles. Due to its ecological relevance *Anabaena* sp. PCC7120 is used in bioassays. Growth endpoints (optical density, fluorescence of chlorophyll a and cell counts) are usually used in these bioassay, which can show low sensitivity to low pollutant concentrations and require long test periods.

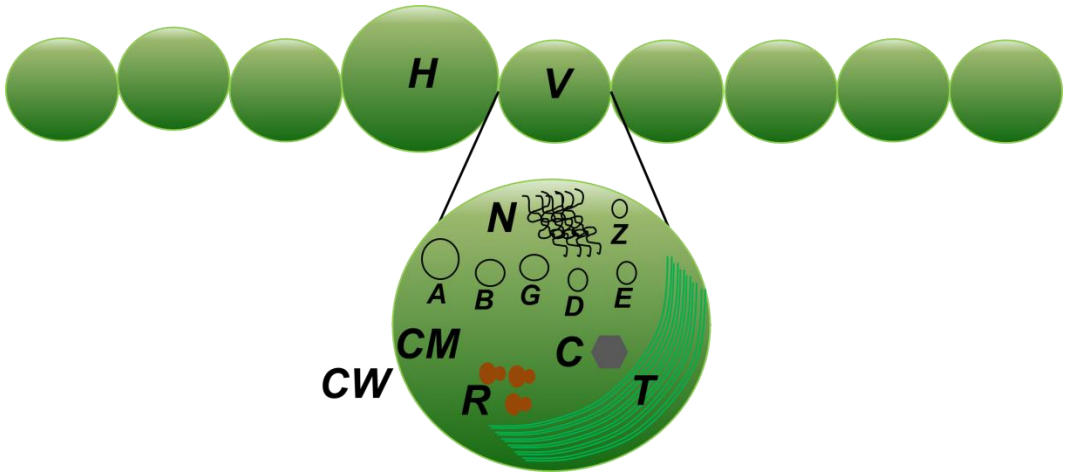

Figure 1.2 Schematic diagram of a typical filament of *Anabaena* sp. PCC7120, H: heterocyst; V: vegetative cell; T: thylakoids; N: nucleoid (chromosome); A: alpha-chromosome; B: beta-chromosome; G: gamma-chromosome; D: delta-chromosome, E: epsilon-chromosome; Z: zeta-chromosome; CW: cell wall; CM: cytoplasmic membrane; C: carboxysome; R: ribosomes.

Fernandez-Piñas and coworkers developed recombinant bioluminescent strain *Anabaena* sp. PCC7120 CPB4337 (*Anabaena* CPB4337) (Fernández-Pinas and Wolk 1994), which has been used in this thesis. This strain is bioluminescent as a consequence of a chromosomal integration of the whole l*uxCDABE* operon from *Photorhabdus luminescens* into *Anabena* sp. PCC7120. *Anabaena* CPB4337 emits an extraordinary high and a stable luminescent signal (Fernández-Pinas and Wolk 1994). Neither growth nor cell viability are affected by the chromosomal integration or bioluminescence expression (Fernández-Pinas and Wolk 1994). The organism is functional in a wide range of pH conditions (Rodea-Palomares et al. 2009b). The bioassays using *Anabaena* CPB4337 have been found to have a very good level of inter- and intra-experimental reproducibility, and it has been successfully tested in environmental matrices of different complexity (García et al. 2013, Rodea-Palomares et al. 2009a, Rosal et al. 2010a). It has been used to study the toxicity of individual and mixtures of pollutants (Rodea-Palomares et al. 2009a, Rodea-Palomares et al. 2009b, Rodea-Palomares et al. 2012, Rodea-Palomares et al. 2010, Rosal et al. 2010a). It has also been used in combination with a battery of organisms of other tropic levels, such as *V. fischeri* and *D. magna*, to study the toxicity of different pollutants (Rosal et al. 2010a). These studies showed that *Anabaena* CPB4337 is a very sensitive organism, particularly to EPs such as fibrates (being for some of them up to two orders of magnitude more sensitive than *V. fischeri*), perfluorinated surfactants, chlorinated by-

products and lipid regulators (Rodea-Palomares et al. 2009a, Rodea-Palomares et al. 2012, Rodea-Palomares et al. 2010, Rosal et al. 2010a). In addition, the luminescent bioassay based on this organism is time-saving, cost effective and of simple operation (Ma et al. 2014, Rodea-Palomares et al. 2009a). Consequently, *Anabaena* CPB4337 can be considered as model to study the effect of EPs in freshwater ecosystems.

1.2.1.2 Bioassays based on algae

For several decades now, algae have been used as model in freshwater toxicology. Algae as primary producers also play a pivotal role in the carbon cycle in freshwater. In this thesis, we used *Pseudokirchneriella subcapitata* and *Chlamydomonas reinhardtii*, which are two of the most commonly algae used in bioassays in freshwater (see table 1.2)

Pseudokirchneriella subcapitata (also known as *Raphidocelis subcapitata* and *Selenastrum capricornutum*) is the primary producer most frequently used in bioassays. *Pseudokirchneriella subcapitata* is a unicellular freshwater green microalga (Nygaard et al., 1986). It belongs to the division Chlorophyta, class Chlorophyceae, order Sphaeropleales, family Selenastraceae, genus *Pseudokirchneriella*. Due to its ease of cultivation, rapid growth and good reproducibility compared with other algae species (Yamagishi et al. 2017b), it is commonly used in standard toxicity tests (OECD, 2006; US-EPA, 2002; ISO 8692, 2004). The bioassays of this alga are based on the inhibition of growth after 72 hours of exposure to the pollutants. *Pseudokirchneriella subcapitata* is highly sensitive to a wide range of individual and mixtures of pollutants (Aruoja et al. 2009, Magdaleno et al. 2015, Pavlic et al. 2005, Tasmin et al. 2014, Yamagishi et al. 2017a, Yamagishi et al. 2017b). Although this alga is widely regulated in standard toxicity tests, the cell biology of *Pseudokirchneriella subcapitata* is poorly understood, which makes difficult to use this organism to study toxicity mechanism (Yamagishi et al. 2017b).

As a consequence of the limited knowledge of the biology of *Pseudokirchneriella subcapitata*, other algae have emerged as model organisms for bioassays to study toxicity mechanisms. *Chlamydomonas reinhardtii* is a model organism in several fields. This is the only alga frequently used in ecotoxicology (see Table 1.2) that has been sequenced, annotated and can be accessed via public databases (including

mitochondrial, chloroplast and nuclear genome); in spite of, there are also ten green algae and three red algae which have complete sequenced genomes (Blaby et al. 2014) (http://www.genome.jp/kegg/catalog/org_list.html).

C. reinhardtii is a unicellular green alga. It belongs to the division Chlorophyta, class Chlorophyceae, order *Volvocales*, family Chlamydomonadacea and genus *Chlamydomonas* (Mussgnug 2015, Pröschold et al. 2001). *Chlamydomonas* genus is widely distributed worldwide, including freshwater ecosystems (Harris 2009). The species of *Chlamydomonas* most commonly used as model organism in bioassays is *C reinhardtii* (Mussgnug 2015). It was isolated in Amherst, Massachusetts, in 1945 by Gilbert M. Smith (Harris 2001, 2009, 2013). Fig. 1.3 shows the schematic diagram of a typical cell of *Chlamydomonas reinhardtii*. Cell wall of *C. reinhardtii* cells is mainly composed of hydroxyproline-rich glycoproteins (Harris 2001, 2009, 2013). *C. reinhardtii* cells feature a singles chloroplast (chlorophyll *a* and *b*), Two contractile vacuoles are located at the anterior end of the cell; the cells also contain mitochondria, an eye-spot (to perceive light information), a pyrenoid and two apical flagella (Harris 2001, 2009, 2013). The vegetative cells are haploid and they can be divided into two mating types (*plus* and *minus*) allowing sexual and asexual cell propagation (Cross and Umen 2015, Mussgnug 2015). Generation times of vegetative cells are of 8 - 12 hours (Blaby et al. 2014, Mussgnug 2015). *C. reinhardtii* can grow in chemoheterotrophic (in dark, using acetate as the organic carbon source) and in photoautotrophic (using light, H_2O and CO_2) conditions (Mussgnug 2015).

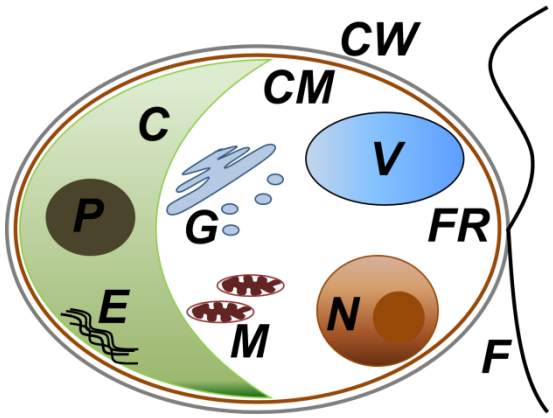

Figure 1.3 Schematic diagram of a typical cell of *Chlamydomonas reinhardtii*, C: chloroplast; E: eyespot; F: flagella; FR, site of flagellar roots; G: Golgi; M: mitochondria; N: nucleus with nucleolus; P: pyrenoid; V: vacuole; CW: cell wall; CM: cytoplasmic membrane.

C. reinhardtii constitutes the most investigated alga (Mussgnug 2015). It is easy to grow under laboratory conditions and to manipulate genetically (Harris 2001, 2009, 2013, Mussgnug 2015). In the last decades, it has been used as a model in studies of photosynthesis, ciliabiogenesis and micronutrient homeostasis (Blaby et al. 2014, Mussgnug 2015). Therefore, it is a well-known organism useful also for ecotoxicology (Harris 2001, 2009, 2013).

Currently, there are a large number of tools to study the effect of toxicity of pollutants on *C. reinhardtii*. At cellular level, several fluorochromes can be used to study a number of cellular parameters, such as ROS (reactive oxygen species) formation, cytoplasmatic and mitochondrial membrane potential, membrane integrity, apoptosis, intracellular pH (pHi), intracellular free calcium, metabolic activity and cellular cycle, in response to pollutants by flow cytometry and confocal microscopy (Esperanza et al. 2015a, Esperanza et al. 2015b, c, 2016). Omics techniques, such as RNA-Seq, have been also applied to study pollutants in *C. reinhardtii* (Esperanza et al. 2015b). The broad knowledge of its genome and its physiology has allowed using *C. reinhardtii* to elucidate the toxicity mechanisms of different pollutants. Several studies related changes in ROS formation, photosynthesis, apoptosis and gene expression in *C reinhardtii* in response to exposure to pollutants (Hu et al. 2014, Jamers et al. 2013, Murik et al. 2014, Petit et al. 2012, Pillai et al. 2014, Pino et al. 2016, Xiong et al. 2017). Consequently, *C. reinhardtii* can be considered as model to study the effect of pollutants in freshwater.

1.2.1.3 Bioassays based on environmental biofilms as model communities in freshwater toxicology

Bioassays based on single species are not useful to understand the effects of pollutants at the community level (Sabater et al. 2007). Therefore, the use of environmental biofilms has been used as a complement of bioassays based on singles species.

Fig. 1.4 shows the diagram of a typical environmental biofilm. Environmental biofilms are communities of microorganisms (algae, cyanobacteria, fungi, bacteria and viruses), also known as periphyton or phytobenthos, located in close physical contact and embedded in an exopolysaccharide matrix (Sabater et al. 2007, Villeneuve et al. 2013).

They are pivotal in freshwater functioning (anabolic and catabolic pathways) (Sabater et al. 2007).

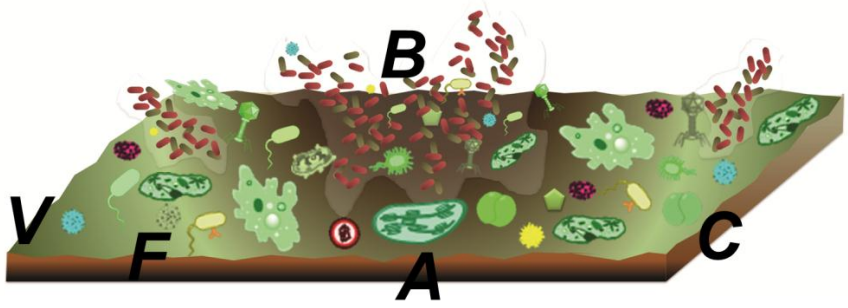

Figure 1.4 Schematic diagram of a typical environmental biofilm. V: virus; F: fungi; B: bacteria; A: algae; C:cyanobacteria.

The effects of pollutants on biofilms are of more ecological relevance since populations can be affected differently proving effects on interaction of populations (Sabater et al. 2007). In the last years, there has been an increase of the toxicological studies based on biofilms. Environmental biofilms have been used as bioassays in freshwater to evaluate the effect of pollutants such as: silver and ZnO nanoparticles, mixtures of pharmaceuticals, triclosan and mixtures of antibiotics (Corcoll et al. 2015, Gonzalez et al. 2015, Guasch et al. 2016, Kim Tiam et al. 2015, Kim Tiam et al. 2014, Lawrence et al. 2015, Proia et al. 2013, Proia et al. 2017, Proia et al. 2016, Sabater et al. 2007, Villeneuve et al. 2013, Xu et al. 2016). Environmental biofilms can be used in experimental systems, such as microcosms, mesocosms and artificial rivers, or *in situ* at various scales (Villeneuve et al. 2013). The impact of pollutants on biofilms can be detected using structural and functional analysis (Sabater et al. 2007) (Villeneuve et al. 2013).

Structural analyses are based on studying the biomass (dry weight, ash-free dry weight or chlorophyll a, focusing on phototrophic communities) per unit of surface area, pigment composition and species composition [Phyto-PAM fluorimetry, denaturing gradient gel electrophoresis (DGGE), emperature gradient gel electrophoresis (TGGE), metagenomic or fluorescence in situ hybridization (FISH)] (Sabater et al. 2007, Villeneuve et al. 2013). The community architecture is usually analysed by scanning electron microscopy (SEM). Species composition does not usually adequately reflect

cause-effect relationship and can required analysing functional properties (Sabater et al. 2007).

Functional analyses are based on photosynthetic measurements (photosynthetic organisms, such as PAM fluorometry, diving PAM fluorometry and O_2-evolution) and metabolic measurements (respiration, using Beta-Glucosidase), enzymatic activities (superoxide dismutase, catalase, peroxidase, glycosidase, phosphatase and aminopeptidase), chemical composition (carbon/nitrogen and nitrogen/phosphorus ratios and -omics (transcriptomic and proteomic) (Sabater et al. 2007, Villeneuve et al 2013).

1.2.2 Bioassays based on intracellular free calcium ($[Ca^{2+}]_i$)

This section explains the role of $[Ca^{2+}]_i$ as a second messenger in eukaryotes (green algae) and prokaryotes (cyanobacteria) and its potential use as an early biomarker of exposure to pollutants.

1.2.2.1 Calcium and life

Ca is an element. It is classified as a divalent metal (Cai et al. 2015). Ca was born when oxygen and neon captured successive α particles in the furnaces of the stars (Clapham 2007).

When the first cells were born in the primordial alkaline ocean, Ca^{2+} concentration was only around 100 nM, which is about one hundred thousand times less than its present concentration. In contrast, Ca was the fifth most abundant element in the Earth`s crust (Case et al. 2007, Kazmierczak et al. 2013). Over time, the concentration of Ca^{2+} in the ocean increased due to influx of Ca^{2+} from riverine, hydrothermal and groundwater seepage in combination with a decrease of seawater alkalinisation. (Kazmierczak et al. 2013, Verkhratsky and Parpura 2014).

The high concentration of Ca^{2+} in the ocean was incompatible with the cellular biochemistry of the first cells. This is due to the very low solubility of the complexes formed by the binding of Ca^{2+} and phosphate (PO_4^{3-}). This leads to the fast precipitation of Ca^{2+} and PO_4^{3-} as calcium phosphate at the typical intracellular pH (Kazmierczak et

al. 2013). As a consequence, the increase of $[Ca^{2+}]_i$ concentration can lead to irreversible damages in the mitochondria, activation of degradative enzymes (such as proteases, nucleases and phospholipases), chromatin condensation, aggregation of proteins (precipitation of proteins) and nucleic acids (RNA/DNA) and can affect the integrity of lipid membranes and the ATP metabolism (precipitation of phosphate) (Case et al. 2007, Kazmierczak et al. 2013, Plattner and Verkhratsky 2016, Verkhratsky and Parpura 2014).

1.2.2.2 The $[Ca^{2+}]_i$ homeostasis system

To prevent these cellular damages, cells developed an effective $[Ca^{2+}]_i$ homeostatic system to keep the levels of $[Ca^{2+}]_i$ in the cytosol low (the same of the primordial alkaline ocean ~100 nM).

This system consisted of decreasing the permeability of the cell envelope through controlled influx mechanisms (Ca^{2+} permeable channels), a high buffering capacity (Ca^{2+} binding proteins and intracellular Ca^{2+} stores) and an effective Ca^{2+} export system (Ca^{2+} pumps and Ca^{2+} exchangers) (Kazmierczak et al. 2013, Marchadier et al. 2016, Verkhratsky and Parpura 2014). Ca^{2+} permeable channels can be classified, according to their activation mechanism, as: voltage-dependent, voltage-independent/ligand-dependent and stretch-activated Ca^{2+} channels (Kudla et al. 2010).

Thanks to $[Ca^{2+}]_i$ homeostatic system, cells of all living beings maintain very low levels of $[Ca^{2+}]_i$ in their cytosol (100 – 200 nM) while the concentration in the milieu is ~10000-100000 times higher (Blackstone 2015, Cai et al. 2015, Case et al. 2007, Edel and Kudla 2015, Shemarova and Nesterov 2014, Stael et al. 2012). Thus, $[Ca^{2+}]_i$ concentration rapidly increases in the cytosol when Ca^{2+} permeable channels are open and $[Ca^{2+}]_i$ concentration can be quickly regulated into cells by export system and buffering capacity (Edel and Kudla 2015). This ancestral $[Ca^{2+}]_i$ machinery is nowadays common to all cells (Cai et al. 2015).

$[Ca^{2+}]_i$ homeostatic system allowed the development of $[Ca^{2+}]_i$ as a ubiquitous second messenger due to its numerous properties: flexible coordination chemistry, high affinity for carboxylate oxygen (which is the most frequent motif in amino acids), less water binding (Ca^{2+} binds water much less tightly than those of Mg^{2+}) and rapid binding

kinetics (Ca^{2+} is the fastest binding agent of all the available divalent ions, binding reactions that are ~100-1000 times faster than Mg^{2+}) (Case et al. 2007, Clapham 2007, Jaiswal 2001, Kazmierczak et al. 2013, Verkhratsky and Parpura 2014). Consequently, Ca^{2+} can easily form complexes with organic acids, membranes and proteins (Kudla et al. 2010).

Both abiotic (e.g., mechanical stress, drought, salinity, osmotic stresses, temperature, light, nutrient limitation include nitrogen starvation in photoautotroph, pollutants) and biotic stressors (e.g., oxidative stress, hormones, pathogens, organism signals) lead to specific $[Ca^{2+}]_i$ signal within the cells, which are the so-called Ca^{2+}-signatures (Barran-Berdon et al. 2011, Batistič and Kudla 2012, Kudla et al. 2010, Leganes et al. 2009, McAinsh and Pittman 2009, Torrecilla et al. 2000, 2004a, Torrecilla et al. 2001, 2004b, Whalley and Knight 2013).

Ca^{2+}-signatures are specific spatial and temporal $[Ca^{2+}]_i$ changes in a certain cell location, which serve to sense and to respond to specific stressors (Agostoni and Montgomery 2014, Whalley and Knight 2013). Ca^{2+}-signatures are defined by the specific combination of parameters, such as amplitude, duration, frequency, rise time, final Ca^{2+} resting levels, recovery time and the source of Ca^{2+}, for each stressor (Berridge et al. 2003, Berridge et al. 2000, Kudla et al. 2010, McAinsh et al. 1997, McAinsh and Pittman 2009, Rudd and Franklin-Tong 2001). Ca^{2+}-signatures are detected, decoded and transmitted or/and propagated to downstream responses through Ca^{2+} sensor proteins (Edel and Kudla 2015, Plattner and Verkhratsky 2016).

Ca^{2+} sensor proteins are commonly characterized for having one or more EF-hand Ca^{2+}-binding motifs, although other Ca^{2+}-binding motifs have been identified. The EF-hand is composed of an acid helix-loop-helix structure with 29-aminoacids; with the central residues forming a turn-loop structure that is responsible for coordination. The loop has high affinity for binding to Ca^{2+}. These structural properties allow the rapid on/off Ca^{2+}-binding, which in turn allows the production of quick responses to changes in the concentration of Ca^{2+} in the cells (Bender and Snedden 2013). Ca^{2+} sensor proteins convert defined Ca^{2+}-signatures into specific downstream reactions through Ca^{2+} dependent phosphorylation events and Ca^{2+} dependent gene regulation through transcriptional factors or direct interaction with promoters (Kudla et al. 2010).

Ca^{2+} sensor proteins are classified into: sensor response [calcium-dependent protein kinases (CDPKs) and calcium-calmodulin-dependent kinase (CCaMKs)], which possess both Ca^{2+}-binding and enzymatic effector domains and sensor relays [calmodulin (CaM) and CaM-like protein (CMLs), which differs from the previous ones in length and/or number of EF-hands], which induce conformational changes that lead to the interaction with other proteins (target protein) regulating their activity (Bender and Snedden 2013, Dodd et al. 2010, Edel and Kudla 2015, Hochmal et al. 2016, Kudla et al. 2010). However, some sensor relays are able to interact and regulate directly the response after suffering conformational changes (Dodd et al. 2010, Kudla et al. 2010). Ca^{2+} sensor proteins through Ca^{2+}-signatures regulate among other processes: gene expression, transcription factors (Kudla et al. 2010), symbiosis signalling, stomatal guard cells opening (McAinsh and Pittman 2009) brain activity modulation, salt tolerance, (Edel and Kudla 2015), metabolic changes, fertilization, proliferation (Berridge et al. 2003), tip growth in pollen tubes and root hair, circadian clock (Dodd et al. 2010), chemotaxis, cell division, biofilm formation, heterocyst differentiation and bacterial cell wall biosynthesis (Marchadier et al. 2016).

1.2.2.3 $[Ca^{2+}]_i$ in environmental relevant microorganisms (cyanobacteria and green algae)

Ca^{2+} also plays an important role as a second messenger in primary producers such as cyanobacteria and green algae (using as model *Chlamydomonas reinhardtii*) (Agostoni and Montgomery 2014, Bickerton et al. 2016, Domínguez et al. 2015, Shemarova and Nesterov 2014, Stael et al. 2012).

1.2.2.3.1 *$[Ca^{2+}]_i$ in cyanobacteria*

Cyanobacteria maintain a tight control on $[Ca^{2+}]_i$ (100 – 200 nM), which implies the existence of a $[Ca^{2+}]_i$ homeostatic system that controls influx and efflux through the membrane (Torrecilla et al. 2000). It has been reported experimental and *in silico* evidences of the presence of a Ca^{2+} homeostasis system in cyanobacteria (Domínguez et al. 2015).

Influxes of Ca^{2+} in cyanobacteria are mediated by mechanosensitive ion MscL channels. Ca^{2+} can penetrate to the cytoplasm through an open MscL (Cox et al. 2013). MscL

have been reported to participate in *Synechocystis* sp. PCC6803 in response to cold and heat treatments (Bachin et al. 2015).

Effluxes of Ca^{2+} in cyanobacteria can be mediated by Ca^{2+}-pumps with the primary structure and biochemical properties close to the P-type Ca^{2+}-ATPase of eukaryotes as identified in *Synechococcus* sp. PCC7942. Another potential P-type Ca^{2+}-ATPase was identified in *Synechocystis* 6803 which acts as a Ca^{2+}-pump equivalent to eukaryotic sarco(endo)plasmic reticulum Ca^{2+}-ATPases (Geisler et al. 1998) and it is the product of *pacL* gene (Berkelman et al. 1994). Futhermore, Ca^{2+}/H^{+} antiporters have been identified in *Synechocystis* sp. PCC6803 and *Aphanothece halophytica* (Waditee et al. 2004). These Ca^{2+}/H^{+} antiporters have been found to be homologous to CAX gene family in *Arabidopsis*. CAX proteins are required for salt tolerance and adaptation of the cells to an alkaline milieu. Additionally, research based on in silico investigation has revealed the presence of a single Ca^{2+}/H^{+} antiporter in the genome sequences of the cyanobacteria *Anabaena* sp. PCC 7120 and *Thermosynechococcus elongatus* BP-1 (Waditee et al. 2004).

Specific stressors induced Ca^{2+} signatures in cyanobacteria (Torrecilla et al. 2000, 2004a, Torrecilla et al. 2001, 2004b). In fact, Ca^{2+}-binding proteins have been found in cyanobacteria. However, none of them have been found to include canonical EF-hand (Domínguez et al. 2015).

Ca^{2+}-binding proteins related with motility were discovered in *Synechococcus* sp. strain WH8102 encoded by *swmA* gene (Brahamsha 1996). The predicted SwmA protein contains a number of Ca^{2+}-binding motifs as well as several potential N-glycosylation sites (Brahamsha 1996). In addition, the role of $[Ca^{2+}]_i$ in heterocyst differentiation has been reported by Torrecilla et al. (2004) and a Ca^{2+}-binding protein involved in this cellular process was discovered in *Anabaena* sp. PCC 7120 encoded by the *ccbp* gene (Shi et al. 2006, Zhao et al. 2005). Degradation of CcbP in vegetative cell led to a release of bound Ca^{2+} that significantly contributed to the increase of $[Ca^{2+}]_i$ during the heterocyst differentiation process (Shi et al. 2006, Zhao et al. 2005). Degradation of CcbP is positively regulated by a serine protease HetR. Transcriptional regulator NtcA increases under nitrogen deficiency conditions. NtcA can bind a fragment of the *ccbP* promoter containing an NtcA-binding sequence in α-ketoglutarate-dependent fashion.

Consequently, $[Ca^{2+}]_i$ is regulated by a collaboration of HetR and NtcA in heterocyst differentiation in *Anabaena* sp. strain PCC 7120 (Shi et al. 2006, Zhao et al. 2005).

Thus, $[Ca^{2+}]_i$ appears to be involved in cyanobacteria in: motility, nitrogen fixation and photosynthesis in response to environment stresses such as heat and cold, osmotic stress, nitrogen depravation, light stresses (including light-to-dark transition), UV irradiation, pH changes, and pollutant (including EPs) (Barran-Berdon et al. 2011, Leganes et al. 2009, Richter et al. 1999, Tiwari et al. 2016, Torrecilla et al. 2000, 2004a, Torrecilla et al. 2001, 2004b, Walter et al. 2016).

2.2.3.2 *$[Ca^{2+}]_i$ in green algae*

The existence of a $[Ca^{2+}]_i$ homeostatic system in algae has been reported (Verret et al. 2010, Wheeler and Brownlee 2008).

Influxes of $[Ca^{2+}]_i$ are mediate by Ca^{2+} channels in green algae. *Ostreococcus lucimarinus* presents four Ca^{2+} channels homologous to voltage-dependent Ca^{2+} channels (VDCC) while *Ostreococcus tauri* has four Ca^{2+} channels homologous to VDCC and one homologous to transient receptor potential channels (TRP). *Micromonas* RCC299 present eight VDCC, five TRP, two cyclic nucleotide-gated channels (CNGC) and six MscS. *Chlamydomonas* genome presents nine VDCC, one inositol (1,4,5)-triphosphate receptors (IP_3R), nineteen TRP, three CNGC and one ionotropic glutamate receptors (GRL) homogolous Ca^{2+} channels (Wheeler and Brownlee 2008). Finally, in *Chlamydomonas reinhardtii* nine VDCC, one GRL, one IP_3R, teen TRP and three CNGC have been identified (Verret et al. 2010).

Ca^{2+}-binding proteins have been also found in green algae. One calmodulin (CaM), eight CaM-like proteins (CMLs), six Ca^{2+} protein kinases (CDPKs) and one calcineurin-like proteins (CBLs) were identified in *Klebsormidum flaccidum*. *Ostreococcus lucimarinus* has one CaM, two CMLs, three CDPKs and one CBLs. *Chlamydomonas reinhardtii* have one CaM, nine CMLs (including CAS) and eight CDPKs (Zhu et al. 2015).

CAS (calcium sensor) is one of the most interesting Ca^{2+}-binding protein found in *Chlamydomonas reinhardtii* is. Given its C-terminal region, it may have

sulfurtransferase or phosphatase activity (in vitro Ca^{2+} activity phosphorylation of CAS) and its N-terminal is involved in Ca^{2+}-binding (Nomura and Shiina 2014, Stael et al. 2012). CAS has been localized in chloroplast thylakoid membranes in *Chlamydomonas reinhardtii* and in CAS-mediated Ca^{2+}-dependent signalling in chloroplast (Nomura and Shiina 2014, Petroutsos et al. 2011). CAS-mediated Ca^{2+} signals are involved in the regulation of high light-stimulated nuclear expression. Specific CAS and Ca^{2+} functions are crucial for light-induced expression of LHCSR3, which constitutes a crucial protein for nonphotochemical quenching. Therefore, it is important for high-light acclimation (Petroutsos et al. 2011). Interestingly, CAS is involved in Ca^{2+}-dependent regulation of cyclic photosynthetic electron flow. CAS is also associated with PGRL1, which is a protein involved in the switch between linear and cyclic electro flow around PSI. CAS also regulates this process in a Ca^{2+}-dependent manner in anaerobic conditions (Terashima et al. 2012). CAS is also involved in cellular adaptation to low light and it is also involved in processes taking place outside the chloroplast (Trippens et al. 2017). In addition, CAS and calmodulin are involved in lipid biosynthesis in *Chlamydomonas reinhardtii* in response to N-starvation regulated by Ca^{2+} signature (Chen et al. 2015). CAS is a Ca^{2+}-mediated regulator of CO_2-concentrating mechanism related genes via a retrograde signal from the pyrenoid in the chloroplast to the nucleus (Wang et al. 2016a). CAS, calcium-dependent lipid-binding protein and Ca^{2+}/calmodulin-dependent protein phosphatase are also involved in the metabolism of lipids in *Chlamydomonas reinhardtii* (Nguyen et al. 2011). In addition, Ca^{2+}-dependent protein Ser/Thr phosphatase activity and Ca-dependent protein Ser/Thr phosphatase regulator change their expression after exposure to TiO_2 nanoparticles (Simon et al. 2013).

In summary, $[Ca^{2+}]_i$ is involved in many cellular responses in *Chlamydomonas reinhardrtii*: phototaxis (Nultsch et al. 1986, Stavis 1974, Stavis and Hirschberg 1973); photostimulation (Schmidt and Eckert 1976); phototaxis related with the eyespot region (Berthold et al. 2008, Harz et al. 1992, Nagel et al. 2002); chemotaxis (Ermilova et al. 1996); mating (Goodenough et al. 1993); gravitaxis (Kam et al. 1999) induction of genes related to chlorophyll biosynthesis and various flagellar responses including deflagellation, flagellar beat, flagellar adhesion during mating and flagella length control (Liang and Pan 2013, Verret et al. 2010, Wakabayashi et al. 2009, Wheeler and Brownlee 2008).

1.2.2.4 Measurements of $[Ca^{2+}]_i$

To assess the role of $[Ca^{2+}]_i$ in organisms it is necessary to count with appropriate tools for measuring the changes of $[Ca^{2+}]_i$. Ca^{2+} indicators can be used for this purpose. They can be classified in: fluorescent dyes, photoproteins, and fluorescent protein Ca^{2+} indicators (Brownlee 2000).

Fluorescent dyes are frequently employed as Ca^{2+} indicators due to their rapid and ease use in different organisms (see table 1.3). These dyes are based on specific Ca^{2+} chelators, such as EGTA and BAPTA. Nowadays, there are a wide variety of commercial fluorescent dyes available: Quin-2/AM, Fura-2/AM, Indo-1/AM, Fluo-3/AM, Fluo-4/AM, Calcium Green-1/AM and Calcium Green-5/AM. One of the most used fluorescence dyes in cyanobacteria and algae is Calcium Green AM (Garcia-Pichel et al. 2010, Prado et al. 2012).

Photoproteins are luminescent indicators. These proteins emit light in a Ca^{2+} dependent manner, being sensitive to physiological $[Ca^{2+}]_i$. Thus, photoproteins can be used to monitor $[Ca^{2+}]_i$ dynamics *in vivo* and in a continuous fashion. In this thesis, we used the photoprotein aequorin, which derives from the jellyfish *Aequorea victoria*. Aequrin is composed of an apoprotein (apoaequorin) and a prostetic group (coelenterazine). Aequorin contains three EF hands motifs and, when Ca^{2+} binds to EF Hand, it produces a conformational change and coelenterazine is oxidized to coelenteramide, which in turns generates light (469 nm) that can be measured using a luminometer. The amount of luminescence emitted by aequorin depends on the $[Ca^{2+}]_i$. This photoprotein is very sensitive to $[Ca^{2+}]_i$ changes, with a dose response curve that begins at around 100 nM $[Ca^{2+}]_i$ and gets saturated above 10 µM $[Ca^{2+}]_i$ (Torrecilla et al. 2000). Therefore, aequorin can be used to monitor $[Ca^{2+}]_i$ dynamics *in vivo* and in a continuous fashion, which allows recording specific Ca^{2+} signatures produced in response to any environmental stimulus, including pollutants.

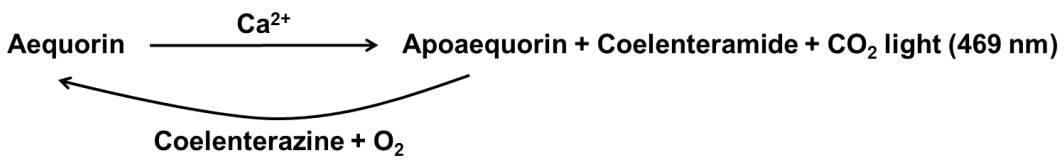

Aequorin gene has been cloned and successfully expressed in animal, plant, and bacterial cells, allowing quantitation of intracellular Ca^{2+} fluxes (Dominguez 2004, Whalley and Knight 2013). Recombinant cells express apoaequrin, while coelentrazine should be exogenously added. In both prokaryotic and eukaryotic microorganisms, apoaequorin has been expressed in *Escherichia coli* (Knight et al. 1991), *Saccharomyces cerevisiae* (Nakajima-Shimada et al. 1991), *Bacillus subtilis* (Herbaud et al. 1998), *Phaeodactylum tricornutum* (Falciatore et al. 2000), *Anabaena* sp. PCC7120 (Torrecilla et al. 2000), *Aspergillus nidulans* (Greene et al. 2002), *Aspergillus awamori* (Kozlova et al. 2005), *Dictyostelium discoideum* (Ludlow et al. 2008), *Mesorhizobium loti* (Moscatiello et al. 2009), *Synechococcus elongatus* (Leganes et al. 2009), *Rhizobium leguminosarum* (Moscatiello et al. 2010), *Neurospora crassa* (Binder et al. 2010b) and *Aspergillus niger* (Binder et al. 2011).

Finally, fluorescent protein Ca^{2+} indicators are based on fluorescent proteins. They are conjugated to GFP, or similar proteins, and calmodulin (CaM) or the CaM-binding peptide M13. Binding of Ca^{2+} causes a conformational change that results in fluorescence resonance energy transfer (FRET) between the different fluorescent proteins, allowing ratio imaging of Ca^{2+} (Bowman et al. 2011, Brownlee 2000).

1.2.2.5 $[Ca^{2+}]_i$ and pollutants

A number of studies show the role of $[Ca^{2+}]_i$ in the perception of environmental changes such as temperature, osmotic stress, nutrient depravation, light stress, UV irradiation, pH changes, hormones or pathogens. In contrast, and despite the fact that pollutants currently constitute some of the most important environmental stressors, the role of $[Ca^{2+}]_i$ in response to those is still poorly understood.

Table 1.3 Concentration of pollutants that evoked changes in the $[Ca^{2+}]_i$ homeostasis systems or $[Ca^{2+}]_i$ in different organisms. The Ca^{2+} indicators are also shown.

Pollutant classes	Pollutants	Cells	Concentrations	Measurements of $[Ca^{2+}]_i$	References
Heavy metals	Al	*Saccharomyces cerevisiae*	1000 μM	Fluo-3/AM	Li et al. (2011)
	Al	Root cells (*Allium cepa*)	800 μM	-	Mohan et al. (2013)
	Al	BY-2 cell line (*Nicotiana tabacum*)	600 μM	Aequorin	Kawano et al. (2003)
	As	*Saccharomyces cerevisiae*	1500 μM	Aequorin	Ferreira et al. (2012)

	As	*Anabaena* sp. PCC7120	5 mg/L	Aequorin	Barran-Berdon et al. (2011) (our group)
	Cd	PC12 cells	5 - 20 µM	Fluo-3/AM	Chen et al. (2011)
	Cd	PC12 cells	1 - 20 µM	Fluo-3/AM	Xu et al. (2011)
	Cd	Cerebral cortical neurons cells (Rat)	5 - 20 µM	Fluo-4/AM	Yuan et al. (2013)
	Cd	Hepatocytes cells (Mouse)	5 - 25 µM	Fluo-3/AM	Wang et al. (2006)
	Cd	NIH 3T3 cells	5 - 15 µM	Aequorin	Biagioli et al. (2005)
	Cd	*Saccharomyces cerevisiae*	500 - 5000 µM	Fluo-3/AM	Wang et al. (2016)
	Cd	Cerebral cortical neurons cells (Rats)	10 - 20 µM	Fluo-4/AM	Lin et al. (2015)
	Cd	*Saccharomyces cerevisiae*	50 – 500 µM	Aequorin	Ruta et al. (2014)
	Cd	Hepatocyte cells (Rat)	2.5 – 10 µM	Fluo-4/AM	Wang et al. (2014)
	Cd	*Anabaena* sp. PCC7120	5 mg/L	Aequorin	Barran-Berdon et al. (2011) (our group)
	Co	*E.coli*	1000 µM	Aequorin	Watkins et al. (1995)
	Ni	*E.coli*	5000 µM	Aequorin	Watkins et al. (1995)
	Cr(VI)	*Oryza sativa*	200 µM	Oregon Green 488 BAPTA-1	Trinhl et al. (2013)
	Cr(VI)	*Anabaena* sp. PCC7120	5 mg/L	Aequorin	Barran-Berdon et al. (2011) (our group)
	Cr(VI)	*Aspergillus awamori*	15 - 260 mg/L	Aequorin	Kozlova et al. (2005)
	Cu	*Eisenia andrei*	1 - 10 µM	-	Gastaldi et al. (2007)
	Cu	Eggs of *Psammechinus miliaris*	6.3 µM	Fura-2/AM	Schäfer et al. (2009)
	Cu	*Ulva compressa*	10 µM	-	Laporte et al. (2016)
	Cu	*Dictyostelium discoideum*	400 µM	Fluo-3/AM	Dondero et al. (2006)
	Cu	*Ulva compressa*	10 µM	Fluo-3/AM	González et al. (2012ab)
	Cu	*Anabaena* sp. PCC7120	5 mg/L	Aequorin	Barran-Berdon et al. (2011) (our group)
	Cu	*Saccharomyces cerevisiae*	100 – 1000 µM	Aequorin	Ruta et al. (2016)
	Hg	*Dictyostelium discoideum*	0.5 µM	Fluo-3/AM	Dondero et al. (2006)
	Hg	Skate hepatocytes cells (*Raja erinacea*)	1 - 1000 µM	Indo-1/AM	Nathanson et al. (1995)
	Hg	*Anabaena* sp. PCC7120	5 – 50 mg/L	Aequorin	Barran-Berdon et al. (2011) (our group)
	Hg	Cerebral cortical neurons cells (Rat)	5 - 100 µM	Fluo-3/AM	Gasso et al. (2001)
	MeHg	ASK cells	2.5µM	-	Nøstbakken et al. (2011)
	MeHg	Cerebral cortical neurons cells (Rat)	10 - 100 µM	Fluo-3/AM	Gasso et al. (2001)
	MeHg	Alveolar macrophages cells (Rat)	7 µM	-	Kuo (2008)
	MeHg	MDCK cells (Canine)	20 µM	Fura-2/AM	Kang et al. (2006)
	MeHg	Sspinal motor neurons cells (Mouse)	0.2 - 1 µM	Fura-2/AM	Ramanathan (2011)
	MeHg	Cerebellar granule cells (Rat)	0.2 - 5 µM	Fura-2	Marty et al. (1997)
	Zn	*Aspergillus awamori*	180 - 1300 mg/L	Aequorin	Kozlova et al (2005)
	Zn	*Anabaena* sp. PCC7120	5 mg/L	Aequorin	Barran-Berdon et al. (2011) (our group)
	Pb	*Danio rerio*	0.02 mg/L	-	Chen et al. 2016
	Pb	*Anabaena* sp. PCC7120	5 mg/L	Aequorin	Barran-Berdon et al. (2011) (our group)
	Pb + decabromodiphenyl ether	*Danio rerio*	0.02 + 0.2 mg/L	-	Chen et al. (2016)
	As + Cd + Pb	Astrocytes cells (Rat)	0.38 + 0.098 + 0.22; 3.8 + 0.98 + 2220 mg/L	Fluo-3/AM	Rai et al (2010)
Pesticides	3, 4-dichloroaniline	RTL-W1 cells	0.1–50 µM	Fura-2 AM	Schweizeret et al. (2011)

	Acrolein	Myocytes trachea cells (Rat)	0.1 -10 μM	Indo-1 AM	Roux et al. (1998)
	AFP_{NN5353}	*Aspergillus niger*	20 mg/L	Aequorin	Binder et al. (2011)
	Dieldrin	Cerebellar granule cells (Mouse)	3 μM	Fluo-3/AM	Babot et al. (2007)
	Diaminochlorotriazine	LβT2 cells	300 μM	Fluo-4/AM	Dooley et al. (2013)
	p,p′-DDE	Sperm cells (Human)	0.000001 – 50 μM	Oregon Green BAPTA-1/AM	Tavares et al. (2013)
	Eugenol	*Saccharomyces cerevisiae*	400 – 1000mg/L	Aequorin	Roberts et al. (2012)
	PAF	*Neurospora crassa*	10 – 100 mg/L	Aequorin	Binder et al. (2010)
	Paraquat	*Chlamydomonas moewusii*	5 – 10 μM	Calcium Green-1,AM	Prado et al. (2012)
Pharmaceuticals	Amiodarone	*Saccharomyces cerevisiae*	5 – 10 μM	Aequorin	Maresova et al. (2008)
	Amiodarone	*Saccharomyces cerevisiae*	20- 80 μM	Aequorin	Muend and Rao.(2008)
	Amiodarone	*Saccharomyces cerevisiae*	15 – 20 μM	Aequorin	Gupta et al. (2003)
	Azalomycin F	*Saccharomyces cerevisiae*	25 – 250 μM	Aequorin	Simkovic et al. (2001)
	Bezafibrate	*Anabaena* sp. PCC7120	5 mg/L	Aequorin	Barran-Berdon et al. (2011) (our group)
	Carvacrol	Glioblastoma cells (Human)	400 – 1000 μM	Fura-2/AM	Liang and Lu, (2012)
	Ciprofloxacin	*Anabaena* sp. PCC7120	5 mg/L	Aequorin	Barran-Berdon et al. (2011) (our group)
	Colistin	Cortex neuronal cells (Chick)	4.3 – 8.3 mg/L	Fura-3/AM	Dai et al. (2013)
	Clofibric acid	*Anabaena* sp. PCC7120	5 mg/L	Aequorin	Barran-Berdon et al. (2011) (our group)
	Fenofibric acid	*Anabaena* sp. PCC7120	5 – 25 mg/L	Aequorin	Barran-Berdon et al. (2011) (our group)
	Gemfibrozil	*Anabaena* sp. PCC7120	5 – 25 mg/L	Aequorin	Barran-Berdon et al. (2011) (our group)
	Gentamicin	Kidney cells (Pig)	100 – 1000 μM	Fura-2/AM	Holohan et al. (1988)
	Geldanamycin	Brain cells (Rat)	5 μM	Indo-1/AM	Sun et al. (2013)
	Naproxen	Renal tubular cells (Canine)	50 -300 μM	Fura-2/AM	Cheng et al. (2015)
	Ofloxacin	*Anabaena* sp. PCC7120	5 mg/L	Aequorin	Barran-Berdon et al. (2011) (our group)
	Triclocarban	Thymocytes cells (Rat)	0.1 – 3 μM	Fluo-3/AM	Miura1 et al. (2014)
	Triclosan	Cardiomyocites cells (Mouse)	10 μM	Fluo-4	Cherednichenko et al. (2012)
	Triclosan	*Dreissena polymorpha*	0.00058 mg/L	-	Riva et al. (2012)
	Triclosan	Thymocytes cells (Rat)	3 μM	Fluo-3-AM	Kawanai et al. (2011)
	Thymol	Renal tubular cells (Canine)	200 - 700 μM	Fura-2/AM	Chang et al. (2014)
	Salicylic acid	*Saccharomyces cerevisiae*	2000 – 5000 μM	Aequorin	Hidetoshi et al. (1998)
	3,5-DPC	*Aspergillus awamori*	0.112 - 112 mg/L	Aequorin	Kozlova et al. (2005)
	Streptomycin + penicillin	Kidney cells (Pig)	100 + 100 mg/L	Fura-2/AM	Bird et al. (1994)
Surfactants	PFOA	Neuron cells (Rat)	100 – 300 μM	Fluo-3/AM	Liu et al. (2011)
	PFOA	*Eisenia fetida*	10 mg/Kg	-	Mayilswami et al. (2016)
	PFOS	Trachea ciliary cells (Mice)	100 μM	Fura-2/AM	Matsubara et al. (2006)
	PFOS	Neuron cells (Rat)	30 – 300 μM	Fluo-3/AM	Liu et al. (2011)
	PFOS	Brain tissue (Male)	1.7 – 15 mg/L	-	Liu et al. (2010a)
	PFOS	Hippocampus (Rat)	3.2 mg/Kg	-	Liu et al. (2010b)
Plasticizer	Bisphenol-A	ERBeta-/- cells (Mice)	0.001 μM	Fura-2/AM	Soriano et al. (2012)
	Bisphenol-A	Islets of Langerhans cells (Mice)	0.001 μM	Fura-2/AM	Soriano et al. (2012)

	Butyl benzyl phthalate	Adrenal medullary cells (Bovine)	10 - 100 μM	Fura-2/AM	Liu et al. (2003)
Polycyclic aromatic hydrocarbons	Benzo(a)pyrene	Peripheral blood mononuclear cells (Human)	1 μM	Atomic Absorption Spectroscopy	Perumal Vijayaraman et al. (2012)
	Benzo(a)pyrene	*Eisenia andrei*	0.1- 10 μM	-	Gastaldi et al. (2007)
	Benzo(a)pyrene	Myometrial PHM1 cell line (Human)	10 μM	Fluo-4/AM	Barhoumi et al. (2006)
	1-nitropyrene	Bronchial epithelial cell line (Human)	10 μM	Fura-2/AM	Mayati et al. (2014)
	3-methylcholanthrene	peripheral blood leukocytes *(Cyprinus carpio)*	0.05 – 20 μM	Indo-1/AM	Reynaud et al. (2003)
Intermediate in the industrial manufacture	Crotonaldehyde	Endothelial cells (Human)	50 - 100 μM	Fluo3/AM	Ryu et al. (2013)
	Crotonaldehyde	Alveolar macrophages cells (Rat)	25 – 100 μM	Fluo-8^{TM}/AM	Yang et al. (2013)
	4-nitrophenol	RTL-W1 cells	4 –20 μM	Fura-2 AM	Schweizer et al. (2011)
	tBOOH	*Saccharomyces cerevisiae*	500 - 1500 μM	Aequorin	Popa et al. (2010)
Flame retardants	6´-OH-BDE-49	PC12 cells	20 μM	Fura-2	Dingemans et al. (2010)
	BDE-47	PC12 cells	20 μM	Fura-2	Dingemans et al. (2010)
	6-OH-BDE-47	PC12 cells	2 - 20 μM	Fura-2	Dingemans et al. (2010)
	5-OH-BDE-47	PC12 cells	5 - 20 μM	Fura-2	Dingemans et al. (2010)
	3-OH-BDE-47	PC12 cells	20 μM	Fura-2	Dingemans et al. (2010)
	4`-OH-BDE-49	PC12 cells	20 μM	Fura-2	Dingemans et al. (2010)
	4-bromophenol	PC 12 cells	300 μM	Fura-2/AM	Hassenklöver et al. (2006)
	2,4 -dibromophenol	PC 12 cells	3 - 300 μM	Fura-2/AM	Hassenklöver et al. (2006)
	2,4,6 - Tibromophenol	PC 12 cells	30 - 300 μM	Fura-2/AM	Hassenklöver et al. (2006)
	2,4,6-Tribromophenol	Eggs of *Psammechinus miliaris*	100 μM	Fura-2/AM	Schafer et al. (2009)
	Tetrabromobisphenol A	TM4 Sertoli cells (Mouse)	5 -60 μM	Fura-2/AM	Ogunbayo et al. (2008)
	Dechlorane plus	*Eisenia fetida*	50 mg/kg	-	Zhang et al. (2014)
PCB	Aroclor 1254	Hippocampus (rats)	10 mg/kg	^{45}Ca	Hilgier et al. (2012)
	PCB 106	Cortical. cells (Mice)	0.1 μM	Fura-2/AM	Londono et al. (2010)
	PCB52	Cerebellar neurons cells (Rat)	1 - 10 μM	Fura-2/AM	Llansola et al. (2010)
	PCB180	Cerebellar neurons cells (Rat)	0.1 – 10 μM	Fura-2/AM	Llansola et al. (2010)
	PCB138	Cerebellar neurons cells (Rat)	1 μM	Fura-2/AM	Llansola et al. (2009)
Endocrine disrupting alkylphenols	Nonylphenol	TM4 testicular Sertoli cell line (Mouse)	3 -100 μM	Fluo-3/AM	Michelangeli et al. (2008)
	Octylphenol	TM4 testicular Sertoli cell line (Mouse)	10 - 100 μM	Fluo-3/AM	Michelangeli et al. (2008)
	Butylphenol	TM4 testicular Sertoli cell line (Mouse)	300 - 1000 μM	Fluo-3/AM	Michelangeli et al. (2008)
Organotin compounds	Dibutyltin	Natural killer cells (Human)	0.001 -0.01 μM	Fura-3/AM	Lane et al. (2009)
	Tri-n-butyltin chloride	*Euglena gracilis Z*	50 μM	Fluo-3/AM	Ohta and Suzuki, (2007)
	Tri-n-butyltin chloride	Hepatocytes cells (Rat)	4 μM	Fura-2/AM	Kawanishi et al. (1999)
	Tributylin	Natural killer cells (Human)	0.05 – 0.5 μM	Fura-3/AM	Lane et al. (2009)
	Tributylin	Hepatocytes cells (*Oncorhynchus mykiss*)	1 - 5 μM	Indo-1/AM	Reader et al. (1994)
	Tributyltin	Cerebra lcortex brain (Rats)	0.3 μM	Fluo-3/AM	Mitra et al. (2013)
Explosive	Cyclotrimethylenetrinitramine (RDX)	*Pimephales promelas*	10 mg/L	-	Gust et al. (2010)

As to date, few studies have reported the role of $[Ca^{2+}]_i$ in response to pollutants in ecologically relevant organisms. In fact, studies are typically focussed on assessing the effect of priority pollutants and antifungals on fungi, rats and human cell lines (Table 1.3).

Most of the studies have been carried out using fluorescent dyes. Especially, Calcium Green-1 AM, Calcium Green-5 AM and Fluo-4/AM have been used to measure $[Ca^{2+}]_i$ homeostasis in response to pollutants (Table 1.3). Other studies have used photoproteins, particularly aequorin, to analyse the changes in $[Ca^{2+}]_i$ response to pollutants such as: antibiotics (Barran-Berdon et al. 2011, Simkovič et al. 2001), anti-inflammatories (Hidetoshi et al. 1998), antiarrhythmic drugs (Gupta et al. 2003a, Maresova et al. 2009a, Muend and Rao 2008b), antifungals (Binder et al. 2011, Binder et al. 2010b, Roberts et al. 2012b), heavy metals (Ferreira et al. 2012b, Ludlow et al. 2008, Watkins et al. 1995), lipid regulators(Barran-Berdon et al. 2011)and inorganic and organic peroxides (Greene et al. 2002, Herbaud et al. 1998). However, the majority of these studies solely were focused on describing the relationship between perturbations of $[Ca^{2+}]_i$ and the presence of a single pollutant and therefore cannot be considered as exposure bioassays.

1.2.2.6 Bioassays based on $[Ca^{2+}]_i$: $[Ca^{2+}]_i$ as a biomarker of exposure to pollutants

The fact that $[Ca^{2+}]_i$ may respond to a variety of environmental stimuli in practically any organism has raised the question of whether $[Ca^{2+}]_i$ might also be useful to identify the presence of pollutants potentially toxic to cells. Recently, bioassays based on the effect of potential pollutants on $[Ca^{2+}]_i$ dynamics have been conducted using different eukaryotic and prokaryotic organisms.

1.2.2.6.1 Bioassays based on $[Ca^{2+}]_i$ in microorganisms

The first bioassay that used $[Ca^{2+}]_i$ to identify pollutants was probably the one reported by Kozlova et al. (2005). In their study, Kozlova et al. (2005), assessed the effect of toxic substances (the heavy metals Cr^{6+} and Zn^{2+} and the phenolic polar narcotic 3,5-dichlorophenol) on the dynamics of cytoplasmic free calcium ($[Ca^{2+}]_c$) in fungus *Aspergillus awamori*, transformed with the apoaequorin gene. The authors studied a series of parameters of the Ca^{2+}-signature in the presence of pollutants. These parameters included: rise time, amplitude, length of transient, final resting level, and

recovery time. Pollutants were preincubated during 5 and 30 min before treatment with 5 mM external $CaCl_2$ and Ca^{2+}-signature was recorded. All the studied pollutants were found to provoke a response in one or more of the studied parameters. Kozlova patented this method based on the eukaryotic biosensor (U.S. Patent Application 20060094002).

Our group used a bioassay based on cyanobacterium *Anabaena* sp. PCC7120 (pBG2001a) and proposed $[Ca^{2+}]_i$ as an early biomarker of exposure to pollutants (Barran-Berdon et al. 2011). *Anabaena* sp. PCC 7120 (pBG2001a) is an ecologically relevant cyanobacterium, which constitutively expresses apoaequorin (Torrecilla et al. 2000). As already described, *Anabaena* sp. PCC 7120 (pBG2001a) has previously been used to study $[Ca^{2+}]_i$ homeostasis in response to heat, cold, salinity, osmotic stress, light-to-dark transitions and heterocyst differentiation (Torrecilla et al. 2000, 2004a, Torrecilla et al. 2001, 2004b).

Barran-Berdon et al. (2011) recorded and analysed the Ca^{2+}-signatures generated by exposure of the cyanobacterium to different groups of environmental priority and some EPs, including metals, organic solvents, naphthalene and pharmaceuticals. They found that, in general, each group of tested chemicals triggered a specific Ca^{2+}-signature in a reproducible and dose-dependent manner. The authors also recorded Ca^{2+} signals triggered by binary mixtures of priority pollutants and a signal induced by a sample of real wastewater, which was mimicked by mixing its main constituents. They also compared Ca^{2+} signals induced by binary mixtures with those resulting from the interaction of binary mixtures using the ecotoxicological bioassay based on *Anabaena* CPB4337 and concluded that *Anabaena* sp. PCC 7120 (pBG2001a) can be used as a tool to predict the nature of the interaction between priority pollutants. Finally, the authors hypothesized that these Ca^{2+} signals could be related to the cellular mechanisms of pollutant perception and ultimately to their toxic mode of action. This organism was used in this thesis to evaluated the use of $[Ca^{2+}]_i$ as an early biomarker of exposure in cyanobacteria to selected EPs applied both singly and combined in mixtures.

1.3. TOXICITY OF MIXTURES OF POLLUTANTS

What is the effect of pollutants in freshwater under realistic conditions? Realistic conditions imply several layers of complexity which complicate problem definition and hypothesis testing. The mixture aspect is intrinsic to environmental pollution. However, the implications of the "mixture" aspects, the experimental methods to study them, and their implications for risk assessment are still under intense investigation (Altenburger et al. 2012, Brack et al. 2015). Presently, the gold standard supporting mixture effect research is fractional additivity methods (Chou 2006, Kortenkamp et al. 2009). Additivity methods are based on the basic idea that the expected effect of a mixture of chemicals can be predicted based on the sum of the fractions of effects of the individual mixture components (Chou 2006, Kortenkamp et al. 2009). Departures from additivity (synergism and antagonism) are defined as deviations from this behaviour (Chou 2006, Kortenkamp et al. 2009).

The mixtures of pharmaceuticals have been of medical concern since ancient times. Drugs which act similarly are often combined to treat a number of diseases as synergistic effects are usually expected. Synergistic drug combinations allow to deliver lower doses to the patient, minimizing adverse effects. In this context, there is a need to define synergism and its opposite, antagonism, which are considered as toxicological interactions in chemical mixtures. There are many definitions of both terms as well as different synonyms. Goldin and Mantel (1957) collected up to seven definitions of synergism with synonyms such as synergy, potentiation, augmentation, sensitization, suppraadditiveness, superadditivity, potentiated summation or positive summation. For antagonisms, terms such as depotentiation, desensitization, infraadditiveness, subadditivity, negative synergy, etc., have been used. Therefore, there was a need for consistent and clear terminology to describe toxicological interactions; in this regard, EPA (1990), Mumtaz and Hertzberg (1993), Hertzberg et al. (1990), EPA (2000) and ATSDR (2004) provided distinct definitions for some of these terms: no apparent influence ("when a component which is not toxic to a particular organ system does not influence the toxicity of a second component on that organ system"); synergism ("when the effect of the mixture is greater than that estimated for additivity on the basis of the toxicities of the components"); potentiation ("when a component that does not have a toxic effect on an organ system increases the effect of a second chemical on that organ

system"); antagonism ("when the effect of the mixture is less than that estimated for additivity on the basis of the toxicities of the components"); inhibition ("when a component that does not have a toxic effect on a certain organ system decreases the apparent effect of a second chemical on that organ system"), and masking ("when the components produce opposite or functionally competing effects on the same organ system, and diminish the effects of each other, or one overrides the effect of the other")(Hertzberg et al. 1999, Mumtaz and Hertzberg 1993).

In the context of the above definitions, toxicological interactions such as synergism and antagonism may be considered as departures from additivity. Berenbaum (1981) already described synergism as the situation where the effect of a drug combination is greater than expected, and antagonism as the situation in which the combination response is less than expected and no or zero interaction as the situation where the drug combination effect is as expected. He also referred to zero interaction as additivity but advised that the term does not imply anything about how the operation of addition is performed(Berenbaum 1981). Goldin and Mantel (1957) described synergism or antagonism when the potency of the mixture/combination is greater or less than can be accounted by the potencies of the individual drugs. When the combination effect is as expected (consistent with the individual drug potencies), the interaction is then additive(Goldin and Mantel 1957).

As stated by Tallarida (2011) and many others, the concept of additivity in drug mixtures is not the simple addition of effects; so that the key question is what is the definition of addivity, zero interaction, or "as expected", as this provides the basis for the assessment of synergism and antagonism. A frame/model for addivity, zero interaction, or "as expected", is needed. The EPA (2000) defined additivity as the situation "when the effect of the combination is estimated by the sum of the exposure levels or the effects of the individual chemicals. The terms 'effect' and 'sum' must be explicitly defined. Effect may refer to the measured response or the incidence of adversely affected organisms. The sum may be a weighted sum (see 'dose addition') or a conditional sum (see 'response addition'). Therefore, there are two mathematical models widely accepted in pharmacology and later in ecotoxicology which are the so-called dose addition (similar joint action) which applies to mixtures of drugs with the same mode of action and response addition (independent joint action) which applies to

mixtures of drugs with different modes of action (Bliss 1939, Loewe and Muischnek 1926). Concentration Addition (CA) or Loewe additivity are synonyms of dose addition, while Independent Action (IA) or Bliss independence are synonymous to response addition.

1.3.1 Concentration Addition (CA)

Compounds with similar modes of action are expected to be mutually exclusive and behave as higher doses of a single compound. Dose addition, or Concentration Addition (CA), is then based on the assumption that all components in the mixture behave as if they are simple dilutions of one another Backhaus et al. (2014). For a mixture of "n" components, the CA concept can be expressed as follows:

$$\frac{\sum_{i=1}^{n} d_i}{D_{x,mix}} = \frac{c_{mix}}{D_{x,mix}} = \sum_{i=1}^{n} \frac{d_i}{D_{x,i}} \tag{1.1}$$

where di is the dose for chemical "i" in the mixture, $D_{x,i}$ the concentration of the "i" component that causes "x" effect for a given endpoint when individually exposed, cmix the total concentration of the mixture, and $D_{x,mix}$ the mixture concentration causing the same effect "x". As cmix = $D_{x,mix}$ the well-known form for CA arises:

$$\sum_{i=1}^{n} \frac{d_i}{D_{x,i}} = 1 \tag{1.2}$$

It is important to point out that, under the model of CA, mixture components below their individual no-effect concentration (NOEC) may nevertheless contribute to the total effect of the mixture.

1.3.2 Independent Action (IA)

In contrast, response addition or Independent Action (IA) applies to chemicals with dissimilar modes of action (Bliss 1939). IA assumes that the mixture components cause a common effect through primary interaction with different target sites (Junghans et al. 2006). It is the case of mutually non-exclusive drugs for which the effect (response), and not the dose, behaves additively. As IA is based on effects, a relevant difference with the CA model is that a mixture component used in a concentration below its NOEC will not contribute to the total effect of the mixture. The mathematical form is as follows:

$$D_{x,mix} = 1 - \prod_{i=1}^{n} \left(1 - D_{x,i}\right) \tag{1.3}$$

1.3.3 Combination index (CI)

Fraser, 1872 was the first to introduce the isobole method to study drug combinations in the field of pharmacology. He used this approach to study drug antagonisms but it serves as a good starting frame to study departures from additivity. The isobole is a graphical method which shows dose combinations of two drugs that yield the same effect; it is a Cartesian coordinate system in which doses of two drugs are represented in the x- and y-axes (Fig. 1.5). Isobolgram can be mathematically expressed as follows (for notation see Equation (1.1)):

$$\frac{d_1}{D_1} + \frac{d_2}{D_2} = 1 \tag{1.4}$$

If for a certain effect level, i.e., 50%, there is no interaction between the two drugs in combination, a straight line connects the intercepts (doses) in the x- and y-axes (isobologram equation = 1) (Fig. 1.5). However, when the line connecting both doses lies below and to the left of the line of additivity (concave up line), synergism is found (isobologram equation <1). When the line connecting both doses lies above and to the

right of the line of additivity (concave-down), antagonism is found (isobologram equation >1) (Fig. 1.5).

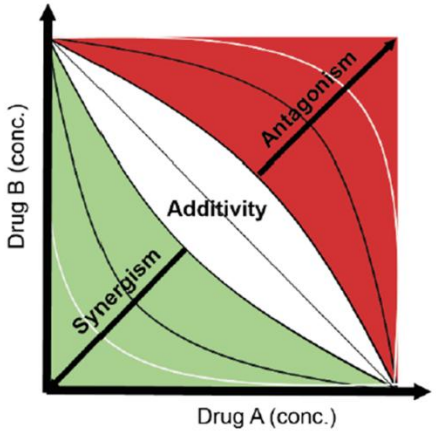

Figure 1.5 Schematic isobologram showing the equi-effective Cartesian plane for the combination of Drug A and Drug B at a specific effect level fa (for example fa = 0.5). For any mixture ratio (A:B), the effect of A + B should be theoretically located on the straight transversal line (the additivity line). The additivity effect can consider uncertainty (depicted by the white region). When the doses of A + B required to get the desired effect (fa) is less than that expected from their theoretical fractional summation of their respective individual effects (see Equation (1.4)), the effect of A + B is synergistic, and their coordinate location in the isobologram Cartesian plane is below the additivity line, depicting synergism. The opposite case indicates antagonism. Figure adapted from Cokol et al. (2011).

The isologram equation may be generalized to n drugs as a sum of fractions:

$$\frac{d_1}{D_1}+\frac{d_2}{D_2}.....+\frac{d_n}{D_n}=1 \tag{1.5}$$

The sum of all fractions has been termed as the Interaction Index (Berenbaum 1981, Syberg et al. 2008) and gives a measure of the degree of synergism or antagonism although it is not clear whether these deviations are statistically significant or not. (Note that Equation (1.5) is in fact equivalent to Equation (1.2) but derived from the isobologram definition). In an effort to evaluate the statistical significance of deviation from the additivity line, Syberg et al. (2008) added an extra parameter to the isobole formula, denoted as λ which described the degree of concavity of the isobole reflecting the degree of synergism/antagonism. In this regard, Carter et al. (1994) already suggested the use of confidence intervals for the additivity line in order to determine

whether true synergism or antagonism held; however, they also pointed out than an estimate of the confidence interval for the mixture should be given to further support the observed interaction.

The isobole is however a graphic method and it seems obvious that with more than 3 components (three-dimensional isobole surface), the graphic is difficult to make and visualization of the effect of mixtures is difficult (Carter Jr and Gennings 1994, Cokol et al. 2011, Tallarida 2011). It is also important to apply the method to as many effect levels as possible as departures from additivity might change with different effect levels. Usually, isoboles are drawn for the 50% effect level. An advanced isobologram representation for extensive data generation as a function of mixture ratio can be found in Cokol et al (2011). Isoboles are generally based on the CA model, however, Berembaum et al. (1981) and Syberg et al. (2008) successfully applied isoboles based on the theory of IA. In fact, as defined by Berenbaum et al. (1981), isoboles do not depend on mechanistic assumptions and are independent of the shapes of the dose-response curves so that they might apply for both CA and IA models of additivity. Further extension of the isobole method is the Isobologram-Combination Index developed by Chou and Talalay et al. (1984), Chou and Martin et al. (2005) and Chou et al. (2006). The Combination Index (CI) equation/theorem, also known as the multiple drug-effect equation, was derived from the median-effect principle of the mass-action law (Chou and Talaly 1977). The medium-effect principle or equation is also called the general theory of dose and effect that demonstrates that there is a univocal relationship between dose and effect independently of the number of substrates or products and of the mechanism of action or inhibition (Chou 2006). Chou and coworkers, after years of progression and development, formulated the general median-effect Equation (1.6) which they claim as a unified theory (derived from over 300 mechanistically distinct equations of biomedical sciences) of dose and effect which linearizes dose-effect curves with different potencies and shapes. This equation is a simple way to relate dose and effect showing that dose and effect are de facto interchangeable:

$$\frac{fa}{fu} = \left(\frac{D}{D_m} \right)^m \tag{1.6}$$

where D is the dose, Dm is the dose for 50% effect, fa is the fraction affected by dose D, fu is the unaffected fraction (fa = 1 − fu), and m is the slope of the dose-effect curve which depicts the shape of the curve (m = 1, >1, and <1 indicate hyperbolic, sigmoidal, and flat sigmoidal curve, respectively). Therefore, the method takes into account both the potency (Dm) and slope (m) parameters. If Equation (1.6) is rearranged, then:

$$D = D_m \cdot [fa/(1 - fa)]^{1/m} \tag{1.7}$$

The Dm and m values for each drug are easily determined by the median-effect plot: x = log (D) versus y = log (fa/fu) which is based on the logarithmic form of Equation (1.7). In the median-effect plot, m is the slope and Dm is the median-effect dose (antilog of the x-intercept of the median effect plot). The conformity of the data to the median-effect principle can be ready manifested by the linear correlation coefficient (r) of the data to the logarithmic form of Equation (1.7) (Chou 2006, Chou and Talalay 1984, Chou and Martin 2005). Based on the general median-effect equation, Chou and Talalay et al. (1984) developed the CI equation for the quantification of synergism or antagonism for n-drug combination at x% inhibition:

$$^{n}(CI)_x = \sum_{j=1}^{n} \frac{(D)_j}{(D_x)_j} = \sum_{j=1}^{n} \frac{(D_x)_{1-n} \left\{ [D]_j \Big/ \sum_{1}^{n} [D] \right\}}{(D_m)_j \left\{ (f_{ax})_j \Big/ \left[1 - (f_{ax})_j \right] \right\}^{1/mj}} \tag{1.8}$$

where *n*(CI)*x* is the combination index for *n* drugs at *x*% inhibition; (*Dx*)1−*n* is the sum of the dose of *n* chemicals that exerts *x*% inhibition in combination, $D_j/\sum_1^n [D]$ is the proportionality of the dose of each of *n* chemicals that exerts *x*% inhibition in combination; and (*Dm*)j·{(*fax*)*j*/[1 − (*fax*)*j*]}1/*mj* is the dose of each drug alone that exerts *x*% inhibition. From Equation (1.8), CI < 1, CI = 1, and CI > 1 indicates synergism, additive effect, and antagonism, respectively. An interesting feature of the method is that no previous knowledge about chemical structures or modes of action are needed to quantify the potential interactions between drugs.

1.3.4 CA and IA in bioassays

From the pioneering work of Hermens, et al. 1985, the idea of using the two simple pharmacological concepts of concentration addition (CA) and independent action (IA) as reasonable references to predict combined effects of chemical mixtures gained strong interest in bioassays. These pioneering works, and the follow ups of Faust, were motivated by a lack of a reference framework for mixture research in bioassays which resulted in a general perception of unpredictability of mixture expected toxicity (Altenburger et al. 2013, Backhaus et al. 2000, Junghans et al. 2006).

From 1999, a series of well-designed experiments were planned and developed with three main objectives: (1) to test whether the two existing pharmacological definitions of additivity (CA and IA) were able to offer a reasonable quantitative estimation of the experimental toxicity produced by multicomponent mixtures; (2) to test whether the effects of mixtures of purely similarly and dissimilarly acting chemicals were predicted better by CA and IA additivity models, respectively; and (3) to test whether or not toxicants near or below the statistically significant effect limit contributed to the resulting toxicity of the mixtures (Altenburger et al. 2013).

This series of experiments revealed important key aspects of the pollutants mixtures which changed and defined the subsequent 20 years of mixture research in bioassays. Regarding the first question, CA and IA showed an unexpected strong predictive power of the toxicity of multicomponent mixtures towards relevant model organisms. In general, the experimental toxicity of pollutant mixtures deviated less than a factor of two of the predictions based on the reference models (CA and IA) (Altenburger et al. 2000, Junghans et al. 2006). In fact, it was demonstrated that IA prediction always underestimated CA predictions and never deviated from CA more than a factor of n (the number of components in the mixtures) (Junghans et al. 2006). Therefore, CA (Loewe additivity) was later proposed as the gold standard for additivity (Kortenkamp et al. 2009).

Regarding the second question, the initial experiments with multicomponent mixtures of Backhaus et al. 2000 with purely similarly acting chemicals (herbicides from the family of PSII inhibitors), and purely dissimilarly acting chemicals (Altenburger et al. 2000)

were more acutely predicted by CA (model for similarly acting chemicals) and IA (model for dissimilarly acting chemicals), respectively. Despite these first insights on the applicability of both models, further research on the goodness of the fit of CA and IA revealed that the criterion on similar/dissimilar modes of action for the selection of the additivity model was not so consistent regarding other model organisms (Teuschler 2007). As reported, some pollutants may present different and unknown modes of action on non-target organisms, such as for example herbicides on amphibians (Rohr et al. 2008). This is especially true for pharmaceutically-active chemicals whose pharmacological mode of action on humans or mammals may be well understood, but whose mechanisms of toxic action on non-target species is generally largely unknown (Teuschler 2007).

Regarding the third point: whether or not toxicants at concentrations near or below their statistically significant effect may contribute to the resulting toxicity of the mixtures; the follow up experiments designed by Junghans et al. (2006), Faust et al. (2001),Walter et al. (2002) were clearly oriented to answer this question: In Faust et al. (2001), 18 purely similarly-acting chemicals (s-triazines) were mixed at their no observed effect concentrations (NOECs) and checked for their combined toxicity to the green alga Scenedesmus vacuolatus. Similarly, Walter et al. (2002) explored the combined toxicity of 11 totally dissimilarly-acting chemicals towards *Scenedesmus vacuolatus*. Interestingly, these works clearly demonstrated that, independently of similar or dissimilar modes of action (CA and IA models, respectively), a mixture of substances below their NOEC was able to produce greater toxicity than any of the individual chemicals, implying that predictions from additivity models, such as IA, are not always right. In fact, those experiments were a clear proof of the "nothing to something" concept, which was strikingly surprising at that time (Altenburger et al. 2013). In addition, the resulting mixture toxicity was accurately predicted by the CA model for similarly acting chemicals, and by IA model for the purely dissimilarly acting chemicals. The last result was unexpected and outmost interesting at this time since the emergence of toxicity in mixtures of purely dissimilarly acting chemicals below their individual NOECs (Faust et al. 2001, Walter et al. 2002) was non-consistent with the theory behind the IA model in the sense that the multiplication of zero effects remains zero (see Equation (1.3)), (note that the effect multiplication in Walter et al. (2002) was performed with the interpolated theoretical effects from the dose-response curves at the

NOEC doses for each individual chemical). After these initial experiments, CA and IA models became more and more popular in ecotoxicology as both theoretical and practical framework which have defined the present foundations of mixture ecotoxicology and mixture risk assessment (Kortenkamp et al. 2009).

1.3.5 CI in bioassays

Rodea-Palomares and co-workers (Rodea-Palomares et al. 2012, Rodea-Palomares et al. 2010, Rosal et al. 2010a) were the first to apply the Combination Index (CI)-Isobologram Equation to study the toxicological interactions of priority and EPs in an ecotoxicological context (using several aquatic organisms). They tested heavy metals, as well as EPs (lipid regulators, chlorinated pollutants, per-fluorinated surfactants and antibiotics) and environmental samples, namely wastewaters, in binary and complex mixtures. As model organisms they used a battery of aquatic organisms, including a natural bioluminescent organism (*Vibrio fischeri*), the recombinant bioluminescent cyanobacterium *Anabaena* CPB4337 and the crustacean *Daphnia magna*. Some of their most interesting findings are that the nature of the interaction between chemicals is strongly dependent on the effect level exerted by the mixture on the organism, so that the same pollutants can act synergistically at low effect levels and antagonistically at high effect levels (Rodea-Palomares et al. 2012, Rodea-Palomares et al. 2010). They also found that EPs with the same pharmacological mode of action (such as fibrates) can strongly interact synergistically in non-target organisms by unknown toxicological modes of action (Rodea-Palomares et al. 2010), and that the nature of the interaction between chemicals is strongly dependent on the test species (Rosal et al. 2010a). They also found that a complex mixture comprising pharmaceuticals and a wastewater from a local treatment plant with more than 30 EPs detected interacted in a synergistic way at all effect levels (Rodea-Palomares et al 2012). This finding is interesting in the context of increasing realism in mixture ecotoxicological research. They proposed that the CI method can be applied in environmental toxicology as a general method to define interactions of potential toxicants in mixtures toward target and non-target organisms.

This is since no previous knowledge on the pharmacological/toxic mechanism of action of the pollutants is needed and that the method may be especially useful for risk assessment strategies that take into account the toxicological interactions of substances

in a mixture. In addition, the CI method offers several graphical representations which have increased power with respect to the classical isobologram method: the fa-CI plots and the polygonogram plots (Chou 2006). As stated, fa-CI plots and the polygonograms are effect-oriented (in contrast to isobolograms, which are dose-oriented). In addition, effect-oriented interactions can be represented for mixtures of any number of components. This attributes are particularly useful for the identification of effect level-dependent departures from additivity, and especially to identify synergistic interactions at low/very low effect levels of pollutants (Rodea-Palomares et al. 2010).

Boltes et al. (2012) used CI to study the toxicity of mixtures of PFOS (perfluorooctane sulphonic acid) with chlorinated chemicals (triclosan and 2,4,6-trichlorophenol) and lipid regulators (two fibrates) towards *P. subcapitata*. They found that PFOS modified the toxicity of all tested compounds independently of their individual toxicity and, most interestingly they found that systematically all the ternary mixtures were more synergistic than their binaries, which again agrees with the notion that the complexity of the mixture tends to increase synergism(Boltes et al. 2012).

Carvalho et al. (2014) also used the CI approach to study the toxicological interactions of 8 preservatives in binary mixtures with an industrial wastewater towards the bacteria *V. fischeri*, *Pseudomonas putida*, the protozoan *Tetrahymena thermophila* and activated sludge. Nine of the binary combinations showed significant interactions as quantified by CI which were under or overestimated by the CA model. Interestingly, the IA model showed a higher predictive power than CA in the biological community of activated sludge.

1.3.6 Fractional approaches (CA, IA and CI): Limitations

Fractional approaches have demonstrated to constitute a reasonable and powerful quantitative framework for the conceptual and practical analysis of chemical mixture effects under "optimal experimental conditions". However, there is an important mismatch between real world conditions on which the conclusions of mixture in bioassays (Artigas et al. 2012, Carvalho et al. 2014, Mason et al. 2007).

.

The practical and sometimes conceptual limitations that the use of fractional approaches and "optimal experimental conditions" take into account are: (A) chemical concentrations at or near the toxicological thresholds of observable effects, (B) mixtures of individually "active" chemicals only, (C) mixtures at limited and very specific component ratios, (D) mixtures and its potential toxicity as a static entities and (E) mixtures evaluated on apical end-points and not considering interactions with other toxicologically relevant non-chemical factors.

(A) Empirical evidences of fractional approaches are presented usually at very high doses: at concentrations on the dose-response range of the individual chemicals, which are far from real world concentrations (usually several orders of magnitude). The basic assumption of fraction linearity remains to be tested regarding the extrapolations from high to very low doses (Mason et al. 2007). However, evidence exists on the non-linearity of the responses below the thresholds of observable monotonic responses. The most common and accepted case is hormesis (Calabrese 2008a, b). Furthermore, there is evidence of compounds resulting in sinusoidal responses along concentrations several orders of magnitude below the threshold of monotonic observable response (including hormesis) (Laetz et al. 2013, McMahon et al. 2011, McMahon et al. 2013, Quinn et al. 2009).

(B) Other of these assumptions is that individually non-active pollutants would never contribute significantly to the resulting chemical mixture effect. Considering the mathematical formulation of additivity, it is clear that it is, in fact, a default assumption (or mathematical limitation) of the present definitions of additivity, since only the chemicals to which "fractions of effect" can be derived, can be included to compute mixture effect predictions. Individually non-active chemicals have, in fact, been suggested to be ignored for riskassessment purposes (Backhaus et al. 2013). However, it is now clear that non-individually active chemicals can substantially modify mixture toxicity (Carvalho et al. 2014, Escher et al. 2013, Fischer et al. 2013).

(C) Mixture ecotoxicology has focused classically in effect-oriented ratios of mixture components rather than in exposure-oriented ratios (Backhaus et al.

2000, Faust et al. 2001, Rodea-Palomares et al. 2010). The problem with realistic mixtures is that their components are normally clearly uneven in potency (Backhaus and Karlsson 2014, Backhaus et al. 2000). Real complex mixtures are more similar to a low component mixture of few chemicals mixed with a highly complex matrix. This kind of mixtures can result in strong interaction effects (Rodea-Palomares et al. 2010, Rosal et al. 2010a). Furthermore, non-additive effects are not uncommon in low-component mixtures. Even trivial mixtures can result in non-expected interacting effects (Cedergreen et al. 2008, Tian et al. 2012).

(D) Dynamics in mixture should consider aspects regarding emission patterns, pollutants partitions, flows, transformation, and degradation. Similarly, it should consider exposure trends, in the sense that exposure may or not be coincident in time (exposure history), and may or may not be continuous (Segner et al. 2014). If the dynamics of components changes the mixtures could result in increased hazard (Baas et al. 2010).

(E) Additivity hypothesis has been tested mainly on apical end-points (such as mortality, growth inhibition, or apical metabolic activities). However empirical evidence is required to elucidate the applicability of fractional approaches and present formulations of additivity on both sub-organismal and supra-organismal end-points (Backhaus and Karlsson 2014). At the sub-organismal level of organization (for example, at the level of gene expression or protein synthesis) (Altenburger et al. 2012), a general problem for the definition of additivity is that the end-points are usually bi-directional: they can be up-regulated and down-regulated (or both, depending on concentration) in response to chemical exposure, and differentially-expressed genes can emerge from single to combined exposures (Vandenbrouck et al. 2009). Since the biological responses violate the basic requirement of monotonicity of the dose-response curves, it is impossible to define a homogeneous and ever-holding fractional effect scale,and, therefore, additivity equations cannot be solved (Scholze et al. 2014).

1.3.7 Global Sensitivity and Uncertainty Analysis (GSUA)

Realistic conditions are characterized by mixture at very low doses and many pollutants. As already described, fractional approaches related dose-response theories do not consider: low-dose, nonlinear/nonadditive, sublethal effects, experimental ratios and presence of non-additive behaviours (only CI). Therefore, the assessment of mixture toxicity in real environmental conditions is still a challenge.

In this context, new tools should be used to assess realistic mixtures, which may consider low-dose, nonlinear/nonadditive, sublethal effects, experimental ratios and presence of non-additive behaviours. Global Sensitivity and Uncertainty Analysis (GSUA) are formal tools for statistical evaluation, which can be used for this purpose.
Uncertainty Analysis propagates uncertainties in input factors onto the model outputs of interest. Sensitivity Analysis studies the strength of the relationship between a given uncertain input and the output. GSUA are divided in "local" and "global", depending on whether high order interaction terms between input factors are considered in the model. Local methods are suited for linear and additive models, while global methods are applicable with no assumption on linearity or additivity (Convertino et al. 2014, Saltelli et al. 2005). From the view point of GSUA, both "chemical by chemical" and "fractional approaches" can be considered as "local methods" and are tied to their own limitations, resulting from building higher levels of complexity from single component information and ignoring interactions and non-linearities raising from the system acting jointly.

Global Methods are suited to study systems from an up-botton strategy, so that the contribution of individual components to the overall toxicity is derived from the complex system acting jointly. The presented approximation has never been applied before to the study of complex mixtures of chemicals.

1.3.7.1 Morris method

The Morris method is a type of GSUA (Morris 1991). It provides a qualitative measure of the importance of each uncertain input factor. It is based on the elementary effects analysis that determines the input factors that have effects that are negligible, linear and

additive, and nonlinear or involved in interactions with other factors (Morris 1991, Saltelli et al. 2005).

For each input factor, two sensitivity measures can be calculated: (1) the mean elementary effect, μ; and (2) the standard deviation of the elementary effects, σ. The former estimates the overall effect (i.e., the importance) of the factor for a given output while the latter estimates the interactions with the other input factors.

Campolongo et al. (2007) suggested to consider the distribution of the absolute values of the elementary effects, $\mu*$ to avoid the canceling effects of opposing signs of the variance since model outputs can be non-monotonic. Although elementary effects are local measures, the method is considered global because the final measure, μ* is obtained by averaging the elementary effects(Campolongo et al. 2007). This averaging eliminates the need to consider the specific points at which they are computed (Saltelli et al. 2005, 2012, Saltelli et al. 1999).

The results of the Morris method are typically presented by plotting σ on the vertical axis and μ* on the horizontal axis for each input factor (Fig. 1.6). The qualitative measure of importance of a given input factor for the model output can be assessed by the horizontal deviation of the $\mu*$ – coordinate from the origin of the (μ*, σ) plane. The presence of interactions on the other hand, is qualitatively measured based on the vertical distance of the σ-coordinate from the origin.

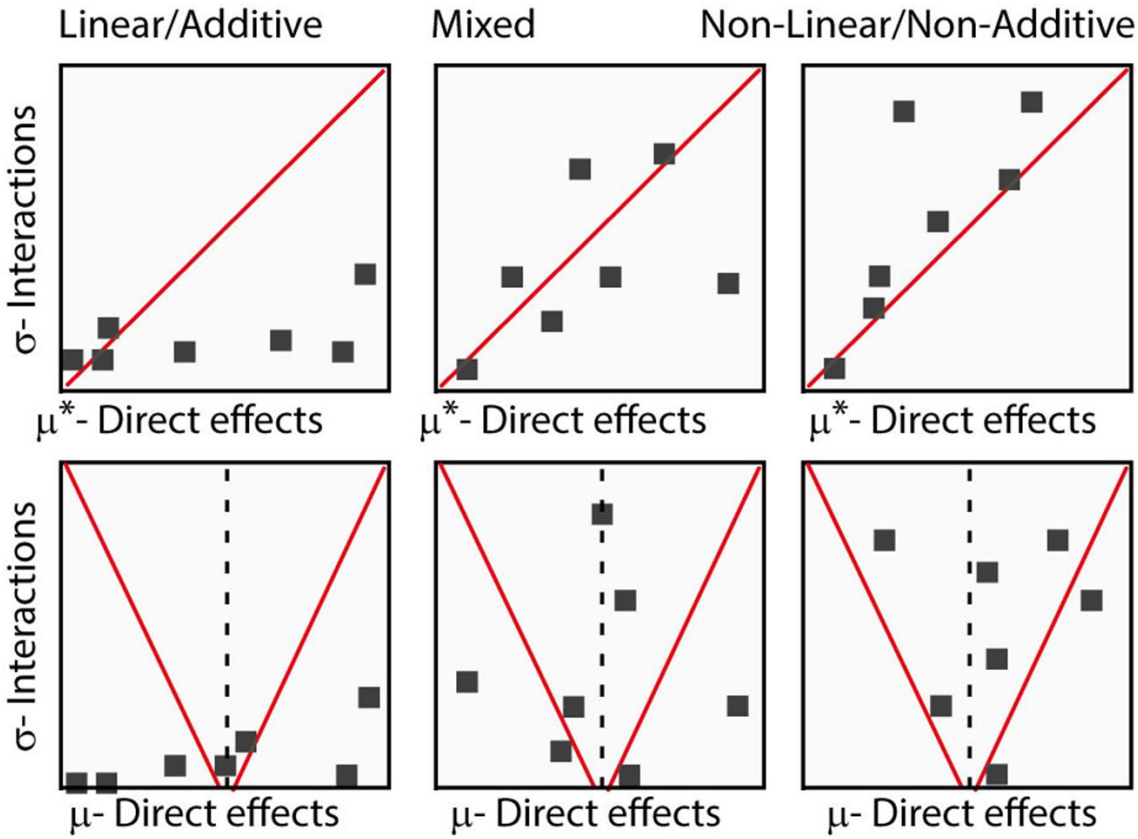

Figure 1.6 GSUA schematic representation of input factor distributions along μ *- σ and μ - σ Cartesian planes for linear/additive,mixed, and nonlinear/nonadditive systems.

The Morris method has the advantage of being computationally less demanding compared to the variance-based analysis. The number of simulations, N, required to perform the Morris method, that is its computational cost, is given as $N = r\,(k + 1)$, where k is the number of input factors, and r is the number of trajectories launched into the input space. Values of r are usually taken in the range of r = 4 to 10.

To study EPs mixtures toxicity with the Morris methods, only mixture information is required, but a precise mixture information.

(1) Work is required to find relevant mixture components (based on EPs occurrence or modelization) considered to generate the mixture components and their concentration levels to be tested (in Morris method, the concentration levels are discrete with, for example 3-4 levels based on the EPs occurrence. Also previously, desired, "external environmental factors" selected in order to evaluate their influence on EP mixture toxicity can be selected. External factors can be "climate factors", like water temperature or light regime; and "water

chemistry" factors, like pH, electrical conductivity and nutrient levels (P+N). External factors can be evaluated in a proposed spatial and temporal scope and clustered to generate a minimum set of reduced "external conditions" for which Morris analysis must be run. For example, 20 pollutants and 4 reduced external conditions can be selected.

(2) A pseudo-Monte Carlo sampling strategy generate a matrix of 10(K+1) mixtures to be tested experimentally (where K is equal to the number of components considered in the mixtures, in which all components and levels are sampled. For example, 20 component mixture, it implies a total of 210 mixture to be evaluated. If information on "reduced external conditions" to get the set of seasonal and water chemistry influence on toxicity want to be considered, Morris data sets (210 mixtures) must be repeated in the selected number of "external conditions".

Although Morris method is semi quantitative in nature, it offer, by the first time, a map of EPs acting under realistic conditions (at environmental concentrations, at environmental ratios and acting jointly). The ranking of importance of EPs in terms of total toxicity generated, and interaction capacity can be obtained for each model organism in each external conditions, and compared with that established based on traditional methodologies (single toxicity and CA/IA additivity predictions).

1.4 REFERENCES

Acuña, V., Aristi, I., Aymerich, I., Barceló, D., Corominas, L., Petrovic, M., Poch, M., Rodríguez-Mozaz, S., von Schiller, D. and Sabater, S. (2015) Emerging Contaminants in River Ecosystems, pp. 143-158, Springer.

Achary, V.M., Parinandi, N.L. and Panda, B.B. (2013) Calcium channel blockers protect against aluminium-induced DNA damage and block adaptive response to genotoxic stress in plant cells. Mutation Research 751(2), 130-138.

Adams, D.G., Bergman, B., Nierzwicki-Bauer, S.A., Duggan, P.S., Rai, A.N. and Schüßler, A. (2013) Cyanobacterial-Plant Symbioses. 359-400.

Agostoni, M. and Montgomery, B.L. (2014) Survival strategies in the aquatic and terrestrial world: The impact of second messengers on cyanobacterial processes. Life 4(4), 745-769.

Ahmed, M.B., Zhou, J.L., Ngo, H.H., Guo, W., Thomaidis, N.S. and Xu, J. (2017) Progress in the biological and chemical treatment technologies for emerging contaminant removal from wastewater: A critical review. Journal of Hazardous Materials 323(Pt A), 274-298.

Altenburger, R., Backhaus, T., Boedeker, W., Faust, M. and Scholze, M. (2013) Simplifying complexity: Mixture toxicity assessment in the last 20 years. Environmental Toxicology and Chemistry 32(8), 1685-1687.

Altenburger, R., Backhaus, T., Boedeker, W., Faust, M., Scholze, M. and Grimme, L.H. (2000) Predictability of the toxicity of multiple chemical mixtures to Vibrio fischeri: mixtures composed of similarly acting chemicals. Environmental Toxicology and Chemistry 19(9), 2341-2347.

Altenburger, R., Scholz, S., Schmitt-Jansen, M., Busch, W. and Escher, B.I. (2012) Mixture toxicity revisited from a toxicogenomic perspective. Environmental Science & Technology 46(5), 2508-2522.

Anderson, B.G. (1944) The toxicity thresholds of various substances found in industrial wastes as determined by the use of Daphnia magna. Sewage Works Journal, 1156-1165.

Ando, T., Nagase, H., Eguchi, K., Hirooka, T., Nakamura, T., Miyamoto, K. and Hirata, K. (2007) A novel method using cyanobacteria for ecotoxicity test of veterinary antimicrobial agents. Environmental Toxicology and Chemistry 26(4), 601-606.

Archer, E., Petrie, B., Kasprzyk-Hordern, B. and Wolfaardt, G.M. (2017) The fate of pharmaceuticals and personal care products (PPCPs), endocrine disrupting contaminants (EDCs), metabolites and illicit drugs in a WWTP and environmental waters. Chemosphere 174, 437-446.

Artigas, J., Arts, G., Babut, M., Caracciolo, A.B., Charles, S., Chaumot, A., Combourieu, B., Dahllöf, I., Despréaux, D. and Ferrari, B. (2012) Towards a renewed research agenda in ecotoxicology. Environmental Pollution 160, 201-206.

Aruoja, V., Dubourguier, H.C., Kasemets, K. and Kahru, A. (2009) Toxicity of nanoparticles of CuO, ZnO and TiO_2 to microalgae Pseudokirchneriella subcapitata. Science of the Total Environment 407(4), 1461-1468.

Baas, J., Jager, T. and Kooijman, B. (2010) Understanding toxicity as processes in time. Science of the Total Environment 408(18), 3735-3739.

Babot, Z., Vilaro, M.T. and Sunol, C. (2007) Long-term exposure to dieldrin reduces gamma-aminobutyric acid type A and N-methyl-D-aspartate receptor function in primary cultures of mouse cerebellar granule cells. Journal of Neuroscience Research 85(16), 3687-3695.

Backhaus, T., Faust, M. and Kortenkamp, A. (2013) Cumulative risk assessment: a European perspective on the state of the art and the necessary next steps forward. Integrated Environmental Assessment and Management 9(4), 547-548.

Backhaus, T. and Karlsson, M. (2014) Screening level mixture risk assessment of pharmaceuticals in STP effluents. water research 49, 157-165.

Backhaus, T., Scholze, M. and Grimme, L. (2000) The single substance and mixture toxicity of quinolones to the bioluminescent bacterium *Vibrio fischeri.* Aquatic Toxicology 49(1), 49-61.

Bachin, D., Nazarenko, L.V., Mironov, K.S., Pisareva, T., Allakhverdiev, S.I. and Los, D.A. (2015) Mechanosensitive ion channel MscL controls ionic fluxes during cold and heat stress in *Synechocystis*. FEMS Microbiology Letters 362(12), fnv090.

Barhoumi, R., Awooda, I., Mouneimne, Y., Safe, S. and Burghardt, R.C. (2006) Effects of benzo-a-pyrene on oxytocin-induced Ca^{2+} oscillations in myometrial cells. Toxicology Letters 165(2), 133-141.

Barran-Berdon, A.L., Rodea-Palomares, I., Leganes, F. and Fernandez-Pinas, F. (2011) Free Ca^{2+} as an early intracellular biomarker of exposure of cyanobacteria to environmental pollution. Anal Bioanal Chem 400(4), 1015-1029.

Batistič, O. and Kudla, J. (2012) Analysis of calcium signaling pathways in plants. Biochimica et Biophysica Acta (BBA) - General Subjects 1820(8), 1283-1293.

Bender, K.W. and Snedden, W.A. (2013) Calmodulin-related proteins step out from the shadow of their namesake. Plant Physiology 163(2), 486-495.

Berenbaum, M.C. (1981) Criteria for analyzing interactions between biologically active agents. Advances in Cancer Research 35, 269-335.

Berkelman, T., Garret-Engele, P. and Hoffman, N.E. (1994) The pacL gene of *Synechococcus* sp. strain PCC 7942 encodes a Ca^{2+}-transporting ATPase. Journal of Bacteriology 176(14), 4430-4436.

Berman-Frank, I., Lundgren, P. and Falkowski, P. (2003) Nitrogen fixation and photosynthetic oxygen evolution in cyanobacteria. Research in Microbiology 154(3), 157-164.

Berridge, M.J., Bootman, M.D. and Roderick, H.L. (2003) Calcium signalling: dynamics, homeostasis and remodelling. Nature Reviews: Molecular Cell Biology 4(7), 517-529.

Berridge, M.J., Lipp, P. and Bootman, M.D. (2000) The versatility and universality of calcium signalling. Nature Reviews: Molecular Cell Biology 1(1), 11-21.

Berthold, P., Tsunoda, S.P., Ernst, O.P., Mages, W., Gradmann, D. and Hegemann, P. (2008) Channelrhodopsin-1 initiates phototaxis and photophobic responses in *Chlamydomonas* by immediate light-induced depolarization. The Plant Cell 20(6), 1665-1677.

Biagioli, M., Pinton, P., Scudiero, R., Ragghianti, M., Bucci, S. and Rizzuto, R. (2005) Aequorin chimeras as valuable tool in the measurement of Ca^{2+} concentration during cadmium injury. Toxicology 208(3), 389-398.

Bickerton, P., Sello, S., Brownlee, C., Pittman, J.K. and Wheeler, G.L. (2016) Spatial and temporal specificity of Ca2+ signalling in *Chlamydomonas reinhardtii* in response to osmotic stress. New Phytologist 212(4), 920-933.

Binder, U., Bencina, M., Eigentler, A., Meyer, V. and Marx, F. (2011) The Aspergillus giganteus antifungal protein AFP_{NN5353} activates the cell wall integrity pathway and perturbs calcium homeostasis. BMC Microbiology 11, 209.

Binder, U., Chu, M., Read, N.D. and Marx, F. (2010a) The antifungal activity of the Penicillium chrysogenum protein PAF disrupts calcium homeostasis in Neurospora crassa. Eukaryotic cell 9(9), 1374-1382.

Binder, U., Chu, M., Read, N.D. and Marx, F. (2010b) The antifungal activity of the Penicillium chrysogenum protein PAF disrupts calcium homeostasis in Neurospora crassa. Eukaryot Cell 9(9), 1374-1382.

Bird, S.D., Walker, R.J. and Hubbard, M.J. (1994) Altered free calcium transients in pig kidney cells (LLC-PK1) cultured with penicillin/streptomycin. In Vitro Cellular & Developmental Biology-Animal 30(7), 420-424.

Blaby, I.K., Blaby-Haas, C.E., Tourasse, N., Hom, E.F., Lopez, D., Aksoy, M., Grossman, A., Umen, J., Dutcher, S., Porter, M., King, S., Witman, G.B., Stanke, M., Harris, E.H., Goodstein, D., Grimwood, J., Schmutz, J., Vallon, O., Merchant, S.S. and Prochnik, S. (2014) The Chlamydomonas genome project: a decade on. Trends Plant Sci 19(10), 672-680.

Blackstone, N.W. (2015) The impact of mitochondrial endosymbiosis on the evolution of calcium signaling. Cell Calcium 57(3), 133-139.

Bliss, C. (1939) The toxicity of poisons applied jointly1. Annals of Applied Biology 26(3), 585-615.

Boltes, K., Rosal, R. and García-Calvo, E. (2012) Toxicity of mixtures of perfluorooctane sulphonic acid with chlorinated chemicals and lipid regulators. Chemosphere 86(1), 24-29.

Bowman, S.M., Drzewiecki, K.E., Mojica, E.R., Zielinski, A.M., Siegel, A., Aga, D.S. and Berry, J.O. (2011) Toxicity and reductions in intracellular calcium levels following uptake of a tetracycline antibiotic in Arabidopsis. Environmental Science & Technology 45(20), 8958-8964.

Brack, W., Altenburger, R., Schuurmann, G., Krauss, M., Lopez Herraez, D., van Gils, J., Slobodnik, J., Munthe, J., Gawlik, B.M., van Wezel, A., Schriks, M., Hollender, J., Tollefsen, K.E., Mekenyan, O., Dimitrov, S., Bunke, D., Cousins, I., Posthuma, L., van den Brink, P.J., Lopez de Alda, M., Barcelo, D., Faust, M., Kortenkamp, A., Scrimshaw, M., Ignatova, S., Engelen, G., Massmann, G., Lemkine, G., Teodorovic, I., Walz, K.H., Dulio, V., Jonker, M.T., Jager, F., Chipman, K., Falciani, F., Liska, I., Rooke, D., Zhang, X., Hollert, H., Vrana, B., Hilscherova, K., Kramer, K., Neumann, S., Hammerbacher, R., Backhaus, T., Mack, J., Segner, H., Escher, B. and de Aragao Umbuzeiro, G. (2015) The SOLUTIONS project: challenges and responses for present and future emerging pollutants in land and water resources management. Science of the Total Environment 503-504, 22-31.

Brahamsha, B. (1996) An abundant cell-surface polypeptide is required for swimming by the nonflagellated marine cyanobacterium Synechococcus. Proceedings of the National Academy of Sciences 93(13), 6504-6509.

Brownlee, C. (2000) Cellular calcium imaging: so, what's new? Trends in Cell Biology 10(10), 451-457.

Bueno, M.J., Gomez, M.J., Herrera, S., Hernando, M.D., Aguera, A. and Fernandez-Alba, A.R. (2012) Occurrence and persistence of organic emerging contaminants and priority pollutants in five sewage treatment plants of Spain: two years pilot survey monitoring. Environmental Pollution (Barking, Essex: 1987) 164, 267-273.

Cai, X., Wang, X., Patel, S. and Clapham, D.E. (2015) Insights into the early evolution of animal calcium signaling machinery: a unicellular point of view. Cell Calcium 57(3), 166-173.

Calabrese, E.J. (2008a) Hormesis and mixtures. Toxicology and Applied Pharmacology 229(2), 262-263.

Calabrese, E.J. (2008b) Hormesis: why it is important to toxicology and toxicologists. Environmental Toxicology and Chemistry 27(7), 1451-1474.

Campolongo, F., Cariboni, J. and Saltelli, A. (2007) An effective screening design for sensitivity analysis of large models. Environmental modelling & software 22(10), 1509-1518.

Carere, M., Polesello, S., Kase, R. and Gawlik, B.M. (2015) Emerging Contaminants in River Ecosystems, pp. 197-215, Springer.

Carter Jr, W. and Gennings, C. (1994) Analysis of chemical combinations: relating isobolograms to response surfaces. Toxicology of Chemical Mixtures: Case Studies, Mechanisms, and Novel Approaches (Yang RSH, ed). San Diego, CA: Academic Press, 643-663.

Carvalho, R.N., Arukwe, A., Ait-Aissa, S., Bado-Nilles, A., Balzamo, S., Baun, A., Belkin, S., Blaha, L., Brion, F. and Conti, D. (2014) Mixtures of chemical pollutants at European legislation safety concentrations: how safe are they? Toxicological Sciences 141(1), 218-233.

Case, R.M., Eisner, D., Gurney, A., Jones, O., Muallem, S. and Verkhratsky, A. (2007) Evolution of calcium homeostasis: from birth of the first cell to an omnipresent signalling system. Cell Calcium 42(4-5), 345-350.

Cedergreen, N., Christensen, A.M., Kamper, A., Kudsk, P., Mathiassen, S.K., Streibig, J.C. and Sørensen, H. (2008) A review of independent action compared to concentration addition as reference models for mixtures of compounds with different molecular target sites. Environmental Toxicology and Chemistry 27(7), 1621-1632.

Clapham, D.E. (2007) Calcium signaling. Cell 131(6), 1047-1058.

Cokol, M., Chua, H.N., Tasan, M., Mutlu, B., Weinstein, Z.B., Suzuki, Y., Nergiz, M.E., Costanzo, M., Baryshnikova, A. and Giaever, G. (2011) Systematic exploration of synergistic drug pairs. Molecular Systems Biology 7(1), 544.

Convertino, M., Muñoz-Carpena, R., Chu-Agor, M.L., Kiker, G.A. and Linkov, I. (2014) Untangling drivers of species distributions: Global sensitivity and uncertainty analyses of MaxEnt. Environmental modelling & software 51, 296-309.

Corcoll, N., Casellas, M., Huerta, B., Guasch, H., Acuna, V., Rodriguez-Mozaz, S., Serra-Compte, A., Barcelo, D. and Sabater, S. (2015) Effects of flow intermittency and pharmaceutical exposure on the structure and metabolism of stream biofilms. Science of the Total Environment 503-504, 159-170.

Cox, C.D., Nomura, T., Ziegler, C., Campbell, A.K., Wann, K.T. and Martinac, B. (2013) Selectivity mechanism of the mechanosensitive channel MscS revealed by probing channel subconducting states. Nature communications 4.

Cross, F.R. and Umen, J.G. (2015) The *Chlamydomonas* cell cycle. Plant Journal 82(3), 370-392.

Chang, H.T., Chou, C.T., Liang, W.Z., Lu, T., Kuo, D.H., Shieh, P., Ho, C.M. and Jan, C.R. (2014) Effects of Thymol on Ca(2)(+) Homeostasis and Apoptosis in MDCK Renal Tubular Cells. Chinese Journal of Physiology 57(2), 90-98.

Chen, H., Hu, J., Qiao, Y., Chen, W., Rong, J., Zhang, Y., He, C. and Wang, Q. (2015) Ca^{2+}-regulated cyclic electron flow supplies ATP for nitrogen starvation-induced lipid biosynthesis in green alga. Scientific Reports 5, 15117.

Chen, L., Zhu, B., Guo, Y., Xu, T., Lee, J.-S., Qian, P.-Y. and Zhou, B. (2016) High-throughput transcriptome sequencing reveals the combined effects of key e-waste contaminants, decabromodiphenyl ether (BDE-209) and lead, in zebrafish larvae. Environmental Pollution 214, 324-333.

Chen, S., Xu, Y., Xu, B., Guo, M., Zhang, Z., Liu, L., Ma, H., Chen, Z., Luo, Y., Huang, S. and Chen, L. (2011) CaMKII is involved in cadmium activation of MAPK and mTOR pathways leading to neuronal cell death. Journal of Neurochemistry 119(5), 1108-1118.

Cheng, H.H., Chou, C.T., Sun, T.K., Liang, W.Z., Cheng, J.S., Chang, H.T., Tseng, H.W., Kuo, C.C., Chen, F.A., Kuo, D.H., Shieh, P. and Jan, C.R. (2015) Naproxen-induced Ca^{2+} movement and death in MDCK canine renal tubular cells. Human and Experimental Toxicology 34(11), 1096-1105.

Cherednichenko, G., Zhang, R., Bannister, R.A., Timofeyev, V., Li, N., Fritsch, E.B., Feng, W., Barrientos, G.C., Schebb, N.H. and Hammock, B.D. (2012) Triclosan impairs excitation–contraction coupling and Ca^{2+} dynamics in striated muscle. Proceedings of the National Academy of Sciences 109(35), 14158-14163.

Chou, T.-C. (2006) Theoretical basis, experimental design, and computerized simulation of synergism and antagonism in drug combination studies. Pharmacological Reviews 58(3), 621-681.

Chou, T.-C. and Talalay, P. (1984) Quantitative analysis of dose-effect relationships: the combined effects of multiple drugs or enzyme inhibitors. Advances in Enzyme Regulation 22, 27-55.

Chou, T.-C. and Talaly, P. (1977) A simple generalized equation for the analysis of multiple inhibitions of Michaelis-Menten kinetic systems. Journal of Biological Chemistry 252(18), 6438-6442.

Chou, T. and Martin, N. (2005) CompuSyn for drug combinations: PC software and user's guide: a computer program for quantitation of synergism and antagonism in drug combinations, and the determination of IC_{50} and ED_{50} and LD_{50} values. ComboSyn, Paramus, NJ.

Dai, C., Zhang, D., Li, J. and Li, J. (2013) Effect of colistin exposure on calcium homeostasis and mitochondria functions in chick cortex neurons. Toxicology Mechanisms and Methods 23(4), 281-288.

Dingemans, M.M., van den Berg, M., Bergman, A. and Westerink, R.H. (2010) Calcium-related processes involved in the inhibition of depolarization-evoked calcium increase by hydroxylated PBDEs in PC12 cells. Toxicological Sciences 114(2), 302-309.

Dodd, A.N., Kudla, J. and Sanders, D. (2010) The language of calcium signaling. Annual Review of Plant Biology 61, 593-620.

Dominguez, D.C. (2004) Calcium signalling in bacteria. Molecular Microbiology 54(2), 291-297.

Domínguez, D.C., Guragain, M. and Patrauchan, M. (2015) Calcium binding proteins and calcium signaling in prokaryotes. Cell Calcium 57(3), 151-165.

Dondero, F., Jonsson, H., Rebelo, M., Pesce, G., Berti, E., Pons, G. and Viarengo, A. (2006a) Cellular responses to environmental contaminants in amoebic cells of the slime mould Dictyostelium discoideum. Comparative Biochemistry and Physiology Part C: Toxicology & Pharmacology 143(2), 150-157.

Dondero, F., Jonsson, H., Rebelo, M., Pesce, G., Berti, E., Pons, G. and Viarengo, A. (2006b) Cellular responses to environmental contaminants in amoebic cells of the slime mould *Dictyostelium discoideum*. Comparative Biochemistry and Physiology: Toxicology & Pharmacology 143(2), 150-157.

Dooley, G.P., Tjalkens, R.B. and Hanneman, W.H. (2013) The atrazine metabolite diaminochlorotriazine suppresses LH release from murine LbetaT2 cells by suppressing GnRH-induced intracellular calcium transients. Toxicol Res (Camb) 2(3), 180-186.

Ebele, A.J., Abou-Elwafa Abdallah, M. and Harrad, S. (2017) Pharmaceuticals and personal care products (PPCPs) in the freshwater aquatic environment. Emerging Contaminants 3(1), 1-16.

Edel, K.H. and Kudla, J. (2015) Increasing complexity and versatility: how the calcium signaling toolkit was shaped during plant land colonization. Cell Calcium 57(3), 231-246.

Ermilova, E.V., Chekunova, E.M., Zalutskaya, Z.M., Krupnov, K.R. and Gromov, B.V. (1996) Isolation and characterization of chemotaxis mutants of Chlamydomonas reinhardtii. Current Microbiology 32(6), 357-359.

Escher, B.I., van Daele, C., Dutt, M., Tang, J.Y. and Altenburger, R. (2013) Most oxidative stress response in water samples comes from unknown chemicals: the need for effect-based water quality trigger values. Environmental Science & Technology 47(13), 7002-7011.

Esperanza, M., Cid, Á., Herrero, C. and Rioboo, C. (2015a) Acute effects of a prooxidant herbicide on the microalga *Chlamydomonas reinhardtii*: Screening cytotoxicity and genotoxicity endpoints. Aquatic Toxicology 165, 210-221.

Esperanza, M., Seoane, M., Rioboo, C., Herrero, C. and Cid, Á. (2015b) Análisis por RNAseq de la respuesta de la microalga *Chlamydomonas reinhardtii* al estrés producido por el herbicida atrazina, pp. 174-175, Universidad de La Rioja.

Esperanza, M., Seoane, M., Rioboo, C., Herrero, C. and Cid, Á. (2015c) *Chlamydomonas reinhardtii* cells adjust the metabolism to maintain viability in response to atrazine stress. Aquatic Toxicology 165, 64-72.

Esperanza, M., Seoane, M., Rioboo, C., Herrero, C. and Cid, Á. (2016) Early alterations on photosynthesis-related parameters in *Chlamydomonas reinhardtii* cells exposed to atrazine: A multiple approach study. Science of the Total Environment 554, 237-245.

Esteban, S., Moreno-Merino, L., Matellanes, R., Catala, M., Gorga, M., Petrovic, M., Lopez de Alda, M., Barcelo, D., Silva, A., Duran, J.J., Lopez-Martinez, J. and Valcarcel, Y. (2016) Presence of endocrine disruptors in freshwater in the northern Antarctic Peninsula region. Environmental Research 147, 179-192.

Fairbairn, D.J., Karpuzcu, M.E., Arnold, W.A., Barber, B.L., Kaufenberg, E.F., Koskinen, W.C., Novak, P.J., Rice, P.J. and Swackhamer, D.L. (2016) Sources and transport of contaminants of emerging concern: A two-year study of occurrence and spatiotemporal variation in a mixed land use watershed. Science of the Total Environment 551-552, 605-613.

Falciatore, A., d'Alcalà, M.R., Croot, P. and Bowler, C. (2000) Perception of environmental signals by a marine diatom. Science 288(5475), 2363-2366.

Faust, M., Altenburger, R., Backhaus, T., Blanck, H., Boedeker, W., Gramatica, P., Hamer, V., Scholze, M., Vighi, M. and Grimme, L. (2001) Predicting the joint algal toxicity of multi-component s-triazine mixtures at low-effect concentrations of individual toxicants. Aquatic Toxicology 56(1), 13-32.

Fernández-Pinas, F. and Wolk, C.P. (1994) Expression of luxCD-E in Anabaena sp. can replace the use of exogenous aldehyde for in vivo localization of transcription by luxAB. Gene 150(1), 169-174.

Ferreira, R.T., Silva, A.R., Pimentel, C., Batista-Nascimento, L., Rodrigues-Pousada, C. and Menezes, R.A. (2012a) Arsenic stress elicits cytosolic Ca^{2+} bursts and Crz1 activation in *Saccharomyces cerevisiae*. Microbiology 158(Pt 9), 2293-2302.

Ferreira, R.T., Silva, A.R.C., Pimentel, C., Batista-Nascimento, L., Rodrigues-Pousada, C. and Menezes, R.A. (2012b) Arsenic stress elicits cytosolic Ca^{2+} bursts and Crz1 activation in Saccharomyces cerevisiae. Microbiology 158(9), 2293-2302.

Fischer, B.B., Pomati, F. and Eggen, R.I. (2013) The toxicity of chemical pollutants in dynamic natural systems: the challenge of integrating environmental factors and biological complexity. Science of the Total Environment 449, 253-259.

Garcia-Pichel, F., Ramirez-Reinat, E. and Gao, Q. (2010) Microbial excavation of solid carbonates powered by P-type ATPase-mediated transcellular Ca^{2+} transport. Proceedings of the National Academy of Sciences of the United States of America 107(50), 21749-21754.

García, J.A.L., Grijalbo, L., Ramos, B., Fernández-Piñas, F., Rodea-Palomares, I. and Gutierrez-Mañero, F.J. (2013) Combined phytoremediation of metal-working fluids with maize plants inoculated with different microorganisms and toxicity assessment of the phytoremediated waste. Chemosphere 90(11), 2654-2661.

Gassó, S., Cristofol, R.M., Selema, G., Rosa, R., Rodríguez-Farré, E. and Sanfeliu, C. (2001) Antioxidant compounds and Ca^{2+} pathway blockers differentially protect against methylmercury and mercuric chloride neurotoxicity. Journal of Neuroscience Research 66(1), 135-145.

Gastaldi, L., Ranzato, E., Capri, F., Hankard, P., Peres, G., Canesi, L., Viarengo, A. and Pons, G. (2007) Application of a biomarker battery for the evaluation of the sublethal effects of pollutants in the earthworm Eisenia andrei. Comparative Biochemistry and Physiology: Toxicology & Pharmacology 146(3), 398-405.

Gavrilescu, M., Demnerova, K., Aamand, J., Agathos, S. and Fava, F. (2015) Emerging pollutants in the environment: present and future challenges in biomonitoring, ecological risks and bioremediation. N Biotechnol 32(1), 147-156.

Geisler, M., Koenen, W., Richter, J. and Schumann, J. (1998) Expression and characterization of a Synechocystis PCC 6803 P-type ATPase in E. coli plasma membranes. Biochimica et Biophysica Acta (BBA)-Biomembranes 1368(2), 267-275.

Geissen, V., Mol, H., Klumpp, E., Umlauf, G., Nadal, M., van der Ploeg, M., van de Zee, S.E.A.T.M. and Ritsema, C.J. (2015) Emerging pollutants in the environment: A challenge for water resource management. International Soil and Water Conservation Research 3(1), 57-65.

Goldin, A. and Mantel, N. (1957) The employment of combinations of drugs in the chemotherapy of neoplasia: a review. Cancer Research 17(7), 635-654.

Gonzalez, A., Cabrera Mde, L., Henriquez, M.J., Contreras, R.A., Morales, B. and Moenne, A. (2012a) Cross talk among calcium, hydrogen peroxide, and nitric oxide and activation of gene expression involving calmodulins and calcium-dependent protein kinases in Ulva compressa exposed to copper excess. Plant Physiology 158(3), 1451-1462.

Gonzalez, A., Cabrera Mde, L., Mellado, M., Cabello, S., Marquez, S., Morales, B. and Moenne, A. (2012b) Copper-induced intracellular calcium release requires extracellular calcium entry and activation of L-type voltage-dependent calcium channels in *Ulva compressa*. Plant Signal Behav 7(7), 728-732.

Gonzalez, A.G., Mombo, S., Leflaive, J., Lamy, A., Pokrovsky, O.S. and Rols, J.L. (2015) Silver nanoparticles impact phototrophic biofilm communities to a considerably higher degree than ionic silver. Environmental Science and Pollution Research International 22(11), 8412-8424.

Gonzalo, S., Rodea-Palomares, I., Leganes, F., Garcia-Calvo, E., Rosal, R. and Fernandez-Pinas, F. (2015) First evidences of PAMAM dendrimer internalization in microorganisms of environmental relevance: A linkage with toxicity and oxidative stress. Nanotoxicology 9(6), 706-718.

Goodenough, U.W., Shames, B., Small, L., Saito, T., Crain, R.C., Sanders, M.A. and Salisbury, J.L. (1993) The role of calcium in the *Chlamydomonas reinhardtii* mating reaction. Journal of Cell Biology 121, 365-365.

Greene, V., Cao, H., Schanne, F.A. and Bartelt, D.C. (2002) Oxidative stress-induced calcium signalling in Aspergillus nidulans. Cellular Signalling 14(5), 437-443.

Guasch, H., Ricart, M., López-Doval, J., Bonnineau, C., Proia, L., Morin, S., Muñoz, I., Romaní, A.M. and Sabater, S. (2016) Influence of grazing on triclosan toxicity to stream periphyton. Freshwater Biology 61(12), 2002-2012.

Gupta, S.S., Ton, V.-K., Beaudry, V., Rulli, S., Cunningham, K. and Rao, R. (2003a) Antifungal activity of amiodarone is mediated by disruption of calcium homeostasis. Journal of Biological Chemistry 278(31), 28831-28839.

Gupta, S.S., Ton, V.K., Beaudry, V., Rulli, S., Cunningham, K. and Rao, R. (2003b) Antifungal activity of amiodarone is mediated by disruption of calcium homeostasis. Journal of Biological Chemistry 278(31), 28831-28839.

Gust, K.A., Wilbanks, M.S., Guan, X., Pirooznia, M., Habib, T., Yoo, L., Wintz, H., Vulpe, C.D. and Perkins, E.J. (2011) Investigations of transcript expression in fathead minnow (Pimephales promelas) brain tissue reveal toxicological impacts of RDX exposure. Aquatic Toxicology 101(1), 135-145.

Hagemann, M., Kern, R., Maurino, V.G., Hanson, D.T., Weber, A.P., Sage, R.F. and Bauwe, H. (2016) Evolution of photorespiration from cyanobacteria to land plants, considering protein phylogenies and acquisition of carbon concentrating mechanisms. J Exp Bot 67(10), 2963-2976.

Harris, E.H. (2001) Chlamydomonas as a model organism. Annual Review of Plant Biology 52(1), 363-406.

Harris, E.H. (2009) The Chlamydomonas sourcebook: introduction to *Chlamydomonas* and its laboratory use, Academic Press.

Harris, E.H. (2013) The *Chlamydomonas* sourcebook: a comprehensive guide to biology and laboratory use, Elsevier.

Harz, H., Nonnengasser, C. and Hegemann, P. (1992) The photoreceptor current of the green alga Chlamydomonas. Philosophical Transactions of the Royal Society of London B: Biological Sciences 338(1283), 39-52.

Hassan, S.H., Van Ginkel, S.W., Hussein, M.A., Abskharon, R. and Oh, S.E. (2016) Toxicity assessment using different bioassays and microbial biosensors. Environ Int 92-93, 106-118.

Hassenklöver, T., Predehl, S., Pilli, J., Ledwolorz, J., Assmann, M. and Bickmeyer, U. (2006) Bromophenols, both present in marine organisms and in industrial flame retardants, disturb cellular Ca^{2+} signaling in neuroendocrine cells (PC12). Aquatic Toxicology 76(1), 37-45.

Heimann, K. and Cirés, S. (2015) Handbook of Marine Microalgae: Biotechnology Advances, pp. 501-515, Academic Press.

Henderson, C. and Pickering, Q.H. (1963) Use of fish in the detection of contaminants in water supplies. Journal (American Water Works Association) 55(6), 715-720.

Herbaud, M.-L., Guiseppi, A., Denizot, F., Haiech, J. and Kilhoffer, M.-C. (1998) Calcium signalling in Bacillus subtilis. Biochimica et Biophysica Acta (BBA)-Molecular Cell Research 1448(2), 212-226.

Hertzberg, R.C., Rice, G. and Teuschler, L.K. (1999) Methods for health risk assessment of combustion mixtures. Hazardous waste incineration: evaluating the human health and environmental risks, 105-148.

Hidetoshi, I., TSUJI, F.I., ISOBE, M., UOZUMI, N. and Shoshi, M. (1998) Salicylic acid induces a cytosolic Ca^{2+} elevation in yeast. Bioscience, Biotechnology, and Biochemistry 62(5), 986-989.

Hilgier, W., Lazarewicz, J.W., Struzynska, L., Frontczak-Baniewicz, M. and Albrecht, J. (2012) Repeated exposure of adult rats to Aroclor 1254 induces neuronal injury and impairs the neurochemical manifestations of the NMDA receptor-mediated intracellular signaling in the hippocampus. Neurotoxicology 33(1), 16-22.

Hochmal, A.K., Zinzius, K., Charoenwattanasatien, R., Gäbelein, P., Mutoh, R., Tanaka, H., Schulze, S., Liu, G., Scholz, M. and Nordhues, A. (2016) Calredoxin represents a novel type of calcium-dependent sensor-responder connected to redox regulation in the chloroplast. Nature communications 7.

Hoiczyk, E. and Hansel, A. (2000) Cyanobacterial cell walls: news from an unusual prokaryotic envelope. Journal of Bacteriology 182(5), 1191-1199.

Holohan, P.D., Sokol, P.P., Ross, C.R., Coulson, R., Trimble, M.E., Laska, D. and Williams, P. (1988) Gentamicin-induced increases in cytosolic calcium in pig kidney cells (LLC-PK1). Journal of Pharmacology and Experimental Therapeutics 247(1), 349-354.

Hu, C., Luo, Q. and Huang, Q. (2014) Ecotoxicological effects of perfluorooctanoic acid on freshwater microalgae *Chlamydomonas reinhardtii* and *Scenedesmus obliquus*. Environmental Toxicology and Chemistry 33(5), 1129-1134.

Hughes, S.R., Kay, P. and Brown, L.E. (2013) Global synthesis and critical evaluation of pharmaceutical data sets collected from river systems. Environmental Science & Technology 47(2), 661-677.

Jackson, H.W. and Brungs, W.A. (1966) Biomonitoring of industrial effluents.

Jaiswal, J.K. (2001) Calcium — how and why? Journal of Biosciences 26(3), 357-363.

Jamers, A., Blust, R., De Coen, W., Griffin, J.L. and Jones, O.A. (2013) An omics based assessment of cadmium toxicity in the green alga *Chlamydomonas reinhardtii*. Aquatic Toxicology 126, 355-364.

Jiang, J.-Q., Zhou, Z. and Sharma, V.K. (2013) Occurrence, transportation, monitoring and treatment of emerging micro-pollutants in waste water — A review from global views. Microchemical Journal 110, 292-300.

Jiang, J.J., Lee, C.L. and Fang, M.D. (2014) Emerging organic contaminants in coastal waters: anthropogenic impact, environmental release and ecological risk. Mar Pollut Bull 85(2), 391-399.

Junghans, M., Backhaus, T., Faust, M., Scholze, M. and Grimme, L. (2006) Application and validation of approaches for the predictive hazard assessment of realistic pesticide mixtures. Aquatic Toxicology 76(2), 93-110.

Kam, V., Moseyko, N., Nemson, J. and Feldman, L.J. (1999) Gravitaxis in *Chlamydomonas reinhardtii*: characterization using video microscopy and computer analysis. International journal of plant sciences 160(6), 1093-1098.

Kaneko, T. (2001) Complete Genomic Sequence of the Filamentous Nitrogen-fixing Cyanobacterium *Anabaena* sp. Strain PCC 7120. DNA Research 8(5), 205-213.

Kang, M.S., Jeong, J.Y., Seo, J.H., Jeon, H.J., Jung, K.M., Chin, M.R., Moon, C.K., Bonventre, J.V., Jung, S.Y. and Kim, D.K. (2006) Methylmercury-induced toxicity is mediated by enhanced intracellular calcium through activation of phosphatidylcholine-specific phospholipase C. Toxicology and Applied Pharmacology 216(2), 206-215.

Kawanai, T. (2011) Triclosan, an environmental pollutant from health care products, evokes charybdotoxin-sensitive hyperpolarization in rat thymocytes. Environmental Toxicology and Pharmacology 32(3), 417-422.

Kawanishi, T., Asoh, H., Kato, T., Uneyama, C., Toyoda, K., Teshima, R., Ikebuchi, H., Ohata, H., Momose, K. and Hayakawa, T. (1999) Suppression of calcium oscillation by tri-n-butyltin chloride in cultured rat hepatocytes. Toxicology and Applied Pharmacology 155(1), 54-61.

Kawano, T., Kadono, T., Furuichi, T., Muto, S. and Lapeyrie, F. (2003) Aluminum-induced distortion in calcium signaling involving oxidative bursts and channel regulation in tobacco BY-2 cells. Biochemical and Biophysical Research Communications 308(1), 35-42.

Kazmierczak, J., Kempe, S. and Kremer, B. (2013) Calcium in the Early Evolution of Living Systems: A Biohistorical Approach. Current Organic Chemistry 17(16), 1738-1750.

Kim Tiam, S., Laviale, M., Feurtet-Mazel, A., Jan, G., Gonzalez, P., Mazzella, N. and Morin, S. (2015) Herbicide toxicity on river biofilms assessed by pulse amplitude modulated (PAM) fluorometry. Aquatic Toxicology 165, 160-171.

Kim Tiam, S., Morin, S., Pesce, S., Feurtet-Mazel, A., Moreira, A., Gonzalez, P. and Mazzella, N. (2014) Environmental effects of realistic pesticide mixtures on natural biofilm communities with different exposure histories. Science of the Total Environment 473-474, 496-506.

Knight, M.R., Campbell, A.K., Smith, S.M. and Trewavas, A.J. (1991) Recombinant aequorin as a probe for cytosolic free Ca2+ in Escherichia coli. FEBS Letters 282(2), 405-408.

Knoll, A.H. (2015) Paleobiological Perspectives on Early Microbial Evolution. Cold Spring Harbor Perspectives in Biology 7(7), a018093.

Kokkali, V. and van Delft, W. (2014) Overview of commercially available bioassays for assessing chemical toxicity in aqueous samples. TrAC Trends in Analytical Chemistry 61, 133-155.

Kolpin, D.W., Skopec, M., Meyer, M.T., Furlong, E.T. and Zaugg, S.D. (2004) Urban contribution of pharmaceuticals and other organic wastewater contaminants to streams during differing flow conditions. Science of the Total Environment 328(1-3), 119-130.

Komárek, J. (2015) Review of the cyanobacterial genera implying planktic species after recent taxonomic revisions according to polyphasic methods: state as of 2014. Hydrobiologia 764(1), 259-270.

Kortenkamp, A., Backhaus, T. and Faust, M. (2009) State of the art report on mixture toxicity. Contract 70307, 2007485103.

Kozlova, O., Zwinderman, M. and Christofi, N. (2005) A new short-term toxicity assay using *Aspergillus awamori* with recombinant aequorin gene. BMC Microbiology 5(1), 40.

Kudla, J., Batistic, O. and Hashimoto, K. (2010) Calcium signals: the lead currency of plant information processing. Plant Cell 22(3), 541-563.

Kuo, T. (2008) The influence of methylmercury on the nitric oxide production of alveolar macrophages. Toxicology and Industrial Health 24(8), 531-538.

Kuzmanovic, M., Ginebreda, A., Petrovic, M. and Barceló, D. (2015) Contaminants of Emerging Concern in Mediterranean Watersheds. 46, 27-45.

Laetz, C.A., Baldwin, D.H., Hebert, V., Stark, J.D. and Scholz, N.L. (2013) Interactive neurobehavioral toxicity of diazinon, malathion, and ethoprop to juvenile coho salmon. Environmental Science & Technology 47(6), 2925-2931.

Lane, R., Ghazi, S.O. and Whalen, M.M. (2009) Increases in cytosolic calcium ion levels in human natural killer cells in response to butyltin exposure. Archives of Environmental Contamination and Toxicology 57(4), 816-825.

Laporte, D., Valdes, N., Gonzalez, A., Saez, C.A., Zuniga, A., Navarrete, A., Meneses, C. and Moenne, A. (2016) Copper-induced overexpression of genes encoding antioxidant system enzymes and metallothioneins involve the activation of CaMs, CDPKs and MEK1/2 in the marine alga Ulva compressa. Aquatic Toxicology 177, 433-440.

Lawrence, J.R., Topp, E., Waiser, M.J., Tumber, V., Roy, J., Swerhone, G.D., Leavitt, P., Paule, A. and Korber, D.R. (2015) Resilience and recovery: the effect of triclosan exposure timing during development, on the structure and function of river biofilm communities. Aquatic Toxicology 161, 253-266.

Leganes, F., Forchhammer, K. and Fernandez-Pinas, F. (2009) Role of calcium in acclimation of the cyanobacterium *Synechococcus elongatus* PCC 7942 to nitrogen starvation. Microbiology 155(Pt 1), 25-34.

Li, X., Qian, J., Wang, C., Zheng, K., Ye, L., Fu, Y., Han, N., Bian, H., Pan, J., Wang, J. and Zhu, M. (2011) Regulating cytoplasmic calcium homeostasis can reduce aluminum toxicity in yeast. PloS One 6(6), e21148.

Liang, W.Z. and Lu, C.H. (2012) Carvacrol-induced [Ca^{2+}]i rise and apoptosis in human glioblastoma cells. Life Sciences 90(17-18), 703-711.

Liang, Y. and Pan, J. (2013) Regulation of flagellar biogenesis by a calcium dependent protein kinase in Chlamydomonas reinhardtii. PloS One 8(7), e69902.

Liu, P.-S., Lin, C.-M., Pan, C.-Y., Kao, L.-S. and Tseng, F.-W. (2003) Butyl benzyl phthalate blocks Ca^{2+} signaling and catecholamine secretion coupled with nicotinic acetylcholine receptors in bovine adrenal chromaffin cells. Neurotoxicology 24(1), 97-105.

Liu, X., Jin, Y., Liu, W., Wang, F. and Hao, S. (2011) Possible mechanism of perfluorooctane sulfonate and perfluorooctanoate on the release of calcium ion from calcium stores in primary cultures of rat hippocampal neurons. Toxicology in Vitro 25(7), 1294-1301.

Liu, X., Liu, W., Jin, Y., Yu, W., Liu, L. and Yu, H. (2010a) Effects of subchronic perfluorooctane sulfonate exposure of rats on calcium-dependent signaling molecules in the brain tissue. Archives of Toxicology 84(6), 471-479.

Liu, X., Liu, W., Jin, Y., Yu, W., Wang, F. and Liu, L. (2010b) Effect of gestational and lactational exposure to perfluorooctanesulfonate on calcium-dependent signaling molecules gene expression in rats' hippocampus. Archives of Toxicology 84(1), 71-79.

Loewe, S. and Muischnek, H. (1926) Über kombinationswirkungen. Naunyn-Schmiedeberg's Archives of Pharmacology 114(5), 313-326.

Londono, M., Shimokawa, N., Miyazaki, W., Iwasaki, T. and Koibuchi, N. (2010) Hydroxylated PCB induces Ca^{2+} oscillations and alterations of membrane potential in cultured cortical cells. Journal of Applied Toxicology 30(4), 334-342.

Low-Decarie, E., Fussmann, G.F. and Bell, G. (2014) Aquatic primary production in a high-CO2 world. Trends Ecol Evol 29(4), 223-232.

Ludlow, M.J., Traynor, D., Fisher, P.R. and Ennion, S.J. (2008) Purinergic-mediated Ca^{2+} influx in Dictyostelium discoideum. Cell Calcium 44(6), 567-579.

Luo, Y., Guo, W., Ngo, H.H., Nghiem, L.D., Hai, F.I., Zhang, J., Liang, S. and Wang, X.C. (2014) A review on the occurrence of micropollutants in the aquatic environment and their fate and removal during wastewater treatment. Science of the Total Environment 473-474, 619-641.

Llansola, M., Montoliu, C., Boix, J. and Felipo, V. (2010) Polychlorinated Biphenyls PCB 52, PCB 180, and PCB 138 Impair the Glutamate− Nitric Oxide− cGMP Pathway in Cerebellar Neurons in Culture by Different Mechanisms. Chemical Research in Toxicology 23(4), 813-820.

Ma, X.Y., Wang, X.C., Ngo, H.H., Guo, W., Wu, M.N. and Wang, N. (2014) Bioassay based luminescent bacteria: interferences, improvements, and applications. Science of the Total Environment 468-469, 1-11.

Magdaleno, A., Saenz, M.E., Juarez, A.B. and Moretton, J. (2015) Effects of six antibiotics and their binary mixtures on growth of Pseudokirchneriella subcapitata. Ecotoxicology and Environmental Safety 113, 72-78.

Malatinszky, D., Steuer, R. and Jones, P.R. (2017) A Comprehensively Curated Genome-Scale Two-Cell Model for the Heterocystous Cyanobacterium Anabaena sp. PCC 7120. Plant Physiology 173(1), 509-523.

Mandaric, L., Celic, M., Marcé, R. and Petrovic, M. (2015) Introduction on Emerging Contaminants in Rivers and Their Environmental Risk. 46, 3-25.

Marchadier, E., Oates, M.E., Fang, H., Donoghue, P.C., Hetherington, A.M. and Gough, J. (2016) Evolution of the Calcium-Based Intracellular Signaling System. Genome Biology and Evolution 8(7), 2118-2132.

Maresova, L., Muend, S., Zhang, Y.-Q., Sychrova, H. and Rao, R. (2009a) Membrane hyperpolarization drives cation influx and fungicidal activity of amiodarone. Journal of Biological Chemistry 284(5), 2795-2802.

Maresova, L., Muend, S., Zhang, Y.Q., Sychrova, H. and Rao, R. (2009b) Membrane hyperpolarization drives cation influx and fungicidal activity of amiodarone. Journal of Biological Chemistry 284(5), 2795-2802.

Marty, M.S. and Atchison, W.D. (1997) Pathways mediating Ca2+ entry in rat cerebellar granule cells following in vitro exposure to methyl mercury. Toxicology and Applied Pharmacology 147(2), 319-330.

Mason, A.M., Borgert, C.J., Bus, J.S., Mumtaz, M.M., Simmons, J.E. and Sipes, I.G. (2007) Improving the scientific foundation for mixtures joint toxicity and risk assessment: Contributions from the SOT mixtures project—Introduction. Toxicology and Applied Pharmacology 223(2), 99-103.

Mateo, P., Leganés, F., Perona, E., Loza, V. and Fernández-Piñas, F. (2015) Cyanobacteria as bioindicators and bioreporters of environmental analysis in aquatic ecosystems. Biodiversity and Conservation 24(4), 909-948.

Matsubara, E., Harada, K., Inoue, K. and Koizumi, A. (2006) Effects of perfluorinated amphiphiles on backward swimming in Paramecium caudatum. Biochemical and Biophysical Research Communications 339(2), 554-561.

Mayati, A., Le Ferrec, E., Holme, J.A., Fardel, O., Lagadic-Gossmann, D. and Øvrevik, J. (2014) Calcium signaling and β2-adrenergic receptors regulate 1-nitropyrene induced CXCL8 responses in BEAS-2B cells. Toxicology in Vitro 28(6), 1153-1157.

Mayilswami, S., Krishnan, K., Megharaj, M. and Naidu, R. (2016) Gene expression profile changes in *Eisenia fetida* chronically exposed to PFOA. Ecotoxicology 25(4), 759-769.

McAinsh, M.R., Brownlee, C. and Hetherington, A.M. (1997) Calcium ions as second messengers in guard cell signal transduction. Physiologia Plantarum 100(1), 16-29.

McAinsh, M.R. and Pittman, J.K. (2009) Shaping the calcium signature. New Phytol 181(2), 275-294.

McKnight, U.S., Rasmussen, J.J., Kronvang, B., Binning, P.J. and Bjerg, P.L. (2015) Sources, occurrence and predicted aquatic impact of legacy and contemporary pesticides in streams. Environmental Pollution (Barking, Essex: 1987) 200, 64-76.

McMahon, T.A., Halstead, N.T., Johnson, S., Raffel, T.R., Romansic, J.M., Crumrine, P.W., Boughton, R.K., Martin, L.B. and Bohr, J.R. (2011) The fungicide chlorothalonil is nonlinearly associated with corticosterone levels, immunity, and mortality in amphibians. Environmental Health Perspectives 119(8), 1098.

McMahon, T.A., Romansic, J.M. and Rohr, J.R. (2013) Nonmonotonic and monotonic effects of pesticides on the pathogenic fungus Batrachochytrium dendrobatidis in culture and on tadpoles. Environmental Science & Technology 47(14), 7958-7964.

Michelangeli, F., Ogunbayo, O.A., Wootton, L.L., Lai, P.F., Al-Mousa, F., Harris, R.M., Waring, R.H. and Kirk, C.J. (2008) Endocrine disrupting alkylphenols: structural requirements for their adverse effects on Ca^{2+} pumps, Ca^{2+} homeostasis & Sertoli TM4 cell viability. Chemico-Biological Interactions 176(2), 220-226.

Mitra, S., Gera, R., Siddiqui, W.A. and Khandelwal, S. (2013) Tributyltin induces oxidative damage, inflammation and apoptosis via disturbance in blood-brain barrier and metal homeostasis in cerebral cortex of rat brain: an in vivo and in vitro study. Toxicology 310, 39-52.

Miura, Y., Chen, X., Yamada, S., Sugihara, A., Enkhjargal, M., Sun, Y., Kuroda, K., Satoh, M. and Oyama, Y. (2014) Triclocarban-induced change in intracellular Ca(2)(+) level in rat thymocytes: cytometric analysis with Fluo-3 under Zn(2)(+)-free conditions. Environmental Toxicology and Pharmacology 37(2), 563-570.

Morris, M.D. (1991) Factorial sampling plans for preliminary computational experiments. Technometrics 33(2), 161-174.

Moscatiello, R., Alberghini, S., Squartini, A., Mariani, P. and Navazio, L. (2009) Evidence for calcium-mediated perception of plant symbiotic signals in aequorin-expressing Mesorhizobium loti. BMC Microbiology 9(1), 206.

Moscatiello, R., Squartini, A., Mariani, P. and Navazio, L. (2010) Flavonoid-induced calcium signalling in Rhizobium leguminosarum bv. viciae. New Phytologist 188(3), 814-823.

Muend, S. and Rao, R. (2008a) Fungicidal activity of amiodarone is tightly coupled to calcium influx. FEMS Yeast Res 8(3), 425-431.

Muend, S. and Rao, R. (2008b) Fungicidal activity of amiodarone is tightly coupled to calcium influx. FEMS yeast research 8(3), 425-431.

Mumtaz, M. and Hertzberg, R. (1993) The status of interactions data in risk assessment of chemical mixtures. Hazard assessment of chemicals 8, 47-79.

Muñoz, I., López-Doval, J.C., Ricart, M., Villagrasa, M., Brix, R., Geiszinger, A., Ginebreda, A., Guasch, H., de Alda, M.J.L., Romaní, A.M., Sabater, S. and Barceló, D. (2009) Bridging levels of pharmaceuticals in river water with biological community structure in the llobregat river basin (northeast spain). Environmental Toxicology and Chemistry 28(12), 2706-2714.

Murik, O., Elboher, A. and Kaplan, A. (2014) Dehydroascorbate: a possible surveillance molecule of oxidative stress and programmed cell death in the green alga *Chlamydomonas reinhardtii*. New Phytologist 202(2), 471-484.

Murray, K.E., Thomas, S.M. and Bodour, A.A. (2010) Prioritizing research for trace pollutants and emerging contaminants in the freshwater environment. Environmental Pollution (Barking, Essex: 1987) 158(12), 3462-3471.

Mussgnug, J.H. (2015) Genetic tools and techniques for *Chlamydomonas reinhardtii*. Applied Microbiology and Biotechnology 99(13), 5407-5418.

Nagel, G., Ollig, D., Fuhrmann, M., Kateriya, S., Musti, A.M., Bamberg, E. and Hegemann, P. (2002) Channelrhodopsin-1: a light-gated proton channel in green algae. Science 296(5577), 2395-2398.

Nakajima-Shimada, J., Iida, H., Tsuji, F.I. and Anraku, Y. (1991) Monitoring of intracellular calcium in Saccharomyces cerevisiae with an apoaequorin cDNA expression system. Proceedings of the National Academy of Sciences 88(15), 6878-6882.

Nathansoni, M., Mariwallai, K., Ballatori, N. and Boyeri, J. (1995) Effects of Hg2+ on cytosolic Ca^{2+} in isolated skate hepatocytes. Cell Calcium 18(5), 429-439.

Nguyen, H.M., Baudet, M., Cuine, S., Adriano, J.M., Barthe, D., Billon, E., Bruley, C., Beisson, F., Peltier, G. and Ferro, M. (2011) Proteomic profiling of oil bodies isolated from the unicellular green microalga Chlamydomonas reinhardtii: with focus on proteins involved in lipid metabolism. Proteomics 11(21), 4266-4273.

Noguera-Oviedo, K. and Aga, D.S. (2016) Lessons learned from more than two decades of research on emerging contaminants in the environment. Journal of Hazardous Materials 316, 242-251.

Nomura, H. and Shiina, T. (2014) Calcium signaling in plant endosymbiotic organelles: mechanism and role in physiology. Molecular plant 7(7), 1094-1104.

Nostbakken, O.J., Goksoyr, A., Martin, S.A., Cash, P. and Torstensen, B.E. (2012) Marine n-3 fatty acids alter the proteomic response to methylmercury in Atlantic salmon kidney (ASK) cells. Aquatic Toxicology 106-107, 65-75.

Nultsch, W., Pfau, J. and Dolle, R. (1986) Effects of calcium channel blockers on phototaxis and motility of Chlamydomonas reinhardtii. Archives of Microbiology 144(4), 393-397.

Ogunbayo, O.A., Lai, P.F., Connolly, T.J. and Michelangeli, F. (2008) Tetrabromobisphenol A (TBBPA), induces cell death in TM4 Sertoli cells by modulating Ca 2+ transport proteins and causing dysregulation of Ca 2+ homeostasis. Toxicology in Vitro 22(4), 943-952.

Ohta, M. and Suzuki, T. (2007) Participation of the inositol phospholipid signaling pathway in the increase in cytosolic calcium induced by tributyltin chloride intoxication of chlorophyllous protozoa *Euglena gracilis* Z and its achlorophyllous mutant SM-ZK. Comparative Biochemistry and Physiology: Toxicology & Pharmacology 146(4), 525-530.

Osorio, V., Larranaga, A., Acena, J., Perez, S. and Barcelo, D. (2016) Concentration and risk of pharmaceuticals in freshwater systems are related to the population density and the livestock units in Iberian Rivers. Science of the Total Environment 540, 267-277.

Pal, A., Gin, K.Y., Lin, A.Y. and Reinhard, M. (2010) Impacts of emerging organic contaminants on freshwater resources: review of recent occurrences, sources, fate and effects. Science of the Total Environment 408(24), 6062-6069.

Pal, A., He, Y., Jekel, M., Reinhard, M. and Gin, K.Y. (2014) Emerging contaminants of public health significance as water quality indicator compounds in the urban water cycle. Environ Int 71, 46-62.

Panda, B., Basu, B., Acharya, C., Rajaram, H. and Apte, S.K. (2017) Proteomic analysis reveals contrasting stress response to uranium in two nitrogen-fixing Anabaena strains, differentially tolerant to uranium. Aquatic Toxicology 182, 205-213.

Pandey, S., Rai, R. and Rai, L.C. (2012) Proteomics combines morphological, physiological and biochemical attributes to unravel the survival strategy of Anabaena sp. PCC7120 under arsenic stress. Journal of Proteomics 75(3), 921-937.

Pavlic, Z., Vidakovic-Cifrek, Z. and Puntaric, D. (2005) Toxicity of surfactants to green microalgae Pseudokirchneriella subcapitata and Scenedesmus subspicatus and to marine diatoms Phaeodactylum tricornutum and Skeletonema costatum. Chemosphere 61(8), 1061-1068.

Perumal Vijayaraman, K., Muruganantham, S., Subramanian, M., Shunmugiah, K.P. and Kasi, P.D. (2012) Silymarin attenuates benzo(a)pyrene induced toxicity by mitigating ROS production, DNA damage and calcium mediated apoptosis in peripheral blood mononuclear cells (PBMC). Ecotoxicology and Environmental Safety 86, 79-85.

Petit, A.-N., Debenest, T., Eullaffroy, P. and Gagné, F. (2012) Effects of a cationic PAMAM dendrimer on photosynthesis and ROS production of Chlamydomonas reinhardtii. Nanotoxicology 6(3), 315-326.

Petroutsos, D., Busch, A., Janßen, I., Trompelt, K., Bergner, S.V., Weinl, S., Holtkamp, M., Karst, U., Kudla, J. and Hippler, M. (2011) The chloroplast calcium sensor CAS is required for photoacclimation in *Chlamydomonas reinhardtii*. The Plant Cell 23(8), 2950-2963.

Pillai, S., Behra, R., Nestler, H., Suter, M.J.-F., Sigg, L. and Schirmer, K. (2014) Linking toxicity and adaptive responses across the transcriptome, proteome, and phenotype of Chlamydomonas reinhardtii exposed to silver. Proceedings of the National Academy of Sciences 111(9), 3490-3495.

Pino, M.R., Muniz, S., Val, J. and Navarro, E. (2016) Phytotoxicity of 15 common pharmaceuticals on the germination of Lactuca sativa and photosynthesis of Chlamydomonas reinhardtii. Environmental Science and Pollution Research International 23(22), 22530-22541.

Plattner, H. and Verkhratsky, A. (2016) Inseparable tandem: evolution chooses ATP and Ca^{2+} to control life, death and cellular signalling. Philosophical Transactions of the Royal Society of London. Series B: Biological Sciences 371(1700).

Popa, C.V., Dumitru, I., Ruta, L.L., Danet, A.F. and Farcasanu, I.C. (2010) Exogenous oxidative stress induces Ca^{2+} release in the yeast *Saccharomyces cerevisiae*. FEBS J 277(19), 4027-4038.

Prado, R., Rioboo, C., Herrero, C. and Cid, Á. (2012) Screening acute cytotoxicity biomarkers using a microalga as test organism. Ecotoxicology and Environmental Safety 86, 219-226.

Proia, L., Osorio, V., Soley, S., Kock-Schulmeyer, M., Perez, S., Barcelo, D., Romani, A.M. and Sabater, S. (2013) Effects of pesticides and pharmaceuticals on biofilms in a highly impacted river. Environmental Pollution (Barking, Essex: 1987) 178, 220-228.

Proia, L., Romani, A. and Sabater, S. (2017) Biofilm phosphorus uptake capacity as a tool for the assessment of pollutant effects in river ecosystems. Ecotoxicology 26(2), 271-282.

Proia, L., von Schiller, D., Sanchez-Melsio, A., Sabater, S., Borrego, C.M., Rodriguez-Mozaz, S. and Balcazar, J.L. (2016) Occurrence and persistence of antibiotic resistance genes in river biofilms after wastewater inputs in small rivers. Environmental Pollution (Barking, Essex: 1987) 210, 121-128.

Pröschold, T., Marin, B., Schlösser, U.G. and Melkonian, M. (2001) Molecular Phylogeny and Taxonomic Revision of Chlamydomonas (Chlorophyta). I. Emendation of Chlamydomonas Ehrenberg and Chloromonas Gobi, and Description of Oogamochlamys gen. nov. and Lobochlamys gen. nov.** In memory of Hanus Ettl (19311997), promoter of the systematics of thegenus. Protist 152(4), 265-300.

Quinn, B., Gagné, F. and Blaise, C. (2009) Evaluation of the acute, chronic and teratogenic effects of a mixture of eleven pharmaceuticals on the cnidarian, Hydra attenuata. Science of the Total Environment 407(3), 1072-1079.

Rai, A., Maurya, S.K., Khare, P., Srivastava, A. and Bandyopadhyay, S. (2010) Characterization of developmental neurotoxicity of As, Cd, and Pb mixture: synergistic action of metal mixture in glial and neuronal functions. Toxicological Sciences 118(2), 586-601.

Ramanathan, G. and Atchison, W.D. (2011) Ca2+ entry pathways in mouse spinal motor neurons in culture following in vitro exposure to methylmercury. Neurotoxicology 32(6), 742-750.

Reader, S., Steen, H.B. and Denizeau, F. (1994) Intracellular calcium and pH alterations induced by tri-n-butyltin chloride in isolated rainbow trout hepatocytes: a flow cytometric analysis. Archives of Biochemistry and Biophysics 312(2), 407-413.

Reynaud, S., Duchiron, C. and Deschaux, P. (2003) 3-Methylcholanthrene inhibits lymphocyte proliferation and increases intracellular calcium levels in common carp (Cyprinus carpio L). Aquatic Toxicology 63(3), 319-331.

Ribeiro, A.R., Nunes, O.C., Pereira, M.F. and Silva, A.M. (2015a) An overview on the advanced oxidation processes applied for the treatment of water pollutants defined in the recently launched Directive 2013/39/EU. Environ Int 75, 33-51.

Ribeiro, A.R., Pedrosa, M., Moreira, N.F., Pereira, M.F. and Silva, A.M. (2015b) Environmental friendly method for urban wastewater monitoring of micropollutants defined in the Directive 2013/39/EU and Decision 2015/495/EU. Journal of Chromatography A 1418, 140-149.

Richter, P., Krywult, M., Sinha, R.P. and Häder, D.-P. (1999) Calcium signals from heterocysts of Anabaena sp. after UV irradiation. Journal of Plant Physiology 154(1), 137-139.

Riva, C., Cristoni, S. and Binelli, A. (2012) Effects of triclosan in the freshwater mussel Dreissena polymorpha: a proteomic investigation. Aquatic Toxicology 118-119, 62-71.

Roberts, S.K., McAinsh, M. and Widdicks, L. (2012a) Cch1p mediates Ca^{2+} influx to protect Saccharomyces cerevisiae against eugenol toxicity. PloS One 7(9), e43989.

Rodea-Palomares, I., Fernández-Piñas, F., González-García, C. and Leganés, F. (2009a) Use of lux-marked cyanobacterial bioreporters for assessment of individual and combined toxicities of metals in aqueous samples. Handbook on Cyanobacteria: Biochemistry, Biotechnology and Applications, 283-304.

Rodea-Palomares, I., González-García, C., Leganés, F. and Fernández-Piñas, F. (2009b) Effect of pH, EDTA, and anions on heavy metal toxicity toward a bioluminescent cyanobacterial bioreporter. Archives of Environmental Contamination and Toxicology 57(3), 477.

Rodea-Palomares, I., Leganés, F., Rosal, R. and Fernández-Pinas, F. (2012) Toxicological interactions of perfluorooctane sulfonic acid (PFOS) and perfluorooctanoic acid (PFOA) with selected pollutants. Journal of Hazardous Materials 201, 209-218.

Rodea-Palomares, I., Petre, A.L., Boltes, K., Leganés, F., Perdigón-Melón, J.A., Rosal, R. and Fernández-Piñas, F. (2010) Application of the combination index (CI)-isobologram equation to study the toxicological interactions of lipid regulators in two aquatic bioluminescent organisms. water research 44(2), 427-438.

Rohr, J.R., Schotthoefer, A.M., Raffel, T.R., Carrick, H.J., Halstead, N., Hoverman, J.T., Johnson, C.M., Johnson, L.B., Lieske, C. and Piwoni, M.D. (2008) Agrochemicals increase trematode infections in a declining amphibian species. Nature 455(7217), 1235-1239.

Rosal, R., Rodea-Palomares, I., Boltes, K., Fernandez-Pinas, F., Leganes, F. and Petre, A. (2010a) Ecotoxicological assessment of surfactants in the aquatic environment: combined toxicity of docusate sodium with chlorinated pollutants. Chemosphere 81(2), 288-293.

Rosal, R., Rodriguez, A., Perdigon-Melon, J.A., Petre, A., Garcia-Calvo, E., Gomez, M.J., Aguera, A. and Fernandez-Alba, A.R. (2010b) Occurrence of emerging pollutants in urban wastewater and their removal through biological treatment followed by ozonation. Water Res 44(2), 578-588.

Roux, E., Hyvelin, J.-M., Savineau, J.-P. and Marthan, R. (1998) Calcium signaling in airway smooth muscle cells is altered by in vitro exposure to the aldehyde acrolein. American Journal of Respiratory Cell and Molecular Biology 19(3), 437-444.

Rudd, J.J. and Franklin-Tong, V.E. (2001) Unravelling response-specificity in Ca2+ signalling pathways in plant cells. New Phytologist 151(1), 7-33.

Ruta, L.L., Popa, C.V., Nicolau, I. and Farcasanu, I.C. (2016) Calcium signaling and copper toxicity in Saccharomyces cerevisiae cells. Environmental Science and Pollution Research International 23(24), 24514-24526.

Ruta, L.L., Popa, V.C., Nicolau, I., Danet, A.F., Iordache, V., Neagoe, A.D. and Farcasanu, I.C. (2014) Calcium signaling mediates the response to cadmium toxicity in Saccharomyces cerevisiae cells. FEBS Letters 588(17), 3202-3212.

Ryu, D.S., Yang, H., Lee, S.E., Park, C.S., Jin, Y.H. and Park, Y.S. (2013) Crotonaldehyde induces heat shock protein 72 expression that mediates anti-apoptotic effects in human endothelial cells. Toxicology Letters 223(2), 116-123.

Sabater, S., Guasch, H., Ricart, M., Romani, A., Vidal, G., Klunder, C. and Schmitt-Jansen, M. (2007) Monitoring the effect of chemicals on biological communities. The biofilm as an interface. Anal Bioanal Chem 387(4), 1425-1434.

Saltelli, A., Ratto, M., Tarantola, S. and Campolongo, F. (2005) Sensitivity analysis for chemical models. Chemical Reviews 105(7), 2811-2828.

Saltelli, A., Ratto, M., Tarantola, S. and Campolongo, F. (2012) Update 1 of: Sensitivity analysis for chemical models. Chemical Reviews 112(5), PR1-PR21.

Saltelli, A., Tarantola, S. and Chan, K.-S. (1999) A quantitative model-independent method for global sensitivity analysis of model output. Technometrics 41(1), 39-56.

Sarmah, A.K., Meyer, M.T. and Boxall, A.B.A. (2006) A global perspective on the use, sales, exposure pathways, occurrence, fate and effects of veterinary antibiotics (VAs) in the environment. Chemosphere 65(5), 725-759.

Sauvé, S. and Desrosiers, M. (2014) A review of what is an emerging contaminant. Chemistry Central Journal 8(1), 15.

Schafer, S., Bickmeyer, U. and Koehler, A. (2009) Measuring Ca2+-signalling at fertilization in the sea urchin Psammechinus miliaris: alterations of this Ca2+-signal by copper and 2,4,6-tribromophenol. Comparative Biochemistry and Physiology: Toxicology & Pharmacology 150(2), 261-269.

Schirrmeister, B.E., Gugger, M. and Donoghue, P.C. (2015) Cyanobacteria and the Great Oxidation Event: evidence from genes and fossils. Palaeontology 58(5), 769-785.

Schmidt, J.A. and Eckert, R. (1976) Calcium couples flagellar reversal to photostimulation in Chlamydomonas reinhardtii. Nature 262(5570), 713-715.

Scholze, M., Silva, E. and Kortenkamp, A. (2014) Extending the applicability of the dose addition model to the assessment of chemical mixtures of partial agonists by using a novel toxic unit extrapolation method. PloS One 9(2), e88808.

Schopf, J.W. (1993) Microfossils of the Early Archean Apex chert: new evidence of the antiquity of life. Science 260(5108), 640-646.

Schweizer, N., Kummer, U., Hercht, H. and Braunbeck, T. (2011) Amplitude-encoded calcium oscillations in fish cells. Biophysical Chemistry 159(2-3), 294-302.

Segner, H., Schmitt-Jansen, M. and Sabater, S. (2014) Assessing the impact of multiple stressors on aquatic biota: the receptor's side matters, ACS Publications.

Shemarova, I.V. and Nesterov, V.P. (2014) [Ca2+ signaling in prokaryotes]. Mikrobiologiia 83(5), 511-518.

Shi, H., Cheng, X., Wu, Q., Mu, R. and Yinfa, M. (2012) Assessment and removal of emerging water contaminants. Journal of Environmental & Analytical Toxicology 2.

Shi, Y., Zhao, W., Zhang, W., Ye, Z. and Zhao, J. (2006) Regulation of intracellular free calcium concentration during heterocyst differentiation by HetR and NtcA in Anabaena sp. PCC 7120. Proceedings of the National Academy of Sciences 103(30), 11334-11339.

Simkovič, M., Lakatoš, B., Tsuji, F., Muto, S. and Varečka, Ľ. (2001) The Effect of Azalomycin F on Ca2 homeostasis in Trichoderma viride and Saccharomyces cerevisiae. General Physiology and Biophysics 20, 131-144.

Simon, D.F., Domingos, R.F., Hauser, C., Hutchins, C.M., Zerges, W. and Wilkinson, K.J. (2013) Transcriptome sequencing (RNA-seq) analysis of the effects of metal nanoparticle exposure on the transcriptome of Chlamydomonas reinhardtii. Applied and Environmental Microbiology 79(16), 4774-4785.

Singh, P.K., Rai, S., Pandey, S., Agrawal, C., Shrivastava, A.K., Kumar, S. and Rai, L. Cadmium and UV-B induced changes in proteome and some biochemical attributes of Anabaena sp. PCC7120.

Soriano, S., Alonso-Magdalena, P., Garcia-Arevalo, M., Novials, A., Muhammed, S.J., Salehi, A., Gustafsson, J.A., Quesada, I. and Nadal, A. (2012) Rapid insulinotropic action of low doses of bisphenol-A on mouse and human islets of Langerhans: role of estrogen receptor beta. PloS One 7(2), e31109.

Stael, S., Wurzinger, B., Mair, A., Mehlmer, N., Vothknecht, U.C. and Teige, M. (2012) Plant organellar calcium signalling: an emerging field. J Exp Bot 63(4), 1525-1542.

Stavis, R.L. (1974) The effect of azide on phototaxis in Chlamydomonas reinhardi. Proceedings of the National Academy of Sciences 71(5), 1824-1827.

Stavis, R.L. and Hirschberg, R. (1973) Phototaxis in Chlamydomonas reinhardtii. The Journal of cell biology 59(2), 367-377.

Stebegg, R., Wurzinger, B., Mikulic, M. and Schmetterer, G. (2012) Chemoheterotrophic growth of the Cyanobacterium Anabaena sp. strain PCC 7120 dependent on a functional cytochrome c oxidase. Journal of Bacteriology 194(17), 4601-4607.

Sun, F.-C., Shyu, H.-Y., Lee, M.-S., Lee, M.-S. and Lai, Y.-K. (2013) Involvement of calcium-mediated reactive oxygen species in inductive GRP78 expression by geldanamycin in 9L rat brain tumor cells. Int J Mol Sci 14(9), 19169-19185.

Syberg, K., Elleby, A., Pedersen, H., Cedergreen, N. and Forbes, V.E. (2008) Mixture toxicity of three toxicants with similar and dissimilar modes of action to Daphnia magna. Ecotoxicology and Environmental Safety 69(3), 428-436.

Tallarida, R.J. (2011) Quantitative methods for assessing drug synergism. Genes & Cancer 2(11), 1003-1008.

Tasmin, R., Shimasaki, Y., Tsuyama, M., Qiu, X., Khalil, F., Okino, N., Yamada, N., Fukuda, S., Kang, I.J. and Oshima, Y. (2014) Elevated water temperature reduces the acute toxicity of the widely used herbicide diuron to a green alga, Pseudokirchneriella subcapitata. Environmental Science and Pollution Research International 21(2), 1064-1070.

Tavares, R.S., Mansell, S., Barratt, C.L., Wilson, S.M., Publicover, S.J. and Ramalho-Santos, J. (2013) p,p'-DDE activates CatSper and compromises human sperm function at environmentally relevant concentrations. Human Reproduction 28(12), 3167-3177.

Terashima, M., Petroutsos, D., Hüdig, M., Tolstygina, I., Trompelt, K., Gäbelein, P., Fufezan, C., Kudla, J., Weinl, S. and Finazzi, G. (2012) Calcium-dependent regulation of cyclic photosynthetic electron transfer by a CAS, ANR1, and PGRL1 complex. Proceedings of the National Academy of Sciences 109(43), 17717-17722.

Ternes, T.A., Joss, A. and Siegrist, H. (2004) Peer reviewed: scrutinizing pharmaceuticals and personal care products in wastewater treatment, ACS Publications.

Teuschler, L.K. (2007) Deciding which chemical mixtures risk assessment methods work best for what mixtures. Toxicology and Applied Pharmacology 223(2), 139-147.

Thompson, S.L., Manning, F.C. and McColl, S.M. (2002) Comparison of the toxicity of chromium III and chromium VI to cyanobacteria. Bulletin of Environmental Contamination and Toxicology 69(2), 286-293.

Tian, D., Lin, Z., Yu, J. and Yin, D. (2012) Influence factors of multicomponent mixtures containing reactive chemicals and their joint effects. Chemosphere 88(8), 994-1000.

Tiwari, A., Singh, P. and Asthana, R.K. (2016) Role of calcium in the mitigation of heat stress in the cyanobacterium Anabaena PCC 7120. Journal of Plant Physiology 199, 67-75.

Torrecilla, I., Leganes, F., Bonilla, I. and Fernandez-Pinas, F. (2000) Use of recombinant aequorin to study calcium homeostasis and monitor calcium transients in response to heat and cold shock in cyanobacteria. Plant Physiology 123(1), 161-176.

Torrecilla, I., Leganes, F., Bonilla, I. and Fernandez-Pinas, F. (2004a) A calcium signal is involved in heterocyst differentiation in the cyanobacterium Anabaena sp. PCC7120. Microbiology 150(Pt 11), 3731-3739.

Torrecilla, I., Leganés, F., Bonilla, I. and Fernández-Piñas, F. (2001) Calcium transients in response to salinity and osmotic stress in the nitrogen-fixing cyanobacterium Anabaena sp. PCC7120, expressing cytosolic apoaequorin. Plant, Cell & Environment 24(6), 641-648.

Torrecilla, I., LeganÉS, F., Bonilla, I. and FernÁNdez-PiÑAs, F. (2004b) Light-to-dark transitions trigger a transient increase in intracellular Ca2+ modulated by the redox state of the photosynthetic electron transport chain in the cyanobacterium Anabaena sp. PCC7120. Plant, Cell & Environment 27(7), 810-819.

Trinh, N.N., Huang, T.L., Chi, W.C., Fu, S.F., Chen, C.C. and Huang, H.J. (2014) Chromium stress response effect on signal transduction and expression of signaling genes in rice. Physiologia Plantarum 150(2), 205-224.

Trippens, J., Reißenweber, T. and Kreimer, G. (2017) The chloroplast calcium sensor protein CAS affects phototactic behaviour in Chlamydomonas reinhardtii (Chlorophyceae) at low light intensities. Phycologia 56(3), 261-270.

Valcarcel, Y., Alonso, S.G., Rodriguez-Gil, J.L., Castano, A., Montero, J.C., Criado-Alvarez, J.J., Miron, I.J. and Catala, M. (2013) Seasonal variation of pharmaceutically active compounds in surface (Tagus River) and tap water (Central Spain). Environmental Science and Pollution Research International 20(3), 1396-1412.

Valitalo, P., Kruglova, A., Mikola, A. and Vahala, R. (2017) Toxicological impacts of antibiotics on aquatic micro-organisms: A mini-review. Int J Hyg Environ Health.

Van Mooy, B., Krupke, A., Dyhrman, S., Fredricks, H., Frischkorn, K., Ossolinski, J., Repeta, D., Rouco, M., Seewald, J. and Sylva, S. (2015) Major role of planktonic phosphate reduction in the marine phosphorus redox cycle. Science 348(6236), 783-785.

Vandenbrouck, T., Soetaert, A., van der Ven, K., Blust, R. and De Coen, W. (2009) Nickel and binary metal mixture responses in Daphnia magna: molecular fingerprints and (sub) organismal effects. Aquatic Toxicology 92(1), 18-29.

Vandermeersch, G., Lourenco, H.M., Alvarez-Munoz, D., Cunha, S., Diogene, J., Cano-Sancho, G., Sloth, J.J., Kwadijk, C., Barcelo, D., Allegaert, W., Bekaert, K., Fernandes, J.O., Marques, A. and Robbens, J. (2015) Environmental contaminants of emerging concern in seafood--European database on contaminant levels. Environmental Research 143(Pt B), 29-45.

Verkhratsky, A. and Parpura, V. (2014) Calcium signalling and calcium channels: evolution and general principles. European Journal of Pharmacology 739, 1-3.

Verret, F., Wheeler, G., Taylor, A.R., Farnham, G. and Brownlee, C. (2010) Calcium channels in photosynthetic eukaryotes: implications for evolution of calcium-based signalling. New Phytologist 187(1), 23-43.

Villeneuve, A., Montuelle, B., Pesce, S. and Bouchez, A. (2013) Encyclopedia of Aquatic Ecotoxicology, pp. 443-456, Springer.

Waditee, R., Hossain, G.S., Tanaka, Y., Nakamura, T., Shikata, M., Takano, J., Takabe, T. and Takabe, T. (2004) Isolation and functional characterization of Ca2+/H+ antiporters from cyanobacteria. Journal of Biological Chemistry 279(6), 4330-4338.

Wagner, C. and Løkke, H. (1991) Estimation of ecotoxicological protection levels from NOEC toxicity data. water research 25(10), 1237-1242.

Wakabayashi, K.i., Ide, T. and Kamiya, R. (2009) Calcium-dependent flagellar motility activation in Chlamydomonas reinhardtii in response to mechanical agitation. Cytoskeleton 66(9), 736-742.

Walter, H., Consolaro, F., Gramatica, P., Scholze, M. and Altenburger, R. (2002) Mixture toxicity of priority pollutants at no observed effect concentrations (NOECs). Ecotoxicology 11(5), 299-310.

Walter, J., Lynch, F., Battchikova, N., Aro, E.-M. and Gollan, P.J. (2016) Calcium impacts carbon and nitrogen balance in the filamentous cyanobacterium Anabaena sp. PCC 7120. J Exp Bot 67(13), 3997-4008.

Wang, J., Zhu, H., Liu, X. and Liu, Z. (2014) Oxidative stress and Ca(2+) signals involved on cadmium-induced apoptosis in rat hepatocyte. Biological Trace Element Research 161(2), 180-189.

Wang, L., Yamano, T., Takane, S., Niikawa, Y., Toyokawa, C., Ozawa, S.-i., Tokutsu, R., Takahashi, Y., Minagawa, J. and Kanesaki, Y. (2016a) Chloroplast-mediated regulation of CO2-concentrating mechanism by Ca2+-binding protein CAS in the green alga Chlamydomonas reinhardtii. Proceedings of the National Academy of Sciences 113(44), 12586-12591.

Wang, S., Chen, L. and Xia, S. (2007) Cadmium is Acutely Toxic for Murine Hepatocytes: Effects on Intracellular Free Ca^ sup 2+^ Homeostasis. Physiological Research 56(2), 193.

Wang, X., Yi, M., Liu, H., Han, Y. and Yi, H. (2016b) Reactive oxygen species and Ca2+ are involved in cadmium-induced cell killing in yeast cells. Canadian Journal of Microbiology 63(999), 1-7.

Wannigama, D.L., Agrawal, C. and Rai, L. (2012) A Comparative study on proteomic and biochemical alterations in the cyanobacterium Anabaena sp. PCC 7120 under short term exposure of abiotic stresses: Pesticide, Salinity, Heavy metal and UV-B.

Watkins, N., Knight, M., Trewavas, A. and Campbell, A. (1995) Free calcium transients in chemotactic and non-chemotactic strains of Escherichia coli determined by using recombinant aequorin. Biochemical Journal 306(3), 865-869.

Whalley, H.J. and Knight, M.R. (2013) Calcium signatures are decoded by plants to give specific gene responses. New Phytol 197(3), 690-693.

Wheeler, G.L. and Brownlee, C. (2008) Ca 2+ signalling in plants and green algae–changing channels. Trends in Plant Science 13(9), 506-514.

Whitton, B.A. and Potts, M. (2012) Introduction to the Cyanobacteria. 1-13.

Xiong, J.Q., Kurade, M.B., Kim, J.R., Roh, H.S. and Jeon, B.H. (2017) Ciprofloxacin toxicity and its co-metabolic removal by a freshwater microalga Chlamydomonas mexicana. Journal of Hazardous Materials 323(Pt A), 212-219.

Xu, B., Chen, S., Luo, Y., Chen, Z., Liu, L., Zhou, H., Chen, W., Shen, T., Han, X., Chen, L. and Huang, S. (2011) Calcium signaling is involved in cadmium-induced neuronal apoptosis via induction of reactive oxygen species and activation of MAPK/mTOR network. PloS One 6(4), e19052.

Xu, Y., Wang, C., Hou, J., Dai, S., Wang, P., Miao, L., Lv, B., Yang, Y. and You, G. (2016) Effects of ZnO nanoparticles and Zn(2+) on fluvial biofilms and the related toxicity mechanisms. Science of the Total Environment 544, 230-237.

Yamagishi, T., Horie, Y. and Tatarazako, N. (2017a) Synergism between macrolide antibiotics and the azole fungicide ketoconazole in growth inhibition testing of the green alga Pseudokirchneriella subcapitata. Chemosphere 174, 1-7.

Yamagishi, T., Yamaguchi, H., Suzuki, S., Horie, Y. and Tatarazako, N. (2017b) Cell reproductive patterns in the green alga Pseudokirchneriella subcapitata (=Selenastrum capricornutum) and their variations under exposure to the typical toxicants potassium dichromate and 3,5-DCP. PloS One 12(2), e0171259.

Yang, B.-c., Pan, X.-j., Yang, Z.-h., Xiao, F.-j., Liu, X.-y., Zhu, M.-x. and Xie, J.-p. (2013) Crotonaldehyde induces apoptosis in alveolar macrophages through intracellular calcium, mitochondria and p53 signaling pathways. The Journal of toxicological sciences 38(2), 225-235.

Yuan, Y., Jiang, C.Y., Xu, H., Sun, Y., Hu, F.F., Bian, J.C., Liu, X.Z., Gu, J.H. and Liu, Z.P. (2013) Cadmium-induced apoptosis in primary rat cerebral cortical neurons culture is mediated by a calcium signaling pathway. PloS One 8(5), e64330.

Zhang, L., Ji, F., Li, M., Cui, Y. and Wu, B. (2014) Short-term effects of Dechlorane Plus on the earthworm Eisenia fetida determined by a systems biology approach. Journal of Hazardous Materials 273, 239-246.

Zhang, Y., Geißen, S.-U. and Gal, C. (2008) Carbamazepine and diclofenac: Removal in wastewater treatment plants and occurrence in water bodies. Chemosphere 73(8), 1151-1161.

Zhao, W., Guo, Q. and Zhao, J. (2007a) A membrane-associated Mn-superoxide dismutase protects the photosynthetic apparatus and nitrogenase from oxidative damage in the Cyanobacterium Anabaena sp. PCC 7120. Plant and Cell Physiology 48(4), 563-572.

Zhao, W., Ye, Z. and Zhao, J. (2007b) RbrA, a cyanobacterial rubrerythrin, functions as a FNR-dependent peroxidase in heterocysts in protection of nitrogenase from damage by hydrogen peroxide in Anabaena sp. PCC 7120. Molecular Microbiology 66(5), 1219-1230.

Zhao, Y., Shi, Y., Zhao, W., Huang, X., Wang, D., Brown, N., Brand, J. and Zhao, J. (2005) CcbP, a calcium-binding protein from Anabaena sp. PCC 7120, provides evidence that calcium ions regulate heterocyst differentiation. Proceedings of the National Academy of Sciences of the United States of America 102(16), 5744-5748.

Zheng, Z., Omairi-Nasser, A., Li, X., Dong, C., Lin, Y., Haselkorn, R. and Zhao, J. (2017) An amidase is required for proper intercellular communication in the filamentous cyanobacterium Anabaena sp. PCC 7120. Proceedings of the National Academy of Sciences of the United States of America 114(8), E1405-E1412.

Zhu, X., Dunand, C., Snedden, W. and Galaud, J.-P. (2015) CaM and CML emergence in the green lineage. Trends in Plant Science 20(8), 483-489.

OBJECTIVES

OBJECTIVES

The present Thesis aims at studying the biological effects of the so-called "emerging pollutants" (EPs), particularly pharmaceuticals, on aquatic photosynthetic organisms of high ecological relevance, namely cyanobacteria and microalgae.

EPs co-occur with many other pollutants in environmental compartments. Therefore, aquatic organisms may be exposed to mixtures of pollutants. While the individual concentrations of these pollutants in aquatic environments may be low, the combined concentrations could result in significant toxicity to aquatic organisms. Besides, as chemicals in a mixture may either not interact or interact synergistically or antagonistically, it is essential for risk assessment strategies to investigate the potential interactions in mixtures and also which of the pollutants in the mixtures may be the main drivers of the observed biological effects. Thus, an evaluation of the individual and combined toxicity of pharmaceuticals towards the organisms will be performed and main toxicity drivers in a complex mixture will be identified.

Bioassays to evaluate the effect of pollutants on living beings may evaluate pollutant exposure and/or toxicity. Bioassays based on biomarkers of exposure can provide information on perception by cells/organisms of certain pollutants, route of action, and sometimes, even the source of exposure. A challenge for biomarkers is the ability to relate the presence of pollutants in the environment with a valid prediction of a subsequent hazard to the cell/organism. Intracellular free Ca^{2+}, $[Ca^{2+}]_i$, is a second messenger known to be involved in the perception and signaling of many abiotic stresses, including pollution. The validity of $[Ca^{2+}]_i$ as an intracellular biomarker of exposure to selected EPs applied both singly and combined will be evaluated as well as the role of Ca^{2+} in the global cellular response to a model EPs.

Specific objectives:

1. To evaluate the response of cyanobacteria and green algae to selected EPs applied both singly and combined. Study of the potential interactions of EPs in mixture toxicity assays.

2. To identify which pollutants are the main drivers of toxicity in multi-pollutant mixtures. For this purpose, Global Sensitivity and Uncertainty Analysis (GSUA) will be used.

3. To evaluate the use of $[Ca^{2+}]_i$ as an early biomarker of exposure in cyanobacteria to selected EPs applied both singly and combined in mixtures; and to analyze whether the recorded Ca^{2+} signals induced by mixtures may determine the nature of the interaction between EPs in the mixture, whether synergistic or antagonistic, well before toxicity is evident.

4. To analyze the role of $[Ca^{2+}]_i$ in the cellular response of the green alga *Chlamydomonas reinhardtii* to the model EPs Triclosan. A mechanistic study will be undertaken combining flow cytometry protocols, physiological analysis as well as gene expression analysis.

CHAPTER 2: TOXICITY OF FIVE ANTIBIOTICS AND THEIR MIXTURES TOWARDS PHOTOSYNTHETIC AQUATIC ORGANISMS: IMPLICATIONS FOR ENVIRONMENTAL RISK ASSESSMENT

2.1 INTRODUCTION

Antibiotics are biologically active molecules with an increasing use in both human and veterinary medicine. These pharmaceuticals play a major role in livestock industries and modern agriculture, which use them as therapeutics and growth promoters in livestock production, as feed additives in fish farms and to prevent crop damage induced by bacteria (Sarmah et al. 2006); although since 2006 antibiotics have been forbidden as growth promoters in animal feed in the EU. From the antibiotics administered to animals, a large proportion is excreted without metabolizing and is dispersed with the manure used for soil amendment, eventually reaching surface waters (Elmund et al. 1971). A large portion of the antibiotics administered in fish farms (70-80%) has been reported to reach the environment (Schneider 1994; Hektoen et al. 1995).

The major pathway whereby residual antibiotics from human use enter the environment is the effluent of wastewater treatment plants (WWTP) as conventional plants are relatively inefficient in completely removing pharmaceuticals (McArdell et al. 2003; Göbel et al. 2005; Xu et al. 2007; Rosal et al. 2010b). Antibiotic contamination of the natural environment has been reported in many countries in Europe, North America and Asia, all classes of antibiotics having been detected in river water (Kolpin et al. 2002; Kolpin et al. 2004; Batt et al. 2006; Xu et al. 2007; Yang et al. 2008; Ginebreda et al. 2009; Tamtam et al. 2009; Watkinson et al. 2009), seawater (Gulkowska et al. 2007; Xu et al. 2007), groundwater (Hirsch et al. 1999; Lindsey et al. 2001; Sacher et al. 2001), drinking water (Zuccato et al. 2000), sediments (Kerry et al. 1996; Kim and Carlson 2007), agricultural soils due to dispersion of sewage sludge and manure (Sarmah et al. 2006), biota (Dolliver et al. 2007; Kong et al. 2007) ,and WWTP effluents (Costanzo et al. 2005; Batt et al. 2006; Watkinson et al. 2009; Gros et al. 2010; Rosal et al. 2010b). Although recorded environmental levels are usually low, at ng L^{-1} to µg L^{-1} in waters (see Table S2.1 under Supplementary Information) and µg kg^{-1} to mg kg^{-1} in soils and sediments, antibiotics are considered to be “pseudopersistant” contaminants due to their continued release into the environment and permanent presence (Daughton and Ternes 1999; Hernando et al. 2006).

Although the major concern of antibiotics is associated with the development of resistance mechanisms by bacteria and its implications in human health, their sustained release to different environmental compartments and their bioactive properties also raise serious concerns about the toxicity of antibiotics to non-target organisms (Migliore et al. 1997; Halling-Sørensen et al. 1998; Baguer et al. 2000; Halling-Sørensen et al. 2000). Algae and cyanobacteria play a crucial role in aquatic ecosystems. They are primary producers which supply nutrients for the rest of the aquatic biota (Greenberg et al. 1992). Cyanobacteria, in addition, are prokaryotes and are thus considered as sensitive organisms to antibiotics (Maul et al. 2006). In fact, the European Medicines Evaluation Agency (EMEA) explicitly recommends the use of cyanobacteria for effect testing of antimicrobials due to their sensitivity (EMEA 2006).

Different classes of antibiotics have been detected simultaneously in environmental compartments (Kolpin et al. 2004; Li et al. 2009; Watkinson et al. 2009; Suzuki and Hoa 2012). Therefore, aquatic organisms may be exposed to mixtures of antibiotics. While the individual concentrations of antibiotics in aquatic environments may be low, the combined concentrations could result in significant toxicity to aquatic organisms. Besides, as chemicals in a mixture may either not interact or interact synergistically or antagonistically, it is essential to investigate the potential interactions in mixtures of antibiotics of different classes (Cleuvers 2003; Teuschler 2007; Rodea-Palomares et al. 2010). This issue has important implications in terms of environmental toxicity and risk assessment strategies, which are often carried out considering the individual effect and additive behaviour. This may severely underestimate the risk associated with antibiotic mixtures as well as mixtures of antibiotics with other pharmaceuticals and anthropogenic contaminants (Kolpin et al. 2002).

The aim of the present study was to evaluate the individual and combined toxicity to the green alga *Pseudokirchneriella subcapitata* and the recombinant bioluminescent filamentous cyanobacterium *Anabaena* CPB4337 of five antibiotics from different classes: amoxicillin (β-lactam), erythromycin (macrolide), tetracycline (tetracycline) and the quinolones norfloxacin and levofloxacin. All of them have a variety of uses in human and veterinary medicine (Table S2.1). In order to identify and quantify the nature of the interactions between the antibiotics, binary and multicomponent mixtures of them were prepared and tested. Results were analyzed by the method of the

combination index (CI)-isobologram equation which we have previously used to study pollutant interactions (Rodea-Palomares et al. 2010; Rosal et al. 2010a; Boltes et al. 2012; Rodea-Palomares et al. 2012). In this paper, we also report a first approach of risk assessment of the antibiotic mixtures for the aquatic environment based on currently available exposure data (Table S2.1) and our toxicity results.

2.2 MATERIALS AND METHODS

2.2.1 Chemicals

The antibiotics used in this study belong to different classes and were selected based on their use and occurrence in the aquatic environment (Table S2.1). The following five antibiotics were selected: amoxicillin (AMO), erythromycin (ERY) and levofloxacin (LEV), purchased from TCI Chemicals; tetracycline (TET) purchased from Sigma-Aldrich; and norfloxacin (NOR) purchased from Fluka. Amoxicillin is a β-lactam with a bactericidal action, it inhibits bacterial cell-wall synthesis. Erythromycin is a macrolide which exerts its antibiotic effects by binding irreversibly to the 50S subunit of bacterial ribosome interfering with bacterial protein synthesis. Tetracycline also inhibits bacterial protein synthesis by preventing the association of aminoacyl-tRNA with the bacterial ribosome. Norfloxacin and levofloxacin are quinolones, which inhibit bacterial DNA gyrase, preventing DNA replication.

The purity of each antibiotic was AMO ≥ 90%, ERY ≥ 98%, LEV ≥ 98%, TET ≥ 98%, NOR ≥ 98%. Except ERY, which was dissolved in methanol, stock solutions of antibiotics were made in high purity water obtained from a Milipore Mili-Q system with a resistivity of at least 18MΩ cm at 25ºC. The antibiotics were stored in the dark and 4 ºC. The dilutions of each antibiotic and their corresponding mixtures were freshly prepared before each experiment with a careful monitoring of solution pH. It was ensured that pH did not change significantly during the experiments. For the case of ERY, the final concentration of methanol in the assay media was always below 0.005% (v/v), which did not result in any significant effect on the bioluminescence of *Anabaena* CPB4337 or the growth rate of *Pseudokirchneriella subcapitata.*

2.2.2 Stability of antibiotics

Initial concentrations and stability of antibiotics under bioassay conditions were examined according to the (OECD 2008) guidance. Analyses have been performed in assay media both in the absence of cells and in the presence of either the cyanobacterium or the green alga in a course-time study up to 72-h exposure. The stability assessment was performed using HPLC-diode array liquid chromatography and TSQ Quantum LC-MS triple quadrupole as follows. HPLC analyses were used to

determine the exposure concentration of TET, LEV and NOR and were performed using a HPLC Agilent Technologies equipped with a diode array detector. The column used was a reversed phase Kromasil 5u 100A C18 analytical column. The mobile phase was a mixture of acetonitrile and acidified water with H_3PO_4 (20:80), adjusted to pH 3 with NaOH 2 M. UV detection was as follows: LEV, 272 nm, NOR and TET, 292 nm. LC-MS QqQ was used to determine the exposure concentration of ERY using an Ascentis express C18 5 cm x 2.1 mm x 2.7 um analytical column. The mobile phase was acetonitrile and water acidified with 0.1% formic acid (50:50).

No significant differences were found between the nominal and measured exposure concentrations for ERY, NOR and LEV either in the presence or absence of the green alga and the cyanobacterium. Therefore, throughout the present study, their nominal concentrations were used for data analyses. AMO was previously reported to be highly unstable in aqueous solutions due to hydrolysis involving the opening of the β-lactam ring (Perez-Parada et al. 2011). Immediately after being put in solution, within a period of minutes, AMO degraded completely and for that reason we used the nominal concentration. This behavior has already been observed by others (Pérez-Parada et al., 2011). The hydrolysis probably produced a set of intermediary products that are not characterized but might also be toxic to aquatic organisms. For TET, compared to the nominal value, and expressed as percentage, the average measured concentrations (in abiotic conditions) were 53.6, 28.6 and 14.3 after 24, 48 and 72 h, respectively. The exposure concentrations were calculated as follows:

$$D^{TET} = \int_0^{72h} c_{TET}\, dt \qquad (2.1)$$

In what follow, D^{TET} was used instead of nominal concentrations, C_{TET}, according to the OECD guidance (OECD 2008). The integral of Eq. 2.1 was solved using a numerical approximation fed with C_{TET} values recorded every 24 h.

2.2.3 Toxicity bioassays

The antibiotic concentrations tested ranged from 0.01 to 1500 mg/L for AMO; 0.01 to 100 mg/L for NOR; 0.01 to 200 mg/L for LEV; 0.01 to 100 mg/L for TET and 0.001 to 10 mg/L for ERY.

Anabaena sp. PCC 7120 strain CPB4337 (hereinafter *Anabaena* CPB4337), which bears in the chromosome a Tn5 derivative with *luxCDABE* from the luminescent terrestrial bacterium *Photorhabdus luminescens* (formerly *Xenorhabdus luminescens*), was used in this study as a bioreporter of antibiotic toxicity. This strain shows a high constitutive self-luminescence with no need to add exogenous aldehyde (Fernandez-Pinas and Wolk 1994). The toxicity bioassays using *Anabaena* CPB4337 are based on the inhibition of constitutive luminescence caused by the presence of a toxic substance; this endpoint is related to metabolic activity of the organism as toxicants affecting the metabolism of the bacterium reduce luminescence. *Anabaena* CPB4337 was routinely grown at 28ºC in the light, ca. 65 µmol photons m^2 s^{-1} on a rotary shaker in 150mL AA/8 (Allen and Arnon 1955) (Table S2.2), supplemented with nitrate (5mM) (hereinafter AA/8 + N) in 250 ml Erlenmeyer flask for 3 days. The strain was grown in liquid cultures with 10 µg/mL of neomycin sulfate (Nm). Toxicity assays were performed as follows: cyanobacterial cultures grown as described were centrifuged, washed twice and resuspended in fresh medium at OD_{750nm} = 2.5. 640 µL of the corresponding antibiotic solution were added to transparent sterile 24-well microtiter plates, followed by 160 µL of 5-fold concentrated AA/8 + N and 200 µL of *Anabaena* CPB4337, prepared as described, were added to the wells to reach a final OD_{750nm} = 0.5. The 24-well microtitter plates were kept at room temperature (28ºC) and light ca. 65 µmol photons m^2 s^{-1} on a rotary shaker during 72 h of exposure. For luminescence measurements, 100 µL of each sample were transferred to an opaque white 96-well microtiter plate. Luminescence was recorded in a Centro LB 960 luminometer during 10 min. Three independent experiments with quadruplicate samples were carried out for all *Anabaena* toxicity assays. Copper sulfate ($CuSO_4$) was selected as reference toxicant for calibration in all assays. The calibration allows one to calculate the mean EC_{50} values (the median effective antibiotic concentration that causes a 50% effect with respect to a non-treated control) of copper in order to refuse or accept the experiment if those EC_{50} values fall in or out of the 95% of confidence limits previously fixed for this reference toxicant (USEPA 1994; 2002). To achieve this, five copper dilutions were tested by quadruplicate in control wells of each assay.

Algal beads of *P. subcapitata* and growing media (Table S2.3) were purchased from MicroBioTest Inc. (Belgium). The determination of multigenerational exposure toxicity was performed following the algal growth inhibition test described in OECD TG 201

open system (OECD 2006). The de-immobilization of algal cells was conducted according to the manufacturer's recommendations. Algal cells were first cultured in 25 mL shaken flasks in which growth was assessed by following optical density at 670 nm. The prescribed amount of cells (final cellular density of 0.1) was then transferred to 96-well clear disposable microplates and was exposed to pollutants during the logarithmic growth phase. The total volume occupied was 200 uL. *P. subcapitata* growth was monitored for 72 h, measuring chlorophyll fluorescence, which excitation/emission wavelengths are 450/672 nm, in a Fluoroskan Ascent EL (Thermo Scientific) microplate reader. Plates were incubated in a growing chamber at 22 ± 2ºC under continuous light. Each concentration was replicated four times in three independent series of assays.

2.2.4 Experimental design of antibiotic mixtures

Solutions of antibiotics were used singly and in binary and 4- or 5-antibiotic mixtures. Algal and cyanobacterial cells were treated with serial dilutions of each chemical individually and in combinations prepared with a fixed constant ratio (1:1) based on the individual EC_{50} values (mg/L). Five to seven dilutions (serial dilution factor = 2) of each antibiotic and combination plus one control were tested in three independent experiments with quadruplicate samples as described elsewhere (Rodea-Palomares et al. 2010).

2.2.5 Median-Effect and combination index (CI)-isobologram equations for determining individual and combined toxicities

The response to toxic exposure in *Anabaena* CPB4337 and in *Pseudokirchneriella subcapitata* tests was estimated using the median-effect equation based on the mass action law, (Chou and Talalay 1984):

$$\frac{f_a}{f_u} = \left(\frac{D}{D_m} \right)^m \qquad (2.2)$$

Where D is the dose, D_m is the dose for 50% effect (EC_{50}), f_a is the fraction affected by dose D (e.g., 0.75 if cell bioluminescence/growth is inhibited by 75%), fu is the

unaffected fraction (therefore, $f_a = 1\text{-}f_u$), and m is the coefficient of the sigmoidicity of the dose-effect curve: $m = 1$, $m > 1$, and $m < 1$ indicate hyperbolic, sigmoidal, and flat sigmoidal dose-effect curve, respectively. Therefore, the method takes into account both the potency (D_m) and shape (m) parameters. Eq. 2.2 may be rearranged as follows:

$$D = D_m \left(\frac{f_a}{1 - f_a} \right)^{\frac{1}{m}} \tag{2.3}$$

The D_m and m values for each individual compound or mixture were determined by the median-effect plot: x = log (D) versus y = log (f_a/f_u) which is based on the logarithmic form of Eq. 2.2. In the median-effect plot, m is the slope and $D_m = 10^{-(\text{y-intercept})/\text{m}}$. The conformity of the data to the median-effect principle can be ready assessed by the linear correlation coefficient (r) of the fitting to Eq. 2.3 (Chou 2006).

These parameters were then used to calculate doses of individual compound and their mixtures required to produce various effect levels according to Eq 2. For each effect level, combination index (CI) values were then calculated according to the general combination index equation for n-chemical combination at x% inhibition (Chou 2006):

$${}^{n}(CI)_x = \sum_{j=1}^{n} \frac{(D)_j}{(D_x)_j} = \sum_{j=1}^{n} \frac{(D_x)_{1-n} \left\{ \dfrac{[D]_j}{\sum_{1}^{n}[D]} \right\}}{(D_m)_j \left\{ \dfrac{(f_{ax})_j}{\left[1-(f_{ax})_j\right]} \right\}^{1/mj}} \tag{2.4}$$

where ${}^{n}(\text{CI})_x$ is the combination index for n chemicals at x% inhibition; $(\text{D}_x)_{1\text{-}n}$ is the sum of the dose of n chemicals that exerts x% inhibition in combination, $\{[D_j]/\sum_1^n[D]\}$ is the proportionality of the dose of each of n chemicals that exerts x% inhibition in

combination; and $(D_m)_j \{(f_{ax})_j/[1-(f_{ax})_j]\}^{1/mj}$ is the dose of each drug alone that exerts *x*% inhibition. From Eq. 2.4, CI < 1, CI = 1 and CI > 1 indicates synergism, additive effect and antagonism, respectively.

2.2.6 Analysis of results

A non-linear fitting was performed to derive individual and mixture dose-effect parameters using the Levenberg-Marquardt algorithm to Eq. 2.2. To compute EC_{10} (the median effective antibiotic concentration that causes a 10% effect with respect to a non-treated control) and EC_{20} (the median effective antibiotic concentration that causes a 20% effect with respect to a non-treated control) in *P. subcapitata* assays for which the inhibition did not reach the median effect value (D_m in Eq. 2.2), a reparametrization was deemed necessary to reduce multicollinearity. For it, we substituted D_m in Eqs 2 and 3 by EC_{20} or EC_{10} in the following modified forms of Eq. 2.2:

$$\frac{f_a}{f_u} = \frac{1}{9}\left(\frac{D}{EC_{10}}\right)^m \tag{2.5}$$

$$\frac{f_a}{f_u} = \frac{1}{4}\left(\frac{D}{EC_{20}}\right)^m \tag{2.6}$$

This procedure allowed reaching efficient non-linear regression with adequate standard deviations for the estimators. The calculation of EC_{50} (the median effective antibiotic concentration that causes a 50% effect with respect to a non-treated control) for *P. subcapitata* exposed to TET, the data for which lie outside the range of validity of the median effect equation (Eq. 2.2), was performed using a linear interpolation method that did not assume any particular dose–effect model (USEPA 2002). Not special transformations or reparametrization of Eq. 2.2 were needed for estimation of dose-effect relationship parameters for *Anabaena* CPB4337 since whole dose-effect curves were obtained for the tested antibiotics and their mixtures.T he computer program CompuSyn (Chou 2005) was used for calculation of the EC_x (the median effective antibiotic concentrations that cause x% effect with respect to a non-treated control) and combination Index values (CI) of the different mixtures in the whole range of effect levels.

2.2.7 Mixture toxicity predictions based on CA, IA and CI equations

Experimental toxicity of the antibiotic mixtures were computed based on the predictive equations of the two most widely used definitions of additivity, that is, Concentration Addition (CA) (equation 5) and Independent Action (IA) (equation 6). (Faust et al. 2001; Altenburger et al. 2004). CA is based on the assumption that mixture components have the same sites and similar mode of action (MOA), and is computed by equation (Altenburger et al. 2004):

$$ECx_{mix} = \left(\sum_i^n \frac{p_i}{EC_{xi}}\right)^{-1} \quad (2.7)$$

Where ECx_{mix} is the effect concentration of the mixture provoking x% effect, EC_{xi} is the concentration of the component *i* provoking the same effect (x%) as the mixture when applied individually, and p_i is the molar ratio of the *i*th component in the mixture.

IA is based on the assumption that mixture components have dissimilar MOA. The following equation applies for IA (Altenburger et al. 2004).

$$E(c_{mix}) = 1 - \prod_{i=1}^{n}\left(1 - E(c_i)\right) \quad (2.8)$$

Where c_{mix} and $E(c_{mix})$ are the total concentration and total effect of the mixture, respectively, and $E(c_i)$ is the effect of the *ith* component with the concentration c_i in the mixture. The c_i in Eq. (2.6) can be replaced by (p_i *x* c_{mix}). The $E(c_i)$ can be calculated from the function that described the concentration-response curve of the ith component (Altenburger et al. 2004; Qin et al. 2010).

The predictive equation based on CI (that is considering deviations from additivity as CI values) was computed as follows:

$$ECx_{mix} = \left(\sum_i^n \frac{p_i}{EC_{xi} \times CI_{x\ comp}}\right)^{-1} \quad (2.9)$$

Where ECx_{mix} is the effect concentration of the mixture provoking x% effect, EC_{xi} is the concentration of the component *i* provoking the same effect (x%) as the mixture when applied individually, p_i is the molar ratio of the *i*th component in the mixture and CI_x *comp* is the computed Combination Index value for the mixture at the x level of effect (x% or *fa*) from the experimental toxicity curve of the mixture. Note that equation 9 is easily derived from Equation 7 since CI and CA methods share the same definition of additivity (Loewe additivity) (Chou 2006).

2.2.8 Risk quotients assessment of antibiotic mixtures

Risk quotients (RQs) try to estimate the actual potential ecological risk (probability of an expected effect, i.e. potential danger, caused by an environmental concentration) of a pollutant. This quotient is calculated as the ratio between Predicted Environmental Concentrations (PEC) or Measured Environmental Concentrations (MEC) and Predicted No Effect Concentrations (PNEC) (Sanderson et al. 2003; Von der Ohe et al. 2011).

The lowest predicted no effect concentrations (PNEC) for single compounds and mixtures were combined with the highest available measured environmental concentrations (MEC) from the literature (Table S2.1). Risk quotients (RQ) were then estimated as follows (Sanderson et al. 2003; Von der Ohe et al. 2011):

$$RQ = \frac{MEC}{PNEC} \qquad (2.10)$$

A PNEC value for a given antibiotic mixture was derived dividing the EC_{50} values by an assessment factor of 1000 (Sanderson et al. 2003; EMEA 2006; Von der Ohe et al. 2011). Highest MEC values (Table S2.1) converted to µmol/L were summed up to give a corresponding mixture concentration. RQ higher than one suggests that an ecological impact is expected for the given antibiotic mixture.

2.3 RESULTS AND DISCUSSION

2.3.1 Toxicity of individual antibiotics

Table 2.1 shows EC_{10}, EC_{20} and EC_{50} values of the five antibiotics tested individually and in binary and complex mixtures. After an exposure of 72 h to AMO, the green alga *P. subcapitata* showed no effect at concentrations up to 1500 mg/L (less than 10% growth inhibition), indicating that this antibiotic was not toxic to the green alga.

Table 2.1 Dose-effect parameters and main Combination Index (CI) values of: amoxicillin (AMO), erythromycin (ERY), levofloxacin (LEV), norfloxacin (NOR) and tetracycline (TET); individually and of their binary and multi-component combinations for *Pseudokirckneriella subcapitata* and *Anabaena sp.* CPB4337 tests.

	Pseudokirckneriella subcapitata						*Anabaena sp.* CPB4337					
	Dose-effect parameters (mg/L)			CI Values			Dose-effect parameters (mg/L)			CI Values		
	EC_{10}	EC_{20}	EC_{50}	f_a = 0.10	f_a = 0.20	f_a = 0.50	EC_{10}	EC_{20}	EC_{50}	f_a = 0.10	f_a = 0.20	f_a = 0.50
AMO	> 1500	> 1500	>1500	-	-	-	6.16 ± 3.5	15.1± 3.2	56.3 ± 2.5	-	-	-
ERY	0.036 ± 0.016	0.082 ± 0.023	0.35 ± 0.03	-	-	-	0.005 ± 0.004	0.009± 0.003	0.022 ± 0.003	-	-	-
LEV	0.93 ± 0.30	4.5 ± 0.6	> 120[c]	-	-	-	1.1 ± 0.4	1.9 ± 0.4	4.8 ± 0.4	-	-	-
NOR	10.9 ± 1.2	20.6 ± 1.0	> 80[d]	-	-	-	1.2 ± 0.5	2.1 ± 0.6	5.6 ± 0.5	-	-	-
TET	0.032 ± 0.008	0.10 ± 0.01	3.31 ± 0.96	-	-	-	2.5 ±0.7	3.5 ± 0.7	6.2 ± 0.8	-	-	-
ERY+LEV	1.3 ± 0.3	23 ± 0.3	> 20.4[e]	2.5	1.2	0.42	0.87 ± 0.3	1.3 ± 0.3	2.5 ± 0.2	1.4	1.2	0.95
ERY+NOR	3.0 ± 0.6	5.8 ± 0.7	18.2 ± 1.5	0.82	0.70	0.54	0.96 ± 0.5	1.7 ± 0.6	4.5 ± 0.7	1.1	1.2	1.2
ERY+TET	0.0046 ± 0.0024	0.021 ± 0.007	0.27 ± 0.04	0.33	0.40	0.60	0.28 ±0.11	0.67 ±0.13	3 ± 0.3	0.23	0.36	0.79
LEV+NOR	1.1 ± 0.4	2.9 ± 0.7	15.0 ± 1.3	0.28	0.24	0.25	1.3 ± 0.5	2.0 ± 0.5	4.3 ± 0.4	1.1	0.98	0.8
LEV+TET	0.34 ± 0.10	0.89 ± 0.14	4.6 ± 0.5	0.84	0.52	0.24	0.37 ± 0.12	0.63 ± 0.24	1.6 ± 0.3	0.21	0.24	0.28
NOR+TET	1.9 ± 0.5	3.5 ± 0.3	9.2 ± 0.9	1.2	0.59	0.22	1.9 ± 0.4	2.7 ± 0.4	5.1 ± 0.5	1.2	1	0.87
4 AB[a]	1.7 ± 0.4	3.9 ± 0.5	16.0 ± 2.0	1.1	0.69	0.37	-	-	.	-	-	-
AMO+ERY	-	-	-	-	-	-	9.4 ± 5.2	16.2 ± 5.5	41 ± 3.5	2	1.4	1
AMO+NOR	-	-	-	-	-	-	8.9 ± 4.0	14.5 ± 4.1	33.1 ± 3.3	2	1.5	1
AMO+LEV	-	-	-	-	-	-	7.7 ± 2.3	11.4± 2.1	22.4 ± 1.5	1.5	1	0.5
AMO+TET	-	-	-	-	-	-	1.8 ± 0.6	2.9 ± 0.5	6.5 ± 0.5	0.33	0.25	0.2
5 AB[b]	-	-	-	-	-	-	5.2 ± 1.2	7.2 ± 0.8	12. 4± 0.8	1.5	1.1	0.7

[a] ERY+ LEV+ NOR+TET; [b] ERY+ LEV+ NOR+TET+AMO; [c] *fa* = 0.42 at 120 mg/L; [d] *fa* = 0.39 at 80 mg/L; [e] *fa* = 0.488 at 20.4 mg/L (20.0 mg LEV/L, 0.4 mg ERY/L)

For ERY, a clear concentration-response relationship was obtained and demonstrated to be highly toxic with an EC_{50}= 0.35 ± 0.03 mg/L and a very low EC_{10}, in the range of µg/L. In the case of the quinolones, NOR and LEV displayed flat and incomplete concentration-response curves (Fig. 2.1).

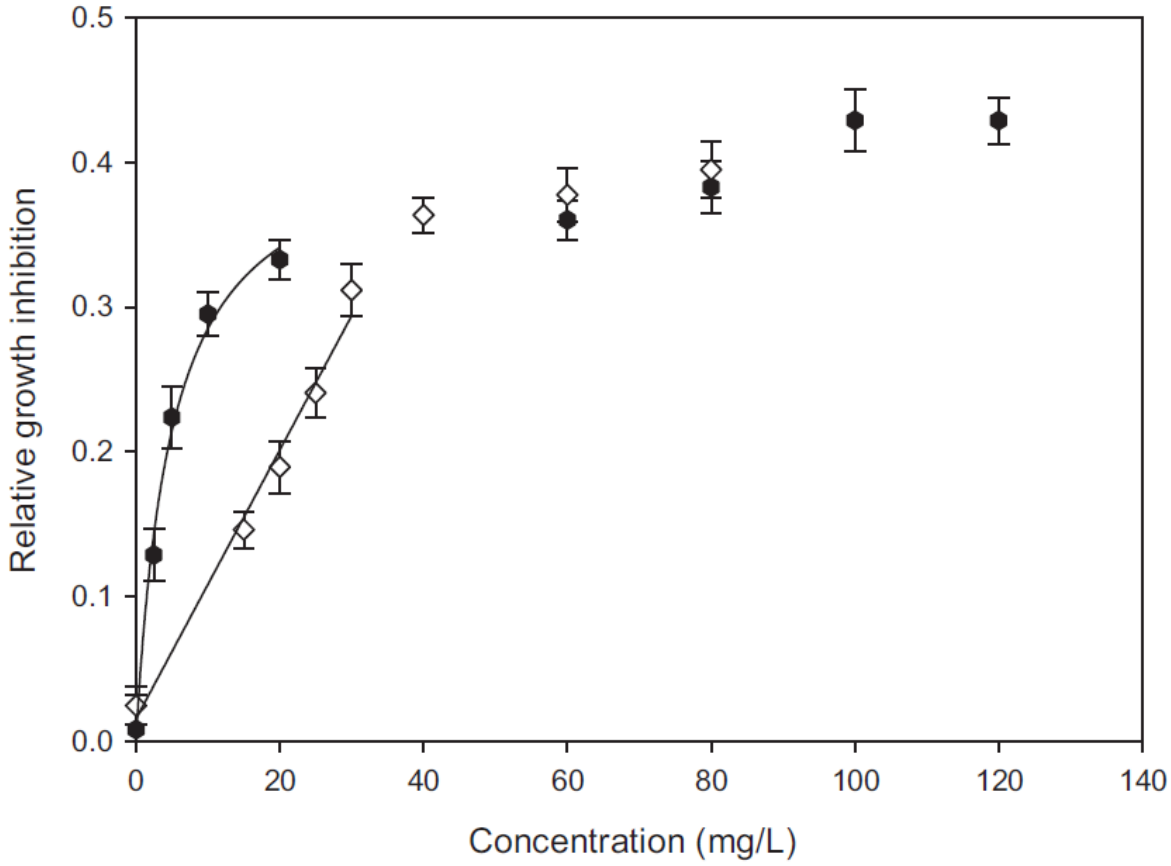

Figure 2.1 Incomplete dose-response curves of antibiotics for *Pseudokirchneriella subcapitata*. Dose-response curves of levofloxacin (◇) and norfloxacin (⬢) for *Pseudokirchneriella subcapitata*. Solid lines represent the fitting to the median effect equation. Error bars correspond to 95% confidence intervals.

This represents a plateau with respect to cell growth rate, the reduction of which did not progressed for drug dosage above 40 mg/L approximately. The reason for this behavior is more probably due to the role played by antibiotic transporters which regulate the influx, efflux and intracellular concentration of antibiotics (Van Bambeke et al. 2003b). In both cases, the fitting to the dose-effect equations was performed only for the lower effect levels. The data shown in Table 2.1 correspond to the fitting of the lower exposures and were calculated using Eqs. 5 and 6. Based on EC_{10} and EC_{20} values, LEV was more toxic than NOR to the green alga; however, EC_{50} was > 80 mg/L for NOR

and > 120 mg/L for LEV. TET proved very toxic for the green alga with a exposure concentration (D^{TET} as indicated in Eq. 2.1) as low as 32 ± 8 µg/L producing a measurable effect (EC_{10}); EC_{50} for TET, calculated as indicated before, was 3.31 ± 0.96 mg/L.

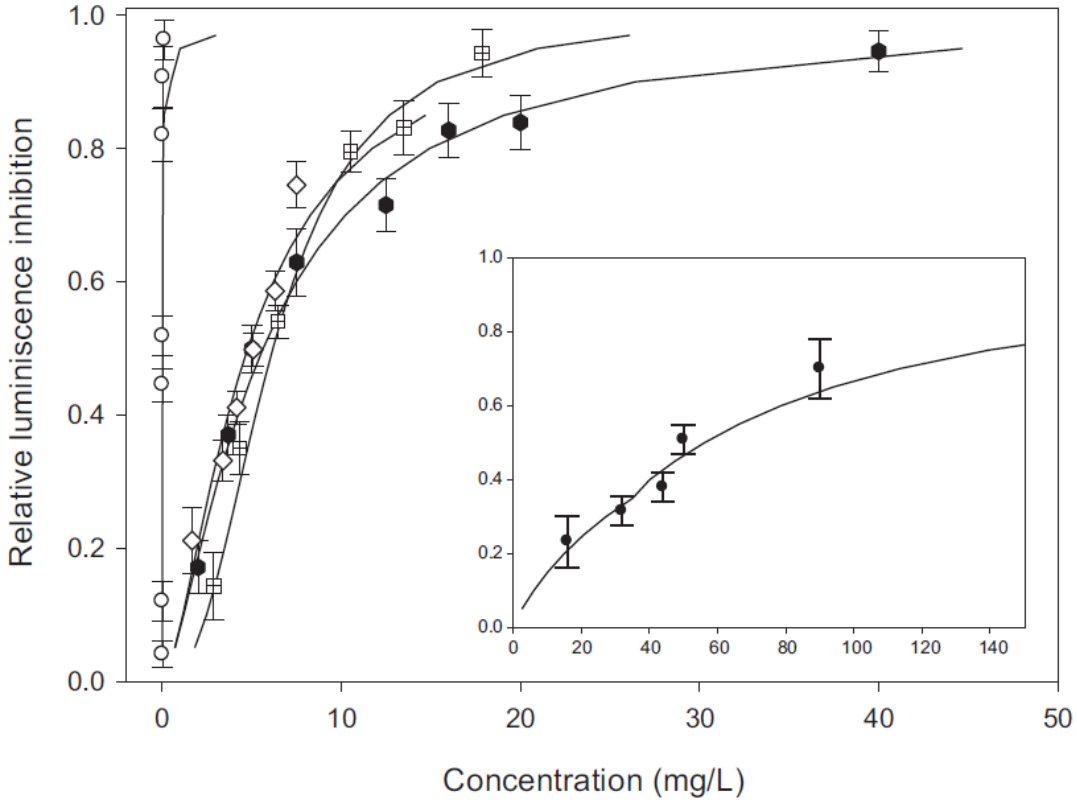

Figure 2.2 Dose-response curves of antibiotics for *Anabaena* CPB4337**.** Dose-response curves of amoxicillin (●; inset), norfloxacin (⬢), levofloxacin (◇), tetracycline (⊞) and erythromycin (○) for *Anabaena* CPB4337. Solid lines represent the fitting to the median effect equation.

With regards to the cyanobacterium, complete concentration-response relationships could be recorded for the 5 tested antibiotics after an exposure of 72 h (Fig. 2.2). The EC_{50} values ranged between 0.022 mg/L and 56.3 mg/L with an order of toxicity as follows: ERY > LEV > NOR > TET > AMO. It should be noticed that, like in the case of the green alga, ERY showed a measurable effect at a concentration as low as 5 µg/L (EC_{10}). The results indicated that the cyanobacterium, most probably due to its prokaryotic nature, is in general, more sensitive than the green alga to the tested antibiotics. Several other researchers found similar results with unicellular cyanobacteria and green algae (Harrass et al. 1985; Lutzhoft et al. 1999; Halling-Sørensen et al. 2000). Although the green alga is a non-target organism for

antimicrobials, the observed toxicity exerted by some antibiotics could be, at least in part, due to the cyanobacterial nature of the chloroplasts which makes these plastids susceptible as potential antibiotic targets (McFadden and Roos 1999); the antiplastidic effects of several antibiotics has been quantified at concentrations well above 1 mg/L (Ebringer 1972; Nicolas 1981). Furthermore, an effect on mitochondria might also account for part of the observed toxic effect in the green alga.

From the tested antibiotics, ERY for both the alga and the cyanobacterium, could be classified as "very toxic to the aquatic life" (Regulation EC No. 1272/2008 on classification, labelling and packaging of substances and mixtures, Category I, EC_{50} < 1 mg/L). In fact, this antibiotic shows measurable effects in both organisms at concentrations in the µg/L, close to measured environmental concentrations (see Table S2.1).

Most authors have found that β-lactams antibiotics such as AMO do not affect green algae (Lutzhoft et al. 1999; Halling-Sørensen et al. 2000; Eguchi et al. 2004), most probably due to the mode of action of this antibiotic which specifically inhibits bacterial cell wall synthesis. Studies on ERY toxicity to the aquatic environments report EC_{50} values ranging between 0.02 mg/L for green algae (Eguchi et al. 2004; Isidori et al. 2005); similar to the one found for the cyanobacterium in this report), and 1000 mg/L for the fish *Danio rerio* with EC_{50} values around 20 mg/L for rotifers, crustacean and invertebrates (Isidori et al. 2004). For LEV, an EC_{50} (after 7-days of exposure) of 7.9 mg/L was reported for the unicellular cyanobacterium *Microcystis aeruginosa* (Robinson et al. 2005), which is slightly higher than the one found for *Anabaena* in this study. A similar value was also reported for the green alga *P. subcapitata* (Robinson et al. 2005). In this report, a much higher øEC_{50} was obtained for LEV in the same alga (> 80 mg/L). There are not many published data on NOR toxicity; an EC_{50} value of 22 µg/L has been reported for the marine bacterium *Vibrio fischeri* (Backhaus et al. 2000) and EC_{50} values of 16.6 mg/L and 10.4 have been reported for the green algae *P. subcapitata* and *Chlorella vulgaris*, respectively (Eguchi et al. 2004). Again, these are significantly lower than those reported here. For TET, EC_{50} values of 0.09 mg/L and 2.2 mg/L have been found for the unicellular cyanobacterium *M. aeruginosa* and the green alga *P. subcapitata*, respectively (Halling-Sørensen et al. 2000), which, for the cyanobacterium, is lower than the one reported in this study.

From the results in previous reports (Halling-Sørensen et al. 2000; Robinson et al. 2005) except for LEV, the unicellular cyanobacterium *M. aeruginosa* appears to be more sensitive to antibiotics than the filamentous *Anabaena* CPB4337, although due to the scarcity of data, more research is needed. However, it should be noted that both the exposure time (7 days for the unicellular vs. 3 days for *Anabaena*) and the toxicity endpoint (growth vs. bioluminescence) were different. In the case of the green alga, the observed discrepancies between our results and those published could be due to the different endpoints used to measure growth which might influence the outcome; we used chlorophyll fluorescence while Eguchi et al. (2005) and Isidori et al. (2005) used cell counts; besides, in the case of the quinolones it could also be due to the flat and incomplete dose-response curves obtained for both quinolones in this work; nevertheless, quite discrepant results have also been reported for LEV toxicity to *Lemna* species with EC_{50} ranging from 0.8 mg/L to 51 mg/L after 7 days of exposure measuring different endpoints such as frond number, growth rate or pigment content (Brain et al. 2004; Robinson et al. 2005).

2.3.2 Toxicological interactions of the tested antibiotics in mixtures

Table 2.1 shows the effective concentrations EC_{10}, EC_{20} and EC_{50} as well as predicted CI values at these effect levels of binary, 4-antibiotic (for the green alga, as AMO was not toxic, it was not included in the mixture assays) and 5-antibiotic (for the cyanobacterium) mixtures. As shown in the table, the binary mixture ERY-TET displayed a considerable toxic effect, particularly for the green alga and at environmentally relevant concentrations (Table S2.1). In fact, in binary as well as in multi-antibiotic mixtures, ERY and to a lesser extent TET, were assayed at near environmental concentrations (see Table S2.1, also Table S2.4 for information of individual concentrations of antibiotics in the mixture effective concentrations). The data show that both antibiotics, when present in mixtures, may exhibit a toxic effect even at very low concentrations.

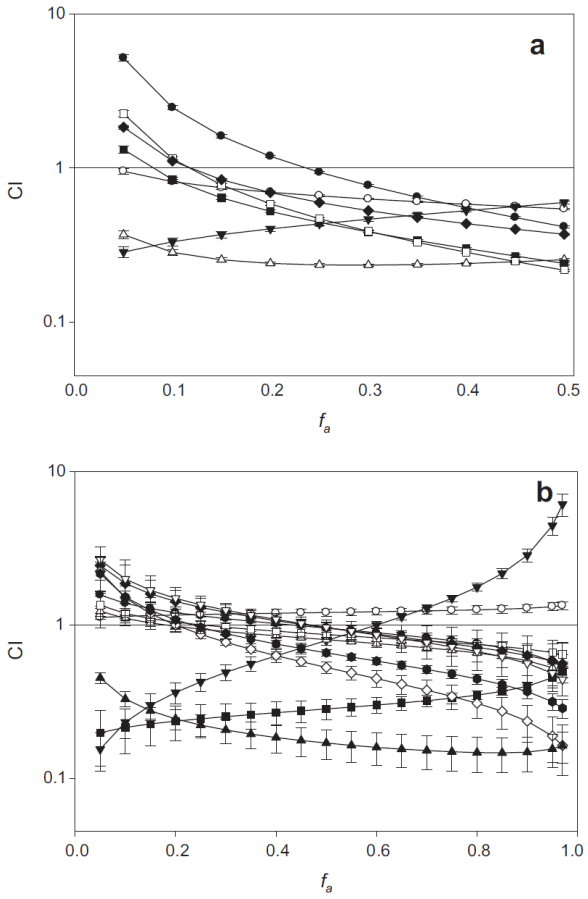

Figure 2.3. Combination index Plot (f_a- *CI plot*) for binary and multi-antibiotic mixtures for *Pseudokirchneriella subcapitata* test (a) and *Anabaena* CPB4337 test (b): ERY+LEV (—●—), ERY+NOR (—○—), ERY+TET (—▼—), LEV+NOR (—△—), LEV+TET (—■—), NOR+TET (—□—), AMO+ERY (—◇—), AMO+LEV (—⬢—), AMO+TET (—▽—), AMO+NOR (—▲—), ERY+LEV+NOR+TET (—◆—), ERY+LEV+NOR+TET+AMO (—◆—). CI values are plotted as a function of the fractional inhibition of bioluminescence/growth (f_a) by computer simulation (CompuSyn). CI< 1, = 1 and > 1 indicates synergism, additive effect and antagonism, respectively. At least three independent experiments with two replicates were used. The vertical bars indicate 95% confidence intervals for CI values based on SDA (Sequential Deletion Analysis) (Chou and Martin, 2005). AMO = Amoxicillin; TET = Tetracycline; ERY = Erythromycin; LEV = Levofloxacin; NOR = Norfloxacin.

The Combination Index (CI) quantifies the nature of the interaction between antibiotics at any effect level. Fig. 2.3 shows the f_a-CI plots of binary (Fig. 2.3a) and multi-antibiotic mixtures (Fig. 2.3b). The f_a- CI plot depicts the CI value versus f_a (the effect level or fraction of luminescence/growth inhibited with respect to the control). Due to the fact that complete concentration-response relationship could not be recorded for the green alga for some antibiotics, the maximum effect level (f_a) shown in the figures of

the green alga is 0.5. Average Combination Index (CI) values for the 3 representative EC values (EC_{10}, EC_{20} and EC_{50}) are shown in Table 2.1.

For the green alga (Fig. 2.3a), the ERY-LEV combination showed a clear antagonism at low f_a levels, becoming synergistic at f_a values above 0.3. The ERY-NOR combination was nearly additive in the whole range of effect levels. The ERY-TET mixture showed a clearly synergistic interaction, particularly at very low f_a values, becoming slightly less synergistic at higher values. The LEV-TET combination was nearly additive at very low effect levels becoming clearly synergistic at f_a values above 0.1. The LEV-NOR mixture was clearly synergistic in the whole range of f_a levels while the NOR-TET combination showed antagonism at very low to low f_a values which changed into synergism at higher effect levels. The 4-antibiotic mixture was nearly additive at very low effect levels and clearly synergistic at effect levels above 0.1. The global picture of antibiotic interactions in the green alga is that synergism clearly predominated.

For the cyanobacterium (Fig. 2.3b), a somewhat more heterogeneous pattern of interactions emerged. The ERY-LEV combination showed antagonism at very low to low effect levels which turned into a near additive behavior at f_a levels above 0.4. The ERY-NOR combination was nearly additive in the whole range of effect levels. The ERY-TET combination was clearly synergistic at very low effect levels which turned into a strong antagonism above a f_a value of 0.6. The NOR-TET combination showed a pattern similar to the one of ERY-LEV combination with slight antagonism at very low to low effect levels, approaching additivity at medium effect levels and slightly synergistic at the higher effect levels. The LEV-NOR combination showed a tendency of interactions similar to that of NOR-TET although at very low to low effect levels it approached the additivity line. The LEV-TET combination showed a strong synergistic interaction in the whole range of f_a levels. The AMO-ERY and AMO-NOR combinations showed a similar pattern of interactions with strong antagonism at f_a values below 0.6 which became slightly synergistic at higher effect levels; the AMO-LEV combination also showed strong antagonism at low effect levels but became slightly synergistic at f_a levels above 0.2. The AMO-TET combination was strongly synergistic in the whole range of f_a values. The 5-antibiotic mixture followed a pattern of interactions quite similar to the one found for the 4-antibiotic mixture in the green alga with antagonism at low effect levels which turned into synergism at f_a values above

0.25. The global pattern of interactions that emerged in the cyanobacterium showed that at very low effect levels, antagonism predominated in most binary mixtures with the exception of 3 mixtures with tetracycline: TET-AMO, TET-ERY and TET-LEV, which were synergistic. At higher effect levels the tendency was similar to that observed in the green alga and synergism became the predominant interaction. It should be noticed that in both cell systems, the ERY-TET combination showed strong synergism at very low to low effect levels, emphasizing again that this could be a quite toxic combination in the environment, even when both antibiotics are present at very low concentrations as already discussed. For the cyanobacterium, two other combinations could be potentially dangerous for their synergistic interactions: the AMO-TET and LEV-TET. For the green alga, the LEV-NOR combination could also be dangerous due to the synergistic interactions found at low effect levels. For both organisms, the multi-antibiotic mixtures were also synergistic at relatively low effect levels (above f_a=0.10 for the green alga and f_a= 0.25 for the cyanobacterium), indicating increased toxicity towards both aquatic organisms when all the tested antibiotics co-occur.

An important feature of the observed antibiotic interactions in both organisms is that the nature of the interaction change with the effect level and with the test organism. We have already found this behavior with other pollutants interactions (Rodea-Palomares et al. 2010; Rosal et al. 2010a; Rodea-Palomares et al. 2012). A possible explanation of this phenomenon might be that at low effect levels, cells are less affected by the pollutants and antagonism/synergism may be explained by specific modes of action; thus, antagonism could be due to competition for uptake/ same binding sites or suppression of the toxic effect of one drug by another while synergism could be explained by mechanisms of drug combinations such as “facilitating actions” meaning that secondary actions of one drug enhances the activity or level of another drug in the mixture or alternatively “complementary actions” when drugs act at the same target at different sites, at overlapping sites or at different targets of the same pathway (Jia et al., 2009); at high effect levels, cells may be heavily affected and toxicity may be increased by an unspecific way of action not probably related to the pharmacological mechanism; at high effect levels, cells membranes may be damaged allowing the bulk entry of toxicants; under these situations, synergism, considered as the combined action of pollutants which increase toxicity by unspecific mode of action, may predominate as we

have previously found for the combined action of heavy metals (Rodea-Palomares et al. 2009) o fibrates (Rodea-Palomares et al. 2010).

The CI method allows quantitative determination of synergism or antagonism but does not give information on the mechanism by which the interactions occur (Chou 2006). However, it should be taken into account that toxicological interactions may be influenced not only by the toxic mode of action but also by pharmacokinetic properties and biological sensitivity (already discussed under toxicity of individual antibiotics). Research on pharmacokinetic properties of antibiotics (absorption, accumulation, distribution and elimination) have mostly focused in invertebrates and fish (Samuelsen 2006; Li et al. 2009) with no similar studies been conducted with algae or cyanobacteria; antibiotic efflux pumps found in prokaryotic and eukaryotic cells play a fundamental role in the modulation of absorption, cellular accumulation and elimination of antibiotics (Van Bambeke et al. 2003a; Van Bambeke et al. 2003b); drug efflux pump genes are present in the genomes of sequenced cyanobacteria (http://genome.kazusa.or.jp/cyanobase/); similarly, multiple antibiotic resistance genes have been found in chloroplasts (Conte et al. 2009); further research is needed to understand the role of these systems in the pharmacokinetics of antibiotics in both algae and cyanobacteria.

The individual mechanisms of action of the 5 tested antibiotics towards their target organisms, prokaryotes, are well known and may be useful to try to explain, at least, some of the observed interactions in the cyanobacterium. However, in the green alga, a eukaryotic organism, the mechanisms of toxicity are probably unrelated to the known mechanism of action in prokaryotes, although, as already mentioned, direct effects on chloroplasts and mitochondria cannot be discarded.

For the cyanobacterium, the nearly additive behavior of the LEV-NOR combinations at f_a levels below 0.5 (Fig. 2.2b) could perhaps be explained by their identical specific mechanism of action: inhibition of bacterial DNA gyrase. Similarly, (Backhaus et al. 2000) found that the mixture toxicity of 10 quinolones to *Vibrio fischeri* followed the concept of concentration addition. (Christensen et al. 2006) also reported that the combination of 2 quinolones, flumequine and oxolinic acid, behaved additively in activated sludge microorganisms. In the green alga, the LEV-NOR combination was

strongly synergistic in the whole range of effect levels. Based on these antibiotics' mechanisms of action, the interaction should have been additive as in the case of *Vibrio*, sludge microorganisms and *Anabaena*. Interestingly, (Yang et al. 2008) also found synergism as the interaction of a norfloxacin-ciprofloxacin binary mixture at an effect level of 0.5 in *P. subcapitata*. The authors indicate that, as the green alga is not a target organism, it is very difficult to explain the interaction. Whatever the mechanism, their results and ours indicate that quinolones appear to interact synergistically in this green alga and this could be environmentally relevant.

The observed strong synergistic interaction between ERY and TET (at f_a levels below 0.6) (Fig. 2.3b) in the cyanobacterium could be explained by the complementary action of both antibiotics in prokaryotic protein synthesis as indicated by (Jia et al. 2009) in their extensive review of mechanisms of drug interactions. Synergism was also found for this antibiotic combination in the green alga (Fig. 2.3a). Perhaps an effect on the chloroplast and mitochondrial ribosomes may explain the observed interaction. (Christensen et al. 2006) also found synergistic effects of a similar mixture, oxytetracycline and erythromycin, in this green alga. The fact that, as reported before , both antibiotics when applied individually, both in the cyanobacterium and the green alga, provoked measurable toxicity at concentrations close to measured environmental concentrations indicates that the observed synergism might represent an ecological risk when the two antibiotics co-occur in aquatic environments.

The patterns of interactions found in the rest of binary mixtures cannot be easily explained in terms of the known mechanisms of antibiotic action. The multi-antibiotic mixtures interactions cannot be explained in terms of mechanisms either. Besides, there are not many reports in the literature which have studied the nature of interactions of this kind of complex mixtures. (Yang et al. 2008) studied the combined effects of 12 antibacterial agents on *P. subcapitata* finding that antagonistic effects predominated at certain antibiotic concentrations. Here, we report antagonism of the multi-component mixtures at very low to low effect levels, with synergism clearly predominating at higher effect levels (Fig. 2.3a). As discussed earlier, this may have important implications in the aquatic environment.

Regarding multi-component mixtures like the 4- and 5-antibiotic mixtures of this work, an interesting feature of the CI method is that knowledge on the component-component type of interaction is not required to assess the overall interaction resulting of a complex mixture (Chou 2006), however more complex studies can be performed based on the CI method in order to identify the component-component interaction contribution to the overall resulting interaction; for example, when analyzing a ternary mixture (A + B + C), it can be considered as a binary mixture composed by (A + B) + C and similarly with other combinations (Chou 2006). This problem could also be assessed by regression analysis where the CI values of the multi-component mixture of interest are regressed against the CI values of the different binary mixtures (Rodea-Palomares et al. 2010; Rodea-Palomares et al. 2012).

2.3.3 Experimental and predicted toxicity of the antibiotic mixtures under CA, IA and CI methods

In order to validate the antibiotic interactions predicted by the combination index (CI) in the different antibiotic mixtures, we have generated predicted dose-response curves of the antibiotic mixtures based on the classical models used in toxicology to predict the expected toxicity of mixtures under additivity: Concentration addition (CA) and Independent Action (IA). We have also generated predicted dose-response curves of the different mixtures based on the CI values obtained at the different f_a levels of the mixtures. Fig. 2.4 shows predicted dose response curves under CA, IA and CI models together with experimental values for four representative antibiotic mixtures of both the cyanobacterium (Fig. 2.4a-d) and the green alga (Fig. 2.4e-f).

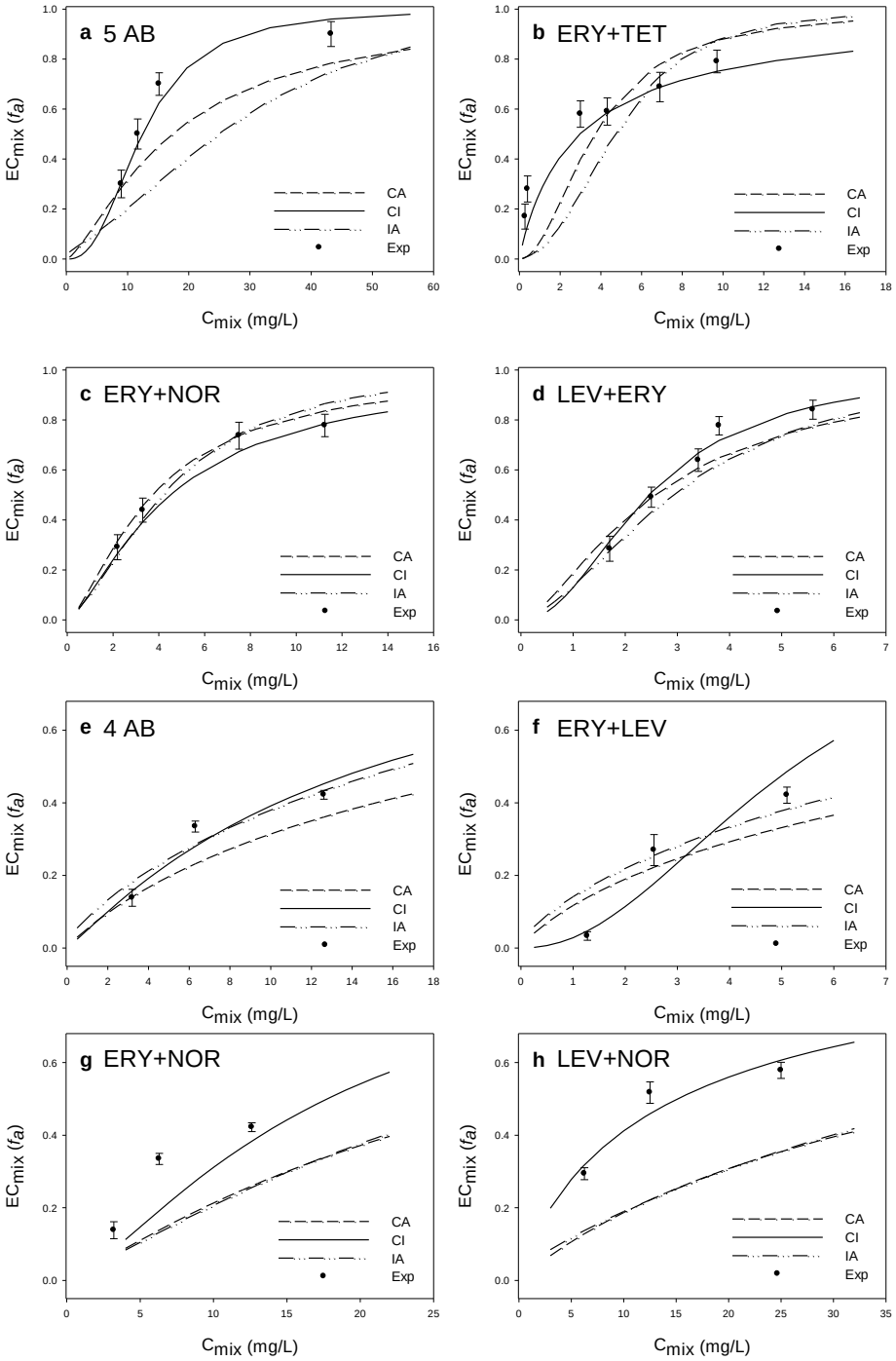

Figure 2.4 Experimental toxicity values (Exp) and predicted dose-response curves of representative antibiotic mixtures based on Concentration Addition (CA), Independent Action (IA) and Combination Index (CI) models for *Anabaena* CPB4337 test (a, b, c and d) and *Pseudokirchneriella subcapitata* test (d, e, f and g). 5 AB = ERY+LEV+NOR+TET+AMO, 4 AB = ERY+LEV+NOR+TET. Exp = Mean ± SD.

Experimental and predicted toxicity values under CA, IA and CI models for all tested mixtures can be found in supplementary Information (Table S2.5). As can be seen in the

figure, in general the prediction of CI method seems to fit more accurately the real experimental toxicity values for both organisms in those effect levels (f_a) of mixtures where CI method predicted departures from additivity (Fig. 2.3); for example, analyzing the 5 AB mixture in the cyanobacterium (Fig. 2.4a), at effect levels above 0.5, and the ERY + TET mixture (Fig. 2.4b) at low effect levels ($f_a < 0.5$), it can be seen that CA and IA did not predict the observed experimental deviation from additivity (towards synergism) which was accurately predicted by CI. A similar pattern can be observed in the ERY + NOR and LEV + NOR combinations for the green algae (Fig. 2.4g and h, respectively). When analyzing the predicted toxicity under CA, IA and CI at mixture effect levels where CI method predicted additivity (CI values near to 1; Fig. 2.3), the three methods CA, IA and CI offered a close and very similar predictions of the expected toxicity of the mixtures, as can be seen in the ERY + NOR and ERY + LEV combinations in the cyanobacterium (Fig. 2.4c,d, respectively), and at the lowest effect levels in the 4 AB and ERY + NOR mixtures in the green algae (Fig. 2.4e, g, respectively).

When comparing the experimental and predicted toxicities of all the tested mixtures based on these three models (CA, IA and CI) (Supplementary Information Table S2.5), it can be seen that, in general, the predicted toxicity of the mixtures according to CI is closer than that of CA and IA to that of experimental toxicity values in those mixtures where CI method predicted departures from additivity, specially in synergistic interactions (Fig. 2.3). However, it has been detected that in some of the mixtures of the cyanobacterium the three methods have underestimated the actual synergism of the mixtures: LEV + NOR and NOR + TET combinations are even more synergistic than that expected based on CI calculations, and the mixture NOR + TET, classified as near additive by the CI method was in fact synergistic as experimental toxicity values are above those predicted by the CI model. Therefore the CI method predicted with a very low error rate (only 1, the NOR-TET combination in the cyanobacterium, of 18 mixtures was wrongly evaluated as near additive when in fact was synergistic, see Supplementary Information Table S2.5) deviations from additivity of mixtures with different degrees of complexity. Furthermore, by taking in to account the estimated CI values of the different antibiotic mixtures, the CI method improved the predictive power of the classical additivity models CA and IA. The possibility of using CI values to get accurate predictions of toxicity in synergistic mixtures is a promising tool for assessing

the real toxicity of mixtures of chemicals. In fact, Cedergreen et al, (2008) performed an extensive statistical analysis of the accuracy of both CA and IA models in predicting the actual toxicity of binary mixtures of chemicals (from pesticides to pharmaceuticals) with 185 independent data sets including 98 different mixtures; they found that approximately half of the experimental toxicity could not be correctly described with either of the two models. They also concluded that when quantifying the maximal synergism and antagonism, none of them proved to be significantly better than the other. Therefore, we can conclude that currently there is a lack of a basic methodology to accurately predict the actual toxicity of about half of the possible mixture situations, since CA and IA models by definition ignore synergism.

2.3.4. Risk quotients assessment of antibiotic mixtures

The RQs for antibiotic mixtures were derived from dividing the MEC by the PNEC. The MEC used in this work were maximum actual environmental measured concentrations reported in surface waters and wastewater effluents (Table S2.1). The procedure aims to assess risk considering unfavorable situations (higher environmental concentrations). The PNEC were obtained by dividing the EC_{50} of the mixtures by a safety factor of 1000 (Von der Ohe et al. 2011). Table 2.2 shows the RQs of binary, 4 and 5-antibiotic mixtures for both *Anabaena* CPB4337 and *P. subcapitata*. The RQs for individual antibiotics are also provided. As shown in the table, the TET + ERY combination was above the threshold value of 1 both in the green alga and the cyanobacterium for wastewater effluents. This mixture posed an ecological risk for both organisms considering today´s pattern of antibiotic use, which is more pronounced for the green alga. As already mentioned, this mixture showed strong synergism at low effect levels in both organisms, emphasizing the danger associated with it. In fact, RQs for individual antibiotics (Table 2.2) also indicated a potentially high ecological risk of ERY for both organisms and of TET towards the green alga. For the cyanobacterium, the NOR-ERY and TET-LEV combinations in wastewater effluents presented values closer to one, indicating a narrow safety margin for these mixtures. It should be noted that the multi-antibiotic mixtures RQs were below 1 in both organisms, indicating that, at actual environmental levels, these mixtures do not pose an ecological risk. As expected RQ values in effluent wastewater were significantly higher than those found in surface waters.

Table 2.2 Risk quotients (RQ) based on MEC and PNEC for the 5 antibiotics for *Anabaena sp.* CPB4337 and *Pseudokirchneriella subcapitata*.

Components	Surface water	Wastewater effluent	*Anabaena sp.* CPB4337			*Pseudokirchneriella subcapitata*		
	MEC (µM)	MEC (µM)	PNEC (µM)	RQ surface water	RQ wastewater effluent	PNEC (µM)	RQ surface water	RQ wastewater effluent
AMO+ERY	0.001889[ac]	0.009096[df]	1.1214	0.0016844	0.008111	-	-	-
NOR+ERY	0.003788[bc]	0.013289[df]	0.0141	0.26854	0.9421	0.05683	0.06666	0.2338
NOR+AMO	0.005304[ba]	0.011528[dd]	0.09172	0.05783	0.1257	-	-	-
LEV+ERY	0.000429[cc]	0.005601[cf]	0.006766	0.06333	0.8279	-	-	-
LEV+AMO	0.001944[ca]	0.003840[cd]	0.06131	0.03171	0.06263	-	-	-
LEV+NOR	0.003843[cb]	0.008034[cd]	0.01285	0.299	0.62503	0.04587	0.08378	0.1751
TET+ERY	0.000434[dc]	0.008579[df]	0.006674	0.06505	1.285	0.0005676	0.765	15.12
TET+AMO	0.001950[da]	0.006818[dd]	0.01754	0.1112	0.3888	-	-	-
TET+NOR	0.003849[db]	0.011011[dd]	0.01389	0.2772	0.7929	0.02861	0.1345	0.3848
TET+LEV	0.000489[dc]	0.003323[dc]	0.003904	0.1254	0.8512	0.01251	0.03914	0.2657
4 AB[g]	0.004278[bcdc]	0.016612[dcdf]	-	-	-	0.04857	0.08807	0.3420
5 AB[h]	0.005980[abcdc]	0.020280[ddcdf]	0.03395	0.1761	0.5973	-	-	-
AMO	0.001702[a]	0.003667[e]	0.154	0.01104	0.0238	-	-	-
NOR	0.003602[b]	0.007861[e]	0.01753	0.2053	0.4482	0.04635[i]	0.0777	0.1696
LEV	0.000242[c]	0.000173[c]	0.01328	0.0182	0.013	0.01245[i]	0.01942	0.01387
TET	0.000248[d]	0.003150[e]	0.01395	0.01774	0.2258	0.0001362[i]	1.817	23.12
ERY	0.000187[c]	0.005429[f]	0.00003	6.227	181.1	0.0002568[i]	0.7269	21.138

[a] Barbara Kasprzyk-Hordern et al 2008; [b] A.J. Watkinson et al 2009; [c] Joon-Woo Kim et al 2009; [d] H.W. Leung et al 2011; [e] D.W. Kolpin et al 2002; [f] José L. Rodriguez-Gil et al 2010; [g] ERY +LEV+ NOR +TET; [h] ERY +LEV+ NOR +TET+AMO; [i] PNEC based on individual EC_{20}

There are not many studies in the literature that report calculations of RQs for antibiotics/pharmaceuticals mixtures. Brain et al. (2004) evaluated the effect of 8 pharmaceuticals including 3 antibiotics and found significant ecological risk for 2 aquatic macrophytes. In a subsequent study, Brain et al. (2005) reported that the mixture of 4 tetracyclines did pose a risk for the same macrophytes. For individual antibiotics, sulfamethoxazole, sulfathiazole, chlortetracycline, oxytetracycline and AMO were found to pose an ecological risk to aquatic ecosystems (Park and Choi 2008). Gros et al. (2010) reported that ERY was hazardous for *Daphnia* and sulfamethoxazole and TET to algae. Isidori et al. (2005) also found that macrolides, which included ERY, was the antibiotic class most harmful to the environment. Our results and others indicate that

ERY and TET both individually and in binary mixtures may pose a significant risk for aquatic ecosystems.

In this work, toxicological interactions of antibiotics were performed for the first time based on Combination Index (CI) analysis. This methodology allowed to identify a general tendency to synergism in complex antibiotic mixtures, and specially to identify tetracycline as a synergistic-inducer component. Correction of additivity predictions based on CA and IA with the information provided by the CI method allowed, for the first time to accurately predict the actual toxicity of synergistic mixtures. This study also identified the erythromycin and tetracycline combination as a potential ecological threat based on today's pattern of use of these antibiotics.

2.4. CONCLUSIONS

We performed individual and combined antibiotic toxicity tests in representative photosynthetic aquatic organisms. The cyanobacterium, due to its prokaryotic nature, was in general more sensitive than the green alga to the tested antibiotics. Toxicological interactions studies using the Combination Index (CI) method indicated that synergism was predominant in binary and multi-component mixtures under real scenarios of contamination. Especially remarkable was the synergism found in almost all mixtures which included tetracycline as a component. CI method proved to give a more accurate prediction of the actual toxicity of synergistic mixtures than that offered by CA and IA. When risk assessment of antibiotic mixtures was performed, the combination of erythromycin and tetracycline presented a RQ value which exceeded 1, posing a potential ecological risk for aquatic organisms with today's pattern of use of both antibiotics.

2.5. REFERENCES

Altenburger, R., Walter, H. and Grote, M. (2004) What Contributes to the Combined Effect of a Complex Mixture? Environmental Science & Technology 38(23), 6353-6362.

Allen, M.B. and Arnon, D.I. (1955) Studies on nitrogen-fixing blue grenn algae. I Growth and nitrogen fixation by *Anabaena cylindrica* Lemm. Plant Physiol 30, 366-372.

Backhaus, T., Scholze, M. and Grimme, L.H. (2000) The single substance and mixture toxicity of quinolones to the bioluminescent bacterium Vibrio fischeri. Aquatic Toxicology 49(1-2), 49-61.

Baguer, A.J., Jensen, J. and Krogh, P.H. (2000) Effects of the antibiotics oxytetracycline and tylosin on soil fauna. Chemosphere 40(7), 751-757.

Batt, A.L., Bruce, I.B. and Aga, D.S. (2006) Evaluating the vulnerability of surface waters to antibiotic contamination from varying wastewater treatment plant discharges. Environmental Pollution 142(2), 295-302.

Boltes, K., Rosal, R. and García-Calvo, E. (2012) Toxicity of mixtures of perfluorooctane sulphonic acid with chlorinated chemicals and lipid regulators. Chemosphere 86(1), 24-29.

Brain, R.A., Johnson, D.J., Richards, S.M., Hanson, M.L., Sanderson, H., Lam, M.W., Young, C., Mabury, S.A., Sibley, P.K. and Solomon, K.R. (2004) Microcosm evaluation of the effects of an eight pharmaceutical mixture to the aquatic macrophytes Lemna gibba and Myriophyllum sibiricum. Aquatic Toxicology 70(1), 23-40.

Brain, R.A., Wilson, C.J., Johnson, D.J., Sanderson, H., Bestari, K., Hanson, M.L., Sibley, P.K. and Solomon, K.R. (2005) Effects of a mixture of tetracyclines to Lemna gibba and Myriophyllum sibiricum evaluated in aquatic microcosms. Environmental Pollution 138(3), 425-442.

Cleuvers, M. (2003) Aquatic ecotoxicity of pharmaceuticals including the assessment of combination effects. Toxicology Letters 142(3), 185-194.

Conte, S., Stevenson, D., Furner, I. and Lloyd, A. (2009) Multiple antibiotic resistance in Arabidopsis is conferred by mutations in a chloroplast-localized transport protein. Plant Physiol 151(2), 559-573.

Costanzo, S.D., Murby, J. and Bates, J. (2005) Ecosystem response to antibiotics entering the aquatic environment. Marine Pollution Bulletin 51(1-4), 218-223.

Chou, T.C. and Talalay, P. (1984) Quantitative analysis of dose-effect relationships: the combined effects of multiple drugs or enzyme inhibitors. Advances in Enzyme Regulation 22, 27-55.

Chou, T.C.M., N. (2005) CompuSyn for Drug Combinations: PC Software and User´s Guide: A Computer Program for Quantification of Synergism and Antagonism in Drug Combinations and the Determination of IC50 and ED50 and LD50 Values., ComboSyn, Inc., Paramus, NJ.

Chou, T.C. (2006) Theoretical basis, experimental design, and computerized simulation of synergism and antagonism in drug combination studies. Pharmacological Reviews 58(3), 621-681.

Christensen, A.M., Ingerslev, F. and Baun, A. (2006) Ecotoxicity of mixtures of antibiotics used in aquacultures. Environmental Toxicology and Chemistry 25(8), 2208-2215.

Daughton, C.G. and Ternes, T.A. (1999) Pharmaceuticals and personal care products in the environment: Agents of subtle change? Environmental Health Perspectives 107, 907-938.

Dolliver, H., Kumar, K. and Gupta, S. (2007) Sulfamethazine uptake by plants from manure-amended soil. Journal of Environmental Quality 36(4), 1224-1230.

Ebringer, L. (1972) Are plastids derived from prokaryotic microorganism-action of antibiotics on chloroplasts of Euglena-gracilis. Journal of General Microbiology 71(1), 35-52.

Eguchi, K., Nagase, H., Ozawa, M., Endoh, Y.S., Goto, K., Hirata, K., Miyamoto, K. and Yoshimura, H. (2004) Evaluation of antimicrobial agents for veterinary use in the ecotoxicity test using microalgae. Chemosphere 57(11), 1733-1738.

Elmund, G.K., Morrison, S.M., Grant, D.W. and Nevins, M.P. (1971) Role of excreted chlortetracycline in modifying decomposition process in feedlot waste. Bulletin of Environmental Contamination and Toxicology 6(2), 129-&.

EMEA (2006) European Chemical Agency. Guideline on the Environmental Risk Assessment of Medicinal products for human use. Doc ref. EMEA/CHMP/SWP/4447/00.

Faust, M., Altenburger, R., Backhaus, T., Blanck, H., Boedeker, W., Gramatica, P., Hamer, V., Scholze, M., Vighi, M. and Grimme, L.H. (2001) Predicting the joint algal toxicity of multi-component s-triazine mixtures at low-effect concentrations of individual toxicants. Aquatic Toxicology 56(1), 13-32.

Fernandez-Pinas, F. and Wolk, C.P. (1994) Expression of luxCD-E in Anabaena sp. can replace the use of exogenous aldehyde for in vivo localization of transcription by luxAB. Gene 150(1), 169-174.

Ginebreda, A., Muñoz, I., de Alda, M.L., Brix, R., López-Doval, J. and Barceló, D. (2009) Environmental risk assessment of pharmaceuticals in rivers: Relationships between hazard indexes and aquatic macroinvertebrate diversity indexes in the Llobregat River (NE Spain). Environment International 36(2), 153-162.

Göbel, A., Thomsen, A., McArdell, C.S., Joss, A. and Giger, W. (2005) Occurrence and sorption behavior of sulfonamides, macrolides, and trimethoprim in activated sludge treatment. Environmental Science & Technology 39(11), 3981-3989.

Greenberg, B.M., Huang, X.D. and Dixon, D.G. (1992) Applications of the aquatic higher plan *Lemna gibba* for ecotxicological risk assessment. Journal of Aquatic Ecosystem Health 1, 147-155.

Gros, M., Petrovic, M., Ginebreda, A. and Barceló, D. (2010) Removal of pharmaceuticals during wastewater treatment and environmental risk assessment using hazard indexes. Environment International 36(1), 15-26.

Gulkowska, A., He, Y., So, M.K., Yeung, L.W.Y., Leung, H.W., Giesy, J.P., Lam, P.K.S., Martin, M. and Richardson, B.J. (2007) The occurrence of selected antibiotics in Hong Kong coastal waters. Marine Pollution Bulletin 54(8), 1287-1293.

Halling-Sørensen, B., Nors Nielsen, S., Lanzky, P.F., Ingerslev, F., Holten Lützhoft, H.C. and Jorgensen, S.E. (1998) Occurrence, fate and effects of pharmaceutical substances in the environment- A review. Chemosphere 36(2), 357-393.

Halling-Sørensen, B., Lutzhoft, H.C.H., Andersen, H.R. and Ingerslev, F. (2000) Environmental risk assessment of antibiotics: comparison of mecillinam, trimethoprim and ciprofloxacin. Journal of Antimicrobial Chemotherapy 46, 53-58.

Harrass, M.C., Kindig, A.C. and Taub, F.B. (1985) Responses of blue-green and green algae to streptomycin in unialgal and paired culture. Aquatic Toxicology 6(1), 1-11.

Hektoen, H., Berge, J.A., Hormazabal, V. and Yndestad, M. (1995) Persistence of antibacterial agents in marine-sediments. Aquaculture 133(3-4), 175-184.

Hernando, M.D., Mezcua, M., Fernández-Alba, A.R. and Barceló, D. (2006) Environmental risk assessment of pharmaceutical residues in wastewater effluents, surface waters and sediments. Talanta 69(2), 334-342.

Hirsch, R., Ternes, T., Haberer, K. and Kratz, K.-L. (1999) Occurrence of antibiotics in the aquatic environment. Science of The Total Environment 225(1-2), 109-118.

Isidori, M., Lavorgna, M., Nardelli, A. and Parrella, A. (2004) Integrated environmental assessment of Volturno River in South Italy. Science of The Total Environment 327(1-3), 123-134.

Isidori, M., Lavorgna, M., Nardelli, A., Pascarella, L. and Parrella, A. (2005) Toxic and genotoxic evaluation of six antibiotics on non-target organisms. Science of The Total Environment 346(1-3), 87-98.

Jia, J., Zhu, F., Ma, X., Cao, Z.W., Li, Y.X. and Chen, Y.Z. (2009) Mechanisms of drug combinations: interaction and network perspectives. Nat Rev Drug Discov 8(2), 111-128.

Kerry, J., Slattery, M., Vaughan, S. and Smith, P. (1996) The importance of bacterial multiplication in the selection, by oxytetracycline-HCl, of oxytetracycline-resistant bacteria in marine sediment microcosms. Aquaculture 144(1-3), 103-119.

Kim, S.C. and Carlson, K. (2007) Quantification of human and veterinary antibiotics in water and sediment using SPE/LC/MS/MS. Analytical and Bioanalytical Chemistry 387(4), 1301-1315.

Kolpin, D.W., Furlong, E.T., Meyer, M.T., Thurman, E.M., Zaugg, S.D., Barber, L.B. and Buxton, H.T. (2002) Pharmaceuticals, hormones, and other organic wastewater contaminants in US streams, 1999-2000: A national reconnaissance. Environmental Science & Technology 36(6), 1202-1211.

Kolpin, D.W., Skopec, M., Meyer, M.T., Furlong, E.T. and Zaugg, S.D. (2004) Urban contribution of pharmaceuticals and other organic wastewater contaminants to streams during differing flow conditions. Science of The Total Environment 328(1-3), 119-130.

Kong, W.D., Zhu, Y.G., Liang, Y.C., Zhang, J., Smith, F.A. and Yang, A. (2007) Uptake of oxytetracycline and its phytotoxicity to alfalfa (Medicago sativa L.). Environmental Pollution 147(1), 187-193.

Li, B., Zhang, T., Xu, Z. and Fang, H.H.P. (2009) Rapid analysis of 21 antibiotics of multiple classes in municipal wastewater using ultra performance liquid chromatography-tandem mass spectrometry. Analytica Chimica Acta 645(1-2), 64-72.

Lindsey, M.E., Meyer, M. and Thurman, E.M. (2001) Analysis of trace levels of sulfonamide and tetracycline antimicrobials, in groundwater and surface water using solid-phase extraction and liquid chromatography/mass spectrometry. Analytical Chemistry 73(19), 4640-4646.

Lutzhoft, H.C.H., Halling-Sorensen, B. and Jorgensen, S.E. (1999) Algal toxicity of antibacterial agents applied in Danish fish farming. Archives of Environmental Contamination and Toxicology 36(1), 1-6.

Maul, J.D., Schuler, L.J., Belden, J.B., Whiles, M.R. and Lydy, M.J. (2006) Effects of the antibiotic ciprofloxacin on stream microbial communities and detritivorous macroinvertebrates. Environmental Toxicology and Chemistry 25(6), 1598-1606.

McArdell, C.S., Molnar, E., Suter, M.J.F. and Giger, W. (2003) Occurrence and fate of macrolide antibiotics in wastewater treatment plants and in the Glatt Valley Watershed, Switzerland. Environmental Science & Technology 37(24), 5479-5486.

McFadden, G.I. and Roos, D.S. (1999) Apicomplexan plastids as drug targets. Trends in Microbiology 7(8), 328-333.

Migliore, L., Civitareale, C., Brambilla, G. and DiDelupis, G.D. (1997) Toxicity of several important agricultural antibiotics to Artemia. Water Research 31(7), 1801-1806.

Nicolas, P. (1981) Sensitivity of Euglena gracilis to chloroplast-inhibiting antibiotics, and properties of antibiotic-resistant mutants. Plant Sci Lett 22, 309-317.

OECD (2006) OECD/201 Guidelines for the testing of chemicals. Freshwater algal and cyanobacteria, growth inhibition test.

OECD (2008) Guidelines for the Testing of Chemicals, No.23: Guidance Document on Aquatic Toxicity Testing of Difficult Subtances and Mixtures, PDF Edition (ISSN 1607-310X), 18th Addendu.

Park, S. and Choi, K. (2008) Hazard assessment of commonly used agricultural antibiotics on aquatic ecosystems. Ecotoxicology 17(6), 526-538.

Perez-Parada, A., Aguera, A., Gomez-Ramos, M.D., Garcia-Reyes, J.F., Heinzen, H. and Fernandez-Alba, A.R. (2011) Behavior of amoxicillin in wastewater and river water: identification of its main transformation products by liquid chromatography/electrospray quadrupole time-of-flight mass spectrometry. Rapid Communications in Mass Spectrometry 25(6), 731-742.

Qin, L.-T., Liu, S.-S., Zhang, J. and Xiao, Q.-F. (2010) A novel model integrated concentration addition with independent action for the prediction of toxicity of multi-component mixture. Toxicology 280(3), 164-172.

Robinson, A.A., Belden, J.B. and Lydy, M.J. (2005) Toxicity of fluoroquinolone antibiotics to aquatic organisms. Environmental Toxicology and Chemistry 24(2), 423-430.

Rodea-Palomares, I., Fernández-Piñas, F., González-García, C. and Leganes, F. (2009) Use of lux-marked cyanobacterial bioreporters for assessment of individual and combined toxicities of metals in aqueous samples. In: Handbook on Cyanobacteria: Biochemistry, Biotechnology and Applications., Nova Science Publishers, Inc. , New York. USA. .

Rodea-Palomares, I., Petre, A.L., Boltes, K., Leganés, F., Perdigón-Melón, J.A., Rosal, R. and Fernández-Piñas, F. (2010) Application of the combination index (CI)-isobologram equation to study the toxicological interactions of lipid regulators in two aquatic bioluminescent organisms. Water Research 44(2), 427-438.

Rodea-Palomares, I., Leganés, F., Rosal, R. and Fernández-Piñas, F. (2012) Toxicological interactions of perfluorooctane sulfonic acid (PFOS) and perfluorooctanoic acid (PFOA) with selected pollutants. Journal of Hazardous Materials 30(201-202), 209-218.

Rosal, R., Rodea-Palomares, I., Boltes, K., Fernández-Piñas, F., Leganés, F. and Petre, A. (2010a) Ecotoxicological assessment of surfactants in the aquatic environment: Combined toxicity of docusate sodium with chlorinated pollutants. Chemosphere 81(2), 288-293.

Rosal, R., Rodriguez, A., Perdigón-Melón, J.A., Petre, A., García-Calvo, E., Gómez, M.J., Agüera, A. and Fernández-Alba, A.R. (2010b) Occurrence of emerging pollutants in urban wastewater and their removal through biological treatment followed by ozonation. Water Research 44(2), 578-588.

Sacher, F., Lang, F.T., Brauch, H.J. and Blankenhorn, I. (2001) Pharmaceuticals in groundwaters - Analytical methods and results of a monitoring program in Baden-Wurttemberg, Germany. Journal of Chromatography A 938(1-2), 199-210.

Samuelsen, O.B. (2006) Pharmacokinetics of quinolones in fish: A review. Aquaculture 255(1â€“4), 55-75.

Sanderson, H., Johnson, D.J., Wilson, C.J., Brain, R.A. and Solomon, K.R. (2003) Probabilistic hazard assessment of environmentally occurring pharmaceuticals toxicity to fish, daphnids and algae by ECOSAR screening. Toxicology Letters 144(3), 383-395.

Sarmah, A.K., Meyer, M.T. and Boxall, A.B.A. (2006) A global perspective on the use, sales, exposure pathways, occurrence, fate and effects of veterinary antibiotics (VAs) in the environment. Chemosphere 65(5), 725-759.

Schneider, J. (1994) Problems related to the usage of veterinary drugs in aquaculture-a review. Química analítica 13(suppl. 1), S34-S42.

Suzuki, S. and Hoa, P.T.P. (2012) Distribution of quinolones, sulfonamides, tetracyclines in aquatic environment and antibiotic resistance in Indochina. Frontiers in Microbiology 3, 67.

Tamtam, F., Mercier, F., Eurin, J., Chevreuil, M. and Le Bot, B. (2009) Ultra performance liquid chromatography tandem mass spectrometry performance evaluation for analysis of antibiotics in natural waters. Analytical and Bioanalytical Chemistry 393(6-7), 1709-1718.

Teuschler, L.K. (2007) Deciding which chemical mixtures risk assessment methods work best for what mixtures. Toxicology and Applied Pharmacology 223(2), 139-147.

USEPA (1994) Short-term methods for estimating the chronic toxicity of effluents and receiving waters to freshwaters organism, U.S. Environmental Protection Agency.

USEPA (2002) Methods for Measuring the Acute Toxicity of Effluents and Receiving Waters to Freshwater and Marine Organism, United Estates Environmental Protection Agency.

Van Bambeke, F., Glupczynski, Y., PlÃ©siat, P., PechÃ¨re, J.C. and Tulkens, P.M. (2003a) Antibiotic efflux pumps in prokaryotic cells: occurrence, impact on resistance and strategies for the future of antimicrobial therapy. Journal of Antimicrobial Chemotherapy 51(5), 1055-1065.

Van Bambeke, F., Michot, J.-M. and Tulkens, P.M. (2003b) Antibiotic efflux pumps in eukaryotic cells: occurrence and impact on antibiotic cellular pharmacokinetics, pharmacodynamics and toxicodynamics. Journal of Antimicrobial Chemotherapy 51(5), 1067-1077.

Von der Ohe, P.C., Dulio, V., Slobodnik, J., De Deckere, E., Kühne, R., Ebert, R.-U., Ginebreda, A., De Cooman, W., Schüürmann, G. and Brack, W. (2011) A new risk assessment approach for the prioritization of 500 classical and emerging organic microcontaminants as potential river basin specific pollutants under the European Water Framework Directive. Science of The Total Environment 409(11), 2064-2077.

Watkinson, A.J., Murby, E.J., Kolpin, D.W. and Costanzo, S.D. (2009) The occurrence of antibiotics in an urban watershed: from wastewater to drinking water. Science of The Total Environment 407(8), 2711-2723.

Xu, W.-h., Zhang, G., Zou, S.-c., Li, X.-d. and Liu, Y.-c. (2007) Determination of selected antibiotics in the Victoria Harbour and the Pearl River, South China using high-performance liquid chromatography-electrospray ionization tandem mass spectrometry. Environmental Pollution 145(3), 672-679.

Yang, L.H., Ying, G.G., Su, H.C., Stauber, J.L., Adams, M.S. and Binet, M.T. (2008) Growth-inhibiting effects of 12 antibacterial agents and their mixtures on the freshwater microalga Pseudokirchneriella subcapitata. Environmental Toxicology and Chemistry 27(5), 1201-1208.

Zuccato, E., Calamari, D., Natangelo, M. and Fanelli, R. (2000) Presence of therapeutic drugs in the environment. The Lancet 355(9217), 1789-1790.

CHAPTER 3: HIDDEN DRIVERS OF LOW-DOSE PHARMACEUTICAL POLLUTANT MIXTURES REVEALED BY THE NOVEL GSA-QHTS SCREENING METHOD

3.1 INTRODUCTION

How can the effects of long-term exposure to low concentrations of PPCPs (Pharmaceutical and Personal Care Products) mixtures be assessed on non-target organisms? This question was recently ranked as number 1 among the 22 scientific priorities regarding PPCPs in the environment as part of a "big question exercise" hosted by SETAC (Society of Environmental Contamination and Toxicology) involving more than 500 environmental scientists from 57 countries (Rudd et al., 2014). PPCPs are widely released into the aquatic environment, where they mix at low concentrations over extended periods of time via diverse pathways, resulting in a very complex fate (Daughton and Ternes, 1999; Boxall et al., 2004; Rudd et al., 2014). Despite their ubiquity, the effects of PPCPs in the environment are not well understood (Boxall et al., 2012; Daughton and Ternes, 1999; Rudd et al., 2014). Part of the difficulties in the elucidation of the risks associated with PPCPs pollution arise from the different nature of their effects with respect to classical acutely toxic pollutants. PPCPs consistently produce sublethal effects even at low concentrations (Pomati et al., 2008; Brodin et al., 2013; Klaminder et al., 2014; Daughton and Ternes, 1999; Boxall et al., 2012), but usually do not present clear evidence of lethality even at unrealistically high doses (Daughton and Ternes, 1999; Boxall et al., 2012; Brodin et al., 2013). Sublethal effects are important since they eventually impact natural systems via direct or cascading effects (Rohr et al., 2008; Halstead et al., 2014; Brodin et al., 2013; Klaminder et al., 2014). The complexity of PPCP fate and their sublethal effects pose important challenges to our present understanding of pollutant mixture effects (Carvalho et al., 2014; Artigas et al., 2012; Klaminder et al., 2014). Null additive models such as Concentration Addition (CA) are usually considered to be a reliable hypothesis to accurate mixture effect predictions (Altenburger et al., 2013; Kortenkamp et al., 2009; Backhaus and Faust, 2012). CA and its related dose-response theory does not consider low-dose non-linear/non-additive sublethal effects (Calabrese and Baldwin, 2003; Fagin, 2012). The current assumption that effects cannot be understood below a certain threshold, usually the 10-20 % relative effect named as the "grey-zone" (Kortenkamp et al., 2009), has limited the study of the sublethal region of the dose-response curves. Preliminary evidence indicates that significant sublethal effects may occur at doses well below the *grey-zone*, both for individual chemicals and mixtures (Laetz et al., 2009; Madureira et al., 2012; Chung et al., 2011; Fagin, 2012; Carvalho et al., 2014; Pomati et

al., 2008) although these findings are criticized due to large uncertainties of existing experimental methods (Backhaus, 2014; Kortenkamp et al., 2009; Fagin, 2012).

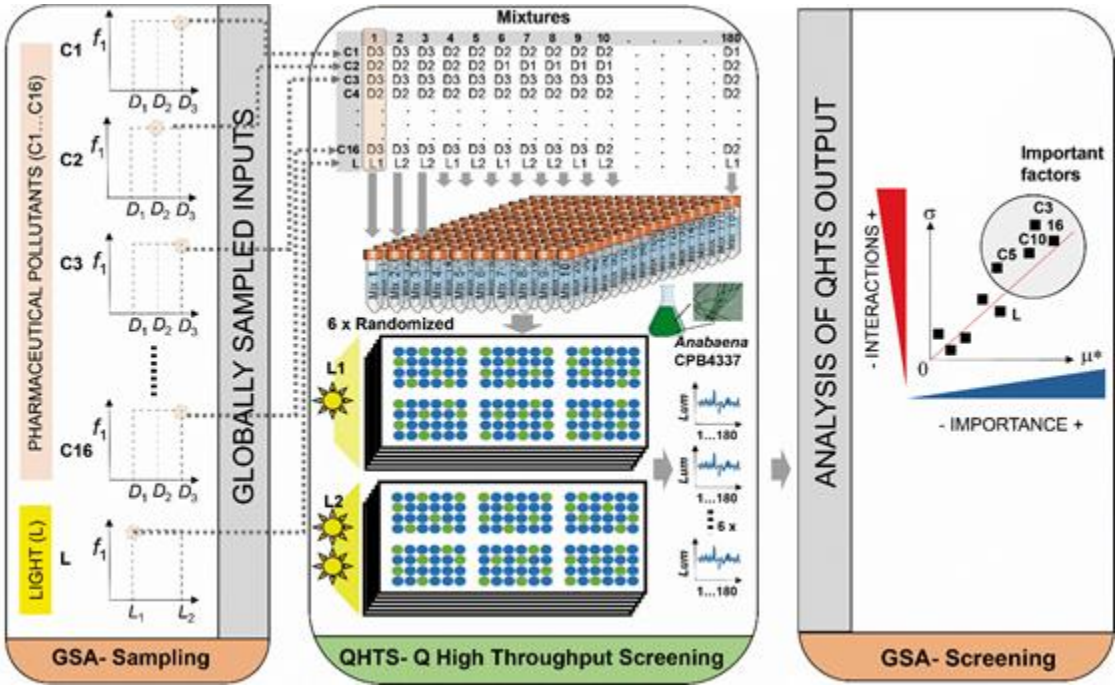

Figure 3.1. *GSA-QHTS* experimental framework. The novel approach couples *Global Sensitivity Analysis* with *Quantitative High Throughput Screening* (*GSA-QHTS*) to understand the main effects and interactions of combinations of diverse input factors, such as chemicals, biotic or abiotic factors, etc. In the present study, *GSA-QHTS* was applied to study the effects on *A.* CPB4337 of mixtures of 16 PPCPs (C1 to C16) at environmentally realistic low-doses (D_1 – D_3) and the influence of light intensity, an abiotic factor. The steps of the framework are highlighted: Parsimonious GSA-Sampling, to generate an experimental design template; QHTS, with randomized biological replication; GSA-Screening of the importance and interactions of input factors controlling biological response.

To address the current limitations in the study of sublethal effects of low-dose PPCP mixtures, we propose a novel tool consisting of coupling *Global Sensitivity Analysis* with *Quantitative High Throughput Screening* (*GSA-QHTS*). *GSA-QHTS* provides a novel perspective for chemical effect assessments by taking advantage of the family of computational GSA techniques to guide experimental design and data analysis of QHTS laboratory experiments (see Fig. 3.1). In general, GSA apportions the observed variability of the system response (output) onto the system´s drivers (inputs), in terms of both direct (1st order) and interactions (higher order) effects. This quantifies the relative importance (sensitivity) of the system's inputs without any a priori assumption on the

nature of the system´s internal processes (such as additivity, linearity or threshold effects (Saltelli et al., 2012, 2005). Among GSA techniques, the Elementary Effects (EEs) Method (Morris, 1991) relies on small number of samples and provides easy to interpret statistics that describe the direct effects of input factors (μ and $\mu*$), and their interactions (σ) (Saltelli et al., 2005, 2012). Here GSA is used to produce cost-effective (parsimonious) experimental templates that reasonably match present QHTS capacities used in ecotoxicology. As a representative freshwater biological system, we used a high throughput configuration of a bioluminescent whole-cell biosensor that detects metabolic toxicity based on a freshwater cyanobacterium (*Anabaena sp.* PCC7120 CPB4337; hereinafter *A.* CPB4337) (Rodea-Palomares et al., 2009). Cyanobacteria are focal primary producers in aquatic systems that take part in carbon and nitrogen cycling (Whitton and Potts, 2000). The EEs Method (see S3.1 for a details description) was applied to generate a set of realistic low-dose mixtures of commonly found PPCPs in freshwater, and characterize their relative importance and interactions (if any). Light intensity was also included in the analysis to illustrate the ability of *GSA-QHTS* to account for not only chemical factors, but also combined effects with other environmental stressors. Finally, novel results of factor importance and interactions obtained with the *GSA-QHTS* framework were critically compared with those from classical additive effect mixture models, and validated on up-scaled experimental freshwater benthic microbial communities.

3.2 MATERIALS AND METHODS

3.2.1 Chemicals

PPCPs and dose levels were selected based on a meta-analysis of PPCP occurrence in Spanish freshwaters (details in S3.2). The 16 PPCPs included in the present study encompassed: a) antibiotics: erythromycin (ERY, C10; Fluka > 95%) and ofloxacin (OFLO, C11; Sigma Aldrich 99.9%); b) β-Blockers: atenolol (ATE, C1; Sigma Aldrich 91%), bezafibrate (BEZA, C2; Sigma Aldrich ≥98%) and gemfibrozil (GEM, C4; Sigma Aldrich >99%); c) stimulants: nicotine (NICO, C12; Sigma Aldrich 99%) and caffeine (CAFE, C13; Sigma Aldrich > 99%); d) analgesics: ketoprofen (KETO, C8; TCI > 98%), ibuprofen (IBU, C7; Sigma Aldrich ≥ 98%), paracetamol (PARA, C9; Sigma Aldrich 99%), and diclofenac (DICLO, C6; Sigma Aldrich ≥98% (sodium salt)); e) diuretics: furosemide (FURO, C3; Sigma Aldrich ≥98%) and hydrochlorothiazide (HYDRO, C5; Sigma Aldrich ≥ 99%); f) an antidepressant: venlafaxine (VENLA, C14; TCI >98%); and g) anticonvulsants: carbamazepine (CARBA, C16; Sigma Aldrich ≥ 98%) and primidone (PRIMI, C15; Sigma Aldrich ≥ 98%). CAS nº and pharmacological family are summarized in S3.3. Additional information on preparation, handling of stock solutions and chemical stability can be found in S3.2.

3.2.2 GSA-QHTS

The Global Sensitivity Analysis technique known as the Elementary Effects (EEs) Method, or "Morris Method" (Morris, 1991; Saltelli et al., 2005, 2012) was used as the GSA framework (Fig. 3.1) to (1) guide the experimental plan to establish a parsimonious set of k = 17 input factors (mixtures and experimental light condition) to perform *QHTS* (GSA-Sampling), and (2) compute EEs Sensitivity screening measures μ (or μ^*) and σ (GSA-Screening). The EEs method (Morris, 1991) scores the relative importance and interactions of *k* input factors according to the marginal changes (elementary effects) that they produce in the output variable (relative bioluminescence) when they are changed one at a time at discrete levels with all the other factors present (Saltelli et al., 2005, 2012). The EEs method is qualitative in nature and can be applied to assess the relative importance of each of the *k* input factors in the context of all other

factors varying at the same time. Additional information on the EEs method is summarized in (Khare et al., 2015; Saltelli et al., 2012, 2005).

3.2.3 GSA-Sampling

To compute elementary effects, Morris (Morris, 1991) proposed to sample *t* random trajectories across the *k*-dimensional space of the input factors, varying one factor at a time at *r* discrete levels within the input factor probability distributions. Typically, *t* = 10 produces satisfactory results (Sabbagh et al., 2013). The number of experimental units (*N*) to perform the EEs analysis is given by:

$$N = t\,(k + 1) \tag{3.1}$$

In our case, GSA-Sampling was performed for a total of 17 input factors (16 pharmaceutical pollutants and 1 abiotic factor, light intensity), resulting in $N = 10\ (17 + 1) = 180$ experimental units. As discrete levels for the input factors, three doses ("*D"* in Fig. 3.1) of each PPCP were selected based on statistical descriptors (median of means, mean of maxima, maximum of maxima) of their environmental concentrations. Light intensity (L) was fixed at two physiological levels (see QHTS below). Discrete uniform (DU) probability distribution functions were used to represent input factor level probabilities. An enhanced Sampling for Uniformity method (Khare et al., 2015)with an oversampling size of 1000 was used to optimize the sampling quality (uniformity, spread and time). The experimental design template of the 180 Experimental Units used in the QHTS experiment can be found in S3.4.

3.2.4 QHTS: Bioactivity determinations based on *Anabaena* sp. PCC7120 CPB4337

Once the experimental template is defined by GSA-Sampling, a biological receptor is interrogated for each of the 180 mixtures with the corresponding light intensity (Fig. 3.1). *A.* CPB4337 was used as biological receptor (González-Pleiter et al., 2013; Rodea-Palomares et al., 2009). *A.* CPB4337 is a genetically engineered *whole-cell* cyanobacterial biosensor which constitutively produces bioluminescence (Rodea-Palomares et al., 2009). Changes in the bioluminescence signal was used as surrogate end-point of metabolic toxicity (Sorensen et al., 2006; Rodea-Palomares et al., 2009).

Standard growth and maintenance conditions were followed (Rodea-Palomares et al., 2009; González-Pleiter et al., 2013). Exposure experiments were performed in continuously shaken 24-well transparent plastic microtiter plates (González-Pleiter et al., 2013). Each plate contained 6 control wells plus 18 treatment wells. The total number of plates by experiment (N) was 11 for the mixture experiments and 10 for the individual exposure experiments. 12 independent experiments (6 for mixture exposure and 6 for individual exposure) were performed. In addition, other 6 independent experiments were performed for dose-response curve determinations of erythromycin and ofloxacin and venlafaxine. In each experiment, a total random experimental design was used satisfying that in each plate, 6 control + 18 treatments would be allocated. The treatments in each plate, and the positions inside the plates were totally and independently randomized for each independent experiment. The intra-experimental replication for control observations was at least 66 observations by experiment (6 by plate). Treatments were not replicated intra-experimentally. Inter-experimental replication was for instance 6 for treatment observations and 12 for control observations. Plates were incubated for 24 h in physiological light conditions: L1 (Ca.35 μmol photons m^2/s), L2 (Ca.65 μmol photons m^2/s). 6 independent experiments were performed with randomized experimental designs. Bioluminescence measurements were performed in 96-well white microtiter plates essentially as reported (González-Pleiter et al., 2013). Bioluminescence was normalized to the mean control response of each individual plate (n = 6) and expressed as relative bioluminescence.

Experiments were performed in 24 well plates. Each plate contained 6 control wells plus 18 treatment wells. The total number of plates by experiment (N) was 11 for the mixture experiments and 10 for the individual exposure experiments. 12 independent experiments (6 for mixture exposure and 6 for individual exposure) were performed. In addition, other 6 independent experiments were performed for dose-response curve determinations of Erythromycin and Ofloxacin. In each experiment, a total random experimental design was used satisfying that in each plate, 6 control + 18 treatments would be allocated. The Treatments in each plate, and the positions inside the plates were totally and independently randomized for each independent experiment. The intra-experimental replication for control observations was at least 66 observations by experiment (6 by plate). Treatments were not replicated intra-experimentally. Inter-

experimental replication was for instance 6 for treatment observations and 12 for control observations.

3.2.5 GSA-Screening

For each factor (x_i, $i = 1...k$) and level ($j = 1...r$), *QHTS* generated an experimental output value *Y*. A factor's elementary effect ($u_{j,i}$) is computed as:

$$u_i = \frac{Y\left(x_1,...,x_i+\Delta x_i,...,x_k\right)-Y\left(x_1,...,x_k\right)}{\Delta x_i} \tag{3.2}$$

The mean and standard deviation of the elementary effects u_i over the *r* levels for each factor produces three sensitivity measurements: μ, the mean of the elementary effects; μ^*, the mean of the absolute value of the elementary effects; and σ, the standard deviation of the elementary effects. μ^* and μ estimate the overall direct (first-order) effect of a factor. Both statistics are calculated because μ accounts for directionality of the effects (positive or negative) but can suffer from compensation of opposing sign effects leading to apparent low importance, while the absolute values in μ^* compensate for this artifact but do not provide directionality. σ estimates the higher-order characteristics of the parameter. Although elementary effects (u_i) are local sensitivity measurements, their moments μ, μ^* and σ are considered global measurements since they are computed across the variation space of all input factors, defined by their provability distributions (Saltelli et al., 2005, 2012).

3.2.6 Individual effect of PPCPs and mixture effect prediction based on additive CA model

The bioactivity of each of the 16 PPCPs at the 2 different light conditions was evaluated individually at each of the 3 dose levels defined by their statistical descriptors (*median of means, mean of maxima, maximum of maxima*) (see *QHTS* section). In addition, their bioactivity was also evaluated at 10 mgL^{-1} at the 2 different light conditions as a first tier toxicity screening. Complete dose-response curves were assessed for erythromycin (C10), ofloxacin (C11) and venlafaxine (C14). 6 independent experiments were performed with randomized experimental design. Experimental conditions and bioluminescence measurements were those explained for *QHTS* before. Mixture effect

predictions were computed based on the well-known predictive arrangement of CA equation as described in (Faust et al., 2001) (details in S3.1, section 3.3).

3.2.7 Effects of selected mixtures on experimental benthic microbial communities

An overview of the ecological scaling-up experiment involving experimental benthic microbial communities can be found in Fig. 3.6. (see later, under Results) River benthic microbial community *inocula* were obtained from a nearby unpolluted stream (Llémena River, Girona, Spain). A set of 10–12 cobbles were collected from a riffle area, and scraped for their biofilm microbial communities. The inocula were used to colonize rough glass substrata in laboratory conditions for 15 days. Nutrients, light and temperature were controlled (details in S3.2). Microbial communities were exposed during 7 days to 3 low-dose PPCP mixtures (Mix16, Mix16-4, and Mix16/10). Mix 16 was the most potent of the 180 mixtures (See S3.1, section 2.2.1). Mix 16-4 was identical to Mix 16 in components and doses except without the PPCPs C16, C3, C10 and C5, while Mix 16/10 was a 10-fold dilution of Mix 16. The effect of the mixtures was evaluated on a series of community level metabolic end-points (the photosynthetic parameters Fo; the dark-adapted basal fluorescence; F, the light-adapted steady state fluorescence; Ymax, the maximum photosynthetic efficiency of PSII and Yeff, the effective quantum yield of PSII; as well as the extracellular enzymatic activities β-glucosidase and alkaline phosphatase) that covered both autotrophic and heterotrophic global fitness indicators suited to study the effects of chemical pollution on freshwater benthic microbial communities (Ricart et al., 2009; Corcoll et al., 2012). Further details of experimental methods can be found in S3.2.

3.2.8 Experimental design and statistical analysis

Basic quality control of data and data analysis were performed in R version 3.1.2 and R-Studio, version 0.98.1091 (see S3.1, section 1.2.1 for details). For the QHTS experiments, sample sizes for treatments were fixed to $n = 6$. Analysis of Variance (ANOVA) was used to study difference of means. Two sided test was used with a minimum testing level for statistical significance (alpha) set to 0.05, with exact *p-values* reported in the text and figures. When multiple testing was performed, Tukey's 'Honest Significant Difference' method with a correction for unbalance experimental design

(Herberich et al., 2010) was used. When multiple testing was limited to the comparison of treatments with a single reference, the correction of Dunnet was used (Dunnett, 1955). Power (1-β) in all ANOVA analysis was > 0.8 for relevant effect sizes (see S3.1 for detail). Bootstrapped 95% confidence intervals were calculated by the bias-corrected and accelerated interval (bca) method (Davison and Hinkley, 1997) (see S3.1, section 2.2.1 for details). EEs method computation was performed using the enhanced sampling for uniformity (eSU) approach (Khare et al., 2015) with a publicly-available MATLAB toolbox (eSU) (see S3.1, section 2.2.3 for details). Dose response curves and derived parameters were computed using the *drc* package for R (Ritz and Streibig, 2005). The mixture effect predictions according to the CA model were computed using a freely-available R-script developed by the authors (R Scripts) (see S3.1, section 3.4 for details). Analysis of CA model fitness with observed data was performed using the publicly-available FITEVAL software implemented in MATLAB (FITEVAL; Ritter and Muñoz-Carpena, 2013). For the model benthic microbial community experiments, sample sizes for treatments were fixed to n = 3. Time-dependent multivariate responses of the freshwater benthic experimental communities were analyzed using Multivariate Generalized Linear Models (GLM_{MV}) (Szöcs et al., 2015) with the "mvabund" package for R, version 3.10.4 (Wang et al., 2012). Statistical significance of individual or nested GLM_{MV} model fits was evaluated by Analysis of Deviance (Warton, 2011) and multivariate test statistics were constructed using a Wald statistic (Wang et al., 2012), where *p*-values were approximated by resampling rows by the method of residual permutation as described in (Szöcs et al., 2015) (see S3.1, section 4 for detail). Power was in general > 0.76 for relevant effect sizes. Extended information on the performed analysis as well as a non-exhaustive list of R packages used in the study can be found in S3.1.

3.3 RESULTS AND DISCUSSION

3.3.1 Generating a low-dose PPCP mixture experimental design based on the EE method

For a total of 17 input factors (16 PPCPs and light intensity), the EEs sampling produced an array of 180 unique mixtures. The selected set of PPCPs included most families of pharmaceutical pollutants occurring broadly in freshwaters such as antibiotics, lipid regulators, stimulants, analgesics, hypertension regulators and psychiatric drugs (Aus der Beek et al., 2015; Hughes et al., 2013). Individual PPCP doses in the mixtures ranged from 25.5 ngL^{-1} to 40780.0 ngL^{-1}, differing by nearly 3 orders of magnitude along their 3 selected environmentally realistic discrete dose levels (*median of means, mean of maxima and maximum of maxima*, Fig. 3.2A). The frequency of input factors levels in the mixtures was near uniform (Fig. 3.2B) honoring the discrete uniform (DU) sampling probability distribution used in GSA-Sampling (see methods). In addition, mean dose distribution of the 16 PPCPs along the 180 mixtures occurred in the ngL^{-1} to μgL^{-1} range defining a robust exposure-oriented array of environmentally realistic dose combinations (Fig. 3.2C). The total PPCP doses of the mixtures presented a bimodal frequency distribution (Fig. 3.2D) with a minimum total dose of 25490 ngL^{-1} and a maximum dose of 123500 ngL^{-1}, indicating a slight bias towards the maximum values of environmental occurrence (Aus der Beek et al., 2015; Hughes et al., 2013). This is a drawback of the inter-level uniformity of dose distance required to optimize GSA-screening computation. However, it was considered appropriate based on the short term exposure duration (24h) of the *QHTS* experiment involving *A*. CPB4337.

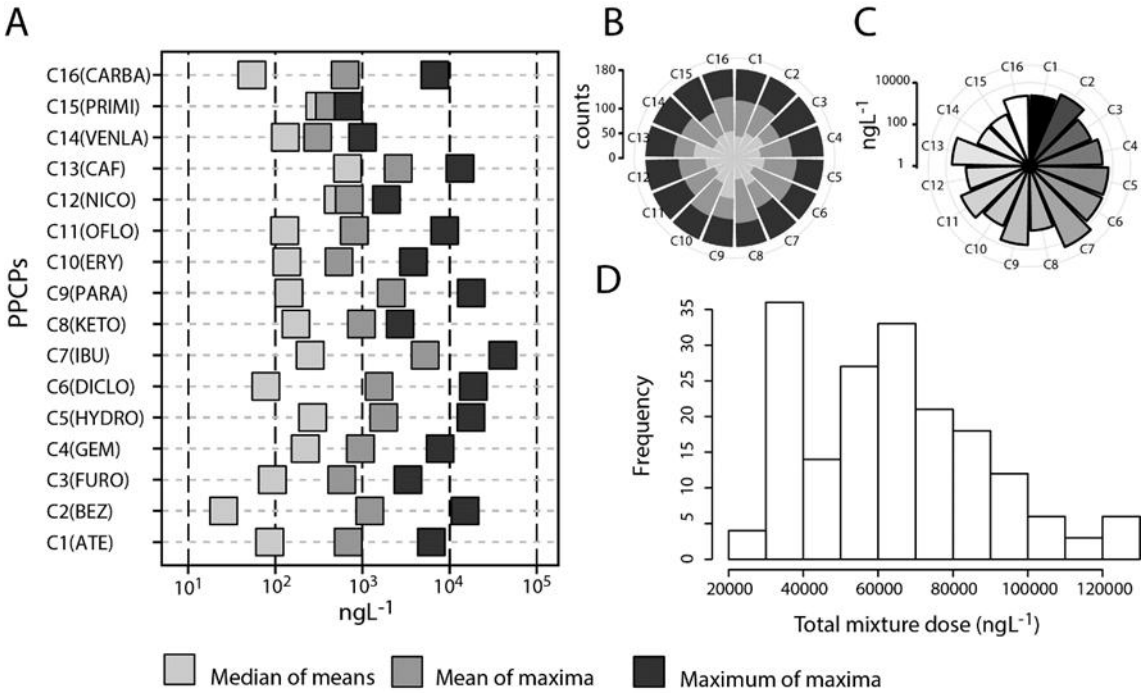

Figure 3.2 Low-dose PPCP mixture experimental design template. (A) Discrete dose levels (ngL^{-1}) of each of the 16 PPCPs (C1-C16) included in the low-dose mixtures. The 3 discrete levels were the *median of means*, the *mean of maxima*, and the *maximum of maxima* of each PPCP in freshwater. (B) Sampling frequency of the three discrete levels for the 16 PPCPs (C1 to C16) across the 180 mixtures. (C) Mean dose of each PPCP along the 180 low dose mixtures. (D) Frequency distribution of sum of PPCPs doses (ngL^{-1}) within each of the 180 low dose mixtures.

3.3.2 Exposure to low-doses of PPCPs produced significant sublethal effects

The *QHTS* results showed statistically significant alterations of the bioluminescence (surrogated end-point of metabolic toxicity (Sorensen et al., 2006; Rodea-Palomares et al., 2009)) of *A.* CPB4337 (Fig. 3.3A; One-Way ANOVA $p < 0.001$). The response of the organism to both PPCPs alone or in mixtures was significantly different (one-way ANOVA, Tukey HSD $p< 0.001$) (Fig. 3.3B). In fact, the median response of *A.* CPB4337 after the exposure to individual PPCPs shifted to an increased bioluminescence (hormesis (Calabrese and Baldwin, 2003)) while exposure to PPCP mixtures produced a median response towards a reduction of the bioluminescence signal (metabolic toxicity).

The median effect of a substantial number of mixtures (67 out of 180) was significantly different from the control median response as shown by the no overlapping of the

bootstrapped 95% confidence intervals (Krzywinski and Altman, 2013) (Fig. 3.3C). Overall, the observed sublethal mixture exposure to PPCPs was in the *grey-zone* of the dose-response curves (Kortenkamp et al., 2009) (median and maximum bioluminescence inhibition of 6.25% and 21.5%, respectively). The magnitude of the observed mixture sublethal effects (lower that 30% effect, Fig. 3.3B) are in good agreement with a growing body of literature reporting significant individual or mixture sublethal effects of PPCPs at low realistic doses (ngL^{-1} to μgL^{-1}) in a variety of organisms (Richards et al., 2004; Galus et al., 2013; Pomati et al., 2006; JM et al., 2014; Pomati et al., 2008; Brodin et al., 2013; Carvalho et al., 2014; Madureira et al., 2012; Chung et al., 2011). The non-chemical factor light intensity did not affect individual exposure to PPCPs (one-way ANOVA $p = 0.132$) (Fig. 3.3C), but did in mixture exposures ($p = 0.000198$) (Fig. 3.3D), indicating that light intensity may be a factor playing a significant role in mixture effects of PPCPs to *A.* CPB4337.

Light intensity is a critical factor not only for the metabolic activity of primary producers, but for the environmental fate, transformation and bioactivity of many chemicals including PPCPs (Stahl Jr. et al., 2013; Boxall, 2010; Yan and Song, 2014). However, the interaction of light, as that of other environmental factors, on the ecological effects of PPCPs and other chemical pollutants is still an unresolved issue in terms of global significance (Landis et al., 2014; Artigas et al., 2012).

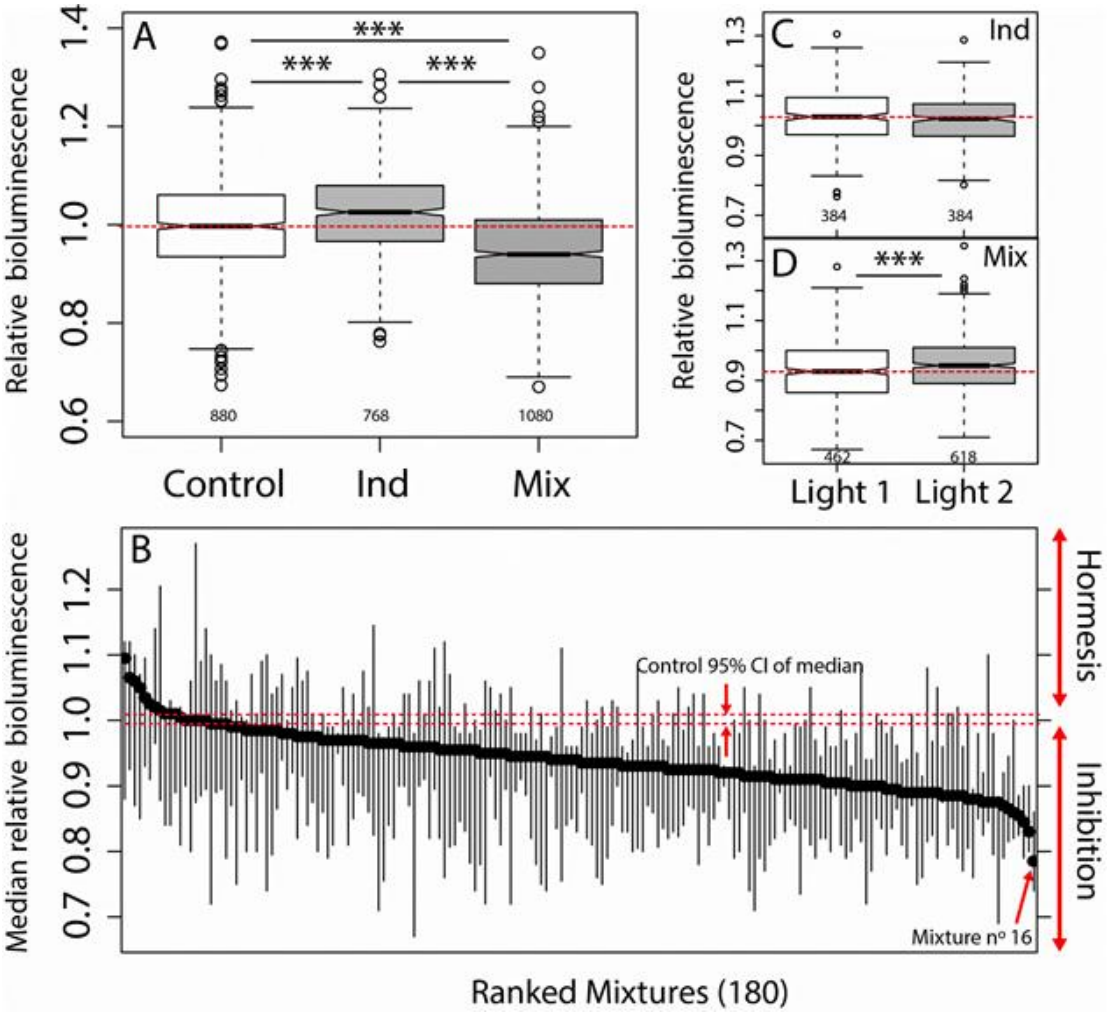

Figure 3.3 Exposure to *low-doses* of PPCPs produced significant sublethal effects. (A) Notched box-plot for relative bioluminescence of *A.* CPB4337 control observations (n =880), individual PPCP exposure (Ind) (n =768) and exposure to mixtures (Mix) (n =1080). (B) Median relative bioluminescence level of *A.* CPB4337 exposed to the 180 mixtures with respect to control levels (relative bioluminescence = 1). Mixtures are ranked in decreasing order based on median relative bioluminescence values. Vertical lines are bootstrapped (n = 999) 95% Confidence Intervals for the median. Horizontal red dashed lines are bootstrapped 95% Confidence Intervals for control median relative bioluminescence level (n = 999). The most potent mixture, no. 16, is highlighted. (C, D) Notched box-plots sorted by light intensity (L1 and L2) for relative bioluminescence of *A.* CPB4337 exposed to individual PPCPs (Ind) (n =768) and mixtures of PPCPs (Mix) (n =1080), respectively. The notches extend to +/-1.58 IQR/$n^{1/2}$ (IQR: interquartile range), where no overlapping of notches among boxes offers evidence of statistically significant differences among their medians (Mcgill et al., 2012). Statistically significant differences were tested by one-Way ANOVA and marked as follows: '***' 0.001 '**' 0.01 '*' 0.05 '·' 0.1.

3.3.3 The classical additive mixture approach does not predict the sublethal effects of low-dose PPCPs mixtures

According to *Loewe* additivity (Loewe, 1928), the foundation of the mixture Concentration Addition (CA) null model (Kortenkamp et al., 2009), each mixture component contributes to the total mixture effect with fractions of doses that can be summed up if the shapes of each mixture component's individual dose response curve is known (Faust et al., 2001). A key theoretical assumption of CA is that infinitely low doses result in infinitely decreasing effects. Therefore, mixture components below a statistical threshold of effect (No Observed Effect Concentration, NOEC) can still contribute to mixture effects, but in a linear and additive way (Kortenkamp et al., 2009). An important practical limitation of CA is that only chemicals individually displaying dose-response curves can be considered in the model (Junghans et al., 2006; Rodea-Palomares et al., 2015).

A first-tier high-dose (10 mgL^{-1}) benchmarking of the toxicity of the 16 PPCPs was performed to identify candidate PPCPs for dose-response curve derivation (Fig. 3.4A). From the 16 PPCPs, only two antibiotics, C10 (erythromycin) and C11 (ofloxacin), resulted in strong (near 90%) bioluminescence inhibition of *A.* CPB4337. C14 (venlafaxine) and C8 (ketoprofen) resulted in weak (less than 20%) inhibition and hormesis, respectively (one-way ANOVA, *Dunnet* test, $p < 0.05$).

Dose-response curves were derived for those PPCPs exhibiting inhibition (C10, C11 and C14, Fig. 3.4B) and the rest of the PPCPs were ignored for further mixture effect modeling based on CA (Backhaus and Faust, 2012). Based on the unique C10:C11:C14 ratio in each of the 180 low-dose mixtures, predicted mixture dose-response curves were modeled (Fig. 3.4C) and additive mixture effects were predicted and compared to the observed experimental mixture effects (Fig. 3.4D). CA predicted near no effect (from 0 to 0.026% inhibition) for all the 180 mixtures in contrast with the observed range of experimental effects (inset in Fig. 3.4D).

The departure of data from the 1:1 reference line (Fig. 3.4D) confirms the inability of the additive null models to predict the observed effects (NSE = -1.766), where NSE = 1 represents perfect agreement (Ritter and Muñoz-Carpena, 2013).

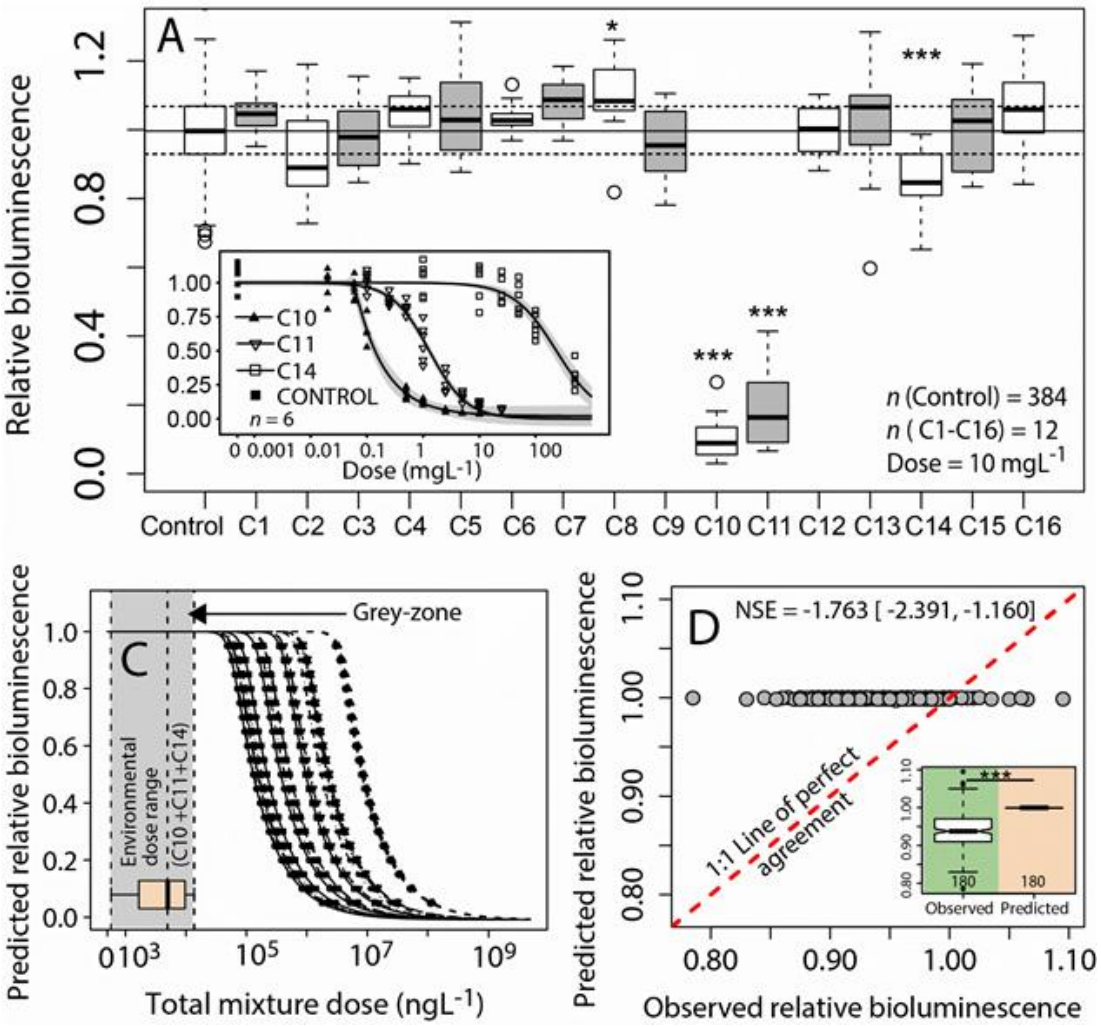

Figure 3.4 The Null additive mixture models does not predict the sublethal effects of low dose PPCP mixtures. (A) Individual effects of PPCPs (C1 to C16) on *A.* CPB4337 relative bioluminescence at 10 mgL^{-1}. Horizontal lines represent the control´s median, Q25 and Q75 relative bioluminescence. Significance codes: '***' 0.001 '**' 0.01 '*' 0.05. (B) Dose-response curves for factors C10 (erythromycin), C11 (ofloxacin) and C14 (venlafaxine). Lines and symbols represent fitted non-linear models (5-parameters log-logistic models) and experimental data, respectively. (C) Modeled mixture dose-response curves for 21 unique C10:C11:C14 ratios present in the sampled 180 PPCP mixtures. The Boxplot shows the 180 low dose mixture´s dose range (D) Observed vs predicted 1:1 plot (Ritter and Muñoz-Carpena, 2013) for the 180 low-dose mixture effects as predicted by the Concentration Addition (CA) additivity model. Note that only the contributions of C10 (erythromycin), C11 (ofloxacin) and C14 (venlafaxine) are considered by the models. NSE: Nash- Sutcliffe Efficiency coefficient with 95% CI in brackets. Inset shows the distribution of observed and predicted luminescence values for the 180 mixtures.

3.3.4 GSA-QHTS identified hidden drivers of low-dose mixture sublethal effects

The graphical representation of GSA statistics (μ, σ) or ($\mu*$, σ) in a Cartesian plane provides a ranking of input factor importance or direct effects (i.e separation from origin along the μ–axis), and interaction effects (i.e separation from origin along the σ–axis).

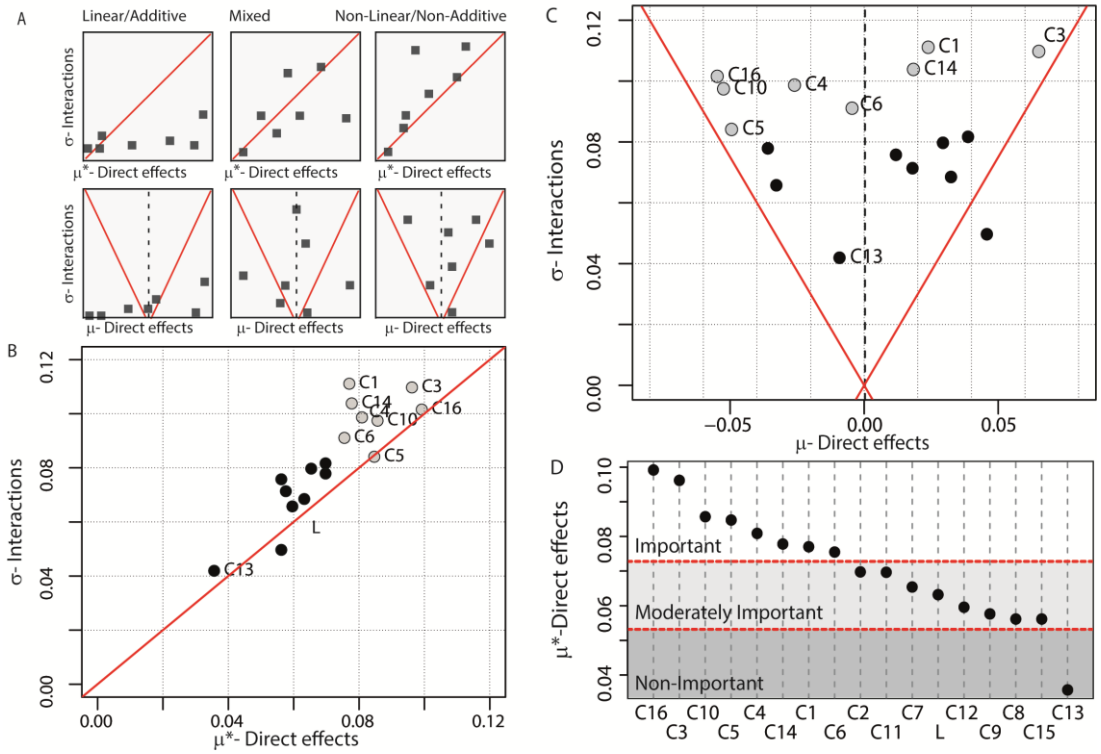

Figure 3.5 *GSA-QHTS* is able to characterize global drivers of low-dose mixture sublethal effects. (A) GSA schematic representation of input factor distributions along $\mu*$–σ and μ–σ Cartesian planes for Linear/Additive, Mixed, and Non-Linear/Non-Additive Systems. (B, C) GSA results in the $\mu*$–σ and μ–σ Cartesian plots, respectively, for the 17 input factors (16 PPCPs (C1 to C16) and Light intensity (L)) analyzed in the present study. Red lines indicate the limits for linear-additive systems. For clarity, only important and non-important input factors are identified in the figure. Hollow symbols indicate important factors (larger separation from the $\mu*$–σ or μ–σ plane origin). (D) Ranked input factors by importance ($\mu*$) showing the proposed limits (red dashed lines) for important, moderately important and non-important factors.

According to the general distribution pattern of the input factors on the $\mu*$ - σ and μ - σ Cartesian planes, systems can be generally classified as Linear/Additive, Mixed, and

Non-linear/Non-additive (Fig. 3.5A) (Morris, 1991). The transition to a Non-linear/Non-additive system is denoted by all the input factors systematically scoring above the 45^{o} line in the μ^{*} - σ plot (Chu-Agor et al., 2011), and in between the $\mu \pm 2\sigma$ reference lines in the μ - σ plot (Morris, 1991) (right panels in Fig. 3.5A). Based on this, it is clear from Fig. 3.5B, C that in our experiments, the response to low dose mixtures of PPCPs was non-linear/non-additive.

The comparison between direct elementary effects calculated as average of absolute values (μ^{*}, Fig. 3.5B) or of with their individual signs (μ, Fig. 3.5C) indicates that effects of some of the PPCPs were also non-monotonic (i.e. could increase or decrease bioluminescence consecutively at increasing doses). For example, C6 in Fig. 3.5B is shown among the group of most important factors (rightmost in x-axis) based on absolute value effects (μ^{*}) while in Fig. 3.5C it is shown close to 0 (no direct effects) based on the arithmetic mean of effects (μ), i.e. +/- effects cancel out in the mean. According to their ranked μ^{*} direct effects (Fig. 3.5D) only half of the chemicals were most important in controlling low dose sublethal effects of the PPCP mixtures, while one of them (C13) was negligible. Interestingly, half of the chemicals exhibited overall effect of bioluminescence inhibition ($\mu < 0$), and the other half of bioluminescence induction or hormesis ($\mu > 0$).

As a complementary line of evidence, Two-Way ANOVA was performed for each group of input factors (most important: C16, C3, C10, C5, C4, C14, C1, C6; and less important: C11, C7, L, C12, C9, C8, C15 and C13). In the most important group, 7 of the 8 factors were found to participate in first or second order significant terms (ANOVA, $p < 0.05$), whereas no significant term was found to any first or second order term for the less important factors group (S3.1, section 2.2.4). Although ANOVA only explored first and second order terms, the results corroborate the ranking of factor importance and interactions identified by EEs, where the latter also considers simultaneously higher order interactions (Saltelli et al., 2005).

Both the EEs method and Two-Way ANOVA confirm that there was structured information in the sublethal effects observed with the 180 low-dose PPCP mixtures, and not just stochastic noise as assumed by the *grey-zone* hypothesis (Kortenkamp et al.,

2009). In addition, the EEs method revealed (and ANOVA confirmed) that the nature of sublethal effects from low-dose PPCP mixtures were non-linear/non-additive, which explains why additive null models for chemical mixtures failed in their predictions (Fig. 3.4D). According to Fig. 3.4A, only 2 of the 16 PPCPs (erythromycin (C10) and ofloxacin (C11)), and to a lesser extent venlafaxine (C14) were potential candidates to drive any low-dose mixture effect.

However, despite being important factors (especially erythromycin, which ranked 3th in global importance according to *GSA-QHTS*, Fig. 3.5C), 7 other PPCPs were found to be as, or even more, important in low-dose mixtures (Fig. 3.5D). These mixture drivers remained hidden to the high-dose benchmarking (Fig. 3.4A), and therefore hinder the predictions of the null additive models (Fig. 3.4D). These results indicate that a simple linear/additive chemical risk assessment approach may overlook a substantial number of chemicals that may be critical under real low-dose environmental conditions. *GSA-QHTS* advances preliminary observations suggesting non-linear/non-additive effects resulting from low-dose mixtures of PPCPs (Pomati et al., 2008; Carvalho et al., 2014; JM et al., 2014). The new framework adds substantial value by allowing a robust, global and comparative understanding of chemical drivers and their effects that remained defective until now (Rudd et al., 2014; Teuschler et al., 2002; Pomati et al., 2008; Carvalho et al., 2014).

Finally, the EEs method was effective when discriminating the importance of chemical factors and other non-chemical stressors. For example, in spite of the apparent significant contribution of light to low-dose PPCP mixture effects (Fig. 3.3D), its global importance was negligible (Fig. 3.5D). This provides a direct comparison of diverse factors in a common scale metric, addressing an unresolved, yet urgent, demand in ecotoxicology (Segner et al., 2014; Beketov and Liess, 2012; Artigas et al., 2012).

3.3.5 Important drivers of mixture bioactivity identified by *GSA-QHTS* are also relevant at higher ecological complexity scales

We performed an ecological scaling-up mesocosm experiment to assess the generalizability of the factors identified as important by the *GSA-QHTS* (Fig. 3.6).

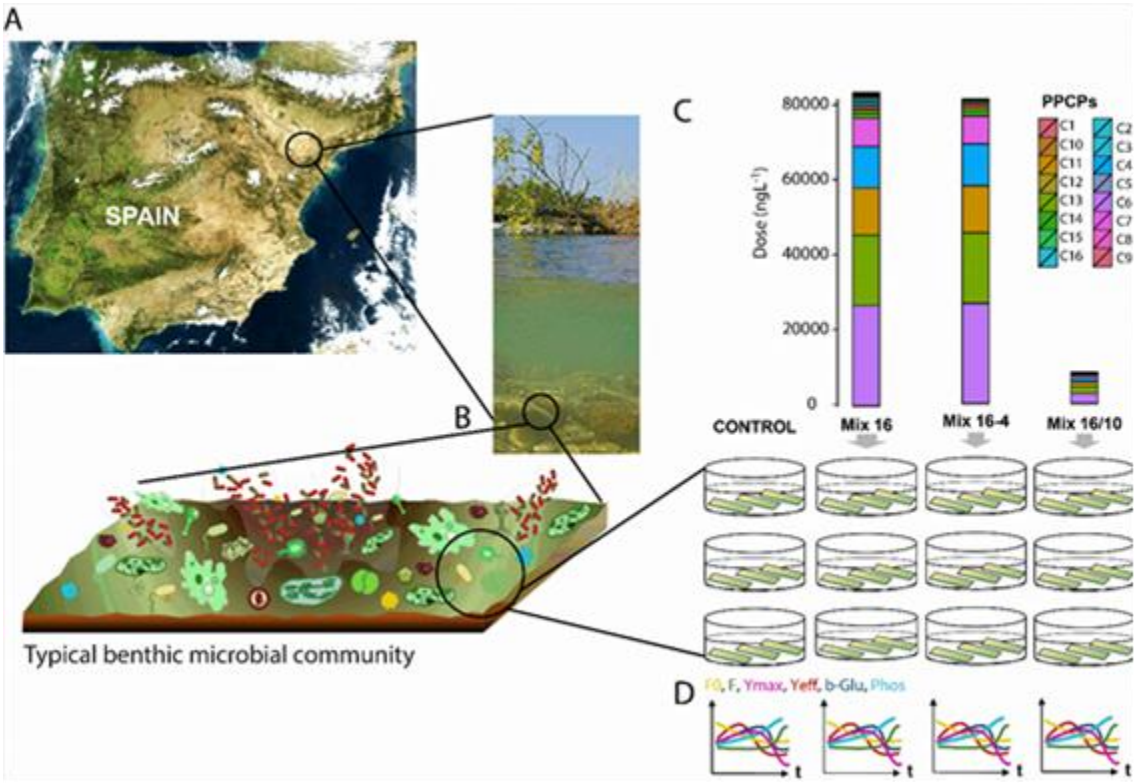

Figure 3.6. Ecological scaling-up experiment. (A) River benthic microbial community inocula were obtained from a nearby unpolluted stream in the Llémena River (Girona, Spain). Schematic benthic microbial community modified from (Egan et al., 2013) (B) A set of cobbles were scraped for their microbial communities, which were used to colonize rough glass substrata in laboratory conditions. (C) Experimental microbial communities were exposed to 3 low dose PPCP mixtures (Mix16, Mix16-4 and Mix16/10, see Methods). (D) Selected community level endpoints (F0, F, Ymax, Yeff, β-Glu and Phos, see Methods) covered both autotrophic and heterotrophic global fitness indicators and were monitored as a function of time.

Multivariate Generalized Linear Models (GLM_{MV}) (Szöcs et al., 2015) revealed a statistically significant interaction between the factors *treatment* (Control, Mix16, Mix16-4 and Mix16/10) and *time* (model 1 in Table 3.1; ANOVA, Wald $p = 0.03$), but no effects from *treatment* or *time* separately. Changes in model communities were expressed mainly on the effective quantum yield of photosystem II, (Yeff) and *β*-glucosidase activity (*β*-Glu) (S3.1, Section 4), indicating relevant effects on both the autotrophic and heterotrophic components of the microbial community.

Table. 3.1. ANOVA Table summaries of multivariate generalized linear models (GLM_{MV}). GLM_{MV} models were fitted to the response of experimental freshwater benthic communities exposed to selected PPCP low-dose mixtures and sequential analysis of deviance (ANODEV) was performed. MV data used to build each GLMMV include the six community-level metabolic end points measured: F_0, the dark-adapted basal fluorescence; F, the light-adapted steady state fluorescence; Ymax, the maximum photosynthetic efficiency of photosystemII (PSII); Y_{eff}, the effective quantum yield of PSII; beta-Glu, beta-glucosidase; and Phos, alkaline phosphatase. The experiment included two factors: treatment (four levels) and time of exposure (three levels). Treatment levels were as follows: control (n = 5);Mix 16 (n = 3), PPCPmixture 16; Mix 16-4 (n = 3),mixture 16 without the fourmost important PPCPs from GSA results; and Mix 16/10 (n = 3), mixture 16 diluted 10 times. Time levels were as follows: 24, 36, and 120 hours of exposure for each treatment (n = 4). Therefore, the total number of samples was n = 42. The null hypothesis (H_0) for the Wald test is that the reduction in model residual deviance is 0. Res. df, residual degrees of freedom; df diff., degrees of freedom difference added by the sequential inclusion of each term of the model.

GLM_{MV} Model	Res. *df*	*df*. diff	Wald	*p*(>Wald)[2]
model 1 (full model): *treatment*time*				
Intercept	41			
treatment	38	3	6.59	0.45
time	36	2	13.05	0.86
*treatment*time*	30	6	17.16	0.01**
model 2 (control only): *time*				
Intercept	14			
time	12	2	10.03	0.01**
model 3 (Mix16 only): *time*				
Intercept	8			
time	6	2	15.75	0.54
model 4 (Mix16-4 only): *time*				
Intercept	8			
time	6	2	162.2	0.04*
model 5 (Mix16/10 only): *time*				
Intercept	8			
time	6	2	18.18	0.61

Significance codes are '**' 0.01, '*' 0.05.

Mixture effects were unraveled by fitting individual GLM_{MV} (models 2 to 5 in Table 3.1) with *time* as an explanatory factor. We found that *time* was significant in Control and Mix 16-4 treatments (ANOVA, Wald p = 0.01 and 0.04, respectively), but not in Mix 16 and Mix 16/10 (p = 0.54 and p = 0.61, respectively), indicating that the 4 most important PPCPs in the full Mix16 blocked the temporal evolution of the metabolic processes of the freshwater benthic communities.

The insensitivity to *time* reflects reduced dynamic behavior and increased temporal autocorrelation that are common symptoms of microbial community stress, lethality and ecological shifts (Dai et al., 2012; Carpenter et al., 2008; Faust et al., 2015). Interestingly, the removal of the 4 important PPCPs was more effective in preventing effects than a 10-fold dilution (Mix 16/10), even although they accounted for less than a 3 % of the total PPCPs dose of the mixture (Fig. 3.6). These results confirms that sublethal effects at the population level can drive disruptive effects at the community level (Carvalho et al., 2014; Rohr et al., 2008).

3.3.6. Main findings

Contrary to current scientific practice (Kortenkamp et al., 2009; Backhaus and Faust, 2012; Altenburger et al., 2013), typical high-dose benchmarking failed to identify the complete set of low-dose mixture effect drivers and the bioactivity of the mixtures was not predicted by the null additive mixture models. The novel *GSA-QHTS* framework was effective at screening the importance of PPCP pollutants at environmentally realistic low-dose mixtures and to identify the main drivers of PPCP sublethal effects. *GSA-QHTS* revealed that observed mixture effects were not random, but driven by a specific subset of PPCPs via nonlinear and/or non-additive effects. This confirms previous evidence of unexpected low-dose effects of PPCPs (Laetz et al., 2013; Carvalho et al., 2014; Pomati et al., 2008; Madureira et al., 2012; Chung et al., 2011) and offers an alternative explanation to the source of the mixture effects typically unaccounted for by additivity assumptions in environmental samples (Escher et al., 2013). The ecological scaling-up experiment illustrated how these hidden PPCPs identified by *GSA-QHTS* at the population level also were responsible for disruptive effects at the community level. Since real world exposure to chemical pollution of natural systems is often dominated by low-dose complex mixtures combined with other biotic and abiotic stressors, we may underestimate the actual risk of chemical pollution with current methods.

3.3.7 Limitations and further research

The results of this work are limited to the specific biological system used as model and provide a first tier phenomenological screening for the effect of low dose of PPCPs in freshwater systems. Further research should include other biological systems in order to

get a wider picture of the generalizability of our findings. An identification of the mechanisms behind the effects of the focal pharmaceuticals requires extension of the *GSA-QHTS* to receptor-mediated biological tests designed to unravel mechanistic pathways of stressor effects (Huang et al., 2016). GSA results are sensitive to a meaningful *a-priori* and *realistic* selection of both input factors and ranges, or GSA may result in misleading conclusions (Saltelli et al., 2012, 2005). A limitation of the present application of the *GSA-QHTS* is that the EEs method, due to its reduced sampling intensity, provides a *qualitative* ranking of the relative importance of the drivers studied. As life sciences high-throughput capacity advance, alternative *quantitative* GSA variance-decomposition methods (Cukier et al., 1978; Saltelli et al., 1999; Sobol, 1993) that require a larger number of samples can be implemented. This will allow the quantitative apportioning of the total variance of the effects onto the individual or combinations of input factors studied (Saltelli et al., 2012, 2005). Armed with the identification of main drivers provided by the GSA-QHTS approach and mechanistic understanding based on receptor mediated analysis, further research should include the development of new conceptual and modelling approaches to predict and integrate non-linear/non-additive effects of chemical pollution within the "big picture" of large-scale ecological systems (Beketov and Liess, 2012; Artigas et al., 2012).

3.4 CONCLUSIONS

As a reliable and robust approach, GSA-QHTS could be of interest to scientists designing experiments to test effects of combined stressors, not only chemical but also physical and biological stressors, therefore crossing the border of different disciplines. The present work has foundational implications not only for ecotoxicology, but also biological and medical sciences as it provides a new experimental framework to approach complexity under realistic conditions.

3.5 REFERENCES

Altenburger, R., Backhaus, T., Boedeker, W., Faust, M., and Scholze, M. (2013). Simplifying complexity: Mixture toxicity assessment in the last 20 years. Environ Toxicol Chem 32: 1685–1687.

Artigas, J. et al. (2012). Towards a renewed research agenda in ecotoxicology. Environmental Pollution 160: 201–206.

Aus der Beek, T., Weber, F.-A., Bergmann, A., Hickmann, S., Ebert, I., Hein, A., and Küster, A. (2015). Pharmaceuticals in the environment - global occurrences and perspectives. Environmental toxicology and chemistry / SETAC.

Backhaus, T. (2014). Medicines, shaken and stirred: a critical review on the ecotoxicology of pharmaceutical mixtures. Philosophical transactions of the Royal Society of London. Series B, Biological sciences 369: 20130585-.

Backhaus, T. and Faust, M. (2012). Predictive environmental risk assessment of chemical mixtures: a conceptual framework. Environmental science & technology 46: 2564–2573.

Beketov, M.A. and Liess, M. (2012). Ecotoxicology and macroecology – Time for integration. Environmental Pollution 162: 247–254.

Boxall, A.B.., Fogg, L.., Blackwell, P.., Kay, P., Pemberton, E.., and Croxford, A. (2004). Veterinary medicines in the environment. Reviews of environmental contamination and toxicology 180: 1–91.

Boxall, A.B.A. et al. (2012). Pharmaceuticals and personal care products in the environment: what are the big questions? Environmental health perspectives 120: 1221–1229.

Boxall, A.B.A. (2010). Veterinary medicines and the environment. Handbook of Experimental Pharmacology 199: 291–314.

Brodin, T., Fick, J., Jonsson, M., and Klaminder, J. (2013). Dilute concentrations of a psychiatric drug alter behavior of fish from natural populations. Science (New York, N.Y.) 339: 814–815.

Calabrese, E.J. and Baldwin, L.A. (2003). Toxicology rethinks its central belief. Nature 421: 691–692.

Carpenter, S.R., Brock, W.A., Cole, J.J., Kitchell, J.F., and Pace, M.L. (2008). Leading indicators of trophic cascades. Ecology letters 11: 128–138.

Carvalho, R.N. et al. (2014). Mixtures of chemical pollutants at European legislation safety concentrations: how safe are they? Toxicol Sci 141: 218–233.

Chu-Agor, M.L., Muñoz-Carpena, R., Kiker, G., Emanuelsson, A., and Linkov, I. (2011). Exploring vulnerability of coastal habitats to sea level rise through global sensitivity and uncertainty analyses. Environmental Modelling & Software 26: 593–604.

Chung, E., Genco, M.C., Megrelis, L., and Ruderman, J. V (2011). Effects of bisphenol A and triclocarban on brain-specific expression of aromatase in early zebrafish embryos. Proceedings of the National Academy of Sciences 108: 17732–17737.

Corcoll, N., Bonet, B., Leira, M., Montuelle, B., Tlili, A., and Guasch, H. (2012). Light History Influences the Response of Fluvial Biofilms to Zn Exposure. Journal of Phycology 48: 1411–1423.

Cukier, R.I., Levine, H.B., and Shuler, K.E. (1978). Nonlinear sensitivity analysis of multiparameter model systems. Journal of Computational Physics 26: 1–42.

Dai, L., Vorselen, D., Korolev, K.S., and Gore, J. (2012). Generic indicators for loss of resilience before a tipping point leading to population collapse. Science (New York, N.Y.) 336: 1175–1177.

Daughton, C.G. and Ternes, T.A. (1999). Pharmaceuticals and personal care products in the environment: agents of subtle change? Environmental health perspectives 107 Suppl: 907–938.

Davison, A.C. and Hinkley, D. V (1997). Bootstrap Methods and Their Application R. Gill, B.D. Ripley, S. Ross, M. Stein, and D. Williams, eds (Cambridge University Press).

Dunnett, C. (1955). A multiple comparison procedure for comparing several treatments with a control. Journal of the American

Statistical Association 50: 1096–1121.

Egan, S., Harder, T., Burke, C., Steinberg, P., Kjelleberg, S., and Thomas, T. (2013). The seaweed holobiont: understanding seaweed-bacteria interactions. FEMS microbiology reviews 37: 462–76.

Escher, B.I., van Daele, C., Dutt, M., Tang, J.Y.M., and Altenburger, R. (2013). Most Oxidative Stress Response In Water Samples Comes From Unknown Chemicals: The Need For Effect-Based Water Quality Trigger Values. Environmental Science & Technology 47: 7002–7011.

eSU.

Fagin, D. (2012). Toxicology: The learning curve. Nature 490: 462–5.

Faust, K., Lahti, L., Gonze, D., de Vos, W.M., and Raes, J. (2015). Metagenomics meets time series analysis: unraveling microbial community dynamics. Current Opinion in Microbiology 25: 56–66.

Faust, M., Altenburger, R., Backhaus, T., Blanck, H., Boedeker, W., Gramatica, P., Hamer, V., Scholze, M., Vighi, M., and Grimme, L.H. (2001). Predicting the joint algal toxicity of multi-component s-triazine mixtures at low-effect concentrations of individual toxicants. Aquatic Toxicology 56: 13–32.

FITEVAL.

Galus, M., Kirischian, N., Higgins, S., Purdy, J., Chow, J., Rangaranjan, S., Li, H., Metcalfe, C., and Wilson, J.Y. (2013). Chronic, low concentration exposure to pharmaceuticals impacts multiple organ systems in zebrafish. Aquatic toxicology (Amsterdam, Netherlands) 132–133: 200–211.

González-Pleiter, M., Gonzalo, S., Rodea-Palomares, I., Leganés, F., Rosal, R., Boltes, K., Marco, E., and Fernández-Piñas, F. (2013). Toxicity of five antibiotics and their mixtures towards photosynthetic aquatic organisms: Implications for environmental risk assessment. Water Research 47: 2050–2064.

Halstead, N.T., McMahon, T.A., Johnson, S.A., Raffel, T.R., Romansic, J.M., Crumrine, P.W., and Rohr, J.R. (2014). Community ecology theory predicts the effects of agrochemical mixtures on aquatic biodiversity and ecosystem properties. Ecology Letters 17: 932–941.

Herberich, E., Sikorski, J., and Hothorn, T. (2010). A robust procedure for comparing multiple means under heteroscedasticity in unbalanced designs. PloS one 5: e9788.

Huang, R., Xia, M., Sakamuru, S., Zhao, J., Shahane, S.A., Attene-Ramos, M., Zhao, T., Austin, C.P., and Simeonov, A. (2016). Modelling the Tox21 10 K chemical profiles for in vivo toxicity prediction and mechanism characterization. Nature communications 7: 10425.

Hughes, S.R., Kay, P., and Brown, L.E. (2013). Global synthesis and critical evaluation of pharmaceutical data sets collected from river systems. Environmental science & technology 47: 661–677.

JM, Martín, P., Freire, P.F., Peropadre, A., and Hazen, M.J. (2014). Cytotoxic evaluation of a mixture of eight pollutants at environmental relevant concentrations. Revista de Toxicología 31: 172–175.

Junghans, M., Backhaus, T., Faust, M., Scholze, M., and Grimme, L.H. (2006). Application and validation of approaches for the predictive hazard assessment of realistic pesticide mixtures. Aquatic Toxicology 76: 93–110.

Khare, Y.P., Muñoz-Carpena, R., Rooney, R.W., and Martinez, C.J. (2015). A multi-criteria trajectory-based parameter sampling strategy for the screening method of elementary effects. Environmental Modelling & Software 64: 230–239.

Klaminder, J., Jonsson, M., Fick, J., Sundelin, A., and Brodin, T. (2014). The conceptual imperfection of aquatic risk assessment tests: highlighting the need for tests designed to detect therapeutic effects of pharmaceutical contaminants. Environmental Research Letters 9: 84003.

Kortenkamp, A., Backhaus, T., and Faust, M. (2009). State of the art report on mixture toxicity. Final Report to the European Commission under Contract Number 070307/2007/485103/ETU/D.1. (European Commission: Brussels, Belgium).

Krzywinski, M. and Altman, N. (2013). Points of significance: error bars. Nature methods 10: 921–2.

Laetz, C.A., Baldwin, D.H., Collier, T.K., Hebert, V., Stark, J.D., and Scholz, N.L. (2009). The synergistic toxicity of pesticide

mixtures: implications for risk assessment and the conservation of endangered Pacific salmon. Environ Health Perspect 117: 348–353.

Laetz, C.A., Baldwin, D.H., Hebert, V., Stark, J.D., and Scholz, N.L. (2013). Interactive neurobehavioral toxicity of diazinon, malathion, and ethoprop to juvenile coho salmon. Environ Sci Technol 47: 2925–2931.

Landis, W.G., Rohr, J.R., Moe, S.J., Balbus, J.M., Clements, W., Fritz, A., Helm, R., Hickey, C., Hooper, M., Stahl, R.G., and Stauber, J. (2014). Global climate change and contaminants, a call to arms not yet heard? Integr Environ Assess Manag 10: 483–484.

Loewe, S. (1928). Die quantitativen Probleme der Pharmakologie. Ergebnisse der Physiologie 27: 47–187.

Madureira, T.V., Rocha, M.J., Cruzeiro, C., Rodrigues, I., Monteiro, R.A.F., and Rocha, E. (2012). The toxicity potential of pharmaceuticals found in the Douro River estuary (Portugal): evaluation of impacts on fish liver, by histopathology, stereology, vitellogenin and CYP1A immunohistochemistry, after sub-acute exposures of the zebrafish model. Environmental toxicology and pharmacology 34: 34–45.

Mcgill, R., Tukey, J.W., and Larsen, W.A. (2012). Variations of Box Plots. The American Statistician.

Morris, M.D. (1991). Factorial sampling plans for preliminary computational experiments. Technometrics 33: 161–174.

Pomati, F., Castiglioni, S., Zuccato, E., Fanelli, R., Vigetti, D., Rossetti, C., and Calamari, D. (2006). Effects of a Complex Mixture of Therapeutic Drugs at Environmental Levels on Human Embryonic Cells. Environmental Science & Technology 40: 2442–2447.

Pomati, F., Orlandi, C., Clerici, M., Luciani, F., and Zuccato, E. (2008). Effects and Interactions in an Environmentally Relevant Mixture of Pharmaceuticals. Toxicological Sciences 102: 129–137.

R Scripts.

Ricart, M., Barceló, D., Geiszinger, A., Guasch, H., de Alda, M.L., Romaní, A.M., Vidal, G., Villagrasa, M., and Sabater, S. (2009). Effects of low concentrations of the phenylurea herbicide diuron on biofilm algae and bacteria. Chemosphere 76: 1392–1401.

Richards, S.M., Wilson, C.J., Johnson, D.J., Castle, D.M., Lam, M., Mabury, S.A., Sibley, P.K., and Solomon, K.R. (2004). Effects of pharmaceutical mixtures in aquatic microcosms. Environmental Toxicology and Chemistry 23: 1035.

Ritter, A. and Muñoz-Carpena, R. (2013). Performance evaluation of hydrological models: Statistical significance for reducing subjectivity in goodness-of-fit assessments. Journal of Hydrology 480: 33–45.

Ritz, C. and Streibig, J.C. (2005). Bioassay Analysis using R. Journal of statistical softhware 12: 17.

Rodea-Palomares, I., González-García, C., Leganés, F., and Fernández-Piñas, F. (2009). Effect of pH, EDTA, and anions on heavy metal toxicity toward a bioluminescent cyanobacterial bioreporter. Archives of Environmental Contamination and Toxicology 57: 477–487.

Rodea-Palomares, I., González-Pleiter, M., Martín-Betancor, K., Rosal, R., and Fernández-Piñas, F. (2015). Additivity and Interactions in Ecotoxicity of Pollutant Mixtures: Some Patterns, Conclusions, and Open Questions. Toxics 3: 342–369.

Rohr, J.R., Schotthoefer, A.M., Raffel, T.R., Carrick, H.J., Halstead, N., Hoverman, J.T., Johnson, C.M., Johnson, L.B., Lieske, C., Piwoni, M.D., Schoff, P.K., and Beasley, V.R. (2008). Agrochemicals increase trematode infections in a declining amphibian species. Nature 455: 1235–1239.

Rudd, M.A., Ankley, G.T., Boxall, A.B.A., and Brooks, B.W. (2014). International scientists' priorities for research on pharmaceutical and personal care products in the environment. Integr Environ Assess Manag 10: 576–587.

Sabbagh, G.J., Muñoz-Carpena, R., and Fox, G.A. (2013). Distinct influence of filter strips on acute and chronic pesticide aquatic environmental exposure assessments across U.S. EPA scenarios. Chemosphere 90: 195–202.

Saltelli, A., Ratto, M., Tarantola, S., and Campolongo, F. (2005). Sensitivity analysis for chemical models. Chem Rev 105: 2811–2828.

Saltelli, A., Ratto, M., Tarantola, S., and Campolongo, F. (2012). Update 1 of: Sensitivity Analysis for Chemical Models. Chemical Reviews 112: PR1-PR21.

Saltelli, a, Tarantola, S., and Chan, K.P.-S. (1999). A Quantitative Model-Independent Method for Global Sensitivity Analysis of Model Output. Technometrics 41: 39–56.

Segner, H., Schmitt-Jansen, M., and Sabater, S. (2014). Assessing the Impact of Multiple Stressors on Aquatic Biota: The Receptor's Side Matters. Environmental Science & Technology 48: 7690–7696.

Sobol, I.M. (1993). Sensitivity analysis for non-linear mathematical models. Mathematical Modelling and Computational 1: 407–414.

Sorensen, S.J., Burmolle, M., and Hansen, L.H. (2006). Making bio-sense of toxicity: new developments in whole-cell biosensors. Curr Opin Biotechnol 17: 11–16.

Stahl Jr., R.G., Hooper, M.J., Balbus, J.M., Clements, W., Fritz, A., Gouin, T., Helm, R., Hickey, C., Landis, W., and Moe, S.J. (2013). The influence of global climate change on the scientific foundations and applications of Environmental Toxicology and Chemistry: introduction to a SETAC international workshop. Environ Toxicol Chem 32: 13–19.

Szöcs, E. et al. (2015). Analysing chemical-induced changes in macroinvertebrate communities in aquatic mesocosm experiments: a comparison of methods. Ecotoxicology 24: 760–769.

Teuschler, L., Klaunig, J., Carney, E., Chambers, J., Conolly, R., Gennings, C., Giesy, J., Hertzberg, R., Klaassen, C., Kodell, R., Paustenbach, D., and Yang, R. (2002). Support of science-based decisions concerning the evaluation of the toxicology of mixtures: a new beginning. Regul Toxicol Pharmacol 36: 34–39.

Wang, Y., Naumann, U., Wright, S.T., and Warton, D.I. (2012). mvabund - an R package for model-based analysis of multivariate abundance data. Methods in Ecology and Evolution 3: 471–474.

Warton, D.I. (2011). Regularized sandwich estimators for analysis of high-dimensional data using generalized estimating equations. Biometrics 67: 116–23.

Whitton, B.A. and Potts, M. (2000). The Ecology of Cyanobacteria: Their Diversity in Time and Space. Kluwer Academic Publishers. Netherlands: 37–59.

Yan, S. and Song, W. (2014). Photo-transformation of pharmaceutically active compounds in the aqueous environment: a review. Environmental science. Processes & impacts 16: 697–720.

CHAPTER 4: INTRACELLULAR FREE Ca^{2+} SIGNALS ANTIBIOTIC EXPOSURE IN CYANOBACTERIA

4.1 INTRODUCTION

Cyanobacteria are ancient organisms dating from the Precambrian era which constitutes a phylogenetically diverse group of photosynthetic prokaryotes (Rippka et al. 1979) (Potts 1994). Increasing evidence indicate that they are the ancestors of chloroplasts of photoautotrophic eukaryotes (Falcón et al. 2010). They are ubiquitous organisms occupying a diverse range of habitats; (Potts 1994) they have a crucial role both in the N and C cycles and as primary producers; and any negative impact on this group may also negatively affect organisms of higher trophic levels. As any other living being, cyanobacteria possess signal transduction systems to sense and respond to changes in their environment. Intracellular messengers are basic component of the cellular signal transduction toolkits.

Intracellular free Ca^{2+}, $[Ca^{2+}]_i$, is probably the most universal of second messengers in living organisms including prokaryotes (Clapham 1995; Dominguez 2004; Domínguez et al. 2015). A prerequisite for $[Ca^{2+}]_i$ to act as a second messenger is a tight homeostasis of its basal levels which is regulated by Ca^{2+}-binding proteins, Ca^{2+} ATPases, Ca^{2+}/H^+ antiporters and Ca^{2+} pumps in order to avoid the formation of toxic intracellular calcium phosphate precipitates.

Our group was the first to construct a recombinant strain of the freshwater nitrogen-fixing cyanobacterium *Anabaena* sp. PCC 7120 constitutively expressing apoaequorin, *Anabaena* sp. PCC 7120 (pBG2001a), which allows continuous and *in vivo* monitoring of $[Ca^{2+}]_i$; with this strain we demonstrated that cyanobacteria were also able to tightly regulate their basal $[Ca^{2+}]_i$ levels with values in the range of 100-200 nM (Torrecilla et al. 2000); similar to the levels found in other bacteria (Dominguez 2004; Domínguez et al. 2015) and eukaryotic cells (Brini et al. 1995; Knight et al. 1991; Kudla et al. 2010; McAinsh and Pittman 2009). Cells respond to different abiotic and biotic stimuli by transient changes in $[Ca^{2+}]_i$, the specificity of the induced Ca^{2+} signals relies not only in the change of the intracellular calcium concentration. A combination of changes in all Ca^{2+} parameters of the signal such as amplitude, duration, frequency, rise

time, final Ca^{2+} resting levels, recovery time and source of the signal induced by a specific stimulus is referred to as a "Ca^{2+} signature" (Berridge et al. 2003; Berridge et al. 2000; Kudla et al. 2010; McAinsh and Pittman 2009; Rudd and Franklin-Tong 2001). The Ca^{2+} signatures encode information relating to the nature and strength of stimuli in their spatio-temporal dynamics (Kudla et al. 2010; McAinsh and Pittman 2009). In cyanobacteria, we have been able to record and analyse a variety of calcium signatures induced by specific environmental stimuli in this strain as well as in a unicellular cyanobacterium also expressing apoaequorin (Leganes et al. 2009; Torrecilla et al. 2000, 2004a; Torrecilla et al. 2001, 2004b).

There are numerous studies reporting that a wide range of pollutants affect Ca^{2+} homeostasis/signalling in a number of organisms (Huang et al. 2010; Ogunbayo et al. 2008; Wang et al. 2015; Xie et al. 2010; Zou et al. 2015) with microorganisms being underrepresented (Barran-Berdon et al. 2011; Dondero et al. 2006; Kozlova et al. 2005; Ohta and Suzuki 2007; Ruta et al. 2016; Ruta et al. 2014; Schäfer et al. 2009). Regarding specifically antibiotics, there are few studies reporting that antibiotics (mostly aminoglycosides and tetracycline) significantly alter Ca2+ homeostasis in animal and human cell lines (Bird et al. 1994; Dai et al. 2013; Dulon et al. 1989; Holohan et al. 1988; McLarnon et al. 2002).

Our group using the apoaequorin expressing cyanobacterial *Anabaena* strain, *Anabaena* sp. PCC 7120 (pBG2001a), has recorded and analysed Ca^{2+} signatures triggered by a variety of pollutants: cationic an anionic heavy metals, the metalloid As, naphthalene, organic solvents and some pharmaceuticals; we also recorded Ca^{2+} signatures induced by some binary mixtures of the pollutants as well as that induced by a real wastewater sample (Barran-Berdon et al. 2011). It was found that, in general, each group of tested pollutants induced a specific Ca^{2+} signature in a reproducible and dose-dependent way. We hypothesized that the recorded Ca^{2+} signatures might be early biomarkers of exposure to pollutants.
In the present study, we wish to deepen this hypothesis by recording Ca^{2+} signatures induced by antibiotics both applied singly and in combination to the apoaequorin expressing *Anabaena* strain, *Anabaena* sp. PCC 7120 (pBG2001a).

The applied antibiotics were from different classes and mode of action: amoxicillin (β-lactam, AMO); erythromycin (macrolide, ERY); tetracycline (tetracycline, TET) and the quinolones norfloxacin (NOR) and levofloxacin (LEV). All of them highly used in human and veterinary medicine.

In a previous study, we investigated the individual and combined toxicity of these five antibiotics in the transgenic bioluminescent cyanobacterium *Anabaena* sp. PCC 7120 CPB4337 (González-Pleiter et al. 2013). The Combination Index (CI) method was used to identify and quantify the toxicological interactions between the antibiotics in the mixtures finding a heterogeneous patterns of interactions whether synergistic or antagonistic. Thus, in the present study, we aimed at determining the role of $[Ca^{2+}]_i$ in the cellular perception of the presence of antibiotics both singly and combined in the external medium and whether the recorded Ca^{2+} signatures are related with the toxicity and pattern of interactions observed in our previous toxicological study.

4.2 MATERIALS AND METHODS

4.2.1 Chemicals

Amoxicillin (AMO), erythromycin (ERY) and levofloxacin (LEV) were purchased from TCI Chemicals; tetracycline (TET) was purchased from Sigma-Aldrich; and norfloxacin (NOR) purchased from Fluka. The purity of each antibiotic was AMO ≥ 90%, ERY ≥ 98%, LEV ≥ 98%, TET ≥ 98%, NOR ≥ 98%. Except ERY, which was dissolved in methanol, stock solutions of antibiotics were made in high purity water obtained from a Milipore Milli-Q system with a resistivity of at least 18 MΩ cm at 25 ºC. The antibiotics were stored in the dark and -20ºC. The dilutions of each antibiotic and their corresponding mixtures were freshly prepared. For the case of ERY, the final concentration of methanol in the assay media was always below 0.005% (*v*/*v*) which did not affect the performance of *Anabaena* sp. PCC7120 (pBG2001a).

Injection of culture medium induced a quite smaller Ca^{2+} transient in amplitude (peak height of 0.30 ± 0.05 µM) and duration (11 ± 1 sec.) which has been attributed to a small mechanically induced Ca^{2+} increase in *Anabaena* sp. PCC7120 (pBG2001a) (Torrecilla et al. 2000). Native coelenterazine, the apoaequorin cofactor, was purchased from Biotium.

4.2.2 Organism and growth conditions

Anabaena sp. PCC 7120 (pBG2001a) expressing apoaequorin was routinely grown in 250 ml conical flasks containing 100 mL of BG11 medium with 2 mM 4-(2-hydroxyethyl)-1-piperazineethanesulfonic acid (HEPES)/NaOH, pH 7 and 2.5 µg mL^{-1} spectinomycin, with the standard calcium concentration (0.25 mM). Cell cultures were incubated on a rotatory shaker at 28 °C under 65 µE m^{-2} s^{-1} fluorescent white light.

4.2.3 *In vivo* aequorin reconstitution and luminescence measurements

For aequorin luminescence measurements, *in vivo* reconstitution of aequorin was performed by the addition of 2.5 µM coelenterazine to cell suspensions (15 µg mL^{-1} chlorophyll) and incubation for 4 h in darkness and shaking at 28ºC. Before

Ca^{2+} measurements were made, cells were washed twice, firstly in Ca^{2+}-depleted BG11 medium buffered with 2 mM HEPES, pH 7.5, containing 0.5 mM EGTA, and later in Ca^{2+}-depleted BG11 medium to remove excess coelenterazine.(Torrecilla et al. 2000) Cells were finally resuspended in BG11 medium (calcium concentration of 0.25 mM) to carry out the bioassays. Luminescence measurements were made using a digital luminometer with a photomultiplier (BioOrbit 1250). Reconstituted cell suspensions (0.5 mL) in a transparent polystyrene cuvette were placed in the luminometer and luminescence was recorded every 1 s over the duration of the experiment.

Calibration of the $[Ca^{2+}]_i$ changes requires knowledge of the total available amount of reconstituted aequorin in cell suspensions (L_{max}) at any one point in time of the experiment, as well as the running luminescence (L_0). For estimation of total aequorin luminescence, the remaining aequorin was discharged at the end of the experiment by the addition of 0.3 ml of 1 M $CaCl_2$ and 10 % (*v*/*v*) Triton X-100. Rate constants of luminescence (L_0 L_{max}^{-1}), and $[Ca^{2+}]_i$ were calculated by using calibration curves obtained for aequorin extracted from the recombinant strain of *Anabaena* sp. PCC 7120 (pBG2001a) according to Torrecilla *et al*. 2000.(Torrecilla et al. 2000) (Torrecilla et al. 2000).

4.2.4 Cell lysis check

For each of the treatments used in the present study, the occurrence of cell lysis was checked by the following methods: (a) examination by optical microscopy; (b) measurement of luminescence after addition of Ca^{2+} to the medium in which reconstituted cells were present after removing the cells by centrifugation at 23000 g at room temperature for 15 min; (c) measurements of phycobiliproteins in the medium in which reconstituted cells were present after removing the cells by centrifugation at 23000 g at room temperature for 15 min.

4.2.5 Statistical analysis

All data were obtained from a minimum of three repetitions for each assay situation. The Ca^{2+} traces represented in the tables and figures have been chosen to best represent the average result of at least three replicates.

4.3 RESULTS AND DISCUSSION

4.3.1 Ca^{2+} signatures induced in *Anabaena* sp. PCC 7120 (pBG2001a) in response to exposure to antibiotics applied singly

Anabaena sp. PCC 7120 (pBG2001a) cells expressing apo-aequorin were incubated with the cofactor coelenterazine in order to reconstitute a functional aequorin. Then, the cells were placed in a luminometer cuvette, the selected antibiotics were injected and subsequent changes (if any) in $[Ca^{2+}]_i$ were recorded. Antibiotics were tested at their EC_{10} (as a surrogate of the NOEC: very low or negligible effect on growth) and EC_{50} (as sublethal concentration: 50% growth inhibition) according to our previous 72 h toxicity study (González-Pleiter et al. 2013). All the antibiotics at the tested concentrations induced a calcium transient (Table 4.1). The Ca^{2+} signal in all cases was very quick, within seconds of injection.

Transient shape, amplitude, rise time (time from application of the stimulus to maximum amplitude of the response), total transient duration (length of the transient form zero time to the recovery of the resting $[Ca^{2+}]_i$) were the characteristics of the Ca^{2+} signatures recorded. As shown in Table 4.1, all tested antibiotics triggered quick Ca^{2+} transients with the same rise time (2-3 s) but which differed in the amplitude (ranging from 0.36 ± 0.06 µM for ERY at its EC_{10} to 2.80 ± 0.15 µM for NOR at its EC_{50}) and total transient duration (from 32 ± 5 s for AMO at its EC_{10} to >4200 s for TET at its EC_{50}).

Toxic	Transient Shape (x-axis: Time (s); y-axis: [Ca^{2+}] (µM))	Amplitude [Ca^{2+}] (µM)	Rise Time (s)	Total transient duration (s)
AMO 6.2 mg/L (EC_{10})	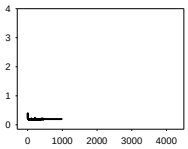	0.40 ± 0.05	2-3	32 ± 5
AMO 56 mg/L (EC_{50})	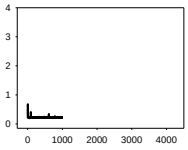	0.59 ± 0.09	2-3	98 ± 11 s
LEV 1.1 mg/L (EC_{10})	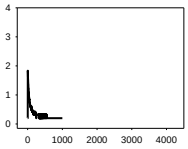	1.84 ± 0.07	2-3	249 ± 77
LEV 4.8 mg/L (EC_{50})	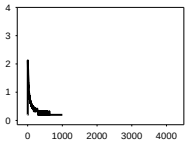	2.13 ± 0.09	2-3	304 ± 59
NOR 2.5 mg/L (EC_{10})	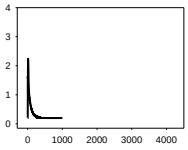	2.24 ± 0.01	2-3	288 ± 22
NOR 6.2 mg/L (EC_{50})	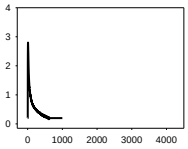	2.80 ± 0.15	2-3	557 ± 142
TET 2.5 mg/L (EC_{10})	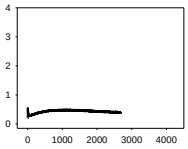	0.55 ± 0.09 0.46 ± 0.08	2-3	>2600
TET 6.2 mg/L (EC_{50})	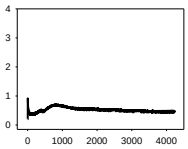	0.92 ± 0.08 0.70 ± 0.12	2-3	>4200
ERY 0.005 mg/L (EC_{10})	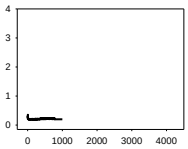	0.36 ± 0.06	2-3	44 ± 12
ERY 0.022 mg/L (EC_{50})	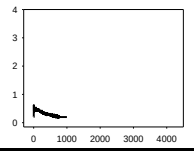	0.63 ± 0.05 0.54 ± 0.08	2-3	664 ± 54

Table 4.1 Ca^{2+} signatures induced by antibiotics. Properties of Ca^{2+} signatures induced by antibiotics (EC_{10} and EC_{50}) in *Anabaena* sp. PCC7120 (pBG2001a).

Regarding shape, in most cases it was characterized by a quick burst of $[Ca^{2+}]_i$, followed by a quick decline reaching a plateau that restored the level of $[Ca^{2+}]_i$

back to resting values (Table 4.1); in the case of TET applied at both concentrations, the Ca^{2+} signature consisted of two consecutive Ca^{2+} transients: one quick and steep spike followed by a bell-shaped transient with lower amplitude but higher duration than the first transient; it should be noted that the amplitude of the second transient was higher for the EC_{50} than for the EC_{10}. In the case of ERY applied at its EC_{50}, there were also two consecutive transients; the second transient had slightly lower amplitude but also higher duration than the first transient.

Although no correlation was found between any of the characteristics of the recorded Ca^{2+} signature and the order of toxicity of the tested antibiotics which was: ERY > LEV > NOR > TET > AMO.(González-Pleiter et al. 2013) It should be noted that antibiotics at the higher concentration tested, EC_{50}, which already inhibited growth by 50%, triggered Ca^{2+} signatures with higher amplitudes, longer transient duration (meaning a longer time to restore $[Ca^{2+}]_i$ basal levels) and the appearance of secondary bell-shaped transients with much longer duration times (case of TET and ERY). This means that $[Ca^{2+}]_i$ may sense differences in antibiotic concentrations even at concentrations causing negligible or very low toxicity (i.e. EC_{10}); this could be essential for the cellular response to the pollutant.

Taken altogether these results show that $[Ca^{2+}]_i$ responds very quickly, within seconds, to antibiotic exposure, the Ca^{2+} signature of each antibiotic differs in amplitude, shape and total transient duration and within each antibiotic also differs with concentration; this suggests that the presence of antibiotics is signalled through immediate $[Ca^{2+}]_i$ transients in the cyanobacterial cytoplasm that may trigger the subsequent cellular response to the pollutant.

In a previous work, our group recorded the Ca^{2+} signatures triggered in *Anabaena* sp. PCC 7120 (pBG2001a) when exposed to 17 chemicals grouped in cations (Zn^{2+}, Pb^{2+}, Cd^{2+}, Cu^{2+} and Hg^{2+}), anions (arsenate and chromate), pharmaceuticals such as lipid regulators (bezafibrate, gemfibrozil, fenofibric acid and clofibric acid) and quinolones (ciprofloxacin and ofloxacin), the PAH naphthalene and the organic solvents acetone, ethanol and toluene.(Barran-

Berdon et al. 2011) For easy comparison, chemicals were tested at the same concentration, 5 mg/L, finding that, in general, each group of chemicals triggered a specific Ca^{2+} signature; in fact the two tested quinolones ciprofloxacin and ofloxacin showed a signature very similar to the quinolones assayed in the present study: LEV and NOR. Furthermore, several chemicals were tested at higher concentrations (shown to be toxic) and they induced Ca^{2+} signatures characterized by broad bell-shaped transients (incapacity to rapidly restore basal cytosolic $[Ca^{2+}]_i$) or by two consecutive transients being the second also broad and bell-shaped. Besides, it was found that Ca^{2+} signatures preceded toxicity in the lights-off bioreporter *Anabaena* CPB4337 as Ca^{2+} signatures were induced within seconds at concentrations much lower than their EC_{50} values. It was concluded that the specific Ca^{2+} signature subsequently induces a signaling pathway which results in an appropriate cellular response to the pollutant which may be adaptation and survival or, when the pollutant is at high concentration, or, the exposure is long, may cause deregulation of Ca^{2+} homeostasis leading to cellular toxicity.

In this regard, Ruta *et al*.2014, 2016 have suggested that the features of the Ca^{2+} signatures may have a significant role in the final cellular response with sudden and sharp Ca^{2+} transients allowing the adaptation to high concentrations of Cd and Cu in apoaequorin- expressing *Saccharomyces cerevisiae* cells while the absence of Ca^{2+} signals or broad ones lead the cells to hypersensitivity and toxicity. They concluded that cells prepared to face high and rapid Ca^{2+} cytosolic waves were fitter for survival.

Kozlova *et al*. 2005 also tried to correlate Ca^{2+} signatures triggered by Cr^{6+}, Zn^{2+} and 3,5-dichlorophenol in apoaequorin-expressing fungus *Aspergillus awamori* with toxicity; for this, they chose length of the Ca^{2+} transients (LT_{50}) to compare with the EC_{50} at 5 and 30 min of the *Aliivibrio fischeri* classical bioluminescent toxicity assay. All toxicants provoked a response in one or more of the studied parameters, but LT_{50} was not the best parameter to compare with the *A. fischeri* bioassay. Therefore, the authors concluded that assessment of a different parameter was needed.

All these results suggest that Ca^{2+} signatures between different pollutants may not correlate with their order of toxicity but that specific Ca^{2+} signatures may serve to discriminate between pollutants and that, within a single pollutant and depending on the concentration, they may serve to tune the cellular response, whether tolerant or hypersensitive.

4.3.2 Ca^{2+} signatures induced by selected mixtures of antibiotics in *Anabaena* sp. PCC7120 (pBG2001a)

Different classes of antibiotics co-occur in environmental compartments (Kolpin et al. 2004; Li et al. 2009; Suzuki and Hoa 2007; Watkinson et al. 2009). Aquatic organisms are thus exposed to the combined action of antibiotics. An important issue of chemical mixtures is the determination of potential interactions between pollutants in a mixture; in this regard, antibiotics in a mixture may not interact (zero interaction or additive effect) or may interact synergistically when the effect of the mixture is greater than that expected from the sum of their individual effects (more-than-additive effects) or antagonistically when the effect of the mixture is less than expected from the sum of individual effects (less-than-additive effect).

In our previous toxicity study, we determined the nature of the interactions between the five antibiotics in binary mixtures and in a multiantibiotic mixture in the bioluminescent strain *Anabaena* sp. PCC 7120 CPB4337 after 72 h of exposure (González-Pleiter et al. 2013). As $[Ca^{2+}]_i$ responds very quickly to individual antibiotics (as shown in Table 4.1) we evaluated whether $[Ca^{2+}]_i$ could also respond to antibiotic binary mixtures and a multiantibiotic mixture so that by comparing the Ca^{2+} signature of the mixture with those of antibiotics when applied singly, patterns of interactions might become evident. We also wanted to assess whether Ca^{2+} signatures of the mixtures could anticipate/predict the toxicological interactions observed at longer times of exposure. For this set of experiments, we selected four binary mixtures that represented different types of toxicological interactions and the five-antibiotic or multiantibiotic mixture (González-Pleiter et al. 2013): two synergistic mixtures at both very low (10%) and median effect levels (50%) which were AMO-TET and LEV-TET; TET-

ERY which was synergistic at very low effect level (10%) but turned into antagonistic at effect levels higher than 60% and AMO-ERY which was antagonistic at both very low (10%) and median effect levels (50%). The multiantibiotic mixture was antagonistic at very low (10%) effect levels, nearly additive at 20-30% effect level, slightly synergistic at 50% effect level and clearly synergistic above this level.

For comparison, the Ca^{2+} signatures induced by the antibiotics when applied individually at the same concentrations (EC_{10} and EC_{50}) as those in the mixtures are shown in Fig. 4.1 and Fig. 4.2. Amplitude of the first transient (some but not all tested antibiotics/concentrations induced a second transient; see Table 4.1) was chosen as the most representative parameter to discern potential interactions between antibiotics in the binary mixtures. Both, the AMO-TET and LEV-TET mixtures, tested at the EC_{10} and EC_{50}, induced a Ca^{2+} signature whose amplitude was higher than the sum of the Ca^{2+} signatures when both pollutants were applied individually, suggesting a more-than-additive effect or synergism; synergism was clearer in the case of the LEV-TET combination (Fig. 4.1).

In the case of the TET-ERY combination, the mixture tested at EC_{10} induced a Ca^{2+} signature with an amplitude higher than the sum of the individual Ca^{2+} signatures suggesting synergism; however, the interaction was clearly antagonistic when tested at the EC_{50}. The ERY-AMO combination, tested at the EC_{10} and EC_{50}, induced a Ca^{2+} signature whose amplitude was lower than the sum of the individual Ca^{2+} signatures suggesting a less-than-additive effect or antagonism (Fig. 4.2).

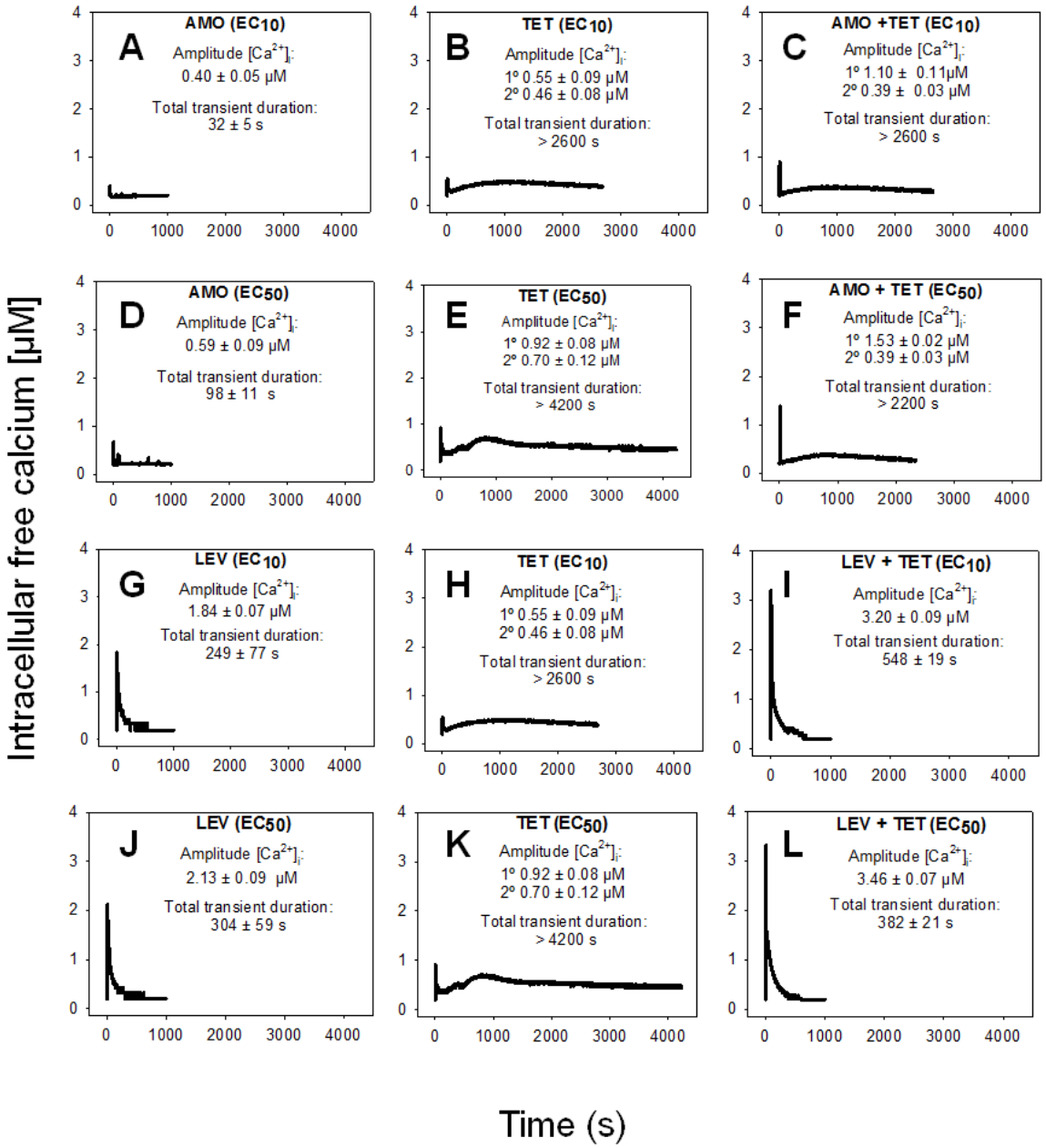

Figure 4.1 Ca^{2+} signatures induced in *Anabaena* sp. PCC 7120 (pBG2001a) in response to antibiotics AMO and TET applied individually and in binary mixture (AMO + TET) at constant ratio 1:1 based on either the EC10s (A to C) or EC50s (D to F) and antibiotics LEV and TET applied individually and in binary mixture (LEV + TET) at constant ratio 1:1 based on either the EC10s (G to I) or EC50s (J to L).

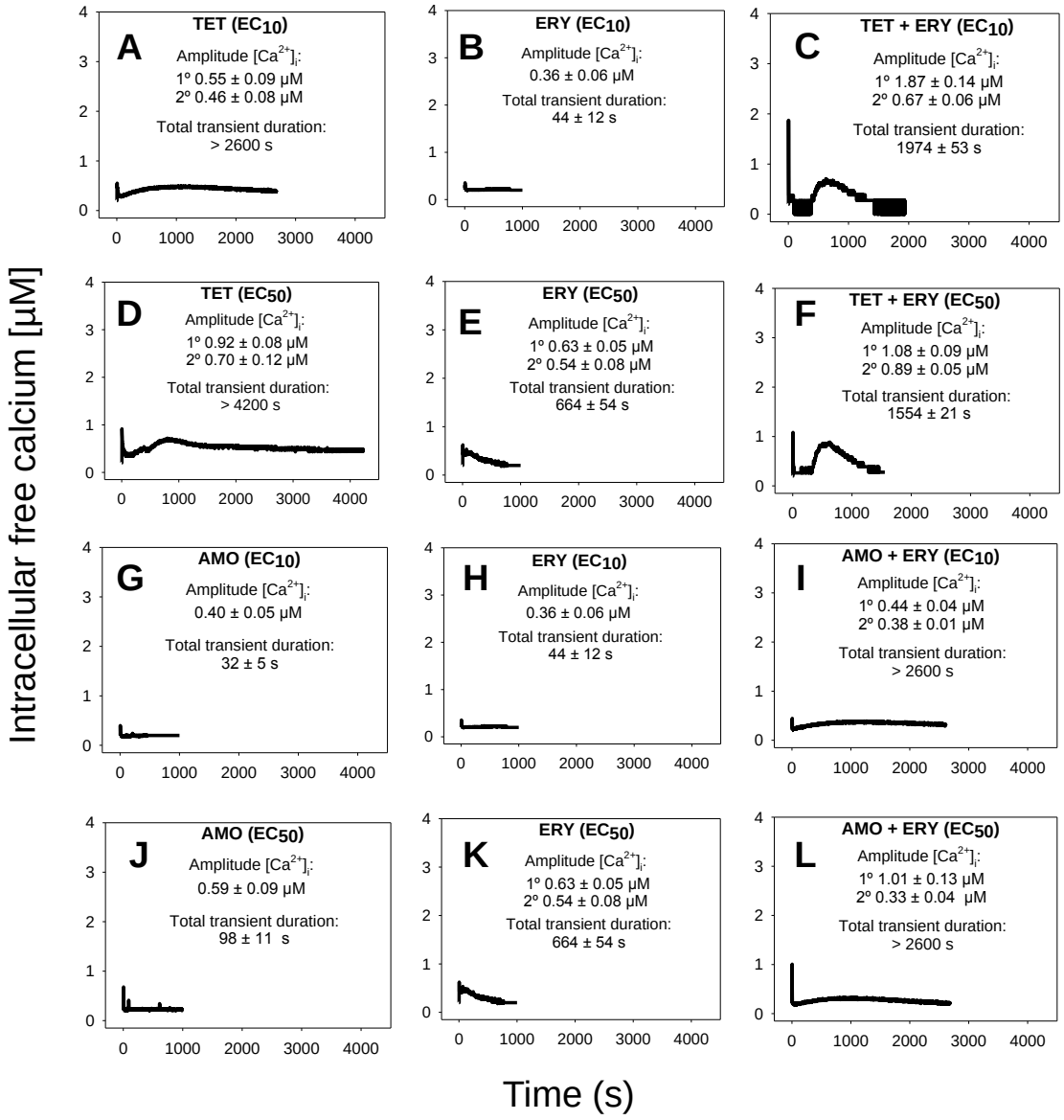

Figure 4.2 Ca^{2+} signatures induced in *Anabaena* sp. PCC 7120 (pBG2001a) in response to antibiotics TET and ERY applied individually and in binary mixture (TET + ERY) at constantratio 1:1 based on either the EC10s (A to C) or EC50s (D to F) and antibiotics AMO and ERY applied individually and in binary mixture (AMO + ERY) at constant ratio 1:1 based oneither the EC_{10s} (G to I) or EC_{50s} (J to L).

Although amplitude was chosen as the reference parameter, it should be noted that the shape of some binary mixtures clearly changed with respect to the individual Ca^{2+} signatures; in the AMO-TET combination, the amplitude of the second TET transient clearly diminished when mixed at their EC_{50}s; in the LEV-TET mixture, the second TET transients disappeared in both combination concentrations (Fig. 4.1). Interestingly, in the TET-ERY combination, the second

TET transient was clearly sharper and shorter in both combination concentrations and in the AMO-ERY mixture, a second transient appeared at both combination concentrations that was larger and with lower amplitude than that of ERY applied at its EC_{50}. The found differences did not clearly correlate with the differences seen when considering the amplitude as reference parameter and, in some cases, they were independent of the tested concentration; so, these differences in shape could indicate that cells are just detecting the specific mixture.

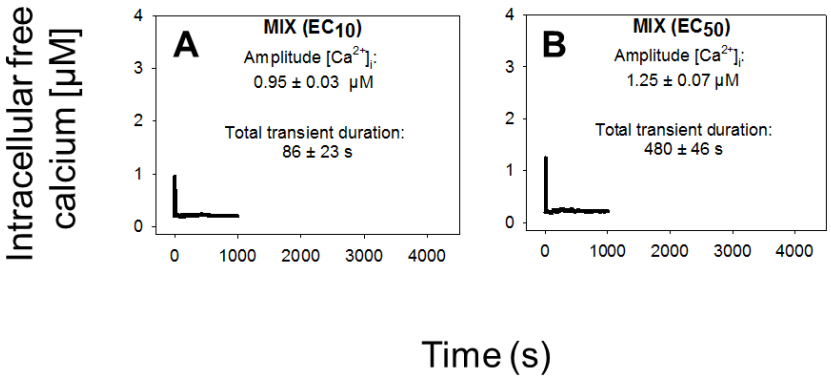

Figure 4.3 Ca^{2+} signatures induced in *Anabaena* sp. PCC 7120 (pBG2001a) in response to the multiantibiotic (five antibiotic) mixture applied at constant ratio 1:1 based on either the EC_{10s} (A) or EC_{50s} (B).

The multiantibiotic mixture, tested at the EC_{10} and EC_{50}, induced Ca^{2+} signatures whose amplitudes were lower than the sum of the individual Ca^{2+} signatures suggesting a less-than-additive effect or antagonism (Fig. 4.3 and Table 4.1). Regarding the shape and for both concentrations, only one quick transient which rapidly returned to basal levels was recorded. As thoroughly discussed by many scientists, the toxicity and, thereby, the risk associated with environmental pollutants is the result of the many interactions of co-occurring pollutants in a given environmental compartment (Rodea-Palomares et al. 2016; Rodea-Palomares et al. 2015). Ca^{2+} signatures in response to mixtures of pollutants could serve as an excellent biomarker for prediction of potential types of interaction, whether synergistic or antagonistic, in exposed organisms.

Our group previously reported that the analysis of the Ca^{2+} signatures induced by binary mixtures of Zn^{2+} plus Cu^{2+}; Zn^{2+} plus the lipid regulator fenofibric acid, Zn^{2+} plus arsenate and the two fibrates fenofibric acid plus bezafibrate could anticipate the toxicological interactions found in toxicity experiments (Barran-Berdon et al. 2011; Rodea-Palomares et al. 2009; Rodea-Palomares et al. 2010). Recently, Ruta *et al*.(2016) reported, in apoaequorin-expressing *Saccharomyces cerevisiae*, that the binary mixture Cu^{2+} and H_2O_2 induced a Ca^{2+} signature sharper and with an amplitude higher than that of individual Ca^{2+} signatures indicating a synergistic interactions between both chemicals in signaling the stress conditions; the authors indicated that the stronger and sharper Ca^{2+} signature induced by the mixture increased the cell chances of survival. In this study, we have found that binary mixtures of antibiotics triggered quick Ca^{2+} signatures that, based on amplitude as the reference parameter to compare with those of the individual Ca^{2+} signatures, could also predict the toxicological interactions found for these antibiotics (González-Pleiter et al. 2013).

In the case of the multiantibiotic mixture only antagonism was found (Fig. 4.3) although in the toxicological experiments a clear synergism was found at medium to high effect levels, this could be explained by the fact that the toxicological experiment was done after 72 h of exposure and cells might be already strongly affected by the antibiotic mixture (González-Pleiter et al. 2013). This would imply that Ca^{2+} signatures are not only early biomarkers/sensors of antibiotic exposure both singly and in mixtures but also that they seem to anticipate the toxicological outcome of the mixture; besides, as suggested by Ruta *et al*. 2016, the specific features of the Ca^{2+} signatures induced by mixtures might perhaps signal whether the cells may survive or not; in this study, we also found that the Ca^{2+} signatures of the mixture were quite different from those of the individual antibiotics although at present we cannot give a clear explanation for these differences. To gain insight into the correct interpretation of the Ca^{2+} signatures triggered by mixtures, a careful and thorough research is needed in more organisms and with more pollutants mixed in realistic scenarios; in this regard, in our previous study by Barran-Berdon *et al*.(2011), we recorded a Ca^{2+} signature triggered by a real wastewater sample that could be mimicked by mixing its main components at their measured environmental concentration.

4.4 CONCLUSIONS

To our knowledge, this is the first report on intracellular free Ca^{2+}, $[Ca^{2+}]_i$, as an early biomarker of antibiotic exposure in the environment. Upon antibiotic exposure, quick (within 2-3 s) and specific Ca^{2+} signatures were recorded. Signatures induced by the different antibiotics differed in amplitude, shape and total transient duration and within the same antibiotic also with the tested concentration with higher amplitude, longer transient duration and in some case the appearance of a second bell-shaped Ca^{2+} signal at the higher concentration tested, EC_{50}.

Ca^{2+} signatures induced by binary mixtures and a multiantibiotic mixture were clearly different from those of the antibiotics applied singly and, using amplitude as a reference parameter, potential interactions between antibiotics in the mixtures could be determined; the Ca^{2+} signatures induced by the mixtures seemed to anticipate the toxicological interactions found at larger times of exposure; thus, well before toxicity is evident.

4.5 REFERENCES

Barran-Berdon, A. L., I. Rodea-Palomares, F. Leganes, and F. Fernandez-Pinas. 2011. Free Ca2+ as an early intracellular biomarker of exposure of cyanobacteria to environmentalpollution. Anal Bioanal Chem 400 (4):1015-1029.

Berridge, M. J., M. D. Bootman, and H. L. Roderick. 2003. Calcium signalling: dynamics, homeostasis and remodelling. Nature Reviews: Molecular Cell Biology 4 (7):517-529.

Berridge, M. J., P. Lipp, and M. D. Bootman. 2000. The versatility and universality of calcium signalling. Nature Reviews: Molecular Cell Biology 1 (1):11-21.

Bird, S. D., R. J. Walker, and M. J. Hubbard. 1994. Altered free calcium transients in pig kidney cells (LLC-PK1) cultured with penicillin/streptomycin. In Vitro Cellular & Developmental Biology-Animal 30 (7):420-424.

Brini, M., R. Marsault, C. Bastianutto, J. Alvarez, T. Pozzan, and R. Rizzuto. 1995. Transfected aequorin in the measurement of cytosolic Ca2+ concentration ([Ca2+] c) A critical evaluation. Journal of Biological Chemistry 270 (17):9896-9903.

Clapham, D. E. 1995. Calcium signaling. Cell 80 (2):259-268.

Dai, C., D. Zhang, J. Li, and J. Li. 2013. Effect of colistin exposure on calcium homeostasis and mitochondria functions in chick cortex neurons. Toxicology Mechanisms and Methods 23 (4):281-288.

Dominguez, D. C. 2004. Calcium signalling in bacteria. Molecular Microbiology 54 (2):291-297.

Domínguez, D. C., M. Guragain, and M. Patrauchan. 2015. Calcium binding proteins and calcium signaling in prokaryotes. Cell Calcium 57 (3):151-165.

Dondero, F., H. Jonsson, M. Rebelo, G. Pesce, E. Berti, G. Pons, and A. Viarengo. 2006. Cellular responses to environmental contaminants in amoebic cells of the slime mould Dictyostelium discoideum. Comparative Biochemistry and Physiology Part C: Toxicology & Pharmacology 143 (2):150-157.

Dulon, D., G. Zajic, J. M. Aran, and J. Schacht. 1989. Aminoglycoside antibiotics impair calcium entry but not viability and motility in isolated cochlear outer hair cells. Journal of Neuroscience Research 24 (2):338-346.

Falcón, L. I., S. Magallón, and A. Castillo. 2010. Dating the cyanobacterial ancestor of the chloroplast. The ISME journal 4 (6):777-783.

González-Pleiter, M., S. Gonzalo, I. Rodea-Palomares, F. Leganés, R. Rosal, K. Boltes, E. Marco, and F. Fernández-Piñas. 2013. Toxicity of five antibiotics and their mixtures towards photosynthetic aquatic organisms: implications for environmental risk assessment. water research 47 (6):2050-2064.

Holohan, P. D., P. P. Sokol, C. R. Ross, R. Coulson, M. E. Trimble, D. Laska, and P. Williams. 1988. Gentamicin-induced increases in cytosolic calcium in pig kidney cells (LLC-PK1). Journal of Pharmacology and Experimental Therapeutics 247 (1):349-354.

Huang, C.-C., R. S. Aronstam, D.-R. Chen, and Y.-W. Huang. 2010. Oxidative stress, calcium homeostasis, and altered gene expression in human lung epithelial cells exposed to ZnO nanoparticles. Toxicology in Vitro 24 (1):45-55.

Knight, M. R., A. K. Campbell, S. M. Smith, and A. J. Trewavas. 1991. Recombinant aequorin as a probe for cytosolic free Ca2+ in Escherichia coli. FEBS Letters 282 (2):405-408.

Kolpin, D. W., M. Skopec, M. T. Meyer, E. T. Furlong, and S. D. Zaugg. 2004. Urban contribution of pharmaceuticals and other organic wastewater contaminants to streams during differing flow conditions. Science of the Total Environment 328 (1):119-130.

Kozlova, O., M. Zwinderman, and N. Christofi. 2005. A new short-term toxicity assay using Aspergillus awamori with recombinant aequorin gene. BMC Microbiology 5 (1):40.

Kudla, J., O. Batistic, and K. Hashimoto. 2010. Calcium signals: the lead currency of plant information processing. Plant Cell 22 (3):541-563.

Leganes, F., K. Forchhammer, and F. Fernandez-Pinas. 2009. Role of calcium in acclimation of the cyanobacterium Synechococcus elongatus PCC 7942 to nitrogen starvation. Microbiology 155 (Pt 1):25-34.

Li, B., T. Zhang, Z. Xu, and H. H. P. Fang. 2009. Rapid analysis of 21 antibiotics of multiple classes in municipal wastewater using ultra performance liquid chromatography-tandem mass spectrometry. Analytica Chimica Acta 645 (1):64-72.

McAinsh, M. R., and J. K. Pittman. 2009. Shaping the calcium signature. New Phytol 181 (2):275-294.

McLarnon, S. J., D. Holden, D. T. Ward, M. N. Jones, A. C. Elliott, and D. Riccardi. 2002. Aminoglycoside antibiotics induce pH-sensitive activation of the calcium-sensing receptor. Biochemical and Biophysical Research Communications 297 (1):71-77.

Ogunbayo, O. A., P. F. Lai, T. J. Connolly, and F. Michelangeli. 2008. Tetrabromobisphenol A (TBBPA), induces cell death in TM4 Sertoli cells by modulating Ca 2+ transport proteins and causing dysregulation of Ca 2+ homeostasis. Toxicology in Vitro 22 (4):943-952.

Ohta, M., and T. Suzuki. 2007. Participation of the inositol phospholipid signaling pathway in the increase in cytosolic calcium induced by tributyltin chloride intoxication of chlorophyllous protozoa Euglena gracilis Z and its achlorophyllous mutant SM-ZK. Comparative Biochemistry and Physiology Part C: Toxicology & Pharmacology 146 (4):525-530.

Potts, M. 1994. Desiccation tolerance of prokaryotes. Microbiological Reviews 58 (4):755-805.

Rippka, R., J. Deruelles, J. B. Waterbury, M. Herdman, and R. Y. Stanier. 1979. Generic assignments, strain histories and properties of pure cultures of cyanobacteria. Microbiology 111 (1):1-61.

Rodea-Palomares, I., F. Fernández-Piñas, C. González-García, and F. Leganés. 2009. Use of lux-marked cyanobacterial bioreporters for assessment of individual and combined toxicities of metals in aqueous samples. Handbook on Cyanobacteria: Biochemistry, Biotechnology and Applications:283-304.

Rodea-Palomares, I., M. Gonzalez-Pleiter, S. Gonzalo, R. Rosal, F. Leganes, S. Sabater, M. Casellas, R. Muñoz-Carpena, and F. Fernández-Piñas. 2016. Hidden drivers of low-dose pharmaceutical pollutant mixtures revealed by the novel GSA-QHTS screening method. Science Advances 2 (9):e1601272.

Rodea-Palomares, I., M. González-Pleiter, K. Martín-Betancor, R. Rosal, and F. Fernández-Piñas. 2015. Additivity and interactions in ecotoxicity of pollutant mixtures: Some patterns, conclusions, and open questions. Toxics 3 (4):342-369.

Rodea-Palomares, I., A. L. Petre, K. Boltes, F. Leganés, J. A. Perdigón-Melón, R. Rosal, and F. Fernández-Piñas. 2010. Application of the combination index (CI)-isobologram equation to study the toxicological interactions of lipid regulators in two aquatic bioluminescent organisms. water research 44 (2):427-438.

Rudd, J. J., and V. E. Franklin-Tong. 2001. Unravelling response-specificity in Ca2+ signalling pathways in plant cells. New Phytologist 151 (1):7-33.

Ruta, L. L., C. V. Popa, I. Nicolau, and I. C. Farcasanu. 2016. Calcium signaling and copper toxicity in Saccharomyces cerevisiae cells. Environmental Science and Pollution Research 23 (24):24514-24526.

Ruta, L. L., V. C. Popa, I. Nicolau, A. F. Danet, V. Iordache, A. D. Neagoe, and I. C. Farcasanu. 2014. Calcium signaling mediates the response to cadmium toxicity in Saccharomyces cerevisiae cells. FEBS Letters 588 (17):3202-3212.

Schäfer, S., U. Bickmeyer, and A. Koehler. 2009. Measuring Ca 2+-signalling at fertilization in the sea urchin Psammechinus miliaris: alterations of this Ca 2+-signal by copper and 2, 4, 6-tribromophenol. Comparative Biochemistry and Physiology Part C: Toxicology & Pharmacology 150 (2):261-269.

Suzuki, S., and P. P. Hoa. 2007. Distribution of quinolones, sulfonamides, tetracyclines in aquatic environment and antibiotic resistance in Indochina. Role and prevalence of antibiosis and the related resistance genes in the environment:45.

Torrecilla, I., F. Leganes, I. Bonilla, and F. Fernandez-Pinas. 2000. Use of recombinant aequorin to study calcium homeostasis and monitor calcium transients in response to heat and cold shock in cyanobacteria. Plant Physiology 123 (1):161-176.

Torrecilla, I., F. Leganes, I. Bonilla, and F. Fernandez-Pinas. 2004a. A calcium signal is involved in heterocyst differentiation in the cyanobacterium Anabaena sp. PCC7120. Microbiology 150 (Pt 11):3731-3739.

Torrecilla, I., F. Leganés, I. Bonilla, and F. Fernández-Piñas. 2001. Calcium transients in response to salinity and osmotic stress in the nitrogen-fixing cyanobacterium Anabaena sp. PCC7120, expressing cytosolic apoaequorin. Plant, Cell & Environment 24 (6):641-648.

Torrecilla, I., F. Leganés, I. Bonilla, and F. Fernández-Piñas. 2004b. Light-to-dark transitions trigger a transient increase in intracellular Ca2+ modulated by the redox state of the photosynthetic electron transport chain in the cyanobacterium Anabaena sp. PCC7120. Plant, Cell & Environment 27 (7):810-819.

Wang, H., Z.-K. Wang, P. Jiao, X.-P. Zhou, D.-B. Yang, Z.-Y. Wang, and L. Wang. 2015. Redistribution of subcellular calcium and its effect on apoptosis in primary cultures of rat proximal tubular cells exposed to lead. Toxicology 333:137-146.

Watkinson, A., E. Murby, D. Kolpin, and S. Costanzo. 2009. The occurrence of antibiotics in an urban watershed: from wastewater to drinking water. Science of the Total Environment 407 (8):2711-2723.

Xie, Z., Y. Zhang, A. Li, P. Li, W. Ji, and D. Huang. 2010. Cd-induced apoptosis was mediated by the release of Ca^{2+} from intracellular Ca storage. Toxicology Letters 192 (2):115-118.

Zou, H., X. Liu, T. Han, D. Hu, Y. Yuan, J. Gu, J. Bian, and Z. Liu. 2015. Alpha-lipoic acid protects against cadmium-induced hepatotoxicity via calcium signalling and gap junctional intercellular communication in rat hepatocytes. The Journal of toxicological sciences 40 (4):469-477.

CHAPTER 5: CALCIUM MEDIATES THE CELLULAR RESPONSE OF *CHLAMYDOMONAS REINHARDTII* TO THE EMERGING AQUATIC POLLUTANT TRICLOSAN

5.1 INTRODUCTION

Calcium is a well-known, ubiquitous and versatile second messenger in eukaryotic as well as prokaryotic cells (Berridge et al., 2003, 2000; Domínguez et al., 2015; Permyakov and Kretsinger, 2009). It regulates crucial cellular processes such as cell cycle, transport, motility, gene expression and apoptosis (Berridge et al., 2003; Case et al., 2007).

In plants and algae, calcium is an essential nutrient; it has both structural (cell wall, membranes, photosystem II) and signaling roles. As most cells, plant cells also keep intracellular resting free Ca^{2+} levels quite low, between 100-200 nM (Hochmal et al., 2015; McAinsh and Pittman, 2009); this tight homeostasis avoids the observed cytotoxicity of high intracellular free Ca^{2+} concentrations (Case et al., 2007).

Between abiotic stressors, environmental pollutants are known to alter Ca^{2+} signaling/homeostasis in many cell systems. Most studies have been done in human and animal cell systems (Huang et al., 2010; Wang et al., 2015; Zou et al., 2015) and very few in eukaryotic microorganisms or organisms of ecological relevance in environmental compartments (Barrán-Berdón et al., 2011; Dondero et al., 2006; Ohta and Suzuki, 2007; Schäfer et al., 2009).

Environmental pollutants are also known to increase the formation of intracellular reactive oxygen species (ROS) (Lushchak, 2011; Xia et al., 2008). In most cell systems, there is a bidirectional interplay between ROS and calcium with calcium regulating ROS production and ROS modulating calcium fluxes (Gilroy et al., 2016, 2014; Görlach et al., 2015) and it is difficult to determine whether Ca^{2+} or ROS lies upstream of the other. Görlach et al (2015) and Gilroy et al (2016) suggested the presence of a self-amplifiable loop between Ca^{2+}-induced ROS increase and ROS-mediated Ca^{2+}-influx which is a key factor for mitochondrial malfunction during Ca^{2+} overload.

Triclosan (TCS; 5-chloro-2-(2,4-dichlorophenoxy)phenol) is an antimicrobial agent which forms part of the so-called personal care products (PCPs) which are receiving increasing attention due to their persistence and toxicity, particularly in the aquatic

environment; at present, TCS is considered as an emerging pollutant of concern and clearly more data regarding its potential toxic effects in the environment are needed for environmental regulations. Its mode of action is the inhibition of enoyl-acyl carrier protein reductase which is involved in bacterial fatty acid synthesis. However, its effects are not restricted to microbes, in mammalian cells it has been found that TCS shows membranotropic effects and behaves as a mitochondrial uncoupler (Ajao et al., 2015; McDonnell and Russell, 1999; Weatherly et al., 2016). Also, over the last years, it has been found that TCS is toxic to many non-target aquatic organisms (Fritsch et al., 2013; Orvos et al., 2002; Riva et al., 2012); microalgae have been found to be very sensitive to this antibacterial agent (Brain et al., 2010; Orvos et al., 2002; Wilson et al., 2003; Yang et al., 2008) although cellular mechanisms responsible of the toxic action have been seldom reported (Ciniglia et al., 2005). There are several studies which have also shown that TCS is able to alter/elevate intracellular free Ca^{2+} levels and to induce ROS formation in animal and human cell lines (Ahn et al., 2008; Cherednichenko et al., 2012; Kawanai, 2011; Palmer et al., 2012; Tamura et al., 2011); however, no such studies have been undertaken with organisms of environmental relevance such as algae. Microalgae as primary producers are a key component of aquatic food chains and any detrimental effect on this group may induce significant alterations in the rest of the ecosystem. *Chlamydomonas reinhardtii* is a unicellular biflagellate green alga which traditionally has served as a model for photosynthesis research and growth in different nutrient conditions, chloroplast structure and function as well as phototaxis and chemotaxis (Blaby et al., 2013; Bonente et al., 2012; Grossman et al., 2007; Harris, 2001; Renberg et al., 2010); it is becoming an important model also for environmental toxicological analyses (Esperanza et al., 2015a, 2015b; Fischer et al., 2010). Regarding calcium signaling, it is particularly relevant in this motile alga which requires rapid signaling networks. Calcium is known to be involved in many cellular responses in *Chlamydomonas*: photoaccumulation (Nultsch et al., 1986; Stavis, 1974); photophobic responses (Schmidt and Eckert, 1976); phototaxis related with the eyespot region (Berthold et al., 2008; Nagel et al., 2002); chemotaxis (Ermilova et al., 1996) ; mating (Goodenough et al., 1993); gravitaxis (Kam et al., 1999) and various flagellar responses including deflagellation (Wakabayashi et al., 2009; Wheeler and Brownlee, 2008).

The hypothesis underlying the present study is that intracellular free calcium mediates the toxic action of TCS in *C. reinhardtii*. To test this, we have undertaken an

investigation of a number of cellular processes that may be affected by 24 h exposure to TCS and have used the intracellular Ca^{2+} chelator BAPTA-AM to study the relationship, if any, between intracellular free Ca^{2+} levels and the *Chlamydomonas* response to TCS. We have investigated the effect of TCS on Ca^{2+} signaling by measuring changes in intracellular free Ca^{2+} and in the expression of Ca^{2+}-related genes; potential oxidative stress and subsequent cellular response was evaluated by measuring ROS formation and the expression of genes involved in the antioxidant cellular response; besides, as it has been largely reported that there is a cross-talk between increased ROS production and increased Ca^{2+} fluxes, the antioxidant compound N-acetylcysteine (NAC) has been used together with BAPTA-AM in an attempt to understand whether the increase of Ca^{2+} precedes and/or modulate the increase of ROS. Other deleterious effects which may be caused by TCS that have been checked include cytoplasmic and mitochondrial membrane potential, changes in intracellular pH, intracellular esterase activity and apoptosis. As the most relevant physiological parameter, photosynthesis performance as well as the expression of photosynthetic genes have been measured. Finally, studies of protein patterns with identifications of relevant proteins altered by TCS exposure have been performed. This study provides novel information on early cellular responses of photosynthetic organisms to pollution and the role of calcium signaling in such responses.

5.2 MATERIALS AND METHODS

5.2.1 Chemicals

TCS was purchased from Sigma-Aldrich (CAS: 3380-34-5, purity ≥ 97.0%). Stock solution of TCS was made in Milli-Q water. TCS was stored in the dark at 4ºC. The dilutions were freshly prepared before each experiment. Exposure concentrations along the experimental lapse time (24 hours) were assumed to be constant based on previous stability studies performed with TCS (Federle and Schwab, 2003).

BAPTA-AM (*N*,*N*`-[1, 2-ethanediylbis(oxy-2,1-phenylene)]bis[*N*-[2-[(acetyloxy)methoxy]-2-oxoethyl]]-,bis[(acetyloxy)methyl]) ester was purchased from Molecular Probes (CAS no 126150-97-8, purity > 98%). BAPTA-AM is an uncharged calcium-binding molecule that can permeate cell membranes and be cleaved by nonspecific esterases, resulting in a charged form that leaks out of the cell very slowly and therefore acts as an intracellular calcium chelator. Stock solution of BAPTA-AM was made in dimethyl sulfoxide (DMSO). BAPTA-AM was stored in the dark at -20ºC. To facilitate cell loading of BAPTA-AM, cells were preincubated with the chelator at a final concentration of 50 µM for 30 min in darkness with shaking before treatment with TCS.

N-acetyl-L-cysteine (NAC) was purchased from Sigma-Aldrich (CAS no 616-91-1, purity ≥ 99%). NAC is an antioxidant; it is the precursor of glutathione synthesis and ROS scavenger. Stock solution of NAC was made in Milli-Q water. NAC was stored in the dark at -20ºC. To facilitate cell loading of NAC, cells were preincubated with the antioxidant at a final concentration of 1 mM for 30 min in darkness with shaking before treatment with TCS.

5.2.2 Microalgal cultures and bioassays

The unicellular green alga *Chlamydomonas reinhardtii* Dangeard (strain CCAP 11/32A mt+) was obtained from the Culture Collection of Algae and Protozoa of Dunstaffnage Marine Laboratory (Scotland, UK). *C. reinhardtii* cells were cultured in Tris-minimal phosphate medium (Harris, 1989) on a rotary shaker set at 150 rpm, under controlled conditions: 22 ± 1 ºC and illuminated with 100 µmol photon m^{-2} s^{-1} under a 12:12 h

light:dark cycle. Cells in mid-logarithmic growth phase were used as inoculum for the different assays. Initial cell density for each experiment was 2×10^5 cells mL^{-1}.

The concentration used in the present study, 13.8 µM, was the EC_{50} after 24 hour exposure to TCS as determined by previous toxicity tests (data not shown). All bioassays were carried out in triplicate and the different analyses were done after 1 and 24 h of TCS exposure.

5.2.3 Flow cytometric analysis (FCM)

FCM analyses of *C. reinhardtii* cells were performed on a Beckman Coulter Gallios flow cytometer fitted with an argon-ion excitation laser (488 nm), a detector of forward scatter (FS), a detector of side scatter (SS) and with four fluorescence detectors with four different wavelength intervals: 505-550 nm (FL1), 550-600 nm (FL2), 600-645 nm (FL3) and >645 nm (FL4, used to estimate cell chlorophyll a content).

Cells were incubated with the appropriate fluorochrome (see supplementary Table S5.1 for details) for each parameter at room temperature and in the dark, after 1 and 24 hours of TCS exposure, prior to analysing by FCM. All fluorochrome stock solutions were prepared in dimethyl sulfoxide (DMSO) and stored at −20 °C, with the exception of the solution of propidium iodide (PI), which was made in Milli-Q water and stored at 4 ºC. The fluorochrome concentrations and incubation times were as those reported by Prado et al. (2012) (Table S5.1).

Three independent experiments with triplicate samples were carried out for each parameter. For all the cytometric parameters studied here, at least 10^4 gated cells were analyzed using Kaluza software version 1.1 (Beckman Coulter).

5.2.4 Lipid peroxidation

Lipid peroxidation was determined in terms of thiobarbituric acid reactive substances (TBARS) following the protocol described by Ortega-Villasante et al. (2005) with minor modifications (Elbaz et al., 2010). Algae were centrifuged (for 5 min at 4500 rpm) and submerged in liquid nitrogen. Frozen pellets were homogenized in 0.5 mL of TCA–TBA–HCl reagent (15 %, w/v) trichloroacetic acid, 0.37 % (w/v) 2-thiobarbituric

acid, 0.25 M HCl, and 0.01 % butylated hydroxytoluene. Absorbance was measured at 535 and 600 nm on a Synergy HT multi-mode microplate reader (BioTek, USA) using 96 well transparent microplates. The amount of TBARS was calculated by using the extinction coefficient of 155 mM^{-1} cm^{-1}. Lipid peroxidation was expressed as MDA relative content.

5.2.5 Chlorophyll determination

Chlorophyll *a* and *b* were extracted from a concentrated algal sample in a 90% acetone aqueous solution and determined by measuring the absorbance of the extract using spectrophotometry at appropriate wavelengths (664 and 647). Chlorophyll concentrations were calculated according to Jeffrey and Humphrey (1975).

5.2.6 Oxygen evolution

Oxygen evolution was measured at 22 ºC under saturating white light (300 µmol photons m^{-2} s^{-1}) with a Clark-type oxygen electrode (Hansatech) according to Leganés et al. (2014). Cells were supplemented with 5 mM $NaHCO_3$, pH 7.5. Photosynthetic rates were expressed as µmol O_2 mg^{-1} Chl h^{-1}.

5.2.7 RT-QPCR

Total RNA was extracted from frozen cell pellets using hot acid (pH 4.5) phenol at 65 ^{o}C (Amresco LLC; VWR Chemicals, USA) followed by extraction with acid hot phenol:chloroform (1:1) and a second extraction with chloroform; subsequent treatment with 1 vol. isopropanol, centrifugation, pellet washing with 70% ethanol and resuspension in DEPC-treated water. Genomic DNA remains were removed using RQ1 RNase-Free DNase (Promega) for 30 min at 37 ^{o}C. Thereafter, RNA was purified using Trizol® (Invitrogen). The concentration of RNA was spectrophotometrically determined in a Nanodrop (Thermo Scientific). cDNA was synthetized from 1 µg of extracted RNA using the iScriptTM cDNA Synthesis Kit from Bio-Rad following manufacturer's instructions. RT-qPCR primers used in this study are indicated in Supplementary Table S5.2. Primers *psbD*F and *psbD*R were designed using the DNASTAR`s Lasergene software.

RT-qPCR was performed on a Techne Quantica apparatus using SYBR Green Master mix (Roche). The 2-ΔΔC (Livak and Schmittgen, 2001) was used to normalize and calibrate transcript values relative to the 18S gene.

5.2.8 Protein isolation and analysis

C. reinhardtii cells were pelleted by centrifugation (for 5 min at 4500 rpm) and frozen in liquid nitrogen. For protein extraction, pellets were grinded using a mortar and liquid nitrogen, and then homogenized in extraction buffer [HEPES 50 mM pH 7.5, 1mM $MgCl_2$, 5 mM EDTA, 1 Mm DTT, protease inhibitor and 1% w/w polyvinylpyrrolidone (PVPP)]. Samples were centrifuged (for 10 min at 10000 rpm) and the supernatant, which constitutes the total protein extract, collected. Protein quantification was performed according to Bradford (1976). Proteins were solubilized using Laemmli buffer boiled at 95ºC for 5 minutes and resolved with sodium dodecyl sulphate polyacrylamide gel electrophoresis (SDS-PAGE) (10%) (Laemmli, 1970). Specific bands were cut out and submitted to the proteomic service of the National Centre for Biotechnology (CNB, Spain) where they were identified by MALDI TOF/TOF tandem mass spectrometry to obtain peptide mass fingerprints. The proteins were identified by comparing peptide mass fingerprints to the NCBInr database for *C. reinhardtii* using the Mascot search engine.

5.2.9 Data analysis

Means and standard deviation values were calculated for each treatment from three independent replicate experiments. To determine significant differences among test treatments, data were statistically analyzed conducting an overall one-way analysis of variance (ANOVA) using R software. A $p < 0.05$ was considered statistically significant. When significant differences were observed, means were compared using the multiple-range Tukey's HSD test. Median values (arbitrary units; a.u.) and standard deviation were calculated for flow cytometry analyses.

5.3 RESULTS

5.3.1 Triclosan-induced alterations in intracellular free Ca^{2+} in *C. reinhardtii*

C. reinhardtii cells were stained with the fluorescent cytoplasmic intracellular free Ca^{2+} (here in after referred as $[Ca^{2+}]_c$) specific indicator Calcium Green-1 to assess by flow cytometry the potential changes in *C. reinhardtii* $[Ca^{2+}]_c$ induced by TCS after 1, 4 and 24 h of exposure (Fig. 5.1).

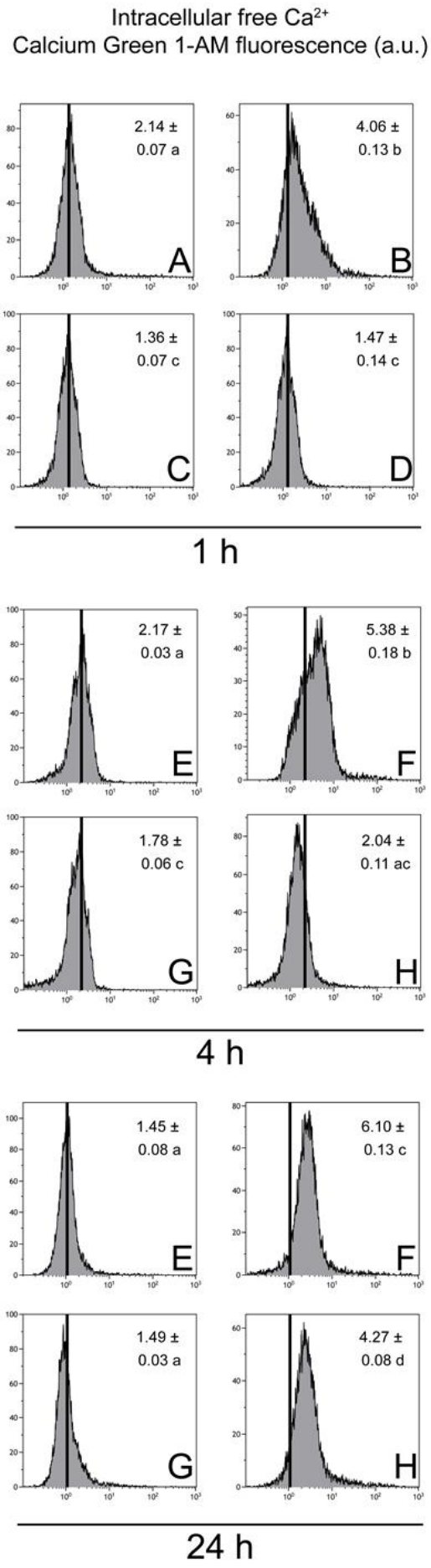

Figure 5.1. Effect of TCS on $[Ca^{2+}]_c$ of *C. reinhardtii* by FCM using the fluorochrome Calcium Green-1, AM. Histograms show the distribution of fluorescence intensity of the CalciumGreen-1 in logarithmic scale among the cells analyzed by FCM (Y-axis: cell number, X-axis: fluorescence intensity in arbitrary units, a.u.). Data are expressed as medianvalues (a.u) ± SD. Treatments with different letters are significantly different (Tukey´ıs HSD, $p < 0.001$). Control (A) and cultures exposed to 13.8 M TCS (B), BAPTA-AM (C) and13.8 M TCS + BAPTA-AM (D) for 1 h. Control (E) and cultures exposed to 13.8 M TCS (F), BAPTA-AM (G) and 13.8 M TCS + BAPTA-AM (H) for 4 h. Control (I) and culturesexposed to 13.8 M TCS (J), BAPTA-AM (K) and 13.8 M TCS + BAPTA-AM (L) for 24 h.

After 1 h of exposure 13.8 µM TCS induced a significant ($p < 0.001$) elevation (87%) in $[Ca^{2+}]_c$ (Fig. 5.1B). Before TCS exposure, cells were pretreated with the intracellular Ca^{2+}-chelator BAPTA-AM. As shown in Fig. 5.1D BAPTA-AM completely avoided the TCS-induced $[Ca^{2+}]_c$ elevation. After 4 h TCS exposure, the elevation increased to around 248% of basal $[Ca^{2+}]_c$ levels (Fig. 5.1F). Pre-incubation with BAPTA-AM completely prevented the observed increase (Fig. 5.1H). After 24 h of exposure, the $[Ca^{2+}]_c$ elevation induced by TCS reached 420% of basal levels with (Fig. 5.1J). Pretreatment with BAPTA-AM partially but significantly ($p < 0.001$) (30 %) avoided the TCS-induced $[Ca^{2+}]_c$ elevation (Fig. 5.1L). BAPTA-AM itself slightly but significantly lowered $[Ca^{2+}]_c$ after 1 h and 4-h exposure (Fig. 5.1C, G) but did not alter basal levels of $[Ca^{2+}]_c$ after 24 h (Fig. 5.1K).

The results indicate that TCS induced a sustained elevation of $[Ca^{2+}]_c$ (up to 24 h) in *C. reinhardtii* significantly altering $[Ca^{2+}]_c$ homeostasis; the intracellular calcium chelator BAPTA-AM completely abolished such $[Ca^{2+}]_c$ elevations at shorter exposure times (1 and 4 h) and partially although significantly after 24 h .

5.3.2 Triclosan-induced ROS formation in *C. reinhardtii*

One of the earlier responses to most pollutants is the formation of ROS (Lushchak, 2011; Ortega-Villasante et al., 2005; Pinto et al., 2003; Pulido-Reyes et al., 2015; Rodea-Palomares et al., 2012; Xia et al., 2008) which, if unbalanced, may cause oxidative stress.

ROS formation was assessed in cells exposed to 13.8 µM TCS after short (1 h) and long (24 h) term exposure. The intracellular calcium chelator BAPTA-AM was used to study the relationship, if any, between $[Ca^{2+}]_c$ changes and ROS formation by TCS. The fluorescent indicator HE was used to determine intracellular superoxide anion by flow cytometry (Fig. 5.2). 1 h exposure to TCS strongly increased intracellular O_2^- levels to around 179% (Fig. 5.2B). BAPTA-AM pretreatment totally prevented the induced increase in O_2^- levels (Fig. 5.2D).

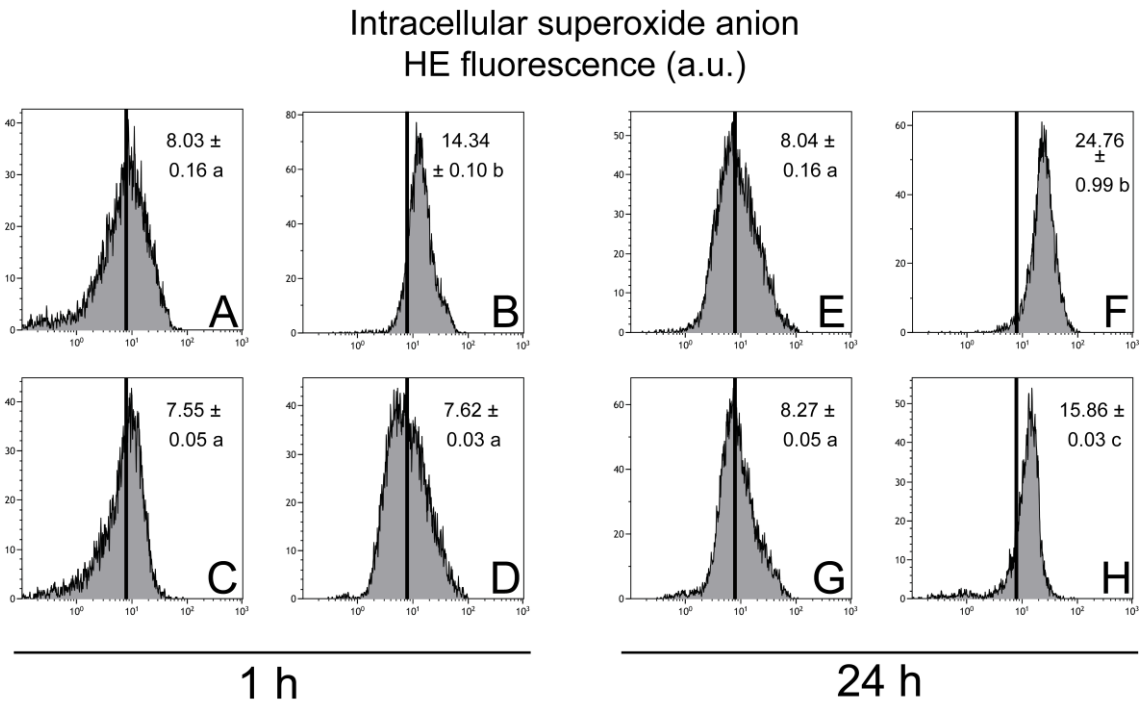

Figure 5.2 . Effect of TCS on intracellular superoxide anion levels of *C. reinhardtii* by FCM using the fluorochrome HE. Histograms show the distribution of fluorescence intensityof HE in logarithmic scale among the cells analyzed by FCM (Y-axis: cell number, X-axis: fluorescence intensity in arbitrary units, a.u.). Data are expressed as median values(a.u.) ± SD. Treatments with different letters are significantly different (Tukey´ıs HSD, $p < 0.001$). Control (A) and cultures exposed to 13.8 M TCS (B), BAPTA-AM (C) and13.8 M TCS + BAPTA-AM (D) for 1 h. Control (E) and cultures exposed to 13.8 M TCS (F), BAPTA-AM (G) and 13.8 M TCS + BAPTA-AM (H) for 24 h. After 24 h exposure, TCS further increased O_2^- levels to 308% of control values (Fig. 5.2E, F). BAPTA-AM pretreatment greatly prevented the observed increase (Fig. 5.2H). BAPTA-AM itself did not have any significant effect on this parameter (Fig. 5.2C, G).

The fluorescent dye DHR123 was used to assess the formation of hydrogen peroxide in TCS-exposed cultures. Intracellular H_2O_2 levels significantly increased (233%; $p < 0.001$) after 1 h of exposure to 13.8 µM TCS (Fig. 5.3B). BAPTA-AM pretreatment completely suppressed the observed TCS-induced increase in H_2O_2 levels (Fig. 5.3D). After 24 h of exposure, 13.8 µM TCS induced a higher formation of intracellular hydrogen peroxide reaching 494% of the control values (Fig. 5.3F). BAPTA-AM significantly ($p < 0.001$) diminished (39%) the observed TCS-induced H_2O_2 formation (Fig. 5.3H). BAPTA-AM itself did not have any significant effect on this parameter (Fig. 5.3C, G).

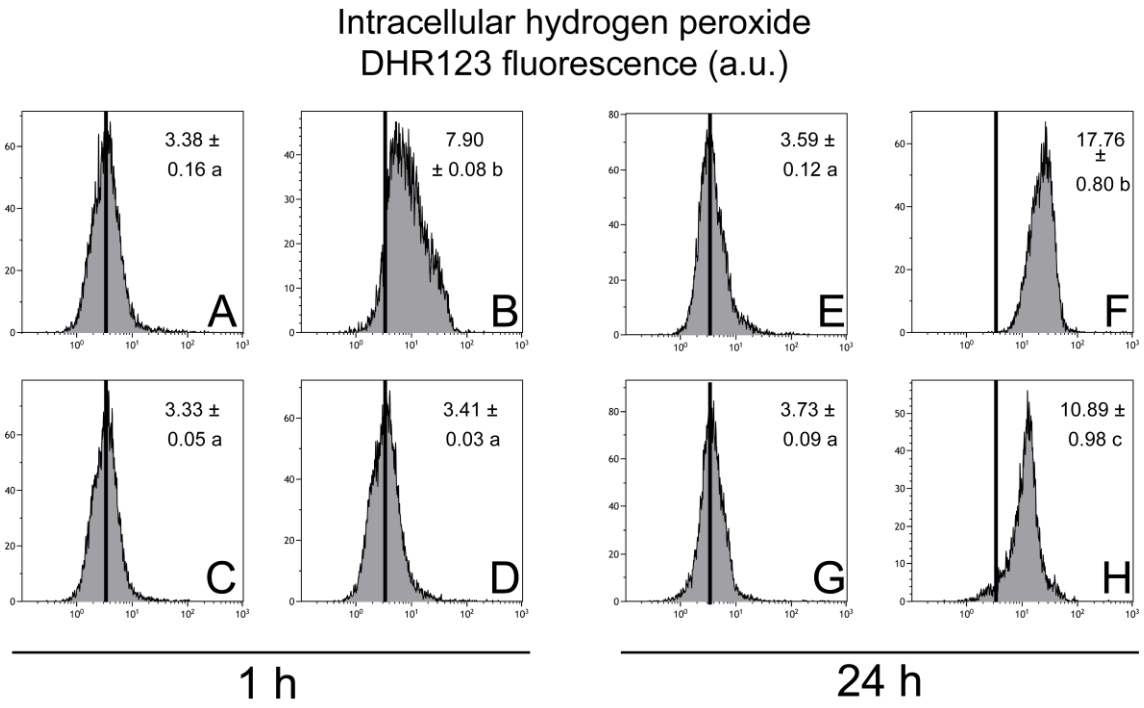

Figure 5.3. Effect of TCS on intracellular hydrogen peroxide levels of C. reinhardtii by FCM using the fluorochrome DHR123. Histograms show the distribution of fluorescenceintensity of DHR123 in logarithmic scale among the cells analyzed by FCM (Y-axis: cell number, X-axis: fluorescence intensity in arbitrary units, a.u.). Data are expressed asmedian values (a.u.) ± SD. Treatments with different letters are significantly different (Tukey´ıs HSD, $p < 0.001$). Control (A) and cultures exposed to 13.8 M TCS (B), BAPTA-AM(C) and 13.8 M TCS + BAPTA-AM (D) for 1 h. Control (E) and cultures exposed to 13.8 M TCS (F), BAPTA-AM (G) and 13.8 M TCS + BAPTA-AM (H) for 24 h.

Summarizing, TCS promoted an extensive formation of ROS such as superoxide anion and hydrogen peroxide in exposed *C. reinhardtii* cells. Pretreatment with the intracellular calcium chelator BAPTA-AM significantly avoided ROS formation implying a role for calcium in intracellular ROS overproduction induced by TCS.

5.3.3 Effects of antioxidant N-acetylcysteine on TCS-induced increases in $[Ca^{2+}]_c$ and ROS formation

To further understand the relationship between TCS-induced calcium homeostasis alterations and oxidative stress due to increased ROS formation, cells were co-treated with the antioxidant N-acetylcysteine (NAC) and TCS and compared to treatment with TCS and BAPTA-AM pretreatment.

NAC is a synthetic precursor of intracellular cysteine and glutathione and is thus considered as an important antioxidant (Zafarullah et al., 2003). NAC was used at a final concentration of 1 mM; although above this concentration ROS formation drastically decreased, it was found that cytotoxicity strongly increased leading to cell lysis (not shown). $[Ca^{2+}]_c$ as well as ROS formation (superoxide anion and hydrogen peroxide) were measured (Fig. 5.4). As Fig. 5.4A shows, after 1 h NAC-TCS co-treatment, $[Ca^{2+}]_c$ significantly ($p < 0.05$) decreased but to a lesser extent than with BAPTA-AM pretreatment which completely prevented $[Ca^{2+}]_c$ increase; after 24 h, NAC-TCS co-treatment slightly attenuated $[Ca^{2+}]_c$ increase as compared to BAPTA-AM pretreatment. NAC and BAPTA by themselves did not have any significant effect on these parameters. Regarding superoxide anion formation, 1 h NAC-TCS co-treatment completely abolished superoxide anion increase induced by TCS; similar to the effect of BAPTA-AM pretreatment; after 24-h, NAC-TCS co-treatment slightly although significantly ($p < 0.05$) attenuated superoxide anion increase but to a lesser extent than BAPTA-AM pretreatment (Fig. 5.4B). Hydrogen peroxide formation under the different treatments followed a similar pattern to that described for superoxide anion formation: NAC-TCS co-treatment completely abolished hydrogen peroxide formation after 1 h and significantly ($p < 0.05$) after 24 h but to a lesser extent than BAPTA-AM pretreatment (Fig. 5.4C).

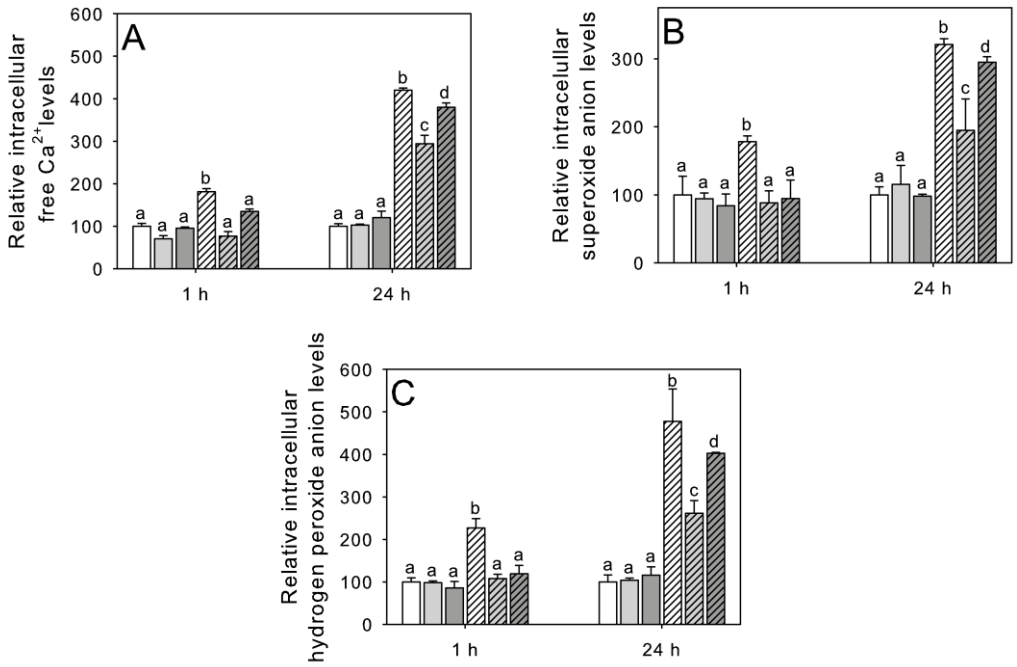

Figure 5.4. Effect of NAC (1 mM) on $[Ca^{2+}]_c$ (A), superoxide anion levels (B) and intracellular hydrogen peroxide levels (C) on *C. reinhardtii* after 1 and 24 h exposure to TCS. Control (▭), BAPTA-AM (▭), NAC (▭), TCS (▨), TCS + BAPTA-AM (▨) and NAC + TCS (▨). Data are expressed as percentage ± SD with respect to control (assigned a value of 100%). Treatments with different letters are significantly different (Tukey´s HSD, $p < 0.05$).

These results support the idea that there is an interconnection between ROS formation (which may lead to oxidative stress) and the observed alteration in $[Ca^{2+}]_c$ induced by TCS.

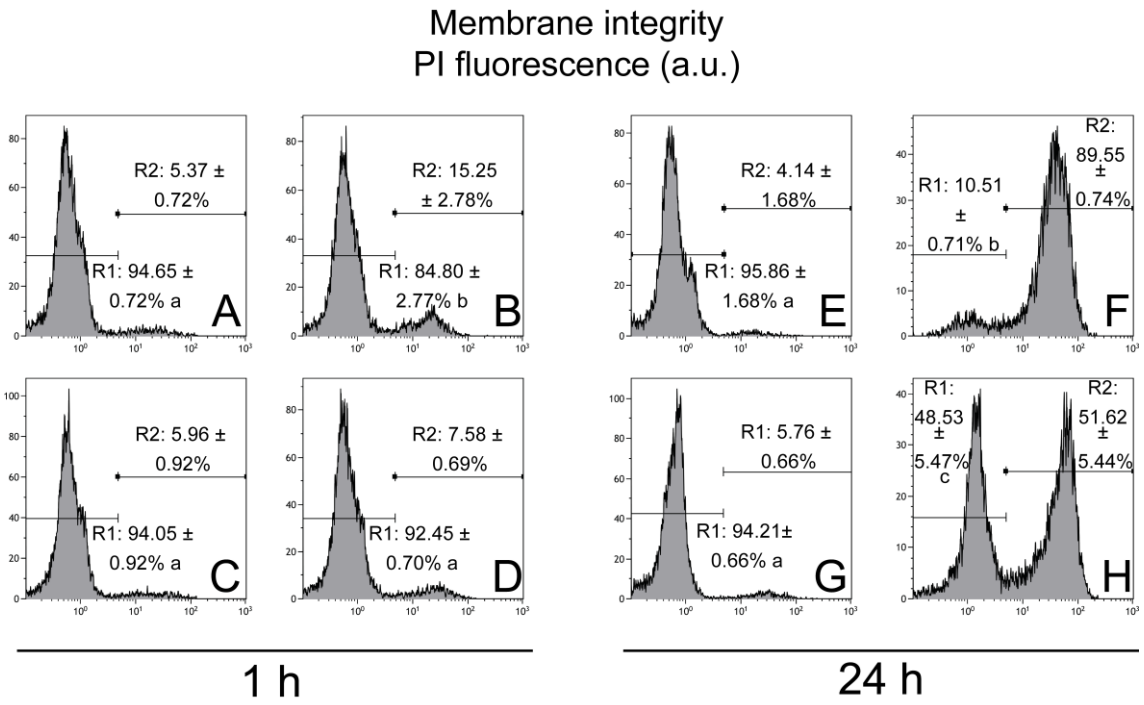

Figure 5.5. Effect of TCS on cell membrane integrity of *C. reinhardtii* by FCM using the fluorochrome PI.

Histograms show the distribution of fluorescence intensity of PI in logarithmic scale among the cells analyzed by FCM (Y-axis: cell number, X-axis: fluorescence intensity in arbitrary units, a.u.). R1 and R2 represent (as percentage) cell subpopulations comprising intact cells (subpopulation R1) and membrane-damaged cells (subpopulation R2) analyzed by FCM, respectively. Treatments with different letters are significantly different (Tukey´s HSD, $p < 0.001$). Control (A) and cultures exposed to 13.8 µM TCS (B), BAPTA-AM (C) and 13.8 µM TCS + BAPTA-AM (D) for 1 h. Control (E) and cultures exposed to 13.8 µM TCS (F), BAPTA-AM (G) and 13.8 µM TCS + BAPTA-AM (H) for 24 h.

5.3.4 TCS alterations in membrane integrity

To check whether TCS may impair membrane integrity, the fluorescent dye PI was used and analyzed by flow cytometry. The flow cytograms showed the presence of two cell subpopulations, R1 and R2, in the control cultures (Fig. 5.5A, E). R1 comprised around 95% of total cells, this region might be considered as intact cells (intact membranes); the R2 subpopulation comprised cells with compromised membranes (less than 5% of total cells). 13.8 µM TCS significantly ($p < 0.001$) affected membrane integrity after 1 h of exposure increasing the R2 subpopulation (the one including damaged cells) to 15% of total cells indicating serious damage to cell membranes. BAPTA-AM pretreatment completely abolished the observed TCS-induced membrane damage. After 24 h of exposure, TCS increased the membrane damaged cells subpopulation to almost 90% of

total cells (Fig. 5.5F). BAPTA-AM pretreatment significantly decreased ($p < 0.001$) the R2 subpopulation to 51% of total cells (Fig. 5.5H). BAPTA-AM itself did not have any significant effect on this parameter (Fig. 5.5C, G).

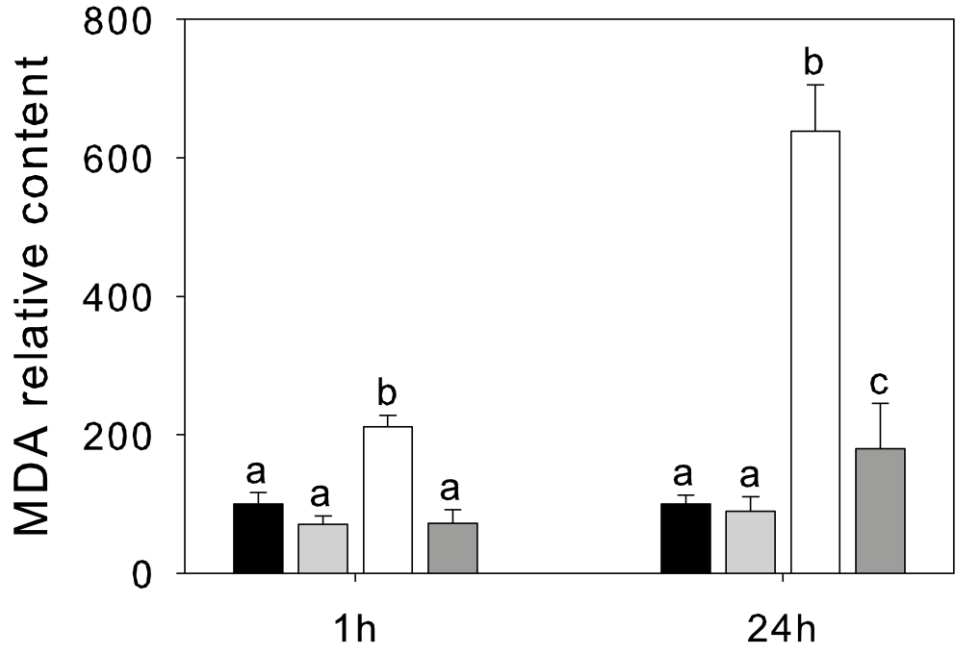

Figure 5.6. Lipid peroxidation levels as MDA relative content of *C. reinhardtii* exposed to treatments after 1 and 24 h of exposure to different treatments. Control (■), BAPTA-AM (▭), TCS (▭) and TCS + BAPTA-AM (▭). Data are expressed as means ± SD. Treatments with different letters are significantly different (Tukey´s HSD, $p < 0.001$).

It was further demonstrated that TCS compromised membrane integrity by measuring the levels of lipid peroxidation; as Fig. 5.6 shows, TCS significantly ($p < 0.001$) increased lipid peroxidation after 1 h of exposure (150% of control cultures); after 24 h of exposure, lipid peroxidation levels reached a value over 600% of that of control culture. BAPTA-AM pretreatment totally prevented lipid peroxidation after 1 h of exposure and significantly ($p < 0.001$) diminished it by three-fold after 24 h exposure. BAPTA-AM itself did not have any significant effect on this parameter (Fig. 5.6). TCS damaged cell membranes of exposed cells which may seriously compromise cell viability. Calcium seems to have a role in this cellular response to the toxicant as suppression/reduction of the $[Ca^{2+}]_c$ elevation by BAPTA-AM significantly decreased TCS-induced membrane damage particularly at the shorter exposure time.

5.3.5 Triclosan-induced alterations in cytoplasmic membrane potential

Previously, it was shown that TCS compromised cytoplasmic membrane integrity which might increase non-specific permeability leading to membrane depolarization. The effect of TCS on cytoplasmic membrane potential of *C. reinhardtii* was studied by flow cytometry using the fluorescent dye $DIBAC_4(3)$ (Fig. 5.7). Flow cytograms showed two clear subpopulations (R1 and R2) in control cells (Fig. 5.7A). R1 was the largest one comprising around 94% of total cells while the R2 subpopulation (showing a slight membrane depolarization) accounted for 5.8% of total cells. After 1 h of exposure, 13.8 µM TCS dramatically increased membrane depolarization (median values of 23.3 a.u. in the TCS treated cultures *vs.* 1 in unexposed controls) of 92% of total cells in culture (R2 subpopulation) (Fig. 5.7B). Pretreatment with BAPTA-AM completely suppressed TCS-induced depolarization (Fig. 5.7D). 24 h of TCS treatment further increased the R2 subpopulation to 95% with levels of membrane depolarization that reached 75 a.u. (median values) (Fig. 5.7F). BAPTA-AM pretreatment significantly ($p < 0.001$) decreased plasma membrane depolarization induced by TCS, both in median values and affected R2 subpopulation, (Fig. 5.7H). BAPTA-AM itself did not have any significant effect on this parameter (Fig. 5.7C, G).

TCS dramatically depolarized cytoplasmic membrane potential. The fact that suppression/reduction of the $[Ca^{2+}]_c$ elevation by BAPTA-AM significantly prevented cytoplasmic membrane depolarization indicated a role of calcium in membrane depolarization induced by TCS.

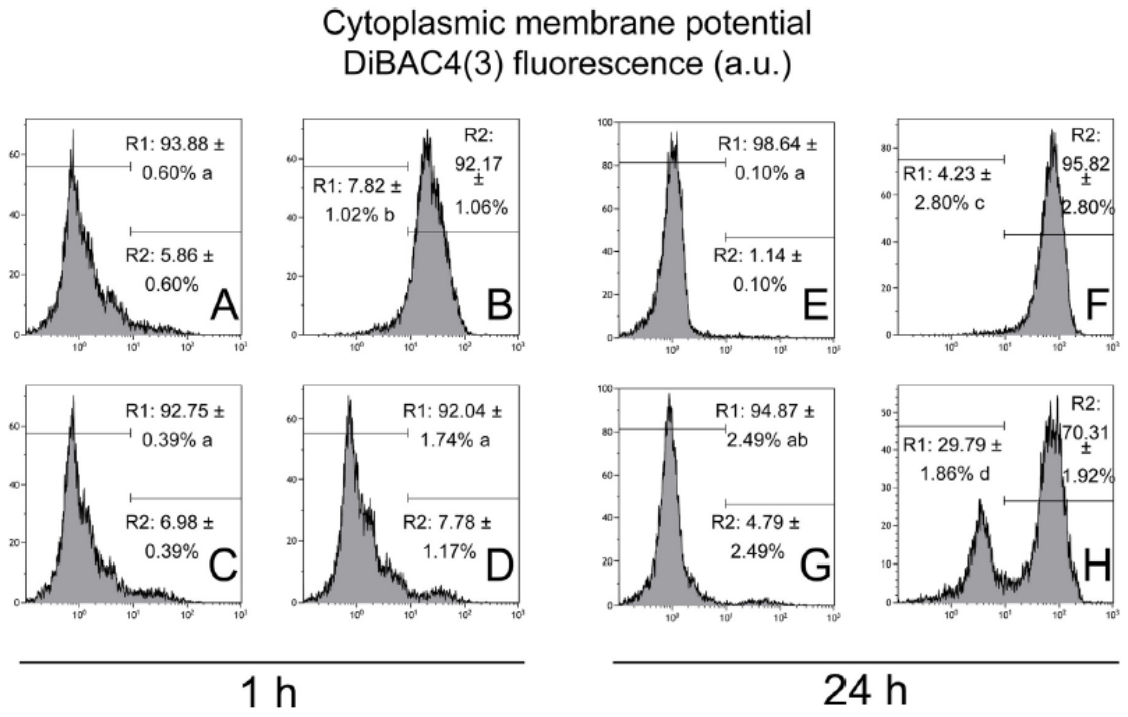

Figure 5.7. Effect of TCS on cell cytoplasmic membrane potential of *C. reinhardti* by FCM using the fluorochrome $DiBAC_4(3)$. Histograms show the distribution of fluorescence intensity of $DiBAC_4(3)$ in logarithmic scale among the cells analyzed by FCM (Y-axis: cell number, X-axis: median values of fluorescence intensity in arbitrary units, a.u.). R1 and R2 represent (as percentage) cell subpopulations comprising cells with non-depolarized cytoplasmic membrane potential (R1) and cells with depolarized cytoplasmic membrane potential (R2) analyzed by FCM, respectively. Treatments with different letters are significantly different (Tukey´s HSD, $p < 0.001$). Control (A) and cultures exposed to 13.8 µM TCS (B), BAPTA-AM (C) and 13.8 µM TCS + BAPTA-AM (D) for 1 h. Control (E) and cultures exposed to 13.8 µM TCS (F), BAPTA-AM (G) and 13.8 µM TCS + BAPTA-AM (H) for 24 h.

5.3.6 Triclosan-induced changes in mitochondrial functions

Mitochondria are not just important in plant bioenergetics and metabolism but also are relevant in cellular processes in response to environmental stresses such as those posed by pollutants. To study potential mitochondria dysfunction induced by TCS exposure, mitochondrial membrane potential and caspase 3/7 activity were assessed by flow cytometry using the fluorescent dyes JC-1 and Cell Event Caspase 3/7 Green Detection reagent, respectively. Although it seems that caspases are not localized in mitochondria; perturbation of mitochondria results in the activation of caspases involved in cell death (Van Loo et al., 2002).

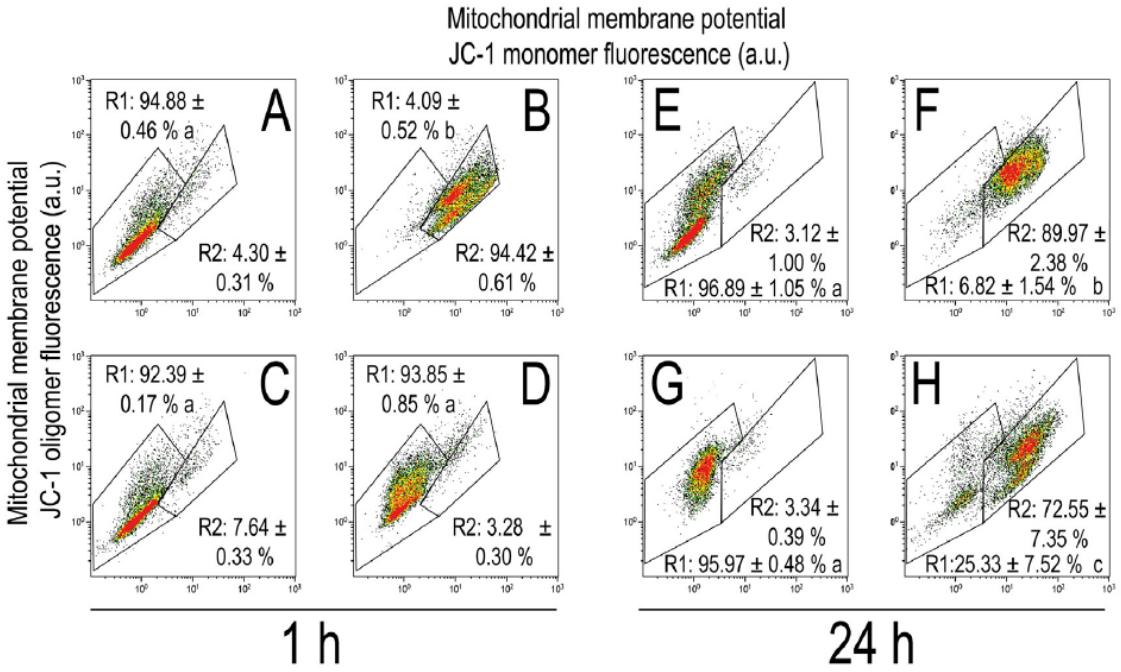

Figure 5.8. Effect of TCS on mitochondrial membrane potential of *C. reinhardtii* by FCM using the fluorochrome JC-1. Dot-plot shows the distribution of fluorescence intensity of the JC-1 monomer fluorescence (a.u.) in logarithmic scale and JC-1 oligomer fluorescence (a.u.) among the cells analyzed by FCM. R1 and R2 represent (as percentage) cell subpopulations comprising cells with non-depolarized mitochondrial membrane potential (R1) and cells with depolarized mitochondrial membrane potential (R2) analyzed by FCM, respectively. Treatments with different letters are significantly different (Tukey´s HSD, $p < 0.001$). Control (A) and cultures exposed to 13.8 µM TCS (B), BAPTA-AM (C) and 13.8 µM TCS + BAPTA-AM (D) for 1 h. Control (E) and cultures exposed to 13.8 µM TCS (F), BAPTA-AM (G) and 13.8 µM TCS + BAPTA-AM (H) for 24 h.

As shown in the flow biparametric cytogram JC1 fluorescence *vs.* cell size (Fig. 5.8); there were two distinct gated regions in each image, denoted as R1 and R2; in the control culture, the R1 gated region stands for cells showing basal JC1 fluorescence values with 94. 88% total cells inside this region; a subpopulation of control cells, R2 (4.30 % total cells) showed higher JC1 values. As shown in Fig. 5.8B and F, 13.8 µM TCS provoked a dramatic membrane potential depolarization at both experimental time points affecting around 95% of total cells (R2 subpopulation). Interestingly, pretreatment with BAPTA-AM completely prevented the observed TCS-induced mitochondrial membrane potential alterations after short time exposure (Fig. 5.8D) and partially but significantly ($p < 0.001$) after longtime exposure (R2 subpopulation

reduced to 72% and R1 increased to 25%) (Fig. 5.8H). BAPTA-AM itself did not have any significant effect on this parameter (Fig. 5.8C, G).

Caspase 3/7 activity (Fig. 5.9) was assayed after 24 h of TCS exposure (1 h of exposure did not show any difference with respect to the control, not shown); as shown in figure 5.9B, TCS caused a drastic increase ($p < 0.001$) in caspase 3/7 activity, up to 450% of the control value (1.81 ± 0.05 *vs.* 0.43 ± 0.0115 median values) in around 83% of total cells in culture identified as R2 subpopulation.

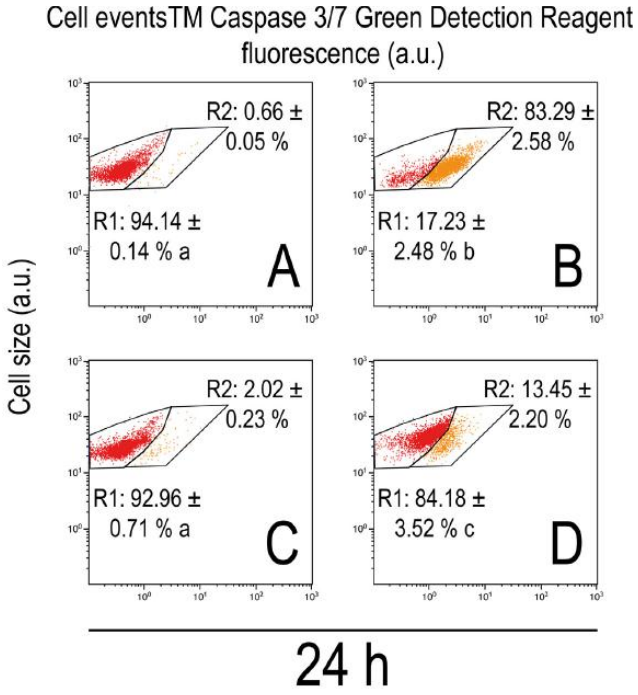

Figure 5.9 Effect of TCS caspase 3/7 activity of *C. reinhardtii* by FCM using the fluorochrome CellEvent™ Caspase-3/7 Green Detection Reagent. Dot-plot shows the distribution of fluorescence intensity of the caspase 3/7 activity in logarithmic scale (arbitrary units; a.u.) and FS among the cells analyzed by FCM. R1 and R2 represent (as percentage) cell subpopulations comprising non-apoptotic cells (R1) and apoptotic cells (R2) analyzed by FCM, respectively. Treatments with different letters are significantly different (Tukey´s HSD, $p < 0.001$). Control (A) and cultures exposed to 13.8 µM TCS (B), BAPTA-AM (C) and 13.8 µM TCS + BAPTA-AM (D) for 24 h.

Pre-Treatment with BAPTA-AM almost completely prevented caspase 3/7 activity induction, with a 41% reduction in activity with respect to the TCS treated cells (1.05 ± 0.0569 *vs*. 1.81 ± 0.05 median values) and 83% reduction in the R2 subpopulation

(Fig. 5.9D). BAPTA-AM itself did not have any significant effect on this parameter (Fig. 5.9C).

TCS provoked important alterations in mitochondrial functions such as marked depolarization and increased caspase 3/7 activity. Calcium also has a role in these processes as abolition/reduction of the $[Ca^{2+}]_c$ elevation by pretreatment with BAPTA-AM largely prevented them.

5.3.7 Triclosan alters intracellular pH (pHi)

Green/red BCECF fluorescence intensity ratio was used to measure pHi by flow cytometry in *C. reinhardtii* exposed to TCS. Fig. 5.10A showed that TCS induced a significant ($p < 0.05$) alkalinization of the cytoplasm after 1 h of exposure; this was totally avoided by pretreatment with BAPTA-AM.

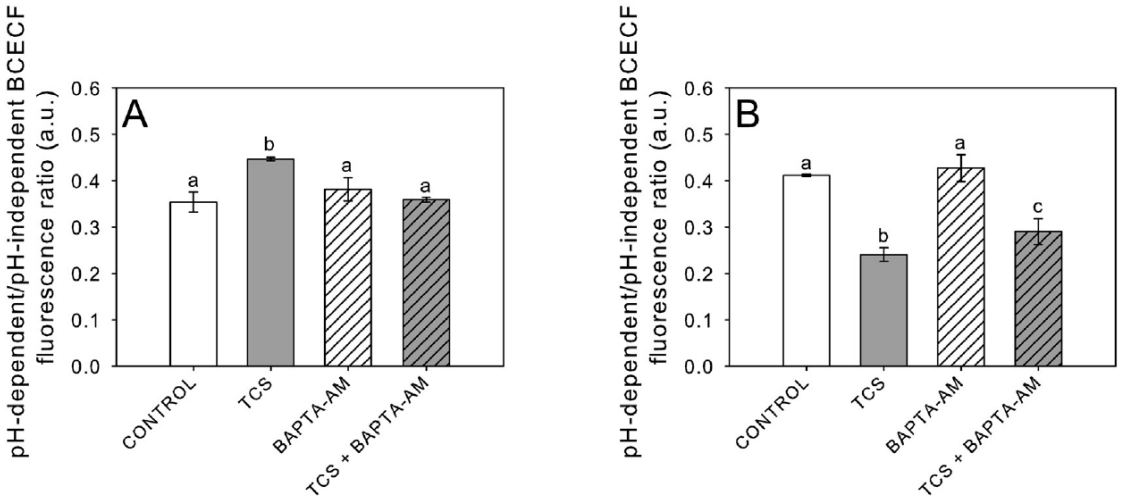

Figure 5.10. Effect of TCS on intracellular pH (pHi) of *C. reinhardtii* by FCM using the fluorochrome BCECF. Data are expressed as the ratio of the fluorescence emitted at 525 nm(pH-dependent BCECF) and 620 nm (pH-independent BCECF). Treatments with different letters are significantly different (Tukey´ıs HSD, $p < 0.05$). Cells exposed to TCS 1 h (A)and 24 h (B).

After 24 h of exposure, instead of alkalinization, a strong acidification of the cytoplasm was observed (Fig. 5.10B) which could be partially although significantly ($p < 0.05$) prevented by BAPTA-AM pretreatment indicating that the drastic observed acidification seemed to be related, at least partially, to the recorded $[Ca^{2+}]_c$ increase. BAPTA-AM itself did not have any significant effect on this parameter (Fig. 5.10A, B).

5.3.8 Triclosan-induced alterations on the metabolic activity of *C. reinhardtii*

The esterase activity analyses (FDA fluorescence monitored by flow cytometry) after 1 h exposure to TCS indicated that metabolic activity was increased around twofold in 65% of total cells in culture while completely inhibited in the remainder 35% of cells (Fig. 5.11B). BAPTA-AM pretreatment significantly ($p < 0.001$) avoided the observed alterations induced by TCS as the metabolic activity increase was not observed and the observed inhibition decreased to 50% (Fig. 5.11D).

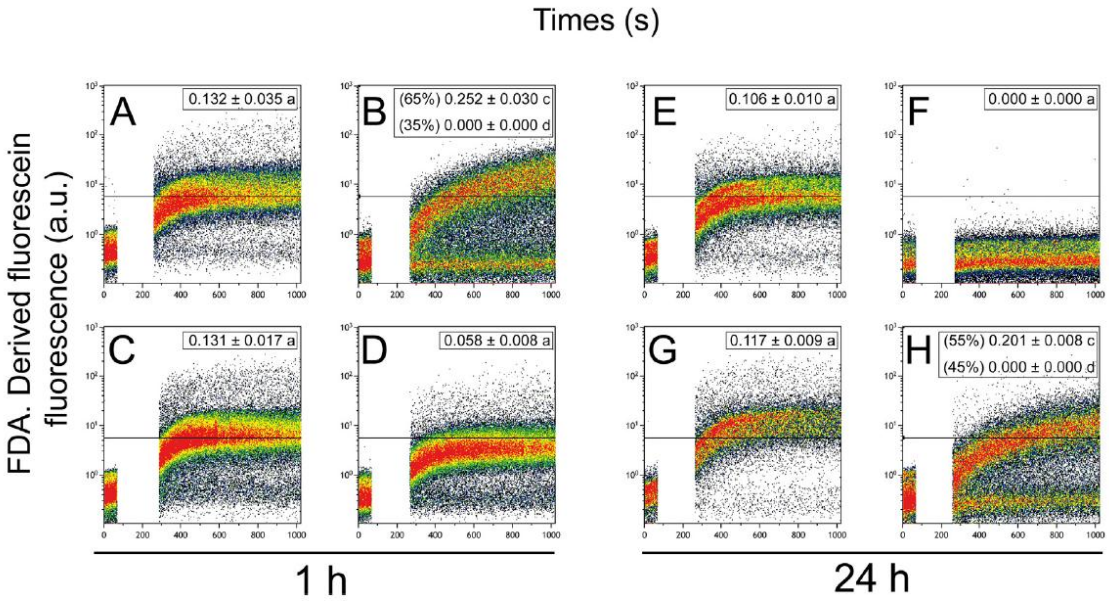

Figure 5.11. Analysis of the effect of TCS on esterase activity (as an index of metabolic activity) through kinetic plots showing the increase of the FDA-derived fluorescein fluorescence as a function of time. Fluorescence generation rates are indicated in arbitrary units per minute (a.u. min^{-1}). Data are expressed as mean values (a.u. min^{-1}) ± SD. Treatments with different letters are significantly different (Tukey´s HSD, $p < 0.001$). Control (A) and cultures exposed to 13.8 µM TCS (B), BAPTA-AM (C) and 13.8 µM TCS + BAPTA-AM (D) for 1 h. Control (E) and cultures exposed to 13.8 µM TCS (F), BAPTA-AM (G) and 13.8 µM TCS + BAPTA-AM (H) for 24 h.

After 24 h of TCS exposure, esterase activity was totally inhibited (Fig. 5.11F). BAPTA-AM pretreatment provoked a twofold increase in the metabolic activity over the control level in 55% of total cells exposed to TCS while 45% of total cell population still showed complete inhibition of the esterase activity (Fig. 5.11H). BAPTA-AM itself

did not have any significant effect on this parameter (Fig. 5.11C, G). Data indicate an involvement of calcium in the cellular response to TCS regarding this crucial parameter.

5.3.9 Photosynthetic responses of *C. reinhardtii* to Triclosan

The photosynthetic performance of 13.8 µM TCS-exposed *C. reinhardtii* was evaluated by measuring O_2 evolution with a Clark-type electrode. Photosynthetic O_2 evolution was significantly ($p < 0.05$) decreased (85% inhibition with respect to unexposed cells) after just 1 h exposure (Table 5.1).

Table 5.1. . Effect of TCS on photosynthetic activity (as O_2 evolution) of *C. reinhardtii*. Data are means ± SD. Treatments with different letters are significantly different (Tukey´s HSD, $p < 0.05$).

Time (hour)	Treatment	O_2 evolution (µmol O_2 mg chl^{-1} h^{-1})
1 h	Control	153.3 ± 0.5 a
	BAPTA-AM	130.3 ± 2.9 a
	TCS	22.2 ± 4.1 b
	TCS + BAPTA-AM	100.6 ± 15.2 c
24 h	Control	250.2 ± 23.7 a
	BAPTA-AM	178.7 ± 7.8 b
	TCS	2.0 ± 1.7 c
	TCS + BAPTA-AM	23.7 ± 1.6 d

Pretreatment with BAPTA-AM significantly ($p < 0.05$) prevented photosynthesis inhibition, as O_2 evolution reached 65% of that of the control culture. After 24 h TCS exposure, pretreatment with BAPTA-AM itself already significantly ($p < 0.05$) decreased O_2 evolution (71% of control value); this could be explained by the fact that calcium is a crucial structural component of photosystem II (PSII) (Vander Meulen et al., 2004). Nevertheless, TCS completely abolished photosynthesis (99.2 inhibition)

which could be partially but significantly ($p < 0.05$) prevented by BATA-AM pretreatment.

5.3.10 Effect of Triclosan on transcription of selected genes involved in photosynthesis, oxidative stress defense, calcium signaling and apoptosis

RT-qPCR was used to determine changes in the expression of selected genes involved in some of these processes as well as in calcium signaling *per* se, in order to gain insight into the molecular mechanisms involved in the observed cellular responses to TCS. As in the previously described experiments, pretreatment with BAPTA-AM allowed to relate changes in gene expression with calcium homeostasis.

Fig. 5.12 shows the effect of 13.8 µM TCS on gene expression of the selected genes after 1 and 24 h exposure. The effect of BAPTA-AM pretreatment is also shown. To determine the effects of TCS on cellular antioxidant defense systems, the expression of the *Fe-SOD*, *Mn-SOD* (encoding superoxide dismutases), *CAT* (encoding a catalase) and *GPX* (encoding a glutathione peroxidase) genes was studied. At short exposure times (1 h), both *Fe-SOD* and *Mn-SOD* expression was downregulated by 70% and 90%, respectively (Fig. 5.12A, B); however, TCS clearly upregulated (1.7-fold) the expression of the *CAT* gene (Fig. 5.12C). BAPTA-AM pretreatment avoided the observed upregulation of *CAT* expression; almost completely avoided the observed decline of the expression of the *Fe-SOD* gene and partially, although significantly ($p < 0.05$), the decrease in the expression of the *Mn-SOD* gene. *GPX* gene expression was not affected by TCS after 1 h exposure (Fig. 5.12D).

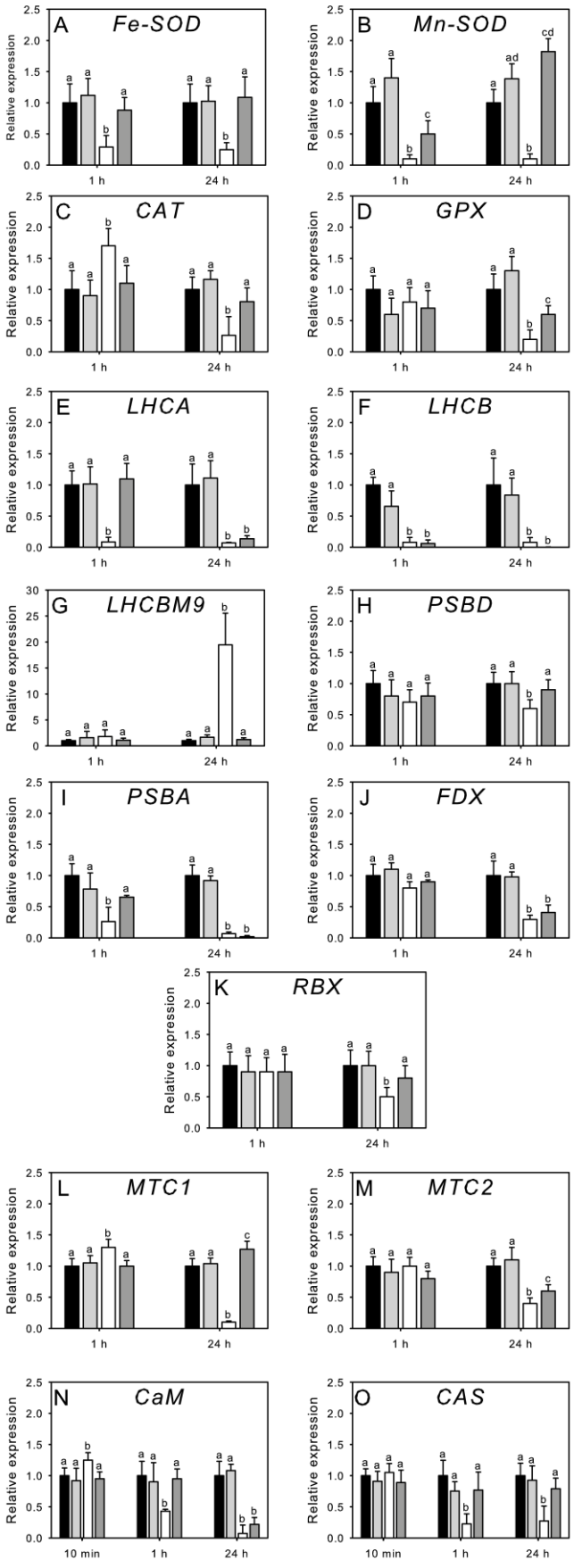

Figure 5.12. Effect of TCS on expression of selected genes after 1 and 24 h of exposure. Control (■), BAPTA-AM (▭), TCS (□) and TCS + BAPTA-AM (▬). Data are represented as relative expression of the genes with respect to the unexposed control (Tukey´s HSD, $p < 0.05$). Control values were set to 1 for easy comparison.

24 h exposure resulted in a drastic decrease, 75% and 90% of *Fe-SOD* and *Mn-SOD* expression, respectively; BAPTA-AM totally prevented the observed gene repression (Figure 5.12A, B). TCS also reduced by 75% *CAT* expression, BAPTA-AM pretreatment almost completely prevented the observed downregulation (Fig. 5.12C). TCS downregulated by 80% the expression of the *GPX* gene; BAPTA-AM pretreatment significantly ($p < 0.05$) prevented the downregulation (Fig. 5.12D). Regarding photosynthesis-related genes, after 1 h exposure, TCS almost completely abolished the expression of *LHCA* and *LHCB* but did not affect the already low level of expression of *LHCBM9*; the three of them encoding proteins involved in the light harvesting complex; pretreatment with BAPTA-AM significantly prevented the observed downregulation of *LHCA* but not *LHBC* expression (Fig. 5.12E, F and G). TCS did not have any significant effect on the expression of *PSBD* encoding PSII D2 protein but significantly ($p < 0.05$) downregulated the expression of *PSBA* encoding PSII D1 protein; this decrease was prevented by pretreatment with BAPTA-AM (Fig. 5.12H, I)*;* also short time exposure to TCS did not have any effect on the expression of the *FDX* (encoding ferredoxin) or *RBX* (encoding RuBisCo large subunit) genes (Fig. 5.12J, K). After 24 h exposure, the effect of TCS on transcription was much stronger for all analyzed photosynthetic genes: there was a drastic decline, between 70-100%, in the expression of *LHCA, LHCB* and *FDX*; BAPTA-AM pretreatment did not prevent this drastic repression in any of these three genes (Fig. 5.12, E, F and J); in the case of *LHCBM9*, instead of gene expression downregulation, TCS induced an extraordinary upregulation of the gene (nineteen-fold); BAPTA-AM pretreatment did not prevent this alteration either (Fig. 5.12G). TCS downregulated the expression of *PSBD* by 40% after 24 h exposure and completely abolished the expression of *PSBA*; pretreatment with BAPTA-AM almost completely prevented the observed decrease in expression of *PSBD* but not that of *PSBA* (Fig. 5.12H, I). *RBX* expression was also reduced by TCS (50%) and in this case BAPTA-AM pretreatment significantly prevented the downregulation (Fig. 5.12K). *MTC1* and *MTC2* encode metacaspases in *C. reinhardtii* (Murik et al., 2014). As shown in Fig. 5.12, *MTC1* was significantly ($p < 0.05$) overexpressed following short-term exposure to TCS but was totally repressed after 24 h exposure; in the case of *MTC2* TCS downregulated its expression by 60% after 24 h exposure. BAPTA-AM pretreatment prevented the downregulation of both genes (Fig. 5.12L, M).

As TCS has been found to quickly increase $[Ca^{2+}]_c$ in the green alga, it was found relevant to study the effect of TCS on the expression of genes involved in calcium signaling in *C. reinhardtii*, namely *CaM* (encoding a calmodulin) and *CAS* (encoding a chloroplast-localized Ca^{2+} sensor). At a very short exposure time (10 min), TCS upregulated by 25% the expression of the *CaM* gene with no effect on the *CAS* gene; after 1 h exposure, TCS significantly ($p < 0.05$) downregulated both genes (60% *CaM* and 75% *CAS* expression); after 24 h exposure, TCS completely abolished *cam* expression but did not decrease *CAS* expression further; BAPTA-AM pretreatment prevented the observed alteration in the expression of both genes except for *CaM* expression after 24 h of exposure (Fig. 5.12N, O). BAPTA-AM itself did not have any significant effect on expression of the selected genes (Fig. 5.12).

5.3.11 Effect of Triclosan on the protein pattern of *C. reinhardtii*

Total cell proteins from homogenates of cells unexposed and exposed to 13.8 µM TCS for 1 and 24 h were analyzed by SDS-PAGE (Supplementary Fig. S5.1). As with previous experiments, pretreatment with BAPTA-AM was done to investigate the role of calcium. After 1 h exposure, no clear alterations in the protein pattern of TCS exposed with respect to unexposed cells were observed. BAPTA-AM by itself did not alter protein patterns either. After 24 h exposure, drastic changes in the protein pattern were detected as many protein bands disappeared in the TCS-treated cultures. Eight protein bands (indicated by arrows in Fig. S5.1) which clearly changed their intensity in the exposed cells and whose alterations were prevented by BAPTA-pretreatment (see below) were further excised and analyzed for identification. The identified proteins in each band with the theoretical and observed Mr and pI are summarized in Table 5.2. As can be seen in the Table, most of the proteins identified are involved in photosynthetic processes: RuBisCo; several proteins of the light harvesting complexes; PSI and PSII proteins, the chloroplast ATP synthase subunit and carbonic anhydrase precursor. As shown by the gene expression profiles (Fig. 5.12), many of the genes involved in photosynthesis underwent important alterations after TCS exposure. Interestingly, glycolysis, a central metabolic pathway which provide energy and also precursors for the synthesis of primary metabolites, was also targeted by TCS such as chloroplast glyceraldehyde-3 phosphate dehydrogenase (with a crucial role in plant metabolism and development (Muñoz-Bertomeu et al., 2010); and fructose-bisphosphate aldolase 1.

Regarding nitrogen metabolism, glutamine synthetase abundance was also decreased by TCS.

Table 5.2. Description of the proteins identified by MALDI TOF/TOF tandem mass spectrometry with scores greater than 58 of cellular extracts of *C. reinhardtii* exposure to TCS after 24 h.

Protein band	GI	Accession number	Score	Description
1	158276701	EDP02472.1	321	Flagellar associated protein
	17380187	P12154	88	Photosystem I P700 chlorophyll a apoprotein A1;PSI-A;PsaA
	131290	P06007	89	Photosystem II D2 protein; PSII D2 protein; Photosystem Q(A) protein
2	131934	P00877	571	Ribulose bisphosphate carboxylase large chain; RuBisCO large subunit
	114513	P26526	128	ATP synthase subunit alpha, chloroplastic; ATP synthase F1 sector subunit alpha
3	74272659	ABA01125	208	Chloroplast glyceraldehyde-3-phosphate dehydrogenase, partial
	378405148	Q42690	90	Fructose-bisphosphate aldolase 1, chloroplastic
	158277729	EDP03496	88	Glutamine synthetase
4	158274405	EDP00188	192	Chlorophyll a-b binding protein of LHCII
	158282426	EDP08178	119	Ribosomal protein S8
5	158282427	EDP08179	264	Light-harvesting protein of photosystem I
	27542569	AAO16495	129	Light-harvesting complex I protein
	158280091	EDP05850	113	Superoxide dismutase [Fe]
	158281602	EDPO7356	86	2-cys peroxiredoxin
	87313229	ABD37911	76	Light-harvesting chlorophyll-a/b binding protein LhcbM2b
6	1323551	AAB19184	365	Carbonic anhydrase precursor
	131389	P11471	366	Oxygen-evolving enhancer protein 2, chloroplastic; OEE2
	158270548	EDO96390	82	Light-harvesting complex II chlorophyll a-b binding protein M3
7	158276701	EDP02472	215	Flagellar associated protein
	131290	P06007	69	Photosystem II D2 protein
8	114513	P26526	210	ATP synthase subunit alpha, chloroplastic
	262527093	BAI48884	153	Large subunit of ribulose-1, 5-bisphosphate carboxylase/oxygenase

Related to antioxidant defense mechanisms, Fe-SOD as well as a peroxiredoxin were both altered by TCS exposure. In fact, gene expression profiles of the *Fe-SOD* gene as well as other antioxidant defense genes already indicated an important downregulation of gene expression by TCS. As described previously, protein band 1 of control cultures

was more intense in TCS-treated cultures. Analysis of this band indicated the presence of a flagellar associated protein; a protein associated to PSI P700 chlorophyll a and PSII D2 protein. Interestingly, when this protein band was analyzed in the TCS-treated culture (denoted as band 7), the protein associated with chlorophyll a in the PSI reaction center disappeared but both the flagellar associated protein and the D2 protein were still present; gene expression analyses of genes *PSBD* (encoding the D2 protein) indicated partial downregulation of this gene under TCS-treatment; thus, expression of this gene was already observed even after 24 h exposure to TCS. The D2 protein is needed for the assembly of a PSII complex and forms part of the D1/D2 reaction center which binds P680, the primary electron donor of PSII as well as several subsequent electron acceptors. Protein pattern analysis showed that proteins belonging mostly to photosynthesis and antioxidant defense mechanisms were targeted by TCS and BAPTA-AM prevented the loss/decrease of such proteins which is in agreement with gene expression studies that indicated significant alterations in the expression of some of these genes.

5.4. DISCUSSION

The major finding of this study is that Triclosan (TCS), an antimicrobial substance, elicits an early and strong toxic response in the green alga *Chlamydomonas reinhardtii* which is mediated by intracellular free calcium, $[Ca^{2+}]_c$. Although several studies have found that TCS is toxic to algae and other aquatic organisms (Capdevielle et al., 2008; Coogan and La Point, 2008; Johansson et al., 2014; Orvos et al., 2002; Wilson et al., 2003; Yang et al., 2008) mechanistic studies are scarce, particularly regarding algae (Ciniglia et al., 2005; Dann and Hontela, 2011; Fritsch et al., 2013; Riva et al., 2012). A combined approach of cellular and physiological analyses as well as gene expression has provided novel insights into toxicological mechanisms of TCS in the green alga.

As an early event, TCS significantly altered $[Ca^{2+}]_c$ homeostasis leading to a sustained increase in basal levels. The disruption of $[Ca^{2+}]_c$ homeostasis was in agreement with the observed alterations in the expression of two genes, *CaM* and *CAS*, involved in calcium signaling in the alga. At very short time of exposure, TCS upregulated *CaM* expression encoding a calmodulin, a calcium sensor protein which initiates an intracellular signaling cascade to acclimate to the environmental insult (Berridge et al., 2003). At longer times of exposure, TCS decreased the expression of both genes impairing the ability of the algae to re-establish their cellular homeostasis. Loss of CAS (chloroplast- localized Ca^{2+} sensor) function has been reported to impair stimulus-induced changes in $[Ca^{2+}]_c$ dynamics (Terashima et al., 2012); in this regard, sustained elevated $[Ca^{2+}]_c$ would eliminate Ca transients caused by other environmental signals which may be essential for the survival of the cells (Dennison and Spalding, 2000; Torrecilla et al., 2000). In most organisms including bacteria, $[Ca^{2+}]_c$ is tightly controlled and alterations in its homeostasis are associated with cellular dysfunction and cell death due to the cytotoxicity of high $[Ca^{2+}]_c$ (Case et al., 2007; Clapham, 2007). Many pollutants increase $[Ca^{2+}]_c$ in a number of cells/organisms (Chen et al., 2011; Ferreira et al., 2012; Laporte et al., 2016; Sivaguru et al., 2004; Wang et al., 2014). TCS at micromolar doses has been found to do so in animal and human cell models (Palmer et al., 2012) but to our knowledge this is the first report in an organism of environmental relevance with a key role as primary producer in aquatic ecosystems. An increase in the level of reactive species, particularly reactive oxygen species (ROS) is a

common response to environmental stress, including pollution (Lushchak, 2011; Pulido-Reyes et al., 2015; Xia et al., 2008). Certain ROS may have a regulatory role in many organisms (D'Autréaux and Toledano, 2007); however, when there is an imbalance between the production of ROS and the cellular antioxidant defense mechanisms, oxidative stress increases leading to membrane integrity disruption, mitochondrial malfunction, apoptosis and eventually cell death (Dan Hess, 2000). In *C. reinhardtii*, TCS strongly triggered the formation of $O_2^{\cdot-}$ and H_2O_2 even at short time exposure that seem to surpass the detoxifying mechanisms of this algae because except for a transient increase in the expression of the *CAT* gene, TCS dramatically downregulated the expression of several antioxidant genes indicating that TCS induced oxidative stress in the green alga.

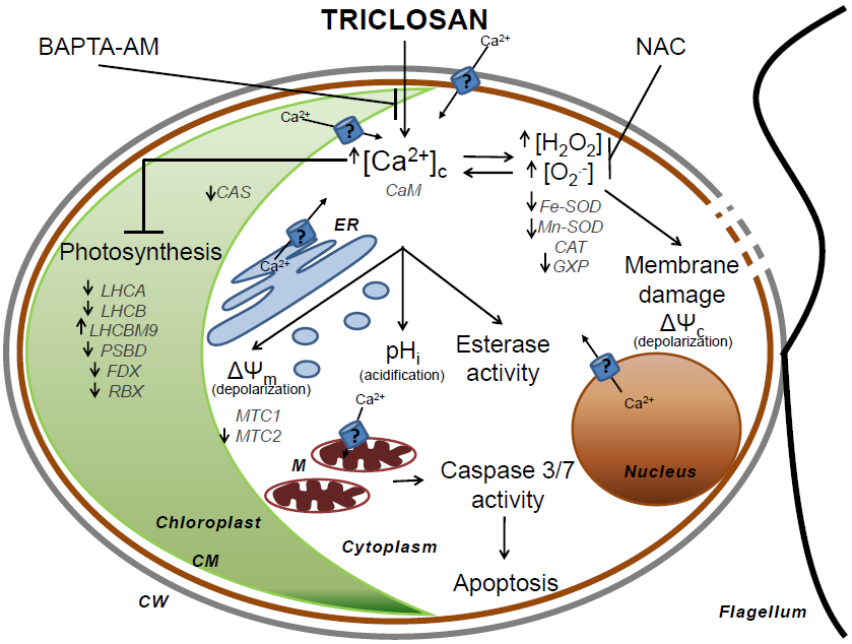

Figure 5.13. Proposed mechanistic scheme for triclosan toxicity in *Chlamydomonas reinhardtii*. Triclosan targets distinct cellular processes through signaling pathways mediated by cytoplasmic calcium ($[Ca^{2+}]_c$) and reactive oxygen species (ROS, including hydrogen peroxide (H_2O_2) and superoxide anions ($O_2^{\cdot-}$). These targeted processes include photosynthesis inhibition, pH acidification, the increase of esterase activity, oxidative stress together with membrane depolarization (mitocondrial ($\Delta\Psi_m$) and cytoplasmic membrane ($\Delta\Psi_c$)) leading to cell apoptosis. Gene expression changes appeared represented by italicized grey letters and arrows indicate the up- or down-regulation of the relative gene expression after triclosan treatment. CaM, CAT and MTC1 genes were upregulated at short time of exposure (10 min or 1 h) and downregulated after 24 h exposure. Genes included in the scheme are described in Table S5.2. CW: cell wall, CM: cytoplasmic membrane; ER: endoplasmic reticulum; M: mitochondria.

$[Ca^{2+}]_c$ prechelation prevented both the formation of ROS and gene downregulation meaning that Ca^{2+} mediates the formation of ROS by TCS. Many studies have linked the formation of ROS with alterations in $[Ca^{2+}]_c$ (Chang et al., 2015; Huang et al., 2010; Xu et al., 2015).

Most probably as the result of ROS overproduction, TCS compromised algal membrane integrity; in human and animal cell models, TCS has been found to induce a membranotropic effect which may impair the functional integrity of the cell membrane (Riva et al., 2012; Villalaín et al., 2001). In fact, ROS induced by TCS can damage cell membrane integrity by lipid peroxidation as demonstrated in this study, which might damage the lipid bilayer that may lead to non-specific membrane ion permeability further facilitating the influx of extracellular Ca^{2+} which may result in the observed sustained elevation of $[Ca^{2+}]_c$; Huang et al. (2010) found similar results when challenging lung cells with ZnO nanoparticles. The relationship or interconnection between oxidative stress and deregulation of $[Ca^{2+}]_c$ is complex and it is difficult to know which event is the first one to trigger the cellular response (Ermak and Davies, 2002); with the use of the $[Ca^{2+}]_c$ chelating agent BAPTA-AM and the antioxidant NAC, we have found an interconnection between ROS production and $[Ca^{2+}]_c$ increase: as the effect of BAPTA-AM is larger and clearly inhibited ROS formation by TCS, it appears that TCS first initiated changes in $[Ca^{2+}]_c$ which subsequently activated ROS production; however as NAC to some extent also inhibited $[Ca^{2+}]_c$ elevation, this might indicate that ROS may also further enhance Ca^{2+} influx in the alga; so that there seems to be a bidirectional interplay between both cellular processes after TCS exposure. In other cell systems, it has been reported that oxidative stress is able to initiate changes in $[Ca^{2+}]_c$ that subsequently activate further production of ROS by i.e. stimulating respiratory chain activity and that these ROS may also further increase $[Ca^{2+}]_c$ by targeting organelle-based calcium channels which may again lead to subsequent increased ROS, forming a self-amplifiable loop, meaning that $[Ca^{2+}]_c$ and ROS signaling systems are intimately integrated (Brown et al., 2004; Ermak and Davies, 2002; Gilroy et al., 2014; Görlach et al., 2015; Singh and Mishra, 2014).

The oxidative damage induced by ROS may negatively impact the photosynthetic machinery as the effect of ROS in photosynthesis is well documented and has been found to damage PSII by inhibiting the repair cycle involving the D1 protein (Latifi et

al., 2009). TCS drastically inhibited algal photosynthesis; $[Ca^{2+}]_c$ play an important role as $[Ca^{2+}]_c$ prechelation significantly prevented this inhibition, particularly after short term exposure. TCS completely abolished the expression of *PSBA* encoding PSII D1 protein. TCS also altered the expression of a number of other genes involved in the photosynthetic process; among these, the gene *LHCBM9* which encodes a major light harvesting polypeptide was highly upregulated by exposure to TCS; a similar effect was found by Petit et al., 2012 in algae exposed to PAMAM dendrimers. LHCBM9 has recently been reported as a protein serving an important protective function during stress conditions stabilizing PSII supercomplexes and promoting efficient light energy dissipation (Grewe et al., 2014).

It has been reported that mitochondria are one of the main targets of oxidative stress leading to cytotoxicity and even apoptosis (Gonzalo et al., 2014; Kowaltowski et al., 1998; Melendez and Davies, 1996; Xu et al., 2015). Besides, elevations in $[Ca^{2+}]_c$ are usually associated with mitochondrial dysfunction by modulating a variety of calcium-sensitive enzymes and by activating the mitochondrial apoptotic pathway (Hajnóczky et al., 2003; Liu et al., 2014; Pathak et al., 2013; Wang et al., 2015; Xie et al., 2010).

Mitochondrial dysfunction is an example of the observed interconnection between $[Ca^{2+}]_c$ and ROS formation: ROS which may be generated in the mitochondria and from other sources may induce cell death basically by depolarizing the mitochondrial membrane potential, $\Delta\Psi_m$ (Ghazizadeh and Nazıroğlu, 2014; Wang et al., 2014). A rise in $[Ca^{2+}]_c$ provokes the subsequent accumulation of Ca^{2+} in mitochondria leading to Ca^{2+} overload which may result in the disruption of mitochondrial functions, dissipation of $\Delta\Psi_m$ and further ROS formation due to redox alterations of the mitochondrial transport chain. This sequence of events may lead to a cell death signal. In this study, TCS strongly depolarized $\Delta\Psi_m$ after short time exposure (1 h) and in the longer-term (24 h), a significant increase in caspase 3/7 activity was found. Both processes were dependent on $[Ca^{2+}]_c$. Although this caspase 3/7 activity assay was performed using substrates designed to be specific for mammalian caspases, increases in this caspase activity associated with the occurrence of cell death in a variety of microalgal species under stress conditions have been reported (Affenzeller et al., 2009; Darehshouri et al., 2008).

How does apoptosis proceed in algal cells? Although during many years it was thought that apoptosis was only present in multicellular organisms (Nedelcu et al., 2011), there is increasing evidence that both prokaryotic and unicellular eukaryotes (from algae to yeast) undergo genetically controlled cell death in response to environmental stress (Bidle et al., 2010; Tchernov et al., 2011). It has been proposed that algae undergo apoptosis as a strategy to survive under unfavorable environmental conditions (Darehshouri et al., 2008). However, the molecular events and mechanisms that trigger apoptosis in unicellular organisms are still unclear (Nedelcu et al., 2011). In this context, metacaspases (MTCs) are structurally similar to animal caspases and have been found to be involved in apoptosis in plants, yeast, protozoa, green algae, dinoflagellates or diatoms (Murik and Kaplan, 2009; Nedelcu, 2009). Two MTCs encoding genes, *MTC1* and *MTC2*, have been identified in *C. reinhardtii* (Murik and Kaplan, 2009; Nedelcu et al., 2011). Murik et al. (2014) recently reported that *MTC1* expression is activated by normal mitochondrial function and oxidative stress while *MTC2* appears to be involved in an alternative route of cell death and in the absence of oxidative stress. In this study it was found that TCS significantly increased the expression of *MTC1* after short-term exposure, although in the long term TCS downregulated both *MTC1* and *MTC2*; gene downregulation was dependent on $[Ca^{2+}]_c$. These results and those of caspase3/7 activation suggest that *C. reinhardtii* cells undergo programmed cell death through mechanisms similar to those found in higher organisms and that TCS triggers a signaling cascade mediated by $[Ca^{2+}]_c$ and $[Ca^{2+}]_c$ -regulated ROS production that ends up in cell death.

As a summary, the current study has improved the understanding of the mechanisms behind the toxicity of pollutants as environmentally relevant as Triclosan emphasizing the role of $[Ca^{2+}]_c$ in mediating Triclosan toxicity (see Fig. 5.13 for a proposed mechanistic scheme). The integration of methodologies like those used in this study, combined with the use of BAPTA-AM or NAC, which modulate $[Ca^{2+}]_c$ and ROS, will be important to better understand the link between these two signal transducers (present in all living organisms), and their subsequent roles in stress responses to pollutants, which include i.e. changes in gene and protein expression, alterations in photosynthesis, and a putative apoptotic response in *Chlamydomonas reinhardtii*.

5.5 REFERENCES

Affenzeller, M.J., Darehshouri, A., Andosch, A., Lütz, C., Lütz-Meindl, U., 2009. Salt stress-induced cell death in the unicellular green alga *Micrasterias denticulata*. Journal of experimental botany 60, 939–54.

Ahn, K.C., Zhao, B., Chen, J., Cherednichenko, G., Sanmarti, E., Denison, M.S., Lasley, B., Pessah, I.N., Kültz, D., Chang, D.P.Y., Gee, S.J., Hammock, B.D., 2008. In vitro biologic activities of the antimicrobials Triclocarban, its analogs, and Triclosan in bioassay screens: receptor-based bioassay screens. Environmental Health Perspectives 116, 1203–1210.

Ajao, C., Andersson, M.A., Teplova, V. V, Nagy, S., Gahmberg, C.G., Andersson, L.C., Hautaniemi, M., Kakasi, B., Roivainen, M., Salkinoja-Salonen, M., 2015. Mitochondrial toxicity of triclosan on mammalian cells. Toxicology Reports 2, 624–637.

Barrán-Berdón, A.L., Rodea-Palomares, I., Leganés, F., Fernández-Piñas, F., 2011. Free Ca^{2+} as an early intracellular biomarker of exposure of cyanobacteria to environmental pollution. Analytical and Bioanalytical Chemistry 400, 1015–1029.

Berridge, M.J., Bootman, M.D., Roderick, H.L., 2003. Calcium: Calcium signalling: dynamics, homeostasis and remodelling. Nature Reviews Molecular Cell Biology 4, 517–529.

Berridge, M.J., Lipp, P., Bootman, M.D., 2000. The versatility and universality of calcium signalling. Nat Rev Mol Cell Biol 1, 11–21.

Berthold, P., Tsunoda, S.P., Ernst, O.P., Mages, W., Gradmann, D., Hegemann, P., 2008. Channelrhodopsin-1 initiates phototaxis and photophobic responses in chlamydomonas by immediate light-induced depolarization. The Plant cell 20, 1665–77.

Bidle, K.A., Haramaty, L., Baggett, N., Nannen, J., Bidle, K.D., 2010. Tantalizing evidence for caspase-like protein expression and activity in the cellular stress response of Archaea. Environmental Microbiology 12, 1161–1172.

Blaby, I.K., Glaesener, A.G., Mettler, T., Fitz-Gibbon, S.T., Gallaher, S.D., Liu, B., Boyle, N.R., Kropat, J., Stitt, M., Johnson, S., Benning, C., Pellegrini, M., Casero, D., Merchant, S.S., 2013. Systems-level analysis of nitrogen starvation-induced modifications of carbon metabolism in a *Chlamydomonas reinhardtii* starchless mutant. The Plant cell 25, 4305–23.

Bonente, G., Pippa, S., Castellano, S., Bassi, R., Ballottari, M., 2012. Acclimation of *Chlamydomonas reinhardtii* to different growth irradiances. The Journal of biological chemistry 287, 5833–47.

Bradford, M.M., 1976. A rapid and sensitive method for the quantitation of microgram quantities of protein utilizing the principle of protein-dye binding. Analytical biochemistry 72, 248–54.

Brain, R.A., Solomon, K.R., Brooks, B.W., 2010. Targets, effects and risks in aquatic plants exposed to veterinary antibiotics, in: Veterinary Pharmaceuticals in the Environment. Chapter 12. pp. 169–189. 012

Brown, D.M., Donaldson, K., Borm, P.J., Schins, R.P., Dehnhardt, M., Gilmour, P., Jimenez, L.A., Stone, V., 2004. Calcium and ROS-mediated activation of transcription factors and TNF-α cytokine gene expression in macrophages exposed to ultrafine particles. American Journal of Physiology - Lung Cellular and Molecular Physiology 286.

Capdevielle, M., Van Egmond, R., Whelan, M., Versteeg, D., Hofmann-Kamensky, M., Inauen, J., Cunningham, V., Woltering, D., 2008. Consideration of exposure and species sensitivity of Triclosan in the freshwater environment. Integrated Environmental Assessment and Management 4, 15. 2007-022.1

Case, R.M., Eisner, D., Gurney, A., Jones, O., Muallem, S., Verkhratsky, A., 2007. Evolution of calcium homeostasis: From birth of the first cell to an omnipresent signalling system. Cell Calcium 42, 345–350. doi:http://dx.doi.org/10.1016/j.ceca.2007.05.001
Chang, H.-T., Chou, C.-T., Kuo, D.-H., Shieh, P., Jan, C.-R., Liang, W.-Z., 2015. The mechanism of Ca^{2+} movement in the involvement of baicalein-induced cytotoxicity in ZR-75-1 human breast cancer cells. Journal of Natural Products 78, 1624–1634.

Chen, E.Y.T., Garnica, M., Wang, Y.-C., Chen, C.-S., Chin, W.-C., 2011. Mucin secretion induced by titanium dioxide nanoparticles. PLoS ONE 6, e16198.

Cherednichenko, G., Zhang, R., Bannister, R.A., Timofeyev, V., Li, N., Fritsch, E.B., Feng, W., Barrientos, G.C., Schebb, N.H., Hammock, B.D., Beam, K.G., Chiamvimonvat, N., Pessah, I.N., 2012. Triclosan impairs excitation-contraction coupling and Ca^{2+} dynamics in striated muscle. Proceedings of the National Academy of Sciences of the United States of America 109, 14158–63.

Ciniglia, C., Cascone, C., Giudice, R. Lo, Pinto, G., Pollio, A., 2005. Application of methods for assessing the geno- and cytotoxicity of Triclosan to *C. ehrenbergii*. Journal of Hazardous Materials 122, 227–232. doi:10.1016/j.jhazmat.2005.03.002
Clapham, D.E., 2007. Calcium Signaling. Cell 131, 1047–1058.

Coogan, M.A., La Point, T.W., 2008. Snail bioaccumulation of triclocarban, triclosan and methyltriclosan in a North Texas, USA, stream affected by wastewater treatment plnat runoff. Environmental Toxicology and Chemistry 27, 1788.

D'Autréaux, B., Toledano, M.B., 2007. ROS as signalling molecules: mechanisms that generate specificity in ROS homeostasis. Nature Reviews Molecular Cell Biology 8, 813–824.

Dan Hess, F., 2000. Light-dependent herbicides: an overview. Weed Science 48, 160–170.

Dann, A.B., Hontela, A., 2011. Triclosan: environmental exposure, toxicity and mechanisms of action. Journal of Applied Toxicology 31, 285–311.

Darehshouri, A., Affenzeller, M., Lütz-Meindl, U., 2008. Cell death upon H(2)O(2) induction in the unicellular green alga Micrasterias. Plant Biology 10, 732–745.

Dennison, K.L., Spalding, E.P., 2000. Glutamate-gated calcium fluxes in *Arabidopsis*. Plant physiology 124, 1511–4.

Domínguez, D.C., Guragain, M., Patrauchan, M., 2015. Calcium binding proteins and calcium signaling in prokaryotes. Cell Calcium 57, 151–165.

Dondero, F., Jonsson, H., Rebelo, M., Pesce, G., Berti, E., Pons, G., Viarengo, A., 2006. Cellular responses to environmental contaminants in amoebic cells of the slime mould *Dictyostelium discoideum*. Comparative Biochemistry and Physiology Part C: Toxicology & Pharmacology 143, 150–157.

Elbaz, A., Wei, Y.Y., Meng, Q., Zheng, Q., Yang, Z.M., 2010. Mercury-induced oxidative stress and impact on antioxidant enzymes in *Chlamydomonas reinhardtii*. Ecotoxicology 19, 1285–1293. 514-z

Ermak, G., Davies, K.J.., 2002. Calcium and oxidative stress: from cell signaling to cell death. Molecular Immunology 38, 713–721.

Ermilova, E. V., Chekunova, E.M., Zalutskaya, Z.M., Krupnov, K.R., Gromov, B. V., 1996. Isolation and Characterization of Chemotaxis Mutants of *Chlamydomonas reinhardtii*. Current Microbiology 32, 357–359.

Esperanza, M., Cid, Á., Herrero, C., Rioboo, C., 2015a. Acute effects of a prooxidant herbicide on the microalga *Chlamydomonas reinhardtii*: Screening cytotoxicity and genotoxicity endpoints. Aquatic Toxicology 165, 210–221.

Esperanza, M., Seoane, M., Rioboo, C., Herrero, C., Cid, Á., 2015b. *Chlamydomonas reinhardtii* cells adjust the metabolism to maintain viability in response to atrazine stress. Aquatic Toxicology 165, 64–72.

Federle, T.W., Schwab, E.L., 2003. Triclosan biodegradation in wastewater treatment plant effluent diluted in various river waters, in: 103rd American Society for Microbiology General Meeting.

Ferreira, I.L., Bajouco, L.M., Mota, S.I., Auberson, Y.P., Oliveira, C.R., Rego, A.C., 2012. Amyloid beta peptide 1–42 disturbs intracellular calcium homeostasis through activation of GluN2B-containing N-methyl-d-aspartate receptors in cortical cultures. Cell Calcium 51, 95–106.

Fischer, B.B., Rüfenacht, K., Dannenhauer, K., Wiesendanger, M., Eggen, R.I.L., 2010. Multiple stressor effects of high light irradiance and photosynthetic herbicides on growth and survival of the green alga *Chlamydomonas reinhardtii*. Environmental Toxicology and Chemistry 29, 2211–2219.

Fritsch, E.B., Connon, R.E., Werner, I., Davies, R.E., Beggel, S., Feng, W., Pessah, I.N., 2013. Triclosan Impairs Swimming Behavior and Alters Expression of Excitation-Contraction Coupling Proteins in Fathead Minnow (*Pimephales promelas*). Environmental Science & Technology 47, 2008–2017.

Ghazizadeh, V., Nazıroğlu, M., 2014. Electromagnetic radiation (Wi-Fi) and epilepsy induce calcium entry and apoptosis through activation of TRPV1 channel in hippocampus and dorsal root ganglion of rats. Metabolic Brain Disease 29, 787–799.

Gilroy, S., Bialasek, M., Suzuki, N., Gorecka, M., Devireddy, A.R., Karpinski, S., Mittler, R., 2016. ROS, Calcium, and Electric Signals: Key Mediators of Rapid Systemic Signaling in Plants. Plant physiology 171, 1606–1615.

Gilroy, S., Suzuki, N., Miller, G., Choi, W.-G., Toyota, M., Devireddy, A.R., Mittler, R., 2014. A tidal wave of signals: calcium and ROS at the forefront of rapid systemic signaling. Trends in Plant Science 19, 623–630.

Gonzalo, S., Llaneza, V., Pulido-Reyes, G., Fernández-Piñas, F., Bonzongo, J.C., Leganes, F., Rosal, R., García-Calvo, E., Rodea-Palomares, I., 2014. A Colloidal Singularity Reveals the Crucial Role of Colloidal Stability for Nanomaterials In-Vitro Toxicity Testing: nZVI-Microalgae Colloidal System as a Case Study. PLoS ONE 9, e109645.

Goodenough, U.W., Shames, B., Small, L., Saito, T., Crain, R.C., Sanders, M.A., Salisbury, J.L., 1993. The role of calcium in the

Chlamydomonas reinhardtii mating reaction. The Journal of cell biology 121, 365–74.

Görlach, A., Bertram, K., Hudecova, S., Krizanova, O., 2015. Calcium and ROS: A mutual interplay. Redox Biology 6, 260–271.

Grewe, S., Ballottari, M., Alcocer, M., D'Andrea, C., Blifernez-Klassen, O., Hankamer, B., Mussgnug, J.H., Bassi, R., Kruse, O., 2014. Light-Harvesting Complex Protein LHCBM9 Is Critical for Photosystem II Activity and Hydrogen Production in Chlamydomonas reinhardtii. The Plant cell 26, 1598–1611.

Grossman, A.R., Croft, M., Gladyshev, V.N., Merchant, S.S., Posewitz, M.C., Prochnik, S., Spalding, M.H., 2007. Novel metabolism in *Chlamydomonas* through the lens of genomics. Current Opinion in Plant Biology 10, 190–198.

Hajnóczky, G., Davies, E., Madesh, M., 2003. Calcium signaling and apoptosis. Biochemical and Biophysical Research Communications 304, 445–454.

Harris, E.H., 2001. *Chlamydomonas* as a model organism. Annual Review of Plant Physiology and Plant Molecular Biology 52, 363–406.

Harris, E.H., 1989. The Chlamydomonas sourcebook: A comprehensive guide to biology and laboratory use. Academic Press, San Diego.

Hochmal, A.K., Schulze, S., Trompelt, K., Hippler, M., 2015. Calcium-dependent regulation of photosynthesis. Biochimica et Biophysica Acta (BBA) - Bioenergetics 1847, 993–1003.

Huang, C.-C., Aronstam, R.S., Chen, D.-R., Huang, Y.-W., 2010. Oxidative stress, calcium homeostasis, and altered gene expression in human lung epithelial cells exposed to ZnO nanoparticles. Toxicology in Vitro 24, 45–55.

Jeffrey, S.W., Humphrey, G.F., 1975. New spectrophotometric method for determining chlorophyll a, b, cl and c2 in algae, phytoplankton, and higher plants. Biochem. Physiol. Pflanz 167, 191–194.

Johansson, C.H., Janmar, L., Backhaus, T., 2014. Triclosan causes toxic effects to algae in marine biofilms, but does not inhibit the metabolic activity of marine biofilm bacteria. Marine Pollution Bulletin 84, 208–212.

Kam, V., Moseyko, N., Nemson, J., Feldman, L.J., 1999. Gravitaxis in *Chlamydomonas reinhardtii* : Characterization using Video Microscopy and Computer Analysis. International Journal of Plant Sciences 160, 1093–1098.

Kawanai, T., 2011. Triclosan, an environmental pollutant from health care products, evokes charybdotoxin-sensitive hyperpolarization in rat thymocytes. Environmental Toxicology and Pharmacology 32, 417–422.

Kowaltowski, A.J., Netto, L.E.S., Vercesi, A.E., 1998. The thiol-specific antioxidant enzyme prevents mitochondrial permeability transition. Evidende for the participation of reactive oxygen species in this mechanism. Journal of Biological Chemistry 273, 12766–12769.

Laemmli, U.K., 1970. Cleavage of structural proteins during the assembly of the head of bacteriophage T4. Nature 227, 680–685.

Laporte, D., Valdés, N., González, A., Sáez, C.A., Zúñiga, A., Navarrete, A., Meneses, C., Moenne, A., 2016. Copper-induced overexpression of genes encoding antioxidant system enzymes and metallothioneins involve the activation of CaMs, CDPKs and MEK1/2 in the marine alga *Ulva compressa*. Aquatic Toxicology 177, 433–440.

Latifi, A., Ruiz, M., Zhang, C.-C., 2009. Oxidative stress in cyanobacteria. FEMS Microbiology Reviews 33.

Leganés, F., Martínez-Granero, F., Muñoz-Martín, M.Á., Marco, E., Jorge, A., Carvajal, L., Vida, T., González-Pleiter, M., Fernández-Piñas, F., 2014. Characterization and responses to environmental cues of a photosynthetic antenna-deficient mutant of the filamentous cyanobacterium *Anabaena* sp. PCC 7120. Journal of Plant Physiology 171, 915–926.

Liu, W., Zhao, H., Wang, Y., Jiang, C., Xia, P., Gu, J., Liu, X., Bian, J., Yuan, Y., Liu, Z., 2014. Calcium–calmodulin signaling elicits mitochondrial dysfunction and the release of cytochrome c during cadmium-induced apoptosis in primary osteoblasts. Toxicology Letters 224, 1–6.

Livak, K.J., Schmittgen, T.D., 2001. Analysis of Relative Gene Expression Data Using Real-Time Quantitative PCR and the 2−ΔΔCT Method. Methods 25, 402–408.

Lushchak, V.I., 2011. Environmentally induced oxidative stress in aquatic animals. Aquatic Toxicology 101, 13–30. 06

McAinsh, M.R., Pittman, J.K., 2009. Shaping the calcium signature. New Phytologist 181, 275–294.

McDonnell, G., Russell, A.D., 1999. Antiseptics and disinfectants: activity, action, and resistance. Clinical microbiology reviews

12, 147–179.

Melendez, J.A., Davies, K.J.A., 1996. Manganese Superoxide Dismutase Modulates Interleukin-1 Levels in HT-1080 Fibrosarcoma Cells. Journal of Biological Chemistry 271, 18898–18903.

Muñoz-Bertomeu, J., Cascales-Miñana, B., Alaiz, M., Segura, J.A., Ros, R., 2010. A critical role of plastidial glycolytic Glyceraldehyde-3-Phosphate Dehydrogenase in the control of plant metabolism and development. Plant Signaling & Behavior 5, 67–69.

Murik, O., Elboher, A., Kaplan, A., 2014. Dehydroascorbate: a possible surveillance molecule of oxidative stress and programmed cell death in the green alga *Chlamydomonas reinhardtii*. New Phytologist 202, 471–484.

Murik, O., Kaplan, A., 2009. Paradoxically, prior acquisition of antioxidant activity enhances oxidative stress-induced cell death. Environmental Microbiology 11, 2301–2309.

Nagel, G., Ollig, D., Fuhrmann, M., Kateriya, S., Musti, A.M., Bamberg, E., Hegemann, P., 2002. Channelrhodopsin-1: a light-gated proton channel in green algae. Science 296.

Nedelcu, A.M., 2009. Comparative genomics of phylogenetically diverse unicellular eukaryotes provide new insights into the genetic basis for the evolution of the programmed cell death machinery. Journal of Molecular Evolution 68, 256–268.

Nedelcu, A.M., Driscoll, W.W., Durand, P.M., Herron, M.D., Rashidi, A., 2011. On the paradigm of altruistic suicide in the unicellular world. Evolution 65, 3–20.

Nultsch, W., Pfau, J., Dolle, R., 1986. Effects of calcium channel blockers on phototaxis and motility of *Chlamydomonas reinhardtii*. Archives of Microbiology 144, 393–397.

Ohta, M., Suzuki, T., 2007. Participation of the inositol phospholipid signaling pathway in the increase in cytosolic calcium induced by tributyltin chloride intoxication of chlorophyllous protozoa *Euglena gracilis* Z and its achlorophyllous mutant SM-ZK. Comparative Biochemistry and Physiology Part C: Toxicology & Pharmacology 146, 525–530.

Ortega-Villasante, C., Rellán-Alvarez, R., Del Campo, F.F., Carpena-Ruiz, R.O., Hernández, L.E., 2005. Cellular damage induced by cadmium and mercury in *Medicago sativa*. Journal of experimental botany 56, 2239–51.

Orvos, D.R., Versteeg, D.J., Inauen, J., Capdevielle, M., Rothenstein, A., Cunningham, V., 2002. Aquatic toxicity of triclosan. Environmental Toxicology and Chemistry 21, 1338–1349.

Palmer, R.K., Hutchinson, L.M., Burpee, B.T., Tupper, E.J., Pelletier, J.H., Kormendy, Z., Hopke, A.R., Malay, E.T., Evans, B.L., Velez, A., Gosse, J.A., 2012. Antibacterial agent triclosan suppresses RBL-2H3 mast cell function. Toxicology and Applied Pharmacology 258, 99–108.

Pathak, N., Mitra, S., Khandelwal, S., 2013. Cadmium induces thymocyte apoptosis via caspase-dependent and caspase-independent pathways. Journal of Biochemical and Molecular Toxicology 27, 193–203.

Permyakov, E.A., Kretsinger, R.H., 2009. Cell signaling, beyond cytosolic calcium in eukaryotes. Journal of Inorganic Biochemistry 103, 77–86.

Petit, A.-N., Debenest, T., Eullaffroy, P., Gagné, F., 2012. Effects of a cationic PAMAM dendrimer on photosynthesis and ROS production of *Chlamydomonas reinhardtii*. Nanotoxicology 6, 315–326.

Pinto, E., Sigaud-kutner, T.C.S., Leitao, M.A.S., Okamoto, O.K., Morse, D., Colepicolo, P., 2003. Heavy metal-induced oxidative stress in algae. Journal of Phycology 39, 1008–1018.

Prado, R., Rioboo, C., Herrero, C., Suárez-Bregua, P., Cid, Á., 2012. Flow cytometric analysis to evaluate physiological alterations in herbicide-exposed *Chlamydomonas moewusii* cells. Ecotoxicology 21, 409–420.

Pulido-Reyes, G., Rodea-Palomares, I., Das, S., Sakthivel, T.S., Leganes, F., Rosal, R., Seal, S., Fernández-Piñas, F., 2015. Untangling the biological effects of cerium oxide nanoparticles: the role of surface valence states. Scientific reports 5, 15613.

Renberg, L., Johansson, A.I., Shutova, T., Stenlund, H., Aksmann, A., Raven, J.A., Gardestrom, P., Moritz, T., Samuelsson, G., 2010. A metabolomic approach to study major metabolite changes during acclimation to limiting CO_2 in *Chlamydomonas reinhardtii*. Plant physiology 154, 187–196.

Riva, C., Cristoni, S., Binelli, A., 2012. Effects of triclosan in the freshwater mussel *Dreissena polymorpha*: A proteomic investigation. Aquatic Toxicology 118, 62–71.

Rodea-Palomares, I., Gonzalo, S., Santiago-Morales, J., Leganés, F., García-Calvo, E., Rosal, R., Fernández-Piñas, F., 2012. An insight into the mechanisms of nanoceria toxicity in aquatic photosynthetic organisms. Aquatic Toxicology 122, 133–143.

Schäfer, S., Bickmeyer, U., Koehler, A., 2009. Measuring Ca^{2+}-signalling at fertilization in the sea urchin *Psammechinus miliaris*: alterations of this Ca^{2+}-signal by copper and 2,4,6-tribromophenol. Comparative biochemistry and physiology. Toxicology & pharmacology : CBP 150, 261–9.

Schmidt, J.A., Eckert, R., 1976. Calcium couples flagellar reversal to photostimulation in *Chlamydomonas reinhardtii*. Nature 262, 713–715.

Singh, S., Mishra, A.K., 2014. Regulation of calcium ion and its effect on growth and developmental behavior in wild type and ntcA mutant of *Anabaena* sp. PCC 7120 under varied levels of $CaCl_2$. Microbiology 83, 235–246.

Sivaguru, M., Yamamoto, Y., Rengel, Z., Ahn, S.J., Matsumoto, H., 2004. Early events responsible for aluminum toxicity symptoms in suspension-cultured tobacco cells. New Phytologist 165, 99–109. doi:10.1111/j.1469-8137.2004.01219.x
Stavis, R.L., 1974. The effect of azide on phototaxis in *Chlamydomonas reinhardtii* (motility) 71, 1824–1827.

Tamura, I., Saito, M., Nishimura, Y., Satoh, M., Yamamoto, H., Oyama, Y., 2011. Elevation of intracellular Ca^{2+} level by Triclosan in rat thymic lymphocytes: Increase in membrane Ca^{2+} permeability and induction of intracellular Ca^{2+} release. Journal of Health Science 57, 540–546.

Tchernov, D., Kvitt, H., Haramaty, L., Bibby, T.S., Gorbunov, M.Y., Rosenfeld, H., Falkowski, P.G., 2011. Apoptosis and the selective survival of host animals following thermal bleaching in zooxanthellate corals. Proceedings of the National Academy of Sciences of the United States of America 108, 9905–9.

Terashima, M., Petroutsos, D., Hüdig, M., Tolstygina, I., Trompelt, K., Gäbelein, P., Fufezan, C., Kudla, J., Weinl, S., Finazzi, G., Hippler, M., 2012. Calcium-dependent regulation of cyclic photosynthetic electron transfer by a CAS, ANR1, and PGRL1 complex. Proceedings of the National Academy of Sciences of the United States of America 109, 17717–22.

Torrecilla, I., Leganés, F., Bonilla, I., Fernández-Piñas, F., 2000. Use of recombinant aequorin to study calcium homeostasis and monitor calcium transients in response to heat and cold shock in cyanobacteria. Plant physiology 123, 161–76.

Van Loo, G., Van Gurp, M., Depuydt, B., Srinivasula, S., Rodriguez, I., Alnemri, E., Gevaert, K., Vandekerckhove, J., Declercq, W., Vandenabeele, P., 2002. The serine protease Omi/HtrA2 is released from mitochondria during apoptosis. Omi interacts with caspase-inhibitor XIAP and induces enhanced caspase activity. Cell Death and Differentiation 9, 20–6.

Vander Meulen, K.A., Hobson, A., Yocum, C.F., 2004. Reconstitution of the photosystem II Ca^{2+} binding site. Biochimica et Biophysica Acta (BBA) - Bioenergetics 1655, 179–183.

Villalaín, J., Mateo, C.R., Aranda, F.J., Shapiro, S., Micol, V., 2001. Membranotropic effects of the antibacterial agent Triclosan. Archives of Biochemistry and Biophysics 390, 128–136.

Wakabayashi, K., Ide, T., Kamiya, R., 2009. Calcium-dependent flagellar motility activation in *Chlamydomonas reinhardtii* in response to mechanical agitation. Cell Motility and the Cytoskeleton 66, 736–742.

Wang, H., Wang, Z.-K., Jiao, P., Zhou, X.-P., Yang, D.-B., Wang, Z.-Y., Wang, L., 2015. Redistribution of subcellular calcium and its effect on apoptosis in primary cultures of rat proximal tubular cells exposed to lead. Toxicology 333, 137–146.

Wang, J., Zhu, H., Liu, X., Liu, Z., 2014. Oxidative Stress and Ca^{2+} Signals Involved on Cadmium-Induced Apoptosis in Rat Hepatocyte. Biological Trace Element Research 161, 180–189.

Weatherly, L.M., Shim, J., Hashmi, H.N., Kennedy, R.H., Hess, S.T., Gosse, J.A., 2016. Antimicrobial agent triclosan is a proton ionophore uncoupler of mitochondria in living rat and human mast cells and in primary human keratinocytes. Journal of applied toxicology : JAT 36, 777–789.

Wheeler, G.L., Brownlee, C., 2008. Ca^{2+} signalling in plants and green algae – changing channels. Trends in Plant Science 13, 506–514.

Wilson, B.A., Smith, V.H., DeNoyelles, F., Larive, C.K., 2003. Effects of three pharmaceutical and personal care products on natural freshwater algal assemblages. Environmental science & technology 37, 1713–9.

Xia, T., Kovochich, M., Liong, M., Mädler, L., Gilbert, B., Shi, H., Yeh, J.I., Zink, J.I., Nel, A.E., 2008. Comparison of the mechanism of toxicity of zinc oxide and cerium oxide nanoparticles based on dissolution and oxidative stress properties. ACS Nano 2, 2121–2134.

Xie, Z., Zhang, Y., Li, A., Li, P., Ji, W., Huang, D., 2010. Cd-induced apoptosis was mediated by the release of Ca^{2+} from

intracellular Ca storage. Toxicology Letters 192, 115–118.

Xu, D., Su, C., Song, X., Shi, Q., Fu, J., Hu, L., Xia, X., Song, E., Song, Y., 2015. Polychlorinated biphenyl quinone induces endoplasmic reticulum stress, unfolded protein response, and calcium release. Chemical Research in Toxicology 28, 1326–1337.

Yang, L.-H., Ying, G.-G., Su, H.-C., Stauber, J.L., Adams, M.S., Binet, M.T., 2008. Growth-inhibiting effects of 12 antibacterial agents and their mixtures on the freshwater microalga *Pseudokirchneriella subcapitata*. Environmental Toxicology and Chemistry 27, 1201.

Zafarullah, M., Li, W.Q., Sylvester, J., Ahmad, M., 2003. Molecular mechanisms of N -acetylcysteine actions. Cellular and Molecular Life Sciences (CMLS) 60, 6–20.

Zou, H., Liu, X., Han, T., Hu, D., Yuan, Y., Gu, J., Bian, J., Liu, Z., 2015. Alpha-lipoic acid protects against cadmium-induced hepatotoxicity via calcium signalling and gap junctional intercellular communication in rat hepatocytes. The Journal of Toxicological Sciences 40, 469–477.

GENERAL DISCUSSION

GENERAL DISCUSSION

The aims of the present thesis were the evaluation of the individual and combined toxicity of EPs, particularly pharmaceuticals, on photosynthetic organisms of high ecological relevance and to validate the role of $[Ca^{2+}]_i$ as an intracellular biomarker of exposure to the individual and combined pharmaceuticals as well as its role in the global cellular response to a model EPs.

Cyanobacteria, *Anabaena* sp. PCC7120 CBP4337 and *Anabaena* sp. PCC7120 pBG2001a, green algae, *Pseudokirchneriella subcapitata* and C*hlamydomonas reinhardtii*, and environmental biofilms (communities of microorganisms) were used in this thesis. All these microorganisms play a key role in the food chain in freshwaters. All of them appear to be sensitive to the pharmaceuticals evaluated in this thesis; therefore, aquatic ecosystems could be affected by pharmaceuticals because negative effects in cyanobacteria and algae could affect the balance of the whole ecosystem (Valitalo et al. 2017).

EPs co-occur with many other pollutants in freshwater. Therefore, aquatic organisms may be exposed to mixtures of pollutants. In the present thesis, it has been evaluated the response of the recombinant bioluminescent filamentous cyanobacterium *Anabaena* sp. PCC7120 CBP4337 and green alga *Pseudokirchneriella subcapitata* to five antibiotics (amoxicilin, erythromycin, levofloxacin, norfloxacin and tetracycline) both singly and combined and their potential interactions in mixture toxicity has been studied.

The five antibiotics tested exert toxic effect towards *Anabaena* sp. PCC7120 CPB4337, especially erythromycin. *Anabaena* sp. PCC7120 CBP4337 appears to be more or equally sensitive than other cyanobacterial strains for erythromycin. It has been reported that other 13 cyanobacterial strains also are sensitive for erythromycin (Ando et al. 2007, Pomati et al. 2004, Prasanna et al. 2010). Only three of them, *Anabaena cylindrica* NIES-19 ($EC_{50\text{ - }6\text{ days}}$ = 0.035 mg/L), *Microcystis aeruginosa* NIES-44 ($EC_{50\text{ - }6\text{ days}}$ = 0.023) and *Mycrocystis wesenbergii* NIES-107 ($EC_{50\text{ - }6\text{ days}}$ = 0.023), were just as sensitive as *Anabaena* sp. PCC7120 CBP4337 ($EC_{50\text{ - }3\text{ days}}$ = 0.022 mg/L), while the other 9 cyanobacterial strains were less sensitive than *Anabaena* sp. PCC7120 CBP4337

(Ando et al. 2007, Pomati et al. 2004, Prasanna et al. 2010). On the other hand, *Anabaena* sp. PCC7120 CBP4337 appears to be less sensitive than other cyanobacteria to amoxicilin, levofloxacin, norfloxacin and tetracycline. It has been reported that other 12 cyanobacterial strains were sensitive to tetracycline (Dias et al. 2015, Halling-Sørensen 2000, Lorenz and Krumbein 1984, Pomati et al. 2004, Prasanna et al. 2010, Yang et al. 2013b), 6 cyanobacterial strains were sensitive for levofloxacin (Prasanna et al. 2010, Robinson et al. 2005, Wan et al. 2014)(Robinson et al 2005; Wang et al 2014; Prasanna et al 2010), 20 cyanobacterial strains were sensitive to norfloxacin (Ando et al. 2007, Dias et al. 2015), 14 cyanobacterial strains were sensitive to amoxicillin (Dias et al. 2015, Liu et al. 2012, Lützhøft et al. 1999). All these cyanobacterial strains appear to be more sensitive than *Anabaena* sp. PCC7120 CBP4337 to amoxicilin, levofloxacin, norfloxacin and tetracycline.

However, it should be noted that both the endpoints and exposure times were different for each bioassay; therefore, it is very hard to compare with each other. The endpoint used to estimate the EC_{50} of the antibiotics on *Anabaena* sp. PCC7120 CBP4337 is based on the inhibition of its constitutive bioluminescence caused by the presence of a toxic substance after 3 days of exposure; this endpoint is related to metabolic activity of the organism as pollutants affecting the metabolism of the cyanobacterium reduce bioluminescence (Fernández-Pinas and Wolk 1994, Rodea-Palomares et al. 2009, Rosal et al. 2010). Other endpoints have been reported to estimate the EC_{50} of the antibiotics on other cyanobacterial strains such as: the inhibition of growth (OD_{655nm}) after 6 days (Ando et al. 2007), the inhibition of growth (Neubauer counting chamber) after 7 days (Liu et al. 2012, the inhibition of in vivo chlorophyll a fluorescence after 5 days {Robinson, 2005 #2164) and the inhibition of chlorophyll fluorescence (extracted using 67% ethanol and determined flurometrically exciting at 430 nm and collecting at 671 nm) after 7 days (Halling-Sørensen 2000, Lützhøft et al. 1999). EC_{50} of antibiotics obtained using *Anabaena* sp. PCC7120 CBP4337 could be higher than EC_{50} of the other cyanobacterial strains due to its endpoint. On the other hand, the different sensitivity could be explained due to exposure times. Exposure time of *Anabaena* sp. PCC7120 CBP4337 was shorter than exposure times reported by other studies. It has been reported that the higher exposure time is usually associated with higher toxicity; therefore, *Anabaena* sp. PCC7120 CBP4337 could be more sensitive if exposure times were shorter. Other studies have not reported the EC_{50} of antibiotics. They only

reported several concentrations and their effect on the growth of cyanobacteria or dose-response curves using different endpoints and exposure times, such as: the inhibition of growth ($OD_{680\ nm}$) after 7 days (Wan et al. 2014, Yang et al. 2013b) and the inhibition of growth ($OD_{750\ nm}$) after 5 days (Pomati et al. 2004). In these cases, if the lower concentrations tested on cyanobacterial strains were lower than the EC_{50} of *Anabaena* sp. PCC7120 CBP4337, it was estimated that *Anabaena* sp. PCC7120 CBP4337 was more sensitive than other cyanobacterial strains. Moreover, it has also been reported minimal inhibitory concentration (MIC) as endpoint for cyanobacteria after exposure to antibiotics, such as minimal inhibitory concentration after 2 - 4 days (Prasanna et al. 2010), minimal inhibitory concentration after 13 days (Dias et al. 2015) and minimal inhibitory concentration after 7 days (Lorenz and Krumbein 1984). However, this endpoint is hardly comparable with EC_{50} and dose-response curves obtained and reported.

The four tested antibiotics, amoxicillin showed no toxicity for the green alga, exerted toxic effect towards *Pseudokirchneriella subcapitata*, especially erythromycin. The EC_{50} of the erythromycin, tetracycline, levofloxacin and norfloxacin obtained using *Pseudokirchneriella subcapitata* in this thesis were lower than ECs_{50} reported by other studies using the same green alga with these antibiotics {Halling-Sørensen, 2000 #2088}(Eguchi et al. 2004, Isidori et al. 2005, Robinson et al. 2005, Yang et al. 2008, Yang et al. 2013b). It should be noted that the endpoints were different for the other bioassays, which also used *Pseudokirchneriella subcapitata*. The endpoint used to estimate the EC_{50} in this thesis was *in vivo* chlorophyll fluorescence, whose excitation/emission wavelengths are 450/672 nm. It has been reported other different endpoints to estimate the EC_{50} of these antibiotics on *Pseudokirchneriella subcapitata* such as: the inhibition of growth (cell count using an automatic hematology analyser and electronic particle dual threshold counter) (Eguchi et al. 2004, Isidori et al. 2005), the inhibition of chlorophyll fluorescence (extracted using 67% ethanol and determined flurometrically exciting at 430 nm and collecting at 671 nm) (Halling-Sørensen 2000), the inhibition of growth (OD_{442nm}) (Yang et al. 2008) and the inhibition of *in vivo* chlorophyll a fluorescence (excitation/emission wavelengths were 340-500/>665 nm) (Robinson et al. 2005). EC_{50} obtained in this thesis for erythromycin and norfloxacin were higher than EC_{50} previously reported. Cell count appears to be an endpoint more sensitive than *in vivo* chlorophyll fluorescence (used in this thesis) on

Pseudokirchneriella subcapitata for erythromycin and norfloxacin (Eguchi et al. 2004, Isidori et al. 2005, Yang et al. 2008), while both inhibition of growth (OD_{442nm}) and the inhibition of chlorophyll fluorescence (extracted using 67% ethanol and determined flurometrically exciting at 430 nm and collecting at 671 nm) appear to be just as sensitive as *in vivo* chlorophyll fluorescence for tetracycline. The EC_{50} obtained in this thesis for tetracycline was similar to the ECs_{50} previosly reported, while EC_{50} obtained in this thesis for norfloxacin and erythromycin were higher than reported (Halling-Sørensen 2000, Yang et al. 2008) probably due to the endpoint used.

Pseudokirchneriella subcapitata appears to be more sensitive than other green algae for antibiotics (Agrawal and Manisha 2007, Eguchi et al. 2004, El-Bassat et al. 2011, Nie et al. 2009). *Pseudokirchneriella subcapitata* was more sensitive than *Chlorella vulgaris* at least for six antibiotics (Agrawal and Manisha 2007, Eguchi et al. 2004, El-Bassat et al. 2011). *Pseudokirchneriella subcapitata* was more sensitive than *Chlorella vulgaris* for erythromycin (Eguchi et al. 2004, El-Bassat et al. 2011). *Pseudokirchneriella subcapitata* also was more sensitive than *Chlorella vulgaris* and *Chlorella variegate* for tetracycline (Agrawal and Manisha 2007). *Pseudokirchneriella subcapitata* also was more sensitive than *Scenedesmus obliquus* for norfloxacin (Nie et al. 2009). On the other hand, *Chlorella vulgaris* appeared more sensitive than *Pseudokirchneriella subcapitata* for norfloxacin (Eguchi et al. 2004). This trend is maintained with other quinolones. Therefore, other green algae appeared to be more sensitive than *Pseudokirchneriella subcapitata* to quinolones and less sensitive than *Pseudokirchneriella subcapitata* to the rest of antibiotics (Valitalo et al. 2017).

Anabaena sp. PCC7120 CBP4337, due to its prokaryotic nature, was in general more sensitive than *Pseudokirchneriella subcapitata* to the tested antibiotics, particularly amoxicillin, which showed no toxicity to the green alga. Norfloxacin and levofloxacin displayed flat and incomplete concentration-response curves to the green alga. In agreement with our results, it has been reported that cyanobacteria are usually more sensitive than green algae to antibiotics (Guo et al. 2016a, b, Qian et al. 2012, van der Grinten et al. 2010). *Microcystis aeruginosa* was more sensitive than *Pseudokirchneriella subcapitata* at least to four antibiotics (trimethoprim, streptomycin, flumequine and sulphamethoxazole) (van der Grinten et al. 2010). *Microcystis aeruginosa* also was more vulnerable than green alga *Chlorella vulgaris* after exposure

to antibiotic streptomycin (Qian et al. 2012). *Synechococcus leopoliensis* and *Anabaena flos-aquae* were more sensitive than *Chlorella vulgaris*, *Pseudokirchneriella subcapitata* and *Desmodesmus subspicatus* for three antibiotics (lincomycin, tylosin and trimethoprim) (Guo et al. 2016a, b). Therefore, cyanobacteria generally are more sensitive than green algae to antibiotics of different class (Valitalo et al. 2017).

The green alga, due to its eukaryotic nature, is a non-target organism for antibiotics; the observed toxicity exerted by some antibiotics could be, at least in part, due to the cyanobacterial nature of the chloroplasts and bacterial nature of mitochondria, which makes them susceptible as potential antibiotic targets.

Chloroplasts play a key role in algae and have a cyanobacterial nature. It has been reported that antibiotics exert toxic effect on photosynthesis in both cyanobacteria and green algae. Erythromycin exerts toxic effect on photosystem I and II in *Microcystis aeruginosa* (Deng et al. 2014). Erythromycin also induced toxic effect on *Pseudokirchneriella subcapitata* inhibiting many photosynthesis-related processes (chlorophyll biosynthesis, net photosynthesis rate, Mg^{2+}-ATPase), the activity of photochemistry, electron transport, photophosphorylation activity and carbon assimilation (Ribulose-1.5-bisphosphate carboxylase content and activity) (Liu et al. 2011a, Liu et al. 2011b). Tetracycline decreased chlorophyll fluorescence index *Fv*/*Fm* in both *M. aeruginosa* (FACHB-942) and *Pseudokirchneriella subcapitata* (Yang et al. 2013b). Levofloxacin decreased chlorophyll content and *Fv*/*Fm* and *Fv*/*Fo* values in *Microcystis flos-aquae* (Wan et al. 2014) and inhibited O_2 evolution and PSII activity in *Synechocystis* sp (Pan et al. 2009). In general, the antibiotics affected the same photosynthetic parameters in both cyanobacteria and green algae; therefore, cyanobacterial nature of the chloroplasts could be the reason that antibiotics exerted toxic effect on green algae, which are non-target organism.

In addition, mitochondria play a key role in algae and they have a bacterial nature. Many pollutants induce stress oxidative on aquatic organisms. Mitochondria are one of the main sources of oxidative stress in eukaryotic cells. It has been reported that antibiotics induced oxidative stress in both cyanobacteria and green algae; therefore, mitochondria could be the target of these antibiotic-inducing oxidative stress. Erythromycin altered ascorbic acid, ascorbate-glutathione cycle and xanthophylls cycle,

the activities of catalase, superoxide dismutase, guaiacol glutathione peroxidase and glutathione-S-transferase and lipid peroxidation on *Pseudokirchneriella subcapitata* (El-Bassat et al. 2011, Nie et al. 2013). Tetracycline also increased the superoxide dismutase activity and lipid peroxidation in *M. aeruginosa* (FACHB-942) and *Pseudokirchneriella subcapitata* (Yang et al. 2013b). Levofloxacin also increased superoxide dismutase, catalase activity and lipid peroxidation in *Microcystins flos-aquae* (Wan et al. 2014). The antibiotics induced oxidative stress in both cyanobacteria and green algae; therefore, the bacterial nature of the mitochondria could be the reason that antibiotic exerted toxic effects on green algae.

Antibiotics may pose a potential ecological risk for aquatic ecosystems with the present environmentally measured concentrations. In our case, especially remarkable were ecological risks for erythromycin in both organisms and tetracycline in green alga. It has been reported that erythromycin may pose a potential ecological risk for green algae, including *Pseudokirchneriella subcapitata*, on aquatic ecosystems with the present environmentally measured concentrations of wastewater effluents, in agreement with our results (Guo et al. 2015, Hernando et al. 2006, Verlicchi et al. 2012). Other antibiotics (larithromycin, trimethoprim, lincomycin, tylosin sulfamethoxazole, azithromycin, clarithromycin, triclosan, cephalotin, gentamycin and vancomycin) may also pose a potential ecological risk for green algae with the present environmentally measured concentrations (Guo et al. 2015, Kosma et al. 2014, Magdaleno et al. 2014, Papageorgiou et al. 2016, Pereira et al. 2015, Verlicchi et al. 2012). However, this thesis is the first report to show the potential ecological risk of tetracycline on green algae. Potential ecological risks based on unicellular cyanobacteria have been reported for amoxicillin, which pose a potential ecological risk on aquatic ecosystems (Guo et al. 2015). Our results showed amoxicillin do not pose potential ecological risk because the results are based on filamentous cyanobacteria, which are less sensitive than unicellular cyanobacteria *Microcystis aeruginosa* and *Synechococcus leopoliensis* for amoxicillin (Guo et al. 2015). Other antibiotics (ofloxacin, sulfamethoxazole, tylosin and enrofloxacin) may also pose a potential ecological risk for cyanobacteria with the present environmentally measured concentrations (Ferrari et al. 2004, Guo et al. 2015, Robinson et al. 2005). However, this thesis is the first report to show the potential ecological risk of erythromycin on cyanobacteria.

Specific combinations of antibiotics may pose a potential ecological risk on aquatic ecosystems with the present environmentally measured concentrations. In our case, the binary erythromycin and tetracycline mixture showed a strong synergism at low effect levels in both organisms in wastewater effluent. It has been reported that mixture of ten antibiotics could pose a potential ecological risk on cyanobacteria with the present environmentally measured concentrations of wastewater effluents in Hong Kong (Leung et al. 2012) and environmental samples that include several antibiotics may also pose potential ecological risk for green algae (Ginebreda et al. 2010). However, they did not study the interaction of antibiotics in mixtures; therefore, they could be underestimating the toxic effect and the ecological risk. Other study analysed the interaction of binary mixtures of antibiotics on *Pseudokirchneriella subcapitata* using Concentration addition (CA) and Independent Action (IA), it has been reported that toxicological interaction of binary mixtures of antibiotics could pose a potential ecological risk for *Pseudokirchneriella subcapitata* with the present environmentally measured concentrations of hospital effluents wastewater in Argentina (Magdaleno et al. 2014). In agreement with our results, they reported that binary mixtures of antibiotics can interact synergistically and, therefore, binary mixtures of antibiotics could be more toxic on aquatic ecosystems than expected. Consequently, mixtures of antibiotics may pose a potential ecological risk for freshwater. However, few studies have reported about the potential ecological risk of mixtures of antibiotics. The role of the interaction of antibiotics in mixtures should be evaluated in order to know their potential ecological risk.

In this thesis, toxicological interactions were studied using the Combination Index (CI) method indicating that synergism was predominant in binary and multi-component mixtures. Especially remarkable was the synergism found in almost all mixtures which included tetracycline as a component in both *Anabaena* sp. PCC7120 CPB4337 and *Pseudokirchneriella subcapitata*. CI method proved to give a more accurate prediction of the actual toxicity of synergistic mixtures than that offered by CA and IA.

It has been reported the toxicological interaction of mixtures of two antibiotics, amoxicillin and spiramycin, on cyanobacterium *Microcystis aeruginosa*. The interactions of the two antibiotics changed from antagonism to synergism with the increasing proportion of spiramycin in the binary mixtures at environmentally relevant

concentrations (Liu et al. 2014). The predictions offered by CA and IA were higher and lower than those observed depending on the ratio of antibiotics in the binary mixtures; in agreement with our results these methods are not good to predict the observed effect. It has been also reported the toxicological interaction of binary mixtures of four antibiotics, cephalotin, ciprofloxacin, gentamycin, and vancomycin, on green alga *Pseudokirchneriella subcapitata* (Magdaleno et al. 2014). The toxicological interactions of binary mixtures were predicted by CA and IA. In all cases a clear synergistic effect was observed, showing that single compound toxicity data are not adequate for the prediction of aquatic toxicities of antibiotic mixtures, in agreement with our results.

In this thesis, the effects of realistic mixtures on photosynthetic organisms were studied using the Morris method. For such purpose, *Anabaena* sp. PCC7120 CPB4337 was exposed to 180 realistic mixtures of 16 pharmaceuticals. Realistic mixtures are characterized by individual pollutant at low doses, which are at or near the toxicological threshold of observable effects (Kortenkamp et al 2008). In fact, our results showed that the median response of *Anabaena* sp. PCC7120 CPB4337 after exposure to 16 individual pharmaceuticals at realistic low-doses was decrease in bioluminescence whereas mixtures produced reduction of the bioluminescence (toxicity). These results agree with those obtained in previous studies, which reported that the toxicity of the mixtures of pharmaceuticals can be higher than the effects of each pharmaceutical individually and that even pharmaceuticals, which do not provoke effects individually, can contribute to toxicity of the mixtures (Backhaus 2014a).

Realistic mixtures are very complex, different chemicals co-occur in environmental compartments in changing ratios (Backhaus and Karlsson 2014). These chemicals in a mixture may either not interact (additivity) or interact, synergistic or antagonistically. CA, a classic model employed in mixture toxicology, and Morris methods, as described above, were used to predict the effect of the 180 realistic mixtures. CA, like CI and IA, is based on the basic idea that the expected effect of a mixture of chemicals can be predicted based on the sum of the fractions of effects of the individual mixture components; therefore CA requires the knowledge of the dose response curves of each of the pollutants (Chou 2006, Faust et al. 2001). In our case, as the 16 individual pharmaceuticals at realistic concentrations showed no toxicity towards *Anabaena* sp. PCC7120 CPB4337, it was necessary to test higher concentrations (1000 times) of the

individual pharmaceuticals than realistic ones in order to identify candidate pharmaceuticals to perform dose-response curves. Three pharmaceuticals (ofloxacin, venlafaxine and erythromycin) showed toxicity at higher concentration and they were selected to carry out the CA. CA predicted nearly no effect (from 0 to 0.026% inhibition) for all the 180 mixtures in contrast with the observed range of experimental effects. This may be due to the fact that CA, like IA, assumes that the components of the mixtures do not interact. However, Morris methods showed interaction between 16 pharmaceuticals in the mixtures. In agreement with these results, it has been reported by Backhaus et al. (2014) that pharmaceuticals in mixtures can interact producing a result different of the expected sum of its effects. However, these authors have also reported that CA can predict effect of mixtures of multi-components. They argue that both synergism and antagonism are confined to mixtures of few components and multi-components mixtures buffer against both interactions (Backhaus 2014b). However, they do not show data to support this hypothesis. They could perform a quantification of the interaction of the components of mixtures in order to confirm that the sum of the interactions is zero. CI could be employed to quantify these interactions (Chou 2006, Rodea-Palomares et al. 2010). Furthermore, unlike IA and CA, CI can be used independently of the mechanism of action of compounds; therefore, it can be employed in this case (Chou 2006). However, like CA and IA, CI requires known dose-response curves of each of the chemicals, which is a great experimental effort for 180 realistic mixtures (Chou 2006). Furthermore, the interaction of components of the mixtures changes according to their ratio, especially in mixtures of pharmaceuticals (Liu et al. 2014). The experimental cost of the study the toxic effects of mixtures with components at different ratio is almost unreachable. On the other hand, the organism may respond to low dose of the chemicals linear or nonlinearly (Calabrese 2008a, b). CA, like IA and CI, assumes linearity. Therefore, another reason by which CA cannot explain the effect of the 180 mixtures, could be because pharmaceuticals display nonlinear responses in the mixtures as showed by the Morris methods. Many studies reported evidence of non-linear responses below the thresholds of observable monotonic responses to pollutants, the most common and accepted case is hormesis (Calabrese 2008a, b). In fact, the median response of *Anabaena* sp. PCC7120 CPB4337 after exposure to 16 individual pharmaceuticals at realistic low doses was an increase in bioluminescence (hormesis), which supported this idea.

Regardless individual effects, it is key to understand which individual components in mixtures are main drivers of the toxicity. Morris method provided a qualitative ranking of the relative importance of the 16 pharmaceuticals and light intensity in realistic mixtures, including factors whose concentration were at the toxicological thresholds of observable effects and those that showed both nonadditivity and nonlinear responses. Another approach based on toxic units (TUs) and quantitative structure-activity relationships (QSARs) have been also employed to provide ranking of the relative importance of the pollutants in mixtures. These approaches are based on CA and IA, therefore, they assumed that components in mixtures do not interact or that the sum of the interactions, at least in multi-components mixtures, is zero (Backhaus 2014a, Backhaus and Karlsson 2014, Kim and Kim 2015a). Backhaus et al (2014) have reported that TUs allow to identify the most important pollutants, which explain the toxicity of mixtures, in effluents of STP. In addition, TUs approaches provided a quantitative ranking of the importance of each of the pollutants unlike the Morris method, which can only do it qualitatively. Backhaus et al. (2014) concluded that, in all cases, 10 mixtures components can explain at least the 95% of the mixtures toxicity (Backhaus and Karlsson 2014). However, TUs approaches required the knowledge of the dose response curves of all the pollutants of the mixtures, which imply not only identifying the components in the mixtures but also to know their toxic effects, unlike the Morris method. Furthermore, TUs, like QSAR, evaluate the low concentration of chemicals, which appear in realistic mixtures, using dose response curve in which the first concentration that appears is several orders of magnitude above the concentration evaluated. Therefore, TUs approaches should assume linear effect even at low concentration, which could affect the ranking in our case (Morris methods showed pharmaceuticals response as non-linear) (Backhaus and Karlsson 2014). In addition, the authors do not check if the toxicity of the mixture is reduced by removing main pollutants, which according to their ranking explains 95% of the toxicity (Backhaus and Karlsson 2014). This would support their hypothesis and demonstrate that the interactions and the linear and nonlinear responses of the pollutants are compensated in mixtures of multi-components. On the other hand, our results support that removing the main drivers of the mixtures identified by Morris method, the toxicity of the mixtures is reduced. On the other hand, QSAR can also be a powerful tool to evaluate the toxicity of mixtures of chemicals due to their reproducibility and wide use as long as it is

assumed that similar molecules have similar activities and linear and non-interacting response of the chemical, at least in multi-components mixtures (Kim and Kim 2015b).

Realistic mixtures include non-chemical factors, such as light and temperature, which should be evaluated. Morris method was useful to evaluate the effect of different light intensity in the mixtures. To our knowledge, TUs approach has not been used to study non-chemical factors, but in theory these approaches could evaluate the non-chemical factors carrying out their dose response curves. Other approaches based on QSAR cannot assess the non-chemicals factors (Kim and Kim 2015b). QSAR are based on the quantitative correlation of the physicochemical properties of molecules with their biological activities, therefore, their rankings do not include non-chemicals (Kim and Kim 2015b). Therefore, Morris method could be useful to test the effects of combined stressors (not only chemicals but also physical and biological stresses) with unknown dose-response curves unlike CI, CA, AI, TUs and QSAR, which required complete dose-responses curves and many other assumptions.

Intracellular free Ca^{2+}, $[Ca^{2+}]_i$, is a second messenger known to be involved in the perception and signaling of many abiotic stresses (Domínguez et al. 2015, Leganes et al. 2009, Shemarova and Nesterov 2014, Torrecilla et al. 2000, 2004a, Torrecilla et al. 2001, 2004b). $[Ca^{2+}]_i$ has also been found to be involved in the response to individual and mixtures of pollutants (see table 1.3). It has been reported that priority and emerging pollutants evoked changes in $[Ca^{2+}]_i$ homeostasis in many organisms, including aquatic organism such as *Chlamydomonas moewusii* (see table 1.3, chapter 1). However, most of these studies (see table 1.3, chapter 1) have only been able to show the effect of pollutants on $[Ca^{2+}]_i$ as a cellular response. Very few of them have assessed the potential usefulness of $[Ca^{2+}]_i$ as a bioassay or as an early biomarker of exposure to pollutants.

In contrast, in this thesis (chapter 4), we used a recombinant bioluminescent strain of the cyanobacterium *Anabaena* sp. PCC 7120, which constitutively expresses the Ca^{2+} binding indicator protein apoaequorin, to evaluate the role of $[Ca^{2+}]_i$ as an early biomarker of exposure to antibiotics. Our group had previously employed this cyanobacterium to study the role of $[Ca^{2+}]_i$ as an early biomarker of exposure in response to other groups of pollutants (Barran-Berdon et al. 2011) and abiotic stresses

(Torrecilla et al. 2000, 2004a, Torrecilla et al. 2001, 2004b). In agreement with these previous studies, the characteristics of the Ca^{2+} signal recorded included transient shape, amplitude, rise time (time from application of the stimulus to maximum amplitude of the response) and total transient duration (length of the transient form zero time to the recovery of the resting $[Ca^{2+}]_i$) (Barran-Berdon et al. 2011). These characteristics give specificity to the Ca^{2+} signal (Ca^{2+} signatures). Likewise, Kozlova et al. (2005) also recorded similar parameters of the Ca^{2+} signal, such as the amplitude, length of transient and final Ca^{2+} resting levels, after exposure to pollutants in order to evaluate the applicability of Ca^{2+} signal as a bioassay using the recombinant apoaequorin expressing fungus *Aspergillus awamori*.

In this thesis, we found that Ca^{2+} signals upon exposure to antibiotics were induced quickly (2-3 seconds). Furthermore, these Ca^{2+} signals were found to be different depending on the antibiotics and the antibiotic concentration. In agreement with these results, our group had previously reported that pollutants triggered specific Ca^{2+} signals and in a dose-dependent manner (Barran-Berdon et al. 2011). Similarly, it has been reported that Ca^{2+} signals were induced in a dose-dependent manner after exposure to pollutants using *Aspergillus awamori* (Kozlova et al. 2005). Other studies have also reported that both fish and rat cellular lines induced Ca^{2+} signals in a dose-dependent manner after exposure to pollutants (see table 1.3, chapter 1). These results support our research findings indicating that antibiotics as well as other pollutants evoked a specific Ca^{2+} signal, which depended on the concentration.

Yet, the role of the Ca^{2+} signal in toxicity is not well understood (Ruta et al. 2016a, Ruta et al. 2014). Ruta et al. (2014, 2016) have suggested that the characteristic of the Ca^{2+} signals may have a significant role in the final cellular response, in this context, quick Ca^{2+} signals may allow the adaptation to high concentrations of pollutants in apoaequorin-expressing *Saccharomyces cerevisiae* cells, while the absence of Ca^{2+} signals or broad ones may lead the cells to toxicity. They concluded that cells prepared to face high and rapid Ca^{2+} cytosolic waves were fitter for survival.

In chapter 2, we determined the nature of the interactions between the five studied antibiotics in binary mixtures and in a multiantibiotic mixture in the bioluminescent strain *Anabaena* sp. PCC 7120 CPB4337 after 72 h of exposure. We evaluated whether

changes in $[Ca^{2+}]_i$ could also be induced by antibiotic binary mixtures and by a multiantibiotic mixture so that by comparing the Ca^{2+} signals of the mixture with those of antibiotics when applied singly, patterns of interactions might become evident. Ca^{2+} signals induced by the mixtures of antibiotics seemed to anticipate the toxicological interactions found at larger times of exposure. Our group also previously compared the recorded Ca^{2+} signal of other pollutants with the values of toxicity interactions of some of the tested pollutants towards *Anabaena* sp. PCC 7120 CPB4337 (Barran-Berdon et al. 2011). In agreement with these results, (Barran-Berdon et al. 2011) and our, Ca^{2+} signatures might predict the nature of interactions of pollutants.

On the other hand, Kozlova et al. (2005) tried to correlate Ca^{2+} signal triggered by pollutants in apoaequorin-expressing fungus *Aspergillus awamori* with toxicity. For these purpose, they compared the amplitude of the changes of Ca^{2+} signals with the EC_{50} of the *Aliivibrio fischeri*, which constitutes a classical bioluminescent toxicity bioassay for pollutants. Their results indicated that the amplitude of Ca^{2+} signals is a less sensitive parameter than the *V. fischeri* luciferase system. The authors, however, highlighted that Ca^{2+} signals consist of many parameters, being therefore possible that some other was more sensitive to toxicity than the amplitude. In addition, they compared the sensitivity of their bioassay, based on eukaryotic cells, with *Aliivibrio fischeri*, which it based on in prokaryotic cells, making these results difficult to compare.

In chapter 5, we studied the role of $[Ca^{2+}]_i$ in the global cellular response to a pollutant. To our knowledge, this study constitutes the first work showing the mechanistic role of $[Ca^{2+}]_i$ in the cellular response to pollutants of organisms of high ecological relevance. As of today, most studies that have evaluated the mechanistic role of $[Ca^{2+}]_i$ in cellular response to pollutants, have been carried out in rat brain cells (Chen et al. 2011, Lin et al. 2015, Marty and Atchison 1998, Mitra et al. 2013, Rai et al. 2010, Sun et al. 2013, Xu et al. 2011, Yuan et al. 2013) and in other cells, such as rat hepatocytes cells (Wang et al. 2014), rat alveolar cells (Yang et al. 2013a), human cells lines (Mayati et al. 2014), fish cells (Reader et al. 1999), *Neurospora crassa* (Binder et al. 2010), *Aspergillus niger* (Binder et al. 2011) and *Saccharomyces cerevisiae* (Ruta et al. 2016b).

We studied the relationship between $[Ca^{2+}]_i$ and the cellular response of *Chlamydomonas reinhardtii* after exposure to model EPs triclosan (TCS). TCS strongly altered $[Ca^{2+}]_i$ homeostasis, which could be prevented by prechelation with BAPTA-AM (an intracellular Ca^{2+} chelator). In other studies, several compounds have been employed to chelate/remove or deregulate $[Ca^{2+}]_i$ in order to understand the relationship between role of $[Ca^{2+}]_i$ and the organism cellular response to pollutants. These compounds can be classified as: Ca^{2+} channel blockers (Binder et al. 2010), calmodulin antagonists (Xu et al. 2011) and intracellular Ca^{2+} chelators (Wang et al. 2014). BAPTA-AM is probably the most frequently used, due to its ability to prevent alterations of $[Ca^{2+}]_i$ homeostasis allowing to study which of the cellular responses after exposure to pollutant depends on alteration of $[Ca^{2+}]_i$ homeostasis and which does not depend on it (Binder et al. 2011, Binder et al. 2010, Chen et al. 2011, Li et al. 2011, Marty and Atchison 1998, Mayati et al. 2014, Mitra et al. 2013, Rai et al. 2010, Reader et al. 1999, Sun et al. 2013, Wang et al. 2014, Xu et al. 2011, Yang et al. 2013a, Yuan et al. 2013).

It has been reported that alteration of the $[Ca^{2+}]_i$ homeostasis is involved in cellular response to pollutants, such as changes in gene expression, increase of oxidative stress, mitochondria malfunction, apoptosis, inhibition of growth and morphological changes, in several organisms (Binder et al. 2011, Binder et al. 2010, Chen et al. 2011, Li et al. 2011, Marty and Atchison 1998, Mayati et al. 2014, Mitra et al. 2013, Rai et al. 2010, Reader et al. 1999, Sun et al. 2013, Wang et al. 2014, Xu et al. 2011, Yang et al. 2013a, Yuan et al. 2013).

Our results showed that TCS induced an increase in the oxidative stress (an imbalance between the production of ROS and the cellular antioxidant defense mechanisms), which was linked to the alteration in $[Ca^{2+}]_i$ homeostasis. This is consistent with other studies where pollutants evoked significant alteration of the $[Ca^{2+}]_i$ homeostasis leading to a sustained increase in basal levels, which seemed to increase oxidative stress (Lin et al. 2015, Rai et al. 2010, Sun et al. 2013, Wang et al. 2014, Xu et al. 2011, Yuan et al. 2013). Most of these studies tested the individual effect of priority pollutant using Cd as model. In addition, Rae et al. (2010) reported that the mixture of three heavy metals increased oxidative stress through sustained alteration of $[Ca^{2+}]$ homeostasis. Moreover, only one study has previously reported the role of $[Ca^{2+}]_i$ in oxidative stress in response

to an emerging pollutant, the antibiotic geldanamycin (Sun et al. 2013). Most probably as the result of oxidative stress, TCS led to mitochondria malfunction and apoptosis. In this regard, Wang et al. (2014) reported that alterations of the $[Ca^{2+}]_i$ homeostasis in response to Cd are linked with mitochondrial depolarization in rat hepatocytes. There are several studies showing the role of $[Ca^{2+}]_i$ in apoptosis in response to individual and mixtures of priority pollutants (Al, Cd and mixtures of Pb + Cd + As) as well as to emerging pollutants (tributyltin and crotonaldehyde) in rat, fish and yeast using different approaches: Western blotting with antibodies, TUNEL assay, caspase-9 and caspase 3/7 activity (Caspase-Glo^{TM}) and Annexin V/PI (Chen et al. 2011, Li et al. 2011, Rai et al. 2010, Reader et al. 1999, Wang et al. 2014, Xu et al. 2011, Yang et al. 2013a, Yuan et al. 2013). However, this thesis constitutes the first study reporting the role of $[Ca^{2+}]_i$ in apoptosis in response to emerging pollutants in a photosynthetic aquatic organism. At a genetic level, TCS significantly altered the expression of *C. reinhardtii* genes involved in calcium signalling (CAS and calmodulin), photosynthesis and oxidative stress, which are strongly linked with the alteration in the $[Ca^{2+}]_i$ homeostasis. This is in agreement with other studies as Li et al. (2011) have reported that the priority pollutant Al down-regulated the expression of genes involved in Ca^{2+} signalling pathway, such as calmodulin and phospholipase C.

The toxic cellular response linked to $[Ca^{2+}]_i$ in response to pollutants can be due to the proven cytotoxicity of increased $[Ca^{2+}]_i$ for a large period of time (Li et al. 2011). It has been shown that sustained increase in $[Ca^{2+}]_i$ basal levels led to irreversible damages in the mitochondria, activation of degradative enzymes (such as proteases, nucleases and phospholipases), chromatin condensation, aggregation of proteins (precipitation of proteins) and nucleic acids (RNA/DNA) and affects the integrity of lipid membranes and the ATP metabolism (precipitation of phosphate) (Case et al. 2007, Kazmierczak et al. 2013, Plattner and Verkhratsky 2016, Verkhratsky and Parpura 2014).

REFERENCES

Agrawal, S.C. and Manisha (2007) Growth, survival and reproduction in Chlorella vulgaris and C. variegata with respect to culture age and under different chemical factors. Folia Microbiologica 52(4), 399-406.

Ando, T., Nagase, H., Eguchi, K., Hirooka, T., Nakamura, T., Miyamoto, K. and Hirata, K. (2007) A novel method using cyanobacteria for ecotoxicity test of veterinary antimicrobial agents. Environmental Toxicology and Chemistry 26(4), 601-606.
Backhaus, T. (2014a) Medicines, shaken and stirred: a critical review on the ecotoxicology of pharmaceutical mixtures. Phil. Trans. R. Soc. B 369(1656), 20130585.

Backhaus, T. (2014b) Medicines, shaken and stirred: a critical review on the ecotoxicology of pharmaceutical mixtures. Philosophical Transactions of the Royal Society of London. Series B: Biological Sciences 369(1656).

Backhaus, T. and Karlsson, M. (2014) Screening level mixture risk assessment of pharmaceuticals in STP effluents. water research 49, 157-165.

Barran-Berdon, A.L., Rodea-Palomares, I., Leganes, F. and Fernandez-Pinas, F. (2011) Free Ca2+ as an early intracellular biomarker of exposure of cyanobacteria to environmental pollution. Anal Bioanal Chem 400(4), 1015-1029.

Binder, U., Bencina, M., Eigentler, A., Meyer, V. and Marx, F. (2011) The Aspergillus giganteus antifungal protein AFPNN5353 activates the cell wall integrity pathway and perturbs calcium homeostasis. BMC Microbiology 11, 209.

Binder, U., Chu, M., Read, N.D. and Marx, F. (2010) The antifungal activity of the Penicillium chrysogenum protein PAF disrupts calcium homeostasis in Neurospora crassa. Eukaryot Cell 9(9), 1374-1382.

Calabrese, E.J. (2008a) Hormesis and mixtures. Toxicology and Applied Pharmacology 229(2), 262-263.

Calabrese, E.J. (2008b) Hormesis: why it is important to toxicology and toxicologists. Environmental Toxicology and Chemistry 27(7), 1451-1474.

Case, R.M., Eisner, D., Gurney, A., Jones, O., Muallem, S. and Verkhratsky, A. (2007) Evolution of calcium homeostasis: from birth of the first cell to an omnipresent signalling system. Cell Calcium 42(4-5), 345-350.

Chen, S., Xu, Y., Xu, B., Guo, M., Zhang, Z., Liu, L., Ma, H., Chen, Z., Luo, Y., Huang, S. and Chen, L. (2011) CaMKII is involved in cadmium activation of MAPK and mTOR pathways leading to neuronal cell death. Journal of Neurochemistry 119(5), 1108-1118.

Chou, T.-C. (2006) Theoretical basis, experimental design, and computerized simulation of synergism and antagonism in drug combination studies. Pharmacological Reviews 58(3), 621-681.

Deng, C.N., Zhang, D.Y. and Pan, X.L. (2014) Toxic effects of erythromycin on photosystem I and II in Microcystis aeruginosa. Photosynthetica 52(4), 574-580.

Dias, E., Oliveira, M., Jones-Dias, D., Vasconcelos, V., Ferreira, E., Manageiro, V. and Canica, M. (2015) Assessing the antibiotic susceptibility of freshwater Cyanobacteria spp. Front Microbiol 6, 799.

Domínguez, D.C., Guragain, M. and Patrauchan, M. (2015) Calcium binding proteins and calcium signaling in prokaryotes. Cell Calcium 57(3), 151-165.

Eguchi, K., Nagase, H., Ozawa, M., Endoh, Y.S., Goto, K., Hirata, K., Miyamoto, K. and Yoshimura, H. (2004) Evaluation of antimicrobial agents for veterinary use in the ecotoxicity test using microalgae. Chemosphere 57(11), 1733-1738.

El-Bassat, R.A., Touliabah, H.E., Harisa, G.I. and Sayegh, F.A. (2011) Aquatic toxicity of various pharmaceuticals on some isolated plankton species. International Journal of Medicine and Medical Sciences 3(6), 170-180.

Faust, M., Altenburger, R., Backhaus, T., Blanck, H., Boedeker, W., Gramatica, P., Hamer, V., Scholze, M., Vighi, M. and Grimme, L. (2001) Predicting the joint algal toxicity of multi-component s-triazine mixtures at low-effect concentrations of individual toxicants. Aquatic Toxicology 56(1), 13-32.

Fernández-Pinas, F. and Wolk, C.P. (1994) Expression of luxCD-E in Anabaena sp. can replace the use of exogenous aldehyde for in vivo localization of transcription by luxAB. Gene 150(1), 169-174.

Ferrari, B., Mons, R., Vollat, B., Fraysse, B., Paxēaus, N., Giudice, R.L., Pollio, A. and Garric, J. (2004) Environmental risk assessment of six human pharmaceuticals: are the current environmental risk assessment procedures sufficient for the protection of the aquatic environment? Environmental Toxicology and Chemistry 23(5), 1344-1354.

Ginebreda, A., Munoz, I., de Alda, M.L., Brix, R., Lopez-Doval, J. and Barcelo, D. (2010) Environmental risk assessment of pharmaceuticals in rivers: relationships between hazard indexes and aquatic macroinvertebrate diversity indexes in the Llobregat River (NE Spain). Environ Int 36(2), 153-162.

Guo, J., Boxall, A. and Selby, K. (2015) Do Pharmaceuticals Pose a Threat to Primary Producers? Critical Reviews in Environmental Science and Technology 45(23), 2565-2610.

Guo, J., Selby, K. and Boxall, A.B. (2016a) Comparing the sensitivity of chlorophytes, cyanobacteria, and diatoms to major-use antibiotics. Environmental Toxicology and Chemistry 35(10), 2587-2596.

Guo, J., Selby, K. and Boxall, A.B. (2016b) Effects of Antibiotics on the Growth and Physiology of Chlorophytes, Cyanobacteria, and a Diatom. Archives of Environmental Contamination and Toxicology 71(4), 589-602.

Halling-Sørensen, B. (2000) Algal toxicity of antibacterial agents used in intensive farming. Chemosphere 40(7), 731-739.
Hernando, M.D., Mezcua, M., Fernandez-Alba, A.R. and Barcelo, D. (2006) Environmental risk assessment of pharmaceutical residues in wastewater effluents, surface waters and sediments. Talanta 69(2), 334-342.

Isidori, M., Lavorgna, M., Nardelli, A., Pascarella, L. and Parrella, A. (2005) Toxic and genotoxic evaluation of six antibiotics on non-target organisms. Science of the Total Environment 346(1-3), 87-98.

Kazmierczak, J., Kempe, S. and Kremer, B. (2013) Calcium in the Early Evolution of Living Systems: A Biohistorical Approach. Current Organic Chemistry 17(16), 1738-1750.

Kim, J. and Kim, S. (2015a) State of the art in the application of QSAR techniques for predicting mixture toxicity in environmental risk assessment. SAR and QSAR in Environmental Research 26(1), 41-59.

Kim, J. and Kim, S. (2015b) State of the art in the application of QSAR techniques for predicting mixture toxicity in environmental risk assessment. SAR and QSAR in Environmental Research 26(1), 41-59.

Kosma, C.I., Lambropoulou, D.A. and Albanis, T.A. (2014) Investigation of PPCPs in wastewater treatment plants in Greece: occurrence, removal and environmental risk assessment. Science of the Total Environment 466-467, 421-438.

Kozlova, O., Zwinderman, M. and Christofi, N. (2005) A new short-term toxicity assay using Aspergillus awamori with recombinant aequorin gene. BMC Microbiology 5(1), 40.

Leganes, F., Forchhammer, K. and Fernandez-Pinas, F. (2009) Role of calcium in acclimation of the cyanobacterium Synechococcus elongatus PCC 7942 to nitrogen starvation. Microbiology 155(Pt 1), 25-34.

Leung, H.W., Minh, T.B., Murphy, M.B., Lam, J.C.W., So, M.K., Martin, M., Lam, P.K.S. and Richardson, B.J. (2012) Distribution, fate and risk assessment of antibiotics in sewage treatment plants in Hong Kong, South China. Environ Int 42, 1-9.
Li, X., Qian, J., Wang, C., Zheng, K., Ye, L., Fu, Y., Han, N., Bian, H., Pan, J., Wang, J. and Zhu, M. (2011) Regulating cytoplasmic calcium homeostasis can reduce aluminum toxicity in yeast. PloS One 6(6), e21148.

Lin, F., Peng, Y.-H., Yang, Q.-H. and Mi, X.-J. (2015) Resveratrol inhibits cadmium induced neuronal apoptosis by modulating calcium signalling pathway via regulation of MAPK/mTOR network. Bangladesh Journal of Pharmacology 10(2), 366.

Liu, B.-y., Nie, X.-p., Liu, W.-q., Snoeijs, P., Guan, C. and Tsui, M.T. (2011a) Toxic effects of erythromycin, ciprofloxacin and sulfamethoxazole on photosynthetic apparatus in Selenastrum capricornutum. Ecotoxicology and Environmental Safety 74(4), 1027-1035.

Liu, B., Liu, W., Nie, X., Guan, C., Yang, Y., Wang, Z. and Liao, W. (2011b) Growth response and toxic effects of three antibiotics on Selenastrum capricornutum evaluated by photosynthetic rate and chlorophyll biosynthesis. Journal of Environmental Sciences 23(9), 1558-1563.

Liu, Y., Gao, B., Yue, Q., Guan, Y., Wang, Y. and Huang, L. (2012) Influences of two antibiotic contaminants on the production, release and toxicity of microcystins. Ecotoxicology and Environmental Safety 77, 79-87.

Liu, Y., Zhang, J., Gao, B. and Feng, S. (2014) Combined effects of two antibiotic contaminants on Microcystis aeruginosa. Journal of Hazardous Materials 279, 148-155.

Lorenz, M.G. and Krumbein, W.E. (1984) Large-scale determination of cyanobacterial susceptibility to antibiotics and inorganic ions. Applied Microbiology and Biotechnology 20(6), 422-426.

Lützhøft, H.-C.H., Halling-Sørensen, B. and Jørgensen, S. (1999) Algal toxicity of antibacterial agents applied in Danish fish farming. Archives of Environmental Contamination and Toxicology 36(1), 1-6.

Magdaleno, A., Juarez, A.B., Dragani, V., Saenz, M.E., Paz, M. and Moretton, J. (2014) Ecotoxicological and genotoxic evaluation of Buenos Aires city (Argentina) hospital wastewater. Journal of Toxicology 2014, 248461.

Marty, M.S. and Atchison, W.D. (1998) Elevations of intracellular Ca2+ as a probable contributor to decreased viability in cerebellar granule cells following acute exposure to methylmercury. Toxicology and Applied Pharmacology 150(1), 98-105.
Mayati, A., Le Ferrec, E., Holme, J.A., Fardel, O., Lagadic-Gossmann, D. and Ovrevik, J. (2014) Calcium signaling and beta2-adrenergic receptors regulate 1-nitropyrene induced CXCL8 responses in BEAS-2B cells. Toxicology in Vitro 28(6), 1153-1157.
Mitra, S., Gera, R., Siddiqui, W.A. and Khandelwal, S. (2013) Tributyltin induces oxidative damage, inflammation and apoptosis via disturbance in blood-brain barrier and metal homeostasis in cerebral cortex of rat brain: an in vivo and in vitro study. Toxicology 310, 39-52.

Nie, X., Gu, J., Lu, J., Pan, W. and Yang, Y. (2009) Effects of norfloxacin and butylated hydroxyanisole on the freshwater microalga Scenedesmus obliquus. Ecotoxicology 18(6), 677-684.

Nie, X.P., Liu, B.Y., Yu, H.J., Liu, W.Q. and Yang, Y.F. (2013) Toxic effects of erythromycin, ciprofloxacin and sulfamethoxazole exposure to the antioxidant system in Pseudokirchneriella subcapitata. Environmental Pollution (Barking, Essex: 1987) 172, 23-32.
Pan, X., Zhang, D., Chen, X., Mu, G., Li, L. and Bao, A. (2009) Effects of levofloxacin hydrochloride on photosystem II activity and heterogeneity of Synechocystis sp. Chemosphere 77(3), 413-418.

Papageorgiou, M., Kosma, C. and Lambropoulou, D. (2016) Seasonal occurrence, removal, mass loading and environmental risk assessment of 55 pharmaceuticals and personal care products in a municipal wastewater treatment plant in Central Greece. Science of the Total Environment 543(Pt A), 547-569.

Pereira, A.M., Silva, L.J., Meisel, L.M., Lino, C.M. and Pena, A. (2015) Environmental impact of pharmaceuticals from Portuguese wastewaters: geographical and seasonal occurrence, removal and risk assessment. Environmental Research 136, 108-119.
Plattner, H. and Verkhratsky, A. (2016) Inseparable tandem: evolution chooses ATP and Ca2+ to control life, death and cellular signalling. Philosophical Transactions of the Royal Society of London. Series B: Biological Sciences 371(1700).

Pomati, F., Netting, A.G., Calamari, D. and Neilan, B.A. (2004) Effects of erythromycin, tetracycline and ibuprofen on the growth of Synechocystis sp. and Lemna minor. Aquatic Toxicology 67(4), 387-396.

Prasanna, R., Madhan, K., Singh, R., Chauhan, A. and Nain, L. (2010) Developing biochemical and molecular markers for cyanobacterial inoculants. Folia Microbiologica 55(5), 474-480.

Qian, H., Li, J., Pan, X., Sun, Z., Ye, C., Jin, G. and Fu, Z. (2012) Effects of streptomycin on growth of algae Chlorella vulgaris and Microcystis aeruginosa. Environmental Toxicology 27(4), 229-237.

Rai, A., Maurya, S.K., Khare, P., Srivastava, A. and Bandyopadhyay, S. (2010) Characterization of developmental neurotoxicity of As, Cd, and Pb mixture: synergistic action of metal mixture in glial and neuronal functions. Toxicological Sciences 118(2), 586-601.
Reader, S., Moutardier, V. and Denizeau, F. (1999) Tributyltin triggers apoptosis in trout hepatocytes: the role of Ca2+, protein kinase C and proteases. Biochimica et Biophysica Acta (BBA) - Molecular Cell Research 1448(3), 473-485.

Robinson, A.A., Belden, J.B. and Lydy, M.J. (2005) Toxicity of fluoroquinolone antibiotics to aquatic organisms. Environmental Toxicology and Chemistry 24(2), 423-430.

Rodea-Palomares, I., Fernández-Piñas, F., González-García, C. and Leganés, F. (2009) Use of lux-marked cyanobacterial bioreporters for assessment of individual and combined toxicities of metals in aqueous samples. Handbook on Cyanobacteria: Biochemistry, Biotechnology and Applications, 283-304.

Rodea-Palomares, I., Petre, A.L., Boltes, K., Leganés, F., Perdigón-Melón, J.A., Rosal, R. and Fernández-Piñas, F. (2010) Application of the combination index (CI)-isobologram equation to study the toxicological interactions of lipid regulators in two aquatic bioluminescent organisms. water research 44(2), 427-438.

Rosal, R., Rodea-Palomares, I., Boltes, K., Fernandez-Pinas, F., Leganes, F. and Petre, A. (2010) Ecotoxicological assessment of surfactants in the aquatic environment: combined toxicity of docusate sodium with chlorinated pollutants. Chemosphere 81(2), 288-293.

Ruta, L.L., Popa, C.V., Nicolau, I. and Farcasanu, I.C. (2016a) Calcium signaling and copper toxicity in Saccharomyces cerevisiae cells. Environmental Science and Pollution Research 23(24), 24514-24526.

Ruta, L.L., Popa, C.V., Nicolau, I. and Farcasanu, I.C. (2016b) Calcium signaling and copper toxicity in Saccharomyces cerevisiae cells. Environmental Science and Pollution Research International 23(24), 24514-24526.

Ruta, L.L., Popa, V.C., Nicolau, I., Danet, A.F., Iordache, V., Neagoe, A.D. and Farcasanu, I.C. (2014) Calcium signaling mediates the response to cadmium toxicity in Saccharomyces cerevisiae cells. FEBS Letters 588(17), 3202-3212.

Shemarova, I.V. and Nesterov, V.P. (2014) [Ca2+ signaling in prokaryotes]. Mikrobiologiia 83(5), 511-518.

Sun, F.C., Shyu, H.Y., Lee, M.S., Lee, M.S. and Lai, Y.K. (2013) Involvement of calcium-mediated reactive oxygen species in inductive GRP78 expression by geldanamycin in 9L rat brain tumor cells. Int J Mol Sci 14(9), 19169-19185.

Torrecilla, I., Leganes, F., Bonilla, I. and Fernandez-Pinas, F. (2000) Use of recombinant aequorin to study calcium homeostasis and monitor calcium transients in response to heat and cold shock in cyanobacteria. Plant Physiology 123(1), 161-176.

Torrecilla, I., Leganes, F., Bonilla, I. and Fernandez-Pinas, F. (2004a) A calcium signal is involved in heterocyst differentiation in the cyanobacterium Anabaena sp. PCC7120. Microbiology 150(Pt 11), 3731-3739.

Torrecilla, I., Leganés, F., Bonilla, I. and Fernández-Piñas, F. (2001) Calcium transients in response to salinity and osmotic stress in the nitrogen-fixing cyanobacterium Anabaena sp. PCC7120, expressing cytosolic apoaequorin. Plant, Cell & Environment 24(6), 641-648.

Torrecilla, I., LeganÉS, F., Bonilla, I. and FernÁNdez-PiÑAs, F. (2004b) Light-to-dark transitions trigger a transient increase in intracellular Ca2+ modulated by the redox state of the photosynthetic electron transport chain in the cyanobacterium Anabaena sp. PCC7120. Plant, Cell & Environment 27(7), 810-819.

Valitalo, P., Kruglova, A., Mikola, A. and Vahala, R. (2017) Toxicological impacts of antibiotics on aquatic micro-organisms: A mini-review. Int J Hyg Environ Health.

van der Grinten, E., Pikkemaat, M.G., van den Brandhof, E.J., Stroomberg, G.J. and Kraak, M.H. (2010) Comparing the sensitivity of algal, cyanobacterial and bacterial bioassays to different groups of antibiotics. Chemosphere 80(1), 1-6.

Verkhratsky, A. and Parpura, V. (2014) Calcium signalling and calcium channels: evolution and general principles. European Journal of Pharmacology 739, 1-3.

Verlicchi, P., Al Aukidy, M., Galletti, A., Petrovic, M. and Barcelo, D. (2012) Hospital effluent: investigation of the concentrations and distribution of pharmaceuticals and environmental risk assessment. Science of the Total Environment 430, 109-118.
Wan, J., Guo, P. and Zhang, S. (2014) Response of the cyanobacterium Microcystis flos-aquae to levofloxacin. Environmental Science and Pollution Research International 21(5), 3858-3865.

Wang, J., Zhu, H., Liu, X. and Liu, Z. (2014) Oxidative stress and Ca(2+) signals involved on cadmium-induced apoptosis in rat hepatocyte. Biological Trace Element Research 161(2), 180-189.

Xu, B., Chen, S., Luo, Y., Chen, Z., Liu, L., Zhou, H., Chen, W., Shen, T., Han, X., Chen, L. and Huang, S. (2011) Calcium signaling is involved in cadmium-induced neuronal apoptosis via induction of reactive oxygen species and activation of MAPK/mTOR network. PloS One 6(4), e19052.

Yang, B.-c., Pan, X.-j., Yang, Z.-h., Xiao, F.-j., Liu, X.-y., Zhu, M.-x. and Xie, J.-p. (2013a) Crotonaldehyde induces apoptosis in alveolar macrophages through intracellular calcium, mitochondria and p53 signaling pathways. The Journal of toxicological sciences 38(2), 225-235.

Yang, L.H., Ying, G.G., Su, H.C., Stauber, J.L., Adams, M.S. and Binet, M.T. (2008) Growth-inhibiting effects of 12 antibacterial agents and their mixtures on the freshwater microalga pseudokirchneriella subcapitata. Environmental Toxicology and Chemistry 27(5), 1201-1208.

Yang, W., Tang, Z., Zhou, F., Zhang, W. and Song, L. (2013b) Toxicity studies of tetracycline on Microcystis aeruginosa and Selenastrum capricornutum. Environmental Toxicology and Pharmacology 35(2), 320-324.

Yuan, Y., Jiang, C.Y., Xu, H., Sun, Y., Hu, F.F., Bian, J.C., Liu, X.Z., Gu, J.H. and Liu, Z.P. (2013) Cadmium-induced apoptosis in primary rat cerebral cortical neurons culture is mediated by a calcium signaling pathway. PloS One 8(5), e64330.

CONCLUSIONES

CONCLUSIONES

1. Los cinco antibióticos (amoxicilina, eritromicina, levofloxacino, norfloxacino y tetraciclina), frecuentemente encontrados en aguas superficiales mostraron toxicidad en los dos organismos fotosintéticos, la cianobacteria recombinante luminiscente *Anabaena* sp. PCC7120 CPB4337 y el alga verde *Pseudokirchneriella subcapitata*. La eritromicina fue el antibiótico más tóxico y la amoxicilina el menos tóxico en ambos organismos. La cianobacteria, debido a su naturaleza procariótica, fue en general más sensible que el alga verde a los antibióticos.

2. El método del "*Combination Index*" (CI) identificó que la sinergia fue la interacción predominante en las mezclas de antibióticos. La tetraciclina interactuó sinérgicamente con los otros antibióticos en la mayoría de mezclas en las que estaba presente. El método del CI proporciono una predicción más exacta de las interacciones toxicológicas observadas en las mezclas de antibióticos que la proporcionada por el "*Concentration addition*" (CA) y el "*Independent action*" (IA), dos métodos ampliamente usados en toxicología de mezclas.

3. La evaluación de riesgo ambiental mostró que las concentraciones que aparecen en las aguas superficiales de eritromicina y de la mezcla eritromicina y tetraciclina, la cual fue fuertemente sinérgica a bajos niveles de efecto, presentan un riesgo potencial de daño para los microrganismos fotosintéticos acuáticos.

4. Mezclas complejas a concentraciones reales, de 16 fármacos combinadas con distintas intensidades de luz, producen toxicidad en la cianobacteria *Anabaena* sp. PCC7120 CPB4337.

5. El "*Concentration addition*" (CA), un método ampliamente empleado en toxicología de mezclas, no fue capaz de predecir los efectos de las mezclas de 16 fármacos combinados con distintas intensidades de luz a concentraciones reales.
6. El método de Morris, un análisis de incertidumbre y sensibilidad global acoplado con un cribado de alto rendimiento (GSUA-QHTS, "*Global Sensitivity*

and Uncertainty Analysis coupled with Quantitative High-throughput Screening") utilizando la cianobacteria recombinante bioluminiscente *Anabaena* sp. PCC7120 CPB4337 fue capaz de identificar los principales contaminantes responsables de la toxicidad de mezclas complejas a concentraciones reales proporcionando una clasificación cualitativa de los mismos basada en su efecto e interacción. Los principales contaminantes responsables de la toxicidad de la mezcla identificados usando el método de Morris fueron confirmados escalando el estudio de la toxicidad de mezclas complejas a concentraciones reales a comunidades microbianas (biopelículas de ríos).

7. El Ca^{2+} libre intracelular $[Ca^{2+}]_i$ fue un buen biomarcador de exposición a antibióticos en la cianobacteria *Anabaena* sp. PCC 7120 pBG2001a, la cual expresa constitutivamente la apoecuorina, una proteína indicadora de unión a Ca^{2+} que permite medir de forma continua e *in vivo* el $[Ca^{2+}]_i$.

8. Los cambios en $[Ca^{2+}]_i$ inducidos por mezclas binarias y complejas de antibióticos fueron capaces de predecir e identificar la naturaleza de las interacciones toxicológicas de las mezclas antes de observarse el efecto tóxico.

9. El $[Ca^{2+}]_i$ tiene un papel clave en la respuesta celular global de *Chlamydomonas reinhardti* tras la exposición al antimicrobiano triclosan.

10. Existe una interrelación entre el $[Ca^{2+}]_i$ y la formación de especies reactivas de oxígeno (EROs) en *Chlamydomonas reinhardti* tras la exposición a triclosan.

ANNEXES: SUPPLEMENTARY MATERIAL

CHAPTER 2: SUPPLEMENTARY MATERIAL

Table S2.1. Occurrence of antibiotics in surface water and wastewater effluents.

Antibiotic	Proportion of the parent compound excreted (%)	Mechanism of action	Group	Molecular weight (g/mol)	Solubility in H_2O (mg/L)	Use	CAS number	pKa	Log Kow	Occurrence in surface water (ng/L)	Occurrence in wastewater effluent (ng/L)	Country	References
Amoxicillin	80 - 90 rates (Mompelat et al. 2009)	Inhibiting the synthesis of bacterial cell walls	B-lactams	365.4	4000	Human Veterinary Aquaculture	26787-78-0	2.4	0.87	68[b]		France	(Dinh et al. 2011)
											66[b]	China	(Leung et al. 2011)
											797[b]		
											1170[b]		
											1340[b]		
											127[b]		
										200[a]	50[a]	Australia	(Watkinson et al. 2009)
										43[a], 13[b]		UK	(Kasprzyk-Hordern et al. 2008))
										552[a], 117[b] 622[a], 149[b] 298[a], 223[b]			
										3.57[c]		Italy	(Zuccato et al. 2010)
										3.77[c]			
										5.57[c]			
										9.91[c]			
Norfloxacin	30 rates (Mompelat et al. 2009)	Inhibition of α sub-unit of the bacterial gyrase	Quinolone	319	178000	Human Veterinary Aquaculture	70458-96-7	6.26 - 8.85	- 1.03	120[c]		USA	(Kolpin et al. 2002)
										37[b]		France	(Dinh et al. 2011)
											75[b]		
											17[b]		
											364[b]	China	(Leung et al. 2011)
											77[b]		
											33[b]		
											1500[b]		
											2510[b]		
											1270[b]		
											2290[b]		
											32.3[b]	Portugal	(Seifrtová et al. 2008)
											81[a]	China	(Xu et al. 2007)
										1150[a]	250[a]	Australia	(Watkinson et al. 2009)
										30[b]	25[b]		
											13.9[b]	China	(Li et al. 2009)
										13.2[c]		France	(Tamtam et al. 2009)
										18.6[c]			
											150[a]	Spain	(Gracia-Lor et al. 2012)
											130[b]		
											330[a]		(Deblonde et al. 2011))

											19.5[b]		
											33[c]	Spain	(Rodriguez-Gil et al. 2010)
											16[c]		
											37[c]		
										8[b]		Spain	(Gros et al. 2009)
										22[a]			
										54[a]	310[a]	Spain	(Gracia-Lor et al. 2011)
										84.6[a]		Spain	(López-Serna et al. 2011)
										89.8[a]			
										22.09[b]			
										22.52[b]			
										15.8[b]		Spain	(Lopez-Serna et al. 2010)
											6.3[b]	Spain	(Köck-Schulmeyer et al. 2011)
											40[c]	France	(Oberlé et al. 2012)
Levofloxacin	75 - 79 human (Croom and Goa 2003)	Inhibition of α sub-unit of the bacterial gyrase	Quinolone	397.83	-	Human aquaculture	100986-85-4	6.2	0.28	87.4[b]	62.4[c]	South Korea	(Kim et al. 2009)
										52[b]			
Tetracycline	80 - 90 rates (Mompelat et al. 2009)	Inhibition of elongation of 30s subunit of ribosome	Tetracycline	444.4	1700	Human Veterinary	60-58-0	3.3–9.6			7.4[b]	France	(Dinh et al. 2011)
											152[b]	China	(Leung et al. 2011)
											14[b]		
											1061[b]		
											1400[b]		
											1150[b]		
											736[b]		
										110[c]		USA	(Kolpin et al. 2002)
											27[b]	Taiwan	(Lin et al. 2009)
										8[a]	24[a]	Luxembourg	(Pailler et al. 2009)
										7[a]			
											170[b]	USA	Karthikeyan et al (2006)
										80[a]	20[a]	Australia	(Watkinson et al. 2009)
											1410[c]	Republic of Korea	(Choi et al. 2007)
											190[c]	USA	(Yang and Carlson 2003)
											89.4[b]	China	(Li et al. 2009)
											340[a]	Spain	(Gros et al. 2010)
										1.2[b]		Spain	(Köck-Schulmeyer et al. 2011)
											1.1[b]		
											0.8[b]		
										110[c]		USA	(Lindsey et al. 2001)
											160[c]	USA	(Yang and Carlson 2003)
											10[c]	France	(Oberlé et al. 2012)

Erythromycin	5 -10 rates (Mompelat et al. 2009)	Inhibition of elongation by binding irreversibly to the 50S subunit of bacterial ribosome	Macrolide	733.9		Human Veterinary Aquaculture	7540-22-9	8.8		4.0[b]		France	(Dinh et al. 2011)
											131[b]		
											4.2[b]		
											760[a]	Spain	(Rosal et al. 2010)
											331[b]		
											80[b]	Spain	(Gracia-Lor et al. 2012)
											120[a]		
											620[a]		(Deblonde et al. 2011)
											230.5[b]		
										111.9[a]		Spain	(López-Roldán et al. 2010)
										32.9[b]			
										70[a]		Spain	(Ginebreda et al. 2009)
										30[b]			
											66[c]	Spain	(Rodriguez-Gil et al. 2010)
											3609[c]		
											3984[c]		
											200[c]		
										30[a]		Spain	(Gros et al. 2006)
										17[b]			
											34[b]	Spain	(Gros et al. 2007)
											29[b]		
											37[b]		
											71[b]		
											21[b]		
											44[b]		
											150[b]	Spain	(Petrovic et al. 2006)
											280[a]		
										15.7[a]		Spain	(López-Serna et al. 2011)
										51.6[a]			
										12.91[b]			
										26.16[b]			
										78[a]	82[a]	Spain	(Gracia-Lor et al. 2011)
										0.4[b]		Spain	(Köck-Schulmeyer et al. 2011)
											1.2[b]		
											6.7[b]		
										10.4[b]		Spain	(Silva et al. 2011)
										42.4[b]			
										9.97[b]			
										14.2[b]			
										21.7[b]			
										15.6[b]			

										137 [b]		South Korea	(Kim et al. 2009)
										75.6 [b]			
										7.4 [b]			
										39.4[b]			
										3.91[c]		Italy	(Zuccato et al. 2010)
										2.88[c]			
										6.81[c]			
										8.12[c]			
										0.78[c]			
										3.51[c]			
										4.62[c]			
										2.82[c]			
											1842[c]	UK	(Ashton et al. 2004)

[a]: Maximum concentration
[b]: Mean concentration
[c]: Individual measured concentration

Ashton, D., Hilton, M. and Thomas, K.V. (2004) Investigating the environmental transport of human pharmaceuticals to streams in the United Kingdom. Science of The Total Environment 333(1-3), 167-184.

Croom, K.F. and Goa, K.L. (2003) Levofloxacin: A Review of its Use in the Treatment of Bacterial Infections in the United States. Drugs 63(24), 2769-2802.

Choi, K.-J., Kim, S.-G., Kim, C.-w. and Kim, S.-H. (2007) Determination of antibiotic compounds in water by on-line SPE-LC/MSD. Chemosphere 66(6), 977-984.

Deblonde, T., Cossu-Leguille, C. and Hartemann, P. (2011) Emerging pollutants in wastewater: A review of the literature. International Journal of Hygiene and Environmental Health 214(6), 442-448.

Dinh, Q.T., Alliot, F., Moreau-Guigon, E., Eurin, J., Chevreuil, M. and Labadie, P. (2011) Measurement of trace levels of antibiotics in river water using on-line enrichment and triple-quadrupole LC-MS/MS. Talanta 85(3), 1238-1245.

Ginebreda, A., Muñoz, I., de Alda, M.L., Brix, R., López-Doval, J. and Barceló, D. (2009) Environmental risk assessment of pharmaceuticals in rivers: Relationships between hazard indexes and aquatic macroinvertebrate diversity indexes in the Llobregat River (NE Spain). Environment International 36(2), 153-162.

Gracia-Lor, E., Sancho, J.V. and Hernández, F. (2011) Multi-class determination of around 50 pharmaceuticals, including 26 antibiotics, in environmental and wastewater samples by ultra-high performance liquid chromatography-tandem mass spectrometry. Journal of Chromatography A 1218(16), 2264-2275.

Gracia-Lor, E., Sancho, J.V., Serrano, R. and Hernández, F. (2012) Occurrence and removal of pharmaceuticals in wastewater treatment plants at the Spanish Mediterranean area of Valencia. Chemosphere 87(5), 453-462.

Gros, M., Petrovic, M. and Barcelo, D. (2007) Wastewater treatment plants as a pathway for aquatic contamination by pharmaceuticals in the ebro river basin (northeast spain). Environmental Toxicology and Chemistry 26(8), 1553-1562.

Gros, M., Petrovic, M. and Barceló, D. (2006) Development of a multi-residue analytical methodology based on liquid chromatography-tandem mass spectrometry (LC-MS/MS) for screening and trace level determination of pharmaceuticals in surface and wastewaters. Talanta 70(4), 678-690.

Gros, M., Petrovic, M. and Barceló, D. (2009) Tracing Pharmaceutical Residues of Different Therapeutic Classes in Environmental Waters by Using Liquid Chromatography/Quadrupole-Linear Ion Trap Mass Spectrometry and Automated Library Searching. Analytical Chemistry 81(3), 898-912.

Gros, M., Petrovic, M., Ginebreda, A. and Barceló, D. (2010) Removal of pharmaceuticals during wastewater treatment and environmental risk assessment using hazard indexes. Environment International 36(1), 15-26.

Kasprzyk-Hordern, B., Dinsdale, R. and Guwy, A. (2008) Multiresidue methods for the analysis of pharmaceuticals, personal care products and illicit drugs in surface water and wastewater by solid-phase extraction and ultra performance liquid chromatography–electrospray tandem mass spectrometry. Analytical and Bioanalytical Chemistry 391(4), 1293-1308.

Kim, J.W., Jang, H.S., Kim, J.G., Ishibashi, H., Hirano, M., Nasu, K., Ichikawa, N., Takao, Y., Shinohara, R. and Arizono, K. (2009) Occurrence of Pharmaceutical and Personal Care Products (PPCPs) in Surface Water from Mankyung River, South Korea. Journal of Health Science 55(2), 249-258.

Köck-Schulmeyer, M., Ginebreda, A., Postigo, C., López-Serna, R., Pérez, S., Brix, R., Llorca, M., Alda, M.L.d., Petrović, M., Munné, A., Tirapu, L. and Barceló, D. (2011) Wastewater reuse in Mediterranean semi-arid areas: The impact of discharges of tertiary treated sewage on the load of polar micro pollutants in the Llobregat river (NE Spain). Chemosphere 82(5), 670-678.

Kolpin, D.W., Furlong, E.T., Meyer, M.T., Thurman, E.M., Zaugg, S.D., Barber, L.B. and Buxton, H.T. (2002) Pharmaceuticals, hormones, and other organic wastewater contaminants in US streams, 1999-2000: A national reconnaissance. Environmental Science & Technology 36(6), 1202-1211.

Leung, H.W., Minh, T.B., Murphy, M.B., Lam, J.C.W., So, M.K., Martin, M., Lam, P.K.S. and Richardson, B.J. (2011) Distribution, fate and risk assessment of antibiotics in sewage treatment plants in Hong Kong, South China. Environment International 42(0), 1-9.

Li, B., Zhang, T., Xu, Z. and Fang, H.H.P. (2009) Rapid analysis of 21 antibiotics of multiple classes in municipal wastewater using ultra performance liquid chromatography-tandem mass spectrometry. Analytica Chimica Acta 645(1-2), 64-72.

Lin, A.Y.-C., Yu, T.-H. and Lateef, S.K. (2009) Removal of pharmaceuticals in secondary wastewater treatment processes in Taiwan. Journal of Hazardous Materials 167(1-3), 1163-1169.

Lindsey, M.E., Meyer, M. and Thurman, E.M. (2001) Analysis of trace levels of sulfonamide and tetracycline antimicrobials, in groundwater and surface water using solid-phase extraction and liquid chromatography/mass spectrometry. Analytical Chemistry 73(19), 4640-4646.

López-Roldán, R., de Alda, M.L., Gros, M., Petrovic, M., Martín-Alonso, J. and Barceló, D. (2010) Advanced monitoring of pharmaceuticals and estrogens in the Llobregat River basin (Spain) by liquid chromatography-triple quadrupole-tandem mass spectrometry in combination with ultra performance liquid chromatography-time of flight-mass spectrometry. Chemosphere 80(11), 1337-1344.

Lopez-Serna, R., Pérrez, S., Ginebreda, A., Petrovic, M. and Barceló, D. (2010) Fully automated determination of 74 pharmaceuticals in environmental and waste waters by online solid phase extraction-liquid chromatography-electrospray-tandem mass spectrometry. Talanta 83(2), 410-424.

López-Serna, R., Petrovic, M. and Barceló, D. (2011) Development of a fast instrumental method for the analysis of pharmaceuticals in environmental and wastewaters based on ultra high performance liquid chromatography (UHPLC)-tandem mass spectrometry (MS/MS). Chemosphere 85(8), 1390-1399.

Mompelat, S., Le Bot, B. and Thomas, O. (2009) Occurrence and fate of pharmaceutical products and by-products, from resource to drinking water. Environment International 35(5), 803-814.

Oberlé, K., Capdeville, M.-J., Berthe, T., Budzinski, H. and Petit, F. (2012) Evidence for a Complex Relationship between Antibiotics and Antibiotic-Resistant Escherichia Coli: From Medical Center Patients to a Receiving Environment. Environmental Science & Technology 46(3), 1859-1868.

Pailler, J.Y., Krein, A., Pfister, L., Hoffmann, L. and Guignard, C. (2009) Solid phase extraction coupled to liquid chromatography-tandem mass spectrometry analysis of sulfonamides, tetracyclines, analgesics and hormones in surface water and wastewater in Luxembourg. Science of The Total Environment 407(16), 4736-4743.

Petrovic, M., Gros, M. and Barcelo, D. (2006) Multi-residue analysis of pharmaceuticals in wastewater by ultra-performance liquid chromatographyâ€“quadrupoleâ€“time-of-flight mass spectrometry. Journal of Chromatography A 1124(1-2), 68-81.

Rodriguez-Gil, J.L., Catalá, M., Alonso, S.G., Maroto, R.R., Valcárcel, Y., Segura, Y., Molina, R., Melero, J.A. and Martínez, F. (2010) Heterogeneous photo-Fenton treatment for the reduction of pharmaceutical contamination in Madrid rivers and ecotoxicological evaluation by a miniaturized fern spores bioassay. Chemosphere 80(4), 381-388.

Rosal, R., Rodriguez, A., Perdigón-Melón, J.A., Petre, A., García-Calvo, E., Gómez, M.J., Agüera, A. and Fernández-Alba, A.R. (2010) Occurrence of emerging pollutants in urban wastewater and their removal through biological treatment followed by ozonation. Water Research 44(2), 578-588.

Seifrtová, M., Pena, A., Lino, C.M. and Solich, P. (2008) Determination of fluoroquinolone antibiotics in hospital and municipal wastewaters in Coimbra by liquid chromatography with a monolithic column and fluorescence detection. Analytical and Bioanalytical Chemistry 391(3), 799-805.

Silva, B.F.d., Jelic, A., López-Serna, R., Mozeto, A.A., Petrovic, M. and Barceló, D. (2011) Occurrence and distribution of pharmaceuticals in surface water, suspended solids and sediments of the Ebro river basin, Spain. Chemosphere 85(8), 1331-1339.

Tamtam, F., Mercier, F., Eurin, J., Chevreuil, M. and Le Bot, B. (2009) Ultra performance liquid chromatography tandem mass spectrometry performance evaluation for analysis of antibiotics in natural waters. Analytical and Bioanalytical Chemistry 393(6-7), 1709-1718.

Watkinson, A.J., Murby, E.J., Kolpin, D.W. and Costanzo, S.D. (2009) The occurrence of antibiotics in an urban watershed: from wastewater to drinking water. Science of The Total Environment 407(8), 2711-2723.

Xu, W.-h., Zhang, G., Zou, S.-c., Li, X.-d. and Liu, Y.-c. (2007) Determination of selected antibiotics in the Victoria Harbour and the Pearl River, South China using high-performance liquid chromatography-electrospray ionization tandem mass spectrometry. Environmental Pollution 145(3), 672-679.

Yang, S. and Carlson, K. (2003) Evolution of antibiotic occurrence in a river through pristine, urban and agricultural landscapes. Water Research 37(19), 4645-4656.
Zuccato, E., Castiglioni, S., Bagnati, R., Melis, M. and Fanelli, R. (2010) Source, occurrence and fate of antibiotics in the Italian aquatic environment. Journal of Hazardous Materials 179(1-3), 1042-1048.

Table S2.2. Composition of the cyanobacterial growth medium AA/8

Component	Final concentration (mM)
KH_2SO_4	0.25
$MgSO_4$	0.125
$CaCl_2$	0.0625
NO_3	5
NaCl	0.5
Na_2-EDTA	0.009625
$FeSO_4$	0.08375
B	0.00053125
Co	0.00002125
Cu	0.00004
Mn	0.00093
Mo	0.00015625
Zn	0.000095
V	0.000025

Table S2.3. Composition of the *P. subcapitata* medium according to OECD Guidelines for the Testing of Chemicals. Guideline TG 201: "Freshwater Alga and Cyanobacteria, Growth Inhibition Test".

Component	Final concentration (mM)
$NaHCO_3$	0.59516724
NH_4Cl	0.28037383
$MgCl_2 \cdot 6(H_2O)$	0.05901736
$CaCl_2 \cdot 2(H_2O)$	0.12238248
$MgSO_4 \cdot 7(H_2O)$	0.06085440
K_2HPO_4	0.00918590
$FeCl_3 \cdot 6(H_2O)$	0.00029595
$Na_2EDTA \cdot 2(H_2O)$	0.00026864
H_3BO_3	0.00299159
$MnCl_2 \cdot 4(H_2O)$	0.00209691
$ZnCl_2$	0.00002201
$CoCl_2 \cdot 6(H_2O)$	0.00000630
$Na_2MoO_4 \cdot 2(H_2O)$	0.00002893
$CuCl_2 \cdot 2(H_2O)$	0.00000006

Table S2.4. Concentration of antibiotics in binary and multicomponent mixtures for *Anabaena* sp. CPB4337 and *Pseudokirchneriella subcapitata*.

Mixture				Individual component concentration in mixture of *Anabaena sp*. CPB4337									
Component	*fa*	Mixture concentration		AMOX		NOR		LEV		TET		ERY	
		mg/L	µM	mg/L	µM	mg/L	µM	mg/L	µM	mg/L	µM	mg/L	µM
A+E	0.1	9.4	25.777	9.418	25.774							0.002	0.003
	0.2	16.2	44.358	16.207	44.354							0.003	0.004
	0.5	41	112.14	40.972	112.129							0.008	0.011
N+E	0.1	0.96	3.003			0.958	3					0.002	0.003
	0.2	1.7	5.287			1.687	5.283					0.003	0.004
	0.5	4.5	14.107			4.501	14.095					0.009	0.012
N+A	0.1	8.9	24.786	8.13	22.25	0.81	2.537						
	0.2	14.5	40.176	13.17	36.043	1.32	4.134						
	0.5	33.1	91.718	30.073	82.302	3.007	9.417						
L+E	0.1	0.87	2.402					0.866	2.396			0.004	0.005
	0.2	1.3	3.535					1.275	3.528			0.005	0.007
	0.5	2.5	6.766					2.44	6.752			0.01	0.014
L+A	0.1	7.7	21.029	7.314	20.016			0.366	1.013				
	0.2	11.4	31.215	10.857	29.713			0.543	1.503				
	0.5	22.4	61.308	21.324	58.358			1.066	2.95				
L+N	0.1	1.3	3.943			0.873	2.734	0.437	1.209				
	0.2	2	6.081			1.347	4.218	0.673	1.862				
	0.5	4.3	12.853			2.847	8.916	1.423	3.938				
T+E	0.1	0.28	0.629							0.279	0.628	0.001	0.001
	0.2	0.67	1.506							0.668	1.503	0.002	0.003
	0.5	3	6.674							2.96	6.661	0.01	0.014
T+A	0.1	1.8	4.857	1.657	4.535					0.143	0.322		
	0.2	2.9	7.824	2.669	7.304					0.231	0.52		
	0.5	6.5	17.537	5.983	16.374					0.517	1.163		
T+N	0.1	1.9	5.174			1.02	3.194			0.88	1.98		
	0.2	2.7	7.353			1.449	4.538			1.251	2.815		
	0.5	5.1	13.887			2.736	8.568			2.364	5.32		
T+L	0.1	0.37	0.903					0.136	0.376	0.234	0.527		
	0.2	0.63	1.537					0.231	0.639	0.399	0.898		
	0.5	1.6	3.904					0.587	1.624	1.013	2.279		
5 AB	0.1	5.2	14.321	4.233	11.585	0.423	1.325	0.212	0.587	0.366	0.824	0.0009	0.001
	0.2	7.2	19.692	5.821	15.93	0.582	1.823	0.291	0.805	0.503	1.132	0.001	0.001
	0.5	12.4	33.95	10.035	27.463	1.004	3.144	0.502	1.389	0.867	1.951	0.002	0.003

Mixture				Individual component concentration in mixture in *Pseudokirchneriella subcapitata*							
Component	*fa*	Mixture concentration		NOR		LEV		TET		ERY	
		mg/L	µM	mg/L	µM	mg/L	µM	mg/L	µM	mg/L	µM
N+E	0.1	3.00	9.37	2.9851	9.3479					0.0149	0.0203
	0.2	5.80	13.02	5.7711	12.9854					0.0289	0.0393
	0.5	18.20	56.83	18.1095	56.7106					0.0905	0.1234
L+E	0.1	1.30	3.56			1.2745	3.5243			0.0255	0.0347
	0.2	23.00	62.97			22.5490	62.3525			0.4510	0.6145
	0.5	-	-			-	-			-	-
L+N	0.1	1.10	3.36	0.8800	2.7558	0.2200	0.6083				
	0.2	2.90	6.82	2.3200	5.2201	0.5800	1.6038				
	0.5	15.00	45.87	12.0000	37.5786	3.0000	8.2956				
T+E	0.1	0.00	0.01					0.0038	0.0086	0.0008	0.0010
	0.2	0.02	0.04					0.0175	0.0394	0.0035	0.0048
	0.5	0.27	0.57					0.2250	0.5063	0.0450	0.0613
T+N	0.1	1.90	5.91	1.8537	5.8048			0.0463	0.1043		
	0.2	3.50	7.88	3.4146	7.6831			0.0854	0.1921		
	0.5	9.20	28.61	8.9756	28.1075			0.2244	0.5049		
T+L	0.1	0.34	0.92			0.3091	0.8547	0.0309	0.0695		
	0.2	0.89	2.42			0.8091	2.2373	0.0809	0.1820		
	0.5	4.60	12.50			4.1818	11.5635	0.4182	0.9409		
4 AB	0.1	1.70	5.16	1.3281	4.1591	0.3320	0.9181	0.0332	0.0747	0.0066	0.0090
	0.2	3.90	11.84	3.0469	9.5414	0.7617	2.1063	0.0762	0.1714	0.0152	0.0208
	0.5	16.00	48.57	12.5000	39.1443	3.1250	8.6412	0.3125	0.7031	0.0625	0.0852

Table S2.5. Experimental EC_x values and predicted EC_x values under Concentration Addition (CA), Independent Action (IA) and Combination Index (CI) predictive equations for the different binary and multi-component mixtures of antibiotics tested for both *P. subcapitata* and *Anabaena sp.* PCC7120 CPB4337.

Mixture	*Pseudokirckneriella subcapitata*					*Anabaena sp.* PCC7120 CPB4337				
	Concentration (mg/L)	Experimental values[1]	Predicted values			Concentration (mg/L)	Experimental values[1]	Predicted values		
			CA	IA	CI			CA	IA	CI
ERY+LEV	1.3	0.03 ± 0.02	0.14	0.17	0.05	1.7	0.29 ± 0.05	0.34	0.28	0.32
	2.6	0.27 ± 0.04	0.22	0.26	0.18	2.5	0.49 ± 0.06	0.49	0.43	0.51
	5.1	0.42 ± 0.02	0.34	0.38	0.49	3.4	0.64 ± 0.07	0.61	0.57	0.67
	-	-	-	-	-	5.6	0.84 ± 0.09	0.77	0.78	0.85
ERY+NOR	5.0	0.13 ± 0.02	0.11	0.11	0.15	2.2	0.29 ± 0.05	0.32	0.26	0.27
	10	0.38 ± 0.04	0.21	0.21	0.31	3.3	0.44 ± 0.05	0.46	0.40	0.39
	20	0.51 ± 0.03	0.37	0.38	0.54	5.5	0.55 ± 0.06	0.64	0.62	0.57
	-	-	-	-	-	11.2	0.78 ± 0.08	0.84	0.87	0.79
ERY+TET	0.015	0.08± 0.02	0.05	0.06	0.12	0.28	0.17 ± 0.05	0.006	0.007	0.10
	0.058	0.39 ± 0.03	0.15	0.17	0.26	0.4	0.28 ± 0.07	0.01	0.01	0.13
	0.23	0.48 ± 0.02	0.36	0.42	0.46	3.0	0.58 ± 0.06	0.40	0.26	0.50
	-	-	-	-	-	9.7	0.79 ± 0.08	0.88	0.88	0.75
LEV+NOR	6.3	0.29 ± 0.02	0.13	0.14	0.32	2.0	0.15 ± 0.03	0.19	0.15	0.20
	13	0.52 ± 0.03	0.22	0.22	0.46	3.3	0.55 ± 0.06	0.34	0.28	0.39
	25	0.58 ± 0.04	0.36	0.36	0.61	5.0	0.74 ± 0.07	0.48	0.43	0.57
	-	-	-	-	-	11.3	0.93 ± 0.09	0.75	0.76	0.86
LEV+TET	0.64	0.089 ± 0.004	0.10	0.14	0.13	0.50	0.23 ± 0.06	0.01	0.01	0.15
	1.3	0.26 ± 0.02	0.16	0.20	0.23	0.91	0.61 ± 0.10	0.03	0.02	0.30
	5.1	0.49 ± 0.03	0.31	0.40	0.55	1.4	0.80 ±0.11	0.1	0.1	0.54
	-	-	-	-	-	3.8	0.93 ± 0.09	0.32	0.21	0.78
NOR+TET	1.3	0.0089 ± 0.006	0.04	0.05	0.01	2.1	0.27 ± 0.06	0.15	0.10	0.13
	2.5	0.026 ± 0.016	0.08	0.09	0.04	4.1	0.68 ± 0.11	0.36	0.25	0.38
	10	0.50 ± 0.03	0.24	0.24	0.62	6.1	0.77 ± 0.10	0.53	0.41	0.60
	-	-	-	-	-	7.5	0.89 ± 0.08	0.62	0.51	0.70
AMO+ERY	-	-	-	-	-	22	0.33 ± 0.07	0.35	0.33	0.28
	-	-	-	-	-	41	0.47 ± 0.06	0.51	0.51	0.50
	-	-	-	-	-	50	0.55 ± 0.09	0.56	0.57	0.57
	-	-	-	-	-	61	0.70 ± 0.08	0.62	0.63	0.65
AMO+NOR	-	-	-	-	-	15	0.23 ± 0.04	0.30	0.28	0.21
	-	-	-	-	-	27.2	0.43 ± 0.07	0.45	0.45	0.42
	-	-	-	-	-	50	0.75 ±0.09	0.62	0.66	0.67
	-	-	-	-	-	75	0.83 ± 0.11	0.72	0.78	0.80
AMO+LEV	-	-	-	-	-	20.1	0.38 ± 0.05	0.32	0.30	0.44
	-	-	-	-	-	27.2	0.72 ± 0.06	0.40	0.38	0.60
	-	-	-	-	-	36.9	0.82 ±0.08	0.48	0.47	0.74
	-	-	-	-	-	75	0.91 ±0.07	0.67	0.71	0.92
AMO+TET	-	-	-	-	-	5	0.36 ± 0.04	0.1	0.1	0.39
	-	-	-	-	-	9.9	0.77 ± 0.08	0.17	0.13	0.67
	-	-	-	-	-	27	0.88 ± 0.10	0.44	0.35	0.92
	-	-	-	-	-	112.5	0.99 ± 0.09	0.84	0.85	0.99
4 AB	3.2	0.14 ± 0.02	0.14	0.18	0.16	-	-	-	-	-
	6.3	0.33 ± 0.03	0.23	0.29	0.28	-	-	-	-	-
	12.6	0.42 ± 0.03	0.36	0.43	0.45	-	-	-	-	-
	-	-	-	-	-	-	-	-	-	-
5 AB	-	-	-	-	-	8.96	0.29 ± 0.04	0.28	0.18	0.31
	-	-	-	-	-	11.7	0.52 ± 0.05	0.37	0.24	0.46
	-	-	-	-	-	15.2	0.71 ± 0.06	0.45	0.31	0.62
	-	-	-	-	-	43.3	0.90 ± 0.07	0.78	0.75	0.96

[1]: Experimental values are shown as mean ± SD.

CHAPTER 3: SUPPLEMENTARY MATERIAL

Supplementary Material S1. Description of Datasets and Guide for data analysis

SUMMARY

This Supplementary Material includes descriptions of the complete data sets and data analysis used in ***Hidden drivers of low-dose pharmaceutical pollutant mixtures revealed by the novel GSA-QHTS screening method***

DATA AND SOFTWARE AVAILABILITY

Data sets, R-scripts and additional material are freely available at:

- Datasets, R scripts, R functions, EEs screening files: https://figshare.com/authors/Ismael_Rodea/624240.
- FITEVAL Software. http://abe.ufl.edu/carpena/software/index.shtml
- Morris SU (Sampling Uniformity). http://abe.ufl.edu/carpena/software/SUMorris.shtml

Contact information:
Dr. Ismael Rodea-Palomares. ismaelropa@gmail.com
Dr. Francisca Fernández-Piñas. francisca.pina@uam.es
Prof. Dr. Rafael Muñoz-Carpena. carpena@ufl.edu

GENERAL OVERVIEW

The sections of the guide are built on homogeneous groups of results and analysis. The sections include a description of the datasets, and a step-by-step analysis using R (mainly but also MATLAB). The analysis covered the results presented in the main body of the article, but also extended descriptions and analysis.
The analysis is built on 4 main data sets:

1. **"GSA.csv":** Raw data from bioluminescence inhibition of *Anabaena* CPB4337 (n = 2728, 40 variables)
2. **"GSA_MEDIAN.csv"**: Aggregated data set including medians of bioluminescence inhibition of *Anabaena* CPB4337 (n = 180, 43 variables)
3. **"ANTIBIOTIC_EC50.csv"**: Raw data from bioluminescence inhibition of *Anabaena* CPB4337 for serial dilutions of the antibiotics Erythromycin and Ofloxacin (n = 144, 10 variables)
4. **"biofilm.csv"**: Raw data from several metabolic end-points measured on freshwater benthic microbial communities exposed to selected PPCP mixtures (n = 42, 6 variables).

1. INDEX

1. GSA dataset. Quality control of raw data, differences control, individual and mixture exposure. Effects of individual exposure to PPCPs. 260

1.1 GSA dataset 260

1.1.2 Variables 260

1.2 GSA.csv data analysis 262

1.2.1. Quality control of data 262

1.2.1.1. Power analysis 262

1.2.1.2. Quality control of "Treatment" observations 265

1.2.1.3. Conclusions from the quality control of GSA.csv dataset 267

1.2.3. Differences by treatment (control, individual exposure and mixture exposure to PPCPS) 268

1.2.4. Effects of light intensity on individual and mixture exposure to PPCPs (Fig. 2 D, E of the manuscript) 273

1.2.5. Effects of individual exposure to high doses of PPCPs (Results presented in Fig. 3A of the manuscript) 275

2. GSA_MIX_MEDIAN. Aggregated data set including medians of bioluminescence inhibition of *Anabaena* CPB4337 and related analysis. 279

2.1 Summary of the GSA_MIX_MEDIAN.csv dataset 279

2.1.1 Variables 279

2.2. GSA_MIX_MEDIAN.csv data analysis 281

2.2.1. Estimating the median effect of the 180 mixtures via bootstrapping 281

2.2.2 Generating the GSA_MIX_MEDIAN.csv dataset 286

2.2.3. Elementary Effects (EEs) Sensitivity Analysis of the GSA_MIX_MEDIAN.csv dataset 286

2.2.3.1. Definition of variables and probability distribution functions for the input factors 287

2.2.3.2. Generation of parameter samples for the method of EEs 287

2.2.3.3. Model evaluation (or biological receptor evaluation in the case of GSA-QHTS) 288

2.2.3.4. Experimental tolerance in the estimation of median effects of the 180 mixtures 288

2.2.3.5. Calculation of sensitivity measures (μ, μ* and σ) 289

2.2.3.5. μ^* - σ and μ - σ Cartesian Plots 290

2.2.4. Two-Way ANOVA of selected input factors on the GSA_MIX_MEDIAN dataset 294

2.2.5. Exploring elementary effects of low dose mixtures experimental design 298

3. ANTIBIOTIC_EC50. 302

3.1 Summary of the ANTIBIOTIC_EC50.csv data set 303

3.1.1 Variables 303
3.2. Fitting individual dose-response models 304
3.3. Estimating the effect of chemical mixtures (in silico mixture effect predictions) 306
3.3.1. Getting chemic 307
3.3.2 Calculating *pi* values 308
3.3.3 Calculating pi/ECxi values 309
3.3.4. In-silico mixture effect predictions (array of dose-response values) for the 21 pi_s 309
3.3.5. Fitting dose-response models to the in-silico dose response arrays of the 21 unique combinations of C10 and C11 and C14 310
3.3.6. Predicting the effect of the 180 low dose PPCPs mixtures based only on C10 and C11 individual dose-response curves 312
3.4. Analyzing the goodness of fit to experimental data of the predictions of the additive model CA using "fiteval" platform 313
4. Effect of selected mixtures on model benthic freshwater microbial communities. 316
4.1 biofilm.csv data set 316
4.1.1 Variables 316
4.2. "biofilm.csv" dataset analysis 317
4.2.1 Analysis of overall time and treatment effect 318
4.2.2 Effects per time and per treatment 324
5. References 330
ANEX 1. Non-exhaustive list of R packages used in the study 332
ANEX 2. Normality test for GSA.csv by "Treatment" 333

1. GSA dataset. Quality control of raw data, differences between control, individual and mixture exposure. Effects of individual exposure to PPCPs.

1.1 GSA dataset

GSA.csv includes raw data from bioluminescence inhibition of *Anabaena* CPB4337 (n = 2728). The dataset consists of 40 variables. The dataset contains the results from 12 independent experiments. 6 of them are the experiments in which *Anabaena* CPB4337 was exposed to 180 complex mixtures of 16 pharmaceutical and personal care products (PPCPs) at low doses. In the other 6 independent experiments, *Anabaena* CPB4337 was exposed to 4 doses of each of the 16 PPCPs individually. All 12 independent experiments included control observations. A summary of the number of observation by case in GSA.csv can be found in **Supplementary Table S3.1.**

Supplementary Table S3.1. Summary of observations by "Case" and "Exp. Group" for GSA.csv data set

n	INDIVIDUAL	MIXTURE	ALL
CONTROL	384	496	880
TREATMENT	768	1080	1848
ALL	1152	1576	2728

1.1.2 Variables

The data set includes 40 variables. A summary of the variables included in the GSA.csv can be found in **Supplementary Table S3.2**.

Supplementary Table S3.2. Summary of the variables included in the GSA.csv dataset.

Var.	**Type**	**Levels**	**Info.**
X	Factor	2728	Observation locator
Exp.	Factor	12	Independent experiment identification
Exp. Group	Factor	2	Determines whether it is an individual or mixture exp.
Case	Factor	2	Determines whether it is a treatment or control observation.
Treatment	Factor	244	Each different treatment (including controls) are identified with a unique number)
C1:C16	Factor	5	Each concentration level for each of the 16 PPCPs is identified from lower to higher: "0": control, "1": median of means, "2": mean of maximum, "3": maximum of maximum, "4": 10 mgL^{-1}
C1.1:C16.1	Numeric	-	The exact concentration (ngL^{-1}) for each of the 16 PPCPs at each of the concentration levels established in C1:C16.
L	Factor	2	Light intensity regime. L1: ca.35 μmol photons m^2/s, L2 ca.35 μmol photons m^2/s
X16	Numeric	-	Sum of the concentrations of PPCPs in each Treatment in ngL^{-1}
Lum	Numeric	-	Bioluminescence signal normalized to control mean bioluminescence (1). A 0.1 difference is equal to a 10% variation

CODE LOCATION: orders to do the analysis and plots presented in this section are in the R script named "Script_GSA_Raw.R".

Complete information on the GSA.csv can be obtained as follows:

```
> #1.1 Quality of control observations
>
> #install.packages(c("qualityTools","car"))
>
> library("qualityTools")
> library("car")

>
> # set paths to your prefered local folders
> Dir.data<-"~/Art-GSA14/ANALISIS_DATA_0615/GSA_EBS_PPCPs_2016/R_DATA"
> Dir.functions<-"~/Art-GSA14/ANALISIS_DATA_0615/GSA_EBS_PPCPs_2016/R_
FUNCTIONS"
> Dir.Scripts<-"~/Art-GSA14/ANALISIS_DATA_0615/GSA_EBS_PPCPs_2016/R_SC
RIPTS"
>
> setwd(Dir.data)
>

> #Loading dataset
> GSA<-read.csv("GSA.csv", header = TRUE, sep=",")# converting interge
rs to factors in PPCP levels
> for (i in seq_along(1:21)){
+         GSA[,i]<-as.factor(GSA[,i])
+ }
> GSA$L<-as.factor(GSA$L)# converting L to factor
> GSA_CONT<-GSA[GSA$Case=="CONTROL",] # subset GSA to get only control
observations

> str(GSA)
'data.frame':  2728 obs. of  40 variables:
 $ X         : Factor w/ 2728 levels "1","2","3","4",..: 1 2 3 4 5 6 7
8 9 10 ...
 $ Exp       : Factor w/ 12 levels "1","2","3","4",..: 1 1 1 1 1 1 1 1
1 1 ...
 $ Exp.Group: Factor w/ 2 levels "INDIVIDUAL","MIXTURE": 2 2 2 2 2 2 2
2 2 2 ...
 $ Case      : Factor w/ 2 levels "CONTROL","TREATMENT": 1 1 1 1 1 1 1
1 1 1 ...
 $ Treatment: Factor w/ 245 levels "0","1","2","3",..: 1 1 1 1 1 1 1 1
1 1 ...
 $ C1        : Factor w/ 5 levels "0","1","2","3",..: 1 1 1 1 1 1 1 1 1
1 ...
 $ C2        : Factor w/ 5 levels "0","1","2","3",..: 1 1 1 1 1 1 1 1 1
1 ...
 $ C3        : Factor w/ 5 levels "0","1","2","3",..: 1 1 1 1 1 1 1 1 1
1 ...
 $ C4        : Factor w/ 5 levels "0","1","2","3",..: 1 1 1 1 1 1 1 1 1
1 ...
 $ C5        : Factor w/ 5 levels "0","1","2","3",..: 1 1 1 1 1 1 1 1 1
1 ...
 $ C6        : Factor w/ 5 levels "0","1","2","3",..: 1 1 1 1 1 1 1 1 1
1 ...
 $ C7        : Factor w/ 5 levels "0","1","2","3",..: 1 1 1 1 1 1 1 1 1
1 ...
 $ C8        : Factor w/ 5 levels "0","1","2","3",..: 1 1 1 1 1 1 1 1 1
1 ...
 $ C9        : Factor w/ 5 levels "0","1","2","3",..: 1 1 1 1 1 1 1 1 1
1 ...
 $ C10       : Factor w/ 5 levels "0","1","2","3",..: 1 1 1 1 1 1 1 1 1
1 ...
 $ C11       : Factor w/ 5 levels "0","1","2","3",..: 1 1 1 1 1 1 1 1 1
1 ...
 $ C12       : Factor w/ 5 levels "0","1","2","3",..: 1 1 1 1 1 1 1 1 1
1 ...
 $ C13       : Factor w/ 5 levels "0","1","2","3",..: 1 1 1 1 1 1 1 1 1
1 ...
 $ C14       : Factor w/ 5 levels "0","1","2","3",..: 1 1 1 1 1 1 1 1 1
1 ...
 $ C15       : Factor w/ 5 levels "0","1","2","3",..: 1 1 1 1 1 1 1 1 1
1 ...
```

```
 $ C16      : Factor w/ 5 levels "0","1","2","3",..: 1 1 1 1 1 1 1 1 1
1 ...
 $ C1.1     : num  0 0 0 0 0 0 0 0 0 0 ...
 $ C2.1     : num  0 0 0 0 0 0 0 0 0 0 ...
 $ C3.1     : num  0 0 0 0 0 0 0 0 0 0 ...
 $ C4.1     : num  0 0 0 0 0 0 0 0 0 0 ...
 $ C5.1     : num  0 0 0 0 0 0 0 0 0 0 ...
 $ C6.1     : num  0 0 0 0 0 0 0 0 0 0 ...
 $ C7.1     : num  0 0 0 0 0 0 0 0 0 0 ...
 $ C8.1     : num  0 0 0 0 0 0 0 0 0 0 ...
 $ C9.1     : num  0 0 0 0 0 0 0 0 0 0 ...
 $ C10.1    : num  0 0 0 0 0 0 0 0 0 0 ...
 $ C11.1    : num  0 0 0 0 0 0 0 0 0 0 ...
 $ C12.1    : num  0 0 0 0 0 0 0 0 0 0 ...
 $ C13.1    : num  0 0 0 0 0 0 0 0 0 0 ...
 $ C14.1    : num  0 0 0 0 0 0 0 0 0 0 ...
 $ C15.1    : num  0 0 0 0 0 0 0 0 0 0 ...
 $ C16.1    : num  0 0 0 0 0 0 0 0 0 0 ...
 $ L        : Factor w/ 2 levels "1","2": 1 1 1 1 1 1 1 1 1 1 ...
 $ X.16     : num  0 0 0 0 0 0 0 0 0 0 ...
 $ Lum      : num  1.096 1.031 0.963 0.939 0.97 ...
```

1.2 GSA.csv data analysis

The data analysis of the GSA.csv data set covers 4 distinct sections: (1) Quality control of data (Section 1.2.1). (2) Analysis of differences by "treatment" (control, individual exposure and mixture exposure to pharmaceuticals) (section 1.2.2; **Fig.3. 2** of the manuscript). (3) Effects of individual exposure to high doses of PPCPs (Section 1.2.4.; **Fig. 3.3A** of the manuscript). (4) Effects of light intensity on individual exposure to PPCPs (Section 1.2.3; **Fig. 3.2 C, D** of the manuscript).

1.2.1. Quality control of data

1.2.1.1. Power analysis

Power of main statistical tests performed in the study were calculated using the package 'pwr' version 1.1-3 (Basic Functions for Power Analysis). The calculation of power is not an easy task, especially when dealing with unbalanced experimental designs and missing terms[1]. One of the main difficulties in calculating power, is that it is calculated for a pre-specified "*effect size*". The effect size is a measurement of the separation between the means of the null and alternative hypothesis in standard deviation units. The simplest definition of effect size is that for a two-sample *t-test* for the difference of two means of two independent samples. The effect size *d* is defined as:

$d = |\mu_1 - \mu_2|/\sigma$

d is therefore a measure of distance normalized to the standard deviation (σ). The relevant effect size parameter is not calculated so straight-forward for multiple group unbalanced One Way or Two-Way ANOVAs tests or for general linear models or generalized linear models. Cohen[1] defined conventional effect sizes (*small, medium, large*) for different statistical tests which simplify the approximation of the power of an statistical test. We used the equivalency of Cohen conventional effect sizes to inform the "*effect size*" parameter required for the different tests performed in the study. Our general approach to approximate power for our statistical tests has been as follows:

1. To identify the relevant "*d*" or "*d*" ranges for the experimental effect sizes observed.

2. To determine the category of conventional *effect size* according to Cohen (*small*, *medium* or *large*)[1] in which the different experimental effect sizes "*d*" fell.
3. Determine the numeric value for the *effect size* parameter required (*d*, *f*, f^2) for the test of interest accordingly to the pre-specified category of conventional *effect size* (*small*, *medium* or *large*) with the function cohen.ES {pwr}.
4. Perform the power analysis with the required function of the 'pwr' package using the conventional *effect size/s* value for the effect size category of interest.

For example see **section 1.2.3**

In general, a power of 0.8 estimated with an alpha of 0.05 is considered acceptable for statistical testing[2]. Lower values may be also acceptable but may indicate a progressively increasing unsuitability to detect false negatives (to detect an effect when it is present).

1.2.1.1. Quality control of control observations

CODE LOCATION: orders to do the analysis and plots presented in this section are in the R script named "Script_GSA_Raw.R".

A basic quality control was performed focused on control observations from the GSA.csv dataset (n = 888). Three main aspects of control observations was studied: homogeneity of the different experiments (n = 12), normality and homoscedasticity.

First we checked normality of control observations (n = 880) by means of a q-q plot.

```
> qqnorm(GSA_CONT$Lum)#, "normal")# q-q normal plot for Lum
> qqline(GSA_CONT$Lum)
```

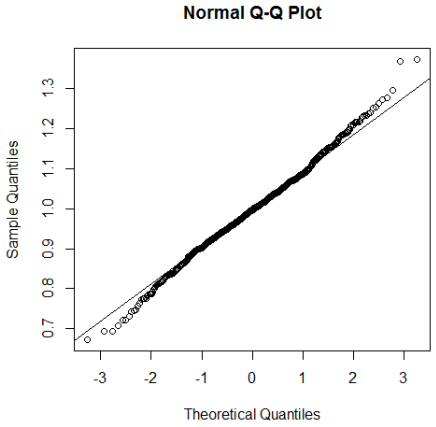

Supplementary Fig. S3.1. Q-Q Plot for "normal" distribution for control observations (n= 880).

As can be seen in the **Supplementary Fig. S3.1** control observations followed a nearly normal distribution with slightly heavy tails

Homogeneity of control observations in the different experimental replicates.

We studied homogeneity of control observations along the twelve experiments by means of boxplots and One-Way ANOVA:

```
> boxplot(GSA_CONT$Lum~GSA_CONT$Exp, notch = TRUE, xlab = "Experiment"
, ylab = "Lum",main="GSA_CONT$Lum~GSA_CONT$Exp")
```

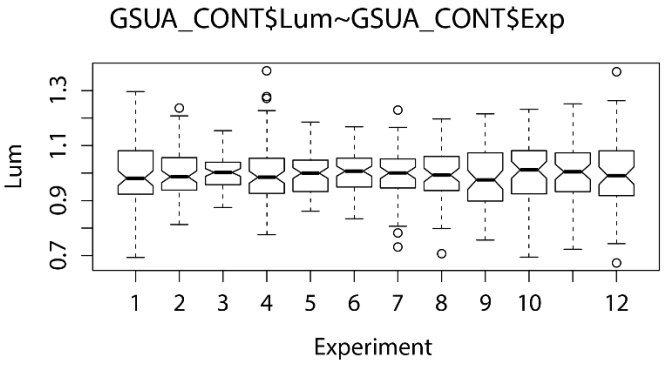

Supplementary Fig. S3.2. Notched box-plot for "Lum" of control observations by "Experiment". The notches extend to +/-1.58 IQR/sqrt(n)[3]

One-Way ANOVA: Bioluminescence level of control observations as a function of "Exp":

```
> anov.1.2.1.2<-aov(GSA_CONT$Lum~GSA_CONT$Exp)# checking for differenc
es among experiments
> anov.1.2.1.2
Call:
   aov(formula = GSA_CONT$Lum ~ GSA_CONT$Exp)

Terms:
                GSA_CONT$Exp Residuals
Sum of Squares      0.019774  8.783118
Deg. of Freedom           11       868

Residual standard error: 0.1005922
Estimated effects may be unbalanced

> Anova(anov.1.2.1.2, type="III", singular.ok = T)
Anova Table (Type III tests)

Response: GSA_CONT$Lum
             Sum Sq  Df   F value Pr(>F)
(Intercept)  83.054   1 8207.8543 <2e-16 ***
GSA_CONT$Exp  0.020  11    0.1777 0.9986
Residuals     8.783 868
---
Signif. codes:  0 '***' 0.001 '**' 0.01 '*' 0.05 '.' 0.1 ' ' 1
```

As can be seen in **Supplementary Fig. S3.2**, control observations of the different experiments were very homogeneous, indicating a good general quality of the experimental data for control observations. Notched overlap in all the boxplot suggesting the absence of statistical significance for the differences in their mean. One-way ANOVA confirmed the absence of statistical significant differences among control datasets by experiments (F value 0.178, Pr >F = 0.9986).

Analysis of equality of variance of Controls by experiment

We used the Brown and Forsyth test [4] test for equality of variance. The Brown and Forsyth test statistic is the *F* statistic resulting from an ordinary one-way analysis of variance on the absolute deviations from the median. For this we used the "HH" package

```
> library("HH")
> hov(Lum~Exp, data=GSA_CONT)

        hov: Brown-Forsyth

data:  Lum
F = 4.7155, df:Exp = 11, df:Residuals = 868, p-value = 4.802e-07
alternative hypothesis: variances are not identical
```

Brown –Forsyth test indicates that there is inequality of variances of control samples depending on the experiment. We print hovPlots to visualize the origin of the non-equality of variances by Experiment (**Supplementary Fig. S3.3).**

```
> hovPlot(Lum~Exp, data=GSA_CONT)
```

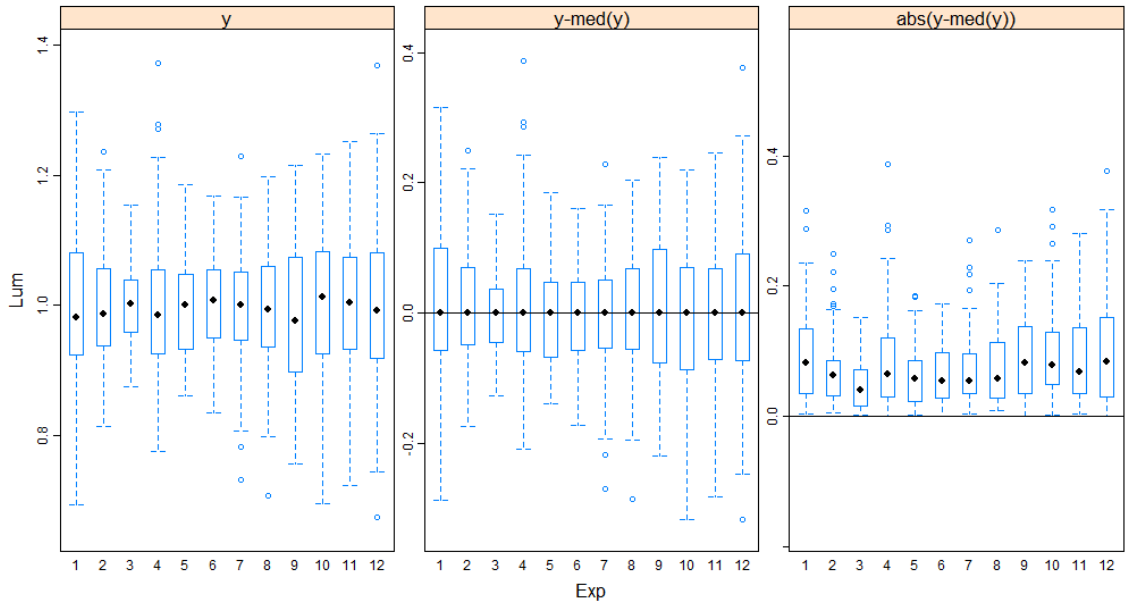

Supplementary Fig. S3.3. hovPlots for Lum~Exp, data=GSA_CONT. Representing boxplots of the mean of Lum (y) by Experiment, Lum- mean(Lum), and absolute value of the deviation Lum- mean(Lum) for the 12 experiments.

Brown and Forsyth test revealed that controls by experiment are not homoscedastic (p = 4.802e-07). As can be seen in the hovPlots (**Supplementary Fig. S3.3**) experiments 3, 5, 6 and 7 have a lower variance than the other 8 experiments, and experiment 1 presented the larger variability.

1.2.1.2. Quality control of "Treatment" observations

Similarly to control observations, "Treatment" data (see **Supplementary Table S3.2**) were tested for normality and heteroscedasticity. Since the number of replicates by level of treatment is small (n = 6), instead of q-q normal plots, Shapiro-Wilk normality test (shapiro.test {stats}) was used for testing normality. Heteroscedasticity was checked based on the Brown and Forsyth test for equality of variance.

```
> GSA_TREAT<-GSA[GSA$Treatment!=0,]#selecting all tratments except lev
el 0
(controls)
> GSA_TREAT<-drop(GSA_TREAT)
> GSA_TREAT<-droplevels(GSA_TREAT)
```

Applying Shapiro test by "treatment":

```
> GSA_TREAT.Shap <- with(GSA_TREAT, tapply(Lum, Treatment, shapiro.tes
t))# apply shapiro.test by level
> str(GSA_TREAT.Shap[[1]])
List of 4
 $ statistic: Named num 0.953
  ..- attr(*, "names")= chr "W"
 $ p.value  : num 0.763
 $ method   : chr "Shapiro-Wilk normality test"
 $ data.name: chr "X[[1L]]"
 - attr(*, "class")= chr "htest"
```

Tabulating results:

```
> GSA_TREAT.lres <- sapply(GSA_TREAT.Shap, `[`, c("statistic","p.value
"))# apply shapiro.test by level
> head(t(GSA_TREAT.lres))
  statistic p.value
1 0.952865  0.7634077
2 0.9028688 0.3911646
3 0.6773077 0.003532857
4 0.9520271 0.7566626
5 0.9473528 0.7188028
6 0.8474926 0.1502042
.
.
.
243 0.9864942 0.9981385
244 0.9858304 0.9975017
```

(Complete output in **ANEX 2**)

Only 12 of the 244 treatments violated the assumption of normality.

Checking for equality of variances in Treatment observations

```
> hov(Lum~Treatment, data=GSA_TREAT)

        hov: Brown-Forsyth

data:  Lum
F = 1.1778, df:Treatment = 241, df:Residuals = 1582, p-value = 0.04176
alternative hypothesis: variances are not identical

> hovPlot(Lum~Treatment, data=GSA_TREAT)
```

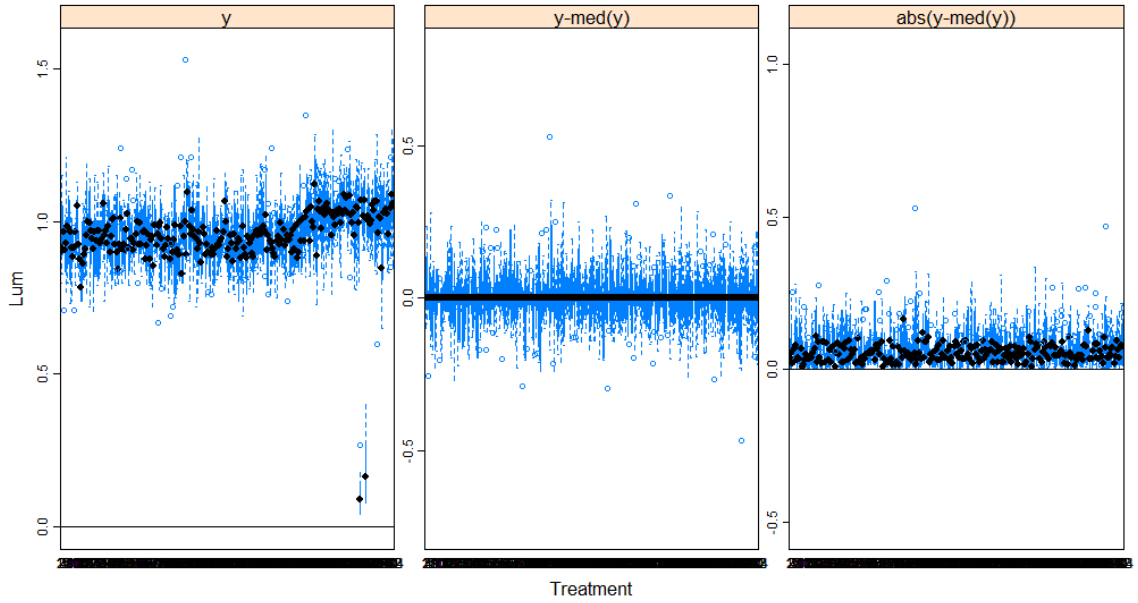

Supplementary Fig. S3.4. hovPlots for Lum~Treatment, data=GSA_TREAT. Representing boxplots of the mean of Lum (y) by Experiment, Lum- mean(Lum), and absolute value of the deviation Lum- mean(Lum) for the 244 Treatments.

According to Brown and Forsyth test, Treatment observations are not homoscedastic (*p-value* = 0.04176). However, they are close to the NULL hypothesis. From the view point of the subsequent analysis, it is important to know whether at least the homogeneous "Exp.Group" = "MIXTURE" is homoscedastic.

```
> GSA_TREAT_Mix<-GSA_TREAT[GSA_TREAT$Exp.Group=="MIXTURE",]
> hov(Lum~Treatment, data=GSA_TREAT_Mix)

        hov: Brown-Forsyth

data:  Lum
F = 0.8472, df:Treatment = 179, df:Residuals = 900, p-value = 0.9162
alternative hypothesis: variances are not identical
```

Exp.Group = "MIXTURE" is homoscedastic (Brown-Forsyth test, *p-value* = 0.9162).

1.2.1.3. Conclusions from the quality control of GSA.csv dataset

GSA.csv dataset includes the dependent variable "Lum" collected from a total of 12 independent biological replicates (independent experiments). The data set is divided in two main Experimental groups: "MIXTURE" and "INDIVIDUAL" referring to mixture and individual exposure, respectively. Both Experimental groups have two main cases: "CONTROL" and "TREATMENT" which refers to control observations or treated organisms, respectively. Control observations (n=880) were normally distributed with slightly heavy tails based on the visualization of normal q-q plot when analyzed by "Experiment" (n =12) (**Supplementary Fig. S3.1**). Boxplots by experiment appeared homogeneous (**Supplementary Fig. S3.2**), and no statistical significant differences were found for the means among experiments (ANOVA, F value 0.178, Pr >F = 0.999). However variances of control data sets among experiments were not homogeneous (Brown-Forsyth test, *p* = 4.802e-07). The inequality

in experimental variance was caused mainly by a group of experiments (3, 5, 6 and 7) which presented lower variance than the rest of experiments. Therefore, despite we consider the general quality of the control observations as acceptable, inequality of variances need to be considered when performing parametric statistics such as ANOVA. "Treatment" observations (n = 1848) were collected along 244 treatments (180 mixtures and 64 individual treatments). In general treatment observations were normal (only 12 of the 244 treatments were statistically significant in the Shapiro-Wilk normality test). Lum was not homoscedastic by "Treatment" when considering the whole "Treatment" categories (mixtures + individual exposure observations). However, when equality of variances was studied considering only "Mixture" Experimental group, the data set was found to be homoscedastic (Brown-Forsyth test, p = 0.9162). This property is very important since the "Mixture" Experimental group is both normal and homoscedastic which justifies further parametric analysis such as ANOVA.

1.2.3. Differences by treatment (control, individual exposure and mixture exposure to PPCPS)

CODE LOCATION: orders to do the analysis and plots presented in this section are in the R script named "Script_GSA_Raw.R".

The first relevant question on the GSA.csv dataset in the article is whether the exposure to low doses of PPCPs is able to induce differential biological effects with respect to Control observations. To check this hypothesis, first we compared "Control", "individual exposure" and "mixture exposure" effect on bioluminescence of *Anabaena* CPB4337 via boxplot visualization:

Preparing the data set:

```
> # 2.1 Boxplot Control, individual, mixture
> #subseting the dataframe: first by "Case" and "Exp.Group" we split c
ontrol, individual
> #and mixture observations
> GSA_C<-GSA[GSA$Case=="CONTROL",]
> GSA_T<-GSA[GSA$Case=="TREATMENT",]
> GSA_Mix<-GSA_T[GSA_T$Exp.Group=="MIXTURE",]
> GSA_Ind<-GSA_T[GSA_T$Exp.Group=="INDIVIDUAL",]#GSA_Ind is more compl
icated
> #since it includes observations of individual expossure to high dose
s (10mg/L, C1..Cn = "4") which

> #we want to remove from this analysis

> GSA_Ind<-GSA_Ind[GSA_Ind$C1!="4"| GSA_Ind$C2!="4"| GSA_Ind$C3!="4"
+                  | GSA_Ind$C4!="4"| GSA_Ind$C5!="4"| GSA_Ind$C6!="
4"| GSA_Ind$C7!="4"
+                  | GSA_Ind$C8!="4"| GSA_Ind$C9!="4"| GSA_Ind$C10!=
"4"| GSA_Ind$C11!="4"
+                  | GSA_Ind$C12!="4"| GSA_Ind$C13!="4"| GSA_Ind$C14
!="4"| GSA_Ind$C15!="4"| GSA_Ind$C16!="4",]
> GSA_Ind<-droplevels(GSA_Ind)

> # we generate a new dataframe only with treatment and Lum values
> Figure<-data.frame("Treat"=factor(), "Lum" = numeric())
> Treat <-c(rep("Control",880), rep("Ind", 768), rep("Mix", 1080))
> Figure<-data.frame("Treat"=Treat, "Lum" = c(GSA_C$Lum, GSA_Ind$Lum,
GSA_Mix$Lum))
```

Boxplots for visualizing differences between "Control", individual exposure to PPCPs and mixture exposure to PPCPs:

```
> boxplot(Lum~Treat, notch = TRUE, data=Figure, col=(c("white","grey",
"darkgrey")),
```

```
+         xlab="Case", ylab="Lum",ylim =c(0.6,1.4), cex.lab=1.2, cex.a
xis= 1.2)
```

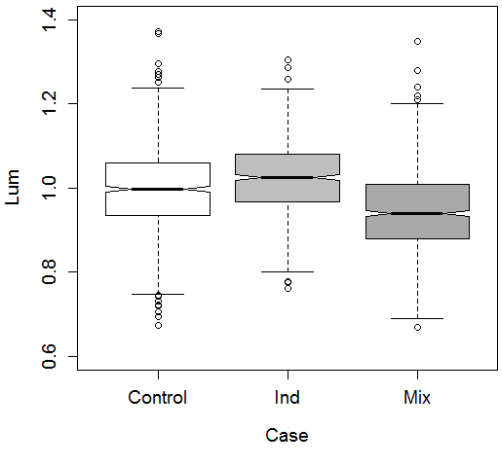

Supplementary Fig. S3.5. Notched box-plot for "Lum" of control observations (n =880), Individual exposure to PPCPs (n =768) and exposure to mixtures of PPCPs (n =1080). The notches extend to +/-1.58 IQR/sqrt(n) [3]

Box plots suggest statistically significant differences in "Lum" as a function of the exposure to PPCPs. To confirm this observation, we performed a One-Way ANOVA:

```
> #Test for statistical significance of mean differences
> anov.1<-aov(Lum~Treat, Fig.)
> anov.1
Call:
   aov(formula = Lum ~ Treat, data = Fig.)

Terms:
                    Treat Residuals
Sum of Squares   2.941171 23.825315
Deg. of Freedom         2      2531

Residual standard error: 0.09702268
Estimated effects may be unbalanced
194 observations deleted due to missingness

> Anova(anov.1, type="III", singular.ok = T)##correction for Type-III
sums of squares due to unbalanced design
Anova Table (Type III tests)

Response: Lum
            Sum Sq   Df  F value    Pr(>F)
(Intercept) 874.84    1 92935.88 < 2.2e-16 ***
Treat         2.94    2   156.22 < 2.2e-16 ***
Residuals    23.83 2531
---
Signif. codes:  0 '***' 0.001 '**' 0.01 '*' 0.05 '.' 0.1 ' ' 1

 > TukeyHSD(anov.1)
  Tukey multiple comparisons of means
    95% family-wise confidence level

Fit: aov(formula = Lum ~ Treat, data = Fig.)

$Treat
                  diff         lwr         upr p adj
Ind-Control  0.02771134  0.01550414  0.03991855 3e-07
Mix-Control -0.05475375 -0.06508627 -0.04442123 0e+00
Mix-Ind     -0.08246510 -0.09421763 -0.07071257 0e+00
```

```
> #The number of observations is unbalanced. We can used a more conser
vative post-hoc test
> # a correction of Tuckey HSD for unbalanced, and non-homoscedastic d
ata sets:
> #ANOVA + Test de Tukey Esther Herberich correction
> #Herberich E, Sikorski J, Hothorn T (2010) A Robust Procedure for Co
mparing Multiple Means under Heteroscedasticity in Unbalanced Designs.
PLoS
> #ONE 5(3): e9788. doi:10.1371/journal.pone.0009788.

> library(sandwich)
> anov.2 <- aov(Lum~Treat, Figure)
> anov.2_glht <- glht(anov.2, mcp (Treat = "Tukey"), vcov = vcovHC)
> Anova(anov.2, type="III", singular.ok = T)##correction for Type-III
sums of squares due to unbalanced design
Anova Table (Type III tests)

Response: Lum
            Sum Sq   Df  F value    Pr(>F)
(Intercept) 874.84    1 92935.88 < 2.2e-16 ***
Treat         2.94    2   156.22 < 2.2e-16 ***
Residuals    23.83 2531
---
Signif. codes:  0 ‘***’ 0.001 ‘**’ 0.01 ‘*’ 0.05 ‘.’ 0.1 ‘ ’ 1
> summary(anov.2_glht)

         Simultaneous Tests for General Linear Hypotheses

Multiple Comparisons of Means: Tukey Contrasts


Fit: aov(formula = Lum ~ Treat, data = Figure)

Linear Hypotheses:
                     Estimate Std. Error t value Pr(>|t|)
Ind - Control == 0  0.027711   0.004960   5.587   <1e-07 ***
Mix - Control == 0 -0.054754   0.004536 -12.072   <1e-07 ***
Mix - Ind == 0     -0.082465   0.004731 -17.430   <1e-07 ***
---
Signif. codes:  0 ‘***’ 0.001 ‘**’ 0.01 ‘*’ 0.05 ‘.’ 0.1 ‘ ’ 1
(Adjusted p values reported -- single-step method)

> plot(TukeyHSD(anov.2)
```

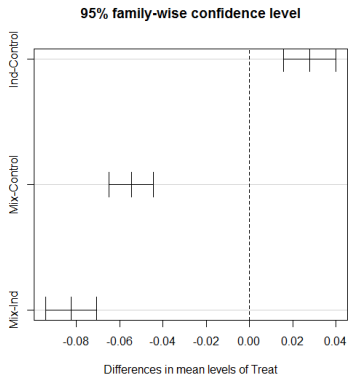

Supplementary Fig. S3.6. Confidence interval for the difference of means according to anova.2_glht model.

Power Analysis

For power analysis calculation we proceed with the steps described in section **1.2.1.1.**

```
> #Power analysis
> #install.packages("pwr")#power analysis utilities
> library("pwr")
```

Calculate sd:

```
> x.sd.1<-mean(sapply(split(Fig.[,2],Fig.$Treat), sd, simplify = TRUE,
na.rm=TRUE)) #mean sd of the 3 cases
> x.sd.1
[1] 0.0955262
```

Calculate mean effects:

```
> x.mean.1<-sapply(split(Fig.[,2],Fig.$Treat), mean, simplify = TRUE,
na.rm=TRUE) #estimating means by Treat
> x.mean.1
  Control       Ind       Mix
0.9970653 1.0247767 0.9423116


> #We calcuate the effect size "d" for the minimum distance in the exp
eriment (control-Ind. Pairwise)
> d.1<-abs((x.means.1[1]-x.means.1[2])/(x.sd.1))
> d.1
  Control
0.2900915
```

Cohen size for "d" = 0.29; approximately *"medium"* (0.25)

```
> cohen.ES(test = "anov", size = "medium")#Cohens category

     Conventional effect size from Cohen (1982)

           test = anov
           size = medium
    effect.size = 0.25

> #Cohens category "medium"
> pwr.anova.test(k=3, n = 768, f = 0.25, sig.level = 0.05, power = NUL
L)

     Balanced one-way analysis of variance power calculation

              k = 3
              n = 768
              f = 0.25
      sig.level = 0.05
          power = 1

NOTE: n is number in each group
```

#########

Just to check that 2 random groups of controls do not produce statistically significant differences

```
> #just a check that 2 groups of controls do not produces statisticall
y significant differences
> GSA_C1<-GSA_C$Lum[1:440]
> GSA_C2<-GSA_C$Lum[441:880]
> Group<-factor(c(rep("C1",440),rep("C2", 440)))
> GSA_CG<-data.frame("Group"=Group, "Lum"=c(GSA_C1,GSA_C2))
>
```

```
> boxplot(Lum~Group, notch = TRUE, data=GSA_CG, col=(c("white","grey",
"darkgrey")),
+         xlab="Case", ylab="Lum",ylim =c(0.6,1.4), cex.lab=1.2, cex.a
xis= 1.2)
```

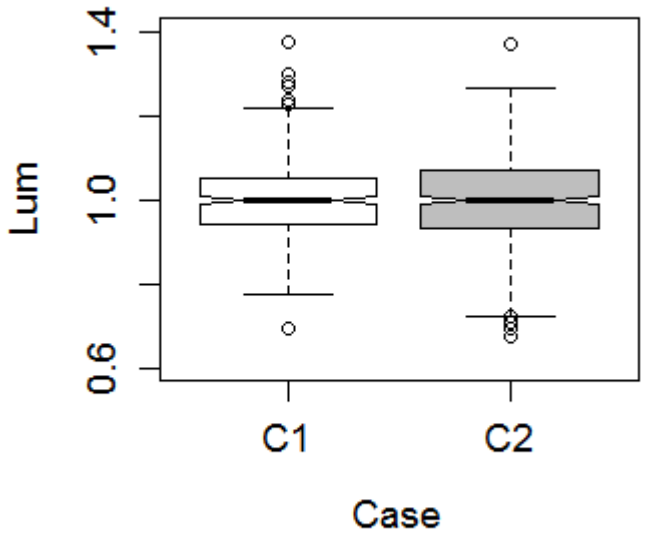

Supplementary Fig. S3.7. Notched box-plot for "Lum" of control observations (n =880), Divided in 2 aleatory groups C1 (n =440) and C2 (n =1080). The notches extend to +/-1.58 IQR/sqrt(n) [3]

Testing differences via One-Way ANOVA:

```
> anov.3<-aov(Lum~Group, GSA_CG)
> anov.3
Call:
   aov(formula = Lum ~ Group, data = GSA_CG)

Terms:
                    Group Residuals
Sum of Squares  0.007187  8.795705
Deg. of Freedom        1       878

Residual standard error: 0.1000894
Estimated effects may be unbalanced

> Anova(anov.3, type="III", singular.ok = T)##correction for Type-III
sums of squares due to unbalanced design
Anova Table (Type III tests)

Response: Lum
             Sum Sq  Df    F value Pr(>F)
(Intercept) 439.93   1 43914.6857 <2e-16 ***
Group         0.01   1     0.7174 0.3972
Residuals     8.80 878
---
Signif. codes:  0 '***' 0.001 '**' 0.01 '*' 0.05 '.' 0.1 ' ' 1
> TukeyHSD(anov.3)
  Tukey multiple comparisons of means
    95% family-wise confidence level

Fit: aov(formula = Lum ~ Group, data = GSA_CG)

$Group
              diff         lwr         upr     p adj
```

```
c2-c1 -0.005715631 -0.01895978 0.007528514 0.3972216
```

One-Way ANOVA confirms the statistical significant differences between control, individual and mixture exposure F =156.2 (Pr(>F) = 2e-16 ***. In fact both individual and mixture exposure resulted in opposite effects on bioluminescence of *Anabaena* CPB4337 which were statistically significantly different among themselves (p<0.001) and with respect to control observations (p<0.001). Both boxplots and ANOVA confirm that there are statistically significant differences between the two aleatory groups of control observations.

1.2.4. Effects of light intensity on individual and mixture exposure to PPCPs (Fig. 3.2 D, E of the manuscript)

In this section, the idea was to check whether light intensity, an important regulator of the metabolic activity of photosynthetic organisms, has any influence on the observed effects of PPCPs on *Anabaena* CPB4337 when exposed to them both individually or in mixtures.

CODE LOCATION: orders to do the analysis and plots presented in this section are in the R script named "Script_GSA_Raw.R"

First we compare the responses by means of boxplots:

```
> #Section 3: Effect of light intensity
> #Data set: GSA
>
> #individual effect of PPCP
> boxplot(Lum~L, notch = TRUE, data=GSA_Ind, col=(c("white","Grey")),
ylim=c(0.65, 1.35)
+         , xlab=NULL, ylab="R.Lum", cex.lab=1.2, cex.axis= 1.2)# effe
ct of light level on
> #mixture exposure
> boxplot(Lum~L, notch = TRUE, data=GSA_Mix, col=(c("white","grey")),
ylim=c(0.65, 1.35),
+         xlab=NULL, ylab="R.Lum", cex.lab=1.2, cex.axis= 1.2)
```

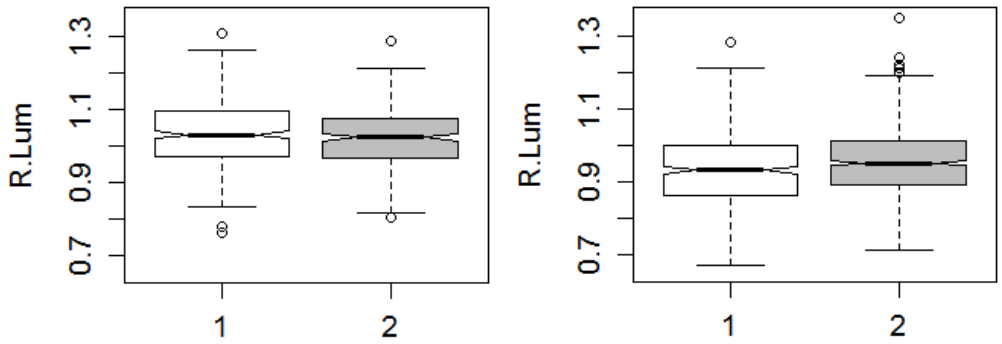

Supplementary Fig. S3.8. Notched box-plot for "Lum" for treatment observations shorted by L level (1 and 2). Left panel: Individual exposure to PPCPs (n = 768). Right panel: Mixture exposure to PPCPs (n = 1080). The notches extend to +/-1.58 IQR/sqrt(n) [3]

Checking for significance of Light effect via One-Way ANOVA

```
> #ANOVA
> #individual effect of PPCP
> anov.4<-aov(Lum~L, GSA_Ind)# One-Way ANOVA light as explanatory vari
able for
> anov.4
```

```
Call:
   aov(formula = Lum ~ L, data = GSA_Ind)

Terms:
                        L Residuals
Sum of Squares  0.017191  4.318219
Deg. of Freedom        1       572

Residual standard error: 0.0868869
Estimated effects may be unbalanced
194 observations deleted due to missingness
> Anova(anov.4, type="III", singular.ok = T)
Anova Table (Type III tests)

Response: Lum
             Sum Sq  Df    F value Pr(>F)
(Intercept) 305.676   1 40490.4372 <2e-16 ***
L             0.017   1     2.2772 0.1318
Residuals     4.318 572
---
Signif. codes:  0 ‘***’ 0.001 ‘**’ 0.01 ‘*’ 0.05 ‘.’ 0.1 ‘ ’ 1
> #mixture exposure
> anov.5<-aov(Lum~L, GSA_Mix)# One-Way ANOVA light as explanatory vari
able for
> anov.5
Call:
   aov(formula = Lum ~ L, data = GSA_Mix)

Terms:
                         L Residuals
Sum of Squares   0.136536 10.550477
Deg. of Freedom         1      1078

Residual standard error: 0.0989297
Estimated effects may be unbalanced
> Anova(anov.5, type="III", singular.ok = T)##correction for Type-III
sums of squares due to unbalanced design
Anova Table (Type III tests)

Response: Lum
            Sum Sq   Df   F value    Pr(>F)
(Intercept) 398.99    1 40766.872 < 2.2e-16 ***
L             0.14    1    13.951 0.0001975 ***
Residuals    10.55 1078
---
Signif. codes:  0 ‘***’ 0.001 ‘**’ 0.01 ‘*’ 0.05 ‘.’ 0.1 ‘ ’ 1
```

Notched boxplots (**Supplementary Fig. S3.8**) indicated and One-Way ANOVA confirmed that there is no influence of light intensity (L) in the effect produced by PPCP on the bioluminescence (lum) of A. CPB4337 when applied individually (One-Way ANOVA, Pr(>F) = 0.132), but there is an influence under mixture exposure (One-Way ANOVA, Pr(>F) = 0.000198).

Power analysis

```
> #Power analysis
> #install.packages("pwr")#power analysis utilities
> #library("pwr")
> #We have to calculate the effect size "d" (in units of the sd). For
this we will aproximate both
> #for the whole experiment. We assumed the worst case scenario: the m
inimum effect size, and the minimum "n"
>
> x.sd.2<-mean(sapply(split(GSA_Mix[,40],GSA_Mix$L), sd, simplify = TR
UE, na.rm=TRUE)) #mean sd of the 3 cases
> x.means.2<-sapply(split(GSA_Mix[,40],GSA_Mix$L), mean, simplify = TR
UE, na.rm=TRUE) #estimating means by Treat
```

```
>
> #We calcuate the effect size "f" for the minimum distance in the exp
eriment (control-Ind. Pairwise)
> d.2<-abs((x.means.2[1]-x.means.2[2])/(x.sd.2))
> d.2
        1
0.2302539
```

Cohen size for "d" = 0.29; approximately *"medium"* (0.25)

```
> cohen.ES(test = "anov", size = "medium")

     Conventional effect size from Cohen (1982)

           test = anov
           size = medium
    effect.size = 0.25

> #Cohens category "medium"
> pwr.anova.test(k=3, n = 768, f = 0.25, sig.level = 0.05, power = NUL
L)

     Balanced one-way analysis of variance power calculation

              k = 3
              n = 768
              f = 0.25
      sig.level = 0.05
          power = 1

NOTE: n is number in each group
```

1.2.5. Effects of individual exposure to high doses of PPCPs (Results presented in Fig. 3.3A of the manuscript)

In this section we analyze the effect of the exposure of *Anabaena* CPB4337 to 10 mgL^{-1} of each of the 16 PPCPs in individual exposure via boxplot and ANOVA coupled with Dunnett Contrasts for Multiple Comparisons of Means [5].

CODE LOCATION: orders to do the analysis and plots presented in this section are in the R script named "Script_GSA_Raw.R"

Preparing the dataset:

```
> #Section 4. 10mgL (Individual effect of 10 mgL-1 of the 16 pharmaceu
ticals)
> ##DATASET GSA
> #Fig. 3a. Individual effects of 16 PPCP at 10 mgL-1
> #In this part we are gona take advance of the variables Exp.Group an
d Treatment to short
> #the dataset and make the plots.
> #first we subset by Exp.Group
> GSA_IND<-subset(GSA, Exp.Group=="INDIVIDUAL", )
> GSA_IND<-droplevels(GSA_IND)
> GSA_IND_L4<-subset(GSA_IND, C1=="0"| C1=="4"|C2=="0"| C2=="4"|C3=="0
"| C3=="4"|
+                                C4=="0"| C4=="4"| C5=="0"| C5=="4"| C6==
"0"| C6=="4"| C7=="0"| C7=="4"|
+                                C8=="0"| C8=="4"| C9=="0"| C9=="4"|C10==
"0"| C10=="4"| C11=="0"| C11=="4"|
+                                C12=="0"| C12=="4"| C13=="0"| C13=="4"|
C14=="0"| C14=="4"| C15=="0"| C15=="4"|
+                                C16=="0"| C16=="4")# we select just the
levels "0" (control) and "4"(10 mgL-1)
```

```
> #of each factor (Cx)
>
> GSA_IND_L4<-droplevels(GSA_IND_L4)
> attach(GSA_IND_L4)
> GSA_IND_L4.ord<-GSA_IND_L4[order(Treatment),]#order by treatment
> detach(GSA_IND_L4)
```

Assigning factor names:

```
> GSA_IND_L4.ord$Treatment<-revalue(GSA_IND_L4.ord$Treatment, c("0"="0
", "184"="C1",
+                                                                "188
"="C2","192"="C3","196"="C4", "200"="C5","204"="C6","208"="C7","212"="
C8",
+                                                                "216
"="C9","220"="C10","224"="C11","228"="C12","232"="C13","236"="C14","24
0"="C15",
+                                                                "244
"="C16"))# change the names of the variables
> # we want to present an idea of the departure from control levels, f
or this, we are going to
> #add three ablines to the plot (the median of the control observatio
ns, and the extent of the notches
> #of control boxplots. The notches extend to +/-1.58 IQR/sqrt(n) (McG
ill et al. 1978)
> #McGill, R., Tukey, J. W. and Larsen, W. A. (1978) Variations of box
plots. The American Statistician 32, 12-16.
```

Calculating statistical summaries for "Control" group:

```
> Ind.control<-subset(GSA_IND_L4.ord, Treatment=="0")
>
> median(Ind.control$Lum)
[1] 0.9962469
> summary(Ind.control$Lum)
   Min. 1st Qu.  Median    Mean 3rd Qu.    Max.
 0.6736  0.9288  0.9962  0.9946  1.0680  1.3680
```

The boxplot:

```
boxplot(Lum~Treatment, notch = FALSE, data=GSA_IND_L4.ord, col=(c("whi
te","grey")), xlab="Factor", ylab="R.Lum",ylim =c(0.0,1.3),cex.lab=1.2
, cex.axis= 1.2)
abline(h=c(0.9288,1.0680), lty=c(3,3), col="red") #Control´s 1st and 3
rd Qu.
abline(h=0.9962, lty=1)#Control´s median
```

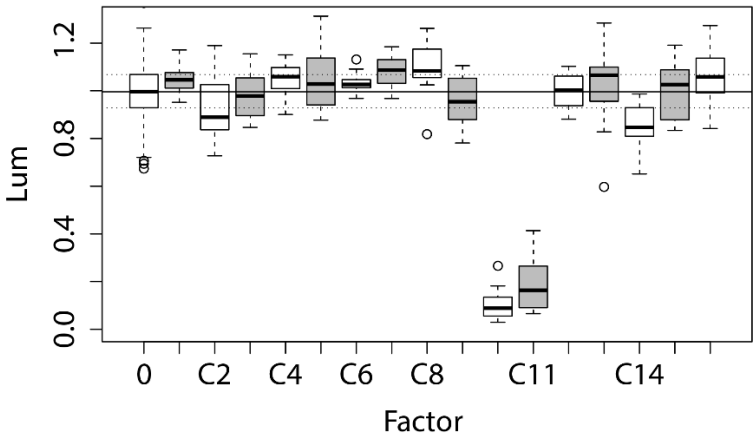

Supplementary Fig. S3.9. Boxplots of Lum as a function of factors (PPCPs) (C1:C16). Straight line and dashed lines are the median, Q25 and Q75 of control observations of the GSA$Exp.Group="INDIVIDUAL" of GSA.csv dataset (n = 384).

Boxplots suggest statistically significant effects for some factors. We formally test for statistically significant differences with respect to control observations via the Dunnett test, which is suitable to perform many-to-one comparisons [5].

```
> anov.5=aov(Lum~Treatment, data=GSA_IND_L4.ord)
> anov.5
Call:
   aov(formula = Lum ~ Treatment, data = GSA_IND_L4.ord)

Terms:
                Treatment Residuals
Sum of Squares  17.362195  6.713478
Deg. of Freedom        16       559

Residual standard error: 0.1095892
Estimated effects may be unbalanced
> Anova(anov.5, type="III", singular.ok = T)
Anova Table (Type III tests)

Response: Lum
             Sum Sq  Df   F value    Pr(>F)
(Intercept) 379.89   1 31631.778 < 2.2e-16 ***
Treatment    17.36  16    90.354 < 2.2e-16 ***
Residuals     6.71 559
---
Signif. codes:  0 ‘***’ 0.001 ‘**’ 0.01 ‘*’ 0.05 ‘.’ 0.1 ‘ ’ 1
> test.dunnett.1 =glht(anov.5, linfct = mcp(Treatment = "Dunnett"))
> summary(test.dunnett.1)

         Simultaneous Tests for General Linear Hypotheses

Multiple Comparisons of Means: Dunnett Contrasts


Fit: aov(formula = Lum ~ Treatment, data = GSA_IND_L4.ord)

Linear Hypotheses:
               Estimate Std. Error t value Pr(>|t|)
C1 - 0 == 0   0.053509   0.032126   1.666 0.798111
C2 - 0 == 0  -0.070301   0.032126  -2.188 0.373456
C3 - 0 == 0  -0.016044   0.032126  -0.499 1.000000
C4 - 0 == 0   0.056055   0.032126   1.745 0.739232
C5 - 0 == 0   0.057750   0.032126   1.798 0.697046
C6 - 0 == 0   0.040237   0.032126   1.252 0.976229
C7 - 0 == 0   0.085293   0.032126   2.655 0.122245
C8 - 0 == 0   0.098925   0.032126   3.079 0.034190 *
C9 - 0 == 0  -0.038784   0.032126  -1.207 0.983124
C10 - 0 == 0 -0.890178   0.032126 -27.709  < 1e-05 ***
C11 - 0 == 0 -0.798588   0.032126 -24.858  < 1e-05 ***
C12 - 0 == 0  0.003620   0.032126   0.113 1.000000
C13 - 0 == 0  0.025749   0.032126   0.801 0.999834
C14 - 0 == 0 -0.141758   0.032126  -4.413 0.000196 ***
C15 - 0 == 0  0.005175   0.032126   0.161 1.000000
C16 - 0 == 0  0.073117   0.032126   2.276 0.311239
---
Signif. codes:  0 ‘***’ 0.001 ‘**’ 0.01 ‘*’ 0.05 ‘.’ 0.1 ‘ ’ 1
(Adjusted p values reported -- single-step method)
```

One-Way ANOVA (Pr<F =<2e-16 ***) confirms that there are statistically significant effects among treatments (C0:C16). Dunnett test confirms that C8 (p = 0.034), C10, C11 and C14 ($p < 0.001$) effects are significantly different from those of control group.

Power analysis

```
> #Power analysis
> #install.packages("pwr")#power analysis utilities
> #library("pwr")
> #We have to calculate the effect size "d" (in units of the sd). For
this we will aproximate both
> #for the whole experiment. We assumed the worst case scenario: the m
inimum effect size, and the minimum "n"
>
> x.sd.3<-mean(sapply(split(GSA_IND_L4.ord[,40],GSA_IND_L4.ord$Treatme
nt), sd, simplify = TRUE, na.rm=TRUE)) #mean sd of the 3 cases
> x.sd.3
[1] 0.09985951
> x.means.3<-sapply(split(GSA_IND_L4.ord[,40],GSA_IND_L4.ord$Treatment
), mean, simplify = TRUE, na.rm=TRUE) #estimating means by Treat
> x.means.3
        0        C1        C2        C3        C4        C5        C6
C7        C8
0.9946358 1.0481452 0.9243348 0.9785916 1.0506912 1.0523858 1.0348725
1.0799293 1.0935604
       C9       C10       C11       C12       C13       C14       C15
C16
0.9558513 0.1044577 0.1960478 0.9982559 1.0203844 0.8528782 0.9998112
1.0677525
> #We calcuate the effect size "f" for the minimum distance in the exp
eriment (control-Ind. Pairwise)
> d.3<-abs((x.means.3[8]-x.means.3[2])/(x.sd.3))
> d.3
       C7
0.3182884
> cohen.ES(test = "anov", size = "medium")

     Conventional effect size from Cohen (1982)

           test = anov
           size = medium
    effect.size = 0.25

> cohen.ES(test = "anov", size = "large")

     Conventional effect size from Cohen (1982)

           test = anov
           size = large
    effect.size = 0.4

> #Cohens category "medium"
> pwr.anova.test(k=17, n = 12, f = 0.25, sig.level = 0.05, power = NUL
L)

     Balanced one-way analysis of variance power calculation

              k = 17
              n = 12
              f = 0.25
      sig.level = 0.05
          power = 0.5340678

NOTE: n is number in each group

> pwr.anova.test(k=17, n = 12, f = 0.4, sig.level = 0.05, power = NULL
)

     Balanced one-way analysis of variance power calculation

              k = 17
              n = 12
              f = 0.4
      sig.level = 0.05
          power = 0.9646119
```

```
NOTE: n is number in each group
```

Despite the power is less than 0.8 for small effect sizes, it is still a moderately high power (0.53) as to trust the results from the test since Dunnett test is conservative and restricts a lot the number of pair-wise comparisons with respect to other post-hoc tests. Anyway, the effect sizes of C10, C11 are higher > 0.4, and therefore the power is very good for detecting their effects (power > 0.96461).

2. GSA_MIX_MEDIAN. Aggregated data set including medians of bioluminescence inhibition of *Anabaena* CPB4337 and related analysis.

In the present part of the guide we are going to generate the "**GSA_MIX_MEDIAN.csv**" dataset. "**GSA_MIX_MEDIAN.csv**" is an aggregated dataset from GSA.csv which contains the same independent variables, and four dependent variables: the empirical medians of Lum values of the original raw dataset "GSA.csv", the bootstrapped estimated medians and the lower and upper 95% confidence intervals for the median (estimated by a bootstrapping procedure, see 2.2.1). The rational of generating such a dataset is because Elementary Effects (EEs) Screening is executed on a single central descriptor of the output sample [6]. We chose the median of the output population for each "treatment" (the 180 mixtures) as central descriptor to perform EEs screening since it is most robust to outliers than the mean.

In addition to generate the "**GSA_MIX_MEDIAN.csv**", all the analysis supporting the results presented in the manuscript based on the median values of mixture effects are also described in detail in the present section. It includes (1) the analysis of the effects of the 180 mixtures on bioluminescence inhibition of *Anabaena* CPB4337 mixture by mixture (section 2.2.1) (2) The results from the Two-Way ANOVA for "Important" and "Non-Important" factors sets (section 2.2.4). (3) In addition, for convenience, in section 2.2.5 it is also included the analysis and code used to generate **Fig. 3.2** of the manuscript on "The parsimonious low dose PPCPs mixture experimental design".

CODE LOCATION: orders to do the analysis and plots presented in this section are in the R script named "Script-GSA_MEDIAN.R"

2.1 Summary of the GSA_MIX_MEDIAN.csv dataset

Supplementary Table S3.3. Summary of observations by Case and Exp. Group for GSA_MIX_MEDIAN dataset

n	INDIVIDUAL	MIXTURE	ALL
CONTROL	0	0	0
TREATMENT	0	180	180
ALL	0	180	180

2.1.1 Variables

The data set includes 42 variables. A summary of the variables included in the **GSA_MIX_MEDIAN.csv** can be found in **Supplementary Table S3.4**.

Supplementary Table S3.4. Summary of the variables included in the **GSA_MIX_MEDIAN.csv** dataset.

Var.	Type	Levels	Info.
X	Factor	180	Observation locator
Exp.	Factor	1	Independent experiment identification
Exp. Group	Factor	2	Determines whether it is an individual or mixture exp.
Case	Factor	2	Determines whether it is a treatment or control observation.
Treatment	Factor	180	Each different treatment (including controls) are identified with a unique number)
C1:C16	Factor	3	Each concentration level for each of the 16 PPCPs is identified from lower to higher: "0": control, "1": median of means, "2": mean of maximum, "3": maximum of maximum, "4": 10 mgL^{-1}
C1.1:C16.1	Numeric	-	The exact concentration (ngL^{-1}) for each of the 16 PPCPs at each of the concentration levels established in C1:C16.
L	Factor	2	Light intensity regime. L1: ca.35 µmol photons m^2/s, L2 ca.35 µmol photons m^2/s
X16	Numeric	-	Sum of the concentrations of PPCPs in each Treatment in ngL^{-1}
emp.med	Numeric	-	Empirical median bioluminescence signal (n=6) normalized to control values of the 6 independent experiments. Control value is 1. A 0.1 difference is equivalent to a 10% variation
est.med	Numeric	-	Median estimated via bootstrapping
est.L	Numeric	-	Lower 95% confidence interval for the median estimated via bootstrapping
Est.U	Numeric	-	Upper 95% confidence interval for the median estimated via bootstrapping

Complete information on the GSA_MIX_MEDIAN.csv can be obtained as follows:

CODE LOCATION: orders to do the analysis and plots presented in this section are in the R script named "Script-GSA_MEDIAN.R"

```
> GSA_MIX_MEDIAN<-read.csv("GSA_MIX_MEDIAN.csv", header = TRUE, sep=",
")# converting intergers to factors in PPCP levels
> setwd("~/Art-GSA14/ANALISIS_DATA_0615/Data_Sets/Dataset-final")# set
wd to the folder
> #where you saved "GSA.csv" file
>
> GSA_MIX_MEDIAN<-read.csv("GSA_MIX_MEDIAN.csv", header = TRUE, sep=",
")# converting intergers to factors in PPCP levels
> GSA_MIX_MEDIAN<-GSA_MIX_MEDIAN[2:43]
> for (i in seq_along(1:20)){
+         GSA_MIX_MEDIAN[,i]<-as.factor(GSA_MIX_MEDIAN[,i])
+ }
> GSA_MIX_MEDIAN$L<-as.factor(GSA_MIX_MEDIAN$L)# converting L to facto
r
```

```
> str(GSA_MIX_MEDIAN)
'data.frame':  180 obs. of  42 variables:
 $ Treatment: Factor w/ 180 levels "1","2","3","4",..: 1 10 100 101 10
2 103 104 105 106 107 ...
 $ Exp      : Factor w/ 6 levels "1","2","3","4",..: 1 1 1 1 1 1 1 1 1
1 ...
 $ Exp.Group: Factor w/ 1 level "MIXTURE": 1 1 1 1 1 1 1 1 1 1 ...
 $ Case     : Factor w/ 1 level "TREATMENT": 1 1 1 1 1 1 1 1 1 1 ...
 $ C1       : Factor w/ 3 levels "1","2","3": 3 2 1 1 1 1 1 1 1 1 ...
 $ C2       : Factor w/ 3 levels "1","2","3": 2 1 2 2 2 2 2 2 2 2 ...
 $ C3       : Factor w/ 3 levels "1","2","3": 3 3 3 3 3 3 3 3 3 3 ...
```

```
 $ C4       : Factor w/ 3 levels "1","2","3": 2 2 3 3 3 3 3 3 3 3 ...
 $ C5       : Factor w/ 3 levels "1","2","3": 2 1 1 1 1 1 2 2 2 2 ...
 $ C6       : Factor w/ 3 levels "1","2","3": 2 2 2 2 2 2 2 2 2 2 ...
 $ C7       : Factor w/ 3 levels "1","2","3": 3 3 1 1 1 2 2 2 2 2 ...
 $ C8       : Factor w/ 3 levels "1","2","3": 2 1 3 3 3 3 3 3 3 3 ...
 $ C9       : Factor w/ 3 levels "1","2","3": 1 1 1 1 1 1 1 1 1 2 ...
 $ C10      : Factor w/ 3 levels "1","2","3": 2 1 3 3 3 3 3 3 3 3 ...
 $ C11      : Factor w/ 3 levels "1","2","3": 2 3 2 2 1 1 1 1 1 1 ...
 $ C12      : Factor w/ 3 levels "1","2","3": 3 3 3 3 3 3 3 3 3 3 ...
 $ C13      : Factor w/ 3 levels "1","2","3": 3 3 1 1 1 1 1 1 2 2 ...
 $ C14      : Factor w/ 3 levels "1","2","3": 2 3 2 2 2 2 2 3 3 3 ...
 $ C15      : Factor w/ 3 levels "1","2","3": 1 1 3 3 3 3 3 3 3 3 ...
 $ C16      : Factor w/ 3 levels "1","2","3": 3 2 3 2 2 2 2 2 2 2 ...
 $ C1.1     : num  8819 981 123 123 123 ...
 $ C2.1     : num  1733.6 36.5 1733.6 1733.6 1733.6 ...
 $ C3.1     : num  4759 4759 4759 4759 4759 ...
 $ C4.1     : num  1355 1355 11125 11125 11125 ...
 $ C5.1     : num  2505 383 383 383 383 ...
 $ C6.1     : num  2216 2216 2216 2216 2216 ...
 $ C7.1     : num  58315 58315 359 359 359 ...
 $ C8.1     : num  1391 246 3875 3875 3875 ...
 $ C9.1     : num  204 204 204 204 204 ...
 $ C10.1    : num  770 194 5501 5501 5501 ...
 $ C11.1    : num  1152 12541 1152 1152 183 ...
 $ C12.1    : num  2696 2696 2696 2696 2696 ...
 $ C13.1    : num  18829 18829 965 965 965 ...
 $ C14.1    : num  437 1434 437 437 437 ...
 $ C15.1    : num  464 464 982 982 982 ...
 $ C16.1    : num  9683 907 9683 907 907 ...
 $ L        : Factor w/ 2 levels "1","2": 1 2 1 1 1 1 1 1 1 1 ...
 $ X.16     : num  115328 105560 46195 37420 36450 ...
 $ emp.med  : num  0.9 0.885 0.945 0.91 0.965 0.93 0.865 0.98 0.96 0.8
9 ...
 $ est.med  : num  0.9 0.885 0.945 0.91 0.965 0.93 0.865 0.98 0.96 0.8
9 ...
 $ est.L    : num  0.8 0.87 0.72 0.78 0.825 ...
 $ est.U    : num  0.93 0.96 1.05 1.05 1.1 0.96 0.93 1.05 1.01 0.95 ..
```

2.2. GSA_MIX_MEDIAN.csv data analysis

CODE LOCATION: orders to do the analysis and plots presented in this section are in the R script named “Script_GSA-Raw.R”, “dotplot.error.IRP.R”, “overlap.fun.R”.

2.2.1. Estimating the median effect of the 180 mixtures via bootstrapping

In order to perform the Morris Analysis on the best possible dataset, we estimated median effects of the 180 mixtures via bootstrapping using the “boot” package [7]

```
#SECTION1: Generating GSA_MEDIAN.csv dataset
#Dataset: GSA.csv
#GSA_MEDIAN.csv will include the median values of Lum by Treatment fro
m GSA$Exp.Group
#=="MIXTURE". The median and confidence intervals for the median will
be generated by
#bootstrapping using the "boot" package.
##Bootstrapping of medians
#Description: functions and datasets for bootstrapping from the
#book "Bootstrap Methods and Their Applications" by A. C. Davison and
#D. V. Hinkley (1997, CUP).
# with boot {boot} Generate R bootstrap replicates
# with boot.ci {boot} Nonparametric Bootstrap Confidence Intervals are
generated
```

Loading “boot” package:

```
#install.packages("boot")
library (boot) #required "boot" package.
#subsetting GSA to GSA_MIX (just mixture observations)
```

Loading the dataset:

```
> #install.packages("boot")
> library (boot) #required "boot" package.
> #subsetting GSA to GSA_MIX (just mixture observations)
>
> Dir.data<-"~/Art-GSA14/ANALISIS_DATA_0615/GSA_EBS_PPCPs_2016/R_DATA"
> Dir.functions<-"~/Art-GSA14/ANALISIS_DATA_0615/GSA_EBS_PPCPs_2016/R_
FUNCTIONS"
> Dir.Scripts<-"~/Art-GSA14/ANALISIS_DATA_0615/GSA_EBS_PPCPs_2016/R_SC
RIPTS"
>
> setwd(Dir.data)# setwd to the folder where you saved "GSA.csv" file
>
> GSA<-read.csv("GSA.csv", header = TRUE, sep=",")# converting interge
rs to factors in PPCP levels
> GSA<-GSA[2:40]
> for (i in seq_along(1:20)){
+         GSA[,i]<-as.factor(GSA[,i])
+ }
> GSA$L<-as.factor(GSA$L)# converting L to factor
```

Selecting mixture observations:

```
GSA_MIX<-GSA[GSA$Case=="TREATMENT",]
GSA_MIX<-GSA_MIX[GSA_MIX$Exp.Group=="MIXTURE",]
GSA_MIX<-droplevels(GSA_MIX)
```

We need to generate the statistic function that we want to bootstrap (the median in this case)

```
med <- function(x,i) median(x[i])# definition of the statistical fucti
on to be bootstrapped: median
#function of x and i where x is the vector and i each element of the v
ector
```

We need to apply the boot {boot} function to all the 180 Treatments in GSA_MIX

```
> set.seed(20)# this is required to fix the starting random number gen
erator
> boot.GSA_MIX<-tapply(GSA_MIX$Lum, GSA_MIX$Treatment, boot, statistic
= med, R = 999, simplify = TRUE)
> #applying boot function over the 180 levels of the factor "GSA$Treat
ment" in the GSA data.frame
> # For this we used tapply {base}.
> # this generates a nested list (2 levels): (1) a list with as much e
lements as levels in level.
> #(2) a list of 180 elements
> str(boot.GSA_MIX[[1]])#visualized the first element of the list
List of 11
 $ t0       : num 0.9
 $ t        : num [1:999, 1] 0.9 0.975 0.9 0.89 0.945 0.88 0.85 0.8 0.
9 0.9 ...
 $ R        : num 999
 $ data     : num [1:6] 0.8 0.9 0.96 0.9 0.99 0.88
 $ seed     : int [1:626] 403 624 -1950722512 -1329105807 622001022 -1
569273369 -347641604 1904205261 1064633898 -936373853 ...
 $ statistic:function (x, i)
  ..- attr(*, "srcref")=Class 'srcref'  atomic [1:8] 1 8 1 33 8 33 1 1
  .. .. ..- attr(*, "srcfile")=Classes 'srcfilecopy', 'srcfile' <envir
onment: 0x00000000040489d0>
 $ sim      : chr "ordinary"
 $ call     : language FUN(data = X[[1L]], statistic = ..1, R = 999)
```

```
 $ stype    : chr "i"
 $ strata   : num [1:6] 1 1 1 1 1 1
 $ weights  : num [1:6] 0.167 0.167 0.167 0.167 0.167 ...
 - attr(*, "class")= chr "boot"
```

Once we have the list containing all the bootstrapped medians (boot.GSA_MIX), we can calculate the 95% confidence intervals for the medians with the function boot.ci {boot}. The function allows to estimate non-parametric bootstrapped confidence intervals based on 6 different methods (see boot package information):

```
> set.seed(20)# this is required to fix the starting random number gen
erator
> boot.ci.GSA_MIX<-lapply(boot.GSA_MIX, boot.ci, conf = 0.95, type = "
all")
There were 50 or more warnings (use warnings() to see the first 50)[1]
```

[1](This warnings are related to the estudentized intervals. Not a problem since we are not using them)

Generating 95% Confidence Intervals for the medians:

```
> #Generating confidence intervals for the median by Treatment for fou
r different methods:
> #"norm", "basic", "perc" and "bca".
> #The output is a nested a nested list of 180 elements
> str(boot.GSA_MIX[[1]])#visualized the first element of the list (the
)
List of 11
 $ t0       : num 0.9
 $ t        : num [1:999, 1] 0.9 0.975 0.9 0.89 0.945 0.88 0.85 0.8 0.
9 0.9 ...
 $ R        : num 999
 $ data     : num [1:6] 0.8 0.9 0.96 0.9 0.99 0.88
 $ seed     : int [1:626] 403 624 -1950722512 -1329105807 622001022 -1
569273369 -347641604 1904205261 1064633898 -936373853 ...
 $ statistic:function (x, i)
  ..- attr(*, "srcref")=Class 'srcref'  atomic [1:8] 1 8 1 33 8 33 1 1
  .. .. ..- attr(*, "srcfile")=Classes 'srcfilecopy', 'srcfile' <envir
onment: 0x00000000040489d0>
 $ sim      : chr "ordinary"
 $ call     : language FUN(data = X[[1L]], statistic = ..1, R = 999)
 $ stype    : chr "i"
 $ strata   : num [1:6] 1 1 1 1 1 1
 $ weights  : num [1:6] 0.167 0.167 0.167 0.167 0.167 ...
 - attr(*, "class")= chr "boot"
```

Plotting qq-plots, histograms and jack after jackknife plots:

```
> plot(boot.GSA_MIX[[1]])# q-q plots and histograms of the bootstrappe
d medians by mixture (in this case Mixture 1)
> jack.after.boot(boot.GSA_MIX[[1]])# same for jacknife
```

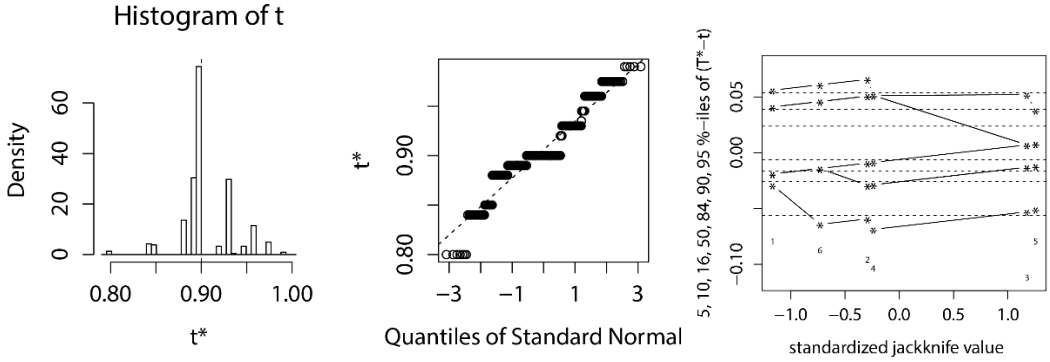

Supplementary Fig. S3.10. Histogram (Left panel), normal q-q plot (central panel) and jack after jackknife plot (right panel) for bootstrapped medians (R = 999) of Lum values for the sample of bootstrapped medians for "treatment" = 1.

Supplementary Fig. S3.10 shows quality plots for bootstrapped medians for the example case of "treatment" = 1. As can be seen, the distribution of bootstrapped medians (n=999) followed a near normal distribution as shown both in the histogram and the Normal qq-plot. In general bootstrapped medians followed an acceptable normal distribution.

Therefore we proceed to extract the data of interest (the estimated medians and the 95% confidence intervals) from the list "boot.GSA_MIX" and "boot.ci.GSA.mix". For this, it is required to source in R the function "values.fun.R".

```
> setwd(Dir.functions)# set wd to the folder where you saved the funct
ions
> source("values.fun.R")#source the function "values.fun.R"
> source("dotplot.error.IRP.R")#source the function "dotplot.error.IRP
.R"
> source("overlap.fun.R")#source the function "overlap.fun".R# takes t
wo arguments (dataset, control)
```

To estimate the 95% CIs we decided to use the Bias-Corrected and accelerated interval (bca) in boot.ci{boot}. The "bca" combines the transformation preserving property of the adjusted percentile method and the good coverage properties of the studentized bootstrap confidence intervals. It is a percentile method, where the quantiles to be obtained from the bootstrapped distribution are a function of bias-correction and acceleration terms. Both of these adjustments, along with the percentile-based method give the bca interval good coverage properties and a transformation preserving property [7].

We can generate a data.frame including the measured and bootstrapped median, as well as the lower and upper 95% confidence intervals for the median:

```
> x<-(values.fun("bca",GSA_MIX, boot.GSA_MIX, boot.ci.GSA_MIX))#genera
te a data.frame
> #with four variables: "Treatment", emp.med, est.med
> head(x)
  Treatment emp.med est.med est.L est.U
1         1   0.900   0.900 0.800 0.930
2         2   0.915   0.915 0.860 1.050
3         3   0.965   0.965 0.710 0.980
4         4   0.905   0.905 0.820 0.990
5         5   0.930   0.930 0.805 1.085
6         6   0.985   0.985 0.800 1.000
```

We decided to plot bootstrapped medians and 95% confidence intervals of the different Treatments and analyze the degree of overlapping with the 95% bootstrapped confidence intervals of the "control" observations. For this we first estimated bootstrapped median and 95% confidence intervals of control observations as follows:

```
> #estimating control median and 95% confidence intervals by the same
procedure that for Treatments
> GSA_CONT<-GSA[GSA$Case=="CONTROL",]
> set.seed(20)# this is required to fix the starting random number gen
erator
> boot.GSA_CONT<-boot(data = GSA_CONT$Lum, statistic = med, R = 999)#
R bootstrap replicates of
> #the statistic (med in the present case).
> set.seed(20)# this is required to fix the starting random number gen
erator
> boot.ci.GSA_CONT<-boot.ci(boot.GSA_CONT, conf = 0.95, type = "all")#
ci95% stimates for the median
```

```
Warning message:
In boot.ci(boot.GSA_CONT, conf = 0.95, type = "all") :
  bootstrap variances needed for studentized intervals
> #extracting empirical median and estimated median and ci 95% ("bca"
method)
> boot.ci95.GSA_CONT<-c(boot.GSA_CONT[[1]], median(boot.GSA_CONT[[2]])
, boot.ci.GSA_CONT$bca[[4]], boot.ci.GSA_CONT$bca[[5]])
> #IMPORTANT: Change boot.ci.GSA_CONT$bca for the type of ci.95 estima
tion used in "values.fun"
> #a vector (mun[1:4]) with the empirical median, the median of the 99
9 median stimates, and the lowe and upper CI95% stimates
> boot.ci95.GSA_CONT
[1] 0.9970461 0.9970461 0.9894975 1.0041401
```

To plot the results we used a built in function with facilitates the display of dotplots with error bars "dotplot.errors" it can be sourced from "dotplot.error.IRP.R" which is a personal version of the original one by Kozak M [8].

```
> #dotplots with error bars being 95% CI
> #"dotplot.error.IRP.R" is a modification of the original script publ
ish by
> #Kozak M. (Communications in Biometry and Crop Science Vol. 5, No. 2
, 2010, pp. 69-77)
> #ordering the data.frame
>
> all_GSA_MED.plot<-data.frame("group"=c(1:180),"lower"= x$est.L, "est
"= x$est.med,"upper"= x$est.U)
> #reference line control median and 95%confidence interval
>
> #visually inspect the variability of the bootstrapped median and ci.
95 of the 180 mixtures
> dotplot.errors(all_GSA_MED.plot, type.bar = "CI", end.length = 0.00,
reorder.groups = TRUE,
+                reordering = "decreasing", reference.line = c(0.99704
61, 1.0045065),
+                horizontal = FALSE, cex.axis=2)#IMPORTANT: Reference
line is the est.med, and the lowe and upper CI95% stimates for control
observations
```

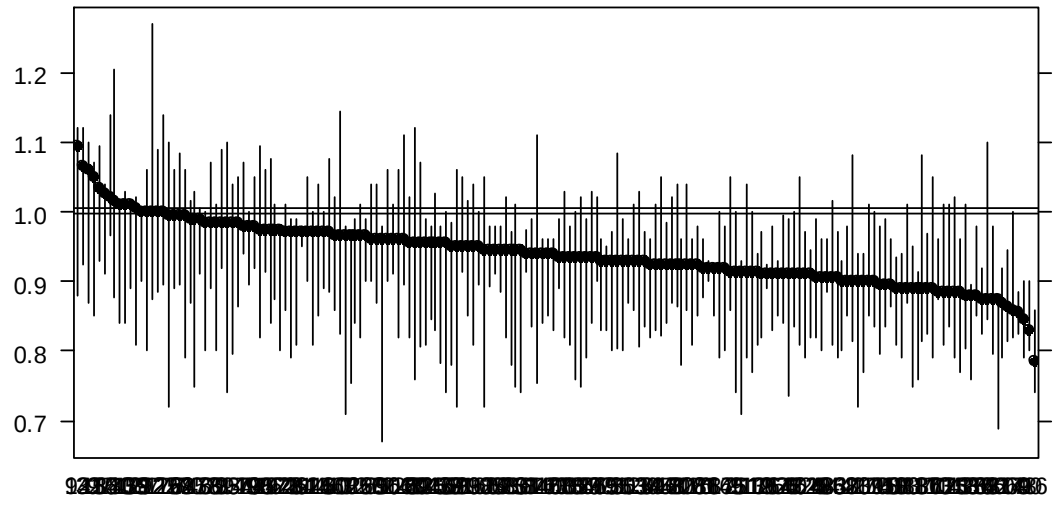

Supplementary Fig. S3.11. Bootstrapped (R=999) medians and 95% confidence intervals for the 180 Treatments (increasing). Dots are the bootstrapped median estimates, vertical lines are

the bca 95% confidence intervals for the median, horizontal lines are the bca 95% confidence intervals for control observations (R=999).

We can identify the mixtures whose 95% confidence intervals do not overlap with those of control group (those mixtures with an individually statistically significant effect with respect to control group (alpha = 0.05). For this, it is necessary to source the function "overlap.fun" from "overlap.fun.R":

```
> #calculate the number of mixtures which do not overlap with control
95%ci.
> #"overlap.fun" takes two arguments (dataset, control)
> y<-overlap.fun(all_GSA_MED.plot, boot.ci95.GSA_CONT)# number of mixt
ures whose ic.95% do not overlap with those of control
> nrow(y[y$ci.overlap=="FALSE",])
[1] 67
> y.false<-y[y$ci.overlap=="FALSE",] #print the mixtures statistically
significantly (alpha=0.05) from control obervations
> head(y.false[order(y.false$est),])
    group     lower   est upper ci.overlap
16     16 0.7400000 0.785 0.860       FALSE
90     90 0.8000000 0.830 0.900       FALSE
43     43 0.7900000 0.845 0.900       FALSE
69     69 0.8250000 0.855 0.885       FALSE
104   104 0.8150000 0.865 0.945       FALSE
127   127 0.7900776 0.870 0.920       FALSE
```

The number of mixtures significantly different from control group is 67, the most potent mixture is mixture 16.

2.2.2 Generating the GSA_MIX_MEDIAN.csv dataset

To generate the "GSA_MIX_MEDIAN.csv" we take advantage of the architecture of the GSA.csv dataset: the first 180 rows correspond to the observations corresponding to the 180 mixtures of the Experiment 1. To generate the GSA_MIX_MEDIAN data.frame we just select from the GSA_MIX data.frame rows 1:180 (the 180 mixtures) and columns 1:38 (the independent variables). Then we merge them by "treatment" with the "x" dataset which contains the bootstrapped median effects and the 95% confidence intervals of the 180 mixtures

```
> #generating "GSA_MIX_MEDIAN" dataset
> #Finally we can generate GSA_MIX_MEDIAN (a data set including median
Lum values and their ci95%
> #together with all the independent variables)
> GSA_MIX_MEDIAN<-merge(GSA_MIX[1:180,1:38],x,by="Treatment")

write.csv(GSA_EBS_out, file="GSA_EBS_out.csv", row.names=F)
```

General info of the dataset can be found in section 2.1.

2.2.3. Elementary Effects (EEs) Sensitivity Analysis of the GSA_MIX_MEDIAN.csv dataset

The elementary Effects Sensitivity Analysis was computed using "Morris SU (Sampling Uniformity) code" available at http://abe.ufl.edu/carpena/software/SUMorris.shtml. "Morris SU (Sampling Uniformity) code" is a suit of MATLAB functions which allows to perform both, parameter samples for the method of Elementary Effects (EEs) (EE_Sampler_Mapper Package),

and to calculate sensitivity measures from a set of model/experimental outputs according to the method of EEs [9] (EE_SensitivityMeasures_Package) [10].

The process involves 4 steps:

(1) Definition of variables and appropriate probability distribution functions for the input factors
(2) Generation of parameter samples according to the method of EEs
(3) Model evaluation (or biological receptor evaluation in the case of *GSA-QHTS*)
(4) Calculation of sensitivity measures (μ, μ^* and σ)

2.2.3.1. Definition of variables and probability distribution functions for the input factors

EEs method works on discrete levels of input factors [9]. In the present work there were only two groups of variables: the pharmaceutical pollutants (C1 to C16) and the environmental factor "light intensity" (L). C1 to C16 had three levels each (1, 2, 3) consisting in three dose levels: *median of means* (Level 1), *median of maxima* (Level 2) and *maximum of maxima* (Level 3). For Light intensity two levels were chosen (L1 and L2). For further information on the criteria for the selection of these factor levels see **Supplementary Material S2**. A discrete uniform (DU) probability distribution was chosen to describe probability distribution of both pharmaceutical pollutants and light intensity. An identical DU probability distribution function with 4 levels (0.25 probability) was chosen for all the PPCPs (C1 to C16), while DU probability distribution function with 2 levels (0.5 probability) was chosen for light intensity. DU probability distributions were chosen since they are used as a pragmatic solution when no or scarce information is available on the true probability distributions of input factors [10]. The "New sample Generation" function of the "statistical preprocessor" utility of Simbab v2.2 software (freely available at https://ec.europa.eu/jrc/en/samo/simlab) was used to define the input factors and to assign the probability distributions. This information was stored in a '*.fac' file which contained the number of parameters (NumFact), the default distribution truncation values and the distribution type and distribution characteristics for each parameter as required by EE_Sampler_Mapper Package. In our case, the file is named "GSA_QHTS.fac" available at https://figshare.com/authors/Ismael_Rodea/624240.

2.2.3.2. Generation of parameter samples for the method of EEs

EE_Sampler_Mapper Package is a set of MATLAB functions that generate parameter samples for the method of Elementary Effects/Morris method [9]. The function 'Fac_Sampler.m' generates parameter samples in unit hyperspace and then transforms them according to the specified probability distributions. For further theoretical details see [10,11]

'Fac_Sampler.m' has the following Syntax:

[Factor_Samples] = Fac_Sampler(facfile,SS,OvrSamSiz,NumLev,NumTraj)

Where

(1) *facfile*: this is '*.fac' file which shall contain following information
  (a) number of parameters (NumFact)
  (b) default distribution truncation values
  (c) distribution type and distribution characteristics for each parameter

(Generated in the previous step)

(2) *SS*: Sampling Strategy. In the present work, the Method of enhanced sampling for uniformity (eSU) was used.

(3) *OvrSamSize*: Oversampling Size. For SU and eSU an OverSamSize > 1000 is recommended. In the present work a oversampling size:1000 was used
(4) *NumLev*: Number of parameter levels. In EE literature various values for number of levels have been suggested. However, standard practice is to use even number of levels usually 4, 6 or 8. For SU and eSU by default NumLev = 4.

(5) *NumTraj*: Number of trajectories to be generated. In EE literature recommended value for number of trajectories vary from as little as 2 to as large as 100. In our case, *NumTraj* = 10.

(Extended information on EEs method can be found in [10]).

'Fac_Sampler.m' function generates a "Factor_Sample.xlsx" file in which each column corresponds to a factor, and in which factor name is specified on the first row. In addition, a FacSamChar.txt file is generated including the characteristics used for generating the sample:

First Line: Sampling Strategy – OT, MOT, SU or eSU
Second Line: Oversampling Size
Third Line: Number of levels
Fourth Line: Number of trajectories
Fifth Line: Number of factors "Factor_Sample.xlsx" and "FacSamChar.txt"

In or case "FacSamChar.txt" and "GSA_QHTS_sam.xlsx" available at https://figshare.com/authors/Ismael_Rodea/624240.

2.2.3.3. Model evaluation (or biological receptor evaluation in the case of GSA-QHTS)

Generally speaking, studied model output should be evaluated for all the input factors' combinations present in "Factor_Sample.xlsx". In *GSA-QHTS*, the selected biological receptor measured end-point (in our case bioluminescence of *Anabaena* CPB4337) is evaluated in all the experimental combinations defined in "Factor_Sample.xlsx". In our case, the 180 mixtures distributed among the two light intensity levels. The result of this evaluation is the response of *Anabaena* CPB4337 to the 180 PPCP mixtures and light conditions. These data are in fact stored in "GSA.csv" file, and summarized as median of the responses in the GSA_MIX_MEDIAN dataset. For the purpose of the present analysis, GSA_MIX_MEDIAN$est.med was stored as "GSA_QHTS_out.csv" and transformed to "*.xlsx" and saved as "GSA_QHTS_out.xlsx".

2.2.3.4. Experimental tolerance in the estimation of median effects of the 180 mixtures

GSA analysis is built on unique values of a "model output". In the present study, the median of the bioluminescence values across the 6 independent experiments were used as central measure estimate of the sample median. With $n = 6$, the tolerance (T) in the estimation of the population true median is calculated as follows:

$$N = Z^2_{0.5\alpha}\, \sigma^2/d^2 \qquad (1)$$ [12]

Where N is the sample size, $Z_{0.5\alpha}$ is the normalized difference from the mean

If we consider the distance d in terms of σ; $d = \delta \cdot \sigma$; by rearrange:

$$\delta = (Z^2_{0.5\alpha}/N)^{1/2} \qquad (2)$$

For an alpha = 0.05; $Z_{0.5\alpha} = 1.960$

$\delta = (1.960^2/N)^{1/2}$ (3)

For $N = 6$; $\delta = 0.8001666$

Therefore, median bioluminescence for the treatments are estimated with a tolerance T = 0.8 *sd*

To calculate the tolerance in the estimation of median bioluminesnce for the different treatments:

```
> x<-split(GSA[,40], GSA$Treatment)
> x.sds<-summary(sapply(x, sd, simplify = TRUE))
> x.sds<-sapply(x, sd, simplify = TRUE)
> x.tol<-x.sds*0.8
```

```
> hist(x.tol, xlim= c(0.01, 0.2), xlab= "tolerance", main= NULL)
> boxplot(x.tol, ylim= c(0.01, 0.2))
> median(x.tol, na.rm = TRUE)
[1] 0.07127038
> summary(x.tol)
   Min. 1st Qu.  Median    Mean 3rd Qu.    Max.    NA's
0.02112 0.05439 0.07127 0.07324 0.08938 0.19640       2
> abline(h=c(0.0712,0.08938), lty=2)
> text(0.67,0.08, "50%, Median = 0.0727")
> text(0.67,0.1, "75%, 3rd Qu. = 0.0893")
```

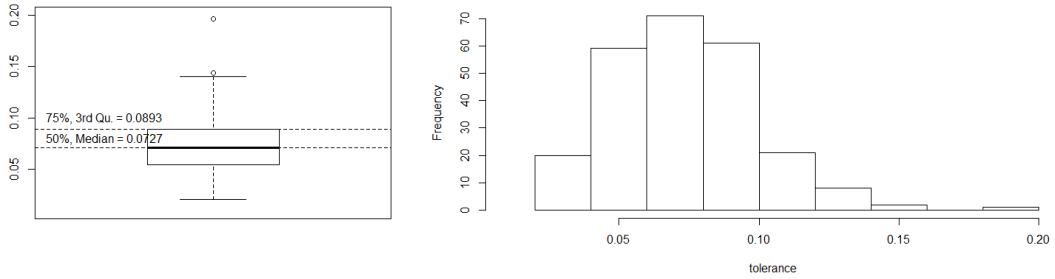

Fig. S3.12 (A) Boxplot and **(B)** Histogram showing the distribution of the Tolerance level in the estimation of median values for "lum" for the 180 treatment.

Therefore, we have a median tolerance (T) in the estimation of true medians for the treatments of 0.0727 bioluminescence relative units. And we estimate the 75% of the treatment effects with a tolerance equal or better than 0.08938.

2.2.3.5. Calculation of sensitivity measures (μ, μ* and σ)

To compute elementary effects Morris [9] proposed to sample *t* random trajectories across the *k*-dimensional space of the input factors, varying one factor at a time at *r* discrete levels of the input factors probability distributions. For each factor ($i = 1,k$) and level ($j = 1,r$), *QHTS* generated an experimental output value *Y*. A factor's elementary effect ($u_{j,i}$) is computed as:

$$u_i = \frac{Y\left(x_1,...,x_i+\Delta x_i,...,x_k\right)-Y\left(x_1,...,x_k\right)}{\Delta x_i} \quad (1)$$

For each factor, three sensitivity measurements are computed: μ*:* the mean of the elementary effects, μ*: the mean of the absolute value of the elementary effects, and σ: the standard deviation of the elementary effects. μ* and μ estimate the overall direct (first-order) effect of a factor. σ estimates the higher-order characteristics of the parameter. Although elementary effects (u_i) are local measurements, μ, μ* and σ are considered global measurements since they are independent of the specific points of computation [6]

For this we used the EE_SensitivityMeasures_Package, which is a is a set of Matlab functions that calculates sensitivity measures for the method of Elementary Effects/Morris method [9], available at http://abe.ufl.edu/carpena/software/SUMorris1.shtml.

'EE_SenMea_Calc.m' is the main function that user needs to call from MATLAB command line. Calculated measures include modified sensitivity measures - μ* and σ and original measure μ proposed by Morris [9].

The function´s syntax is as follows:

EE_SenMea_Calc ('Factor_Sample.xlsx ',' Factor_Sample.txt',' Factor_Sample_Output.xlsx')

Inputs:
(1) *Fac_Sam_File*: This is an '*.xlsx' file containing factor/parameter samples. This file is generated by SU *Fac_Sampler* package for factor sample generation. In our case "GSA_QHTS_sam.xlsx"

(2) *Fac_Sam_Char*: This is a text '*.txt' file which contains following information
(a) Sampling Strategy (line 1)
(b) Over Sampling Size (line 2)
(c) Number of factor levels (line 3)
(d) Number of trajectories (line 4)
(e) Number of factors (line 5)

This file is generated along with 'Factor_Sample.xlsx' file by Factor_Sampler_Mapper package for factor sample generation. In our case: "FacSamChar.txt"

(3) *Mod_Out_File*: This is an '*.xlsx' file containing model outputs arranged column-wise. Output names should be specified in the first row. In our case, "GSA_QHTS_out.xlsx", variable name: "emp.Lum"

EE_SenMea_Calc() generates an "*EE_SA_Measures.txt" file which includes* Sensitivity measures based on the method of Elementary for each model input. In our case "EE_SA_Measures.txt" available also as *.csv file: "GSA_Morris_S_MedianLum.csv".

2.2.3.5. μ^* - σ and μ - σ Cartesian Plots

The visualization of the dataset and the plots was performed in R:
CODE LOCATION: orders to do the analysis and plots presented in this section are in the R script named "Script-GSA_MEDIAN.R"

```
> #SECTION 2. MORRIS SCORES ANALYSIS AND PLOTS
>
> ##This scripts DO NOT PERFORM EEs Analysis. Code and intructions to
do it are available
> #at: http://abe.ufl.edu/carpena/software/SUMorris1.shtml
> #The present code is intended to explore results from EEs and produc
e the plots
>
> setwd(Dir.data)# setwd to the folder
> Morris.Scores<-read.csv(file = "GSA_Morris_S_MedianLum.csv", sep =";
", dec =".")
> colnames(Morris.Scores) <-c("facname","muS","mu","sigma" )
> attach(Morris.Scores)
> Morris.Scores<-(Morris.Scores[order(muS),])#ordering by mu* increasi
ng
> detach(Morris.Scores)
> Morris.Scores
```

```
   facname    muS      mu  sigma
13     C13 0.0357 -0.0092 0.0419
8       C8 0.0562  0.0119 0.0757
15     C15 0.0562  0.0457 0.0497
9       C9 0.0576  0.0180 0.0714
12     C12 0.0596 -0.0327 0.0657
17      L1 0.0632  0.0324 0.0685
7       C7 0.0654  0.0294 0.0797
11     C11 0.0697 -0.0360 0.0779
2       C2 0.0698  0.0388 0.0817
6       C6 0.0755 -0.0045 0.0911
1       C1 0.0770  0.0238 0.1111
14     C14 0.0778  0.0184 0.1038
4       C4 0.0809 -0.0260 0.0986
5       C5 0.0847 -0.0494 0.0841
10     C10 0.0857 -0.0525 0.0974
3       C3 0.0962  0.0652 0.1097
16     C16 0.0992 -0.0548 0.1016
```

Getting the μ^* - σ plot:

```
> #mu*-sigma EEs plot
> plot(Morris.Scores$muS, Morris.Scores$sigma, xlim= c(0, 0.12), ylim=
c(0, 0.12),
+      cex=1.2, pch= 16)
> text(Morris.Scores$muS[10:17], Morris.Scores$sigma[10:17], labels= M
orris.Scores$facname[10:17], cex = 0.7, pos=4, offset=0.4) #texting on
ly important factors
> text(Morris.Scores$muS[c(1,3)], Morris.Scores$sigma[c(1,3)], labels=
Morris.Scores$facname[c(1,3)], cex = 0.7, pos=4, offset=0.4)# #texting
the two less important factors
> abline(h=c(0.02, 0.04, 0.06, 0.08, 0.1, 0.12), lty=3, lwd=0.5)
> abline(v=c(0.02, 0.04, 0.06, 0.08, 0.1, 0.12), lty=3, lwd=0.5)
> abline(0, 1,lty=1, lwd=1.5, col = "black")# drowing the 1:1 line of
interacting systems
```

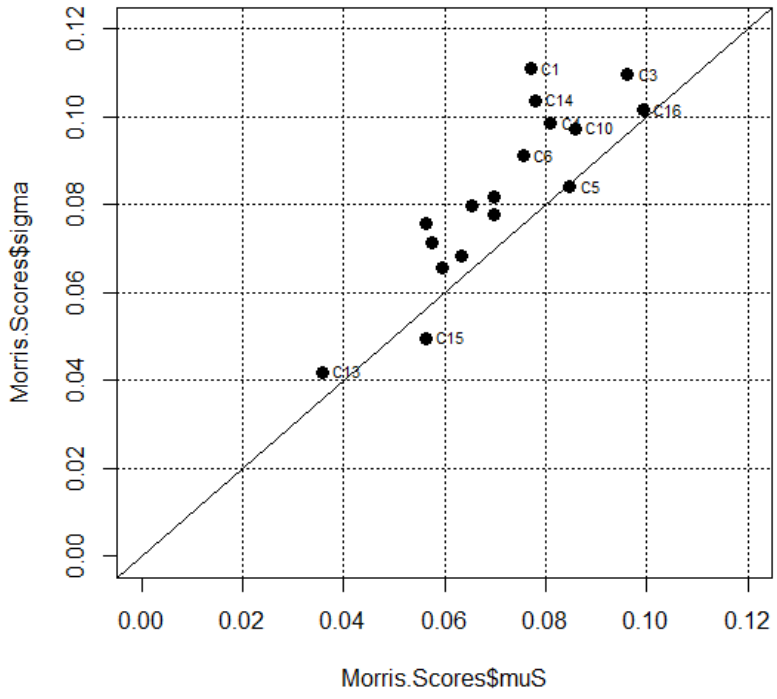

Supplementary Fig. S3.13. EEs $\mu*$ - σ plot for the 17 studied input factors (16 PPCPs and Light Intensity). The straight line is the 1:1 reference which defines the transition to non-linear/non –additive systems

Supplementary Fig. S3.13 presents the Morris sensitivity estimates $\mu*$ (the mean of the absolute value of the elementary effects of each input factor) in the *x-axis*, and σ (the standard deviation of the elementary effects of each input factor) in the *y-axis*. $\mu*$ informs on the global importance (first order plus higher order effects) of each input factor in the context of all other input factors present, while σ estimates the specific contribution of higher order effects of each input factor (non-linearities and interactions) [10,11]. The straight line in the plot delimited the transition between additive/linear systems (input factors below the straight line) and non-linear/non-additive systems. When input factors are located mainly below the straight line: the system is dominated mainly by first order effects, therefore the system is linear/additive. When input factors are located both above and below the straight line, the system is mixed with some factors contributing linearly and others with important non-linear/non-additive contributions. Finally, when input factors located mainly above the straight line, the system is dominated by higher order effects of the input factors. From **Supplementary Fig. S3.13**, it is clear that the *Anabaena* CPB4337 response to low dose mixtures of PPCPs is not dominated by linear/additive effects, but by relevant higher order contributions of the input factors.

The rank of importance of the input factors is usually established based on $\mu*$ [6] since it is an absolute value indicator and therefore, contributions of opposing sign when estimating u_i are not cancelled (main criticism in using μ for raking importance as originally proposed by Morris [9].

Ranking factor importance (ranked-$\mu*$ dotplot):

```
> library(Hmisc)
> dotchart2(Morris.Scores$muS,labels=Morris.Scores$facname, horizontal
= FALSE,dotsize = 2, lty=2, lwd=2, xlab="mu*", ylab= "Factor", gcolor=
"black", cex.axis=1.2)
> abline(h=0.072,lty=3, lwd=2, col = "red")
> abline(h=0.054,lty=3,lwd=2, col = "red")
> abline(h=0.087,lty=3, col = "red")
```

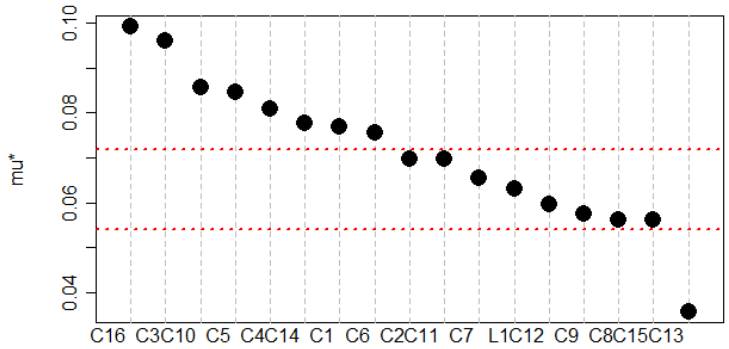

Supplementary Fig. S3.14. Ranked input factors by importance (μ∗). The arbitrary limits for important, moderately important and non-important factors is presented as red dashed straight lines

Supplementary Fig. S3.14 showed input factors ranked based on their importance (μ∗). we established an arbitrary value for "important" factors at μ∗ = 0.072, as well as that for

non-important factors at 0.054. Three groups of input factors can be identified according to their importance: "important" input factors (in order of importance based on $\mu*$): C16 (CARBA), C3 (FURO), C10 (ERY), C5 (HYDRO), C4 (GEM), C14 (VENLA), C1 (ATE), C6 (DICLO) and. "Moderately important" input factors: C9 (PARA), C12 (NICO), C8 (KETO), L (Light) and C15 (PRIM). Non-contributing input factors: C13 (CAFE).

Getting the μ - σ plot:

```
> #mu-sigma EEs plot
> plot(Morris.Scores$mu, Morris.Scores$sigma, xlim= c(-0.08, 0.08), yl
im= c(0, 0.12),
+      cex=1.2, pch= 16)
> text(Morris.Scores$mu[10:17], Morris.Scores$sigma[10:17], labels= Mo
rris.Scores$facname[10:17], cex = 0.7, pos=4, offset=0.4)
> text(Morris.Scores$mu[c(1,3)], Morris.Scores$sigma[c(1,3)], labels=
Morris.Scores$facname[c(1,3)], cex = 0.7, pos=4, offset=0.4)
>
> abline(h=c(0.02, 0.04, 0.06, 0.08, 0.1, 0.12), lty=3, lwd=0.5)
> abline(v=c(-0.08, -0.02, -0.04, -0.06, 0.02, 0.00, 0.04, 0.06, 0.08,
0.1, 0.12), lty=3, lwd=0.5)
> abline(0, 1.5,lty=1, lwd=1.5, col = "red")
> abline(0, -1.5,lty=1, lwd=1.5, col = "red")
```

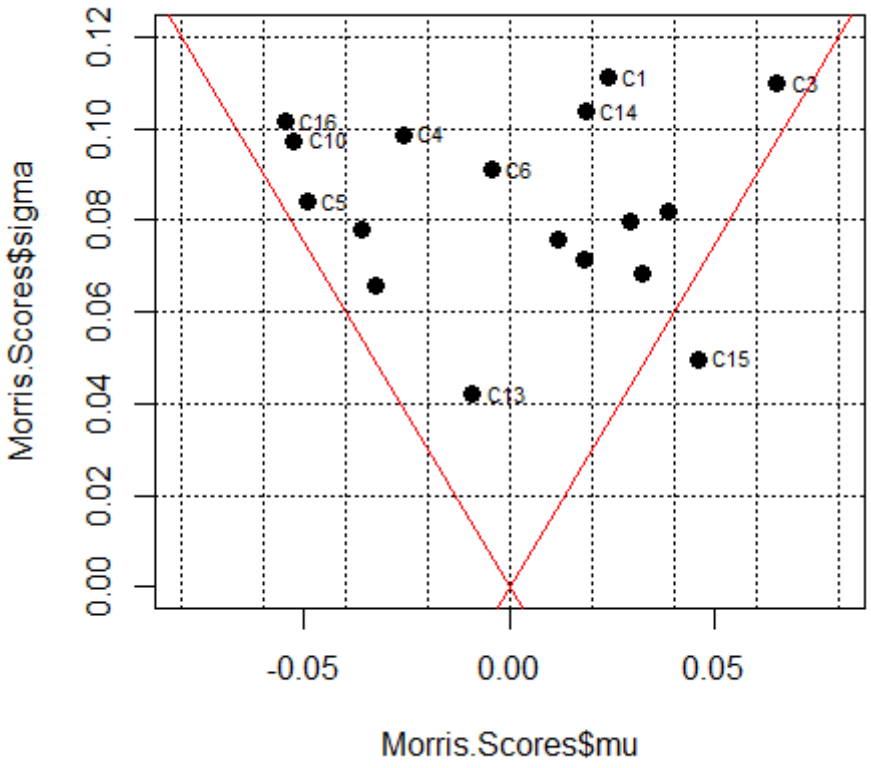

Supplementary Fig. S3.15. EEs μ - σ plot for the 17 studied input factors (16 PPCPs and Light Intensity). The straight lines are the $\pm 2 \cdot \sigma$ limit for additive systems.

Supplementary Fig. S3.15 shows Morris μ–σ Cartesian plots, being μ the mean of the elementary effects of the input factors, and σ their standard deviations). μ–σ Cartesian plots allows to identify the overall directionality (if any) of the elementary effects of the input factors.

That is, whether they mainly contribute towards bioluminescence inhibition or hormesis in a consistent way. From the important factors identified in **Supplementary Fig. S3.13,** and based on their μ–σ scores in **Supplementary Fig. S3.15**, C16 (CARBA), C10 (ERY), C4 (GEM) and C5 (HYDRO) globally contributed towards metabolic toxicity ($\mu < 0$), while C3 (FURO), C1 (ATE) and C14 (VENLA) globally contributed to hormesis ($\mu > 0$). C6 (DICLO) with a μ value near to 0, and high σ, had contributions which depended strongly on the other factors present (strong non-linear or interacting effects).

At this point it is interesting to note that the units of μ^*, μ and σ are the same as those of the output variable. They summarized the marginal (differential) variation in the output variable (in this case bioluminescence level) which can be attributed to marginal changes in each input variable. Therefore for example, μ^*, μ, σ parameters for C16 can be interpreted as that C16 marginal changes in dose level produced roughly a mean absolute marginal change in bioluminescence level near 10%, with a standard deviation of near 10%, and a mean change value of near – 5% (bioluminescence inhibition). C10 produced roughly a mean absolute marginal change in bioluminescence level also near 10%, with a standard deviation of near 10% (both C16 and C10 are nearly important explaining mixture effect variation along the 180 mixtures). However C10 presented a mean change value of near + 5% (hormesis). In fact C10 (ERY) is working more as a protecting pharmaceutical in those dose ranges than as a toxicant. Therefore *GSA-QHTS* allows to dissect and integrate important and dynamic information behind the effect or the absence of effect of a mixture [13]

2.2.4. Two-Way ANOVA of selected input factors on the GSA_MIX_MEDIAN dataset

In the present section, we perform the analysis of variance (Two-Way ANOVA) for two different groups of input factors. The first group includes the 8 input factors which got the highest µ*-sigma scores in the EEs sensitivity screening (see **Supplementary Table S3.3** and **Supplementary Fig. S3.14**). These factors are (in decreasing order of importance): C16, C3, C10, C5, C4, C14, C1 and C6. The second group of input factors includes the 8 input factors which got the lowest µ*-sigma scores in the Morris sensitivity screening (see **Supplementary Table S3.3** and **Supplementary Fig. S3.14**). These factors are (in decreasing order of importance): C11, C7, L, C12, C9, C8, C15 and C13.

CODE LOCATION: orders to do the analysis and plots presented in this section are in the R script named "Script-GSA_MEDIAN.R"

```
> GSA_MIX_MEDIAN<-read.csv("GSA_MIX_MEDIAN.csv", header = TRUE, sep=",
")# converting intergers to factors in PPCP levels
> GSA_MIX_MEDIAN<-GSA_MIX_MEDIAN[2:40]
> for (i in seq_along(1:20)){
+         GSA_MIX_MEDIAN[,i]<-as.factor(GSA_MIX_MEDIAN[,i])
+ }
> GSA_MIX_MEDIAN$L<-as.factor(GSA_MIX_MEDIAN$L)# converting L to facto
r
```

To execute the Two-Way ANOVA:

```
#Two-Way ANOVA on the most important factors group
Anov.1 <- (aov(emp.med ~ C16*C3*C10*C5*C4*C14*C1*C6, data=GSA_MIX_MEDI
AN))
Anov.1.s<-Anova(Anov.1, type="III", singular.ok = T)
> Anov.1.s
Anova Table (Type III tests)

Response: emp.med
                              Sum Sq Df F value    Pr(>F)
```

```
(Intercept)                0.000284  1  0.2014  0.654688
C16                        0.001158  2  0.4100  0.664889
C3                         0.004223  2  1.4953  0.229704
C10                        0.004870  2  1.7246  0.184081
C5                         0.003109  2  1.1009  0.337023
C4                         0.010122  2  3.5843  0.031787 *
C14                        0.005169  2  1.8303  0.166282
C1                         0.002980  2  1.0552  0.352376
C6                         0.013154  2  4.6582  0.011884 *
C16:C3                     0.016319  4  2.8893  0.026652 *
C16:C10                    0.006901  3  1.6291  0.188201
C3:C10                     0.013392  4  2.3712  0.058256 .
C16:C5                     0.013520  4  2.3938  0.056316 .
C3:C5                      0.008526  4  1.5096  0.206085
C10:C5                     0.012935  4  2.2902  0.065770 .
C16:C4                     0.006231  4  1.1032  0.360022
C3:C4                      0.002967  4  0.5253  0.717359
C10:C4                     0.001184  4  0.2097  0.932444
C5:C4                      0.005011  4  0.8872  0.475027
C16:C14                    0.002908  4  0.5148  0.725000
C3:C14                     0.013741  4  2.4330  0.053095 .
C10:C14                    0.040096  4  7.0994  5.154e-05 ***
C5:C14                     0.007820  4  1.3846  0.245626
C4:C14                     0.000626  1  0.4436  0.507108
C16:C1                     0.011567  3  2.7308  0.048477 *
C3:C1                      0.003387  2  1.1995  0.306115
C10:C1                     0.004952  2  1.7537  0.178990
C5:C1                      0.000545  1  0.3863  0.535821
C4:C1                      0.002852  1  2.0198  0.158715
C14:C1                               0
C16:C6                     0.015191  3  3.5862  0.016798 *
C3:C6                      0.003016  2  1.0681  0.347961
C10:C6                     0.019108  3  4.5111  0.005391 **
C5:C6                                0
C4:C6                                0
C14:C6                               0
C1:C6                                0
…
…
Residuals                  0.127077 90
---
Signif. codes:  0 ‘***’ 0.001 ‘**’ 0.01 ‘*’ 0.05 ‘.’ 0.1 ‘ ’ 1
```

```
> plot(Anov.1)
```

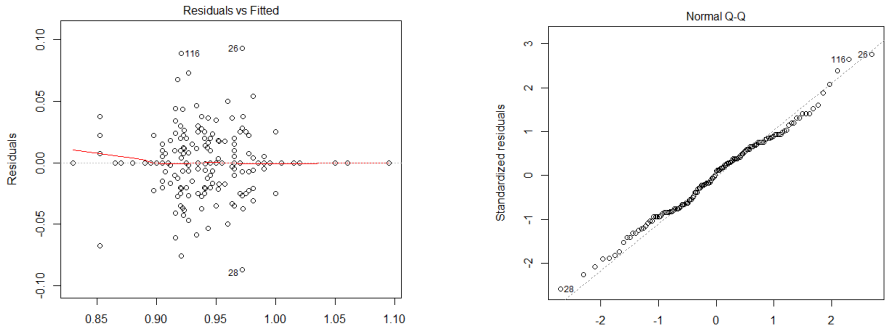

Supplementary Fig. S3.16. Diagnostic plots of **Anov.1** model.

The Two-Way ANOVA for the “Non-Important” factors set:

```
Anov.2 <- (aov(emp.med ~ C11*C7*L*C12*C9*C8*C15*C13, data=GSA_MIX_MEDI
AN))
Anov.2.s<-Anova(Anov.2, type="III", singular.ok = T)
```

```
> Anov.2.s
Anova Table (Type III tests)

Response: emp.med
                              Sum Sq Df F value  Pr(>F)
(Intercept)                 0.009587  1  4.6707 0.03334 *
C11                         0.004440  2  1.0816 0.34343
C7                          0.003809  2  0.9279 0.39913
L                           0.000002  1  0.0011 0.97353
C12                         0.006714  2  1.6356 0.20058
C9                          0.000026  2  0.0062 0.99377
C8                          0.004087  2  0.9956 0.37354
C15                         0.006657  2  1.6216 0.20330
C13                         0.002252  2  0.5487 0.57962
C11:C7                      0.002950  2  0.7186 0.49020
C11:L                       0.002574  2  0.6269 0.53654
C7:L                        0.005461  2  1.3302 0.26957
C11:C12                     0.004959  4  0.6040 0.66072
C7:C12                      0.008460  4  1.0304 0.39604
L:C12                       0.004740  2  1.1547 0.31977
C11:C9                      0.001948  4  0.2372 0.91664
C7:C9                       0.008649  4  1.0534 0.38435
L:C9                        0.005268  2  1.2833 0.28214
C12:C9                      0.010447  4  1.2725 0.28673
C11:C8                      0.011087  4  1.3505 0.25754
C7:C8                       0.008427  4  1.0265 0.39806
L:C8                        0.005558  2  1.3540 0.26342
C12:C8                      0.006246  4  0.7608 0.55352
C9:C8                       0.007710  4  0.9391 0.44512
C11:C15                     0.002710  3  0.4402 0.72482
C7:C15                      0.005592  4  0.6811 0.60687
L:C15                       0.008064  2  1.9645 0.14619
C12:C15                     0.008075  4  0.9835 0.42070
C9:C15                      0.002969  4  0.3617 0.83529
C8:C15                                0
C11:C13                     0.003747  3  0.6086 0.61115
C7:C13                      0.002032  3  0.3299 0.80371
L:C13                       0.000010  1  0.0047 0.94551
C12:C13                     0.000033  2  0.0081 0.99191
…

…

C16:C3:C10:C5:C4:C14:C1:C6            0
Residuals                   0.127077 90
---
Signif. codes:  0 ‘***’ 0.001 ‘**’ 0.01 ‘*’ 0.05 ‘.’ 0.1 ‘ ’ 1
```

Plotting model diagnostics:

```
Plot(Anov.2)
```

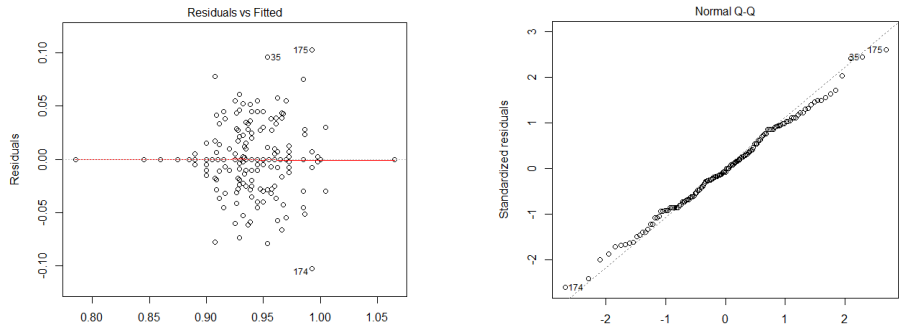

Supplementary Fig. S3.17. Diagnostic plots of **Anov.4** model.

```
> #Power analisys
> #We calculate power for first and second order terms of the Two-Way
ANOVA
> #for the different dfs available (unbalanced experimental design) an
d for
> #the three standard effect sizes according to Cohen (1988)
> #Effect sizes according to cohen
> #small: 0.02
> #medium: 0.15
> #large: 0.35
> #first order terms:
> #dfs: 1, 2
> #second order terms:
> #dfs: 1,2,3,4
> #u = degrees of freedom for numerator (Dfs of the term)
> #v = degrees of freedomfor denominator a*b(n-1); levels(A)=3, levels
(B)=3, n=180/(3*3)
> #f2
> #effect size
> cohen.ES(test = "f2", size = "small")

     Conventional effect size from Cohen (1982)

           test = f2
           size = small
    effect.size = 0.02

> cohen.ES(test = "f2", size = "medium")

     Conventional effect size from Cohen (1982)

           test = f2
           size = medium
    effect.size = 0.15
```

Cohen effect size small (f2 = 0.02)

```
> pwr.f2.test(u=4, v=3*3*((180/9)-1), f2 = 0.02, sig.level = 0.05, pow
er = NULL)

     Multiple regression power calculation

              u = 4
              v = 171
             f2 = 0.02
      sig.level = 0.05
          power = 0.2761652
```

Cohen effect size small (f2 = 0.065)

```
> pwr.f2.test(u=4, v=3*3*((180/9)-1), f2 = 0.065, sig.level = 0.05, po
wer = NULL)

     Multiple regression power calculation

              u = 4
              v = 171
             f2 = 0.065
      sig.level = 0.05
          power = 0.7676784
```

Cohen effect size small (f2 = 0.15)

```
> pwr.f2.test(u=4, v=3*3*((180/9)-1), f2 = 0.15, sig.level = 0.05, pow
er = NULL)

     Multiple regression power calculation
```

```
              u = 4
              v = 171
             f2 = 0.15
      sig.level = 0.05
          power = 0.9910435
```

Despite the power is less than 0.8 for the conventional "small effect size" (f2=0.02), it is however high for a f2 value slightly higher (f2=0.065), power = 0.7676. Power is very good for medium conventional effect sizes (equivalent to *d* = 0.3 sd).

2.2.5. Exploring elementary effects of low dose mixtures experimental design

This section includes orders to generate the plots in manuscript´s **Fig. 3.1**. We are going to explore composition and PPCPs dose distributions in the 180 low dose mixtures generated by the EEs input factor samples (section 2.2.3). For convenience we will start working on the data from the GSA_MIX_MEDIAN data set.

CODE LOCATION: orders to do the analysis and plots presented in this section are in the R script named "Script-GSA_MEDIAN.R"

First we isolate isolate the "unique" dose levels of each PPCP with a for loop:

```
> #This section requires packages "reshape2" and "ggplot2"
>
> library(reshape2)
> library(ggplot2)
>
> Factors.conc<-GSA_MIX_MEDIAN[,21:36]#taking the factor´s concentrati
on
> Factors.levels<-GSA_MIX_MEDIAN[,5:20]#taking the factor´s levels
>
> for (i in seq_along (1:16)) {
+         a<-paste("C",i, sep="")
+         b<-unique(Factors.conc[,i])#selecting unique concentrations
+         b<-b[order(b)]
+         assign(a,b)
+         }
> #generating a data.frame (conc.L which includes for each PPCP the "v
ariable" colum, each
> #conc. level ("Level" colum), and the actual concentration ("value"
colum)))
> Level<-(c(1,2,3))
> conc<-as.data.frame(cbind(Level, C1, C2, C3, C4, C5, C6, C7, C8, C9,
C10, C11, C12, C13, C14, C15, C16))
> conc$Level<-as.factor(conc$Level)
> colnames(conc)<-c("Level","1","2","3","4","5","6","7","8","9","10","
11","12","13","14","15","16")
> conc.L<-melt(conc)
Using Level as id variables
> conc.L$variable<-as.numeric(conc.L$variable)
```

Generating the concentration level plot for the 16 PPCPs (**Fig. 3.1a** of the manuscript):

```
> #concentation level plot
> plot<-ggplot(conc.L, aes(value, variable))
> plot<-plot + scale_y_continuous(breaks = c(1,2,3,4,5,6,7,8,9,10,11,1
2,13,14,15,16))
> plot<-plot + geom_vline(xintercept = c(10, 100, 1000, 10000, 100000)
, linetype="longdash")
> plot<-plot + geom_hline(yintercept = 1:16, linetype="longdash", colo
ur="grey")
> plot<-plot + geom_point(size=7, shape=22, colour="black", label=FALS
E, aes(fill=factor(Level)))
```

```
> plot<-plot + scale_x_log10(limits=c(8, 110000), breaks = c(10, 100,
1000, 10000,100000))
> plot<-plot + theme_bw()
> plot<-plot + theme(panel.grid.major = element_blank(), panel.grid.mi
nor = element_blank())
> plot<-plot + scale_fill_grey(start=0.8, end=0.2)
> plot
```

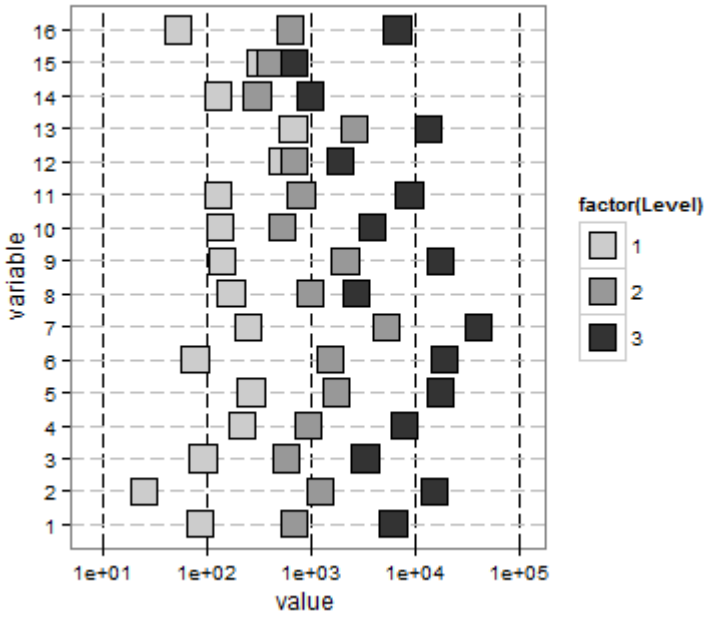

Supplementary Fig. S3.18. Dose ranges of PPCPs (ngL-1). "Variable" are the 16 PPCPs C1 to C16, and "factor(Level)" are the three discrete dose levels (1, 2, 3) median of means, mean of maxima and maximum of maxima for each PPCP.

As can be seen in **Supplementary Fig. S3.18** the doses of the PPCPs ranged along near three orders of magnitude (from near tens/hundreds of ngL^{-1} to near hundreds/thousands of ngL^{-1}). Mean inter-level variation was around 1 order of magnitude.

Frequency distribution of total dose of the 180 mixtures:

```
hist(GSA_MIX_MEDIAN$X.16)# The frequency distribution of the total sum
of PPCPs (ng/L) in the 180 mixtures
```

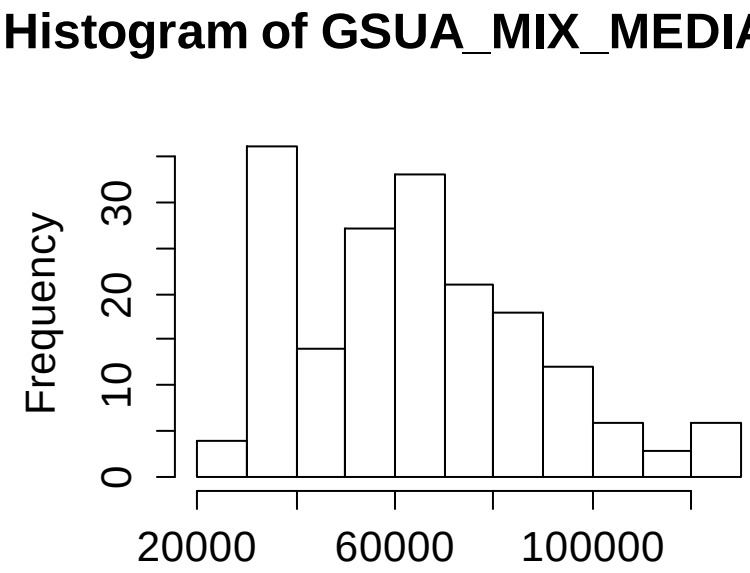

Fig. S3.19. Histogram of the frequency distribution of the total (summation) of the 16 PPCPs in the 180 mixtures

Exact composition of the 180 mixtures can be found in **Supplementary Material S4**. Total dose frequency of PPCPs presented a bimodal frequency with a first mode occurring at near 30000 ngL^{-1} and a second one at 65000 ngL^{-1}. The Q_{25} and Q_{75} of total mixture dose were 42710 ngL^{-1} and 79970 ngL^{-1}, respectively. The minimum and maximum were 25490 ngL^{-1} and 123500 ngL^{-1}, respectively. Total dose frequency distribution resulted slightly biased towards typically reported maximum of occurrence [14,15] as a drawback of the maximization of inter level distance. This is a drawback of EEs Method, since it works on marginal changes in the output variable, it needs factor levels that actually can produce marginal changes in the output variable when input level changes from level to level.

Generating rose plots:

For this we will use "ggplot2" package

```
> #Rose plots
> #Rose plot for frequencies of levels of the 16 PPCPs in the 180 mixt
ures
> #Now we work with the levels of the PPCPs
> GSA_Lev<-cbind(GSA_MIX_MEDIAN[,1], GSA_MIX_MEDIAN[,5:20])
> colnames(GSA_Lev)<-c("Mix","C1","C2","C3","C4","C5","C6","C7","C8","
C9","C10","C11","C12","C13","C14","C15","C16")
>
> for (i in 2:17) {
+         GSA_Lev[,i]<-as.numeric(GSA_Lev[,i])
+ }
> GSA_Lev_melt<-melt(GSA_Lev)
Using Mix as id variables
> GSA_Lev_melt$Mix<-as.integer(GSA_Lev_melt$Mix)
> GSA_Lev_melt$value<-as.factor(GSA_Lev_melt$value)
>
> plot<-ggplot(GSA_Lev_melt, aes(variable, fill=value))
> plot<-plot + geom_bar()
> plot<-plot + coord_polar()
> plot<-plot + theme_bw()
```

```
> plot<-plot + theme(panel.grid.major = element_blank(), panel.grid.mi
nor = element_blank())
> plot<-plot + scale_fill_grey(start=0.8, end=0.2)
> plot
```

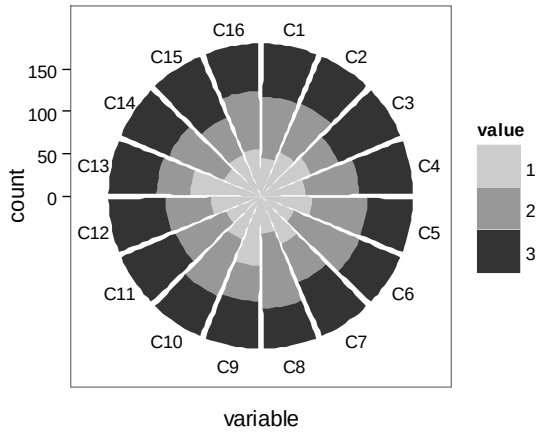

Supplementary Fig. S3.20. Rose plot presenting the relative abundance (counts) of each PPCP (variable) and level (value) of each PPCP in the 180 mixtures

The Roseplot for concentrations:

```
> #Roseplot for concentrations

>
> GSA_Conc<-cbind(GSA_MIX_MEDIA
> colnames(GSA_Conc)<-c("Mix","C1","C2","C3","C4","C5","C6","C7","C8",
"C9","C10","C11","C12","C13","C14","C15","C16")
>
> #install.package(plyr)
> library(plyr)
>
> GSA_Conc_melt<-melt(GSA_Conc)
Using Mix as id variables
> GSA_Conc_melt$Mix<-as.integer(GSA_Conc_melt$Mix)
> mm <- ddply(GSA_Conc_melt, "variable", summarise, value = mean(value
))# mean concentration of
> #PPCPs in the 180 mixtures
> #GSA_Conc_melt$value<-as.factor(GSA_Conc_melt$value)
> plot<-ggplot(mm, aes(x = factor(variable), y = value))
> plot<-plot + geom_bar(stat = "identity",colour="black", aes(fill=fac
tor(variable)))
> plot<-plot + scale_fill_grey(start = 0.0, end = 1.0)
> plot<-plot + coord_polar()
> #plot<-plot + scale_y_continuous(breaks = c(750, 9000, 16000))
> plot<-plot + scale_y_log10(limits=c(1, 20000))
> plot<-plot + theme(axis.text=element_text(size=12))
> plot<-plot + theme_bw()
> #plot<-plot + theme(panel.grid.major = element_blank(), panel.grid.m
inor = element_blank())
> #plot<-plot + scale_fill_grey()
> plot
```

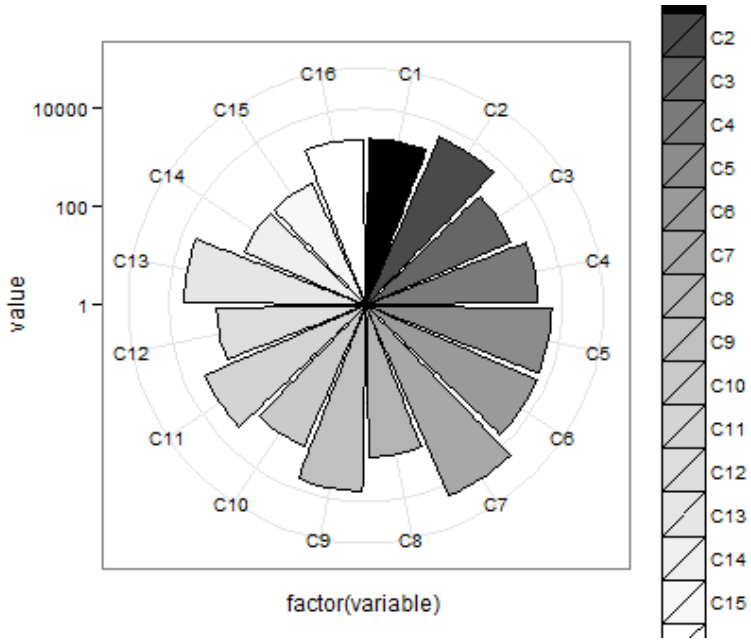

Supplementary Fig. S3.21. Rose plot presenting the mean concentration (value) of each PPCP (variable) in the 180 mixtures

Supplementary Fig. S3.21 and Supplementary Fig. S3.20 summarized as rose plots the factor and level frequency distribution of each PPCP in the 180 mixtures, and the mean concentration of each PPCP in the 180 mixtures respectively. As can be seen in **Supplementary Fig. S3.21**, frequency distributions of input factors and levels were near homogeneous along the 180 mixtures due to the DU sampling probability distribution. However, since each level of the DU distribution corresponded to a different concentration level reassembling actual environmental concentration of each PPCP, the mean dose distribution of the 16 PPCPs along the 180 mixtures ranged from ngL^{-1} to $mgL^{-1.}$

3. ANTIBIOTIC_EC50.

In the present section Concentration Addition (CA) model is used to predict mixture effect of the 180 mixtures based on individual chemical information only [16]. Specifically, we will model the expected bioluminescence level of *Anabaena* CPB4337 exposed to the 180 mixtures considering that (1) only ERY (C10), OFLO (C11) and VELA (C14) will contribute to mixture effect. (2) They will contribute to total mixture effect in accordance to the predictive form of CA equation [17]. For this, individual dose-response curves should be first experimentally assessed and fitted by a dose-response model. Experimental dose-response data for *Anabaena* CPC4337 exposed to ERY, OFLO and VENLA individually is available in the ANTIBIOTIC_EC50.csv dataset.

3.1 Summary of the ANTIBIOTIC_EC50.csv data set

3.1.1 Variables

"ANTIBIOTIC_EC50.csv" includes 204 observations of 11 independent variables (both numeric and factors) and 1 dependent variable (numeric). A summary of the variables included in the ANTIBIOTIC_EC50.csv can be found in **Supplementary Table S3.5.**

Supplementary Table S3.5. Summary of observations by "Exp. Group" for ANTIBIOTIC_EC50.csv dataset

n	CONTROL	ERY (C10)	OFLO (C11)	VENLA (C14)	ALL
OBSERVATIONS	72	48	48	36	204

Supplementary Table S3.6. ANTIBIOTIC_EC50.csv dataset.

Var.	Type	Levels	Info.
Exp.	Factor	1	In this case it refers to the median of the 6 raw data
Case	Factor	2	Determine whether the observation is a Control or not
Exp. Group	Factor	2	Determines whether it is an individual or mixture exp.
Treatment	Factor	13	Each different treatments (1 control, 6 ERY, 6 OFLO)
Conc	numeric	-	Concentration of the chemical (mgL^{-1})
C10,C11,C14	Factor	5	Dose level C10 and C11 (mgL^{-1}). Numeric
C10.1,C11.1, C14.1	Numeric	-	Dose level C10 and C11(mgL^{-1}) (as factor)
Lum	Numeric	-	Bioluminescence signal normalized to control values. Control value is 1. A 0.1 difference is equivalent to a 10% variation

Complete information on the dataset can be obtained:

CODE LOCATION: orders to do the analysis and plots presented in this section are in the R script named "Script_CA_Prediction.R"

```
> #1º SECTION: Fitting dose response curves to individual chemicals
> #DATA SET: ANTIBIOTIC_EC50.csv
>
> setwd(Dir.data)# setwd to the folder where you saved "R-DATA" folder
>
> ANTIBIOTIC_EC50<-read.csv("ANTIBIOTIC_EC50.csv", header = TRUE, sep=
";")# converting intergers to factors in PPCP levels
> ANTIBIOTIC_EC50$Exp<-as.factor(ANTIBIOTIC_EC50$Exp)
> ANTIBIOTIC_EC50$Treatment<-as.factor(ANTIBIOTIC_EC50$Treatment)
>
> head(ANTIBIOTIC_EC50)
  Exp    Case Exp.Group Treatment Conc C10 C11 C14 C10.1 C11.1 C14.1       Lum
1   1 CONTROL    CONTROL         0    0   0   0   0     0     0     0 0.9028870
2   1 CONTROL    CONTROL         0    0   0   0   0     0     0     0 0.8535957
3   1 CONTROL    CONTROL         0    0   0   0   0     0     0     0 0.8355839
4   1 CONTROL    CONTROL         0    0   0   0   0     0     0     0 1.1634032
5   1 CONTROL    CONTROL         0    0   0   0   0     0     0     0 1.1147318
6   1 CONTROL    CONTROL         0    0   0   0   0     0     0     0 0.9639565
> tail(ANTIBIOTIC_EC50)
    Exp      Case Exp.Group Treatment Conc C10 C11 C14 C10.1 C11.1 C14.1       Lum
199   1 TREATMENT     VENLA        22  500 500   0   0     0     0   500 0.4640633
200   2 TREATMENT     VENLA        22  500 500   0   0     0     0   500 0.3261596
201   3 TREATMENT     VENLA        22  500 500   0   0     0     0   500 0.2072841
202   4 TREATMENT     VENLA        22  500 500   0   0     0     0   500 0.2650545
203   5 TREATMENT     VENLA        22  500 500   0   0     0     0   500 0.3243946
204   6 TREATMENT     VENLA        22  500 500   0   0     0     0   500 0.2926664
```

3.2. Fitting individual dose-response models

In this section we are going to fit non-linear models to the dose-response data in **"ANTIBIOTIC_EC50.csv"** using "drc" package[18]. The final objective is to be able to estimate the ECx for any desired effect level "x" for C10, C11 and C14.

CODE LOCATION: orders to do the analysis and plots presented in this section are in the R script named "Script_CA_Prediction.R", "GetECx.R"

Loading "drc" package:

```
> # Fitting drms (dose response models for OFLO and ERY)
> #install.packages("drc")
> library("drc")
```

We are going to fit 5 parameters log logistic models (LL.5 model in *drc* package) to the data. # There are many more models available in "drc" for fitting experimental dose-response data. We select 5 parameter log logistic models since they got very high raking in IAC criteria for all the chemicals independently of the marked shape differences among chemicals (see **Supplementary Fig. S3.21**). More advance methods of model selection are available under the function mselect {drc}.

```
> chem.m1<-drm(Lum~Conc, Exp.Group, data = ANTIBIOTIC_EC50, fct=LL.5(f
ixed = c(NA, 0, 1, NA, NA)))
Control measurements detected for level: CONTROL
> #This way we apply the same non-linear regression function to all th
e chemicals
> #we fit just 2 parameters log-logistic models. However more complex
metodology is
> #available using mselect {drc} function
> summary (chem.m1)#information on the fitted model parameters

Model fitted: Generalized log-logistic (ED50 as parameter) (3 parms)

Parameter estimates:

          Estimate Std. Error    t-value p-value
b:C11.1  1.9568758  0.5437764  3.5986771  0.0004
b:C10.1 15.5543716 18.0977688  0.8594635  0.3911
b:C14.1  2.0159007  0.9495947  2.1229063  0.0350
e:C11.1  0.5672540  0.1794415  3.1612192  0.0018
e:C10.1  0.0570027  0.0046396 12.2862086  0.0000
e:C14.1 58.4125839 28.5887256  2.0432035  0.0424
f:C11.1  0.4209126  0.1810373  2.3250049  0.0211
f:C10.1  0.0485195  0.0578798  0.8382811  0.4029
f:C14.1  0.2687619  0.1891828  1.4206464  0.1570

Residual standard error:

 0.09698944 (195 degrees of freedom)

> ##ggplot
> ##Fitting the same models that in chem.m1 but separatelly
> chem.m1.1<-drm(Lum~Conc, data = ANTIBIOTIC_EC50[ANTIBIOTIC_EC50$Exp.
Group=="ERY",], fct=LL.5(fixed = c(NA, NA, 1, NA, NA)))
> chem.m1.2<-drm(Lum~Conc, data = ANTIBIOTIC_EC50[ANTIBIOTIC_EC50$Exp.
Group=="OFO",], fct=LL.5(fixed = c(NA, NA, 1, NA, NA)))
> chem.m1.3<-drm(Lum~Conc, data = ANTIBIOTIC_EC50[ANTIBIOTIC_EC50$Exp.
Group=="VENLA",], fct=LL.5(fixed = c(NA, NA, 1, NA, NA)))
>
> # new dose levels as support for the line
> newdata <- expand.grid(Conc=exp(seq(log(0.0005), log(1000), length=1
00)))
> # predictions and confidence intervals
> pm <- predict(chem.m1.1, newdata=newdata, interval="confidence")
> # new data with predictions chem.m1.1
> newdata$p <- pm[,1]
```

```
> newdata$pmin <- pm[,2]
> newdata$pmax <- pm[,3]
>
> newdata.2 <- expand.grid(Conc=exp(seq(log(0.0005), log(1000), length
=100)))
> # predictions and confidence intervals
> pm.2 <- predict(chem.m1.2, newdata=newdata.2, interval="confidence")
> # new data with predictions chem.m1.2
> newdata.2$p <- pm.2[,1]
> newdata.2$pmin <- pm.2[,2]
> newdata.2$pmax <- pm.2[,3]
>
> newdata.3 <- expand.grid(Conc=exp(seq(log(0.0005), log(1000), length
=100)))
> # predictions and confidence intervals
> pm.3 <- predict(chem.m1.3, newdata=newdata.3, interval="confidence")
> # new data with predictions chem.m1.3
> newdata.3$p <- pm.3[,1]
> newdata.3$pmin <- pm.3[,2]
> newdata.3$pmax <- pm.3[,3]
>
> # plot curve
> library(ggplot2)
>
> ANTIB_GGPLOT<-ANTIBIOTIC_EC50
> nrow(ANTIB_GGPLOT[ANTIB_GGPLOT$Case=="CONTROL",])
[1] 72
> #sampling 6 example control observations
> num<-c(seq(1,72,1))
> set.seed(1000)
> Exam.Cont<-sample(num,6)
> Exam.Cont
[1] 24 54  8 48 36  5
> ANTIB_GGPLOT<-ANTIB_GGPLOT[c(24,54,8,48,36,5,73:204),]
> # need to shift conc == 0 a bit up, otherwise there are problems wit
h coord_trans
> ANTIB_GGPLOT$Conc[ANTIB_GGPLOT$Case == "CONTROL"] <- 0.0005
>
> # plotting the curve
> ggplot(ANTIB_GGPLOT, aes(Conc, Lum)) +
+         geom_point(aes(shape = factor(Exp.Group)), size = 2.5)+
+         scale_shape_manual(values = c(15, 17, 6, 0))+
+         #stat_summary (mapping = aes(group = Exp.Group, shape =Exp.G
roup), fun.data = "mean_sdl", size = .5)+
+         geom_ribbon(data=newdata, aes(x=Conc, y=p, ymin=pmin, ymax=p
max), alpha=0.2) +
+         geom_line(data=newdata, aes(x=Conc, y=p)) +
+         geom_ribbon(data=newdata.2, aes(x=Conc, y=p, ymin=pmin, ymax
=pmax), alpha=0.2) +
+         geom_line(data=newdata.2, aes(x=Conc, y=p)) +
+         geom_ribbon(data=newdata.3, aes(x=Conc, y=p, ymin=pmin, ymax
=pmax), alpha=0.2) +
+         geom_line(data=newdata.3, aes(x=Conc, y=p)) +
+         scale_x_continuous(breaks=c(0.0005,0.001, 0.01,0.1, 1, 10, 1
00)) +
+         scale_y_continuous(breaks=c(0.00,0.25,0.5,0.75,1.00)) +
+         coord_trans(x="log") +
+         theme_bw()+
+         theme(panel.grid.major = element_blank(), panel.grid.minor =
element_blank(), axis.text = element_text(size = 20), axis.title = ele
ment_text(size = 30)) +
+         xlab("Dose (mg L-1)") + ylab("Relative bioluminescence")
```

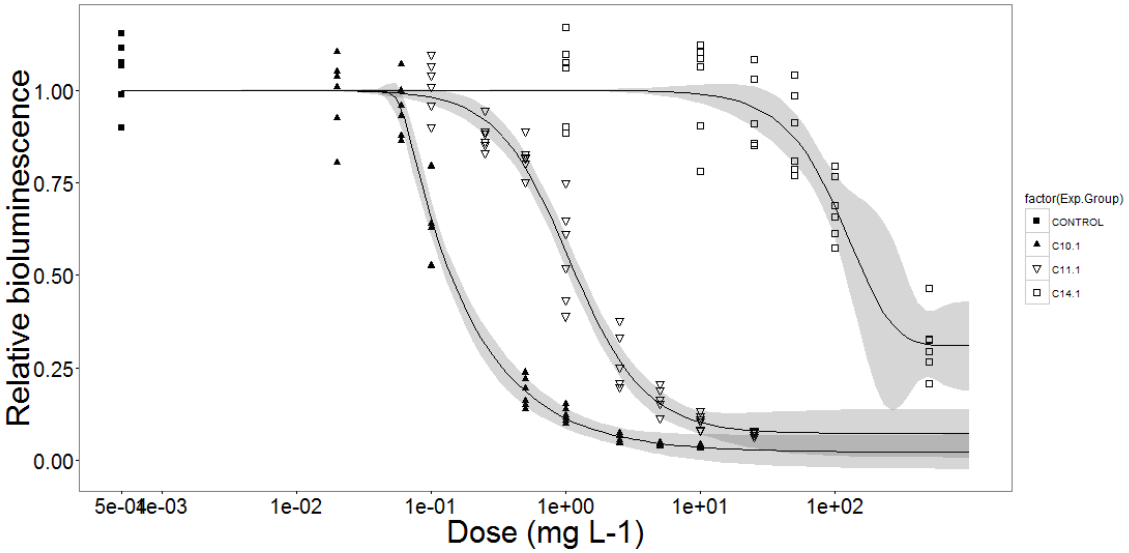

Supplementary Fig. S3.22. Dose-response data and fitted LL2 drm models (chem.1) to the experimental data. Note only a comparative (*n*) of control observations were sampled to be shown in the Figure.

Now we can get EDx values to any affect/s levels that we want based on the generated *drm* model (chem.m1) using GetECx{drc} (Note that chem.1 includes ERY, OFLO and VENLA models). In this case we will ask for an array of 19 ECx of each one:

```
> #Getting EDx values for each individual chemcical
> # required to source the function (GetECx)
> List.ECx<-GetECx(Data=ANTIBIOTIC_EC50, drm=chem.m1, Chem.var= "Exp.G
roup", Chem = "ALL",E.Level=5)
> # It generates a list containing n matrices 19x2 including the Estim
ate concentration
> #and std. Error for each efect level
> head(List.ECx)
 [[1]]
           Estimate  Std. Error
C10.1:5  0.05936013 0.004350188
C10.1:10 0.06503495 0.004043052
C10.1:15 0.07053769 0.004494833
C10.1:20 0.07656382 0.004894055
C10.1:25 0.08343934 0.005242092
C10.1:30 0.09143869 0.005646283
C10.1:35 0.10087655 0.006217862
C10.1:40 0.11216432 0.007076667
C10.1:45 0.12587136 0.008371112
....

....

C14.1:70   535.95947   132.923407
C14.1:75   752.47284   239.617310
C14.1:80  1137.78565   473.246128
C14.1:85  1936.49591  1067.775280
C14.1:90  4094.24743  3074.466802
C14.1:95 14717.21470 16197.846626
```

3.3. Estimating the effect of chemical mixtures (in silico mixture effect predictions)

Now we start to build the functions that will allow us to predict the combined effect of ERY and OFLO based on the Concentration Addition (CA). For this we will build on the predictive form of the Loewe additivity equation as deducted by Faust and coworkers [17] (Eq. 2)

$$EC_{xmix} = \left[\sum_{n}^{i=1} \frac{p_i}{ECx_i} \right]^{-1} \qquad (2)$$

Where *pi* is the relative proportion with respect to the total mixture concentration cmix of the concentration of the chemical i (ci). Therefore, pi=ci/cmix. ECxi is the concentration of the chemical i that alone produce an effect of x%. ECxmix, is therefore the mixture concentration that produces a total fractional effect x. Therefore, by calculating the quotients (Pi/ECxi)j for each chemical "i", effect level "x" and fractional ration "pi" we can get the predicted mixture effects for any mixture concentration (*EC*xmix).

A schematic summary of the calculation steps required to compute modeled mixture effect as programmed in the R script "Script_CA_prediction.R" is shown in **Supplementary Fig. S3.22**.

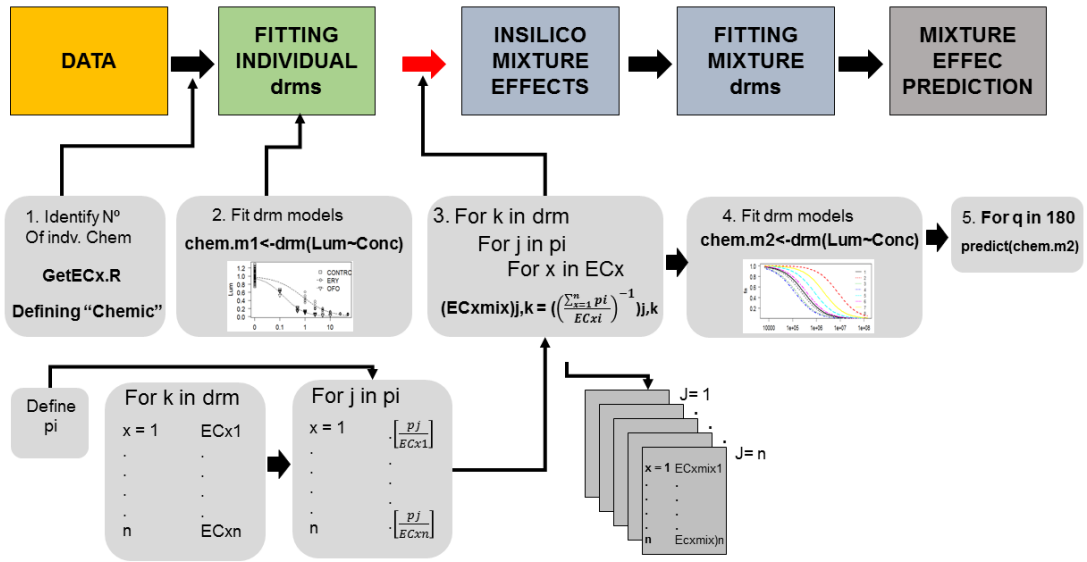

Supplementary Fig. S3.23. Schematic representation of the calculation sequence required to predict chemical mixture effects.

```
> #2º SECTION: Estimating the effect of chemical mixtures
>
> #2.1 calculating the quotients (Pi/ECxi)j for any component i in any
fractional ratio j
> #2.1.1 calculating pi:
> #pi is the fraction of each mixture component in the mixture
>
> levels(ANTIBIOTIC_EC50$Exp.Group) <- c("CONTROL", "C10.1", "C11.1")#
change notation
```

3.3.1. Getting chemic

"Chemic" serves to identify the number of individual chemicals to build on the mixture predictions

```
> levels(ANTIBIOTIC_EC50$Exp.Group) <- c("CONTROL", "C10.1", "C11.1", "C14.1")
#change notation
>
> get.chemic<- function (Data, Chem.var, Chem= ALL){
+         Chemic<-c(character())#asigning Chemic (the number and names of the
chemicals
+         #to be evaluated by EDx function)
+         if (Chem=="ALL"){
+                 Get.name<-function (Data, colname) return (Data[[colname]])
+                 Chem.var<-Get.name(Data, Chem.var)
+                 Chemic<-levels(Chem.var)
+                 Chemic<-Chemic[Chemic!="CONTROL"]
+         }else {
+                 Chemic <- Chem
+         }
+         Chemic
+ }
>
> Chemic<-get.chemic(ANTIBIOTIC_EC50,Chem.var="Exp.Group", Chem="ALL" )
> Chemic
[1] "C10.1" "C11.1" "C14.1"
```

Therefore, Chemic identifies that there are two different chemicals in the dataset.

3.3.2 Calculating *pi* values

From here we start to take into account the actual concentrations of C10 and C11 in the 180 mixtures:

```
> #Now we need to work on GSA_MIX_MEDIAN.csv data set
> GSA_MIX_MEDIAN<-read.csv("GSA_MIX_MEDIAN.csv", header = TRUE, sep=",
")# converting intergers to factors in PPCP levels
> GSA_MIX_MEDIAN<-GSA_MIX_MEDIAN[2:40]
> for (i in seq_along(1:20)){
+          GSA_MIX_MEDIAN[,i]<-as.factor(GSA_MIX_MEDIAN[,i])
+ }
> GSA_MIX_MEDIAN$L<-as.factor(GSA_MIX_MEDIAN$L)# converting L to facto
r
```

Now we calculate p_i (fractional ratio of each component in the mixture for each mixture). Those fractional ratios (p_is) define unique combinations of the chemicals (in this case of C10 and C11) in the mixtures. For each unique combination, an in-silico dose-response array of data will be generated. Note that the script works on "Chemic", therefore it allows to work with more than two chemical components.

To calculate p_is:

```
> b<-subset(GSA_MIX_MEDIAN, select=c(Chemic))
> sum.ci<-apply(b, MARGIN = 1, sum)
>
> for (i in seq_along(Chemic)){
+          a<-paste(Chemic[i],"pi", sep="")
+          c<-subset(b, select=Chemic[i])
+          d<-c/sum.ci
+          colnames(d)<-a
+          b<-cbind(b,d)
+ }#we have generate a data.frame containing pi for each component che
mical for each mixture
> head(b)
    C10.1   C11.1   C14.1    C10.1pi    C11.1pi    C14.1pi
1  538.31  805.65  305.54 0.32634738 0.48842073 0.18523189
2  135.50 8770.00 1003.00 0.01367513 0.88509865 0.10122622
```

```
3 3847.00  805.65  305.54 0.77588798 0.16248873 0.06162329
4 3847.00  805.65  305.54 0.77588798 0.16248873 0.06162329
5 3847.00  128.00  305.54 0.89871839 0.02990277 0.07137884
6 3847.00  128.00  305.54 0.89871839 0.02990277 0.07137884
```

3.3.3 Calculating pi/ECxi values

Now we are going to calculate the fractions p_i/ECx_i for each unique combination of C10 and C11 present in the 180 mixtures

The function to do this:

```
> #2.1.2 calculating Pi/ECxi
> # we will calculate pi/ECxi for each element of the List.ECx object
> pi<-as.data.frame(unique(b[,4:6]))# calculating pi
> ##IMPORTANT: Change the range of data in "b[,4:6]" to the actual col
ums in your
> #data which contains pis. It will depend on the number of chemicals
in the mixtures
>
> List.ECx.pi.out<-list(c())#generating an empty list
> List.ECx.pi<-List.ECx#we are going to fill up the original Lis.ECx l
ist with the
> #calculated pi/ECxi
> for (i in seq_along(List.ECx.pi)){#removing the errors column since
we are not using it
+        List.ECx.pi[[i]]<-List.ECx.pi[[i]][,1]
+ }
>
> for (i in seq_along(pi[,1])){#for each level in pi (6 levels)
+          for (j in seq_along(List.ECx.pi)){#2 levels C10 (ERY) and C1
1 (OFLO)
+                  for(k in seq_along(List.ECx.pi[[j]][])){#effect leve
ls
+                            List.ECx.pi[[j]][[k]]<-pi[[i,1]]/List.ECx[[j
]][[k]]
+                            List.ECx.pi.out[[i]]<-List.ECx.pi#filing the
list. It is
+                            #a list of j outputs containing pi/ECxi for
each pi and
+                            #mixture component
+                  }
+          }
+ }
```

The result from the function is a list of 21 lists of two elements which contain pi/ECxi values (19 values) for each p_i and ECx level.

```
> str(List.ECx.pi.out)
List of 21
 $ :List of 3
  ..$ : Named num [1:19] 5.5 5.02 4.63 4.26 3.91 ...
  .. ..- attr(*, "names")= chr [1:19] "ERY:5" "ERY:10" "ERY:15" "ERY:20" ...
  ..$ : Named num [1:19] 1.634 1.094 0.845 0.691 0.581 ...
  .. ..- attr(*, "names")= chr [1:19] "OFO:5" "OFO:10" "OFO:15" "OFO:20" ...
  ..$ : Named num [1:19] 0.01211 0.00804 0.00613 0.00492 0.00405 ...
  .. ..- attr(*, "names")= chr [1:19] "VENLA:5" "VENLA:10" "VENLA:15" "VENLA:2
0" ...
…

…
```

3.3.4. In-silico mixture effect predictions (array of dose-response values) for the 21 pi_s

Now we are going to predict in-silico dose-response values for each of the 9 unique combinations of C10 of C11 and C14 (p_is). This way, we generate 9 arrays of effect levels and fractional effects for each of the 21 fractional combinations of C10, C11 and C14 (later, we will be able to fit *drm* models, see below)

```
> #2.2 predicted mixture dose-response curves for i pi levels (mixtures with a
unic
> #combination ofcomponents and pi)
> #pi contains the the conc. fractions of the total conc. of each of the compo
nents
> #(colums) of each of the unique mixtures (rows)
> #for each mixture, ECxmix=(sum(pi/ECxi))^-1
> #them for each mixture i and each effect level x we can compute ECxi mix
>
> List.ECx.mix<-list(c())#generating the list
> for (i in seq_along(List.ECx.pi.out)){
+         List.ECx.pi.out[[i]]<-as.data.frame(List.ECx.pi.out[[i]])#convert li
st in data.frame
+         List.ECx.mix[[i]]<-apply(List.ECx.pi.out[[i]], 1, sum)#sum(pi/ECxi)
+         List.ECx.mix[[i]]<-(1/List.ECx.mix[[i]])*1000000#sum(pi/ECxi))^-1, f
rom mgL-1 to ngL-1
+         }
```

The result is a new list (List.ECx.mix) which contains the 19 ECx values (ngL^{-1}) for the 21 different unique combinations of ERY and OFLO

```
> head(List.ECx.mix)
[[1]]
    ERY:5    ERY:10    ERY:15    ERY:20    ERY:25    ERY:30    ERY:35
ERY:40    ERY:45    ERY:50
 139970.8  163402.5  182557.2  201690.5  222405.3  245759.5  272771.1
304653.0  343012.7  390111.6
   ERY:55    ERY:60    ERY:65    ERY:70    ERY:75    ERY:80    ERY:85
ERY:90    ERY:95
 449281.7  525661.9  627606.5  769602.4  978968.3 1313465.8 1917517.5
3266331.5 8111282.3

[[2]]
    ERY:5    ERY:10    ERY:15    ERY:20    ERY:25    ERY:30    ERY:35
ERY:40    ERY:45    ERY:50
  3340306   3899487   4356601   4813203   5307548   5864880   6509491
7270331   8185758   9309742
   ERY:55    ERY:60    ERY:65    ERY:70    ERY:75    ERY:80    ERY:85
ERY:90    ERY:95
 10721794  12544556  14977391  18366025  23362396  31344946  45760218
77948722 193570094

…
…
…
```

3.3.5. Fitting dose-response models to the in-silico dose response arrays of the 21 unique combinations of C10 and C11 and C14

Now we can fit dose response models (*drm*s) to the predicted dose-response arrays of the 21 combinations of C10, C11 and C14 as follows:

Preparing the data set:

```
> #2.3. Fitting mixture dose-response models
> E.Level<-5#fix E.Level as in Get.ECx function
> fa<-1-(seq_along(List.ECx.mix[[1]])*E.Level/100)#the effect levels o
f the mixture. In 0-1 scale. 1-(fa):this
> #is since we don´t want the effect level (inhibition), but viability
(in 1 to 0) sacale.
```

```
> #where 1 is the control viability and 0 in the maximum possible effe
ct
> ID<-seq_along(pi[,1])#mixture ID in accordance with unic(pi)
> Data.Ecx.mix<-unlist(List.ECx.mix, use.names=FALSE)#mixture conc. pr
oducing each effect level
> Frame.ECx.mix<-data.frame(ID=c(integer()), fa=c(integer()), ECx.mix=
c(numeric()))
>
> ID<-as.vector(mapply(rep, ID, length(fa)))
> fa<-(rep(fa,length(ID)))
> ECx.mix<-Data.Ecx.mix
> e.1<-cbind(ID, fa, ECx.mix)
> Frame.ECx.mix<-rbind(Frame.ECx.mix,e.1)
>
>
```

Fitting the dose-response models (also LL5 log logistic models):

```
> summary (chem.m2)#information on the fitted model parameters

Model fitted: Generalized log-logistic (ED50 as parameter) (4 parms)

Parameter estimates:

        Estimate  Std. Error     t-value p-value
b:1   5.5935e+00  1.2577e-02  4.4473e+02       0
b:2   5.5900e+00  1.2567e-02  4.4481e+02       0
b:3   5.5901e+00  1.2567e-02  4.4483e+02       0
b:4   5.5899e+00  1.2566e-02  4.4485e+02       0
b:5   5.5901e+00  1.2569e-02  4.4474e+02       0
b:6   5.5902e+00  1.2568e-02  4.4479e+02       0
b:7   5.5861e+00  1.2546e-02  4.4526e+02       0
b:8   5.6151e+00  1.2682e-02  4.4278e+02       0
b:9   5.5904e+00  1.2563e-02  4.4498e+02       0
…
…
f:15  1.4803e-01  4.4495e-04  3.3270e+02       0
f:16  1.4779e-01  4.4412e-04  3.3278e+02       0
f:17  1.4810e-01  4.4530e-04  3.3259e+02       0
f:18  1.4804e-01  4.4497e-04  3.3271e+02       0
f:19  1.4809e-01  4.4515e-04  3.3268e+02       0
f:20  1.4805e-01  4.4495e-04  3.3273e+02       0
f:21  1.4804e-01  4.4492e-04  3.3273e+02       0

Residual standard error:

 0.0008370345 (7497 degrees of freedom)

> plot(chem.m2, type=c("bars"), cex=1.2, cex.axis=1.2,cex.legend=0.9,
cex.lab=1.2, col=TRUE, pch=c(0,1,6), lwd= 2)
```

Plotting the 9 dose response models:

```
> #Plotting predicted dose-response curves for the 21 C10:C11:C14 rati
ons according to the null mixture model Concentration Addition (CA)
>
> #setting plotting parameters
> mar.plot<-c(c(5, 4, 2, 2))
> par(mar=mar.plot)
> par(fig=c(0,1,0,1), new=FALSE)
> #plotting
> plot(chem.m2, type=c("all"), xlim=c(500,5e+09), ylim=c(0, 1.1), cex=
1, cex.axis=2, cex.lab=2,
+      cex.legend=1, lwd= 1.2, bp=100, xttrim=FALSE, xt=c(500, 1000, 1
e+04, 1e+05, 1e+06, 1e+07, 1e+08),
+      xlab= "Total mixture dose ngL-1",
+      ylab="Predicted relative bioluminescence", col=FALSE)
```

```
> #adding the dose ranges (C10+C11+C14 total doses) for the 180 chemic
al mixtures
> summary(sum.ci)
   Min. 1st Qu.  Median    Mean 3rd Qu.    Max.
    569    1650    4958    5602    9614   13620
> abline(v=c(569, 4958, 13620), lwd=1.2, lty=2, col=c("black", "black"
, "black"))
> par(fig=c(0,1,0.1,0.5), new=TRUE)
> boxplot(log(sum.ci), cex=2, cex.axis=2,cex.legend=2, cex.lab=2,axes=
FALSE, horizontal=TRUE, log="y", ylim=c(6.21,22.3327))
```

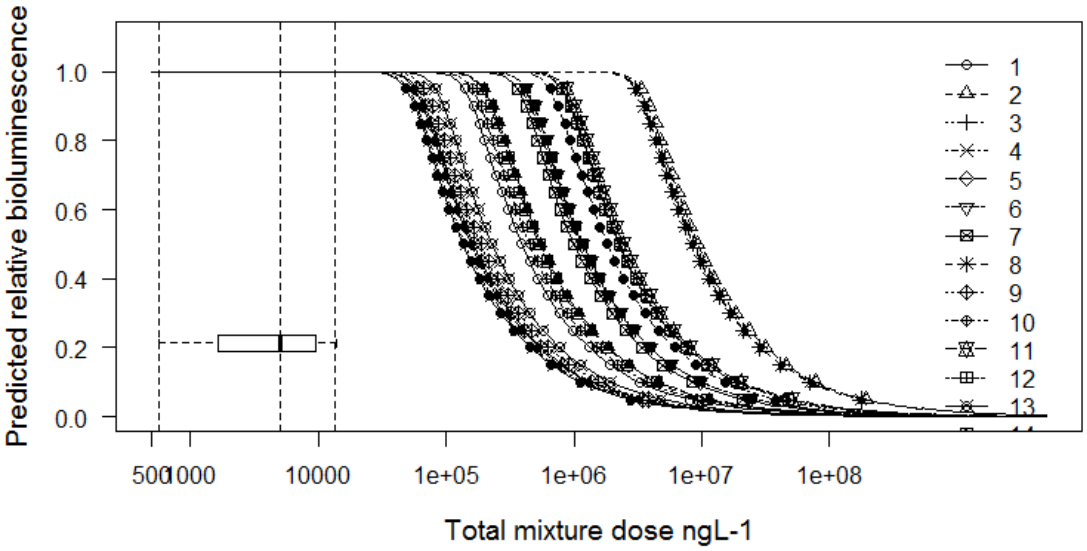

Supplementary Fig. S3.24. The 21 dose-response models (LL.5 models) fitted to the in-silico predicted dose-response patterns of the 21 unique combinations of C10, C11 and C14.

3.3.6. Predicting the effect of the 180 low dose PPCPs mixtures based only on C10 and C11 individual dose-response curves

Now having the predicted dose-response curves of the 21 fractional combinations of C10 and C11 present in the 180 mixtures, we can actually predict the expected effect of each of the 180 PPCPs mixtures. For this, we have to identify the specific pi of each mixture, and predict the effect for a specific concentration of C10+C11 using the built-in function "predict" {drc} of the drc package:

First we calculate C10+C11+C14 (ngL^{-1}):

```
> #SECTION3: Predicting the effect of the 180 mixture
> #For predict the effect of the 180 chemical mixtures, we will use th
e function predict{drc}
>
> #in the data.frame "pi" we have the 21 unique fractional ratios of t
he 180 mixtures
>
> #we will reuse the "b" data.frame which includes de individual conce
ntrations of
> #the factors incuded in "chemic", and their respective pi. It includ
es the number of
```

```
> #unique mixture inthe data set in the same order than the lists and
ID number in
> #Frame.ECx.mix and Chem.m2
>
> sum.ci<-as.numeric(c(apply(b[,seq_along(Chemic)], 1, sum)))# calcula
ting sumCi
> b$sum.ci<-sum.ci
```

Predicting effects:

```
> pi.pred<-unique(b)# a more complet verion of pi data.frame
> Lum.pred<-predict(chem.m2, data.frame(pi.pred[,ncol(pi.pred)]),
+                                ID= c("1", "2" , "3" , "4" ,"5", "6", "7", "8",
"9", "10", "11", "12",
+                                     "13", "14", "15", "16", "17", "18", "19",
"20", "21"))
> #prediction for each of the elements of pi.pred, according to its respective
non-linear model
> #fitted and stored in "chem.m2".
```

Manipulating the data.frame:

```
> pi.pred$Lum.pred<-Lum.pred#joining pi.pred with the predictions of e
ffect according to additivity model
> b.pred <- merge(b,pi.pred, by=c("C10.1", "C11.1", "C14.1","C10.1pi",
"C11.1pi", "C14.1pi", "sum.ci"))# asigning the predicted effect to the
180 mixtures
> #we merge the data sets according to "sum.ci" which is unique for ea
ch mixture ratio
```

We can see the result ("Lum.pred" is the predicted bioluminescence of each of the 180 mixtures):

```
> head(b.pred)
  C10.1 C11.1   C14.1   C10.1pi   C11.1pi   C14.1pi  sum.ci Lum.pred
1 135.5   128 1003.00 0.1069878 0.1010659 0.7919463 1266.50        1
2 135.5   128 1003.00 0.1069878 0.1010659 0.7919463 1266.50        1
3 135.5   128  305.54 0.2381203 0.2249403 0.5369394  569.04        1
4 135.5   128  305.54 0.2381203 0.2249403 0.5369394  569.04        1
5 135.5   128  305.54 0.2381203 0.2249403 0.5369394  569.04        1
6 135.5   128  305.54 0.2381203 0.2249403 0.5369394  569.04        1
```

```
> GSA_MIX_MEDIAN_pred<-cbind(GSA_MIX_MEDIAN, b.pred$Lum.pred)# merging
with the original data.frame where observed effects are stored
> colnames(GSA_MIX_MEDIAN_pred) [40] <-"Lum.pred"
```

3.4. Analyzing the goodness of fit to experimental data of the predictions of the additive model CA using "fiteval" platform

In the present section, we evaluate the accuracy of CA additivity predictions based on the fiteval model fitness evaluation framework [19]. For this we used the freely available tool "fiteval" http://abe.ufl.edu/carpena/software/fiteval.shtml. The framework proposed the combined use of graphical tools (The 1:1 agreement plot), absolute value error statistics (Root mean square error) and normalized goodness-of-fit statistics (Nash-Sutcliffe Efficiency coefficient, NSE) to evaluate model fitness and to avoid ambiguity in model fitness evaluation.

First we can check how accurate it is the CA prediction bioluminescence of *Anabaena* CPB4337 versus the experimental bioluminescence:

```
> library("reshape2")
> box<-melt(GSA_MIX_MEDIAN_pred[,39:40])
No id variables; using all as measure variables
```

```
> colnames(box)<-c("CASE", "Lum")
> boxplot(box$Lum~box$CASE, notch=T)
Warning message:
In bxp(list(stats = c(0.83, 0.91, 0.9375, 0.97, 1.05, 0.99999999443647
1,  :
  some notches went outside hinges ('box'): maybe set notch=FALSE
```

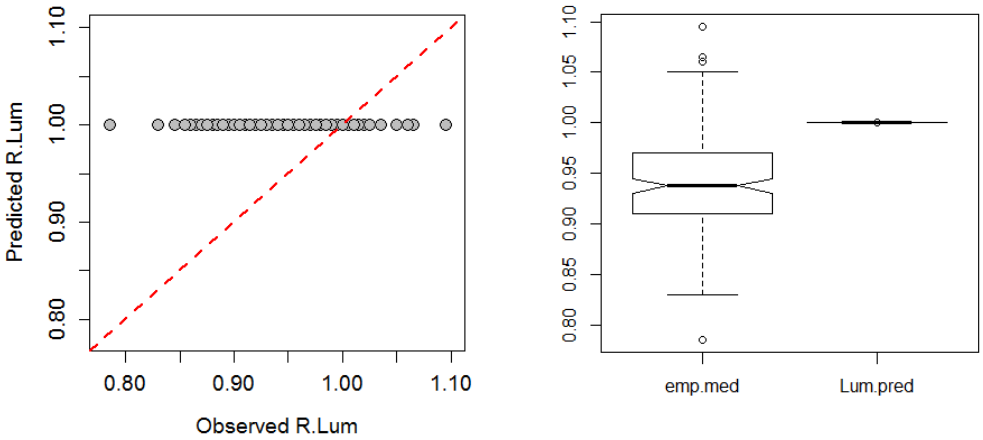

Supplementary Fig. S3.25. Observed vs predicted bioluminescence values (R.Lum) of *Anbaen a* CPB4337 to the 180 low dose mixtures of PPCPs. Red line depicts the 1:1 line of perfect mod el agreement [19] (**A**) and a Boxplot (**B**)

We can check for statistical significant differences

```
> anov.1<-aov(box$Lum~box$CASE)# checking for differences among expper
iments
> anov.1
Call:
   aov(formula = box$Lum ~ box$CASE)

Terms:
                box$CASE Residuals
Sum of Squares   0.32400   0.36755
Deg. of Freedom        1       358

Residual standard error: 0.03204178
Estimated effects may be unbalanced
> summary(anov.1)
             Df Sum Sq Mean Sq F value Pr(>F)
box$CASE      1 0.3240   0.324   315.6 <2e-16 ***
Residuals   358 0.3676   0.001
---
Signif. codes:  0 ‘***’ 0.001 ‘**’ 0.01 ‘*’ 0.05 ‘.’ 0.1 ‘ ’ 1
```

It is evident that modeled response looks a bit insensitive with respect to experimental outcome. However we want to test it in a formal way using FITEVAL framework. For this we generate the “*.csv” file from “GSA_MIX_MEDIAN_pred” data.frame as follows:

```
> write.csv(GSA_MIX_MEDIAN_pred[,c("emp.med","b.pred$Lum.pred")],
file="Observed_vs_CA.csv")
```

FITEVAL can be executed as standalone application or as a MATLAB function. As a standalone application, it is executed from the command line interface. For evaluating model fitness we only need a “*.csv” file which contains the “observed values” (experimental observations) in one column, and the “predicted values” in other column, as well as the “fitevalconfig.txt” file including the “fiteval” mode of computation.

For our analysis we used the **default** configuration in executing fiteval in the "fitevalconfig.txt" file:

0.65 % Acceptable NSE threshold value
0.80 % Good NSE threshold value
0.90 % Very good NSE threshold value
5 % BiasValue
0 % Compute Legates and McCabe modified Ceff (1=yes,0=no)
1 % Bootstrap method (1= Efrons' bootstrapping, 0= block boostrapping)
10 % FontSizeValue
0 % Do not display graphical output (1=accept)
0 % Take into account observations uncertainty (>0,1,2,3 or 4= yes)
ro % Color and type of marker size
4 % Sizes of the series marker

NOTE: For executing fiteval, both "fitevalconfig.txt" and Observed_vs_CA.in must be in the same folder of "fiteval.exe". The order for execution in the command line interface is as follows

\fiteval Observed_vs_CA.IN

After running FITEVAL, it performs the goodness-of-fit evaluation providing a portable data file (pdf) which contains:

a) A plot of observed vs. computed values illustrating the match on the 1:1 line;
b) The calculation of NSE and RMSE and their corresponding confidence intervals of 95%;
c) The qualitative goodness-of-fit interpretation based on the established classes;
d) A verification of the presence of bias or the possible presence of outliers;
e) The plot of the NSE cumulative probability function superimposed on the NSE threshold class regions;
f) A plot illustrating the evolution of the observed and computed values.

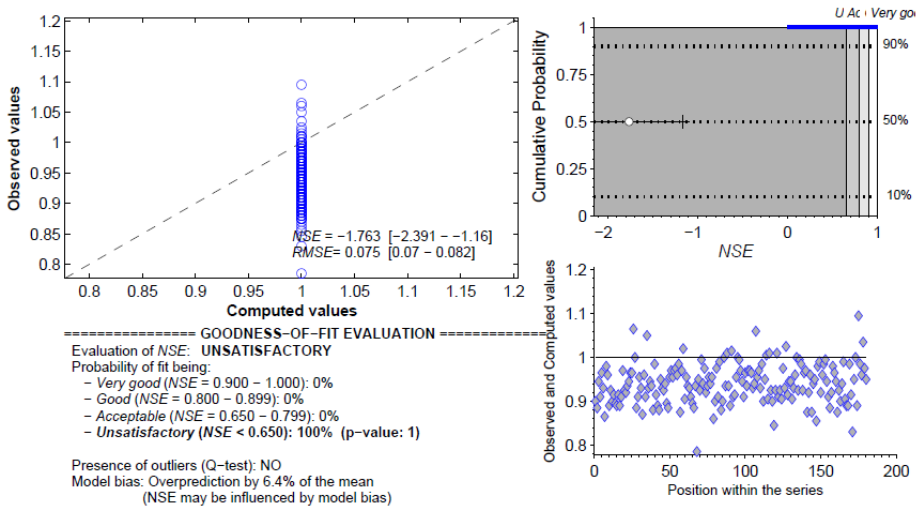

Supplementary Fig. S3.26. "fiteval" report for predicted vs. experimental low dose mixture effects of PPCPs. Upper left, "Observed values" are experimental values of bioluminescence of *Anabaena* CPB4337 exposed to the 180 low dose PPCPs mixtures. "Computed values" are bioluminescence values of *Anabaena* CPB4337 predicted based on CA model assuming that only ERY and OFLO contributed to mixture effect. NSE: Nash- Sutcliffe efficiency coefficient, RMSE: Root mean square error. Bottom left panel is the model fitness evaluation summary. Bottom right is the model performance evaluation plot respect to position

within series. Detailed information on the "FITEVAL" model evaluation framework can be found in [19].

Results of the FITEVAL execution on "Observed_vs_CA.in" are shown in **Supplementary Fig. S3.24.** As can be seen in the **Supplementary Fig. S3.24.** (Upper left), experimental values of bioluminescence of *Anabaena* CPB4337 vs. predicted based on CA model assuming that only ERY and OFLO contributed to mixture effect offers a very poor predictive ability. In fact, CA predictions of mixture effect of the 180 mixtures fell in one of two possibilities: bioluminescence = 1 (no effect) or bioluminescence = 0.97 (3% of inhibition). However it is clear that there is much more variability in mixture experimental data as presented in section 2.2.1. In addition, NSE: -1.763 fell in the unsatisfactory category [19]. Therefore we can state that mixture effect predictions based exclusively on ERY and OFLO contribution assuming a linear and additive contribution poorly modeled the experimental sublethal effects found.

4. Effect of selected mixtures on model benthic freshwater microbial communities.

4.1 biofilm.csv data set

4.1.1 Variables

The "biofilm.csv" dataset includes experimental data of benthic model microbial communities exposed to 4 different treatments for 7 days exposure time. The treatment were Treatment "1" = Control unexposed communities, Treatment "2" = microbial benthic communities exposed to Mix 16 (the most potent mixture identified in **section 2.2.1.**).Treatment "3" = microbial benthic communities exposed to Mix 16-4 (Mix 16 without the 4 most important PPCPs identified by EEs Screening method: C16, C3, C10, C5, C4; **section 2.2.3**). Treatment "3" = biofilm exposed to a 10-fold dilution of Mix 16. The number of observations by Treatment and time can be found in **Supplementary Table S3.7**. The data set includes 42 observations of variables and 9 variables. A summary of the variables included in the biofilm.csv can be found in **Supplementary Table S3.8.**

Supplementary Table S3.7. Summary of observations by Exp. Group for biofilm.csv dataset

	Time	CONTROL	Mix 16	Mix16-5	Mix16/10	All
n	1	5	3	3	3	14
n	2	5	3	3	3	14
n	3	5	3	3	3	14
n	all	15	9	9	9	42

Supplementary Table S3.8. "biofilm.csv" dataset.

Var.	Type	Levels	Info.
vessel	Factor	14	Identification of the experimental mesocosm
treatment	Factor	4	Determines the applied treatment (Control, Mix16, etc.)
time	Factor	3	Time of measurement
Phosphatase[1]	Numeric	-	Phosphatase activity
Glucosidase[2]	Numeric	-	Glucosidase activity
F0[2]	Numeric	-	Basal Chlorophyll fluorescence of photosynthetic organism adapted to dark conditions
Ymax[2]	Numeric	-	Maximum photosynthetic efficiency
F[2]	Numeric		Steady state (light adapted) Chlorophyll fluorescence
Yeff[2]	Numeric		effective quantum yield of PSII or ϕ PSII (Real

			photosynthetic efficiency)

[1]: Heterotrophic metabolism-related end-point. [2]: Autotrophic metabolism-related end-point. Further information on experimental methods and measured end-points can be found in **Supplementary Methods S2**.

4.2. "biofilm.csv" dataset analysis

CODE LOCATION: orders to do the analysis and plots presented in this section are in the R script named "Script_GLMs.R".

"biofilm.csv" dataset is a multivariate time series (**Supplementary Fig. S3.15**). To analyze it we used Multivariate Generalized Linear Models (GLM_{MV}s) as analysis framework as suggested by Szög et al. (2015) [20]. GLM_{MV}s are the extension of GLMs to a multivariate response. As demonstrated recently, GLM_{MV}s may have higher statistical power for time dependent multivariate data compared to multivariate techniques like RDA that commonly have been used by ecologists [20,21]. GLM_{MV}s fit separate GLMs to each dependent variable. The individual GLM are then combined using sum-of-Likelihood-Ratios (PLR) statistic, which allows testing for a significant community response. Univariate responses are directly available because a GLM is fitted to each variable. Contributions of single variables to the community response can be derived from the deviance of the univariate GLMs. Different (nested) models could be fitted and compared. ANOVA test can be performed via permutations in order to take into account the time dependence. Further explanations can be found in the Supplemental Material provided in Szög et al. (2015)[20].

Main model assumptions of GLM_{MV}. Negative binomial regression (used in GLM models) makes 2 key assumptions, both of which can be readily checked by looking for the absence of apparent patterns on a *residual vs. fits* plot[21]. We found that applying a simple 10* to 1000* factor transformation to the dependent variables GLM maximized the matching of GLM model assumption (see diagnostic plot **Supplementary Fig. S3.15.**), so this transformations were applied to the original data previous to analysis**.**

```
> #install.packages(c("reshape2", "ggplot2")
> library("reshape2")
> library("ggplot2")
>
> Dir.data<-"~/Art-GSA14/ANALISIS_DATA_0615/GSA_EBS_PPCPs_2016/R_DATA"
> Dir.functions<-"~/Art-GSA14/ANALISIS_DATA_0615/GSA_EBS_PPCPs_2016/R_
FUNCTIONS"
> Dir.Scripts<-"~/Art-GSA14/ANALISIS_DATA_0615/GSA_EBS_PPCPs_2016/R_SC
RIPTS"
>
> biofilm<-read.csv("biofilm.csv", header = TRUE, sep=",")# converting
intergers to factors in PPCP levels
>
> biofilm<-biofilm[2:10]
> for (i in seq_along(1:3)){
+         biofilm[,i]<-as.factor(biofilm[,i])
+ }# assigning the independent variables as factors
>
> # appliying a 10* to 1000* for transforming the dependent variables
in order to improve
> # the model mean-variance relatioship and error distribution require
ments of GLMs assomptions
> # according to Warton, D. I., Wright, S. T., & Wang, Y. (2012). Dist
ance-based multivariate
> #analyses confound location and dispersion effects. Methods in Ecolo
gy and Evolution, 3(1),
> #89-101. http://doi.org/10.1111/j.2041-210X.2011.00127.x
>
> biofilm[,4]<-biofilm[,4]*10
```

```
> biofilm[,5]<-biofilm[,5]*10
> biofilm[,6]<-biofilm[,6]*10
> biofilm[,7]<-biofilm[,7]*1000
> biofilm[,8]<-biofilm[,8]
> biofilm[,9]<-biofilm[,9]*1000
```

```
> head(biofilm)
  vessel treatment time Phosphatase Glucosidase        F0      Ymax         F     Yeff
1      1         1    1    711.1866    855.4283 1716.6667 363.3333 153.3333 440.6667
2      2         1    1    801.4332    420.0169  983.3333 418.6667 120.0000 461.3333
3      3         1    1    994.0886    347.4483  733.3333 380.0000 133.6667 445.6667
4      4         1    1    525.6993    525.6471 1160.0000 404.3333 151.6667 468.6667
5      5         1    1    594.7944    842.2991 1533.3333 316.3333 122.3333 431.6667
6      6         2    1    535.2175   1903.7339  956.6667 326.6667 111.0000 278.6667
```

4.2.1 Analysis of overall time and treatment effect

To analyze the overall time and treatment of the selected mixtures on the benthic microbial communities, we followed the approach and procedure in Szög et al. (2015)[20]. Basically we prepare the dataset and fit a GLM_{MV}s models in which the multivariate response of the microbial communities are set as a function of the independent variables "time" and "treatment". Later the statistical significance of the terms in the model ANOVA models is tested via permutations.

Now we can visualize the evolution with time of the 6 endpoint using "reshape" and "ggplot2" packages:

Plotting biofilms.csv data by measured variable (end-point) and time

First we manipulate variables:

```
> #Prepare dtaset for ggplot visualization
> biofilm_s<-biofilm[,4:9]
> time=biofilm[,3]
> treatment=biofilm[,2]
> vessel=biofilm[,1]
>
> take=c("Phosphatase", "Glucosidase", "F0", "Ymax", "F", "Yeff")
> abu <- biofilm_s[ , names(biofilm_s) %in% take]
> #abu_t <- round(abu)
> abu_t <- abu
>
```

We generate the "ggplot" object

```
> #install.packages("reshape2")
> library("reshape2")
> library("ggplot2")
> dfm <- melt(data.frame(treatment, time, abu_t), id.vars = c('treatme
nt', 'time'))
> dfm$time <- as.numeric(as.character(dfm$time))
> ggplot(dfm, aes(x = time, y = value, col = treatment)) +
+         geom_point() +
+         #geom_smooth(aes(group = treatment), size=1, se = FALSE) +
+         facet_wrap(~variable, scales = 'free_y') +
+         #geom_vline(aes_string(xintercept = 1), col ="black") +
+         #scale_y_log10() +
+         theme_bw() +
+         ylab("response") +
+         xlab('time')
```

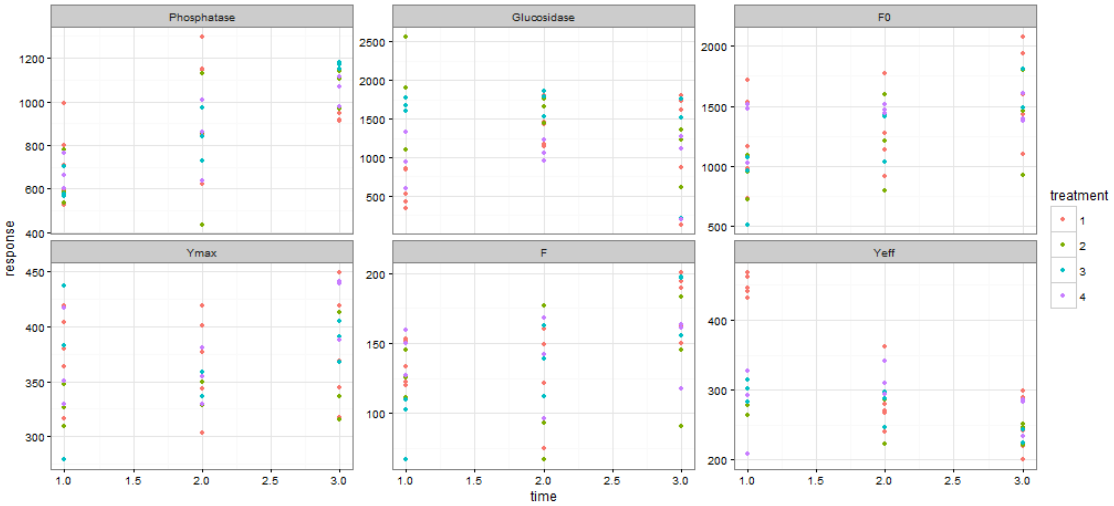

Supplementary Fig. S3.27. Response of 6 community level end-points measured along time as a function of "treatment" on model freshwater benthic microbial communities. (1): CONTROL group, (2): Mix16, (3): Mix16-4, (4) Mix16/10 (for further explanations on the treatments and the measured end-points see **Supplementary Material S2** of the manuscript).

Now we prepare the variables properly to fit the GLM_{MVs} models

```
> #install.packages("utils")
> library(utils)# active package package
> ##subsetting independent variables
> ttd=biofilm[, 1:3]
> biofilm_t <- round(biofilm_s)##round dependent variables
> head(biofilm_t)
  Phosphatase Glucosidase   F0 Ymax   F Yeff
1         711         855 1717  363 153  441
2         801         420  983  419 120  461
3         994         347  733  380 134  446
4         526         526 1160  404 152  469
5         595         842 1533  316 122  432
6         535        1904  957  327 111  279
>
> env <- data.frame(ttd$treatment, ttd$time) ##creating a dataframe in
cluding the two expalining variables
```

Now we apply the GLM_{MV}s to the data set as follows generating a "manyglm" GLM_{MV} model in which the multivariate variable "biofilm_mv" is explained by "treatment", "time" and their interaction "treatment*time":

```
> env <- data.frame(ttd$treatment, ttd$time) ##creating a dataframe in
cluding the two expalining variables
> #install.packages("mvabund")
> library(mvabund)#Statistical Methods for Analysing Multivariate Abun
dance Data
> biofilm_mv <- mvabund(biofilm_t)#converting the dataset in an mvabun
d object
> mod_full <- manyglm(biofilm_mv ~ ttd$treatment*ttd$time, data = env)
#fitting the
> #Fitting Generalized Linear Models for Multivariate data
```

Inspecting the distribution of Residual vs. fitted values for model assumption checking

```
> plot(mod_full)# model visual inspection
```

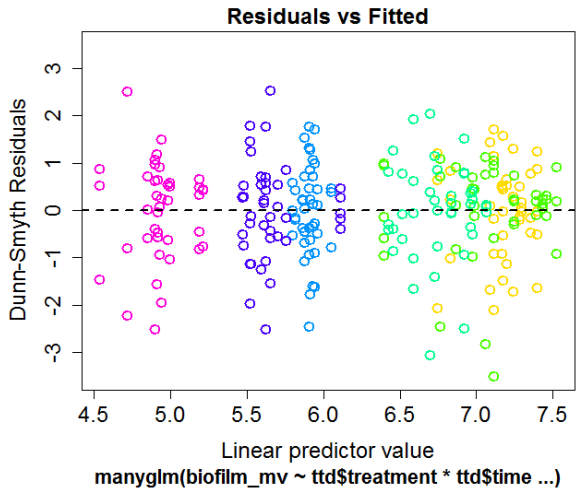

Supplementary Fig. S3.28. Residual vs. fitted values plot

As can be seen in **Supplementary Fig. S3.28**, residuals distribution followed no clear specific pattern. The residuals "bounce randomly" around the 0 line. This suggests that the assumption that the response variable followed the fitted model is reasonable. The residuals roughly form a "horizontal band" around the 0 line. This suggests that the variances of the error terms are equal. No one residual "stands out" from the basic random pattern of residuals. This suggests that there are no outliers. Therefore, we considered appropriated the data transformation used and GLM_{MV} fitted model.

Since "time" is being taken into account, significance of the factors "time" and "treatment" must be studied via permutations[20] based on "vessel" variable. For this, we need to construct a permutation matrix. This matrix is passed directly to anova() instead of passing the permutation design (Further explanations can be found in the Supplementary Material of [20]). For this we used the functions in "vegan" package:

```
> #install.packages("vegan")
> library(vegan)
> #generating permutations
> set.seed(125)# this is required to fix the starting random number ge
nerator
> control <- how(within = Within(type = "none"),plots = Plots(strata =
factor(ttd$vessel), type = "free"), nperm = 99)
> permutations <- shuffleSet(nrow(biofilm_t), control = control)
```

Significance can be tested using the ANOVA function of "mvabund" package. Since our data are not high dimensional (k > n), where n is the number of end-points (6) and k the number of experimental units (experimental vessels, 15), we used cor.type = "R", which uses the unstructured correlation matrix, and the default "Wald" test for statistical inference. Wald is not recommended only in the case of presence/absence data and/or abundant 0 count values. (see help for manyglm{mvabund}.

```
> #testing ANOVA via permutations
> aov_mglm <- anova(mod_full, bootID = permutations, p.uni = "unadjust
ed",  cor.type="R",test = "wald", resamp = "perm.resid")
Using bootID matrix from input.
Time elapsed: 0 hr 0 min 4 sec
```

```
> aov_mglm#view ANOVA Table
Analysis of Variance Table

Model: manyglm(formula = biofilm_mv ~ ttd$treatment * ttd$time, data = env)

Multivariate test:
                      Res.Df Df.diff  wald Pr(>wald)
(Intercept)               41
ttd$treatment             38       3  6.59      0.45
ttd$time                  36       2 13.05      0.86
ttd$treatment:ttd$time    30       6 17.16      0.01 **
---
Signif. codes:  0 ‘***’ 0.001 ‘**’ 0.01 ‘*’ 0.05 ‘.’ 0.1 ‘ ’ 1

Univariate Tests:
                      Phosphatase           Glucosidase              F0
Ymax
                                wald Pr(>wald)        wald Pr(>wald)  wald Pr(>w
ald)  wald
(Intercept)
ttd$treatment                0.593      0.94       2.474      0.08 1.874
0.41 5.096
ttd$time                     6.046      0.97       1.566      0.95 3.861
0.84 4.423
ttd$treatment:ttd$time       2.874      0.36       3.313      0.23 2.438
0.53 3.284
                                    F             Yeff
                      Pr(>wald)  wald Pr(>wald)   wald Pr(>wald)
(Intercept)
ttd$treatment               0.34 1.618      0.62  3.328      0.01
ttd$time                    0.34 3.367      0.91  5.442      0.80
ttd$treatment:ttd$time      0.85 3.353      0.21 12.675      0.01
Arguments:
 Test statistics calculated assuming unconstrained correlation response
P-value calculated using 99 resampling iterations via residual permutation (wi
thout replacement) resampling (to account for correlation in testing.
```

The multivariate test indicates that there is an statistically significant effect of the interaction of treatment and time on the multivariate response of the physiological activities measured on the biofilm community (ANOVA, Pr(>Wald) = 0.01**). The univariate test showed significant main effects of treatment and the interaction of treatment and time for Yeff (effective photosynthetic yield of the primary producers of the microbial community) (Pr(>Wald) = 0.01**), and Glucosidase activity of heterotrophic bacteria of the microbial community for “treatment” variable (Pr(>Wald) = 0.08·) (mild statistical significance).

Power analysis

```
> #Power Analysis of the ANOVA for the model terms in the GLMMV
> #power for the first order terms
> cohen.ES(test = "anov", size = "medium")#Cohens category medium

     Conventional effect size from Cohen (1982)

           test = anov
           size = medium
    effect.size = 0.25

> cohen.ES(test = "anov", size = "large")#Cohens category large

     Conventional effect size from Cohen (1982)

           test = anov
           size = large
    effect.size = 0.4

> #treatment
> pwr.f2.test(u=3, v=38, f2 = 0.15, sig.level = 0.05, power = NULL)#me
dium effect size
```

```
     Multiple regression power calculation

              u = 3
              v = 38
             f2 = 0.15
      sig.level = 0.05
          power = 0.4944788

> pwr.f2.test(u=3, v=38, f2 = 0.4, sig.level = 0.05, power = NULL)#lar
ge effect size

     Multiple regression power calculation

              u = 3
              v = 38
             f2 = 0.4
      sig.level = 0.05
          power = 0.9196398

> #time
> pwr.f2.test(u=3, v=36, f2 = 0.15, sig.level = 0.05, power = NULL)#me
dium effect size

     Multiple regression power calculation

              u = 3
              v = 36
             f2 = 0.15
      sig.level = 0.05
          power = 0.4711834

> pwr.f2.test(u=3, v=36, f2 = 0.4, sig.level = 0.05, power = NULL)#lar
ge effect size

     Multiple regression power calculation

              u = 3
              v = 36
             f2 = 0.4
      sig.level = 0.05
          power = 0.9036476

> #interaction
> pwr.f2.test(u=6, v=30, f2 = 0.15, sig.level = 0.05, power = NULL)#me
dium effect size

     Multiple regression power calculation

              u = 6
              v = 30
             f2 = 0.15
      sig.level = 0.05
          power = 0.3064002

> pwr.f2.test(u=6, v=30, f2 = 0.4, sig.level = 0.05, power = NULL)#lar
ge effect size

     Multiple regression power calculation

              u = 6
              v = 30
             f2 = 0.4
      sig.level = 0.05
          power = 0.7416778
```

In the case of GLM_{MV}s, power to detect small size effects was in general lower (power near 0.5) than in the QHTS experiments due to the lower number of experimental replicates. However

power was very good to detect large effect sizes (> 0.4 sds) (Power > 0.74). Power is anyway the probability of detecting an effect when it exists, meaning that in this analysis, we have lower chances than in QHTS analysis for detecting small effects even if they exist. However with this analysis we were interested in detecting big patterns and not to get detailed inference in a case by case basis. Therefore despite the experiment was slightly underpowered, we consider the power sufficient for the objectives of the analysis.

Checking the relevance of *time* and *treatment* via comparison with reduced nested models

To check the relevance of both variables *time* and *treatment*, we can compare the ANOVA model including "treatment" and "time" as factors with a nested model which includes just "time" or just "treatment":

```
> #we can compare with a model in which the variable "treatment" is re
move
> mod_reduced_t <- manyglm(biofilm_mv ~ ttd$time, data = env)
> aov_mglm.2 <- anova(mod_reduced_t , bootID = permutations, p.uni = "
unadjusted",  cor.type="R",test = "wald", resamp = "perm.resid")
Using bootID matrix from input.
Time elapsed: 0 hr 0 min 1 sec
> aov_mglm.2#view ANOVA Table
Analysis of Variance Table

Model: manyglm(formula = biofilm_mv ~ ttd$time, data = env)

Multivariate test:
            Res.Df Df.diff  wald Pr(>wald)
(Intercept)     41
ttd$time        39       2 12.84          1
.
.
.
(…)

> #we can compare with a model in which the variable "time" is remove
> mod_reduced_Treat <- manyglm(biofilm_mv ~ ttd$treatment, data = env)
> aov_mglm.3 <- anova(mod_reduced_Treat , bootID = permutations, p.uni
= "unadjusted",  cor.type="R",test = "wald", resamp = "perm.resid")
Using bootID matrix from input.
Time elapsed: 0 hr 0 min 1 sec
> aov_mglm.3#view ANOVA Table
Analysis of Variance Table

Model: manyglm(formula = biofilm_mv ~ ttd$treatment, data = env)

Multivariate test:
              Res.Df Df.diff wald Pr(>wald)
(Intercept)       41
ttd$treatment     38       3 6.59      0.45
.
.
.
(…)
```

And we can compare full model with both nested models:

```
> #we can compare with a model in which the variable "treatment" or "t
ime" is removed
> aov_mglm.4 <- anova(mod_full, mod_reduced_t, bootID = permutations,
p.uni = "unadjusted", test = "wald", resamp = "perm.resid")
Using <int> bootID matrix from input.
Time elapsed: 0 hr 0 min 0 sec
```

```
> aov_mglm.4
Analysis of Variance Table

mod_reduced_t: biofilm_mv ~ ttd$time
mod_full: biofilm_mv ~ ttd$treatment * ttd$time

Multivariate test:
              Res.Df Df.diff  wald Pr(>wald)
mod_reduced_t     39
mod_full          30       9 24.02      0.01 **
---
Signif. codes:  0 ‘***’ 0.001 ‘**’ 0.01 ‘*’ 0.05 ‘.’ 0.1 ‘ ’ 1
.
.
.
(…)
```

```
> aov_mglm.5 <- anova(mod_full, mod_reduced_Treat, bootID = permutatio
ns, p.uni = "unadjusted", test = "wald", resamp = "perm.resid")
Using <int> bootID matrix from input.
Time elapsed: 0 hr 0 min 0 sec
> aov_mglm.5
Analysis of Variance Table

mod_reduced_Treat: biofilm_mv ~ ttd$treatment
mod_full: biofilm_mv ~ ttd$treatment * ttd$time

Multivariate test:
                  Res.Df Df.diff  wald Pr(>wald)
mod_reduced_Treat     38
mod_full              30       8 22.98      0.01 **
---
Signif. codes:  0 ‘***’ 0.001 ‘**’ 0.01 ‘*’ 0.05 ‘.’ 0.1 ‘ ’ 1

.
.
.
(…)
```

There is a statistically significant difference between the full model (which includes “time” and “treatment”) and the reduced models (which includes only “time” or “treatment”), confirming that there is a significant effect of the term “treatment” and its interaction with “time” on the biofilm communities’ response.

However, which treatment/treatments are different? What is the effect of “time” on the response of the model communities to the different treatments?

4.2.2 Effects per time and per treatment

Once we know that there is a significant contribution of “treatment” and of the interaction “treatment*time”, we can study the effects of “treatment” in two ways: (1) we can study the occurrence of “treatment” significant effects along individual time points. (2) We can study which treatments produce or not significant changes in the biofilm responses along “time”.

Occurrence of treatment significant effects along individual time points

The concept is the same proposed in [20]. It consists in Looping through time and for every time point fitting and testing an individual ANOVA model.

```
> #1. Occurrence of treatment significant effects along individual tim
e points:
> #The concept is the same proposed in (Szöcs et al. 2015), (and the s
ame function). It consist in Looping
> #through time and for every time point fitting and testing an indivi
dual ANOVA
> #model.
>
```

The function to do it:

```
> mv_per_time <- function(response, treatment, time, nperm = NULL) {
+   df <- data.frame(treatment = treatment, time = time, stringsAsFact
ors = FALSE)
+   out <- NULL
+   for (i in levels(time)) {
+     rsp <- mvabund(response[df$time == i, ])
+     out[[i]]$mod <- manyglm(rsp ~ treatment, data = df[df$time == i,
])
+     out[[i]]$anova <- anova(out[[i]]$mod, nBoot = nperm, p.uni = "un
adjusted",
+                             test = "wald", resamp = "perm.resid", sh
ow.time = "none")
+
+   }
+   return(out)
+ }
>
```

Running the function:

```
> per_time <- mv_per_time(biofilm_mv, env$ttd.treatment, env$ttd.time,
nperm = 99)
```

The output is large (it includes a model with multivariate and univariate responses for every time point) (skipped here). *p*-values from Wald test can be extracted for every week. Remember that the null hypothesis in Wald test is: H0 = the response difference among factor levels is 0.

```
> sapply(per_time, function(y) y$anova$table[2, 4])# extracting the p-
values
   1    2    3
0.03 0.18 0.06
```

Therefore, there are significant effects of treatment on the biofilm community responses at time points 1 (24h) (ANOVA, (Wald>P) = 0.03 and point 3 at $p \leq 0.06$ (for 7 days exposure time), but not at time point 2 (3d). This may suggest an initial strong effect of the mixture treatments, a subsequent adaptation period (3d) and a latter incidence of chronic effects (7d).

Occurrence of treatment significant effects along individual time points

Here the concept is inverted: we are going to loop through treatment and fit for and test an individual ANOVA model for every treatment in which the independent variable is time.

The function to do it:

```
> #2. Occurrence of treatment significant effects along individual tre
atments:
> #Here the concept is inverted to (1): we are going to loop through t
reatment
> #and fit for and test an individual ANOVA model for every treatment
in which the
> #independent variable is time.
> mv_per_treatment <- function(response, treatment, time, nperm = NULL
) {
```

```
+   df <- data.frame(treatment = treatment, time = time, stringsAsFact
ors = FALSE)
+   out <- NULL
+   for (i in levels(treatment)) {
+     rsp <- mvabund(response[df$treatment == i, ])
+     out[[i]]$mod <- manyglm(rsp ~ time, data = df[df$treatment == i,
])
+     out[[i]]$anova <- anova(out[[i]]$mod, nBoot = nperm, p.uni = "un
adjusted",
+                             test = "wald", resamp = "perm.resid", sh
ow.time = "none")
+   }
+   return(out)
+ }
```

And we run the function:

```
> per_treatment <- mv_per_treatment(biofilm_mv, env$ttd.treatment, env
$ttd.time, nperm = 99)
```

With this we can elucidate whether there are or there are not significant changes in the multivariate response of the microbial community for the different treatments along time. However, since microbial communities are dynamical systems and we are studying explicitly the temporal dimension, we have to check first the behavior of the control group: does it change with time?

Detail of GLM fitted to model freshwater microbial community response for the treatment = CONTROL. Both multivariate and univariate models with statistical significance are shown

```
> per_treatment[[1]]#ANOVA table for GLM, Treatment = CONTROL
$mod

Call:  manyglm(formula = rsp ~ time, data = df[df$treatment == i, ])
[1] "negative.binomial"

Nuisance Parameter(s) phi estimated by the PHI method.
Phosphatase  Glucosidase           F0         Ymax            F         Yeff
      0.038        0.253        0.061        0.010        0.023        0.010

Degrees of Freedom: 14 Total (i.e. Null); 12 Residual

                    Phosphatase  Glucosidase  F0       Ymax     F        Yeff
2*log-likelihood:   -196.94      -226.87      -217.07  -154.90  -140.34  -151.22
Residual Deviance:    15.11        15.65        15.16    15.04    15.59    15.54
AIC:                 204.94       234.87       225.07   162.90   148.34   159.22

$anova
Analysis of Variance Table

Model: manyglm(formula = rsp ~ time, data = df[df$treatment == i, ])

Multivariate test:
           Res.Df Df.diff  wald Pr(>wald)
(Intercept)     14
time            12       2 23.56      0.01 **
---
Signif. codes:  0 ‘***’ 0.001 ‘**’ 0.01 ‘*’ 0.05 ‘.’ 0.1 ‘ ’ 1

Univariate Tests:
           Phosphatase           Glucosidase              F0            Ymax                F
                 wald Pr(>wald)        wald Pr(>wald)  wald Pr(>wald)  wald Pr(>wald)  wald Pr(>wa
ld)
(Intercept)
time             2.775       0.05       2.873       0.05 1.899       0.31 0.436       0.93 3.009       0
.03
           Yeff
           wald Pr(>wald)
(Intercept)
time       8.53       0.01
Arguments:
 Test statistics calculated assuming unconstrained correlation response
P-value calculated using 99 resampling iterations via residual permutation (without replacement) res
ampling (to account for correlation in testing.
```

Detail of GLM fitted to model freshwater microbial community response for the treatment = Mix16. Both multivariate and univariate models with statistical significance are shown

```
> per_treatment[[2]]#ANOVA table for GLM, Treatment = Mix16
$mod
```

```
Call:  manyglm(formula = rsp ~ time, data = df[df$treatment == i, ])
[1] "negative.binomial"

Nuisance Parameter(s) phi estimated by the PHI method.
Phosphatase  Glucosidase           F0         Ymax            F         Yeff
      0.057        0.076        0.059        0.007        0.077        0.007

Degrees of Freedom: 8 Total (i.e. Null); 6 Residual

                    Phosphatase  Glucosidase  F0        Ymax      F         Yeff
2*log-likelihood:   -120.395     -133.331     -126.741   -86.698   -89.886   -77.108
Residual Deviance:     9.103        9.123        9.081    17.731     9.126    10.732
AIC:                 128.395      141.331      134.741    94.698    97.886    85.108

$anova
Analysis of Variance Table

Model: manyglm(formula = rsp ~ time, data = df[df$treatment == i, ])

Multivariate test:
            Res.Df Df.diff  wald Pr(>wald)
(Intercept)      8
time             6       2 15.75       0.59

Univariate Tests:
            Phosphatase           Glucosidase              F0            Ymax                F
                  wald Pr(>wald)        wald Pr(>wald)  wald Pr(>wald)  wald Pr(>wald)  wald Pr(>wa
ld)
(Intercept)
time              2.648       0.17       2.549       0.11 2.105       0.28 1.831       0.77 0.922       0
.67
             Yeff
             wald Pr(>wald)
(Intercept)
time         2.622       0.20
Arguments:
 Test statistics calculated assuming unconstrained correlation response
P-value calculated using 99 resampling iterations via residual permutation (without replacement) res
ampling (to account for correlation in testing.
```

In Control group we observed that there are significant changes is the multivariate response along time (ANOVA wald test Pr(>wald) = 0.01). In the univariate test we observe significant changes in Phosphatase, Glucosidase, F and Yeff (ANOVA wald test Pr(>wald) = 0.05, 0.05 and 0.03 and 0.01, respectively). Therefore, we can say that there is a time dependent behavior of Control group, and that it is accounted mainly by time dependent changes in Phosphatase, Glucosidase, F and Yeff.; by contrast, in Mix16 treatment, no statistically significant change was found in the multivariate response of the microbial community along time for both the multivariate response (ANOVA wald test Pr(>wald) = 0.59) or their individual parameters.

An easy way to compare responses of the different treatments is checking whether biofilm exposed to the different mixture treatment present similar changes with respect to control group along time. For this, first we can extract the *p*-values of Wald tests for "time" variable from the ANOVA summaries for the different treatments as follows:

```
> sapply(per_treatment, function(y) y$anova$table[2, 4])# extracting p
-values by treatment
   1    2    3    4
0.01 0.54 0.02 0.61
```

Only treatment "1" (control group) and treatment "3" Mix16-4 present a significant effect of "time" on the microbial community response.

Executing the following commands we can see the summaries of ANOVA tables of the GLM_{MV}s and constituent GLMs for each treatment:

```
> per_treatment[[1]]#ANOVA table for GLM, Treatment = CONTROL
> per_treatment[[2]]#ANOVA table for GLM, Treatment = Mix16
> per_treatment[[3]]#ANOVA table for GLM, Treatment = Mix16-4
> per_treatment[[4]]#ANOVA table for GLM, Treatment = Mix16/10
# Skipped due to space constrains.
```

Supplementary Table S3.9. *p*-values of Wald-test for significance of "time" variable of the ANOVA test for each univariate GLMs fitted to each end-point (Phosphatase, Glucosidase, F0, Ymax, F, Yeff) for each "treatment" with "time" as explanatory variable .

	CONTROL	MIX16	MIX16-4	MIX16/10
Phosphatase	0.05	0.17	0.01	0.05
Glucosidase	0.05	0.11	0.36	0.84
F0	0.25	0.28	0.05	0.81
Ymax	0.93	0.77	0.63	0.17
F	0.03	0.67	0.01	0.84
Yeff	0.01	0.20	0.06	0.38

The information from the ANOVA Table summaries for the GLMs of the different treatments can be found in **Supplementary Table S3.9.** In **Supplementary Table S3.9** we can observe which univariate GLM present statically significance when test for "time" changes for each "treatment" for Wald test. The statistically significant threshold limit was fixed at (Pr(>wald) < 0.05). As can be seen, while Control presented significant changes along time in Phosphatase, Glucosidase, F and Yeff; Treatment "2" (Mix16), did not show any statistically significant change along time in any of the studied parameters. Treatment "3" (Mix16-4) presented significant changes along time in Phosphatase, F0, F and Yeff (ANOVA wald test Pr(>wald) = 0.01, 0.05, 0.01 and 0.06, respectively). Treatment "4" (Mix16/10) present statistically significant changes along time only for Phosphatase activity wald test Pr(>wald) =0.05. Therefore, we can state that (1) "treatment" produced significant effects on the time evolution of physiological end-points of the freshwater biofilm communities. (2) Physiological parameters of "Control biofilm" ("treatment" =1) and those of Mix16-4 ("treatment" =3) evolved with time while those of Mix 16 ("treatment" =2) and Mix 16/10 ("treatment" =4) did not. Therefore, Mix16-4 is more similar to the control group than Mix 16 and Mix 16/10.

These observations are confirmed by a jackard dissimilarity index computation, for this we feed the results on statistical significant positive or negative to a dychotomic variable (0,1):

```
> #With the information on significant differences for "time" in ech t
reatment,
> #we can compare the simmilarity of each treatment regarding which sp
ecific
> #metabolic end-points ("Phospatase", "Glocosidase", etc.) are or not
significantly
> #changing along time. (information in per_treatment [[i]] objects, U
nivariate tests)
>
> #We built a matrix including each treatment and a dychotomic variabl
e with values 0 = not
> #statistically significant (p>0.1), 1= statistically significant)
> DI_control<-as.factor(c(1, 1, 0, 0, 1, 1))
> DI_Mix16<-as.factor(c(0, 0, 0, 0, 0, 0))
> DI_Mix16_4<-as.factor(c(1, 0, 1, 0, 1, 1))
> DI_Mix16_10<-as.factor(c(1, 0, 0, 0, 0, 0))
>
> M<-as.data.frame(t(cbind(DI_control,DI_Mix16,DI_Mix16_4,DI_Mix16_10)
))
> M
            V1 V2 V3 V4 V5 V6
DI_control   2  2  1  1  2  2
DI_Mix16     1  1  1  1  1  1
DI_Mix16_4   2  1  2  1  2  2
DI_Mix16_10  2  1  1  1  1  1
```

```
> vegdist(M, method="jaccard", binary=FALSE, diag=FALSE, upper=FALSE,
na.rm = FALSE)
            DI_control  DI_Mix16 DI_Mix16_4
DI_Mix16     0.4000000
DI_Mix16_4   0.1818182 0.4000000
DI_Mix16_10  0.3000000 0.1428571  0.3000000
```

Jaccard dissimilarity index value (0-1).The higher the index, the higher the dissimilarity. As can be seen, the highest dissimilarities in the microbial community responses occurred between Control and Mix16 treatments (Jaccard= 0.4) but also between Mix16 and Mix16-4 (Jaccard =0.4). Interestingly, Control and Mis16-4 responses were less dissimilar (Jaccard index = 0.18), as were Mix16 and Mix16/10. This confirms the results inferred from the comparisons of the significance of the temporal pattern of the GLMs.

5. References

1. Cohen, J. *Statistical Power Analysis for the Behavioral Sciences (2nd ed.)*. *Statistical Power Analysis for the Behavioral Sciences* **2nd,** (New York: Academic press, 1988).

2. Krzywinski, M. & Altman, N. Points of significance: Power and sample size. *Nat. Methods* **10,** 1139–1140 (2013).

3. Mcgill, R., Tukey, J. W. & Larsen, W. A. Variations of Box Plots. *Am. Stat.* (2012). at <http://www.tandfonline.com/doi/abs/10.1080/00031305.1978.10479236>

4. Brown, M. B. & Forsythe, A. B. Robust Tests for the Equality of Variances. *J. Am. Stat. Assoc.* (2012). at <http://www.tandfonline.com/doi/abs/10.1080/01621459.1974.10482955#.VovxUhXhDIU>

5. Dunnett, C. A multiple comparison procedure for comparing several treatments with a control. *J. Am. Stat. Assoc.* **50,** 1096–1121 (1955).

6. Saltelli, A., Ratto, M., Tarantola, S. & Campolongo, F. Sensitivity analysis for chemical models. *Chem Rev* **105,** 2811–2828 (2005).

7. Davison, A. C. & Hinkley, D. V. *Bootstrap Methods and Their Application*. *Engineering* **42,** (Cambridge University Press, 1997).

8. Kozak, M. dotplots.errors, a new R function to ease the pain of creating dotplots. *Commun. Biometry Crop Sci.* **5,** 69–77 (2010).

9. Morris, M. D. Factorial sampling plans for preliminary computational experiments. *Technometrics* **33,** 161–174 (1991).

10. Khare, Y. P., Muñoz-Carpena, R., Rooney, R. W. & Martinez, C. J. A multi-criteria trajectory-based parameter sampling strategy for the screening method of elementary effects. *Environ. Model. Softw.* **64,** 230–239 (2015).

11. Saltelli, A., Ratto, M., Tarantola, S. & Campolongo, F. Update 1 of: Sensitivity Analysis for Chemical Models. *Chem. Rev.* **112,** PR1–PR21 (2012).

12. Hillel, D. Environmental Soil Physics. *Acad. Press San Diego CA* 771 (1998). doi:10.2134/jeq1999.00472425002800060046x

13. Rodea-Palomares, I., González-Pleiter, M., Martín-Betancor, K., Rosal, R. & Fernández-Piñas, F. Additivity and Interactions in Ecotoxicity of Pollutant Mixtures: Some Patterns, Conclusions, and Open Questions. *Toxics* **3,** 342–369 (2015).

14. Aus der Beek, T. *et al.* Pharmaceuticals in the environment - global occurrences and perspectives. *Environ. Toxicol. Chem.* (2015). doi:10.1002/etc.3339

15. Hughes, S. R., Kay, P. & Brown, L. E. Global synthesis and critical evaluation of pharmaceutical data sets collected from river systems. *Environ. Sci. Technol.* **47,** 661–77 (2013).

16. Junghans, M., Backhaus, T., Faust, M., Scholze, M. & Grimme, L. H. Application and validation of approaches for the predictive hazard assessment of realistic pesticide mixtures. *Aquat. Toxicol.* **76,** 93–110 (2006).

17. Faust, M. *et al.* Predicting the joint algal toxicity of multi-component s-triazine mixtures at low-effect concentrations of individual toxicants. *Aquat. Toxicol.* **56,** 13–32 (2001).

18. Ritz, C. & Streibig, J. C. Bioassay Analysis using R. *J. Stat. software* **12,** 17 (2005).

19. Ritter, A. & Muñoz-Carpena, R. Performance evaluation of hydrological models: Statistical significance for reducing subjectivity in goodness-of-fit assessments. *J. Hydrol.* **480,** 33–45 (2013).

20. Szöcs, E. *et al.* Analysing chemical-induced changes in macroinvertebrate communities in aquatic mesocosm experiments: a comparison of methods. *Ecotoxicology* **24,** 760–769 (2015).

21. Warton, D. I., Wright, S. T. & Wang, Y. Distance-based multivariate analyses confound location and dispersion effects. *Methods Ecol. Evol.* **3,** 89–101 (2012).

ANEX 1. Non-exhaustive list of R packages used in the study

Package	Version	Repository
'qualityTools'. Statistical Methods for Quality Science	1.55	CRAN https://cran.r-project.org/src/contrib/Archive/qualityTools/
'HH'. Statistical Analysis and Data Display: Heiberger and Holland	3.1-31	CRAN https://cran.r-project.org/web/packages/HH/index.html
"plotrix". Various plotting functions	3.6-1	CRAN https://cran.r-project.org/web/packages/plotrix/index.html
"sandwich". Robust Covariance Matrix Estimators	2.3-4	CRAN https://cran.r-project.org/web/packages/sandwich/index.html
"plyr". Tools for splitting, applying and combining data	1.8.3	CRAN https://cran.r-project.org/web/packages/plyr/index.html
"mulcomp". Simultaneous Inference in General Parametric Models	1.4-4	CRAN https://cran.r-project.org/web/packages/multcomp/index.html
"Boot". Bootstrap Functions (originally by Angelo Canty for S)	1.3-13	CRAN https://cran.r-project.org/web/packages/boot/index.html
"Hmisc". Harrell Miscellaneous	3.17-4	CRAN https://cran.r-project.org/web/packages/Hmisc/index.html
'reshape2'. Flexibly Reshape Data: A Reboot of the Reshape Package	1.4.1	CRAN https://cran.r-project.org/web/packages/reshape2/index.html
'ggplot2'. An implementation of the Grammar of Graphics	2.1.0	CRAN https://cran.r-project.org/web/packages/ggplot2/index.html
'drc'. Analysis of dose-response curve data	2.5-12	CRAN https://cran.r-project.org/web/packages/drc/index.html
'utils'. The R Utils Package	3.1.2	CRAN https://cran.r-project.org/web/packages/R.utils/index.html
'mvabund'. Statistical Methods for Analysing Multivariate Abundance Data	3.11.9	CRAN https://cran.r-project.org/web/packages/mvabund/index.html
'vegan'. Community Ecology Package	2.3-	CRAN https://cran.r-project.org/web/packages/vegan/index.html
'pwr'	1.1-3	CRAN https://cran.r-project.org/web/packages/pwr/index.html

ANEX 2. Normality test for GSA.csv by “Treatment”

```
> t(GSA_TREAT.lres)
     statistic p.value
1    0.952865  0.7634077
2    0.9028688 0.3911646
3    0.6773077 0.003532857
4    0.9520271 0.7566626
5    0.9473528 0.7188028
6    0.8474926 0.1502042
7    0.8988828 0.3673684
8    0.8569352 0.178897
9    0.922688  0.5249286
10   0.7900428 0.04772941
11   0.7771389 0.03624455
12   0.863418  0.2012046
13   0.9215106 0.5163068
14   0.9153092 0.4722337
15   0.9551273 0.7815109
16   0.8697972 0.2253976
17   0.8510184 0.1604151
18   0.9366644 0.632455
19   0.9165707 0.4810111
20   0.9599355 0.8192433
21   0.869542  0.2243856
22   0.9181668 0.4922565
23   0.8091382 0.07090881
24   0.9493016 0.7346223
25   0.9136937 0.4611389
26   0.9347663 0.6173788
27   0.8868845 0.3021843
28   0.9342552 0.61334
29   0.8127177 0.07625038
30   0.9629463 0.8421349
31   0.8504883 0.1588424
32   0.9304184 0.583337
33   0.9099395 0.4359982
34   0.8369611 0.1229976
35   0.9926135 0.9945781
36   0.9469607 0.7156167
37   0.9528743 0.7634817
38   0.8980119 0.3623122
39   0.7402758 0.01597366
40   0.8707002 0.2290103
41   0.9927851 0.9948647
42   0.8933048 0.3358671
43   0.8838003 0.2869669
44   0.9277221 0.5626289
45   0.9265592 0.5538048
46   0.9690605 0.8860648
47   0.9348375 0.6179423
48   0.9421427 0.6765071
49   0.8456164 0.1450043
50   0.868278  0.2194267
51   0.9480122 0.7241584
52   0.9715738 0.9028349
53   0.9189526 0.4978496
54   0.7848593 0.04276473
55   0.9751628 0.9251435
56   0.8780977 0.2604347
57   0.8990581 0.3683924
58   0.900681  0.3779711
59   0.9428098 0.6819113
60   0.9360378 0.6274655
61   0.8544141 0.1708101
62   0.9732028 0.9132167
63   0.7365619 0.01466912
```

64	0.9665473	0.8684903
65	0.9487175	0.729884
66	0.868326	0.2196134
67	0.9334874	0.6072898
68	0.9215012	0.5162385
69	0.9367805	0.633381
70	0.9592112	0.8136413
71	0.9775625	0.9388196
72	0.7073392	0.007379758
73	0.7928729	0.05065768
74	0.8907152	0.321952
75	0.9370515	0.6355432
76	0.9079069	0.4227699
77	0.9377107	0.6408121
78	0.7896352	0.04732062
79	0.8385322	0.1267594
80	0.9012992	0.3816664
81	0.7827638	0.04089588
82	0.9822723	0.9622791
83	0.942746	0.681394
84	0.9160024	0.477045
85	0.8223653	0.09250111
86	0.9031044	0.3926048
87	0.8722779	0.2354368
88	0.9974724	0.9995748
89	0.8739306	0.2423274
90	0.8591813	0.1863749
91	0.8450475	0.1434588
92	0.7734307	0.03345026
93	0.7336054	0.0137025
94	0.9039282	0.3976694
95	0.936193	0.6286997
96	0.839672	0.1295515
97	0.971224	0.9005536
98	0.9432925	0.6858246
99	0.9691424	0.886625
100	0.9779901	0.9411421
101	0.9715115	0.90243
102	0.9220072	0.5199334
103	0.9944056	0.997163
104	0.9429292	0.6828785
105	0.9021447	0.3867625
106	0.9787744	0.9453058
107	0.954119	0.7734632
108	0.8868199	0.3018594
109	0.944214	0.6933023
110	0.9006223	0.3776215
111	0.8910559	0.3237573
112	0.9133196	0.458593
113	0.8878362	0.3070051
114	0.9587933	0.8103942
115	0.8874902	0.3052455
116	0.9680186	0.8788702
117	0.9411088	0.6681452
118	0.9516522	0.7536397
119	0.9578673	0.8031626
120	0.9108997	0.4423416
121	0.9363947	0.6303058
122	0.8950474	0.3454833
123	0.8795195	0.2668577
124	0.9528732	0.7634733
125	0.9445842	0.6963083
126	0.96339	0.845448
127	0.9794281	0.94868
128	0.926408	0.5526621
129	0.857697	0.1814041
130	0.9703678	0.8948962
131	0.8423224	0.1362534
132	0.893105	0.3347776
133	0.8873967	0.3047713

134 0.9550715 0.7810666
135 0.7805088 0.03896894
136 0.8753401 0.2483331
137 0.8842526 0.28916
138 0.982125 0.9616198
139 0.9231539 0.5283614
140 0.8983561 0.3643043
141 0.8959572 0.3505852
142 0.9163151 0.4792252
143 0.8775395 0.2579474
144 0.9336016 0.6081882
145 0.9681943 0.8800928
146 0.9461345 0.7089034
147 0.9576988 0.8018412
148 0.872802 0.237604
149 0.946231 0.7096871
150 0.9148927 0.4693577
151 0.9027692 0.3905569
152 0.8927545 0.3328726
153 0.8890992 0.3134947
154 0.9041166 0.3988345
155 0.8924133 0.3310258
156 0.9314043 0.5909893
157 0.8086332 0.07018308
158 0.9572119 0.7980161
159 0.963749 0.8481162
160 0.9476558 0.7212639
161 0.9354552 0.6228369
162 0.8916492 0.3269192
163 0.8417257 0.1347186
164 0.9327102 0.6011883
165 0.9503725 0.7432981
166 0.9395601 0.6556565
167 0.8587898 0.1850527
168 0.924827 0.5407857
169 0.834035 0.1162532
170 0.8625845 0.1982107
171 0.9415791 0.6719473
172 0.9484103 0.727391
173 0.7636735 0.02702034
174 0.7317583 0.01312919
175 0.9059592 0.4103505
176 0.9132082 0.4578365
177 0.8913839 0.3255027
178 0.8830052 0.2831438
179 0.8972899 0.3581586
180 0.9265041 0.5533879
181 0.8809646 0.09017685
182 0.9400284 0.4984395
183 0.9426783 0.5335288
184 0.9674952 0.8828745
185 0.9265346 0.3448231
186 0.978813 0.9784848
187 0.9527509 0.6774826
188 0.9340344 0.4248415
189 0.9853332 0.9969286
190 0.988389 0.9993015
191 0.9090804 0.2076316
192 0.9546772 0.7060127
193 0.9638388 0.8368949
194 0.8947325 0.135629
195 0.9796982 0.9824228
196 0.956469 0.7324912
197 0.9089683 0.2371148
198 0.9660401 0.865237
199 0.9085377 0.2043278
200 0.9598818 0.7821414
201 0.9474549 0.6001261
202 0.8618664 0.05159355
203 0.9472818 0.5976477

204 0.9099993 0.2133433
205 0.9048078 0.1829597
206 0.9470645 0.5945437
207 0.9225165 0.3074502
208 0.9742314 0.9497014
209 0.8259454 0.01876398
210 0.9744622 0.9514925
211 0.9172828 0.2642019
212 0.9090813 0.207637
213 0.9340485 0.425004
214 0.9443677 0.5566301
215 0.9726596 0.9365706
216 0.961808 0.8092991
217 0.9470788 0.5947474
218 0.9401489 0.5000033
219 0.9351347 0.4377206
220 0.8875696 0.1096416
221 0.9622119 0.7989522
222 0.9308477 0.389184
223 0.9152001 0.2486019
224 0.9066351 0.1931413
225 0.9892026 0.9995763
226 0.8912288 0.1222188
227 0.9617596 0.8086271
228 0.9426329 0.5329161
229 0.9249074 0.3292376
230 0.8981298 0.1500422
231 0.8672294 0.06027846
232 0.8979101 0.1490655
233 0.8916869 0.123893
234 0.9424175 0.5300111
235 0.8795227 0.08642134
236 0.9564703 0.7325112
237 0.931239 0.3934298
238 0.9041492 0.1794198
239 0.9401752 0.5003446
240 0.9377677 0.4697064
241 0.9823048 0.9912094
242 0.9288036 0.3676037
243 0.9864942 0.9981385
244 0.9858304 0.9975017

CHAPTER 5: SUPPLEMENTARY MATERIAL

Table S5.1. Concentrations, incubation times and mode of action of fluorochromes used in the FCM analysis.

Fluorochrome	Applications	Mode of action	Stock concentration	Final concentration	Incubation time (min)
Calcium Green-1 AM	Intracellular free Ca^{2+}	Calcium Green-AM is a chemical indicator that diffuses freely into the cells. Once it is inside the cell , non-specific esterases cleave acetate group and Calcium Green-AM binds to intracellular free calcium, exhibiting an increase in green fluorescence (recorded in FL1 channel)	2.6 mg/mL	10.3 µg/mL	120
DHR123	Intracellular levels of hydrogen peroxide	DHR123 passively diffuses across cell membranes. Once that it enters the cell, it can be oxidised, mainly by H_2O_2, in a slow reaction unless catalysed by an enzyme with peroxidase activity, and secondarily by peroxynitrite anion, to form cationic rhodamine 123. This is a fluorescent compound which localises in the mitochondria emitting a bright green fluorescent signal (recorded in FL1 channel)	2 mg/mL	10 µg/mL	40
HE	Intracellular levels of superoxide anion	HE enters the cell, where it is selectively oxidised by superoxides into fluorescent ethidium, which is trapped by intercalating with DNA, resulting in red fluorescent signal (recorded in FL3 channel)	3.154 mg/mL	5 µg/mL	30
PI	Membrane integrity	Due to its polarity, PI is unable to pass through intact cell membranes. However, when the integrity of the cell membranes is damaged, PI is able to enter and to intercalate with double-stranded nucleic acids to produce red fluorescence (recorded in FL3 channel)	1 mg/mL	2.5µg/mL	10
$DiBAC_4(3)$	Cytoplasmic membrane potential	$DiBAC_4(3)$ is lipophilic and shows high fluorescence dynamics upon changes in membrane potential by its Nernstian distribution between the inner and outer medium of the cells. Once the cells are equilibrated with DiBAC4(3), depolarisation increases green fluorescence (recorded in FL1 channel) when the cells are excited with blue light (488 nm excitation laser) as the negatively charged oxonol moves into the cells, where it is bound to intracellular proteins and membranes. Hyperpolarization decreases fluorescence (recorded in FL1 channel). Due to overall negative charge, it is excluded from the mitochondria, so the mitochondrial membrane potential does not interfere with the measurement of the cytoplasmic membrane	0.5 mg/mL	0.5 µg/mL	10

		potential			
JC-1	Mitochondrial membrane potential	JC-1 exhibits potential-dependent accumulation in mitochondria and owns dual emission potential-sensitivity. Fluorescence emission shifts from green (recorded in FL1 channel) to red (recorded in FL2 channel). Mitochondrial depolarization decreases the red/green fluorescence intensity ratio	1 mg/mL	5 µg/mL	20
CellEvent™ Caspase-3/7 Green Detection Reagent	Activity of caspases 3 and 7	Caspase-3/7 is a novel fluorogenic substrate for activated caspases 3 and 7. This is a four amino acid peptide (DEVD) conjugated to a nucleic acid binding dye. Caspase 3/7 diffuses across the cell. If caspase-3 or capase-7 are activated, the DEVD peptide is cleaved, enabling the dye to bind to DNA, producing a bright green fluorogenic response (recovered in FL1 channel)	2 mM	20 µM	60
FDA	Metabolic activity	FDA is lipophilic so it can enter the cells. Inside the cells, its acetate residues are cleaved off by non-specific esterases and the polar hydrophilic fluorescent product green fluorescein is retained by cells (recorded in FL1 channel). The amount of fluorescence increases over time depending on the metabolic activity of non-specific esterases. FDA was added and fluorescence charges recorded continuously during 15 min according to Padro et al., (2012a)	5 mg/mL	0.1 µg/mL	-
BCECF AM	Intracellular pH	BCECF-AM AM diffuses through the cell membrane and intracellular esterases cleave the ester bond, releasing BCECF. When BCECF AM is excited by blue light (488 nm excitation laser), this fluorochrome emits fluorescence with a maximum at 525 nm. In the range of physiological pH, the emission intensity increases with increasing pH. The fluorescence emitted at 620 nm is not pH-dependent. In spite of this wavelength, it is not really an isosbestic point. The ratio of fluorescence emitted at 525 and 620 nm (green/red) was used to analyse pHi in cells stained with BCECF (Koo et al., 2007).	1 mg/L	5 µg/mL	40

Table S5.2. Specific primers for RT-qPCR analysis

Gene	Primer sequence (5`-3`)	Accession Number	Encoding	References
Fe-SOD	CCGCGACTTCGGCAGCCTGG	U22416	Superoxide dismutase-Fe	Luis et al., 2006
	GGTTCACGGCGTTGGGCGAC			
Mn-SOD	CTGGAGCCGCATGTGGATGCC	U24500	Superoxide dismutase-Mn	Luis et al., 2006
	CCCACGGCCTTGTTCAGGTC			
CAT	GGAGGCTGCAGGAAAACTGA	AF016902	Catalase	Petit et al., 2012
	ATTTCCAGCCTGGGCTACCT			
GPX	CGAAGCCGCACATGGTATAGT	AY051144	Glutathione peroxidase	Petit et al., 2012
	TGCTCCAATCACGACCTATTTG			
LHCA	CAAGACGCTAGGGAGGAGTG	AY171231	Light-harvesting complex I protein	Petit et al., 2012
	CCACACAGGTGCCATGTTAG			
LHCB	CGCTGAGCTGAAGGTGAAG	AY171229	Light-harvesting complex II protein	Petit et al., 2012
	GGTGAACTTGGTGGCGTAG			
LHCBM9	AGGCCTTCTGGATGTACCAC	AF479778.1	Major light-harvesting complex II protein m9	Petit et al., 2012
	ATGGTTCTGGACACAACTGC			
PSBD	ATCGGTACATATCAAGAGAA	2716961	Photosystem II protein D2	This study
	CACAAGGGAATAGTAATAAAC			
PSBA	GCTGCTTGGCCGGTAATCGG	X02350	Photosystem II protein D1	Luis et al., 2006
	GGAAGTTGTGAGCGTTACGC			
FDX	GCCTACAAGGTCACCCTGAAGA	L10349.1	Ferredoxin	Petit et al., 2012
	GCAAGAGTAGGGCAGGTCCAG			
RBX	CATCCACCGTGCTATGCACGC	J01399	Rubisco large subunit	Luis et al., 2006
	TACGTCGCCACCTTCACGAGC			
MTC1	GCGGACACCAATAAGCTGT	5722640	Metacaspase	Murik et al., 2014
	CAGTAGCACGCCGTATGTCT			
MTC2	CATCCAGACCGTCATCAAG	5717424	Metacaspase	Murik et al., 2014
	CGTTCTTGTTGCTGCACTC			
CaM	AACGGCACCATTGATTTCC	NW_001843987.1	Calmodulin	Chen et al., 2015
	TCATCTCATCGACCTCCTCC			
CAS	TCAACTCGGGCACCAAGG	AB127959.1	Chloroplast-localized Ca^{2+} sensor	Chen et al., 2015
	CGCCCACCACCACATACAC			
18S	GCCTAGTAAGCGCGAGTCAT	M32703.1	small subunit ribosomal RNA	Chen et al., 2015
	AGCCAAGCTCAATCCGAACA			

Chen, H., Hu, J., Qiao, Y., Chen, W., Rong, J., Zhang, Y., He, C., Wang, Q., 2015. Ca(2+)-regulated cyclic electron flow supplies ATP for nitrogen starvation-induced lipid biosynthesis in green alga. Scientific reports 5, 15117. doi:10.1038/srep15117

Luis, P., Behnke, K., Toepel, J., Wilhelm, C., 2006. Parallel analysis of transcript levels and physiological key parameters allows the identification of stress phase gene markers in Chlamydomonas reinhardtii under copper excess. Plant, Cell and Environment 29,

2043–2054. doi:10.1111/j.1365-3040.2006.01579.x

Murik, O., Elboher, A., Kaplan, A., 2014. Dehydroascorbate: a possible surveillance molecule of oxidative stress and programmed cell death in the green alga *Chlamydomonas reinhardtii*. New Phytologist 202, 471–484. doi:10.1111/nph.12649

Petit, A.-N., Debenest, T., Eullaffroy, P., Gagné, F., 2012. Effects of a cationic PAMAM dendrimer on photosynthesis and ROS production of *Chlamydomonas reinhardtii*. Nanotoxicology 6, 315–326. doi:10.3109/17435390.2011.579628

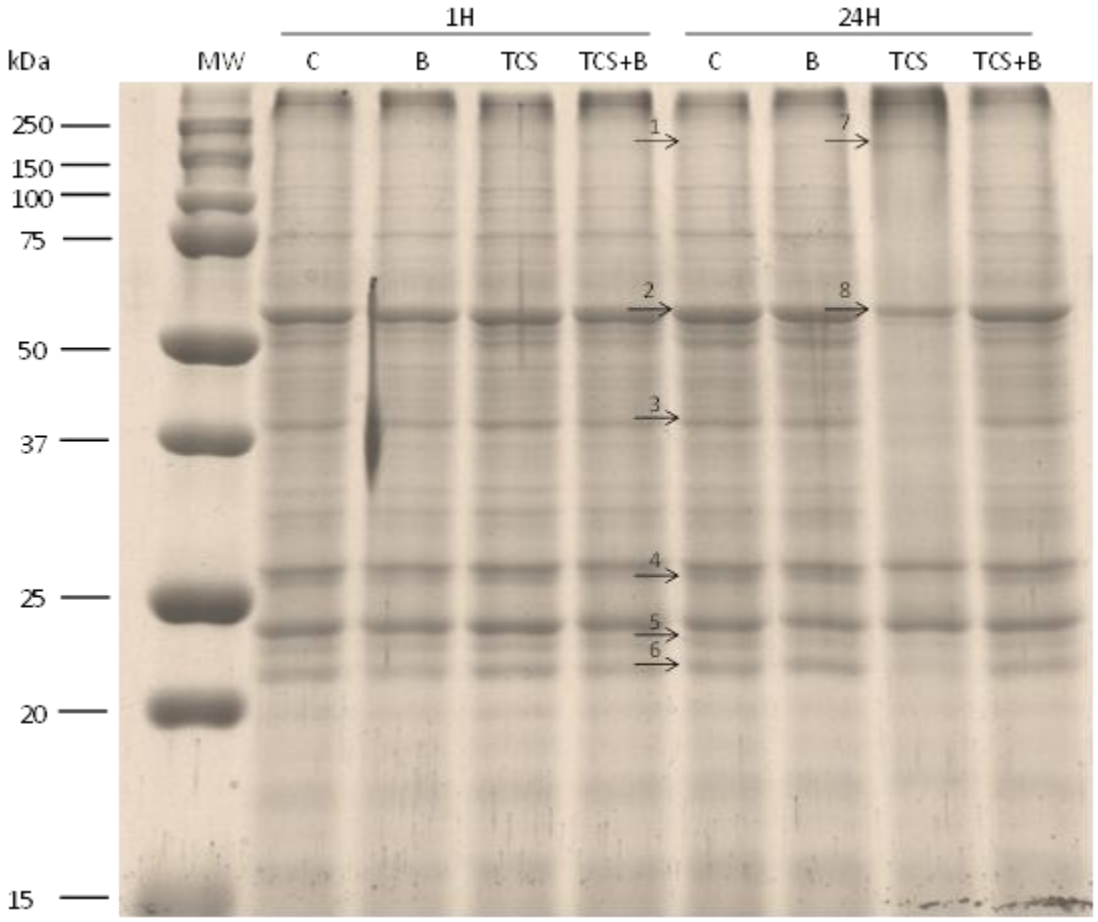

Figure S5.1. Effect of TCS on protein pattern of *C. reinhardtii* cells after 1 and 24 h of exposure. SDS-PAGE of cellular extracts of cells of *C. reinhardtii* exposure to TCS at 1 and 24 h. MW: molecular weight markers (kDa). C: control, B: BAPTA-AM; TCS: triclosan and TCS + B: triclosan + BAPTA-AM. Arrows indicate changes detected in the protein pattern (see text for details)